THE CATHODE RAY OSCILLOSCOPE

J. CZECH · THE CATHODE RAY OSCILLOSCOPE

THE CATHODE RAY OSCILLOSCOPE

THE CATHODE RAY OSCILLOSCOPE

CIRCUITRY AND PRACTICAL APPLICATIONS

621.317.755

BY

J. CZECH

PHILIPS' TECHNICAL LIBRARY

INTERSCIENCE PUBLISHERS, INC.–NEW-YORK

1957

Translated from the German by
G. E. LUTON, A.I.L.

Publisher's note:
A German edition of this book was published by
Verlag für Radio-Foto-Kinotechnik G.m.b.H.
Berlin-Borsigwalde

Printed in the Netherlands

First published in 1957

PREFACE

Experience repeatedly confirms that the practical value of an oscilloscope depends essentially upon how far its most useful potentialities are understood for the wide variety of measurements to which it can be applied. This in turn presupposes a comprehensive knowledge of the way the oscilloscope functions, since its circuit enters into the whole circuit under measurement and its properties determine to a very great extent the most suitable method of measurement to be adopted.

Accordingly, parts I and II of this book are mainly concerned with the structural sections and the mode of operation of the oscilloscope. The circuit descriptions are supported by numerous original oscillograms and part II also deals with the principles which apply when using the oscilloscope in measuring-technique.

In part III a number of examples are considered of measurements taken from actual practice, and the methods used for evaluating the results are discussed in detail. Particular attention is devoted in chapter 15 to measurements on television receivers, showing at the same time how the use of a time base expansion unit allows far greater insight into the details of a signal under investigation than a normal oscillogram.

Part IV is devoted to directions for building a simplified oscilloscope, a high-precision instrument and a simple time-base expansion unit. The circuits described provide an opportunity of considering further details of importance for working with oscilloscopes and for assessing their suitability to perform certain tasks.

This book is above all intended as an introduction for those who are newcomers to the technique of oscillography, a technique which is gaining more and more in importance as time goes by. For this reason I have made exclusive use of original oscillograms in this present work as in all my previous publications, which are also partly reproduced here. I believe that only in this way is it possible to convey that direct impression of the results of measurement which is so important for becoming familiar with the uses of the oscilloscope.

I gladly take this opportunity of thanking all who have lightened the task of preparing this book. I am especially indebted to the managements of the Deutsche Philips GmbH, Valvo GmbH, and the Elektro Spezial GmbH, Hamburg, who placed at my disposal the measuring apparatus and accessories needed for the practical work involved. Acknowledgements are also due to N.V. Philips' Gloeilampenfabrieken, Eindhoven (Holland), who kindly allowed me to make use of information from various sources which are listed in the bibliography. I should also like to express my gratitude to Mr. G. E. Luton

for his English translation and to the members of the Industrial Products Division of Philips Electrical Ltd., London, who gave their help in checking the proofs.

May this book contribute not only to the advancement of the cathode ray oscilloscope on its own territory, electrical engineering, but also to promoting its application in other fields where problems of measurement still await a solution.

J. Czech

Hamburg, December 1956

CONTENTS

PART I

The Cathode Ray Oscilloscope

1. The Cathode Ray Oscilloscope

Structural Sections.

The main structural sections of the oscilloscope, apart from the cathode ray tube itself, are the power supply, the vertical deflection amplifier—Y axis—and the time base or "sweep" generator. This is sometimes combined with a horizontal deflection amplifier—X axis.

A schematic indication of the way the individual sections work together is given in fig. 1–1. The mode of operation and uses of the oscilloscope will be dealt with in detail in the following chapters.

The power supply provides the AC and DC voltages needed for feeding the cathode ray tube and auxiliary circuits.

As the block diagram shows, there is also a synchronizing device, which enables the time-base frequency to be locked with either the vertical deflection voltage, with a voltage supplied from an external source or with the mains voltage, according to choice. Possibilities are also provided for triggering a single time base and for triggering a sweep by a pulse sequence or by a part cycle of a sinusoidal voltage. These processes are dealt with in detail in the chapter on time bases.

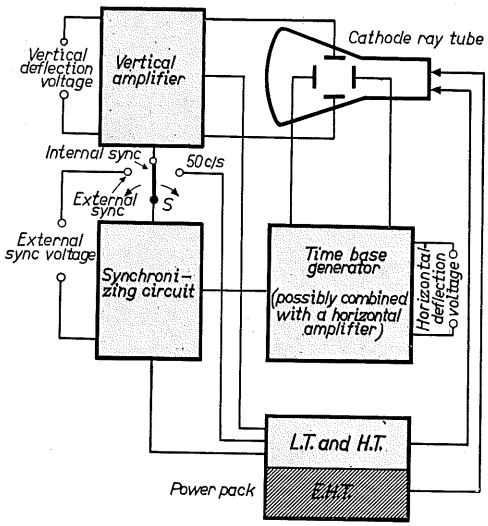

Fig. 1–1.
Schematic layout of the structural sections of a conventional oscilloscope

The synchronizing device is nearly always combined with the time base, both in the circuit and in the structural design. This has been particularly brought out in fig. 1 in order to emphasise its useful possibilities which, as experience shows, are seldom exploited to the full.

Fig. 1–2 shows the exterior of a cathode ray oscilloscope with its control panel. The probe in the input permits a division of the voltage to be measured by a ratio of 20 : 1 before it is fed in correct amplitude and phase to the Y amplifier.

The retractable light-shield with the scale for quantitative evaluation of the patterns is shown pulled back. The heat generated in the apparatus is allowed to escape through vents plentifully provided in the casing.

The structural sections indicated in fig. 1–1 can be seen in figs. 1–3 and 1–4, which show the interior of Philips oscilloscope GM 5653.

Fig. 1–3 gives a view of the mains transformer, the rectifying valves for the anode voltages together with the valves and circuit components for the time base.

Fig. 1–4 shows the other side of the chassis with the valves and circuit components for the vertical deflection amplifier. Below in the centre can be seen a group of electrolytic condensers, whose main function is to provide the filtering for the two cascade rectifiers which generate the E.H.T. for the anodes of the cathode ray tube (See circuit diagram fig. 3–6 page 31). The mains transformer is again visible, as well as two stabilizer valves 85 A1, and valves PL 81 and EF 42 for electronic control.

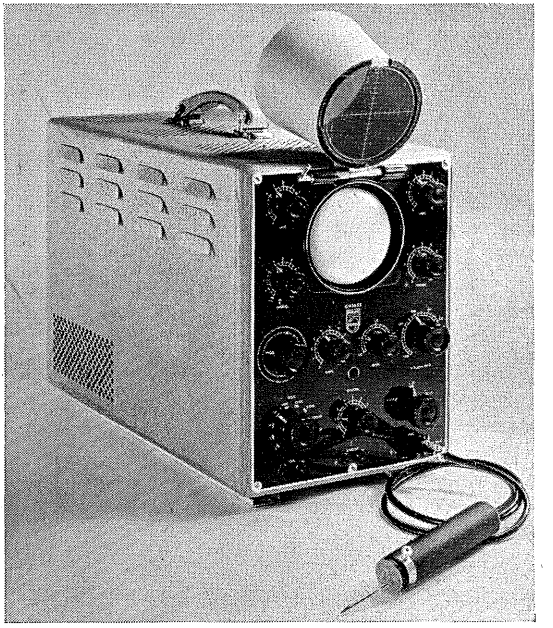

Fig. 1–2.
Front view of Philips oscilloscope "GM 5653/01."

An R.F. choke is located above the transformer for preventing time base harmonics from interfering with radio reception.
These illustrations show that the mains transformer is generously dimensioned. This is necessary to minimize its stray field, which might otherwise cause unwanted deflection of the electron beam. The cathode ray tube is further protected against stray magnetic fields by a high grade mu-metal cylinder.
All sections of the oscilloscope—the cathode ray tube, the power supply, the time base and the deflection amplifiers—will be examined in the following chapters.
The descriptions of oscilloscope construction given in part IV provide further and more detailed examples of rating specifications for the individual circuit components.

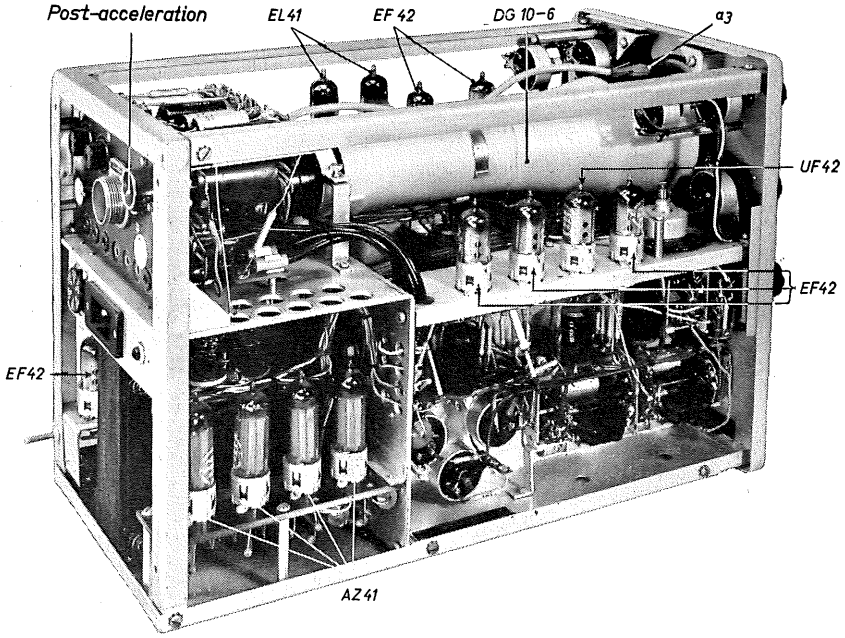

Fig. 1–3.
Interior view of oscilloscope "GM 5653/01", showing time base and power supply sections.

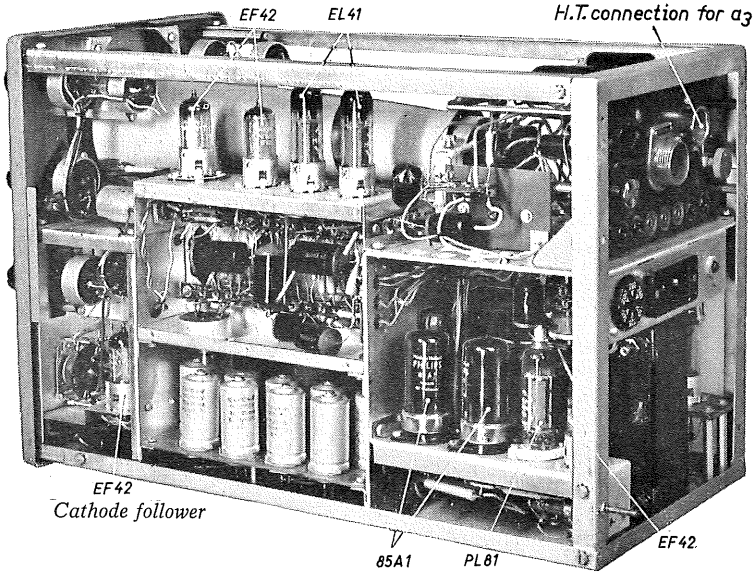

Fig. 1–4.
Interior view showing vertical amplifier.

2. The Cathode Ray Tube[1]

The cathode.

An indirectly heated cathode is generally used as the source of electrons. The electrons are emitted from an oxide coating on the tip of a small nickel cylinder sealed at one end. The coated tip is shown in fig. 2–1*a* as a white surface marked *k*. The filament or "heater" is reproduced in fig. 2–1*b*, the cathode cylinder having been removed. As can be seen, it is bent double. This is done to achieve maximum heating with the most economical means. To insulate it from the cathode, the filament is coated with a layer of kaoline.

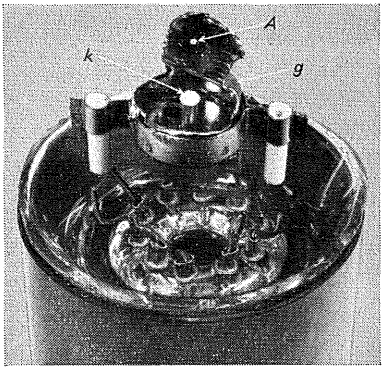

Fig. 2–1*a*. Electrode system showing the cathode of DG 10–6. *k* = electron-emitting layer. *g* = Wehnelt cylinder (opened). *A* = aperture for electron stream.

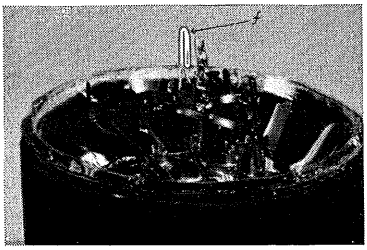

Fig. 2–1*b*. Filament of cathode ray tube DG10–6. Heater supply: 6.3 V/0.3 A.

Electrode arrangement in the cathode ray tube.

In its simplest form a cathode ray tube might be built as indicated in fig. 2–2. Opposite the indirectly heated cathode is a metal disc with an opening in the centre. This is the anode and it is operated at a positive potential to the cathode. The negative electrons emitted by the cathode are attracted by the positive anode. The great majority of the electrons land on the metal disc and return to the cathode via the voltage source. Some, however, accelerated by the attractive force of the anode voltage, pass through the opening in the disc and proceed in a straight line to the screen.

The screen consists of a phosphor-chemical coating on the inside of the large end of the tube which becomes fluorescent when struck by the electron beam. Within certain limits, the brightness of the spot thus produced on the screen is proportional to the density of the electron beam. The colour of the fluorescent glow depends upon the composition of the coating material.

By analogy with radio valves the arrangement of electrodes described corresponds to a diode. To control the magnitude of the electron beam, another electrode is added, consisting of a metal cylinder which is placed around the

[1] The C.R.T. was described by Prof. Braun in 1897, after whom it was at first named the "Braun Tube".

cathode and closed at one end except for one small aperture. This arrangement is represented schematically in fig. 2–3.

This electrode, named the *Wehnelt Cylinder* after its inventor, or quite shortly grid "*g*" by analogy with the amplifying valve, is kept at a negative (*DC*) potential with respect to the cathode. By varying this potential it is possible to control the intensity of the electrons which are attracted by the anode voltage through the opening in the Wehnelt cylinder. The voltage at which the electron beam is just suppressed, or cut off, is known as the grid cut-off voltage. This voltage is given in all tube data published by the manufacturers. In standard commercial tubes it lies between—30 and—100 V.

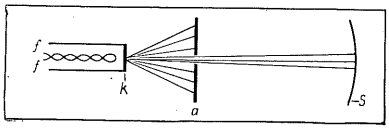

Fig. 2–2.

Simple arrangement of a cathode ray tube; f = filament, k = cathode, a = anode, s = screen

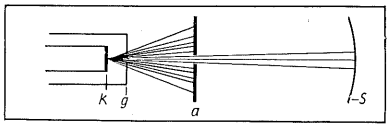

Fig. 2–3. Electrode arrangement of a cathode ray tube with Wehnelt cylinder. k = cathode, g = grid (Wehnelt cylinder), a = anode, s = screen.

With a grid bias of zero volts the electron beam is not influenced and the greatest number of electrons then pass through the aperture in the electrode. Fig. 2–4, a, b and c shows schematically the effect on the electron beam of different grid bias voltages and fig. 2–5 reproduces the actual construction of the Wehnelt cylinder.

It is important to remember that the *voltage on the Wehnelt cylinder must never be positive*, as otherwise grid current will flow and the cathode may be damaged by excessive emission.

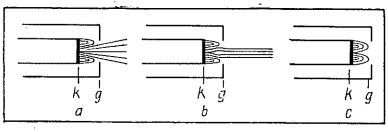

Fig. 2–4. Control of the cathode current of a C.R.T. by means of the Wehnelt cylinder. *a*) 0 bias, maximum electron emission. *b*) Medium bias, medium emission. *c*) Cut-off bias, electron beam suppressed.

Concentrating the electron beam.

The electrons emitted by the cathode represent identical charges; they therefore mutually repel each other and the beam tends to spread out.

It is essential, however, to have as fine a beam as possible, and so special measures are taken to concentrate the electrons into as narrow a beam as can be obtained. It is clear that the beam will be narrower if the electrons are made to travel faster since they will then have less time to scatter before reaching the screen.

Thus, to obtain a small spot on the screen, it is necessary to have the anode

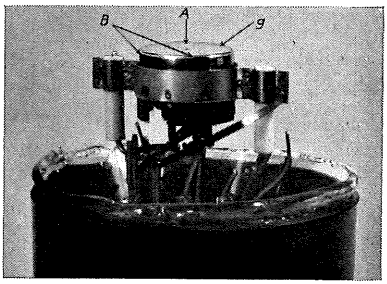

Fig. 2–5. Wehnelt cylinder of a cathode ray tube; g = Wehnelt cylinder, A = aperture for electron beam. B = observation points for assembly.

potential as high as possible. Reasons of economy, however, set a practical limit to this. Only by introducing further electrodes between the anode and the grid can a sufficiently narrow beam be obtained with a reasonable anode voltage. Fig. 2–6*a* illustrates the basic idea of these electrodes. Between anode and grid a cylindrical electrode is added which receives a positive voltage with respect to the cathode, namely about $^1/_3$ of the anode voltage. A potential difference now exists between the anode and the additional electrode amounting to about $^2/_3$ of the anode voltage and a corresponding electrostatic field is set up.

The lines of force of this field are shown in fig. 2–6*a*. The arrows indicate the direction from the lower and the higher potential and also the direction of the force acting on the electrons. The concentrating effect of this new electrode on the electron beam can plainly be recognized. The surfaces that cut the lines of force have an equal potential at all points and are therefore known as "equipotential surfaces". The cross-sections through these are shown as broken lines in fig. 2–6*a*. Comparison with fig. 2–6b makes it clear that these surfaces have the same form as the boundary surfaces of a corresponding optical lens. Their influence on the electron beam is in fact very similar to the influence of an optical lens on rays of light, and thus we speak of "electron optics."

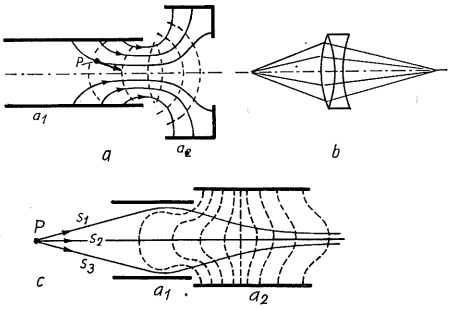

Fig. 2–6. Electron optics – light optics. *a*) Voltage relationship between anode and auxiliary anode and its effect upon the electron beam. *b*) Analogy with a) behaviour of light rays in a glass lens, *c*) influence of electrostatic field upon electron beam.

Varying the voltage on the *focusing* electrode a_1 (fig. 2–6*c*) varies the electrostatic field between anode a_2 and this electrode and thus the concentrative influence on the electron beam.

In this way the spot of light on the screen can be sharply adjusted for definition just as, for instance, an object to be photographed is focused by a camera. Where particularly sharp focusing of the spot is demanded, it is not uncommon in practice to employ not only one "electron lens", but, as in light optics, to use a combination of such lenses, involving a complicated electrode system. Fig. 2–7 shows different stages of spot definition when the voltage on the first (focusing) anode is varied in the region of sharp focus. The spot on the screen shown here is actually the reduced image of the emitting surface of the cathode. It follows from this of course that it must also

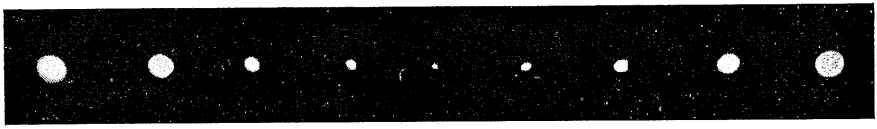

Fig. 2–7. The spot on the screen with different voltages on anode a_1.

be possible to reproduce in this way a *magnified image of the cathode*. With the aid of a suitable electron lens it is in fact possible to achieve magnifications of this sort far exceeding the capabilities of optical microscopes.
Most oscilloscopes are able to reproduce an enlarged image of the cathode on the screen, or of a section, which is determined by the apertures of the electrodes through which the beam passes. When the grid bias is set at zero, i.e. when the tube is "turned on", it only requires a low potential on a_1 to obtain distinctly on the screen a magnified image of the cathode. In this way it is possible to gain an impression of the condition of the cathode in a given tube. "C.R.T. spot photographs" of this sort are shown in fig. 2–8 *a* and *b*.

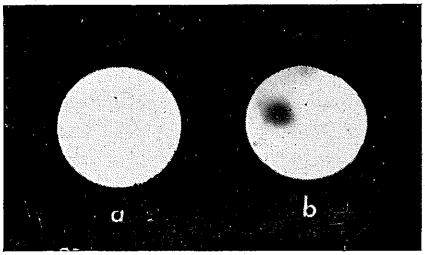

Fig. 2–8. Image of the cathode on the screen of a C.R.T. *a*) Uniformly emitting cathode. *b*) Cathode with an area of low emission.

Deflecting the beam.

The electron beam can be deflected from its path by electromagnetic as well as by electrostatic fields. For *electromagnetic deflection*, two coils are fitted opposite each other over the neck of the tube and the current to deflect the spot on the screen is passed through them. This method of deflecting has the disadvantage that, even using coils with a large numbers of turns, a fair current and therefore relatively high power is needed for deflecting the beam. Moreover, self-induction in the coils may cause extra distortion of a possibly non-sinusoidal alternating current passing through them. Since it is precisely the behaviour of the current which is to be observed, tubes of this sort are only used in television, where known fixed frequencies are used for deflecting the beam.
To deflect the electron beam, and thus the spot on the screen, by *electrostatic* fields, a pair of *deflection plates* is arranged as close behind anode a_2 as possible, in such a way that the electron beam passes centrally between them (when they are not under voltage) and the voltage to be observed is applied to them.

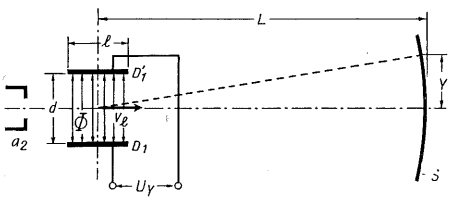

Fig. 2–9. Electrode system for electrostatic deflection. a_2 = anode, D_1, D_1' = deflection plates, S = screen

With the vacuum of the tube as dielectric, the deflection plates constitute in effect a condenser. However, its capacitance together with that of the leads in the tube amounts to only a few micromicrofarads (in practice between 1 and 3 pF) so that the alternating current flowing remains extremely small even up to high frequencies and therefore the load on the source whose output is to be investigated is kept to a minimum.

Electrostatic deflection of the beam is thus particularly suitable for electrical measurements and is almost exclusively used for such purposes.
We shall therefore examine the conditions which apply, making reference to the schematic representation in fig. 2–9. When, for instance, one of these plates is positive, the electron beam will be attracted to it, while it will be repelled by a negative plate. If, however, an alternating voltage is applied to both plates, the electron beam will be alternately attracted and repelled by the plates in a way corresponding exactly to the waveform and polarity of the voltage.
Fig. 2–10*a* shows the positions of the spot when *DC* voltages up to + 100 V are applied to the plates in steps of 25 V, and fig. 2–10*b* shows the trace under otherwise identical conditions with an alternating voltage of 50 $V_{r.m.s.}$ on the plates.

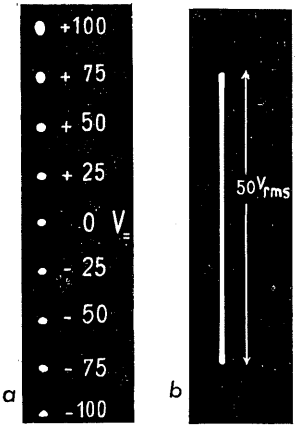

Fig. 2-10. Picture on the screen with *DC* and *AC* deflection *a*) *DC* voltage in steps of 25 V *b*) *AC* voltage 50 $V_{r.m.s.}$

As the alternating voltage moves the spot to and fro on the screen at a speed corresponding to the frequency, the individual positions of the spot can no longer be seen and now appear to the eye as a single luminous line, the length of which corresponds to the positive and negative *amplitudes* of the alternating voltage. The increase in brilliance at the end of this line is due to the fact that the velocity of a sinusoidal voltage falls to zero towards the maximum value, i.e. the speed is fast at the centre of the screen and slow near each end. Since, within certain limits, the screen becomes brighter the more electrons strike it within a given interval of time, the line traced on the screen by a sinusoidal voltage appears brighter at the ends than in the middle. What stands out more than anything in fig. 2–10*a* is that the distance between each position of the spot is absolutely identical for identical increases of voltage. From this the important fact emerges that the *beam deflection is linearly proportional to the deflection voltage.*

Calculating the beam deflection.

The following calculations presuppose that care has been taken in the tube construction to ensure that a sufficiently uniform field exists between the plates within the limits necessary for deflection. After passing through the anode, the average longitudinal velocity of the electrons in the beam is v_l. The amount of work exerted upon the electrons was:

$$W = V_a \cdot e \qquad \text{(a)}$$

(e = charge of electron)
This work must be equal to the kinetic energy, thus:

$$W = V_a \cdot e = \frac{1}{2} \cdot m \cdot v_l^2 \qquad \text{(b)}$$

From this it follows that:

$$v_l^2 = 2 \cdot \frac{e}{m} \cdot V_a \qquad \text{(c)}$$

The electrons now arrive in the field between the deflection plates, whose potential difference is V_Y. The field strength $\mathfrak{S}$ is

$$\mathfrak{E} = \frac{V_Y}{d} \tag{d}$$

The force exerted upon an individual electron is thus:

$$F = \mathfrak{E} \cdot e \tag{e}$$

The transverse acceleration of the electron is therefore equal to:

$$a = \frac{F}{m} = \mathfrak{E} \cdot \frac{e}{m} \tag{f}$$

If the electron remains under the influence of the transverse field for a time t_1, its transverse velocity is:

$$v_Y = a \cdot t_1 = \mathfrak{E} \cdot \frac{e}{m} \cdot t_1 \tag{g}$$

The time t_1 is given by the velocity with which the electron passes through the length l of the deflection plates, thus:

$$t_1 = \frac{l}{v_l} \tag{h}$$

From this it follows that:

$$v_Y = \mathfrak{E} \cdot \frac{e}{m} \cdot \frac{l}{v_l} \tag{i}$$

The electron therefore retains this velocity while passing through the length L, for a time of:

$$t_2 = \frac{L}{v_l} \tag{k}$$

The electron thus covers a distance vertical to the axis of the tube (the deflection from its orginal path) equal to:

$$Y = t_2 \cdot v_Y = \frac{V_Y}{d} \cdot \frac{e}{m} \cdot \frac{l}{v_l} \cdot \frac{L}{v_l} \tag{2-1}$$

If the value of v_l^2 obtained is inserted (c), the deflection on the screen can be expressed by:

$$Y = \frac{1}{2} \cdot \frac{L \cdot l}{V_a \cdot d} \cdot V_Y \tag{2-2}$$

With this formula all values can be calculated needed for deflecting the beam. It also shows that the deflection is linearly proportional to the deflection voltage. A linear fall-off in deflection occurs with increasing anode voltage. As a measure of a tube's deflection characteristics it is usual to indicate how far the spot can be displaced by 1 V deflection voltage. Thus the *deflection sensitivity* can be expressed by the equation:

$$DS = \frac{Y}{V_Y} = \frac{1}{2} \cdot \frac{l}{d} \cdot \frac{1}{V_a} \cdot L \tag{2-3}$$

The *deflection factor* is also commonly used for describing the behaviour of a tube and is expressed by the reciprocal of the deflection sensitivity:

$$DF_{=} = \frac{V_Y}{Y} = \frac{2 \cdot d}{l \cdot L} \cdot V_a = k_{=} \cdot V_a \qquad (2\text{–}4)$$

In this equation k is a tube constant given by d, l and L. The deflection factor indicates what (DC) voltage is needed to deflect the spot over a given unit of length on the screen (e.g. 1 cm.) It increases therefore linearly with the acceleration voltage V_a.
With an AC voltage on the deflection plates, the maximum spot displacement is determined by the peak voltage values. If the voltage is sinusoidal (the peak-to-peak values then correspond to $2 \cdot \sqrt{2}$ times the *r.m.s.* values), the *deflection sensitivity* is equal to:

$$DS_{\sim} = \frac{\sqrt{2} \cdot l \cdot L}{d \cdot V_a} \qquad (2\text{–}5)$$

and the *deflection factor* is:

$$DF_{\sim} = \frac{d}{\sqrt{2} \cdot l \cdot L} \cdot V_a = k_{\sim} \cdot V_a \qquad (2\text{–}6)$$

For tube DG 10–6, to take one example, the tube data give a deflection sensitivity of 0.3 mm/$V_{=}$ for an anode voltage of 2000 V. From (2–3) the deflection is expressed by:

$$Y_{=} = DS_{=} \cdot V_Y \qquad (2\text{–}7)$$

With a DC voltage of 40V, therefore, a deflection of 12 mm is obtained. (10 mm = 1 cm = 0.3937 inch). The deflection factor (for 1 cm) would thus amount in this case to: $\frac{10\ [\text{mm}]}{0.3\ [\text{mm/V}]} = 33^1/_3$ V. In other words, a deflection of 10 mm is achieved with a DC voltage of $33^1/_3$ V. With a sinusoidal voltage the same deflection is achieved with a voltage whose r.m.s. value is $\frac{1}{2 \cdot \sqrt{2}}$ = 0.355 times the DC value. In the example given, therefore, a deflection of 10 mm is achieved by $33^1/_3 \cdot 0.355 = 11.8$ $V_{r.m.s.}$ In pulse technique (television, radar, electronic control etc.) non-sinusoidal voltages are very frequently encountered. Voltages such as these can only be denoted by the oscillogram and the peak-to-peak (V_{pp}) values. The peak voltage is obtained by comparison with a sinusoidal voltage causing the same beam deflection. The *r.m.s.* value of this voltage multiplied by $2 \cdot \sqrt{2} = 2.83$ gives the corresponding V_{pp} value of the voltage being investigated.

Two-dimensional deflection of the beam.

Although cathode ray tubes with only one pair of plates can be put to quite a considerable number of uses, the wide range of applications at the present day first became possible by using tubes with *two pairs of deflection plates*. As

shown in fig. 2–11, the pairs of plates are mounted one behind the other in such a way that one pair deflects the beam at right angles to the other.
Thus deflecting the electron beam in two mutually perpendicular directions corresponds to the customary scientific method of representing the dependence of one quantity upon the values of another by means of rectangular co-ordinates. [2]

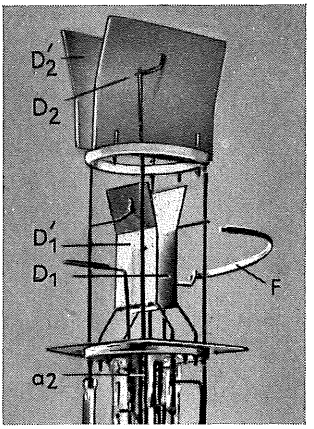

Fig. 2–11. Anode and deflection plates for double electrostatic beam deflection.

In this familiar method, the values of the quantity whose dependence is to be illustrated are shown in the vertical plane, along the Y-axis ("ordinate"), while the values of the reference quantity are shown in the horizontal plane, i.e. along the X-axis ("abscissa"). To use the terms of analysis, y is represented as a function of x, thus:

$$y = f(x) \qquad (2\text{–}8)$$

If the voltage to be examined is applied to the pair of plates for the vertical deflection and if the voltage upon which the dependence is to be shown is applied to the plates for the horizontal deflection, the spot will be moved on the screen in a manner corresponding to the influence of *both* voltages.
In this way it is possible to display the interdependence of two variables. The visible path traced on the screen represents the resultant or the vector sum of the two voltages. Apart from actual electrical voltages, practically any other measurable phenomena can be converted into proportional electrical voltages and displayed on the cathode ray tube by means of a suitable transducer (condenser microphone, photocell, mechanical vibration pick-up, strain gauge, etc.).

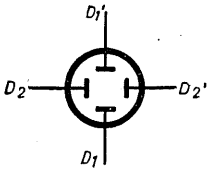

Fig. 2–12. Symbolic representation of a cathode ray tube. D_1, D_1' = Y plates D_2, D_2' = X plates.

It is usual in circuit diagrams to represent the cathode ray tube by the deflection plates only, as shown in fig. 2–12. The remaining electrodes for controlling brilliance, focus etc., are not essential parts of the measurement itself. The photograph reproduced in fig. 2–13*a* gives an example of the positions of the spot when DC voltages are applied in uniform steps of 20 V to the pairs of plates singly and simultaneously.
By reversing the polarity of the voltage source the spot can be moved upward as well as downward. With a voltage on both pairs of plates, row number 3 is situated in *quadrants* I and III and row number 4 in II and IV of the system of co-ordinates. The spots of row 1 lie in a line representing the Y-axis, row 2 represents the X-axis while rows 3 and 4 represent the positions of

[2] Other methods of deflection are, of course, conceivable. In "triographs" for example, (used for investigating the contractions of cardiac muscles) the electron beam is deflected by 3 pairs of plates each displaced at angles of 120° with respect to the other.

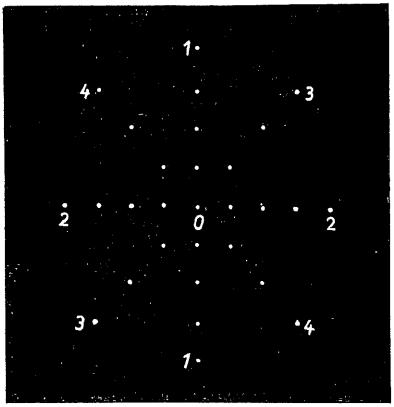

Fig. 2–13a. Spot deflection with *DC* voltage on the plates. *a*) positions of spot on screen. 1) *DC* voltage on *Y* plates only, 2) *DC* voltage on *X* plates only, 3) and 4) *DC* voltage simultaneously on *X* and *Y* plates, with differing polarities.

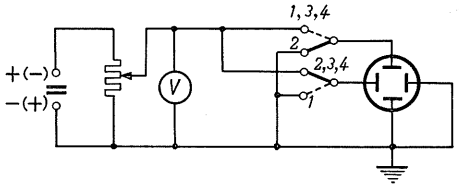

Fig. 2–13b. Circuit for 2–13a. The switch positions correspond to the appertaining rows of spots on the screen.

the spot when the voltages on the *Y* plates and on the *X* plates are changed simultaneously with differing polarities.

If a voltage of 80 V is applied to *both* pairs of plates, the spot is deflected beyond the useful area of the screen.

Particularly noticeable in this photograph is that the deflections along the *Y*-axis for each uniform increase in voltage are greater than along the *X*-axis. Thus, the line of the spots when an equal voltage is applied to both pairs of plates is not, as one might expect, at an angle of 45° but steeper. This is due to the fact that both pairs of plates do not act upon the beam at the same

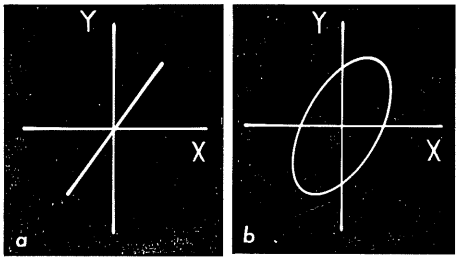

Fig. 2–14. Two alternating voltages on the deflection plates. a) Both voltages reach maximum and minimum simultaneously: they are *in phase*. b) Both voltages do not reach maximum and minimum simultaneously: *a phase shift* exist.

point, because, as can be seen from figs. 2–11 and 2–16, they are arranged one behind the other. The length *L* in formula (2–3) is therefore different for the two axes of deflection, resulting in different values of deflection sensitivity. Fig. 2–14 shows two patterns on the screen produced by two different *AC* voltages with the same frequency applied to both pairs of plates.

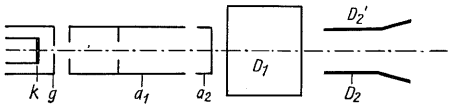

Fig. 2–15. Complete arrangement of electrodes in a C.R.T. k = cathode, g = grid, a_1 = first anode, a_2 = second anode, D_1 = *Y* plate, D_2 D_2' = *X* plates.

A highly significant feature of this method of displaying two interdependent quantities is the ability to represent the behaviour of a given phenomenon

within a given interval of time; that is to say, a quantity can be shown as a function of time ($x = f(t)$). For this purpose it is customary to apply the voltage to be measured to the vertical deflection (Y) plates, while the spot is made to move along the horizontal axis uniformly with time—*linear with time*—by simultaneously applying an appropriate voltage to the *horizontal deflection* (X) *plates* Fig. 2–15 shows schematically the arrangement of electrodes in a C.R.T. with 2 pairs of deflection plates. Fig. 2–16 shows the assembly of electrodes in tube DG 10–6. (See also fig. 2–11).

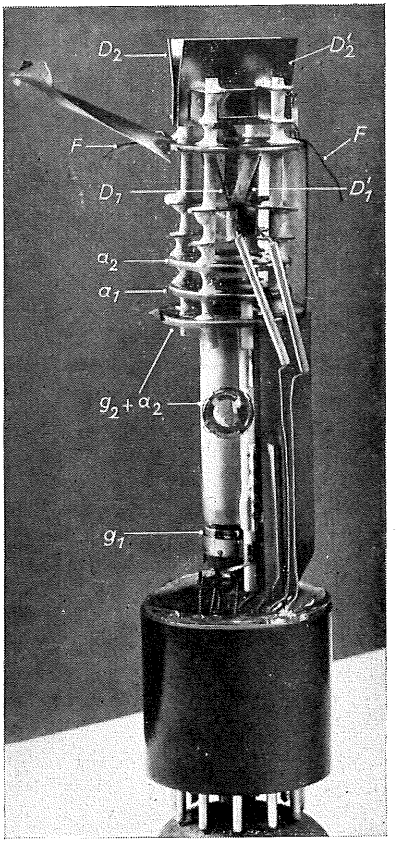

Fig. 2–16. Electrode system of cathode ray tube type DG 10–6.

Connection of the deflection plates.

There must be no voltage difference worth mentioning between the anode and the deflection system, as otherwise the velocity of the electrons will be increased or decreased according to the polarity of the voltage. As the voltage to be measured is usually connected in some way with earth potential, the anode is earthed in cathode ray tubes and not, as is customary in the case of amplifier valves, the cathode. With respect to earth therefore, the cathode is below the anode.

For sharp and undistorted patterns on the screen it is also necessary to consider the operation of the plates with respect to earth. Fig. 2–17, for example, shows a simplified arrangement of the first pair of plates in their circuit relationship with anode a_2. Plate D_1 is connected to earth i.e. with the anode. If there is a potential on the deflection plates, there will be a voltage drop between them that can always be assumed. This means with this circuit, however, that there is not the same potential in the middle of the deflection system. It fluctuates between zero and half of the voltage V_D on the "hot" plate. This results in additional acceleration of the beam following the fluctuations of the deflection voltage.

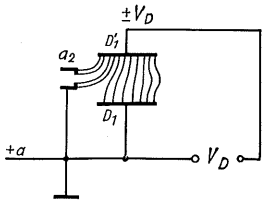

Fig. 2–17. Unbalanced circuit for deflection plates.

The field is distorted as shown in fig. 2–17, being distributed from plate D_1' to plate D_1 and to the anode a_2. As the accelerating field does not originate

from a symmetrical electrode, distortion of the spot takes place on the one hand, and on the other hand much depends upon whether the beam passes nearer to the earthed plate or to the voltage-carrying plate. If it passes nearer to the earthed deflection plate its velocity is not affected. The sensitivity in the X-direction remains unchanged.

If it passes nearer to the "hot" plate (which is positive) it will be accelerated corresponding to V_D. According to formula (2–3) however, this results in a reduction of the deflection sensitivity, as the accelerating voltage is now $V_a + V_D$.

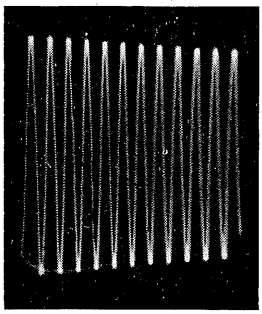

Fig. 2–18. Oscillogram of unbalanced voltage on balanced X plates.

With AC deflection voltages on both pairs of plates, the spot should describe a square or rectangular pattern on the screen. Owing to the voltage asymmetry on the respective plates, the amounts of deflection in the vertical direction vary and the pattern described by the spot becomes trapezoidal, a phenomenon known as *trapezium distortion* and represented in fig. 2–18. These unwanted phenomena (partial defocusing —see spot series in fig. 2–10a—and trapezium distortion) can be wholly avoided in practice by using a deflection system balanced with respect to earth. As shown by fig. 2–19, the lines of the field are symmetrically distributed between the plate, the average field remaining constant.The voltages on the plates now fluctuate symmetrically between only $\pm \frac{V_D}{2}$ so that there is no noticeable deterioration of the spot or trapezium distortion. The deflection system can be balanced by a voltage divider or by centre-tapped transformers as shown in fig. 2–20a and b. As a

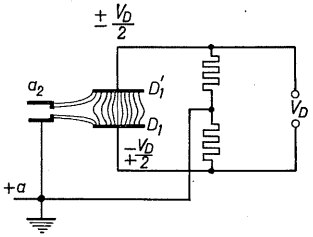

Fig. 2–19. Balanced circuit for deflection plates.

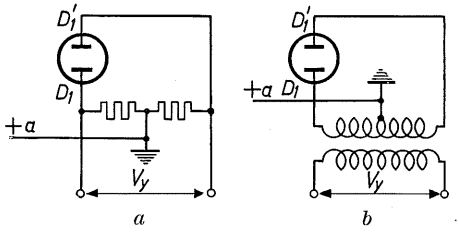

Fig. 2–20. Circuits for balancing the voltage to be measured. a) Balancing by voltage division, using two resistors. b) Balancing by a transformer.

rule, however, amplifier valves in push-pull are used for this purpose. This method is discussed in detail in chapter 5, "Deflection Amplifiers".

For reasons of economy, other means of compensating for these defects were sought by improving the deflection plates and by the use of auxiliary electrodes. This is satisfactory as regards the pair of plates nearer to the screen. The pair of plates nearer to the anode, however, should always have as balanced a

deflection voltage as possible applied to them, unless only small deflections are required or general allowances can be made for the geometry of the pattern. A solution of this sort is indicated in fig. 2–21*a* and *b*. Two small wire hooks have been soldered as auxiliary electrodes- *d*- to the unearthed plate for horizontal deflection. If the voltage on this plate increases in the positive direction, the deflection sensitivity will normally decrease. But this auxiliary electrode also attracts the beam so that the deflection in this direction is greater.
The fact remains that, where high demands are made on pattern geometry, the voltage balance for both pairs of plates must be improved and symmetrical electrodes used for deflection.

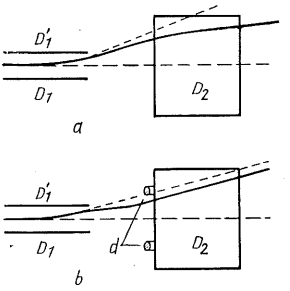

Fig. 2–21. Compensating for trapezium distortion. *a*) Unearthed *X* plate alters the velocity of the beam. *b*) Compensating for loss of sensitivity by means of two auxiliary electrodes *d*.

Load due to deflection plates.

As already mentioned, the deflection plates together with their leads in the tube possess a certain amount of capacitance, small though it may be. With an *AC* voltage on the plates, a current increasing with rising frequency will flow over this capacitance.
Because of the low value of capacitance, however, this current only needs to be taken into account for high frequency measurements. But there is still another way in which the deflection plates represent a certain load upon the voltage source. When the electrons strike the screen their kinetic energy is partly converted into radiant energy, and partly serves to release new electrons from the material of the screen. These are known as secondary electrons. (Secondary emission is brought about intentionally. Details are given in the section dealing with screens.)
The screen electrons constantly strive to move towards higher potentials, which means that they will move to the deflection plates when these have a higher potential at a given moment than the anode. Other electrons (stray electrons) also attach themselves to the deflection plates, so that a compensating current can arise between each pair of plates, resulting in a further load upon the voltage source. In order to avoid these effects, the inside of the glass envelope of the C.R.T. is coated with a colloidal graphite known as "aquadag". By means of two ductile springs (see springs marked "*F*" in figs. 2–11 and 2–16) this coating is connected with the anode and thus to earth. The electrons are thereby conducted to earth and additional load on the voltage source is avoided.
Rough treatment during transport may have caused damage to the contact between the graphite coating and the springs, or even have broken the springs. Defects of this sort can be recognized immediately by the severe distortion of the pattern caused if the screen is touched during operation. It can also happen in such cases that the pattern on the screen becomes erratic. The charge on the screen is no longer able to leak away and after reaching a certain potential, caused by the accumulation of electrons, it breaks down at irregular intervals

determined by the remaining possibilities of escape. It is also possible in this way for "islands" to form, that is to say, areas where no fluorescence occurs. Similar defects are more likely to be found in tubes working on excessively low anode voltages. The potential of the accumulated electrons on the screen is then wholly or in part higher than the accelerating voltage between cathode and anode. For various reasons the *AC* voltage for the vertical deflection plates must be applied via coupling condensers. This is primarily necessary in order to keep the anode *DC* voltage of the *AC* amplifier from the plates. At the same time the deflection plates must always be directly connected to earth via leak resistors, as otherwise they can take on random charges from stray electrons and thus introduce uncertainty into the measurements. The leak resistors should be rated between 1–10 MΩ to keep the load on the voltage source to a minimum.

Influence of electron transit time on deflection sensitivity.

The displacement of the spot on the screen corresponds to the instantaneous value of the *AC* deflection voltage only as long as the electron transit time *within the pair of plates* concerned is sufficiently short with respect to the duration of one cycle. Otherwise the deflection sensitivity will suffer.
The frequency f, at which the deflection sensitivity is reduced by a certain portion p for a plate length l and an anode voltage V_a can be found from the equation:

$$f\,(\mathrm{Mc/s}) = \frac{46 \cdot \sqrt{p \cdot V_a\,(\mathrm{V})}}{l\,(\mathrm{cm})} \qquad (2\text{–}8)$$

In tube DG 10–6, for example, $l = 2$ cm. If, with an anode voltage of 1000 V, a deflection error of 2% — $(p = 0.02)$ — is admitted, the frequency can be calculated as: $f = 46 \cdot \frac{\sqrt{0.02 \cdot 1000}}{2} = 145$ Mc/s approx.
As regards general-purpose tubes, therefore, and especially when working with even higher accelerating voltages, the equation shows that the deflection error remains within limits of accuracy on the screen up to and exceeding 100 Mc/s.
Where the time differences between voltages on both pairs of plates are to be determined (e.g. in phase measurements by ellipses) the transit time of the beam *between both pairs of plates* must be taken into consideration. At high frequencies an error occurs which can be indicated as an additional phase angle.
For a phase error with an angle θ, the frequency f appears from the equation:

$$f\,(\mathrm{c/s}) = \frac{\theta \cdot \sqrt{V_a}}{s_E} \cdot 1.65 \cdot 10^5 \qquad (2\text{–}9)$$

Taking the phase angle of 2° in an elliptical pattern, a frequency $f = 4.2$ Mc/s is obtained when $V_a = 1000$ V and the average distance between plates is $s_E = 2.5$ cm (DG 10–6).

This error in transit time can play an important part in phase measurements in radio engineering and most especially in television and short-wave technique ($f > 3$ Mc/s) [1].

The fluorescent screen.

As already stated, certain chemical substances used as the screen in cathode ray tubes become fluorescent when bombarded by electrons.
The brightness and colour of the light thus emitted depend upon the characteristics of the substance used.
The light is produced by a part of the kinetic energy of the electrons being converted into light energy. The electrons receive their kinetic energy while traversing the voltage drop between cathode and anode. The power inherent in the beam current can accordingly be expressed by the product:

$$N = I_S \cdot V_a \text{ [3]} \qquad (2\text{–}10)$$

and given in Watts or mW.
The amount of light emitted is not only directly proportional to the power of the beam but is also dependent upon the velocity of the beam, and thus upon V_a. For a given product $I_S \cdot V_a$, therefore, more light is obtained from a high anode voltage and small current than from a lower voltage and correspondingly higher current.
An upper limit is set to the brightness by the fact that beam currents exceeding a certain value cause "spot burns", resulting in a loss of efficiency in that part of the screen. It is obvious that this danger is greatest when the area under bombardment is small, i.e. a spot. It should be a rule, therefore, always to keep the beam moving in some way across the screen. But even as a trace, burning can be caused if the screen is subjected to bombardment for a prolonged period, as can often be observed on oscillocopes which have been in use for some time. It is interesting to note that the danger of burning is apparently greater at lower anode voltages.
Whereas it is difficult to produce a screen with a satisfactory life for anode voltages under 500 V, screens of tubes working with anode voltages of several kV are comparatively free from the phenomenon of burning. No complete explanation of this apparent paradox has so far been offered, as the process of energy conversion in the fluorescent screen is not yet sufficiently understood [2].
It is assumed that, with low accelerating voltages, only the upper layer of screen atoms takes part in the conversion of energy. At higher voltages the electrons of the beam penetrate deeper. Therefore deeper layers of the screen will also emit light and thus the specific load on the atoms will not be so great.
The screen is continuously supplied by the electron beam with a negative charge, so that without counter-measures its potential would constantly increase. This charge could have an undesirable effect upon the spot deflection and might even prevent further electrons reaching the screen. However, by

[3] The beam current I_S must never be confused with the anode current Ia_2. It is usually appreciably smaller than the anode current. In tubes without a post-acceleration electrode it can be measured by applying a sufficiently high voltage to one deflection plate to cause the beam to end there.

choosing a suitable luminescent material, the electrons penetrating the screen (primary electrons) can be made to release new electrons, known as *secondary electrons*. The majority of these secondary electrons possess enough energy actually to leave the screen. They then move towards the positive anode, or towards the graphite layer on the inside of the tube, which is also connected to the anode.

In this way they are able to return to the electron source—to the power supply for the C.R.T. anode voltage. A condition of balance results when the number of secondary electrons emitted from the screen equals the number of primary electrons striking the screen. The luminescent layer then assumes a constant potential, which experiments on general purpose tubes have shown to be about 100 V below the accelerating voltage. The maximum possible luminous intensity is thus directly related to the value of the upper limit of potential for a given material. This is known as the "sticking potential".

Every screen has its "sticking potential" beyond which an increase in luminous intensity is no longer possible, even with higher accelerating voltages (unless metal-backed screens are used). The sticking potential is about 8 kV for standard screen materials. A great variety of screen materials is available for producing a luminous trace in practically any desired colour. As, in general, oscillograms are visually observed it is desirable to use a screen whose spectral energy maximum corresponds as far as possible with the spectral sensitivity maximum of the eye.

The maximum sensitivity of the average human eye is about 5500 Å [4] so that screens emitting a greenish-yellow light are the most favourable. With such a screen, a satisfactory brightness of image can be achieved with a smaller beam current than would be necessary for a screen with a less suitable colour of luminescence. This means, of course, that with a greenish-yellow screen the spot appears small and the picture "sharp".

Curves comparing the spectral energy distribution of standard C.R.T. screens and the spectral sensitivity of the human eye are given in fig. 2–22*a* and *b*.

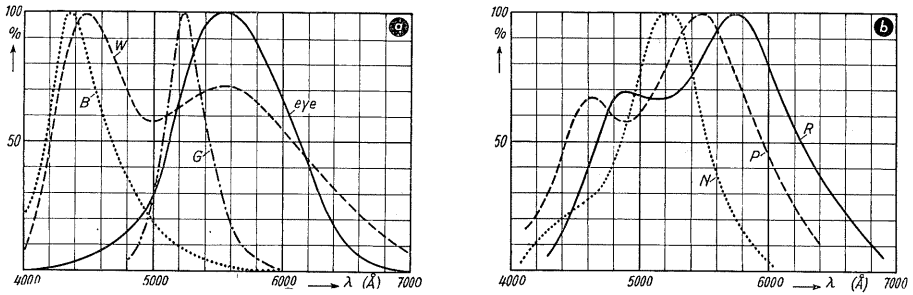

Fig. 2–22. Spectral energy distribution of various screens on Philips cathode ray tubes. *a*) Short and medium persistence screens *b*) Long persistence screens

[4] This depends upon the adaptation of the particular eye. The maximum sensitivity of the average light-adapted eye is around 5550 Å, while for the eye completely adapted to the dark it is about 5070 Å.

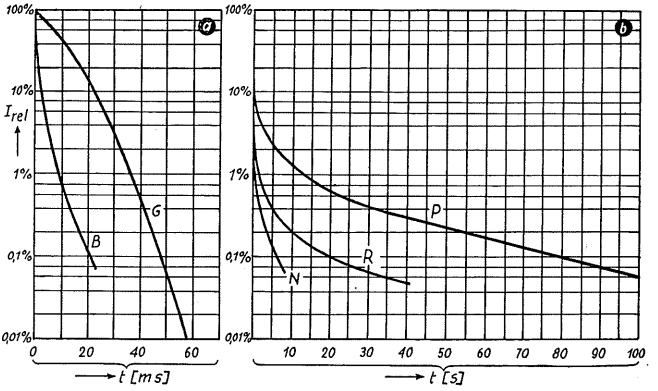

Fig. 2–23. Afterglow intensity in dependence upon time, on screens as in fig. 2–22. *a*) Short and medium persistence tubes (time scale in in millisecs. *b*) Long persistence tubes (time scale in secs.)

A certain period of time is necessary for the screen to be excited into light emission and also for the light to decay after excitation. Whereas the period of excitation is so short that it is for general purposes negligible, the period of phosphorescence (afterglow) usually lasts longer. Long afterglow is of particular advantage for observing the behaviour of non-recurring or slowly moving phenomena, and so special long-persistence screens were developed with a prolonged duration of afterglow. Fig. 2–23*a* and *b* give the persistence characteristic of five different types of screen. The blue fluorescent screen *B* belongs to the short persistence category; after 20 ms the relative brightness has decreased to $\frac{1}{1000}$ th of its original value. Screen *G*, with an afterglow of almost 50 ms more, belongs to the medium persistence category. It should be noted in this context that *G*'s light decreases more slowly at first than that of *R* and *P*. The green fluorescent screen *N* with an afterglow of about 6 secs. belongs to the long persistence category, while *R* is very long (20 secs.) and the double-layer screen *P* extremely long (80 secs.).

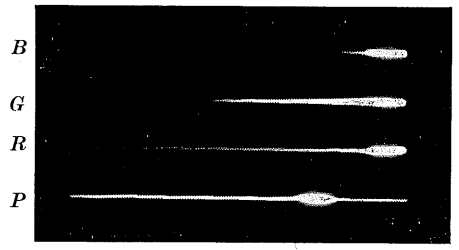

Fig. 2–24. Photographic recording of afterglow on four different screens.

How long the afterglow can be perceived by the observer depends more than anything upon the ambient light. In darkened rooms, traces decayed to $\frac{1}{1000}$ of their original brightness can be seen quite well. The times given apply in these conditions.

A photographic impression of the afterglow is given by the oscillogram in fig. 2–24. For this photograph, the spot was moved from left to right at a speed of approx. 1 m/sec (on the screen) by the time base generator of a standard oscilloscope. Photographs were taken of the afterglow from tubes with screens of different persistence, using in each case an exposure of $^1/_{100}$ sec. Whereas little more than the actual spot could be retained on the *B* screen,

the other types of screen show various lengths of afterglow trace. The *G*-screen, as one would expect from the curve in fig. 2–23, shows a short but initially fairly strong afterglow. The *R*-screen, also corresponding to its persistence curve, shows a sharp initial drop and a longer duration of afterglow. The afterglow effects on the *P*-screen overlapped during the individual periodic movements of the spot, so that the whole length of the trace was recorded, falling off a little from the actual spot onwards during the exposure. Of course, these oscillograms can only give an approximate idea of the persistence of the various screens. When the photographs were taken, the most favourable conditions for each type of screen could not be selected, as otherwise there would have been no basis of comparison. Particularly with regard to the long-persistence screens *R* and *P*, the difference between the luminous intensity upon excitation and that of the afterglow is so great (as shown by the curves in fig. 2–23) that it can hardly be overcome by an ordinary photographic film.

To avoid glare effects on the eyes during the observation of slow-speed phenomena or single transients on long persistence screens, advantage can be taken of the fact that the light emitted as a direct result of excitation (fluorescence) has a colour different from the light given off during afterglow (phosphorescence). If, for instance, a yellow filter is placed over the *P*-screen, the bluish-green light emitted during excitation will be greatly damped and the yellow afterglow trace will stand out more clearly.

Filters of this sort, using the colour of the trace of a particular tube, can be applied with advantage to other screens also. They prevent the ambient light from whitening the whole screen. The ambient light has to penetrate the filter twice (there and back) before it reaches the eye of the observer. For example, if a green filter is used in front of the tube, a bright green oscillogram appears upon the dark green screen. Thus the contrast of an image on the screen is considerably heightened. Care must be taken, however, that the transparency of the filter agrees as far as possible with the spectral energy distribution of the screen, as otherwise loss of light will result.

Photographic recording of oscillograms is possible with all standard types of film. The overall sensitivity as well as the spectral sensitivity in relation to the spectral energy distribution of the screen must naturally be taken into account.

For yellowish-green screens, orthochromatic high sensitivity film is especially suitable; e.g.: *Agfa* "Fluorapid", *Gevaert* "Scopix *G*" etc. High contrast developers must be employed (no soft tones!). For general purposes, standard 30 B.S. (31° Scheiner) (80 ASA) Pan film is used, as this produces a finer grained photograph than the high-sensitivity films mentioned.

Blue *B* screens are useful when, for instance, a short afterglow is needed for moving-film recordings or when a large number of photographs are to be made on cheap recording paper. Low colour-sensitized material has the highest sensitivity in the blue-violet part of the spectrum so that in this case the most favourable conditions are present when a blue fluorescent screen is used [3] [4] [5].

Post-acceleration tubes.

The aim of the tube designer has always been to achieve the brightest possible spot on the screen. This means, of course, that the output of the beam must be as high as possible. By increasing the beam current, a certain increase in brilliance can certainly be obtained, but this soon results in beam-scattering so that the spot becomes unduly large. The only alternative is to increase the anode voltage. If this is stepped up, the brightness of the spot does indeed increase quite considerably, because the higher anode voltage not only boosts the beam output but also improves beam concentration and screen efficiency. Unfortunately, however, the deflection sensitivity deteroriates. This entails very high voltages for beam deflection and thus a costly lay-out in deflection amplifiers. Intensive research has nevertheless shown a way of increasing the spot brightness without causing any appreciable deterioration in the deflection sensitivity [6] [7] [8].

The method is to effect the main acceleration of the beam *after* deflection by using a further anode—a_3. In this way a decline in deflection sensitivity can be largely avoided. If a voltage positive with respect to earth is applied to this electrode, the velocity of the electron beam will be increased after deflection by the accelerating field of the voltage and thus the brilliance of the spot on the screen will be correspondingly increased. Tubes employing this device are known as "post-acceleration tubes".

A certain transverse attractive force exerted by this electrode cannot be avoided, so that the deflection sensitivity does suffer a slight decline. Nevertheless it remains considerably higher than it would be if the anode voltage on a_2 alone were to be raised to the same value.

A cathode ray tube of this type, DG 10–6, is reproduced in fig. 2–25, showing the connection for the post-acceleration voltage and the cone-shaped electrode (graphite layer).

With a potential of 1 kV on a_2 in DG 10–6, the deflection sensitivity declines by only 20% for a post-acceleration potential of 1 kV on a_3 and by $33^1/_3$% for 2 kV.

A distinct increase in luminous intensity and spot sharpness is noticeable if only the ordinary *DC* voltage of 250–400 V for the deflection amplifier and time base supply is applied to a_3. In this case, deflection sensitivity declines by about 5% only.

The increased brightness of the image on the screen due to post-acceleration makes it possible, on ordinary cathode ray tubes, to photograph movements of the spot at speeds of up to about 100 km/sec. It also enables the oscillographic image to be projected on to screens of up to 2 m² [9].

Cathode ray tube data.

Typical operating and limiting characteristics are given for cathode ray tubes as for thermionic valves.

The following data apply to tube DG 10–6.

Table 2–I

Operating characteristics

Filament voltage:	V_f	= 6.3 V (indir.)
Filament current:	I_f	= 0.3 A (*AC* or *DC*)
Anode voltage:*	V_{a3}	= 2000 ... 4000 V
	V_{a2+g2}	= 2000 ... 2000 V
	V_{a1}	= 400 ... 720 V
Grid voltage:	V_g	= —45 ... —100 V
Anodes current:	I_{a2}	= 0 ... 1200 μA
	I_{a1}	= —15 ... +10 μA
Deflection sensitivity (first pair of plates)**	$DS_{D_1D_1'}$	= 0.3 ... 0.25 mm/V
Deflection sensitivity (second pair of plates)	$DS_{D_2D_2'}$	= 0.23... 0.19 mm/V

Capacitances

Grid-cathode	C_{g1}	= 8.0 pF
1st plates (singly) —a_2 (chassis)	C_{D_1}	= 5.8 pF
	$C_{D_1'}$	= 5.8 pF
2nd plates (singly) —a_2 (chassis)	C_{D_2}	= 7.6 pF
	$C_{D_2'}$	= 7.6 pF
1st plates (mutual)	$C_{D_1-D_1'}$	= 1.9 pF
2nd plates (mutual)	$C_{D_2-D_2'}$	= 2.4 pF
Both pairs of plates mutually	$C_{D_1}C_{D_1'}-C_{D_2}C_{D_2'}$	= 0.35 pF

Weight ..... 330 g.

Limiting values (maximum)

Anode voltages***	V_{a3}	= 5000 V
	V_{a2+g2}	= 2500 V
	V_{a1}	= 1000 V
Anode load:	N_{a2+g2}	= 4 W
Grid voltage:	V_g	= 0 V ...—100 V
Voltage on deflection plates	$V_{D_1D_1'}V_{D_2D_2'}$	= 450 V
Load on screen	N_s	= 3 mW/cm²
Leak resistor for deflection plates	$R_{D_1D_1'}R_{D_2D_2'}$	< 5 MΩ
Grid leak	R_{g1}	< 1.5 MΩ

* The tube can also operate with V_{a2} = 1000 V., in which case it is essential to apply a post-acceleration voltage to a_3, connecting it at least to the low voltage positive pole of + 300 V. It is of course better to use a post-acceleration voltage of not less than 1 kV, as in the case of the Oscilloscope FTO 2, described in the appendix. In this way a bright spot is obtained with a comparatively high deflection sensitivity (almost twice as high as with V_{a2} = 2000 V).

** Counted from cathode to anode.

*** The value of V_{a3} refers to the total potential difference between cathode and a_3. If, for instance, there is a potential of 2 kV on a_2, the positive post-acceleration voltage may have a maximum of 3 kV. It should be noted that V_{a2} must be at least half V_{a3}. A voltage relationship V_{a2} = 1kV, V_{a3} = 3kV, would be unfavourable.

Dimensions, base characteristics and a schematic arrangement of the electrodes for tube DG 10–6 are given in fig. 2–26. Characteristic curves of I_{a2} and I_s (beam current) in dependence upon grid voltage are reproduced in fig. 2–27.

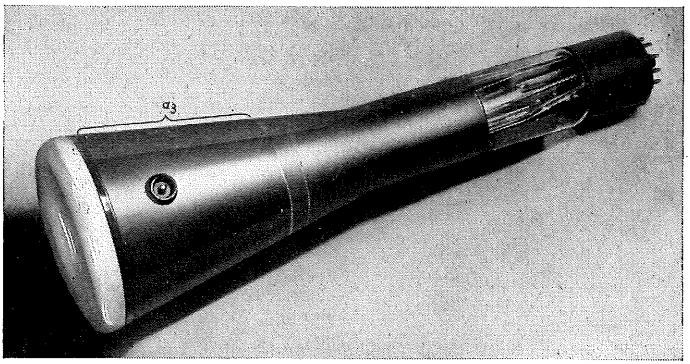

Fig. 2–25. Cathode Ray Tube DG 10–6 with post-acceleration electrode (a_3).

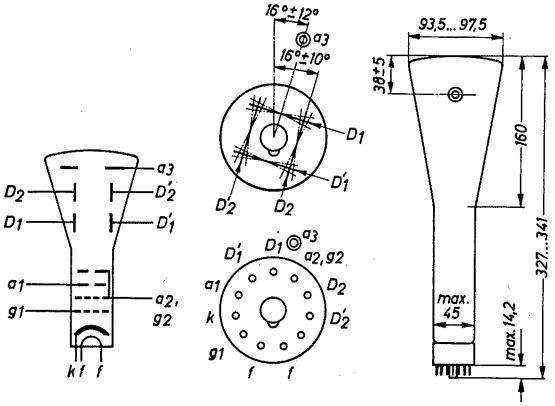

Fig. 2–26. Dimensions and base connections of C.R.T. DG 10–6

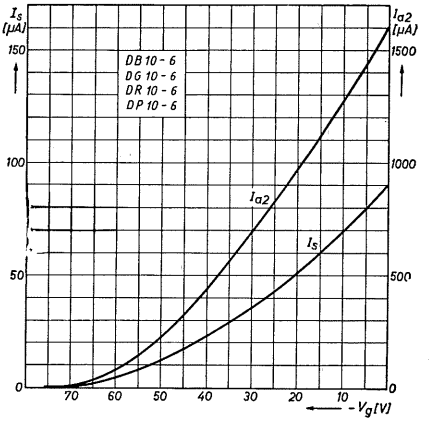

Fig. 2–27. Anode current (I_{a2}) and beam current (I_s) as a function of grid voltage Vg.

In type designations of cathode ray tubes, an attempt was first made with Philips types to provide at the same time information about tube characteristics. The following method of designation applies to standard tubes:

Table 2–II

1st Letter	2nd Letter	Figure preceding the dash
Deflection and Beam Concentration	Screen	Diameter of screen (diagonal in the case of rectangular tubes)
D = double-electrostatic deflection, electrostatic beam concentration M = magnetic deflection in both directions, magnetic beam concentration	B = blue screen, short persistence G = greenish-yellow screen, medium persistence N = green screen, long persistence R = greenish-yellow screen, very long persistence P = bluish-green screen, extremely long persistence, yellow afterglow	7 = tube with useful screen diameter of 7 cm 10 = useful screen dia. 10 cm. 36 = rectangular tube with screen diagonal of 36 cm. 43 = rectangular tube with screen diagonal 43 cm.

The figure following the dash represents a constructional characteristic.

Example: DG 10–6 = double electrostatic deflection, electrostatic beam concentration, greenish-yellow screen of medium persistence and 10 cm useful screen diameter.

3. Power Supply

Construction.

Cathode ray oscilloscopes, like all other electronic measuring instruments, are designed as a rule to operate on *AC* mains voltage only. The secondary of an appropriately rated mains transformer supplies all voltages required. *AC* is used throughout for the valve filaments and this is also provided by suitable windings on the mains transformer. Separate windings are necessary for heating E.H.T. the rectifiers and the cathode ray tube; these must be properly insulated as they are usually at a high potential with respect to the chassis or with respect to other windings. The *DC* voltages for the anodes of the valves in the vertical deflection amplifier and time base sections are generated by full-wave rectification of a corresponding *AC* voltage. For reasons which will be discussed later, considerable currents are needed for vertical deflection amplifiers, particularly for those with a high upper frequency limit. This load usually accounts for the greatest share in the power supply.

Anode voltage for the cathode ray tube.

The high anode voltage needed in cathode ray tubes can be obtained by simple half-wave rectification of a correspondingly high *AC* voltage, or by a voltage doubler or voltage multiplier.[5] Valves suitable for rectification are Philips types 1875, 1876 and 1877, having been developed especially for this purpose. Valve type EY 51 is suitable for smaller currents. PL 81, connected as a diode, can also be used for rectification.

Fig. 3–1 shows the basic circuit of an E.H.T. rectifier. The voltage required for anode a_1 is obtained from a variable voltage divider which permits fine adjustment. The *negative* grid voltage for brilliance control is taken in this circuit from the potentiometer R_5 which is in series with the filter resistor R_1. Additional filtering and decoupling is provided by resistor R_6 and condenser C_3.

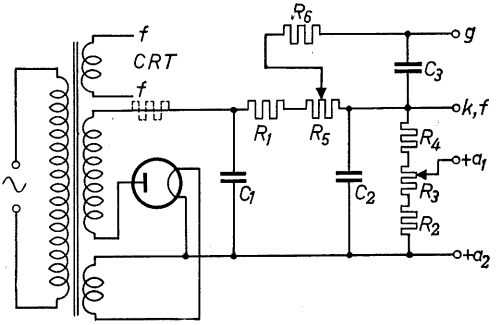

Fig. 3–1. Conventional circuit of an E.H.T. power pack.

Table 3–I on page 36 sets out the circuit component ratings for the most important Philips cathode ray tubes.

As the current consumption of the auxiliary anode seldom exceeds 250–500 μA in practice, a current rating of 1–2 mA suffices for the voltage divider. For this reason the filter element is usually a simple resistor. It is also possible under certain circumstances to obtain satisfactory filtering by means of an appropriately rated reservoir condenser alone. To this end, two or three electrolytic condensers can be connected in series for particularly high operating voltages. For example, the capacitance of 4μF resulting from two condensers each with a rating of 8 μF for 550/660 V permits adequate filtering of a voltage of 1000 V.

It is worth noting that anode voltage fluctuations resulting from ripple have a greater periodic effect upon deflection sensitivity than upon spot focus. This is explained by the fact that the voltage on the auxiliary anode is obtained by division of the anode voltage. As the ratio of anode voltage and auxiliary anode voltage determines the spot sharpness, only large fluctuations in anode voltage can produce a noticeable deterioration of spot focus. The oscillograms in fig. 3–2 illustrate the influence of anode voltage ripple on spot sharpness and deflection sensitivity, showing anode voltage, spot, datum line and the wave shape of a 300 c/s sinusoidal voltage during three periods of ripple voltage. In this case, smoothing was effected by simple reservoir condensers of 0.1 μF and 0.4 μF.

If the fluctuations in deflection sensitivity caused by ripple in the acceler-

[5] Special high-frequency oscillators or pulse generators are used at present for generating E.H.T. in television projection receivers but seldom in standard oscilloscopes. This method of E.H.T. generation will not therefore be treated in this work.

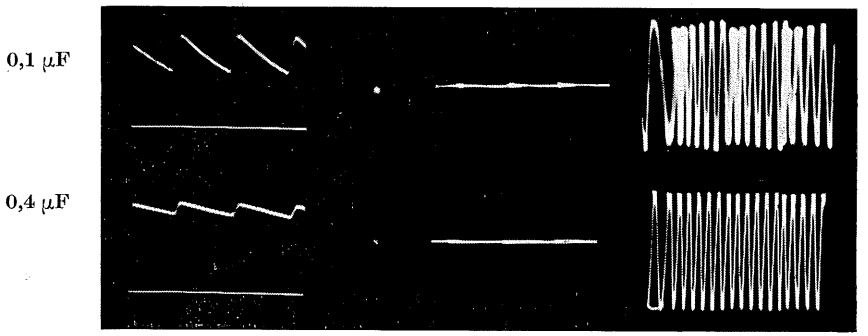

Fig. 3–2. Influence of anode voltage ripple on spot focus and deflection sensitivity

ation voltage are to remain unnoticeable, they must be smaller than $^1/_2$ of the spot diameter. As in good cathode ray tubes the spot diameter is in the order of $^1/_2$ millimetre, the change in beam deflection as a result of ripple must be < 0.25 mm. With a maximum deflection of 75 mm, this corresponds to a permissible ripple of 0.3%, which means a ΔV of only 3.0 V for an anode voltage of 1 kV.

The exact calculation of rectifier and filter specifications has been dealt with comprehensively elsewhere [1] [2] so that it will only be necessary here to touch upon one or two simple aspects for the purpose of orientation. To calculate the ripple voltage, for instance, the following rule-of-thumb formula applies:

$$\Delta V_{(pp)} = 4.5 \cdot \frac{I_{=}\,(\text{mA})}{C\,(\mu\text{F})} \qquad (3\text{–}1)$$

Expressed in words, the ripple voltage equals 4.5 $V_{r.m.s.}$ for 1 mA current and 1 μF capacitance. (For full-wave rectification under identical conditions, $\Delta V = 1.5$ V.) From this equation (3–1), the capacitance C for a given permissible ripple ΔV is:

$$C\,(\mu\text{F}) = 4.5 \cdot \frac{I_{=}\,(\text{mA})}{\Delta V_{pp}} \qquad (3\text{–}2)$$

The process of rectification may now be considered in rather more detail with reference to the oscillograms in fig. 3–3. Fig. 3–3*a* represents two cycles of an alternating voltage on the secondary of the transformer and 3–3*b* shows the half cycles allowed to pass through a rectifier (without a filtering condenser). The oscillogram in 3–3*c* shows the *DC* voltage across a filtering condenser of 0.1 μF drawing 1.5 mA current.

When choosing rectifier valves it is important to ascertain in what way the current passes to the reservoir condenser. As illustrated in fig. 3–3*c*, the condenser charges almost to the peak amplitude of the rectified half cycle. When the voltage pulse is withdrawn, the current drain discharges the condenser until the arrival of the next pulse renews the charge. This means that current can pass through the rectifier valve only within this short period of time, and as the condenser is correspondingly heavily charged, the current

pulses can reach considerable peak values. Fig. 3–3*d* reproduces the pattern of these pulses in the example discussed. To provide a scale for the amplitude, the trace was first recorded of an AC voltage corresponding to a current of 30 mA_{pp}, which shows that the peak value of the charging current pulses is 18 mA.

It may be necessary, especially when using large reservoir condensers, to reduce these current pulses to accord with the permissible value for a particular valve (e.g. for EY 51). This is done by means of a series resistor as shown by dotted lines in fig. 3–1. The condenser then takes longer to charge up but the voltage is prevented from reaching the peak value.

With regard to rating the filter system for the high tension, the following indications may be useful:

If, for instance, the first filter condenser is chosen with a rating of 0.5 μF, then according to the formula (3–1), for a current drain of 1.5 mA, the ripple across this condenser will be:

$$\Delta V = 4.5 \frac{1.5}{0.5} = 13.5 \text{ V}$$

As the permissible ripple voltage must be no more than 3.0 V, smoothing will have to be increased $\frac{13.5}{3.0} = 4.5$ times. For this purpose, a resistor and a further condenser must be connected after the first condenser, as shown in fig. 3–4*a*. As a result of the ripple voltage on C_1, an alternating current flows through resistor R and condenser C_2. The reactance of condenser C_2 should be as small as possible in relation to the resistance of R. In other words, the ripple voltage should as far as possible be wholly across the resistor. In the example given, the ripple on C_2 must be at the most $\frac{1}{4.5}$ of the ripple in C_1. This means, therefore, that the ratio of the total impedance of R and C_2 to the capacitive reactance of C_2 alone must be 5.5 : 1. The reactance of a capacitor is:

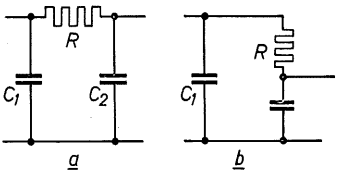

Fig. 3–4. Resistance-capacitance filter.

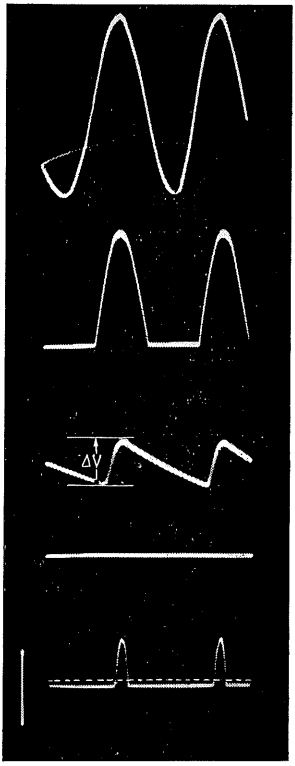

Fig. 3–3. Voltage and current waveforms in anode half-wave rectification. a) AC voltage V_{Tr} on anode winding of transformer (approx: 850 $V_{r.m.s.}$) b) Rectified half-cycles of AC voltage (capacitance C not present) c) DC voltage $V_{=}$, when $C = 0.1$ μF and current drain is 1.5 μA. ΔV = voltage ripple. d) Charging current surges from rectifier to C. The broken line corresponds to the mean value of the constant current drain $I_{=} = 1.5$ mA.

$$X_c = \frac{1}{\omega C} \tag{3-3}$$

(where $\omega = 2\pi f$, f = the frequency of the ripple voltage and C = the capacitance in farads) and therefore the total impedance is:

$$Z = \sqrt{R^2 + \left(\frac{1}{\omega C_2}\right)^2} \tag{3-4}$$

The ratio between these two values, and thus the smoothing of the ripple from C_1, is:

$$\frac{X_c}{Z} = \frac{\frac{1}{\omega C_2}}{\sqrt{R^2 + \left(\frac{1}{\omega C_2}\right)^2}} \tag{3-5}$$

By transposing formula (3–5), equations are obtained which allow the values for R and C_2 to be directly calculated. If the smoothing ratio $\frac{X_c}{Z}$ is called s, the required value of the filter resistor R can be obtained from:

$$R = \frac{1}{\omega C_2} \cdot \sqrt{\frac{1}{s^2} - 1} \tag{3-6}$$

The capacitance C_2, with a given value for R, is obtained from:

$$C_2 = \frac{1}{\omega R} \cdot \sqrt{\frac{1}{s^2} - 1} \tag{3-7}$$

In the example quoted, an increase in smoothing of at least 4.5 has to be achieved. If the capacitance of C_2 is taken as 0.5 μF, then R must be at least 35 kΩ for the filtering desired. With an anode current of 1.5 mA, there will be a *DC* voltage drop across this resistor of 52.5 V. The transformer voltage should therefore be taken correspondingly higher. This voltage drop is not wholly lost to the cathode ray tube supply. It can still be used for grid biasing, as shown in the circuit in fig. 3–1. In a practical case of this sort, the resistor would be rated at 50 kΩ and the voltage drop of 75 V tolerated in order to avoid all hum. The filter components in the circuit in fig. 3–1 have been rated in accordance with these considerations.

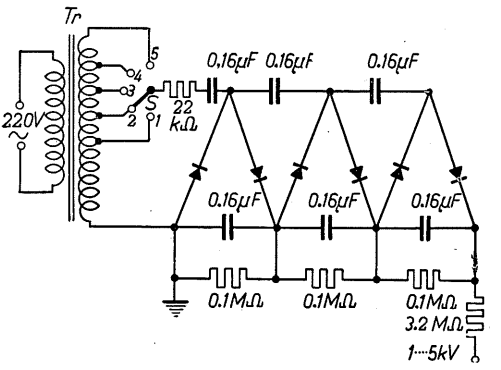

Fig. 3–5. Power supply circuit of the Philips 5 kV post-acceleration unit GM 4188.

As an example of a voltage multiplier circuit for generating the anode voltage for a cathode ray tube, fig. 3–5 reproduces the circuit used in the Philips post-

acceleration apparatus GM 4188. In this circuit, an *AC* voltage from the secondary of the mains transformer is fed to a voltage sextupler with selenium rectifying cells, so that a *DC* voltage of 1, 2, 3, 4 or 5 kV can be taken from the connection plug.
Having regard to the high tension present, the whole rectifying unit is housed in an oil-filled tank.
With this circuit a maximum current of 100 μA can be drawn. When the load is 50 μA and the output voltage 5 kV, the ripple amounts to $<$ 40 V (0.8%).
(As the post-acceleration voltage has considerably less influence on deflection sensitivity than the "pre"-acceleration voltage (Va_2), an appreciably greater ripple is admissible for V_{a3} than for V_{a2}). In order to avoid fluctuations in the screen pattern resulting from the influence of mains surges on anode voltage, electronic stabilization of the extra high tension has recently been introduced similar to that described in the following section [6] (see fig. 3–8).

The high tension supply and electronic stabilization.

Where high currents are needed it is necessary, among other things, to connect two rectifier valves in parallel, as shown in fig. 3–6. As a rule, the vertical deflection amplifier and the time base generator are both fed by the high tension supply. However, as both often have to work on extremely low frequencies (a few cycles or less) and as these must be decoupled, it is of primary importance that the internal resistance of the power supply be low enough even for frequencies as low as these.
Standard filter components are only suitable for this purpose under certain conditions, so that the only satisfactory solution is to use an *electronically stabilized power supply.*
Fig. 3–7 shows the circuit used in the GM 5653 oscilloscope, a circuit which is typical of electronic stabilization in general. Between the filter section of the mains rectifier and the load lies the internal resistance of PL 81, which is connected as a triode. The grid voltage of this valve, which determines its internal resistance, is taken from

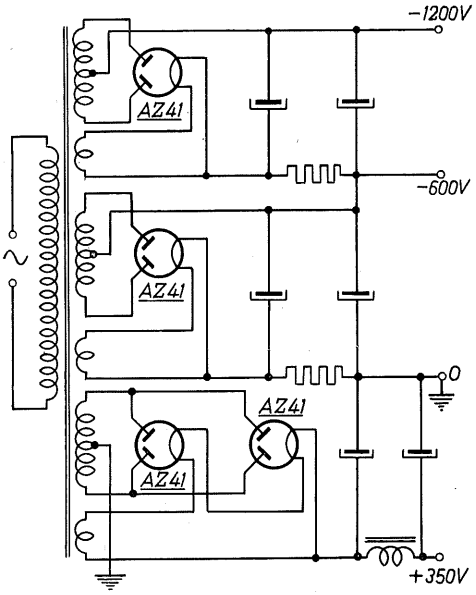

Fig 3–6. Power supply of a large oscilloscope (Philips GM 5653) high tension section: two AZ 41 rectifiers in parallel. Extra high tension section: two full-wave rectifiers AZ41 of 600 V$_{=}$ connected in cascade.

[6] *Philips* Oscilloscope GM 5654.

a voltage divider across the load and controlled and amplified via a high-mu sharp cut-off pentode, EF42. If now for any reason the output voltage from the power supply drops, the voltage on the load would normally drop likewise. However, as soon as the slightest reduction in load voltage occurs, the grid voltage of the controlled valve PL 81 (amplified by EF 42), and thus its internal resistance, is also reduced. This means that the voltage drop across PL 81 is reduced so that the voltage on the load is kept for the most part constant. A change of 10% in the mains voltage changes the load voltage by only some ‰. The constant grid bias for the control valve is supplied by the high-constancy stabilizer valve 85 A 1. (The ignition voltage of this valve changes by no more than 1 V in 5000 hours; the change is usually less than a few tenths of one volt.)

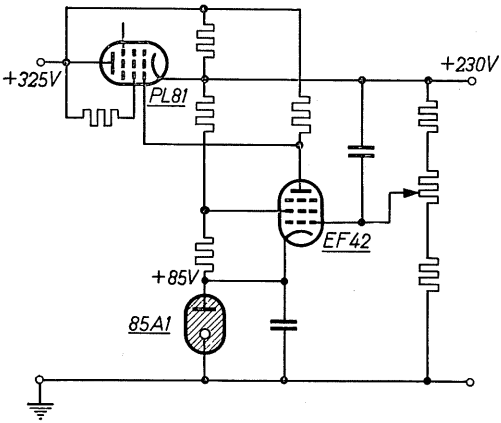

Fig. 3–7. Electronic stabilization of H.T. section

By means of electronic stabilization the output voltage is kept independent of the current drain, while on the other hand the current is kept reasonably independent of the voltage from the power supply. In other words, the internal resistance of the power supply is very small (10...25 Ω), which holds good for all frequencies from zero upwards, right up to the range where the filter condenser in the output acts as a short circuit. This entails, of course, a certain loss of voltage, in the example about 95 V.

Of course, this "expensive" electronically regulated voltage will only be used for those stages which are unable to do without it. The output stages of the vertical deflection amplifier with their large current consumption can be fed directly by the voltage from the filter system. At the most, only the screen grid voltages for these valves (which, in pentodes, determine the anode current) will be kept constant by means of the electronic stabilizer. (See fig. 5–41.)

Electronic stabilization in the E.H.T. supply.

Even when the low tension supply is electronically stabilized, it is still possible for mains voltage fluctuations to affect the size of the pattern on the screen by causing fluctuations in the extra high tension supply for the cathode ray tube. This can only be completely overcome if the extra high tension supply is also electronically stabilized.[7]

Fig. 3–8 gives as an example the power supply circuit for the cathode E.H.T.

[7] Stabilization with "glow stabilizer cascades" has the disadvantage that the voltage source must supply a 50% higher voltage for ionization. A further disadvantage of ordinary gas-discharge tubes is that sudden spontaneous changes in gas pressure or changes in temperature may cause erratic changes in voltage.

of 1200 V in the Philips oscilloscope GM 5654. Pentode PL 81, connected as a diode, serves as the rectifier. The *DC* taken from the 1 μF reservoir condenser must flow through the pentode PL 83 which is connected in the positive lead of this circuit. The second grid of this valve derives its electronically stabilized voltage of +250 V in the manner already described. (See fig. 3–7.) The voltage for the control grid is taken from a voltage divider which lies between the + 250 V and the output E.H.T. of—1200 V. The voltage division is arranged in such a way that the operating point of the valve lies on the desired part of the I_a/V_g characteristic at the nominal mains voltage and under normal load current. As the voltage of this divider is electronically stabilized at + 230 V, any change in the negative output caused by mains voltage surges or varying current drain (brilliance control of the C.R.T.) will produce a corresponding change in the (negative) voltage on the first grid of PL 83. The internal resistance of the valve is thereby altered to such an extent that it opposes all voltage fluctuations in the E.H.T. output.

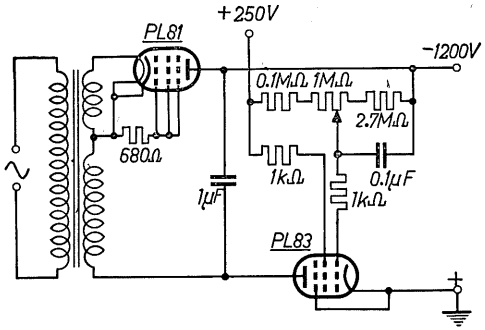

Fig. 3–8. Electronic stabilization of E.H.T. section (Philips GM 5654).

Although in this circuit the control voltage is not, as in the stabilizing circuit given in fig. 3-7, amplified by a further valve, a sufficiently good degree of E.H.T. stabilization is nevertheless achieved, due to the high mutual conductance of PL 83. In this way also, the residual ripple from the reservoir condenser can be quite considerably reduced.

Simplifying the E.H.T. circuit.

For reasons of economy in the power supply, various simplifications in circuitry have come into general use. Examples are shown in figs. 3–9 and 3–10.

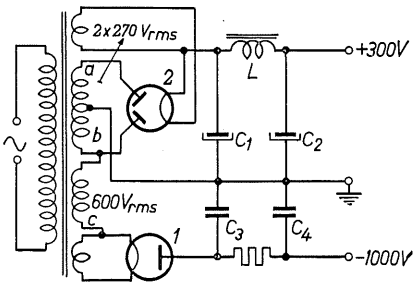

Fig. 3–9. E.H.T. power supply using one half of H.T. winding.

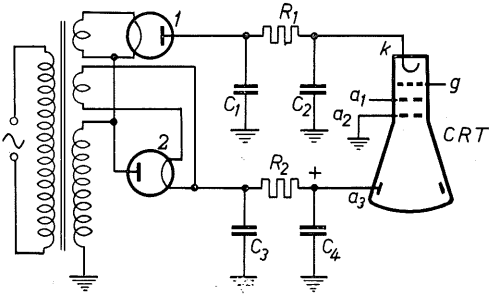

Fig. 3–10. E.H.T. power supply for cathode (–) and post-acceleration electrode (+) from one winding.

Fig. 3–9 illustrates how a part of the **E.H.T.** winding can be saved if one half of the high tension winding *b*) is connected in series with the extra high tension winding *c*). The low current consumption of the **E.H.T.** supply will of course have no effect upon the balance of the high tension supply.
Furthermore, by using two rectifier valves with alternate polarity, one **E.H.T.** winding is able to provide the negative **E.H.T.** for the cathode as well as an equally high positive voltage for the post-acceleration electrode. (See fig. 3–10.) In this circuit, the charging current flows through the rectifier valves during each half cycle alternately.

Beam positioning.

In order to adjust the exact position of the spot on the screen or to displace it when observing asymmetrical patterns, it is necessary to apply appropriate *DC* voltages to the deflection plates. These voltages must be variable up to a certain value on the + and — sides of zero. A suitable voltage can be obtained by connecting a potentiometer across two terminals of the power supply with a sufficiently high positive and negative potential: for example, across — 600 V and + 350 V, as in fig. 3–6.
If the deflection plates have single-pole earthing, the spot can, of course, only be displaced by a *DC* potential on the "hot" plate, as indicated in fig. 3–11*a*.

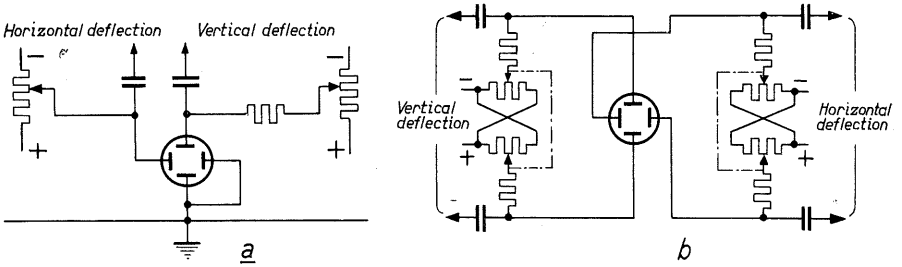

Fig. 3–11. Supply for positioning the spot *a*) for unbalanced deflection plates *b*) for balanced deflection plates

As already described, with unbalanced deflection systems of this sort certain distortions of the pattern on the screen must be expected (trapezium distortion, astigmatism), especially if any large displacement is necessary. Sharply focused patterns entirely free from distortion can be obtained by a balanced deflection system, together with balanced *DC* displacement voltages, as shown in fig. 3–11*b*. For each pair of plates a tandem potentiometer is required whose arms of resistance are oppositely connected. Thus any increase in positive potential on the one plate necessarily sends the potential on the other plate more negative for the same amount. It is important in this context to note that the average potential between the pair of plates must always remain equal to the potential on anode a_2. The centre position of the potentiometer must therefore actually correspond to V_{a2} (usually "0"). If this is not so, (and the spot is also central if, for instance, both plates are at + 15 V) severe astigmatism will appear.

The spot will no longer be round but flattened out in a shape which will also be dependent upon the position of the spot. These points should therefore be borne carefully in mind when rating the power supply components.
In order subsequently to ascertain the electrical centre as exactly as possible, special controls are provided. These make it possible to shift either the average potential of the deflection plates or the potential on anode a_2; the focusing effect is the same. In the hints on construction given in part IV, using the oscilloscope FTO 2 as an example, adjustment can also be made by means of R_{86}.
A device of this sort for post-adjustment of the average plate potential (*astigmatism control*) permits good spot definition even with unbalanced operation of balanced deflection plates [8]. However, as the displacement of the plate potential must always correspond to the average value of the deflection voltage on these plates in order to obtain a sharply focused pattern, this (second) focusing does rather depend upon the amplitude of the deflection voltage. The shift voltage must therefore be post-adjusted accordingly, especially for large variations in deflection voltage.
A further advantage of this device is that it improves the frequency- and phase-response of the deflection amplifier.

Shielding the cathode ray tube

The electron beam can also be influenced by magnetic fields. If no countermeasures were taken, the stray field of the mains transformer would therefore affect the deflection of the spot. In practice this causes an inclined stroke or a loop to appear on the screen instead of a spot (fig. 3–12*a*). If beam deflection is applied, a wave or a ribbon of light appears instead of a trace (fig. 3–12*b* and *c*).
The position of the mains transformer which produces the least disturbance must be found by experiment. To eliminate all remaining magnetic influence,

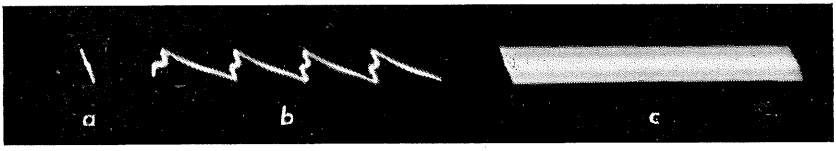

Fig. 3–12. Effect of magnetic interference on the screen.

however, the cathode ray tube must be magnetically shielded. This is best done with a mu metal cylinder. All remanent magnetism must be carefully removed from the shield as otherwise the spot will be pre-deflected from the zero position, resulting in a certain astigmatism.
The presence of remanent magnetism can easily be recognized by eccentric movement of the spot on the screen if the shield is turned around the axis of the tube.

[8] Philips Oscilloscope GM 5660.

Table 3–I (to fig. 3–1, p. 27)

C.R.T.	V_{Tr} [$V_{r.m.s.}$]	Valve	C_1 [μF]	C_2 [μF]	C_3 [μF]	R_1 [kΩ]	R_2 [MΩ]	R_3 [kΩ]	R_4 [kΩ]	R_5 [kΩ]	R_6 [MΩ]	Operating current [mA]
DG 7–5 DG 7–6	850	1876	0.5	0.5	0.5	100	0.5	100	200	50	0.5	1.0
DG 0–6	850*	1876	0.5	0.5	0.5	50	0.42	100	150	50	0.5	1.5
	1500**	1875	0.5	0.5	0.5	50	1.25	300	400	100	0.5	1.0
DG 13–2	1500**	1875	0.5	0.5	0.5	50	1.25	300	400	100	0.5	1.0

* $V_{a2} = V_{a3} = 1000$ V ** $V_{a2} = V_{a3}$ 2000 V.

4. The Time Base Generator

The representation of changing phenomena.

The great significance of the oscilloscope as a measuring instrument is due more than anything else to the fact that it enables the course of changes in a condition over a period of time to be made visible in a singularly clear and comprehensive way. To explain the time base principle in the oscilloscope as simply as possible, it will be best to begin by describing the common scientific method of representing the dependence of a given quantity upon time. In this method it is customary to plot the instantaneous values of a quantity in the perpendicular direction from zero and to plot time in a horizontal direction progressively to the right (along the "time axis"), both in any scale which may be suitable. Positive values are plotted above and negative values below the zero line. Each instantaneous value appears displaced in points to the right according to the length of time which has elapsed between one value and the next, so that if the points are joined together they will form a diagonal line or a curve. This "curve" represents the "function" of the quantity in dependence upon time. To illustrate this, fig. 4–1 shows the course of a sinusoidally changing voltage as a function of time. This method is in such general use that it is customary to speak only of the pattern of the electrical phenomena. Other methods of representation are possible, however, and these will be discussed in the chapter on practical measuring technique.

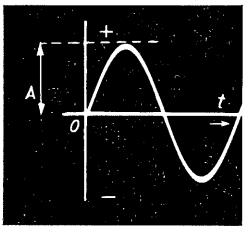

Fig. 4–1. Example of representing a quantity in relation to time. A = amplitude of the quantity to be measured; t = time axis moving progressively to the right.

A particularly important function of the oscilloscope is also to represent the interdependence of two or more different phenomena.

Horizontal deflection for the time base.

In order to get a clear picture from the oscilloscope of the behaviour of a given quantity over a given period of time, it is necessary to be able to observe the

changes of condition long enough for a judgement to be made. This means in other words that the movements of the spot produced by each instantaneous value of the phenomenon being measured must be presented in such a way that the observer sees, or believes he sees, the changes taking place at one and the same time. For this purpose the voltage to be examined is applied to the Y plates so that the spot is deflected vertically by an amount corresponding to the momentary values of the voltage.

A voltage is applied simultaneously to the X plates which increases at a uniform rate, that is, always by the same amount for each moment of time, and this voltage moves the spot to the right at a constant speed across the screen. In other words it deflects the spot "linearly with time". Thus the vertical deflections produced by the signal appear, not in a perpendicular line

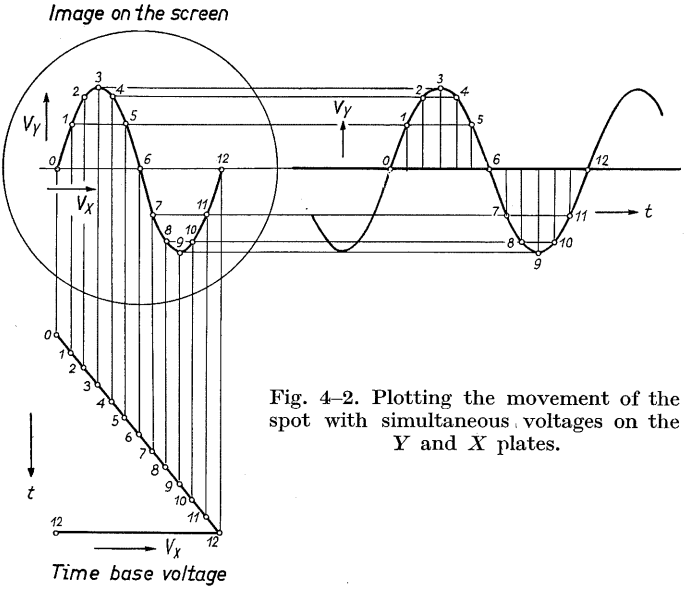

Fig. 4–2. Plotting the movement of the spot with simultaneous voltages on the Y and X plates.

but progressively to the right, one after the other. In this way the spot on the screen describes a curve, completely analogous to the method of representation outlined at the beginning of this chapter, a curve which presents the changes in value of the phenomenon under investigation in dependence upon time. As there would be no point in deflecting the spot horizontally beyond the useful area of the screen, the voltage on the X plates drops to zero when the right-hand edge of the screen is reached and the spot thus returns to its starting point at the left.

The way in which a pattern is formed on the screen as a result of simultaneous vertical and horizontal deflection is explained in fig. 4–2. One complete cycle of the time base voltage is shown subdivided into 12 equal periods of time. Rather more than one complete cycle of the voltage to be applied to the Y plates is shown on the right, with its amplitude plotted against time. Underneath the pattern on the screen the change in the potential on the X plates

is indicated by a linear voltage, whereby time, also beginning from zero, is plotted progressively downwards. If now the individual points from the time base voltage are projected perpendicularly to the screen and if corresponding instantaneous values of the Y voltage are projected horizontally, then the position of the spot on the screen at each moment is given by the points of intersection.

To simplify the illustration, the length of the time base is taken to equal one cycle of the signal applied to the Y plates and both are taken to start simultaneously from zero. The resulting pattern on the screen is one cycle of the signal applied to the Y plates.

With a single time base of this sort, however, no more than an extract of the signal is described once only. Such a system is of practical value solely when relatively slow-moving phenomena have to be studied, and even then it is necessary to use a long-afterglow tube or photographic recording. Only by using a repetitive time base is it possible to study the course of periodically recurring phenomena on the oscilloscope in a generally satisfactory way. If at the same time a synchronizing device is used, whereby the time base is made to be always one or more integral periods of the voltage on the Y plates (i.e. the ratio of the time base frequency to the signal frequency is a whole number), then the spot will always retrace exactly the same path on the screen. As a result, because of the inertia of the human eye and partly because of the afterglow on the screen, the observer sees a stationary pattern.[9]

Generation of the time base voltage.

As we have seen, the horizontal deflection for the time base needs a voltage which will rise linearly with time to an adjustable value and then return rapidly to zero. This process must repeat itself uniformly for as long as may be desired at regular intervals which can also be adjusted. Three cycles of the voltage trend required are shown in fig. 4–3. The voltage-versus-time charac-

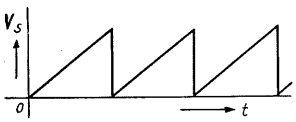

Fig. 4–3. The voltage waveform required for linear time base deflection (sawtooth).

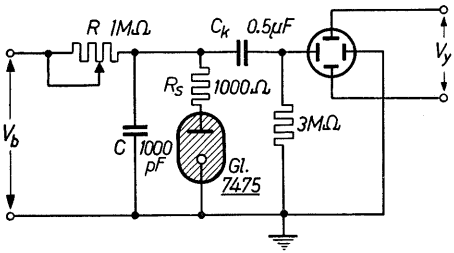

Fig. 4–4. Glow-tube relaxation oscillator for generating time base voltage. R_s resistance for limiting discharge current.

[9] If the time base frequency is lower than about 30 c/s, the image on the screen will begin to flicker. It will flicker more and more distinctly the more the sweep frequency decreases, so that the eye is gradually able to follow the movement of the spot.
The reason why the number of patterns per second needed for a steady oscillogram is greater than the minimum number of pictures per second necessary in cinematography (min. 16 pictures per sec.) is that the picture on the cathode ray tube does not originate as one whole but is produced by the movement of a spot on the screen.

teristic is a "sawtooth" wave-shape, for which reason the time base voltage is referred to sometimes as the "sawtooth sweep" voltage. One of the suitable circuits for generating a voltage of this sort is the "glow-tube relaxation oscillator" or the "neon sawtooth generator", shown in fig. 4–4.

A voltage from a *DC* power source V_b charges condenser C through resistor R. Directly across the condenser is connected a glow tube *Gl*. As soon as the voltage across the condenser reaches the ionizing or "ignition" potential of the tube, the tube becomes conductive and forms a path through which the condenser can discharge until the voltage falls to the de-ionizing or "extinction" potential. The glow tube then stops conducting and the condenser begins to charge up once again. A varying voltage thus exists across the condenser which, as the oscillogram in fig. 4–5*a* shows, has the sawtooth trend required for the time base. (See fig. 4–3). The waveform across the condenser is shown in fig. 4–5*b*.

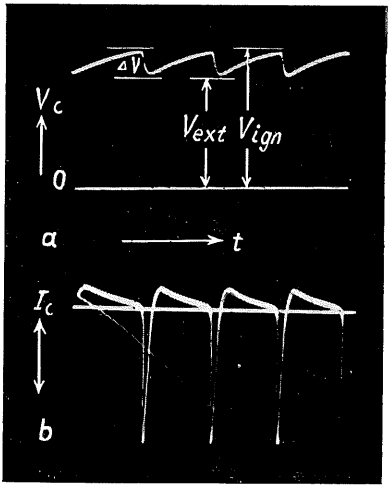

Fig. 4–5. *a*) Waveform of voltage across charging condenser in a glow-tube relaxation oscillator. V_{ign} = ionization potential (ignition voltage); V_{ext} = de-ionization potential (extinction voltage); *b*) waveform of condenser current; charge above zero line; discharge below zero line.

To produce a voltage trend of this kind the discharge period must be so short that no time is left for a further significant charge to build up again through resistor R. Expressed in another way, the RC time constant during discharge must be very small compared with that during charge [1] [2].

The amplitude of the voltage variation ΔV (fig. 4–5*a*) is determined by the difference between the ignition and extinction voltage of the tube. The frequency of this variation may be found approximately from the formula:

$$f = \frac{I_c}{\Delta V \cdot C} \qquad (4\text{–}1)$$

For a particular tube with a fixed voltage ΔV, the frequency is thus given by the average charging current I_c and by the capacitance of condenser C. The current, and therefore the frequency, can be varied by changing the value of resistor R.

To prevent the *DC* voltage V_b from reaching the deflection plates and thereby causing horizontal displacement of the spot, condenser C_k must be connected between glow-tube and deflection plate. To ensure that the *DC* potential on this plate remains at a clearly determined value, the plate should be connected to earth over a leak resistor of between 1 to 10 megohms. The other plate is connected straight to earth. (The glow-tube is thus connected asymmetrically.)

Employing a Philips type 7475 glow-tube, with an ignition voltage of 110 V and an extinction voltage of 85 V, the difference ΔV is 25 V.

It is found when using this circuit that the voltage is insufficient to deflect

the spot horizontally over the whole length of the screen. As fig. 4–5*a* shows, the deflecting voltage is determined by the difference between the ignition and extinction voltages of the tube employed. This voltage difference is relatively small and depends partly upon the type of gas filling used. Fig. 4–6 shows the patterns produced by the time base voltage from a glow-tube sawtooth generator with a sinusoidal signal of suitable frequency simultaneously on the Y plates. Apart from the inadequate length of the trace, it is noticeable in fig. 4–6*a* that the waveforms of the signal become crowded together towards the right. The reason for this is made clear from fig. 4–6*b*, which shows the waveform of the time base voltage itself. As can be seen, the voltage does not rise as it should do, linearly with time, but slows down towards the end of the charge. The instantaneous value of the charging current is determined by the difference between V_b and v_c; because the voltage on the condenser is increasing, this difference becomes progressively smaller so that the charging current decreases likewise (see fig. 4–5*b*). Thus the charging current for any given moment can be calculated from the equation:

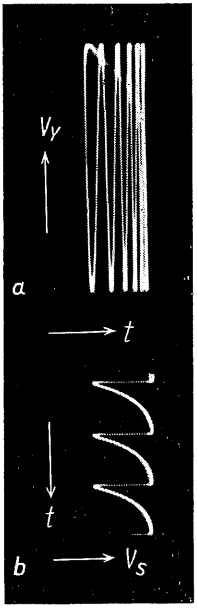

Fig. 4–6. *a*) Pattern on the screen produced by glow-tube sweep generator and sinusoidal input signal. *b*) Waveform of voltage on the X plates.

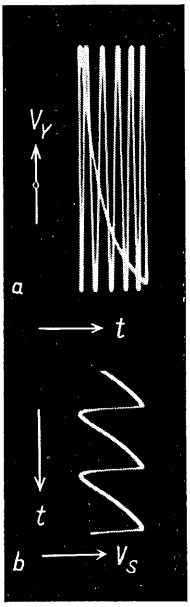

Fig. 4–7. *a*) and *b*) Patterns as in fig. 4–6, but with higher supply voltage V_b.

$$i_c = \frac{V_b - v_c}{R} \qquad (4\text{–}2)$$

For the voltage rise, therefore, the characteristic charging curve of a condenser is obtained as depicted in figs. 4–5*a* and 4–6*b*. The formula for calculating the instantaneous voltage across the condenser is:

$$v_c = V_b \cdot \left(1 - e^{-\frac{t}{RC}}\right) \qquad (4\text{–}3)$$

(in which v_c is the voltage across the condenser after time t, with a battery voltage V_b; e is the base of the natural logarithm $e = 2.718$).

From formula (4–3) it can be derived that the voltage rise will be less curved if V_b is higher. The difference $V_b - v_c$ is then not so much smaller towards the end of the charge as in the first case, so that the charging current remains more constant and the voltage increase across the condenser occurs more uniformly. This improvement is clearly visible in fig. 4–7*a* and *b*. For fig. 4–6, the *DC* voltage $V_b = 150$ V, and for fig. 4–7, $V_b = 250$ V.[10]

[10] These oscillograms were recorded on a DG 9–3 cathode ray tube, with a voltage of approx. 950 V on anode a_2.

As fig. 4–8 shows, useful results can be obtained with this voltage if the demands are not too high. The waveform of two cycles of the input signal can be followed quite distinctly.
It can be seen from these oscillograms, however, that the sawtooth voltage achieved in this way is hardly sufficient. It would certainly be possible to amplify this voltage as is done in other time base circuits, but the glow-tube circuit has other disadvantages, for which reason it is now no longer used, although it served its purpose during the early development of the oscilloscope. It is discussed at this stage because it is useful as an introduction to the generation of sawtooth sweeps. It also offers the opportunity of considering the behaviour of gas discharge tubes, which in itself is not without interest.

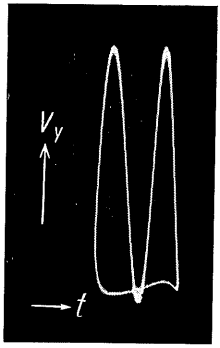

Fig. 4–8. Oscillogram of two cycles of an *AC* voltage with time base deflection as in fig. 4–7*b*.

The requisite amplitude of the time base voltage.

When designing the source of the time base voltage it is first of all necessary to decide on the voltage amplitude required. Since we are concerned with non-sinusoidal waveforms, it will not be possible to measure these with the normal measuring apparatus calibrated in *r.m.s.* values. Having regard to the fact that the deflection path of the spot corresponds to the maximum values of the deflection voltage [11], and moreover that these maximum values must be taken into consideration when rating the voltage source for horizontal deflection, it will be necessary always to calculate the voltage in peak-to-peak (V_{pp}) values.

The deflection voltage required is determined by the deflection sensitivity or the deflection factor of the tube for given operating conditions. (The peak-to-peak voltage V_{pp} is identical with the *DC* voltage $V_{=}$).
According to equation (2–3) the deflection sensitivity is given by $DS_{=} = \frac{X}{V_X}$, in which X is the deflection and V_X is the voltage on the deflection plates.
The voltage necessary for a certain deflection (*DC* voltage $V_{=}$ or V_{pp}) is given by:

$$V_{pp} = \frac{X}{DS_{=}} \qquad (4\text{–}4)$$

To take an example, for tube DG 10–6 with $V_{a2} = V_{a3} = 2$ kV, and with a length of deflection of 80 mm, $V_{pp} = \frac{80}{0.30} = 267\ V_{pp}$.

Time base circuits using a gas triode (thyratron sweep circuits).

Adequate time base voltages can be obtained by using a gas-discharge valve; in addition to the electrodes of the glow tube discussed, this has a control

[11] See chapter 2. "Calculating the beam deflection" and fig. 2–10*b*.

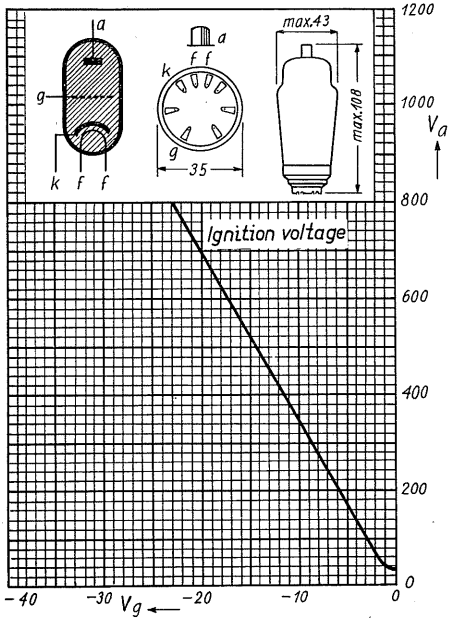

Fig. 4–9. Thyratron ignition characteristic. Arrangement of electrodes in gas triode EC50 with dimensions and base connections.

grid and usually an indirectly-heated cathode. Valves of this sort, which are often used nowadays for generating low frequency sawtooth sweeps, are known as gas triodes or thyratron triodes. Fig. 4–9 shows the gas triode with its three electrodes—the indirectly-heated cathode, the control grid and the anode. After the air has first been evacuated, the glass envelope is filled with an inert gas under low pressure (neon, argon or helium). In the de-ionized state the gas-triode behaves very much like a high vacuum valve. Electrons are emitted by the cathode and these are controlled by the potential existing between grid and cathode. This control potential V_{con}—which may be imagined to be in the plane of the grid—is composed of the grid voltage proper and that part of the anode voltage which *penetrates* through the grid. How large this influence is depends, among other things, upon the geometric dimensions of the grid (number and thickness of the windings of the mesh) and upon the distance from the anode. This penetration is denoted by the symbol D for the German expression "Durchgriff", otherwise known as the *penetration factor*.

The value of the anode voltage penetration is thus: $D \cdot V_a$, so that the control voltage can be expressed by:

$$V_{con} = V_g + V_a \cdot D \tag{4–5}$$

Conversely we may indicate how much greater the influence of the grid voltage changes are on anode current in proportion to the influence of anode voltage changes on anode current. This relationship is a constant of high vacuum valves and is called the *amplification factor*, denoted by the symbol μ. The amplification factor can be expressed as the reciprocal of the penetration factor, thus:

$$\mu = \frac{1}{D} \tag{4–6}$$

When the control voltage is lower than zero, i.e., negative, only very few of the electrons emitted by the cathode are able to penetrate the grid; they are forced back and form a cloud (known as the *space charge*) around the cathode. However, as soon as the control voltage goes positive, e.g. when the anode voltage is increased, the electrons will flow in increasing numbers through

the grid to the anode. As long as the now positive control voltage remains below the ignition or ionizing potential of the particular gas, the electrons in a gas triode wander in a small, ineffective, though measurable stream to the anode. In a high-vacuum valve this current is largely limited by the space charge, which determines the grid-voltage/anode-current characteristic. The moment the control voltage reaches the ionizing potential, however, the gas filling becomes effective. The electrons, now flowing at sufficient speed, ionize molecules of gas and set up a chain reaction whereby new ions and electrons are constantly being formed. The gas thus "ignites", an automatic arc discharge occurs and a strong electron stream begins to flow.
The ions move towards the cathode, where they are mostly absorbed by the electrons in the space charge and become neutral gas molecules again. In this way the space charge rapidly disappears so that the total electron emission of the cathode—the saturation current—would normally be able to flow unhindered to the anode. This current, however, would in itself overload the cathode and, what is more, the excess of positive ions, which can no longer be neutralized by the space charge, would flow to the negative cathode, and indeed especially to the parts emitting the greatest number of electrons. At these points, therefore, the cathode would be damaged by the heat thus released if nothing were done to limit the anode current to the permissible value. This is done by inserting a resistance, either in the anode or the cathode lead. The internal resistance of a gas triode is, at least in the ionized state, extremely low (it is in principle negative), so that it is particularly suitable as a discharge valve in relaxation oscillators for generating a time base voltage.

Controlling the ionizing potential of a gas triode.

If the grid is joined with the cathode, i.e. if the grid potential is zero, then for practical purposes all electrons emitted by the cathode can be attracted through the grid by the positive potential of the anode. Only a small ignition voltage is then necessary for ionization. Taking the helium-filled triode thyratron EC 50 as an example, 35 V are needed. At this potential the discharge—the "arc"—in the valve is only just maintained; it is thus also referred to as the arc potential and denoted by V_{arc}. If the voltage on the grid is not zero but has a certain negative value, a higher anode potential is necessary for ionization. This relationship is shown by the characteristic reproduced in fig. 4–9. The curve indicates how high the anode voltage must be to ionize the gas for a given negative grid voltage. As regards this valve, it can be seen that above about 40 V the anode potential must always be larger by a certain constant factor than the negative grid potential for ionization to take place. This factor will be called the "ignition factor" and represented by the symbol μ by analogy with the amplification factor of amplifier valves, with which it might be compared. Thus:

$$V_a = -\mu \cdot V_g \qquad (4\text{–}7)$$

In our example EC 50, the factor is 35. This means that with a grid bias of —11.4 V, for instance, ionization will occur at an anode potential of 400 V.

If a gas triode is used in the circuit given in fig. 4–4 for discharging the condenser C, as shown in fig. 4–10, it is then possible to control the charging potential of the condenser by simply varying the grid bias.

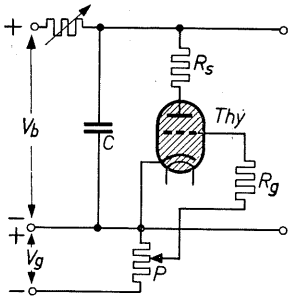

Fig. 4–10. Thyratron relaxation oscillator for generating sawtooth sweep.

The voltage V_s across the condenser (see fig. 4–11), which is the voltage for the time base, varies between the anode potential V_a at the point of ionization and the arc potential V_{arc}, thus:

$$V_s = V_a - V_{arc} \tag{4–8}$$

The potential across the condenser for a certain deflection voltage is thus the sum:

$$V_c = V_a = V_s + V_{arc} \tag{4–9}$$

Fig. 4–11 shows the waveform of the voltage across the condenser obtained when using the circuit in fig. 4–10. If we compare this oscillogram with that in fig. 4–5, a considerable improvement can at once be seen. The residual DC voltage V_{arc} is noticeably smaller as compared with the extinction voltage V_{ext} in fig. 4–5*a*, and V_s is several times larger than ΔV in fig. 4–5. The expression (4–9) must, however, be equal to (4–7), thus:

$$-\mu \cdot V_g = V_s + V_{arc} \tag{4–10}$$

From this is obtained the grid bias required for a specific value of sawtooth voltage:

$$V_g = -\frac{V_s + V_{arc}}{\mu} \tag{4–11}$$

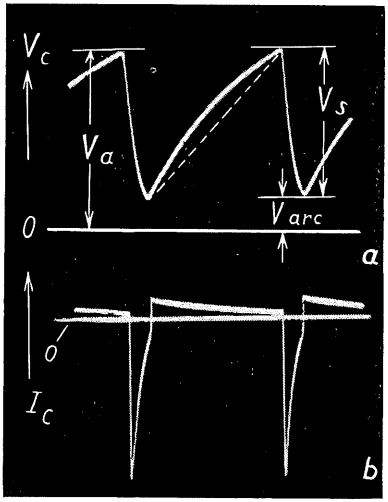

Fig. 4–11. Voltage and current waveforms across condenser C in the circuit given in fig. 4–10.

Fig. 4–12. Oscillogram of sinusoidal input signal with time base generated by thyratron relaxation oscillator given in fig. 4–10.

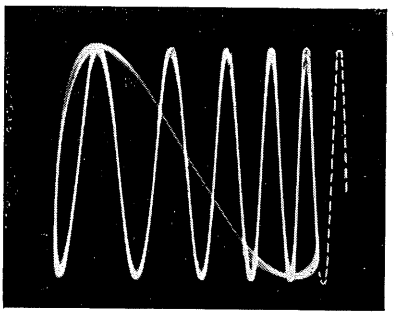

The deflection voltage required for DG 10–6 was calculated from formula (4–4) as 267 V_{pp}. Using thyratron triode EC 50, a negative bias is therefore needed of: $V_g = -\frac{267 + 35}{35} = -8.63$ V.

This value can also be read from the characteristic curve in fig. 4–9. We can now compare the output of the thyratron triode sawtooth generator, figs. 4–11*a* and 4–12, with that of a glow-tube (figs. 4–6*a* and 4–7*a*). It can be seen that, for general purposes, adequate amplitudes of deflection voltages can be obtained using a gas triode, although the time base voltage is still not linear with time.

Linearizing the sawtooth sweep voltage with a pentode.

It is clear from fig. 4–11*a* that to achieve a linear sawtooth waveform, the all too rapid initial voltage rise must be prevented in some way. The charge must increase evenly for each unit of time. This means that the charging resistor must have the property of allowing at all times a constant and adjustable current to pass, even during a falling potential difference. Up to a certain lower voltage limit, this condition is fulfilled by a pentode. Fig. 4–13*a* gives the characteristic curves of an EF 80, showing the dependence of anode current upon anode voltage with various voltages on the second grid as parameter. It can be seen from these curves that, for a given grid voltage, the change in anode current is negligible after a lower limit of approximately 100 V anode potential. (The internal resistance of a pentode, which is high in any case, can be made still higher by introducing negative feedback. In circuits figs. 4–25 and 4–27 and in the circuit for a small oscilloscope given in part IV of this book, negative feedback is effected by means of a non-bypassed cathode resistor.)

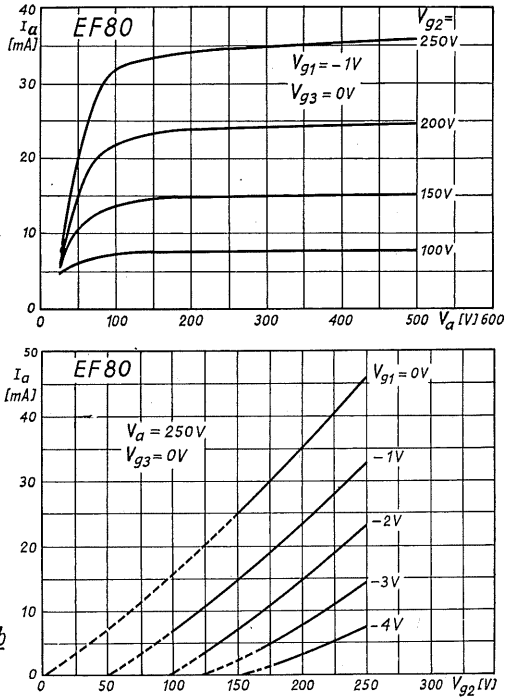

Fig. 4–13. Characteristics of high mutual conductance pentode EF 80; *a*) anode current in dependence upon anode voltage; *b*) anode current in dependence upon screen grid voltage.

Fine adjustment of the time base frequency by the anode current is now possible by controlling the screen grid voltage. Using a potentiometer with a linear characteristic, the resulting curve is practically linear, in contrast to

that obtained by controlling the voltage on the first grid. The curves in fig. 4–13*b* show the dependence of anode current upon screen grid voltage for various voltages on the first grid, again using EF 80 as an example.

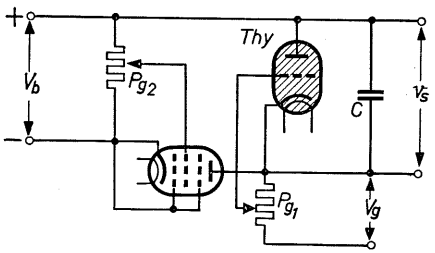

Fig. 4–14. Time base generator with a pentode for controlling charging current. *Thy* = gas triode. P_{g1} = potentiometer for controlling ignition potential; P_{g2} = potentiometer for controlling charging current by varying voltage on second grid of pentode (frequency control).

A circuit for generating the sawtooth sweep voltage by this method is shown in fig. 4–14.

The pentode for controlling the charging current is now connected in the negative lead in order that it may also receive the supply voltages for the charging valve in the correct polarity from voltage source V_b. The way the circuit itself functions is not altered by this in any way.[12] Fig. 4–15*a* shows the waveform of the voltage across the charging capacitor, and fig. 15*b* that of the charging current. The charging current (above the zero line) is now constant and the voltage rise linear. It can be seen from fig. 4–16 that the individual cycles of a sinusoidal signal on the *Y* plates are now evenly spaced.

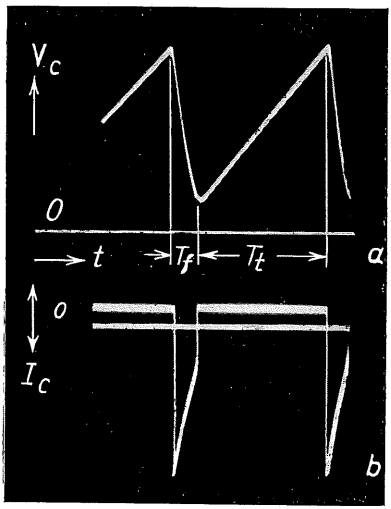

Fig. 4–15. Waveforms of current and voltage across charging condenser C in circuit as in fig. 4–14; *a*) voltage *b*) current.

Fig. 4–16. Oscillogram of sinusoidal input signal with time base generated by circuit in fig. 4–14.

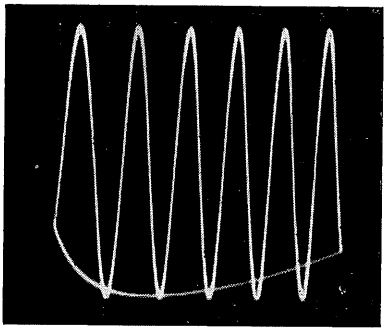

Flyback time.

We have so far assumed that the flyback or retrace of the spot to its starting position, and therefore the discharge of the condenser in the sawtooth sweep circuit, took place in a negligibly small space of time. As can be seen from

[12] Variations of this sort are quite common in time base circuits. Some circuits provide for initially rapid charging and a linear discharge by means of a pentode or a cathode follower.

fig. 4–15*a*, this is not so in practice. The time required for discharge is determined by the resistors in the discharge circuit and by the capacitance of the charging condenser, i.e. by the RC time constant ($t = R \times C$). The charge, and thus the *forward trace* on the screen, takes place during the time T_t, while the discharge—the flyback of the spot—occurs in the time T_f. The duration of the whole horizontal deflection cycle T_X is therefore equal to the sum of forward trace and flyback times:

$$T_X = T_t + T_f \tag{4–12}$$

The number of horizontal deflection cycles in one second—the *time base frequency*—thus appears as the reciprocal of the duration of one horizontal deflection cycle:

$$f_X = \frac{1}{T_X} \tag{4–13}$$

In order to be able to study the waveform of the signal on the Y plates, at least one complete cycle must be visible. The time base frequency is therefore chosen as a rule to be either equal to or a whole fraction of the frequency of the signal to be examined. If the time base frequency is equal to the signal frequency, one complete cycle will appear on the screen; if it is one half of the signal frequency, two cycles will appear, and so on. The total number N_t of cycles of the signal appearing on the screen during the forward trace and flyback of the spot is thus the ratio of the signal frequency f_s to the time base frequency f_X:

$$N_t = \frac{f_S}{f_X} \tag{4–14}$$

The portion attributed to flyback can be seen immediately from the signal frequency. In fig. 4–12, for example, the flyback accounts for about $^3/_4$ of a cycle of the signal frequency (the missing cycle is added in broken lines). With a total of 6 cycles, therefore, the flyback time is: $\frac{^3/_4}{6} = 12^1/_2\,\%$ approx. of the duration of one whole time base cycle.[13]

In general, then, the ratio of the number of cycles attributable to the flyback (N_f) to the total number of visible cycles of the signal (N_t) gives the share of the flyback in the duration of one whole time base cycle.

If we call this ratio Z_f, we get:

$$Z_f = \frac{N_f}{N_t} \tag{4–15}$$

With a resistor in circuit, it can be seen from figs. 4–11 and 4–5 that the condenser charges and discharges according to an exponential function.

Because the flyback interrupts the pattern on the screen, the aim is to keep the flyback time as short as possible. In this circuit it is essentially determined by the limiting resistor for the discharge current through the thyratron. This current falls during discharge from the permissible peak value $I_{a\ max}$ to

[13] In figs. 4–11, 4–12, 4–15 and 4–16, the flyback time was made deliberately long in order to show distinctly the phenomena under discussion. In practice it lies between 1 and 5%. Only at the highest frequency ranges does T_f rise to 20 ... 30%.

zero. It may therefore be assumed with some approximation that the average discharge current is $\frac{I_{a\ max}}{2}$ The period of discharge, i.e. the flyback time T_f, is arrived at in a way similar to formula (4–1)

$$T_f = 2 \cdot \frac{V_X \cdot C}{I_{a\ max}} = 2 \cdot R_s \cdot C \qquad (4\text{–}16)$$

According to formula (4–1) the time T_t required for the trace, i.e. the charging time, is:

$$T_t = \frac{V_X \cdot C}{I_c} \qquad (4\text{–}17)$$

(I_c = average charging current)

The ratio $\frac{T_f}{T_t}$, which approximately corresponds to Z_f for the share of the flyback in the time base cycle, is therefore:

$$\frac{T_f}{T_t} = \frac{2 \cdot I_c}{I_{a\ max}} \qquad (4\text{–}18)$$

Thus, if the flyback is to be small, it is desirable for the charging current to be as low as possible in proportion to the discharge current. However, to obtain a certain time base frequency, we are compelled, following formula (4–1), for a given value of C to choose a correspondingly high value of I_c. At higher frequencies, therefore, a relatively longer flyback time will have to be tolerated.

Moreover, at higher time base frequencies a certain inertia of the gas filling becomes increasingly noticeable. The fact is that a certain time is also necessary for the gas to ionize and thus for C to discharge, so that under some circumstances the flyback time may be several times longer than that calculated from formula (4–16). It is easily conceivable that the complete ionization of the gas filling will be accelerated if, immediately after ignition, the grid is driven sharply negative, because in this way the free ions will more rapidly leak away.

Improved time base circuit with thyratron triode.

Fig. 4–17 reproduces a circuit incorporating improvements on that given in fig. 4–14. The charging pentode is in this case connected across the grid and the cathode of the thyratron.

The time base voltage is controlled by potentiometer P_{g1} by which a suitably high inverse voltage is applied to the grid of the thyratron. When condenser C is discharged, a high potential difference exists between cathode and anode of the charging valve, and the grid of the thyratron is negative with respect to the cathode. As C is charging up, the negative voltage goes more positive and thus the potential difference between grid and cathode of the thyratron decreases until, at a potential corresponding to the ignition characteristic, the gas ionizes. Fig. 4–18 reproduces oscillograms showing the

resultant waveforms of grid and anode voltages of the thyratron with reference to the ignition characteristic. The reduction in grid voltage necessarily corresponds to an increase in anode voltage.
With this circuit it is possible, even at higher time base frequencies, to obtain flyback times approaching those calculated from formula (4–16). Small values

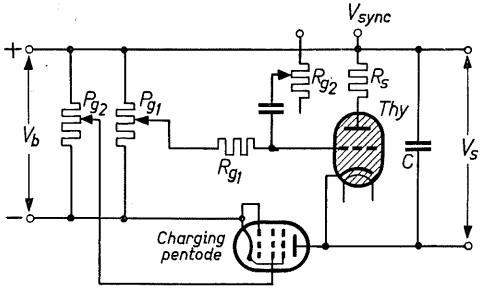

Fig. 4–17. Improved time base generator. The charging element lies between grid and cathode of the thyratron.

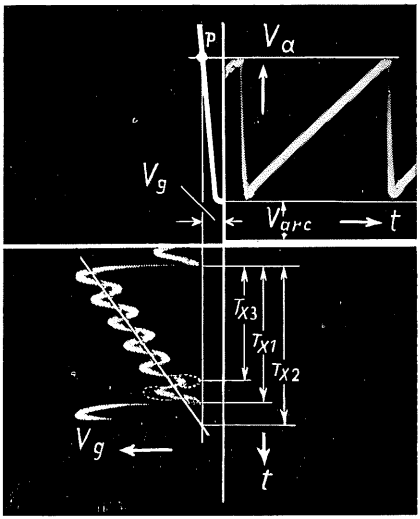

Fig. 4–18. Anode voltage and grid voltage with reference to ignition characteristic of thyratron in circuit fig. 4–17, showing signal superimposed on grid voltage for synchronization.

of capacitance for C must be used at high frequencies. However, this might lead more easily than at higher values for C to interfering voltages straying to the unearthed connection of the charging condenser, which is connected with one of the X plates[14].
For this reason a special heater winding must be provided for the thyratron, and screened from the other windings. Its centre tap is connected to the cathode to avoid stray voltages between the cathode and the filament. As the capacitance of this winding lies parallel to the charging condenser, it must be kept as small as possible by means of a suitably strong insulation barrier.

Maximum time base frequency and thyratron load.

It is understandable that high time base frequencies are needed in order to be able to examine high frequency waveforms.
The relevant data published by the manufacturers refer only to the individual valves (gas-filling, electrodes, dimensions etc.) and should be taken to mean that the indicated frequency is within the reach of the valve in question in a reasonably normal circuit.
The maximum frequency is limited not only by the maximum permissible

[14] The power supply must be rated in such a way that it represents an AC short-circuit for the entire frequency range of the time base. It is then unimportant whether the plus or the minus pole is earthed.

average anode current of the thyratron, by the charging capacitance and by the capacitance lying in parallel with it, but also in another way by the permissible load of the thyratron. The power drawn by the thyratron, if the frequency is not too high, is found from the product: arc voltage × recharging current (the latter is also the mean current through the valve). Thus:

$$N_{thy} = V_{arc} \cdot I_{am} \qquad (4\text{–}19)$$

In high-vacuum valves the power drawn causes heating of the anode (anode dissipation). In thyratrons, however, a part of the current is due to ions wandering to the cathode and giving up their energy there. We may therefore speak of a maximum permissible *cathode load.* For thyratron EC 50 we can calculate from formula (4–19): $N_{EC\ 50} = 35 \times 0.01 = 0.35$ W. However, as already mentioned, some time elapses before the gas filling forms an arc. This means that during this time the voltage on the anode is higher than the arc voltage at low frequencies. As a result, the load on the thyratron is increased, so that at high frequencies overloading can easily occur. For this reason, thyratron time base circuits are employed mainly for low frequencies, where they make it possible to obtain relatively short flyback times. Generally speaking, high-vacuum valves are used for sawtooth sweep circuits, especially for the high frequencies. These circuits will be discussed at a later stage. The following observations on synchronization apply, of course, to time base circuits in general.

Synchronization of time base circuits.

As we saw at the beginning of this chapter, a stationary picture of periodically recurring phenomena can be obtained if the frequency of the time base is exactly the same as, or is an exact whole multiple of, the input signal on the *Y* plates. This is not so easy to bring about by simple adjustment, especially at higher frequencies, so that the pattern on the screen is seen to drift. (During each time base cycle the pattern is displaced either to the left or to the right.) However, it is possible to lock the sawtooth voltage with the signal to be investigated. This is known as *synchronization.* For example, if a portion of the input signal is fed to the grid of the thyratron, it will superimpose itself upon the grid bias. (Figs. 4–17 and 4–18). As long as the grid bias is below the ignition point, the additional voltage will have no influence whatsoever. But as the operating point of the tube approaches the ignition potential—rising anode voltage and falling bias—(fig. 4–18) — the *AC* signal on the grid can cause earlier ionization than would otherwise be the case. The duration of one time base cycle T_{X1} will now be shorter (without synchronization it would be T_{X2}). In other words, the time base frequency will be increased. Referring again to fig. 4–18, if the time base frequency is somewhat lower than $^1/_6$ of the input signal frequency, it will be carried along by the "sync" signal such that ionization will occur at the maximum of the sixth cycle of the signal to be observed. The pattern jumps into step and remains stationary on the screen for six cycles (half a cycle here goes in flyback). In this way it is possible to make the waveforms stationary on the screen up to very high frequencies. In thyratrons, fractions of one volt are quite sufficient for synchronization. If

the sync signal is chosen too high, ionization might be brought about at the fifth cycle of the input signal (dotted cycle in fig. 4–18). This would have the result, however, that the condenser would discharge again at quite a low anode potential so that the time base voltage, and thus the length of the pattern, would be smaller by $^1/_6\,(T_{X3})$. In order to obtain any desired value of sync voltage, variable resistors are connected in the lead to the grid of the thyratron.

Broadly speaking, the electrodes of the thyratron can be considered as interconnected once ionization has set in, and therefore a quite considerable current might flow over the sync voltage sockets. To avoid this, a resistor and condenser should be connected in one of the leads. As general guidance, the resistor R_{g2} should be at least $300 \cdot V_X$. For a 500 V_{pp} time base voltage it must therefore be not lower than 150 kΩ. The sync voltage is usually supplied either by the input signal amplified in the vertical deflection amplifier, by an externally fed signal or by the mains frequency. To avoid mutual interference between time base generator and input signal, special sync amplifiers are used when the demands are particularly high.

To use the oscilloscope correctly it is most important to understand clearly the correct conditions for synchronization. Space will therefore be devoted to its extensive possibilities in the section of this book dealing with the specific applications of the oscilloscope.

Further circuits for linearizing the sawtooth sweep.

When describing the thyratron time base oscillator it was shown in circuits figs. 4–14 and 4–17 how a pentode could be used to obtain a linear increase of the voltage across the charging condenser.

Circuits by means of which an exponentially rising voltage (the charging of a condenser through a resistor) can be subsequently linearized, have achieved considerable importance [3]. They make it possible first to generate a sawtooth voltage in the simplest way and then to linearize it before it is applied to the X plates.

The easiest method of doing this is offered by the curved grid-voltage/anode-current dynamic transfer characteristic of an amplifying valve. By choosing a suitable transfer characteristic, i.e. a suitable operating portion of the curve, it is possible, as fig. 4–19 shows, to obtain a linearly rising voltage on the grid. The drawbacks of this system are that the operating point must be well maintained and the amplitude of the grid voltage must not vary to any great extent.

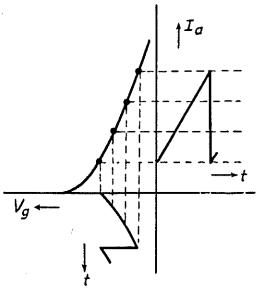

Fig. 4–19. Linearizing the sawtooth voltage by making use of the curved V_g/I_a characteristic of an amplifying valve.

Fig. 4–20*a* shows another possible way of linearizing the charging curve of a condenser. The charging resistor R_L now consists of two resistors, R_1 and R_2, connected in series. The voltage from charging condenser C_L lies on the grid of the cathode follower (1).[15] The voltage across the cathode resistor increases with the

[15] Further details are given in chapter 5. Deflection Amplifiers.

voltage across the charging condenser and is in the same phase. This voltage is now fed back via condenser C_R to the junction between R_1 and R_2. While the condenser is charging up through the resistor, the potential difference between C_L and the positive terminal $+a$ is normally falling. However, in this circuit the voltage from $+a$ has added to it the voltage fed back from the cathode of the valve over condenser C_R, which is itself increasing, so that, if the circuit components are suitably rated, the potential on this terminal remains constant. This means therefore that the voltage across R_1, and thus the charging current, will also remain constant. In this way a quite considerable linearity of the voltage rise across charging condenser C_L is achieved. The discharge occurs in the usual way, that is by means of a thyratron as already described, or by circuits employing high vacuum valves in a manner which will be discussed later. The device employed is indicated by switch S and resistor R_E. A circuit of this sort, which is known in America as the "bootstrap circuit" offers several important advantages by its use of a cathode-follower. The input impedance of a cathode-follower is high, whereas its output impedance is low. For reasons which will be gone into, good linearity of the sawtooth voltage requires that the load on the charging condenser (which is after all the voltage source of the sawtooth sweep) shall be kept as low as possible, i.e. it must have a high ohmic value. On the other hand, the output impedance must be low in order, for one thing, to minimize the adverse influence of stray wiring capacitances at high frequencies. Both these requirements are largely met by this circuit.

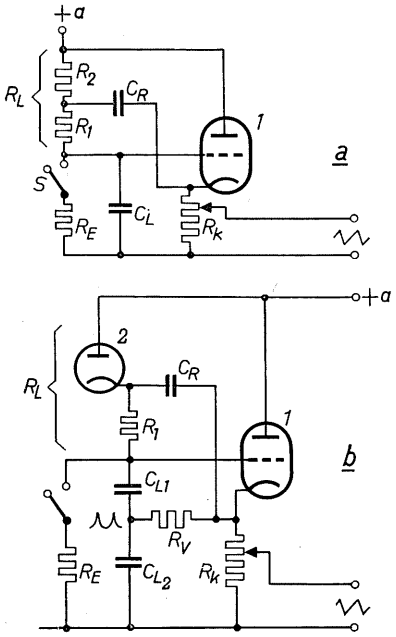

Fig. 4–20
Linearizing the sawtooth voltage by means of a cathode-follower with feedback (Bootstrap circuit). *a*) Basic circuit. *b*) Improved circuit using a diode in the charging circuit and integration network at the charging condenser.

The circuit can be extended as shown in fig. 4–20*b*. A diode takes the place of R_2, so that in the direction from the junction point R_1, C_R and the cathode of valve 2 to the voltage source $+a$ the impedance for practical purposes will be infinitely high. In consequence the voltage coming from cathode resistor R_k via C_R will serve exclusively to increase the potential at this point (the diode cannot load the feed-back voltage). Furthermore, the charging condenser is made up of two separate parts, C_{L1} and C_{L2}. Between the junction point of these two condensers and the cathode of the cathode-follower, a resistor forms an integration network with C_{L2}. The sawtooth signal coming from the cathode produces at this position a parabolic upward-peaking waveform. The potential now upon the grid of the cathode-follower consists of the sawtooth

voltage across C_{L1} and the parabolic voltage across C_{L2}, the peaks of which coincide with the peak of the sawtooth voltage. This enables a great degree of linearity to be obtained. Since the way the circuit components function depends upon the frequency they have to work with, provision must be made for switching over to higher frequency ranges. This entails a more extensive outlay, which is why the circuit as shown in fig. 4–20*b* is used more in television and radar sets than in oscilloscopes [4].
To obtain the lowest possible output impedance, a valve with a high mutual conductance is needed as the cathode follower in these circuits, for which reason steep slope pentodes are used, such as types EF 42, EF 80 etc., which can be connected either as a triode or as a pentode.
When used as a pentode, the screen grid must be decoupled over a condenser at the cathode.
As shown in the time base generator circuit in fig. 4–27, a triode can also serve to linearize the charge. By means of a relatively high cathode resistor, a strong negative feedback current is introduced to keep the charging current constant. These widely used and characteristic examples are only a few of the many circuits either possible or in practical use for obtaining greater linearity of the sawtooth waveform.

Time base circuits using high-vacuum valves.

Although time base frequencies of up to 150 kc/s are possible using gas discharge triodes in the manner described (circuit fig. 4–17), most oscilloscopes nevertheless use high-vacuum valves in the time base generator. Depending on the outlay, they enable sweep frequencies from 250 to 500 kc/s, and even as high as 1 Mc/s, to be produced. These "hard" valve circuits have some features in common with those of the "soft" valves (periodic charging and discharging of a condenser); but otherwise they work on a different circuit principle altogether, very often on what is called the *multivibrator* principle. In most cases the amplitude of the output voltage from these circuits is too low for direct use in time base deflection, and must therefore be amplified before being applied to the X plates.

Multivibrators.

If the amplified voltage of a two-stage RC-coupled amplifier is fed back over a coupling condenser, a circuit is obtained as shown in fig. 4–21*a* which, redrawn as in 4–21*b*, is known as the *multivibrator* after Abraham and Bloch. As drawn, the circuit is not stable; the voltages across both valves swing alternately from one extreme to the other at a frequency determined by the time constants of the coupling components. Because of its action, the multivibrator is also known as the "flip-flop". When, for example, the anode voltage V_{a1} of valve 1 rises for any reason, the grid voltage V_{g2} of valve 2 goes less negative. This causes the anode voltage V_{a2} of valve 2 to drop, and consequently the grid voltage V_{g1} of valve 1 is driven more negative via coupling condenser C_2. As a result, the anode voltage V_{a1} rises still further, and so on, until in this way the grid voltage V_{g1} is driven so negative that the anode

current of valve 1 is cut off and V_{a1} becomes equal to V_b. V_2 is now conducting heavily and no further increase in current is possible, V_{a1} being at a maximum and V_{a2} at a minimum. This state of equilibrium (the anode voltages remain at this value) lasts until, at a moment determined by the circuit time constants, the voltage V_{g1} begins to go less negative. This causes the anode current in valve 1 to rise and the same process repeats itself rapidly in reverse; the voltages "flop" to the other extremes.

It is desirable for the trailing edge of the sawtooth sweep voltage to be as steep as possible; i.e. the flyback time must be short. For this reason, asymmetrical rectangular pulses are generated for time base circuits, whereby one pulse width is made very short. If this asymmetrical rectangular pulse is used to charge a condenser (C_3 in fig. 4–21*b* and C in fig. 4–22), an integration of the rectangular voltage curve results. The linear voltage rise occurs during the long portion and the drop occurs during the short portion of the cycle.

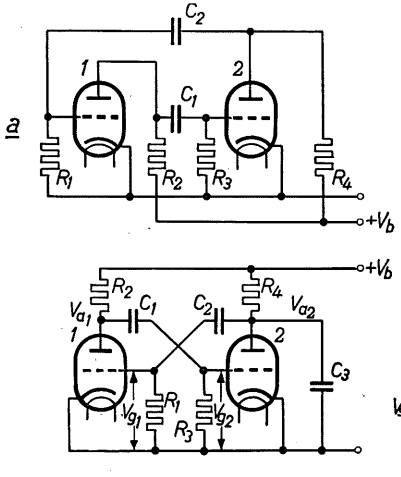

Fig. 4–21

Fig. 4–22

Fig. 4–21. Multivibrator; *a*) output circuit of a two-stage amplifier with feedback coupling; *b*) conventional multivibrator circuit.
Fig. 4–22. Practical circuit of cathode-coupled multivibrator.

A great number of similar circuits have been developed with which it would be impossible to deal in detail within the scope of this book. Double triodes such as the ECC 40 or ECC 81 are predominantly used in these circuits, although pentodes can also be employed with advantage. The cross-connected screen grids then act as the anodes, and the output can be taken from the anodes proper without changes in the load affecting the oscillatory circuit. Occasionally the grid resistors are connected across a positive voltage instead of to the chassis in order to effect a more rapid "flip-flop" action.

The conventional circuit described couples back the anode voltage. For this reason it is known as the *anode-coupled multivibrator.*

The circuit using pentodes is known as the *electron-coupled multivibrator.*

Another widely used circuit is the *cathode-coupled multivibrator*. Here the feedback takes place over the cathode resistor common to both valves. A circuit of this kind is shown in fig. 4–22, which gives the operating data for ECC 40. The frequency is determined by the values of C_g and R_{g1}. Fine adjustment is effected by varying R, though it causes some fluctuation in the output voltage. For higher frequencies both C and C_g must be given different values; C_g should be $^1/_{20}$ to $^1/_{30}$ of the value of C, and for a sawtooth sweep frequency of 50 c/s C should be approximately 0.5 μF. At frequencies up to 1 kc/s the flyback time is about 5% and at frequencies from 10–20 kc/s, about 20%. For both systems the anode current is 2.6 mA.

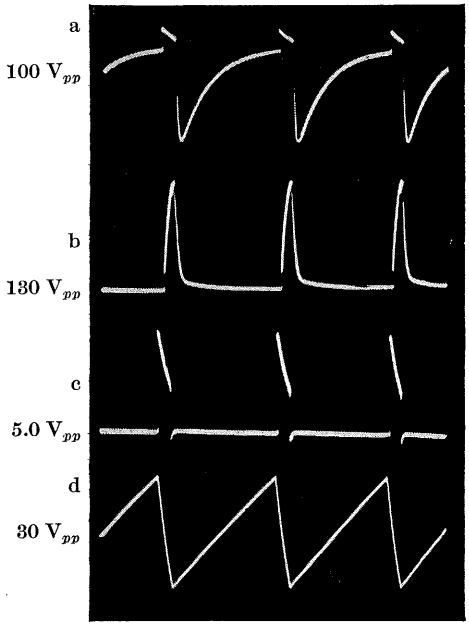

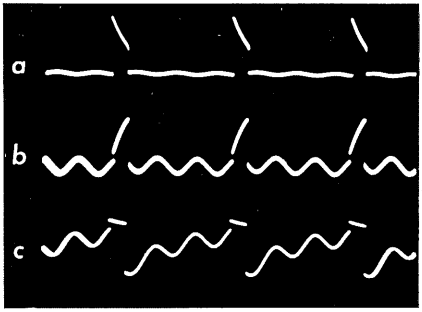

Fig. 4–24. Oscillograms of cathode-coupled multivibrator, synchronized with a sinusoidal voltage ($f_M = f_X = 3$); *a*) common cathode; *b*) anode I; *c*) grid I.

Fig. 4–23. Oscillograms of cathode-coupled multivibrator as in fig. 4–22; *a*) grid I; *b*) anode I; *c*) voltage on common cathode; *d*) sawtooth voltage on aII.

For synchronization, the sync voltage, which must be at least 1V, can be applied to the grid of valve I.

The oscillograms in fig. 4–23 show the waveforms obtained with this circuit. At the circuit component ratings the frequency of the sawtooth sweep was about 350 c/s. In view of the fact that the waveforms are reproduced at similar amplitudes for the purpose of easy comparison, the individual peak-to-peak values are given at the side. In this example, the amplitude of the sawtooth voltage was about 30 V_{pp}, so that further amplification is necessary for adequate spot deflection. The oscillograms in fig. 4–24 show the waveforms at the cathode and anode of valve system II and at the grid of valve system I with a sinusoidal synchronizing voltage of 1050 c/s (three cycles on the screen of the oscilloscope in question).

Triple pentode circuit.

A time base circuit can also be built with three pentodes. This circuit, which was published in 1936, is used with slight modifications in Philips oscilloscopes GM 5653 and GM 5654 for a frequency range of 5 c/s. ... 500 kc/s. The basic circuit diagram is shown in fig. 4–25.
The circuit works as follows:
If to begin with there is a voltage across charging condenser C_L and if at the same time an anode current is flowing in valve 7 such that the voltage drop

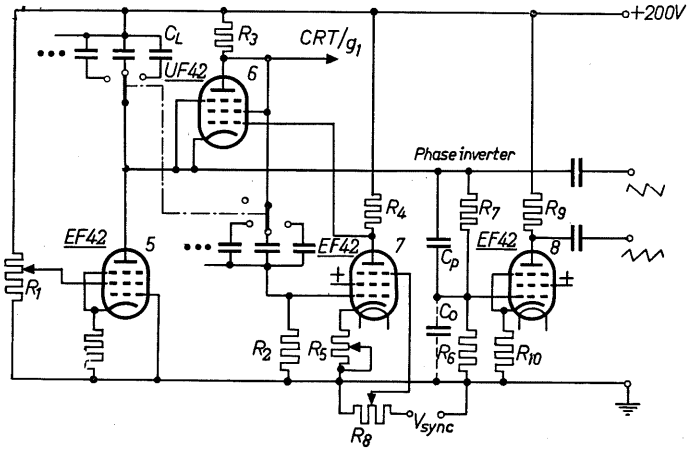

Fig. 4–25. Triple-pentode circuit (oscilloscope GM 5653).

across R_4 is greater than the voltage across C_L, then there will be a negative bias on the grid of valve 6; the valve is cut off and no anode current can flow. C_L therefore charges linearly through the valve, which causes the anode potential on valve 5 to sink, and with it the potential of the interconnected cathode of valve 6. As soon as the potential difference between grid and cathode of valve 6 has become so small that anode current begins to flow, a voltage drop occurs across the load resistor R_3 of valve 6 which is transmitted to the grid of valve 7 via condenser C_k. The anode current of valve 7 falls in consequence, whereby the grid of valve 6 is driven more positive, causing a sudden increase in anode current in this valve. As a result C_L discharges rapidly and the process starts again from the beginning.
Oscillograms depicting this sequence of events are shown in fig. 4–26.
In fig. 4–26*a*, three cycles of the voltage across C_L are reproduced; 4–26*b* shows the discharge current as the voltage on the anode of valve 6, 4–26*c* the voltage on grid 1 of control valve 7 and 4–26*d* the voltage on the anode of this valve.
Coarse frequency adjustment is carried out by switching over to other values of C_L and C_K and fine adjustment by means of controlling the charging current of valve 5 with its screen grid voltage by means of R_1. As the time base deflection must be symmetrical in cathode ray tube DG 10–6, which is used in GM 5653, a phase inversion stage—valve 8—is used. Through the frequency-

compensated voltage divider, consisting of R_6 and R_7 with C_p and C_o, a portion of the sawtooth voltage reaches the grid of valve 8. This voltage then appears amplified at the anode, with its phase shifted 180°.

The amplitude of the voltage is adjusted by varying the cathode resistor R_5, thus varying the anode current of the control valve. Synchronization is effected via the third grid of valve 7; the sync intensity is controlled by potentiometer R_8. The frequency range obtained extends from 5 c/s to 500 kc/s in 10 steps. As the discharge valve in this circuit (fig. 4–25) is connected as a triode, the designation "triple pentode" may not seem appropriate. It became familiar, however, at a time when the third valve was also connected as a pentode and the name has therefore been retained.

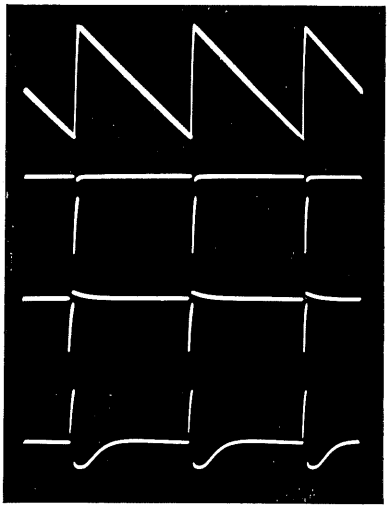

Fig. 4–26. Oscillograms for circuit in fig. 4–25. *a*) Anode of charging valve 5 or voltage across charging condenser. *b*) Anode of discharge valve 6, inversely proportional to discharge current. *c*) Grid 1 of control valve 7. *d*) Anode of control valve 7.

Triple triode circuit.

If a horizontal amplifier is used in the oscilloscope, small amplitudes of voltage may suffice for generating the sawtooth sweep. The time base oscillator can then be simplified. An example of this is the time base generator used in Philips' oscilloscope GM 5659. A circuit is employed which in principle is identical with the triple pentode circuit just described. Although only three triodes are used (the fourth serves to amplify the synchronization signal), a frequency range of 3 c/s — 250 kc/s is achieved, together with good linearity of the output.

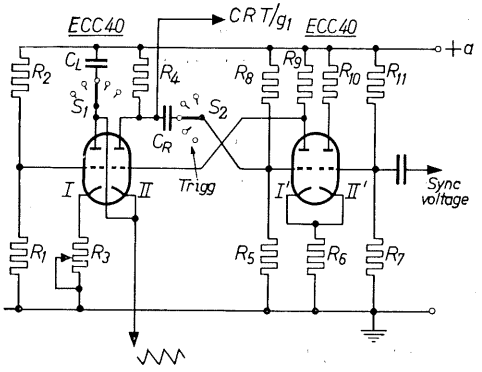

Fig. 4–27.
Triple triode circuit (oscilloscope GM 5659).

The practical circuit is shown in fig. 4–27. Valve system I serves as the charging valve. The current through the cathode resistor R_3 gives rise to a strong negative feedback current which keeps the charging current remarkably constant. By varying R_3, the average value of the charging current

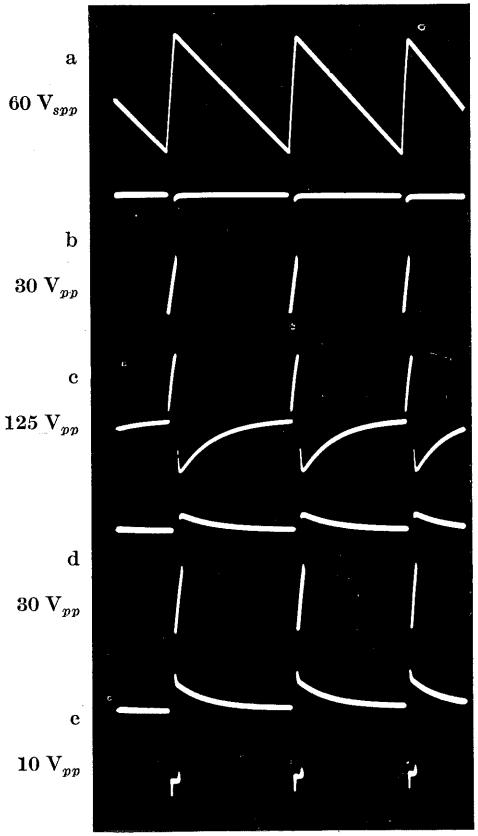

Fig. 4–28. Oscillograms for circuit in fig. 4–27. *a*) Anode of charging valve (I). *b*) Anode of discharge valve (II). *c*) Anode of control valve (I′). *d*) Grid of control valve (I′). *e*) Cathode of control valve (I′ and II′).

varies; this is thus the fine frequency control of the time base. The time frequency ranges are selected by base switching to different values of the charging condenser C_L. During the charging time, valve II is cut off. The grid voltage of this discharge valve is again dependent upon the potential difference between the anode of system I and the anode of system I′ (control valve). As in the case of the circuit in fig. 4–25, here too the sequence is briefly as follows: when condenser C_L charges up, valve II becomes conductive and thus triggers a positive pulse to its own grid via valve I′, whereby condenser C_L rapidly discharges. The oscillograms in figs. 4–28 and 4–29 reproduce the waveforms at the interesting points in this circuit. Fig. 4–28*a* shows the voltage on the anode of valve system I, and thus the voltage curve of the charging condenser. Fig. 4–28*b* shows the voltage on the anode of the discharge valve, which is inversely proportional to the discharge current. This waveform is very useful for brightening the trace, and accordingly for suppressing the flyback if it is also applied to the grid of the cathode ray tube, as it is in this circuit. In *c*), the voltage on the anode of the control valve I′ is shown; the peaks in this waveform are the pulses which trigger the rapid discharge of C_L.

The voltage on the grid of the control valve, which is fundamentally identical with the voltage on the anode of the discharge valve, is reproduced in *d*). In *e*) is shown the voltage on the cathode of the control valve, the shape of which agrees with that of the cathode current.

In the lead from the anode of discharge valve II to the grid of control valve I′ is located switch S_2 with which various values of the coupling condenser C_R can be selected for the frequency range required. Another switching position is provided, marked "Trigg", by means of which this connection can be interrupted. The charging condenser then remains charged up and the circuit is static, the self-oscillating action having been arrested. However, as soon as an *AC* voltage or a rhythmical pulse train is applied to the grid of system II′,

it is coupled into system I′ via cathode resistor R_6. From the anode of this system it passes to the grid of the discharge valve II, and discharge now occurs in the rhythm of the applied pulse. The speed of the time base can then be adjusted independently of the pulse rhythm so that it is possible to expand along the time axis those pulses whose duration is short compared with their frequency of repetition. For this purpose the time base frequency must always be larger then the pulse frequency or the frequency of the *AC* voltage. In the case of a sinusoidal voltage, one half cycle is reproduced expanded along the time axis according to the adjusted speed of the sweep. This method of "time base expansion" in an oscilloscope is known as "triggering". It makes possible, for instance, a time base expansion of 1 ms for the whole width of the pattern in the rhythm of 50 c/s corresponding to a cycle duration of 20 ms. The oscillogram will show a bright spot or dash on the left from which starting point the waveform of the pulse appears, less bright, towards the right.

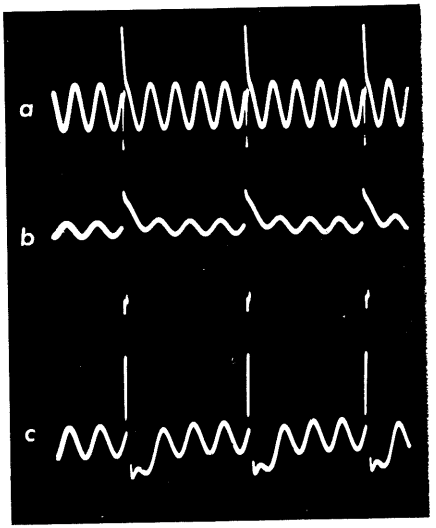

Fig. 4–29.
Oscillograms for circuit in fig. 4–27 with sync voltage. *a*) Grid voltage of sync-amplifier stage (II′). *b*) Cathode (I′ and II′). *c*) Anode of control valve (I′) or grid of discharge valve (II).

In this example, the time base voltage is amplified by a two-stage amplifier consisting of two EF 80's. As an *AC* amplifier of this sort is only capable of undistorted amplification of voltages varying about a zero line, it cannot be used for "single shot" sweeps.

Fig. 4–29 shows the waveforms of a number of voltages, synchronized with an input frequency equal to five times the time base frequency (five cycles on the screen of the oscilloscope in question). The voltage on the grid of system II′ is reproduced in *a*). From this can be seen the form of the input signal and the peaks which are injected by the feedback pulses. The waveform in *b*) corresponds to the cathode voltage and that in *c*) to the voltage on the anode of control valve I′ and thus on the grid of discharge valve II which triggers the discharge. The flyback times in these oscillograms is normal (short), so that the shape of the positive-going pulse cannot be seen so clearly as in fig. 4–28. (For these oscillograms the longest practical flyback times were chosen to make the behaviour of the voltage as clear as possible.)

Blocking oscillator circuits.

In the circuits so far described, the flip-flop action was effected with the *anode current* of the valve. There are a large number of sawtooth circuits in use, however, which employ the *grid current* of a valve for rhythmically

charging a condenser. (In such circuits, the grid current must, of course, remain within permissible limits.)
A suitable circuit can be built, as shown in fig. 4–30*a*, with a triode oscillator, making the inductive coupling between anode and grid so tight that when the coupling M goes beyond the oscillation point, the strong grid current drives the voltage across condenser C in the grid circuit so negative that oscillation is cut off or "blocked". (The operating portion of the curve is no longer steep enough, so that despite tight coupling the conditions for oscillation are no longer fulfilled.) The condenser C can now discharge through the leak resistor; in other words, it becomes less negative. As soon as the negative voltage on the grid is reduced to just above cut-off, anode current begins to

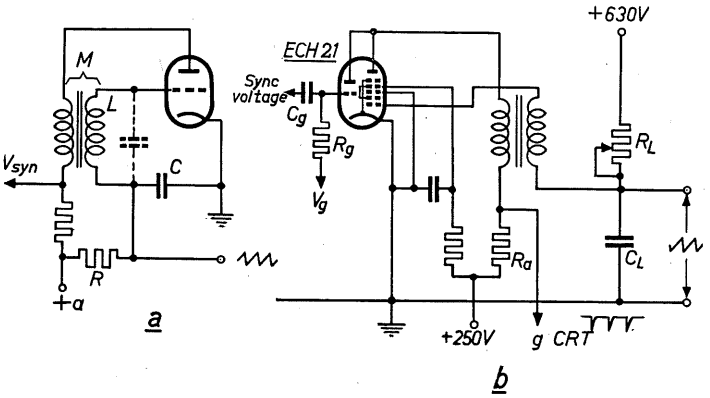

Fig. 4–30.
Blocking oscillator. *a*) Basic circuit with triode. *b*) Circuit with heptode-triode (oscilloscope GM 5655).

flow and oscillation again sets in. The process is then repeated. Every radio amateur knows this process in a regenerative detector; when the feedback is amplified beyond the oscillation point, the receiver begins to growl to an extent depending on the time constants of the grid circuit. If, as is usual in radio practice, the grid resistor R were connected to the cathode, the condenser would only be able to discharge non-linearly, in view of the small voltage across it. If, however, this resistor is connected across a high positive potential, as shown in fig. 4–30*a*, the voltage drop across R will remain constant during the build-up of the charge (the potential difference between charged and discharged condenser C is small compared to the voltage drop across R) so that a good, linear sawtooth voltage is obtained across condenser C.
This circuit is used in Philips Oscilloscope GM 5655, in which the heptode section of a heptode-triode ECH 21,[16] connected as a pentode, acts as the oscillator (see fig. 4–30*b*). The triode section serves to amplify the synchronization signal, for which a smaller voltage suffices than in the simple circuit diagram 4–30*a*, where the sync voltage is fed direct to the anode of the

[16] Valves ECH 81, ECC 81, ECC 83 and ECL 80 can be used for the same purpose.

oscillator. A number of oscillograms recorded from oscilloscope GM 5655 are reproduced in fig. 4–31 to illustrate the way this circuit functions. The voltage on the grid is shown in *a*). It can be seen that when the condenser is charging (negative), the circuit oscillates briefly for a few cycles. The sawtooth voltage across charging condenser C_L is shown by *b*); the condenser short-circuits the high frequency voltage, resulting in a pure, linearly rising sawtooth voltage.

During the high frequency oscillations, short H.F. pulses appear on the anode, as shown in *c*). Rectified L.F. pulses as shown in *d*) can accordingly be taken from the anode resistor to which the circuit capacitances are in parallel. These pulses are fed to the grid of the cathode ray tube where they suppress or "blank" the flyback of the spot. In this apparatus, the time base frequency range is 15 c/s — 25 kc/s. Another Philips circuit, using an ECC 40, is given in fig. 4–32. The valve system I serves, as already described, as the oscillator, while system II linearizes the sawtooth output by the "boot-strap" method, shown in fig. 4–20*a*.

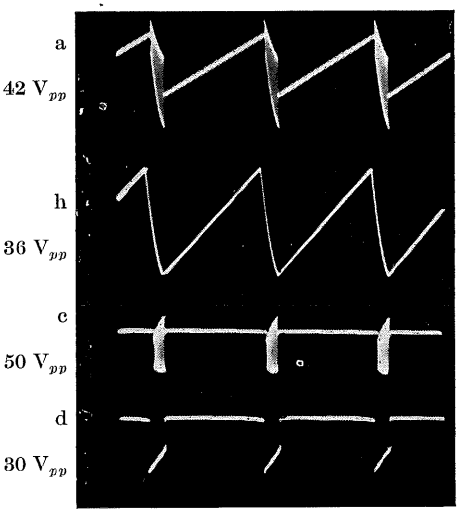

Fig. 4–31. Oscillograms for circuit in fig. 4–30*b*. *a*) Grid 1 of heptode. *b*) Sawtooth voltage across charging condenser. *c*) H.F. pulses on anode. *d*) Pulses across anode resistor R_a

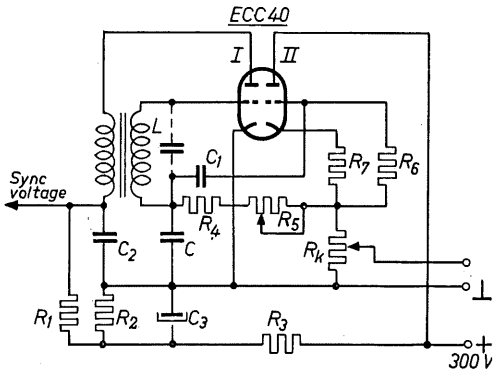

R_1 = 10 kΩ
R_2 = R_3 = 68 kΩ
R_4 = 0.4 MΩ
R_5 = 1.0 MΩ
R_6 = 2.7 MΩ
R_7 = 1 kΩ
R_k = 10 kΩ

C_1 = 0.22 μF
C_2 = 390 pF
C_3 = 4 μF
C = 50000 ····· 150 pF

Fig. 4–32. Blocking oscillator and cathode-follower feedback circuit ("bootstrap" circuit) for additional linearizing, using duotriode ECC 40.

As can be seen in fig. 4–32, the condenser C is not charged by the anode voltage, but by a potential comprising the positive voltage across cathode resistor R_k and the negative build-up of the charge across C to the peak voltage during the blocking process. With the component values given, this voltage has a mean value of 40 + 48 = 88 V.

The reaction coils particularly suitable for this purpose are I.F. filters for about 470 kc/s. Parallel capacitances must obviously be removed as well as all unnecessary connections Care must be taken

that the polarity of the coils is correct. This circuit permits H.F. oscillations of between 4–5 Mc/s. Coarse frequency adjustment is effected by switching over C and fine adjustment by varying R_5. The resistor R_4 is required to ensure the desired oscillating conditions under all circumstances.
The synchronizing voltage is here again superimposed directly upon the anode voltage. If necessary, a separate valve can be used to amplify the sync voltage as, for example, in fig. 4–30*b*.
The data for the circuit components are given in fig. 4–32. If condenser C can be switched in seven stages from 50,000 pF to 150 pF, the sawtooth sweep frequency range will extend from about 20 c/s to 20 kc/s. The output voltage is about 54 V_{pp} for a supply voltage of 300 V. Flyback times lie between 2.5 to 8%, and non-linearity is between – 8.8 and – 5.4%.
In another type of blocking oscillator, the feedback coupling is made even tighter than in the circuit described and the grid circuit is so severely damped that H.F. oscillations cannot arise. The condenser is then charged up, for practical purposes, within one H.F. cycle.
This type of oscillator[17] is very often used in television circuits.
Its mode of operation is illustrated by the oscillograms of fig. 15–16 in chapter 15 on "Investigations on Television Receivers".
In all such oscillator circuits, particular care must be taken to ensure good H.F. decoupling of the time base section from the power supply, as otherwise oscillator radiation may lead to severe interference with radio reception.

The transitron-Miller circuit.

Among the numerous systems of generating a sawtooth voltage by means of one valve—usually a pentode—special significance attaches to the "transitron" circuit [6] [7].
The transitron-Miller circuit (incorporated in the oscilloscope described in chapter 21) is essentially a combination of two circuit ideas.
The sawtooth voltage is generated by the transitron, and the application of the "Miller effect" permits the use of considerably smaller charging capacitances.
The transitron circuit, indicated by Brunetti [8], takes advantage of the fact that at particular values of voltage on the second and third grids of a pentode the screen-current/screen-voltage characteristic has a very steep *negative portion*. The voltage on the first grid must be slightly positive—between 0 and approx. + 0.25 V. The voltages on the second and third grid should be approximately equal and between +40 and +80 V. The potential on the anode is less critical. (In the publication quoted [6] curves are shown for $V_{g2} = V_{g3} = +60$ V with $V_a = 50$ V and 200 V, which differ very little from each other.)
The transitron characteristic is very similar to the dynatron characteristic of a tetrode. In the dynatron, however, the falling portion of the V_a–I_a characteristic is due to the effect of secondary emission of the anode. As this does not occur evenly and in the standard makes is not controlled and certainly not sought after, the valve suppliers generally reject this circuit. With a

[17] This actually is the genuine "blocking" oscillator. The circuit so far discussed is better described as the "squegging" oscillator.

transitron, on the other hand, use is made of the current distribution between the third and second grid. Since this current distribution essentially depends only upon the geometric form of the grids and the voltages applied to them, no fundamental objection is raised against their use. In this circuit, as always, care must be taken that the limiting data for the valves are not exceeded under any possible working condition. The basic transitron circuit is shown in fig. 4–33. The voltage for the third grid appears automatically across the condenser as a result of oscillation. If, as a starting point, we take C_L as discharged, then as the charge builds up through R_L the voltage rises until anode current begins to flow. Owing to the anode current, which is controlled by the second and third grid, C_L will now discharge rapidly. This produces a sawtooth voltage at the anode and an asymmetrical rectangular voltage on the screen grid. With the operating data given in the circuit diagram, for example, a sawtooth voltage of about 30 V_{pp} can be taken off at the anode. In principle, the charging condenser with its resistor could be connected in the grid circuit. The discharge would then take place as grid current, and the voltage variation across the charging condenser would then appear amplified at the anode. Thus only a small variation in grid volts suffices to produce a fundamentally improved linearity and enables a still larger sawtooth voltage to be taken off at the anode, which must now be connected to the voltage source via a coupling resistor. It is large enough to deflect the beam in the cathode ray tube without subsequent amplification.

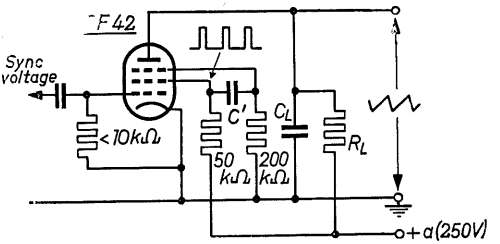

Fig. 4–33. Transitron circuit.

If, however, the charging condenser is connected between grid and anode instead of between grid and cathode, then for a rise in grid voltage of e.g. 1 V, there will be a voltage drop at the anode of G-volts. (G = the gain of this stage). A certain voltage variation between grid and cathode thus produces a $(1 + G)$ times greater variation of the voltage across condenser C_L. For a given charging current to produce a certain voltage variation across the charging condenser, only $\frac{1}{1+G}$ times the capacitance needed when it was connected between grid and cathode is now required.

This effect became known as the *Miller effect* at a time when the influence of the grid-anode capacitance of a triode was being investigated. It does not influence by itself the linearity of the voltage rise, as is sometimes assumed, but merely makes it possible to use considerably smaller capacitances to obtain a nevertheless satisfactory amplitude of voltage.[18]

[18] This apparent amplification of capacitance is also made use of when time bases with a duration in the order of one minute have to be generated. The charging condenser is then connected between the grid of the firststage of a cascade amplifier with an odd number of stages and the anode of the last stage. In this way the same effect can be obtained with a small capacitance as with a capacitance several thousand times larger between grid and cathode.

A basic circuit of this sort, as first indicated by Cocking [9], is shown in fig. 4–34, together with the component values given by Philips for valve EF 50. For a time base frequency of 60 c/s, $C_L = 0.1\ \mu F$ and $C_1 = 4{,}500$ pF. The following currents were measured for a supply voltage of 250 V:

$$I_a = 5.5\ \text{mA} \qquad I_{g2} = 2.4\ \text{mA}$$
$$I_{g1} = 90\ \mu\text{A} \qquad I_{g2} = 4\ \mu\text{A}.$$

The output voltage was 130 V_{pp}, the flyback time 2%, and the deviation from linearity −0.2%.

The pentode EF 42 is especially suitable for this circuit. It is used for this purpose in the oscilloscope described in chapter 21. The oscillograms in fig. 4–35 show the voltage

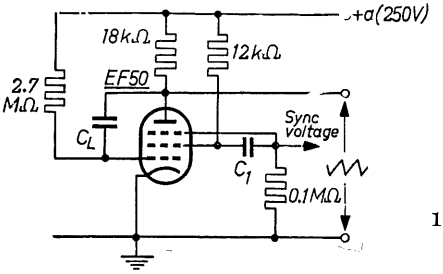

Fig. 4–34.
Transitron-Miller sawtooth generator.

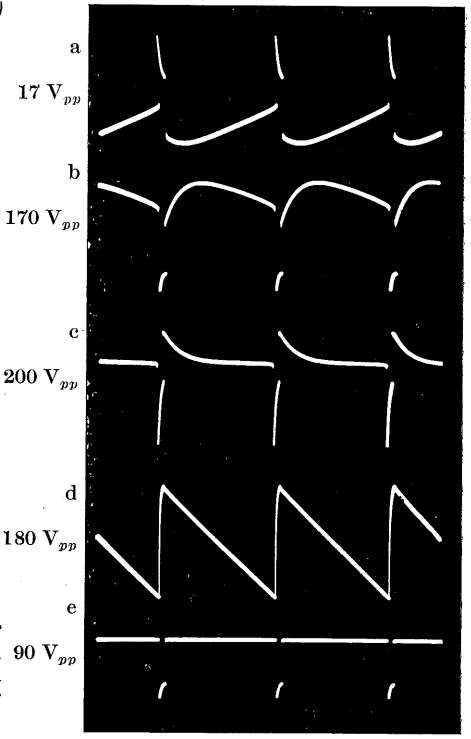

Fig. 4–35. Oscillograms of Transitron-Miller circuit, using valve EF 50. *a*) Grid 1, *b*) grid 2, *c*) grid 3, *d*) sawtooth voltage on anode, *e*) gate voltage from g_2 for suppressing the flyback.

waveforms obtained on an EF 50. The pulse for blanking the return trace (or brightening the forward trace) is taken from the second grid. To ensure uniform brilliance of the spot during the forward trace, the voltage is "clipped" by a biased diode EA 50. The waveform thus obtained is shown in fig. 4–35*e*. It can be seen that the positive part of the cycle is quite flat. This results in an even intensity of brilliance on the screen of the cathode ray tube.

A review of sawtooth generators of particular interest to television engineers, in which detailed descriptions of the way the circuits function are given, may be found in chapter V of the book "Television" by F. Kerkhof and H. W. Werner [10].

Dependence of amplitude control upon frequency.

Many of the circuits familiar at the present time, especially those not using post-amplification (e.g. fig. 4–25) have the drawback that controlling the amplitude of the deflection voltage influences the control of the frequency and vice versa. With the "Transitron-Miller" circuit, in which the oscillator itself works as a "Miller amplifier", the output is taken from the relatively low-ohmic anode resistor. As this can be connected as a potentiometer without noticeable disadvantage, it is possible with this circuit to regulate the amplitude without influencing the frequency.
The same applies also to all circuits using a cathode-follower in the output for extra linearity (see fig. 4–20*a* and *b*). Here, too, the generally low-ohmic cathode resistor in the output can be used to control the amplitude without the frequency being affected.
It is plain, of course, that in all circuits where the sawtooth voltage is subsequently amplified by a wide-band amplifier (e.g. in oscilloscope GM 5659; figs. 4–27 and 5–40) the amplitude of the output on the deflection plates can be controlled by the prescribed adjustment of amplification without influencing the frequency.
In this connection another circuit may be mentioned in which the time base frequency is automatically controlled in such a way that when a certain number of cycles of the input signal is adjusted on the screen, the adjustment remains constant even when the frequency of the input signal changes (up to 1 : 10). When regulating the frequency, readings can be made on a milliammeter which indicates the average charging current. In this circuit the amplitude of the time base voltage also stays constant at the adjusted value. The practical application of this circuit in industrially manufactured apparatus has not so far been made known.

Screening the time base voltage.

The necessity of carefully screening the time base voltage becomes obvious when one considers that it always has a value of several hundred volts and has a high harmonic content, owing to the waveform required (steep voltage drop). Not only when high frequencies are employed but also in the lower frequency ranges (a few hundred cycles) the harmonics falling within the reception bands of radio receivers are considerable. Without satisfactory screening, the harmonics may interfere severely with radio reception. The time base frequency and its harmonics must also be kept away from the *Y* plates and from the input to the vertical deflection amplifier. Otherwise, even without a signal on the *Y* plates, deflection would take place in the vertical direction, and since this occurs simultaneously with the time base deflection, the trace would become twisted or curved. If harmonics alone are responsible for *Y* deflection, a peak appears at one end of the trace.
A number of typical patterns on the screen are given in fig. 4–37, which should make it easier to trace this kind of fault if it arises.
For the reasons described, all leads and components carrying such voltages must be thoroughly screened. Care should be taken, however, to keep the

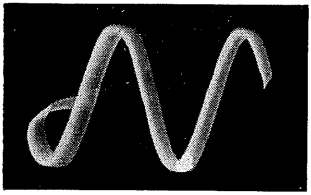

Fig. 4–36. Oscillogram of two cycles of an AC input-signal with the time base voltage distorted by ripple.

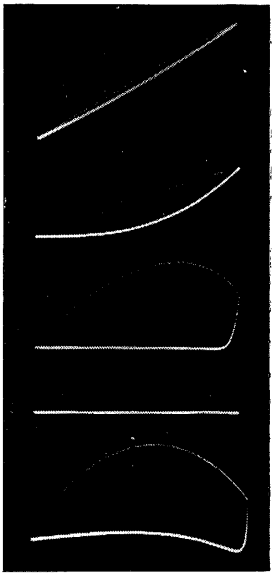

Fig. 4–37. Examples of time base distortion caused by sweep voltage interference on the Y plates. *a*) Time base with simultaneous interference from fundamental and harmonics. *b*) Fundamental of interference voltage attenuated with respect to harmonics (capacitive coupling). *c*) Interference from harmonics only (coupling via small capitance). *d*) Time base without interference. *e*) Y amplifier transmits interfering sweep voltage in wrong phase.

extra wiring capacitance resulting from screening to a minimum to avoid affecting the higher frequencies. A good R.F. choke in the power supply is most advisable.

Blanking the return trace.

As could be seen from some of the oscillograms so far reproduced, the returning spot also leaves a visible trace on the screen. This "flyback" can be especially disturbing at high frequencies, and so circuits have been developed to suppress the electron beam during the flyback time and thus make the return trace invisible. To this end the grid of the cathode ray tube receives a negative pulse during the discharge of the condenser in the time base generator.
A suitable voltage is available at certain points in almost all time base circuits. Mention has been made of these in some of the various circuits already described; see in this connection figs. 4–25, 4–27, 4–30*b* and 4–33, and also the oscillograms of figs. 4–26*b*, 4–28*b*, 4–31*d* and 4–35*e*.

Load on the time base generator and linearity.

In so far as the voltage is not taken from an amplifying stage or a cathode-follower, as in some examples, but straight from the charging condenser, non-linearity can result from a too heavy external load. The additional non-linearity of a condenser charging to a voltage V_X with a current I_L can be approximately given for a total load resistance of R_T by the expression:

$$\textit{Non-linearity due to load} = \frac{V_X}{R_T \cdot I_L}$$

(R_T is the total shunt resistance). If, for example, this ratio should be no more than 10% (i.e. the fraction $^1/_{10}$), then the load resistance R_T will be:

$$R_T = 10 \cdot \frac{V_X}{I_L} \qquad (4\text{–}20)$$

When $V_X = 400\ V_{pp}$ and $I_L = 2.0$ mA, then

$$R_T = 10 \cdot \frac{400}{2 \cdot 10^{-3}} = 2\ \text{M}\Omega$$

This would mean a leak resistor of 4 MΩ and an internal resistance of the charging valve of 4 MΩ. In general, the internal resistance of this valve will not be so high, but by means of negative feedback it is comparatively easy to obtain values of this sort. It is thus advisable in order to obtain lower frequencies not to permit the values to be too low for the control range of the charging current. Again, when the time base frequency is used to control another apparatus (e.g. a wobbulator for representing resonance curves) care must be taken that the load impedance of the apparatus remains sufficiently high, usually at least 5 MΩ. A further prerequisite is that the insulation resistance of the charging condenser dielectric must be high enough to be left out of account. (Time constant: insulation resistance × capacitance > 1000 —MΩ × μF—). Otherwise it would cause much worse non-linearity than that resulting from the influences discussed. For this reason, only first-class condensers should be used in time base generators.

Anode voltage ripple in the time base generator.

The supply voltage for the anodes of the time base valves must have a minimum hum content. Fig. 4–36 shows an oscillogram of two cycles of a sinusoidal voltage with a frequency $\gg 50$ c/s, a sweep voltage amplitude of 350 V_{pp} and a ripple of 6.5%. It is clear from this that the amplitude or ripple in the anode voltage must be smaller than 0.5%. There must therefore be very thorough filtering in the power supply. This is also particularly important in order to avoid undesired synchronization with the mains frequency.

Circuit characteristics.

The electrical efficiency of a time base generator is very often indicated only by the frequency ranges, which are by no means conclusive. It is also important to know what the maximum width of deflection is for a given time base frequency. During one cycle of the sweep, the spot is moved by the deflection voltage V_X from one end of the screen to the other. The faster the rise of V_X, the shorter will be the time T_X required for one cycle of the sweep. The time base allowing the presentation of the most rapidly changing phenomena will be that which permits the greatest rise of voltage in the unit of time, i.e. the highest sweep voltage velocity. This value is obtained from the relationship:

$$\textit{Velocity of sweep voltage} = v_{V_X} = \frac{V_X}{T_X} \tag{4–21}$$

Substituting the duration of deflection by its reciprocal $\left(\frac{1}{T_X} = f_X\right)$—the frequency—the velocity of the sweep voltage appears as the product of time base frequency and voltage amplitude:

$$v_{V_X} = V_X \cdot f_X \tag{4–22}$$

To be able to compare time base generators it is therefore necessary to compare the sweep voltage velocities obtainable. If, for example, with a voltage of 300 V_{pp}, a maximum frequency is given of 40,000 c/s, this means a maximum sweep voltage velocity of: 300 V $\times$ 40,000 c/s $= 12 \cdot 10^6$ V/sec or 12 V/μ sec.

To compare the highest possible time base velocities on the screens of two oscilloscopes, the deflection sensitivity of the cathode ray tubes must be taken into account. The sweep voltage velocity indicates the increase in sweep voltage in the unit of time. The path on the screen covered along the X axis in the unit of time—the speed of deflection along the X axis v_x—is obtained by multiplying together the sweep voltage velocity and the deflection sensitivity of this pair of plates, thus:

$$v_X = f_X \cdot V_{X_{pp}} \cdot DS_= \tag{4–23}$$

The time base frequency and the length of the trace (denoted by X) will usually be known. As the length of the trace is given by $X = V_{X_{pp}} \cdot DS_=$, the time base velocity on the screen is obtained from the product:

$$v_X = f_X \cdot X \tag{4–24}$$

Taking as an example tube DG 7–6, where $V_{X_{pp}} = 300$ V, $f = 40{,}000$ c/s and $DS_= = 0.26$ mm/V, then $40{,}000 \times 300 \times 0.26 = 3.12 \times 10^6$ mm/s $= 0.312 \times 10^6$ cm/sec. This is equal to 0.312 cm/μsec. Of course, the input frequency is quite often known, at least approximately, and therefore it is useful to know the time base frequencies in an oscilloscope. Nevertheless, one should always insist on information on the maximum sweep voltage velocity of a time base generator, or on the maximum velocity of deflection. These values alone truly characterize the efficiency of a time base generator or an oscilloscope. At high frequencies, where the flyback time of the spot (usually blanked) is an important factor, knowledge of these values may reveal that the time base expansion is greater than might have been expected from an indication of the time base frequency alone.

Limiting effect of spot diameter on frequency.

The shortest duration of a changing phenomenon which can still be recognized on an oscilloscope is dependent not only upon the maximum deflection speed of the spot but also upon the diameter of the spot. It may be assumed that the smallest distinguishable value (ΔY_{min}) on the screen of a cathode ray tube is given by the centres of two positions of the spot, the space between

which is equal to the diameter of the single spot (d_s). Therefore the discrimination on the screen can be assumed to be:

$$\Delta Y_{min} = 2 \cdot d_s \tag{4–25}$$

To illustrate these relationships, the oscillogram in fig. 4–38*a* shows a section of a sinusoidal voltage, the frequency of which was chosen such that the spaces between the turning points at the upper and lower ends of the waveform were each equal to the diameter of the spot. In fig. 4–38*b* the section indicated in *a*) is reproduced magnified about $2^1/_2$ times, and *c*) shows the section of an oscillogram with the input frequency doubled. The end points now touch each other[19] and it is no longer possible to distinguish between them. The smallest interval of time of the measured signal which can be distinctly determined—T_{Mmin}—appears from the formulas (4–22), (4–23) and (4–25) as:

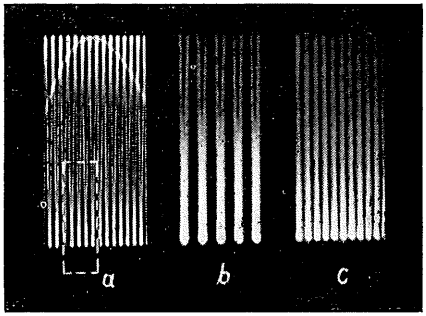

Fig. 4–38. Examples of oscillograms showing limiting effect of spot diameter on sweep frequency.

$$T_{Mmin} = 2 \cdot \frac{d_s}{f_X \cdot V_X \cdot DS_=} = 2 \cdot \frac{d_s}{v_X} \tag{4–26}$$

In the example quoted, taking the spot diameter at 1.0 mm.,[20] a time T_{Mmin} is calculated of:

$$\frac{2 \cdot 1.0}{3.12 \cdot 10^6} = 0.64 \cdot 10^{-6} \text{ sec or } 0.64\ \mu \text{ sec.}$$

The highest frequency of the signal to be measured (f_M) which still has a clearly distinguishable waveform (see fig. 4–38*a*) appears then as the reciprocal of T_{Mmin}:

$$f_{Mmax} = \frac{1}{2} \cdot \frac{v_X}{d_s} \tag{4–27}$$

Turning to the example once again, we get:

$$\frac{3.12 \cdot 10^6}{2 \cdot 1.0} = 1.56 \text{ Mc/s.}$$

Rating the coupling components for the time base generator.

For application to the deflection plates and within the oscillator circuit the time base voltage must often be coupled free of *DC* over *CR* networks. When rating the coupling components it should be remembered that the sawtooth voltage consists of a fundamental with a large number of harmonics having specific

[19] This position might also be used to define the upper frequency limit.
[20] In the turning point.

phase relationships. It is essential therefore for the rating to permit the fundamental plus its harmonics to pass unattenuated and, what is more difficult, without phase distortion. This is only touched on here in passing, as the subject is dealt with in detail in the following chapter on deflection amplifiers.

Special-purpose time bases.

A great number of measurements are concerned with the investigation of *single transients*, for which a non-repetitive or *single shot* time base is needed. A long persistence tube, i.e. with a long afterglow screen, is the most suitable for observing these waveforms, although photographic recordings are indispensable for accurate assessment. To prevent premature exposure resulting from the initially quiescent spot, it must be deflected beyond the screen, or even better, suppressed by a sufficiently high negative potential on the grid of the cathode ray tube. As a rule the spot should also write a portion of the trace *before* the transient to be examined is started. By means of contact relays or suitable valve circuits it is possible at the required intervals first to brighten the beam, then to start the time base (single-shot) and only subsequently to release the signal.
The measures to be taken for this are described in the introduction to the methods of operating oscilloscopes. Guidance is also given in part III of this book in the chapters "Investigating switching phenomena on electric light bulbs" and "Measuring the action of between-lens shutters".
The method of starting rapid time bases by low-frequency pulses—triggering—was mentioned when describing the triple-triode oscillator (circuit in fig. 4–27). The apparatus for greatly expanding the time display about to be described operates on the same principle.
Sinusoidal voltages too can be used to obtain a linear time base. Advantage is taken of the fact that the sinusoidal voltage has a constant speed, i.e. is linear, in the vicinity of the zero cross-over point. Only the rising portion of the sine wave is used. The falling portion is blanked by a voltage 90° out of phase with the sweep voltage applied to the grid of the cathode ray tube. This process is described in detail for a voltage with a frequency of 50 c/s in chapter 22 "A simple time base expansion unit". Since it has so far proved impossible to produce a linear time base directly with frequencies of several megacycles and more, other methods have been sought for generating high frequency sweep voltages. A circuit has been described [13] in which, by using sinusoidal voltages from 60 kc/s to 6 Mc/s a time base expansion is achieved corresponding to linear sweep voltages of frequencies from 0.9 to 90 Mc/s. The field of application for such apparatus is naturally limited to specialized laboratory work.
High-frequency sweep voltages (>1 Mc/s) are very difficult to synchronize with any degree of stability, so that when investigating frequencies above 100 Mc/s we are limited as a rule to photographing oscillograms on a single-shot time base. High-frequency voltages of several thousand megacycles have been recorded in this way. These processes cannot be dealt with in any detail within the scope of this book, but the interested reader is referred to the literature on the subject quoted in the bibliography [13] [14].

Time base generators for extreme expansion of the display.

The normal time base is no longer adequate when it is required to display changes in a condition which are short in relation to the duration of one cycle. In standard oscilloscopes, the maximum amplitude of the sweep voltage is usually just sufficient to deflect the spot over the whole length of the screen. On the other hand, the time base frequency can at the most be equal to the input signal frequency for correct synchronization to be possible. The highest relative expansion of a certain portion of a whole cycle which can be obtained in this way is thus determined by the maximum deflection speed of the spot and by the ratio of the diameter of the screen to the diameter of the spot (see "Limiting effect of spot diameter on frequency", page 68).
To achieve greater expansion of the display on the time base, the following are some of the possibilities known:

1) greatly increased time base frequency;
2) periodic triggering of relatively short sweeps in the rhythm of the fundamental frequency;
3) greatly increased amplitude of sweep voltage.

1. Greatly increased time base frequency

The use which can be made of a time base frequency several times greater than the input signal frequency to expand the display on the screen has already been touched upon in this chapter. Further details are given in chapter 6 (see fig. 6–7 on page 137).
In order to obtain the stationary pattern shown in fig. 6–7, for a time base frequency eleven times higher than the input frequency, it was necessary to over-synchronize; the resulting pattern is therefore not entirely reliable. Abnormal synchronization also caused oblique curtailment of the right-hand edge of the pattern.
Nevertheless, it is possible to achieve good synchronization of a time base frequency several times higher than the input frequency by producing harmonics from the input frequency with a distorting circuit and a suitable filter, and by using these harmonics to synchronize the time base frequency. Oscillograms of this sort always have the disadvantage, however, that they contain all the expanded phases of a cycle in one picture.[21]
This method is only usable, therefore, when the voltage trend is generally constant and manifests merely at one or two short intervals the rapid changes which are to be investigated. It cannot be used for voltages which contain rapid and possibly differing pulses over the entire cycle. In such cases all that appears is an undecipherable maze of lines.

2. Periodic triggering of relatively short sweeps in the rhythm of the fundamental frequency

In high-grade oscilloscopes a triggering device is provided for examining the

[21] This disadvantage could be overcome by using a suitable rectangular pulse to brighten only that cycle of the sweep which contains the interesting portion of the voltage under investigation.

waveforms of pulses. In the triggering position the time base generator is fundamentally static and is started only by the input voltage-pulse itself at any desired time base velocity corresponding to the setting for the appropriate sweep frequency.

The quiescent spot is then visible, usually on the left, as a bright spot or vertical blip (unless it is blanked) and from this point the oscillogram is described, less bright, over the screen to the right. The difference between the luminous intensity of the quiescent spot and that of its trace on the screen is due to the difference in bombardment time on the screen.

With this process it is evident that the beginning of the pulse will not be completely visible, because a certain time—even though fractional—elapses before the time base can start to move across the screen. It is possible, however, to incorporate a delay circuit in the vertical amplifier which ensures that the beginning of the pulse reaches the Y deflection plates after the sweep has already started. This delay circuit must not, of course, distort the input signal in any way.

To investigate a train of different pulses which have a rhythmic repetition frequency (e.g. in television, radar, etc.), a rapid time base of this sort can be suitably triggered by the lower frequency. Naturally this will only allow a section of the whole pulse train in one cycle to be visible on the screen. In order to select at will a certain section of the pulse train for observation, it is necessary to provide for phase control between the triggering pulse and the time base generator, which must allow a 360° phase change within one cycle of the pulse train. This circuit has become known as the "time base expansion unit". It is used particularly for investigating pulse shapes in television engineering.

A more detailed description is given in the following part of this chapter.

3. Greatly increased amplitude of sweep voltage *

In so far as the sweep voltage is obtained through an amplifying stage, the maximum permissible voltage drive of the amplifier valves sets a limit to the time base expansion which can be achieved by increasing the amplitude of the sweep. An expansion of hardly more than ten times the normal time base is possible by these means. Here also it is appropriate to provide a facility for phase control in order to be able to select the desired portion of the phenomena to be observed. The advantage of this method is that its permits, especially where circumstances are limited, the construction of comparatively simple yet very efficient circuits for extreme time base expansion. (see page 77.)

Sawtooth generator for pulse modulation (triggering)

The familiar sawtooth generators are used to produce the deflection voltage for this type of time base expansion too. The individual cycles are not, however, produced continuously by direct synchronization with the input signal, but mostly via a "flip-flop" multivibrator (Eccles-Jordan circuit) [15]. This makes it possible to select the deflection speed independently of the time base frequency. Fig. 4–39 shows the circuit of the time base generator

* For amplifying the sawtooth voltage, DC amplifiers are necessary to prevent displacement of the operating point owing to the rectification effects caused by over-modulation. By the simultaneous application of triggering and sawtooth voltage amplification, unusually large time-base expansions can be obtained. By means of a "delayed sweep" device, any section of a pulse train can be selected and displayed expanded over the whole width of the screen.

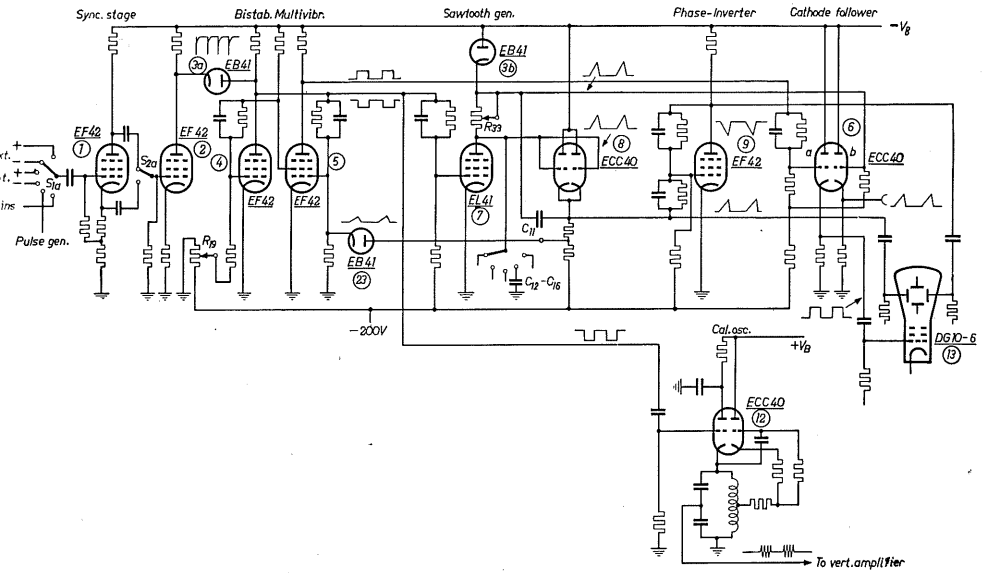

Fig. 4–39. Time base generator for pulse triggering.

used in Philips' type GM 5660 oscilloscope [16]. The sweep circuit consists of the synchronizing stage (valves 1 and 2), the multivibrator (4 and 5), the sawtooth generator proper (3b, 7 and 8) and the phase inverting stage [9]. The sawtooth voltage is generated by charging a condenser (C_{12} . . . C_{16}) through a resistor (R_{33}) and by discharge through a pentode [7]. A modification of the bootstrap circuit in fig. 4–20b is used for linearizing the voltage rise. (The integration network, consisting of R_v and C_{L2}, is not employed.)

The parallel systems of an ECC 40 serve as a cathode follower stage [8]. The voltage appearing on the cathode of this stage is fed via capacitor C_{11} to the junction of resistor R_{33} with diode 3b. This voltage rises with the voltage across the capacitor and thus the voltage rises in the same way at the junction. The result is that the difference between the voltages at the ends of resistor R_{33} remains pratically constant, and so, therefore, does the charging current. In this way the voltage rise across capacitor C_{12} . . . C_{16} is linear with time.

This voltage is fed to the left-hand X plate of the cathode ray tube direct and to the right-hand X plate via a phase-inverter stage [9].

The discharge valve [7] is driven by the multivibrator (4 and 5), which can work either in continuous self-oscillation or in two stable working positions. The anode alternating voltage of the first valve (4) of the multivibrator also lies on the first grid of the discharge valve [7]. During the negative phase of this voltage the discharge valve is cut off, which allows the condenser for generating the sawtooth voltage to charge up. A part of the sawtooth voltage is fed back via a diode [23] to the grid of the second multivibrator

[5], thus ensuring that the change of equilibrium in the multivibrator—which also introduces the discharge again—always occurs at a specific amplitude of the sawtooth voltage. Because of this, the controls for the time constants of the sawtooth generator can be calibrated for durations of deflection independent of the time base frequency.

In this way the deflection over the whole screen can be regulated in five steps of 2 to 5000 μs, corresponding to time base expansions of 0.2 to 500 μs/cm. If the multivibrator is brought into equilibrium by suitably adjusting the grid bias of the first valve [4] with R_{1g}, the flip-flop action, and thus the triggering of the time base, will only be possible by means of synchronous pulses over diode 3_a. After each pulse a complete deflection takes place, upon which incidental voltage surges have no effect. By means of the first valve in conjunction with the coupled switches S_{1a} and S_{1b} a choice can be made, for triggering the time base, between positive and negative pulses, between sinusoidal voltages (including the mains) or between the pulses from the pulse generator incorporated in the apparatus. The rectangular voltage on the anode of the second valve of the multivibrator [5] is fed via a cathode follower [6a] to the grid of the cathode ray tube. In this way the spot on the screen is modulated in intensity; it remains bright for exactly as long as the deflection lasts. (The trigger time for the maximum time-base cycle is 0.25 μs and for the minimum cycle, 0.1 μs.) The time base deflection can thus be pulse-triggered for non-recurring phenonema, or take place in the usual manner either synchronized or non-synchronized. (The modulation time for the triggered time base is about 0.1 μs.)

The waveforms of the most important voltages in this circuit are shown by the oscillograms in Fig. 4–40, which were taken on a type GM 5654 oscilloscope with probe. Those settings were used in which the 1 Mc/s oscillator [12] was switched for time calibration via the amplifier on to the Y plates. This voltage is used for driving the time base generator (internal synchronization). The values of voltage or current are given as peak-to-peak beside the corresponding oscillograms. [22]

The 1 Mc/s voltage is generated with a double triode, type ECC 40 [12]. The grid of the left-hand triode in the circuit diagram receives from the anode of the left-hand valve in the multivibrator a voltage of the waveform shown in oscillogram *d*. During the positive cycles of this voltage the triode is conductive. Its output resistor lies in parallel to the ringing circuit in the cathode lead. As the valve is circuited as a cathode follower, its output resistance is low and has such a damping effect that the ringing circuit is not able to oscillate during the positive cycles. When the voltage goes negative the grid is blocked and the condenser in the ringing circuit is charged by the voltage surge (the current through the inductance cannot rise so rapidly). As there is now no anode current flowing, the circuit is no longer damped, so that the condenser can discharge through the inductance. The circuit now oscillates at its own frequency until the grid goes positive once more. The resultant surge causes the ringing circuit to oscillate again, but the severe damping due to the output resistor of the valve stops the oscillation after only one cycle.

[22] At other settings the waveforms as well as the amplitude of the oscillograms can deviate considerably from those shown.

One part of the choke in the ringing circuit is connected to the cathode lead of the right-hand triode [12], to the grid of which the HF voltage is fed via a condenser from the upper end of the choke. The resultant circuit is a Hartley oscillator. By suitably rating the two resistors in the cathode circuit favourable dedamping can be obtained and the oscillation produced in the ringing circuit falls off quite slowly. [23]

The time base deflection is thus triggered by this voltage over valves [1] and [2], so that in this case the time base generator controls the voltage under test, and this in its turn triggers the time base generator. In other words, inverse coupling takes place over two oscillation generators.

The voltage on the anode of the synchronization valve [3] is shown by oscillogram *b*. The horizontal, thick parts originate from a certain residuum of the 1 Mc/s voltage, which shows that the amplification of this valve was higher than practically necessary. Normally one will only see the pulses visible in the oscillogram.

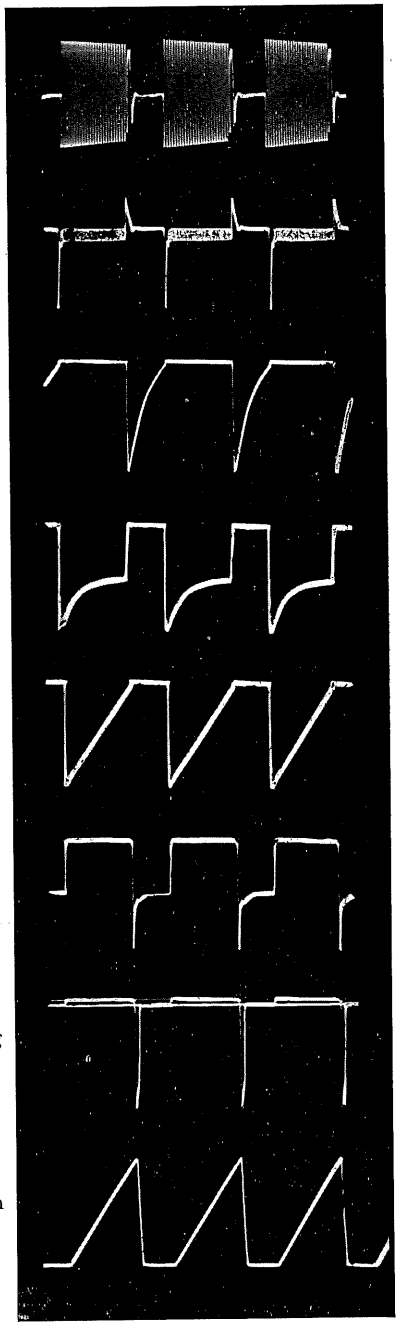

Fig. 4–40. Waveforms in the time base generator as in circuit diagram fig. 4–39.

a)	Voltage on the ringing circuit for the 1 Mc/s time calibration. (Valve 12)	11 V_{pp}
b)	Sync pulse on anode of valve 2	210 V_{pp}
c)	Valve 4, grid voltage	80 V_{pp}
d)	Valve 4, anode voltage	130 V_{pp}
e)	Valve 5, grid voltage	85 V_{pp}
f)	Valve 5, anode voltage	105 V_{pp}
g)	Charging current in condenser (C_{12}...C_{16})	55 mA_{pp}
h)	Valve 8, cathode	140 V_{pp}

[23] This fall-off is more clearly pronounced in oscillogram fig. 4–40a because three time base cycles are shown. In consequence, the train of oscillation, which practically extends over the whole width of the screen, is correspondingly compressed. Slight damping must nevertheless be preserved to ensure that the oscillation is effectively stopped.

Oscillogram *c* shows the voltage on the grid of the multivibrator valve [4] and oscillogram *d* the voltage on the anode of the same valve.

The grid voltage of the second multivibrator valve [5]—oscillogram *e*—is determined by the sawtooth voltage, which is fed back from the cathode of double triode ECC 40 [8], from the condenser (C_{12} . . . C_{16}) and from the anode of the discharge valve EL 41 [7] over diode EB 41 [23]. The waveform of the voltage on the anode of valve [5] is shown in oscillogram *f*.

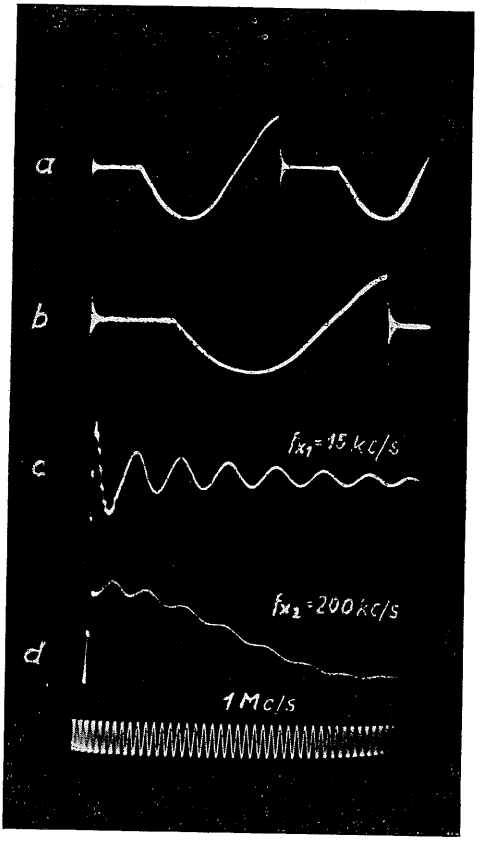

Fig. 4–41. Comparison of normal oscillograms (*a* and *b*) with oscillograms expanded by pulse triggering (*c* and *d*).

Oscillogram *g* shows the form of the charging current in the condenser. This was taken by connecting a resistor of 100 Ohms to the earth side of the condenser and recording the voltage appearing across it. To make a clear distinction between the charging and discharge currents the zero line was recorded separately and added to the picture. The course of the charging current can be seen above the zero line, and below it, the negative current surge during discharge, found by measurement to be 55 mA_{pp}. The average charging current was found to be 3.0 mA. With a total duration of a sawtooth section of about 25 μs (40 kc/s) the discharge current pulse lasted about $1^1/_2$ μs. The time during which the electron beam remains at the left of the screen—spot suppressed—can be recognized as the horizontal part of this oscillogram on the zero line; it is dependent upon the setting of the operating point of the left-hand multivibrator valve [4] (time base equilibrium).

An example of the possibilities of increased time base expansion offered by this circuit is given in fig. 4–41. The oscillograms show the waveform of the voltage on the anode of a grid-controlled thyratron, the anode current being taken from the 50 c/s mains. Oscillograms *a* and *b* represent normal time base frequencies of 25 c/s and 50 c/s respectively. It is particularly evident from oscillogram *b* that after the collapse of the anode voltage (current flow) oscillation takes place. However, the behaviour of the voltage in this part of the oscillogram can only be clearly recognized and assessed in the greatly expanded oscillogram shown under *c*, which was obtained by pulse

triggering. The natural frequency of this damped oscillation was found to be 15 kc/s. It can also be seen that a further damped oscillation is present at the beginning of the voltage curve in this oscillogram. From the even greater time base expansion represented under *d*, to which the picture of a voltage with a frequency of 1 Mc/s has been added for time calibration, the frequency of this oscillation can be determined as about 200 kc/s.

Time base expansion unit.

The assembly of *Philips'* GM 4584 apparatus, which we shall use as an example, is shown in block diagram form in fig. 4–42. The sawtooth voltage for the time base is generated by an EF 80 pentode, connected as a Transitron-Miller oscillator-I. It is applied in antiphase to symmetrical deflection plates after

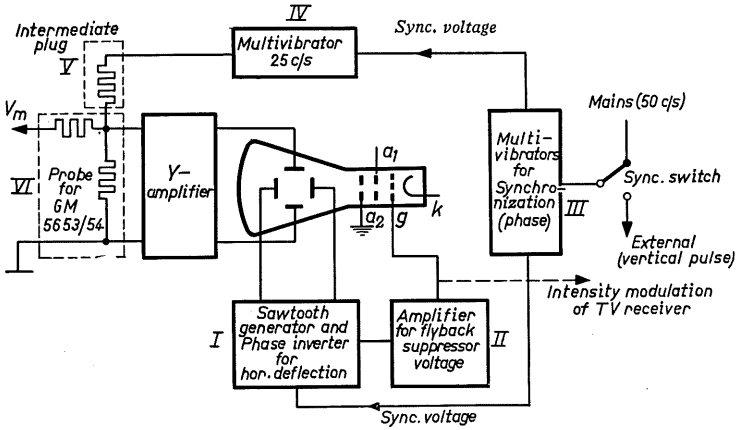

Fig. 4–42. Block diagram of Philips GM 4584 time base expansion unit.

passing through a phase inverter, formed by a section of an ECC 81 double triode. The circuit components of the sawtooth oscillator are rated such that the transitron section can generate a frequency approximately equal to the mains frequency (50 or 60 c/s).

"Miller" capacitors with small ratings (C_L in fig. 4–34) make it possible to achieve at the same time a sawtooth cycle which, unlike that in usual time base oscillators, is essentially shorter than would correspond to the total duration of one cycle of the process to be investigated (50 c/s — 20 ms).

The duration of the sawtooth pulses can be adjusted by switching to different values of capacitance (C_L in fig. 4–34) and can be continuously controlled by the charging resistor (2.7 MΩ in fig. 4–34).

The oscillograms in fig. 4–43 show, each in the starting position of the fine frequency control (longest sawtooth pulse), the voltage waveforms during two cycles (40 ms) of the appropriate range.

The linearly rising portion of the voltage corresponds in *a*) to about $2^1/_4$ ms, in *b*) to about 1 ms and in *c*) to about 0.4 ms.

These voltages are applied to the *X* plates, the normal time base generator of course being switched off. A pulse derived from the same circuit is amplified

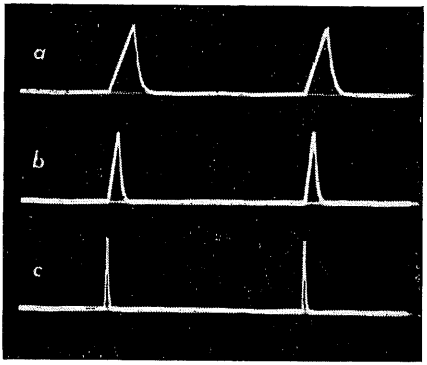

Fig. 4–43. Deflection voltages of the GM 4584 time base expansion unit for various stages of sweep velocity.

via II (second triode ECC 81) and used to modulate the intensity of the beam (brighten the spot) during the time base deflection. With no input signal, all that appears on the screen is a bright spot at the left, since the electron beam is in a state of obeyance for most of the time, corresponding to the zero line in the oscillograms in fig. 4–43. As a rule it is placed outside the screen by a positioning control. The oscillogram is fainter, corresponding to the speed of deflection, and becomes still fainter the shorter the sawtooth pulse is, that is to say, the larger the time base expansion chosen.

In order to be able to select for observation any desired portion of the input signal, a more than 360° phase-changing facility is necessary for synchronization of the time base.

This is done in the following way: a multivibrator—III, ECL 80— is locked in phase with the reference frequency—the mains or the vertical pulse from the source under investigation. The trailing edge of the rectangular pulse from the multivibrator is used, after differentiation, to synchronize with the sawtooth voltage generator.

Thus, by changing the pulse width, the phase of the synchronized pulse can be shifted.

Since with only one multivibrator a phase change of $< 360°$ is obtained, this apparatus uses two multivibrators connected one behind the other. The sync pulse of the first synchronizes the second multivibrator and this locks in with the sawtooth voltage generator. In this way the time base can be adjusted in phase with respect to the reference voltage over more than 400°.

In order to be able to represent separately the voltage waveforms of the composite television pulse of both fields, a third multivibrator is provided—IV, ECL 80— which generates a symmetrical rectangular pulse with exactly half the frequency (25 c/s) of the input signal. This multivibrator too is locked in with the first multivibrator in III. If the output voltage of IV is fed to the input of the vertical deflection amplifier, two lines are obtained one above the other, similar to the result obtained when using an electronic switch. The distance between them is determined by the output voltage of the multivibrator and by the adjusted amplification in the Y amplifier.

In oscilloscopes GM 5653 and GM 5654, a plug—V—together with a probe—VI—forms a resistance T-network. In this way, as indicated in fig. 4–42, the voltage to be measured—V_m—can be added to the rectangular pulse of the 25 c/s multivibrator with sufficient freedom from reaction. The pulse sequences of both fields of the television frame thus appear on the screen of the oscilloscope one above the other. Fig. 4–44*a* shows a double oscillogram of this sort using the smallest time base expansion of the GM 4584 unit. The

phase of the time base voltage was adjusted in such a way as to make the picture of the sync-pulse mixture visible around the vertical blanking pulse. The ranges of adjustment for the time base velocities are approximately as follows for the individual stages:

Stage	*Time base velocity*
I	10.....30 cm/ms
II	23.....80 cm/ms
III	60....150 cm/ms

The "normal" oscillogram of a 50 cycle waveform represents a cycle duration of 20 ms. Thus with a picture width of 8 cm the oscillogram corresponds to a time base velocity of $\frac{8}{20} = 0.4$ cm/ms.

Fig. 4–44. Expanded oscillogram of composite television pulse with: *a*) vertical blanking pulse and *b*) corresponding intensity-modulated lines on television screen.

It follows from this that the GM 4584 time base expansion unit is capable of expanding a normal oscillogram by more than 300 times. Of course, it is to be expected that the brilliance of the pattern on the screen will suffer considerably in consequence. For this reason the cathode ray tube normally works with a high post-acceleration voltage (2 kV).

The intensity-modulating pulse for the linear portion of the sawtooth voltage has a further very useful application. When investigating a composite television pulse, using the time base expansion unit, the pulse sequences during more or less horizontal deflections—the line signals—appear on the screen according to the time base expansion employed. If the intensity-modulating pulse for the oscilloscope is fed simultaneously to the grid of the C.R.T. of the television receiver, a part of the picture corresponding to the oscillogram under observation will be brightened. In this way it is possible to distinguish the lines in the picture appertaining to the pattern on the oscilloscope. Fig. 4–44*b* shows the picture on the television screen appertaining to the oscillogram in fig. 4–44*a*.

As this oscillogram embraces the vertical blanking, which is normally not visible, the vertical frequency was overadjusted to bring the blanking gap into the picture. The first horizontal pulse is identical with the first line (from above) in the intensity-modulated strip. The starting position of the spot appears in this process as vertical blips in the double oscillogram in 4–44*a* (see also fig. 15–34).

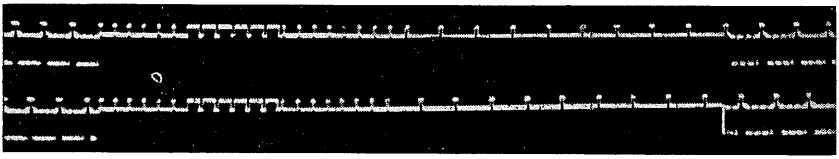

Fig. 4–45. Expanded oscillogram of composite television pulse from the large signal generator GM 2657. (Three recordings joined together.)

As the deflection voltage of the time base expansion unit GM 4584 is greater than is used for deflection over the whole width of the screen, more lines appear intensity-modulated in the receiver picture (below) than line pulses can be seen in the oscillogram. The white arrows in the receiver picture circumscribe the lines actually covered in this way.
Further similar pictures are given in figs. 15–34 to 15–40 in chapter 15, on "Investigations on Television Receivers".
In conclusion, fig. 4–45 reproduces the signal-pulse mixture with vertical blanking signals from the large television signal-generator GM 2657. This picture however is made complete by three oscillograms with large time base

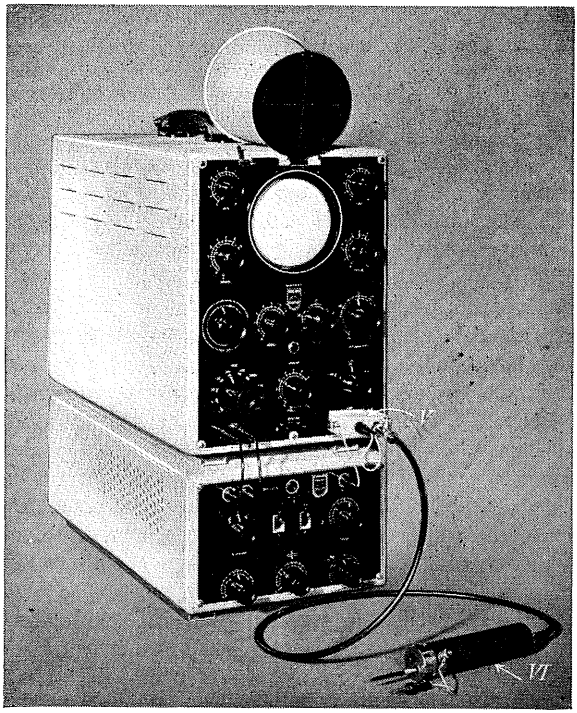

Fig. 4–46. Time base expansion unit GM 4584 with oscilloscope GM 5653

expansion and corresponding phase angles joined together. It can be seen that the vertical synchronizing pulses from this signal generator, in accordance with the CCIR standard, are accompanied by pre- and post-equalizing pulses, and in general satisfy the prescribed conditions.
Mains synchronization cannot be used for large time base expansions, even when the television system is mains-coupled, as phase changes in the mains between synchronising signal-generator and receiver cause the picture to fluctuate to and fro in a horizontal direction. In such cases external synchronization is essential, whether it be from the synchronization separator or from one side of the frame output transformer of the receiver. Using free-running synchronizing signal-generators with quartz crystal control for the sync pulses—completely in accordance with the standards— external synchronization must always be applied.
Fig. 4–46 shows an exterior view of the GM 4584 time base expansion unit together with the GM 5653 oscilloscope in working arrangement.
Obviously, the application of this apparatus is not limited to television practice. It can be used for observing, expanded along the time axis, all other voltage changes with a recurrence frequency of 50–60 c/s. (Relay testing, waveforms of electronic-control circuits, etc.) Reference is made in this connection to figs. 22–1 and 22–6 in chapter 22 "A simple time base expansion unit" [16].

5. Deflection Amplifiers

General.

The cathode ray tube is an ideal device for the static representation of electrical potentials. They can be observed on standard tubes, without perceptible errors of measurement, at frequencies of up to more than 100 Mc/s. For adequate deflection of the beam, however, voltages are necessary which are only seldom available in practical measurements. Amplification is therefore essential in the majority of cases. For this reason oscilloscopes are, as a rule, provided with an amplifier for vertical deflection, and sometimes with an amplifier for horizontal deflection, possibly with a smaller frequency range.

Frequency range.

A vertical amplifier with a frequency rating of about 5 c/s to 20 kc/s suffices for audio frequency measurements. However, in order, to be able to reproduce satisfactorily the harmonics of the voltages under examination, an upper frequency limit of 40 to 50 kc/s is desirable even for audio frequencies.
For high frequency investigations, vertical amplifiers with frequency ratings of up to at least 1 to 3 Mc/s are required, and in television and pulse technique, up to 10–30 Mc/s. Since, for reasons which will be discussed later, an amplifier with a widely extended upper frequency range entails a disproportionate increase in outlay, probes with a demodulating diode or a crystal detector are used for measuring high frequency voltages on ordinary oscilloscopes. If the

H.F. voltage under investigation is modulated by a low frequency signal, this signal appears across the probe and can be observed on the oscilloscope. In so far as the depth of modulation is known, it is possible in this way to get an indirect idea of the magnitude of the high frequency voltage, though not, of course, of its trend. For physiological investigations, measurements of mechanical vibrations and the like, the lower frequency limit must be very low. An *AC* amplifier for vertical deflection has been developed, for instance, with a lower frequency limit of $^1/_{10}$ c/s [1]. Certain measurements require special *DC* ampliers, which must be capable of amplifying without distortion both the *DC* voltages and the desired frequency range of *AC* voltages. Carrier-frequency amplifiers are sometimes used for indicating values of voltage with a *DC* component. Here a carrier frequency is first modulated with the voltage in question, and amplified to the value required. The carrier frequency is then demodulated and the demodulation voltage is fed direct, or via a vertical amplifier, to the deflection plates. Usually, *AC* wide-band amplifiers with *RC* coupling are used in oscilloscopes.

Characteristics of a vertical amplifier.

The fundamental requirement of a vertical amplifier in an oscilloscope is that it should provide the necessary amplification in the frequency range required without causing any perceptible change in the shape of the voltage observed on the screen. This applies not only with respect to a simple, sinusoidally

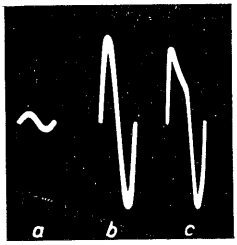

Fig. 5–1. Amplitude distortion; sinusoidal voltage; *a*) unamplified voltage, *b*) amplified voltage with no amplitude disortion, *c*) amplified voltage with amplitude distortion.

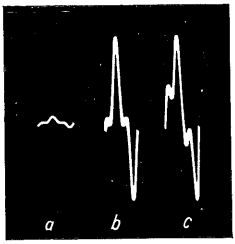

Fig. 5–2. Phase distortion: voltage with third harmonic; *a*) unamplified voltage, *b*) amplification with no phase or amplitude distortion, *c*) the amplitude is undistorted but the phase of the harmonic has been shifted (phase distortion).

varying voltage which must suffer no amplitude distortion, but even more so to phenomena which appear on the screen as the sum of several alternating voltages.

The whole purpose of the oscilloscope is to make changes of this sort visible, but a deflection amplifier which produces additional deformation of a waveform would only have a very limited field of application.

Fig. 5–1a shows one cycle of an unamplified sinusoidal voltage and fig. 5–1b the same voltage amplified tenfold. Fig. 5–1c shows the picture on the screen when amplitude distortion is caused at the same amplification. The oscillograms in fig. 5–2 reproduce the possible effect of an amplifier when two

frequencies are amplified simultaneously. In this instance the input voltage contains a strong third harmonic. Fig. 5–2a represents the unamplified voltage and b) the shape of the voltage amplified in the desired way. Fig. 5–2c shows a voltage amplified by the same amount in which, although there is no amplitude distortion, the relative positions of fundamental and harmonic have become displaced. The *transit time* of both frequencies through the amplifier was not equal, that is to say a *phase shift* occurred. Phase shift is synonymous with time delay, which means that in this case the time delay characteristic of the amplifier is not linear and the output signal is therefore not a true reproduction of the input signal.

The frequency response required of an amplifier is dictated by the range of applications within which it has to work. The output voltage of the amplifier must be large enough in its working range to deflect the spot without noticeable distortion over the whole screen and even, for certain purposes, far beyond it. Moreover, the changes in output voltage must follow the changes in input voltage linearly, or in any other way desired. The amplification must be susceptible of control such that small as well as large input signals can be amplified to produce a pattern of the required size on the screen. It must be possible by means of voltage division in true frequency—and phase—to attenuate a large input voltage in such a way as to exclude the danger of overloading.

To summarize, the following are the principal demands made upon a deflection amplifier for oscilloscopes:

1) a sufficiently high amplification;
2) a satisfactorily uniform amplification within a given frequency range;
3) no noticeable shift between phase relationships for the various frequencies of a given range;
4) a sufficiently high output voltage within the frequency range concerned, without noticeable amplitude distortion;
5) an amplification susceptible of control within definite limits;
6) an output voltage which follows proportionally the trend of the input voltage.

The simultaneous fulfilment of all these requirements, which not infrequently contradict each other in their technical context, demands a very thorough study of the factors involved. Considerations of economy in outlay, which will be discussed later in detail, make it necessary, especially as regards increasing the upper frequency limit, to compromise between technical requirements and tolerable costs.

Amplification with electronic valves.

To help elucidate the effect of amplification, fig. 5–3 shows the basic circuit of an electronic valve with its anode load resistor R_a.

The voltage gain G is equal to the ratio between the output and the input voltage, thus:

$$G = \frac{v_{out}}{v_{in}} \quad [24] \tag{5–1}$$

To calculate the voltage gain obtained with this circuit, it is customary to look upon the valve as the voltage source with an EMF: $\mu \cdot v_{in}$, which drives the anode alternating current i_a through the internal resistance R_i connected in series with the external resistance R_a. However, since in the following considerations a number of impedances will be found in the anode circuit

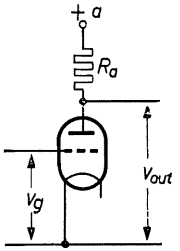

Fig. 5–3. Basic circuit of an electronic valve as amplifier.

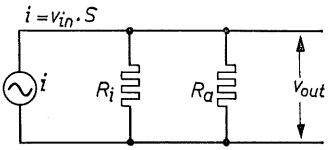

Fig. 5–4. Equivalent circuit of a valve with internal resistance R_i and load resistance R_a.

connected in parallel with the anode load resistor, it will be more appropriate to look upon the valve as the current source, with a constant current:

$$i_a = v_{in} \cdot S \quad [25] \tag{5–2}$$

The result of these considerations is not affected thereby. The corresponding equivalent circuit is given in fig. 5–4. For the current source, the total load resistance R_t is obtained as the value of R_i and R_a in parallel:

$$R_t = \frac{R_i \cdot R_a}{R_i + R_a} \tag{5–3}$$

The AC voltage on the anode is equal to:

$$v_{out} = i_a \cdot \frac{R_i \cdot R_a}{R_i + R_a} \tag{5–4}$$

Taking $i_a = v_{in} \cdot S$ as in formula (5–2), then:

$$v_{out} = v_{in} \cdot S \cdot \frac{R_i \cdot R_a}{R_i + R_a} \tag{5–5}$$

From this, the gain $\frac{v_{out}}{v_{in}} = G$ is given by:

$$G = S \cdot \frac{R_i \cdot R_a}{R_i + R_a} \tag{5–6}$$

For pentodes, R_i is always $> R_a$.

[24] To distinguish the values of AC voltage clearly from those of the operating DC voltages, small letters are used here for the former.
[25] S = slope (mutual conductance).

In wide-band amplifiers, moreover, the anode resistance must be particularly low in order to achieve a high upper frequency limit, so that $R_i > R_a$ usually applies to triodes also.
However, if R_a as opposed to R_i in the denominator of equation (5–6) can be neglected, the gain is then simply:

$$G = S \cdot R_a \qquad (5\text{–}7)$$

Frequency response of the vertical amplifier.

In the frequency ranges in question ($f < 10$ Mc/s) the process of amplification takes place in the valves themselves without power loss or time delay (phase shift). The values S, D and R_i of the valves are free of phase distortion.
As the following observations will show, the decrease in gain at the upper and lower limits is determined solely by the characteristics of the coupling elements between the valves, although, of course, the capacitances of the valves must not be overlooked. Thus, when considering the loss in relative gain from the mean value it is sufficient to limit ourselves to these factors. It will be shown that the gain at the upper and lower frequency limits decreases according to definite functions. It must now be ascertained what decrease in gain is to be considered as permissible.
Taking as a starting point the fact that by reducing the output voltage of an amplifier by 30% (corresponding to 3 db or 0.33 N) the decrease in loudspeaker volume is just imperceptible, it is customary in electro-acoustics to denote that frequency as the limit frequency at which the gain has fallen to $\frac{1}{\sqrt{2}} = 0.707$ of the mid-frequency value.

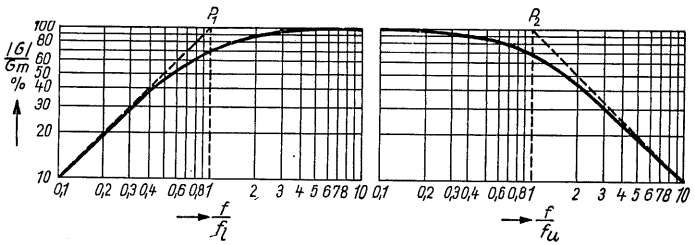

Fig. 5–5. Drop in gain at the ends of the frequency band.

The curves given in fig. 5–5 represent the relative loss in gain at the upper and lower ends of the frequency range. For a drop to the value of 0.707, the cut-off frequency at the lower end is denoted by f_l and at the upper end by f_u. At both ends the relative gain is indicated in fractions of the cut-off frequencies from 1/10 to 10. In accordance with the usage in electro-acoustics, the ordinate scale is logarithmic.
When determining the cut-off frequencies, the stipulation is that the fall-off in gain must be only just imperceptible. This stipulation carried over into oscillography means that the limit must be set by a drop of about 2%.
For assessing the performance of amplifiers in oscilloscopes it is therefore

essential to represent the response as ordinates with a *linear scale*, unless of course the gain for certain purposes is in actual fact logarithmically proportional to the input signal, which is only the case in oscilloscopes designed for specific tasks.

Loss of gain at the lower frequency limit.

The basis for the following considerations is the circuit given in fig. 5–6, representing two stages of a conventional resistance-coupled amplifier. The components determining the frequency limits have been marked with the customary symbols. In addition to these, C_{out} and C_{in} represent respectively the output and input capacitances of the valves, C_s is the stray wiring capacitance and C_r the additional capacitance due to anode reaction. In general the symbols refer to the electrodes in whose path they lie, thus: C_g is the grid condenser, C_k is the cathode condenser, etc.

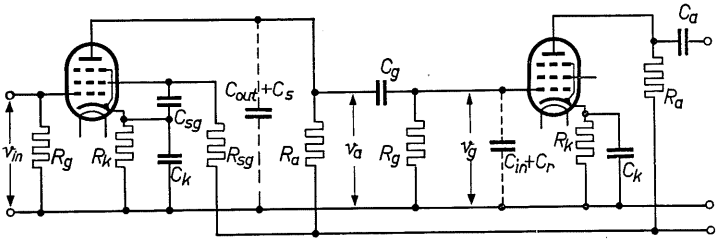

Fig. 5–6. Basic circuit of a two-stage resistance-coupled amplifier.

For the low frequency range, the capacitances (C_{out}, C_s) shunted across the path of amplification can be ignored. They offer such a high impedance to these frequencies that, especially as compared with the anode resistor R_a, they play no part at all. (It is assumed in the first place that C_k in the cathode lead and C_{sg} for decoupling the screen grid are infinitely large. Their influence will be mentioned separately at a later stage.) The resulting equivalent circuit is given in fig. 5–7a. According to formula (5–2) an alternating current $i_a = v_{in} \cdot S$ flows through the anode load resistor, so that from formula (5–5) there will be a voltage across this of:

$$v_a = v_{in} \cdot S \cdot R_a \qquad (5\text{–}8)$$

(This assumes R_i to be $> R_a$)

The grid of the following valve receives this amplified voltage via the grid coupling capacitor C_g. The *AC* voltage produced across the anode resistor results in a current which flows through the series-connected C_g and R_g. Since, however, the capacitive impedance Z_c of C_g is equal to $\frac{1}{\omega \cdot C_g}$ and thus increases with decreasing frequency, in this range the output voltage v_g of this coupling element will be smaller than v_a and will decrease with the frequency. The series circuit of C_g and R_g acts as a (frequency dependent) voltage divider. The drop in output voltage v_g with decreasing frequency—the

"frequency response"—is shown by the curve in fig. 5–7b. It results from the voltage ratio $v_g : v_a$ for the given frequencies. These voltages are related to the circuit impedance, thus:

$$v_g : v_a = R_g : (R_g + Z_c) \qquad (5\text{–}9)$$

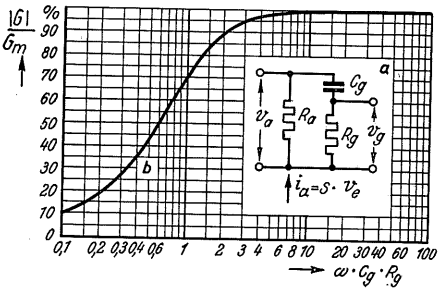

Fig. 5–7. Relative gain (b) obtained with a frequency-dependent coupling network (a).

As a condenser represents an opposition to alternating current, the voltages or the values of resistance and capacitive impedance must be brought into a vectorial relationship when calculating or otherwise treating these ratios. (See following paragraph and fig. 5–9.) The ratio of the voltages $v_g : v_a$ is the "transfer function" of this coupling network. Its value $|U|$ may be derived from the resistance/impedance relationship:

$$|U| = \left|\frac{v_g}{v_a}\right| = \frac{R_g}{\sqrt{R_g^2 + \frac{1}{\omega^2 \cdot C_g^2}}} \qquad (5\text{–}10)$$

From the curve in fig. 5–7b may be derived the actual gain G in relation to the gain G_m in the mid-frequency range (where there is no attenuation). This ratio is also equal to the transfer function of the coupling network, thus:

$$|U| = \frac{|G|}{G_m} \qquad (5\text{–}11)$$

The relative gain is therefore equal to:

$$\frac{|G|}{G_m} = \frac{1}{\sqrt{1 + \frac{1}{\omega^2 \cdot C_g^2 \cdot R_g^2}}} \qquad (5\text{–}12)$$

The gain G is thus:

$$|G| = G_m \cdot |U| \qquad (5\text{–}13)$$

If

$$\omega_l^2 \cdot C_g^2 \cdot R_g^2 = 1$$

then:

$$\frac{|G|}{G_m} = 0.707$$

Therefore $f_l = \frac{\omega_l}{2\pi}$ is the lower-frequency limit of the amplifier. In order to be able to make the widest possible use of the curve in fig. 5–7b the scale for the abscissa was not taken as simply the frequency but as the product $\omega \cdot R_g \cdot C_g$. If $f = \frac{\omega}{2\pi}$ is the frequency under consideration and $f_l = \frac{\omega_l}{2\pi}$ is the lower frequency limit, then as $\frac{\omega \cdot C_g \cdot R_g}{\omega_l \cdot C_g \cdot R_g} = \frac{\omega}{\omega_l} = \frac{f}{f_l}$, instead of the product $\omega \cdot C_g \cdot R_g$ we can take the ratio $\frac{f}{f_l}$ as the scale for the abscissa, (see also figs. 5–5 and 5–27).

In this way the required RC product can be determined for a given frequency and for the permissible drop in gain. At the same time, the curve enables the transfer function, thus the frequency response, to be ascertained for other frequencies, once the RC product, and with it the frequency limit, have been fixed.

If, for example, the drop in gain is not to exceed 5%, then for $\omega \cdot C_g \cdot R_g$ we may read off the value of 3. With a value of 2MΩ for R_g and a frequency $f = 30$c/s, then $C_g = \frac{3}{\omega \cdot R_g} = \frac{3}{2\pi \cdot 30 \cdot 2 \cdot 10^6} = 8000 \cdot 10^{-12}$ F or 8000 pF. (in round figures).

For one third of the frequency, thus $f = 10$ c/s ($\omega \cdot R_g \cdot C_g = 1$) the attenuation is 0.707. This would therefore be the frequency limit. Three times the frequency, i.e. 90 c/s ($\omega \cdot R_g \cdot C_g = 9$) will be transferred practically unattenuated. These considerations, however, apply to one coupling network only. In a deflection amplifier there are always several such coupling networks.

The total transfer function $|U_t|$ of the amplifier, which indicates the drop in gain for a given frequency, is the product of the transfer functions of each stage:

$$|U_t| = |U_1| \cdot |U_2| \cdot |U_3| \text{ etc.} \qquad (5\text{–}14)$$

Phase shift at the lower frequency limit.

In ordinary electro-acoustical amplifiers it is not generally necessary to pay attention to phase relationships, unless special problems have to be solved, such as the rating of phase inversion stages and feedback circuits. In deflection amplifiers for oscilloscopes, on the other hand, high demands are made on the ability of an amplifier to reproduce phase relationships faithfully. One of the most important applications of the oscilloscope is the measurement of phase shifts.

Fig. 5–8*a* shows, together with the characteristic curve, the vectorial relationship of resistance and capacitive reactance and thus of the voltages in the series circuit of R_g and C_g as in fig. 5–7*a*.

The vector of the capacitive reactance X_c of C_g or the voltage v_c is shown as the vertical side (ordinate) of a right angle whose base (ascissa) represents the resistance R_g or the voltage v_g. The *impedance* Z resulting from R_g and X_c results geometrically in the hypotenuse of a right-angled triangle whose small sides are the vectors of R_g and X_c. From fig. 5–9 it can be seen that for different values of $\frac{1}{\omega \cdot C_g}$ and R_g, the vertices of the right-angled triangle formed by the two vectors, v_c and v_g (X_c and R_g) lie on a semi-circle above the vector of v_a (Z). On this semi-circle can be plotted as a scale the points corresponding to the different values of $\omega \cdot C_g \cdot R_g$. The angle formed by the reference vector R_g—(v_g) and the resultant vector Z—(v_a) is known as the *phase angle*, also referred to as the phase shift, phase distortion or phase difference.

A phase shift between two voltages means that the voltages cross the time axis at different times. This time difference can be designated in degrees as the

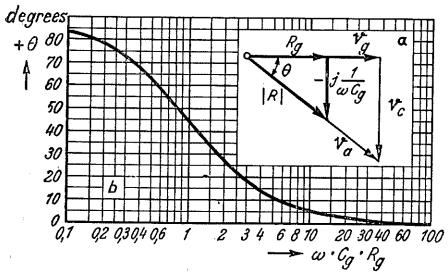

Fig. 5–8. Phase shift *b*) caused by a *CR* network as in fig. 5–7*a* for various values of $\omega \cdot R_g \cdot C_g$ and *a*) vector diagram of voltages and impedances.

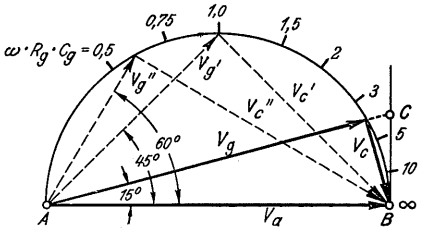

Fig. 5–9. Vector diagrams of *AC* voltages in a coupling network as in the equivalent circuit fig. 5–7*a*.

angle between the two voltage vectors or as a fraction of the total time of alternation —*T*. It is sometimes more convenient to indicate the phase angle by the length of the chord of the arc pertaining to this angle for the radius $r = 1$. As a rotation of the vector by 360° is equal to the duration *T* of one complete cycle, and as this corresponds to the arc 2π, the result for this representation is $360° = T = 2\pi$. The phase angles can thus be expressed also as fractions of π, where $\pi = \frac{T}{2}$.

In the oscillograms (figs. 5–10 and 5–11) the phase shift is best determined as the distance between the zero points where the two voltages being compared cross the time axis. This distance represents the time difference of the voltage vectors which exists between input and output voltage of a coupling element; it is the time expressed in electrical degrees by which one voltage leads or lags the other.

This "phase delay time" τ, is calculated from the formula:

$$\tau = \frac{\theta}{\omega} \qquad (5\text{–}15)$$

The angle θ must be inserted in this formula in radians. Thus $360° = 2\pi = 6.28$ and $\theta_{arc} = \frac{6.28}{360} \cdot \theta° = 0.0175 \cdot \theta°$.

According to formula (5–15) a phase angle of 45° in fig. 5–10*d*, for example, corresponds to a phase delay time of $\tau = \frac{45 \cdot 0.0175}{314} = 2.5$ ms. The phase angle θ can be calculated trigonometrically, thus:

$$\cot \theta = \omega \cdot R_g \cdot C_g \qquad (5\text{–}16)$$

and the angle itself is:

$$\theta = \text{arc cot } \omega \cdot R_g \cdot C_g \qquad (5\text{–}17)$$

The equation (5–17) states that the angle θ is represented by that chord length (arc) for which the cotangential ratio is equal to $\omega \cdot R_g \cdot C_g$. (In fig. 5–9 this ratio is the distance ratio $\overline{AB} : \overline{BC}$ for the angle 15°). Thus for a certain value of $\omega \cdot R_g \cdot C_g$, the angle θ can be read off directly from a table of

trigonometrical functions. In fig. 5–8*b*, moreover, the curve (which basically corresponds to the cotangential function) indicates the trend of the phase angle at the lower frequency limit for different values of $\omega \cdot C_g \cdot R_g$. The arrangement of oscillograms in fig. 5–10 gives an illustration of the relationships discussed. In each case, for different values of $\omega \cdot R_g \cdot C_g$, a section of an oscillogram is given with a whole cycle of the sinusoidal voltage v_a (dotted) with at the same time the corresponding cycle of the grid voltage v_g (full). The values used for these recordings are set out in Table 1. In all cases the grid resistance was 16 kΩ while the capacitance C_g was varied. The frequency was $f = 50$ c/s ($\omega = 2\pi \cdot f = 314$). The phase differences are expressed as fractions of T. From these oscillograms can be read off directly not only the attenuation but also the phase shifts between the voltages v_g and v_a. A law governs the relationship between voltage decline and phase shift through a coupling network. It is:

$$\frac{v_g}{v_a} = \cos \theta \qquad (5\text{–}18)$$

The transfer function is therefore: $U = \cos \theta$ and thus:

$$v_g = v_a \cdot \cos \theta \qquad (5\text{–}19)$$

If both vectors of the voltages across the resistor and the condenser are equal (in fig. 5–9 v'_g and v'_c) then the angle between v'_a and v'_g is 45°. But cos 45° is 0.707 so that this relationship corresponds to the cut-off frequency.
A series of coupling networks in the amplifier results in a phase shift which is equal to the sum of the phase changes of each individual network. Thus:

$$\theta_{total} = \theta_1 + \theta_2 + \theta_3 \text{ etc.} \qquad (5\text{–}20)$$

The influence of phase shifts on an oscillogram of composite voltages.

When all the positions of the spot in the oscillogram of a composite voltage (as in fig. 5–11*a*—full line) are displaced uniformly in one direction along the time axis, the resultant waveform of the voltage trend is in itself unaltered. The sum curve in this oscillogram is composed of the two voltages shown in broken lines.

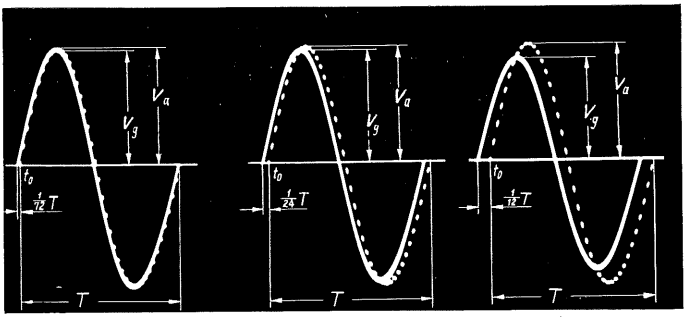

Fig. 5–10. Oscillograms of voltages at the input and output of a *CR* network as in fig. 5–7*a*, for different values of $\omega \cdot R_g \cdot C_g$.

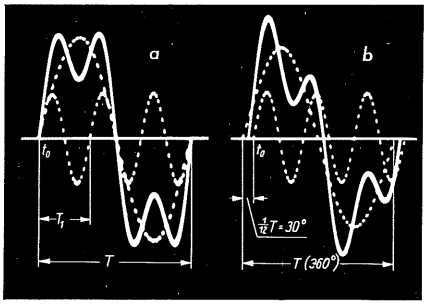

Fig. 5–11. Distortion of a composite *AC* voltage due to a *CR* network. *a*) Sum voltage curve (full) and its components (dotted) in the starting position (fundamental and harmonic in phase). *b*) Distortion due to phase shift in a *CR* network.

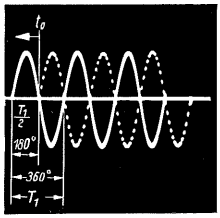

Fig. 5–12. Harmonic of fig. 5–11 in the starting position (full) and shifted in phase by 180° (dotted) for comparison with the oscillogram in fig. 5–10*e*.

Fig. 5–12 shows the waveform of the *harmonic* of fig. 5–11*a* and the same voltage displaced in phase by $180° \left(\frac{T_1}{2}\right)$ (dotted). Fig. 5–10*e* shows a phase shift of the fundamental (apart from the difference in amplitude) of $60° \left(\frac{T}{6}\right)$.

TABLE I (for fig. 5–10)

Quantity	a	b	c	d	e	f	Remarks
$\omega \cdot R_g \cdot C_g$	11.4	3.75	1.73	1.00	0.58	0.27	$= \cot \theta$
$R_g \cdot C_g$	36.8	12.0	5.60	3.20	1.86	0.87	$\times 10^{-3}$ sec
C_g	2.3	0.75	0.35	0.20	0.116	0.054	μF
$\frac{v_g}{v_a}$	1.00	0.97	0.87	0.707	0.50	0.25	$= \cos \theta$
θ	5	15	30	45	60	75	$\theta°$
$R_g = 16\ \mathrm{k}\Omega$; $f = 50$ c/s							

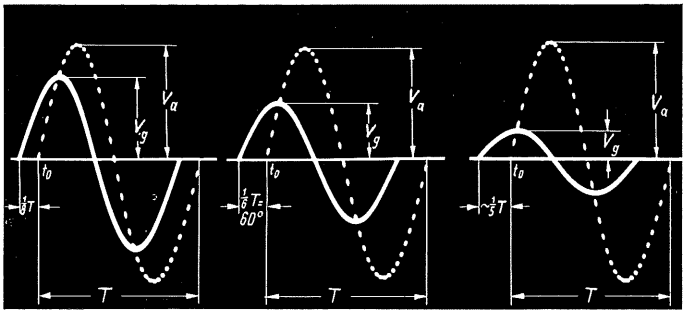

d e f

A comparison of these two oscillograms confirms that a phase shift of three times that of the fundamental is required for the same displacement along the time axis at three times the frequency.
(According to fig. 5–8*b*, in certain parts of the curve there is an almost linear increase in θ at decreasing values of $\cot \theta = \omega \cdot R_g \cdot C_g$.)
If, therefore, the pattern on the screen is to correspond faithfully to the voltage trend, the coupling networks must either cause no phase shift at all or the stipulation must be made:

$$\theta = k \cdot f \qquad (5\text{–}21)$$

where k is a constant.
In practice, however, this can only be achieved, with some approximation, at the upper cut-off frequency (see fig. 5–21*a* and *b*). At the lower end, the reverse is the case. In fig. 5–11*b*, for example, voltage curves are reproduced which, passed through a coupling network, suffer a phase shift of the fundamental of $30° = \frac{T}{12}$. For three times the frequency, the result is, according to formula (5–17), only about one third of the phase shift of the fundamental frequency, thus $10°$ or $\frac{1}{36}$ of T_1.
The duration of one complete cycle of the triple frequency—(T_1 in fig. 5–11*a*) is however only $^1/_3$ of T (10 mm), so that the displacement of the harmonic is only $\frac{1}{108}$ of T, in the original oscillogram about $^1/_3$ mm. It can therefore no longer be perceived, as it only amounts to a fraction of the diameter of the spot. On the other hand, the displacement of the fundamental, for which T on the screen amounted to about 30 mm, was $\frac{T}{12} = 2^1/_2$ mm. The sum of these two curves, now displaced one against the other (full curve in fig. 5–11*b*) is a severely distorted picture of the original voltage trend.
It follows from this that an essential requirement of deflection amplifiers is that they should keep phase shifts as low as possible to prevent noticeable changes in the voltage waveform appearing on the screen. Whereas with a simple sinusoidal voltage a phase shift of 5° is only just perceptible, phase shifts of the fundamental of more than 2° cause distinct distortion of the waveform of composite voltages. Moreover, as a voltage diminution of only 1%

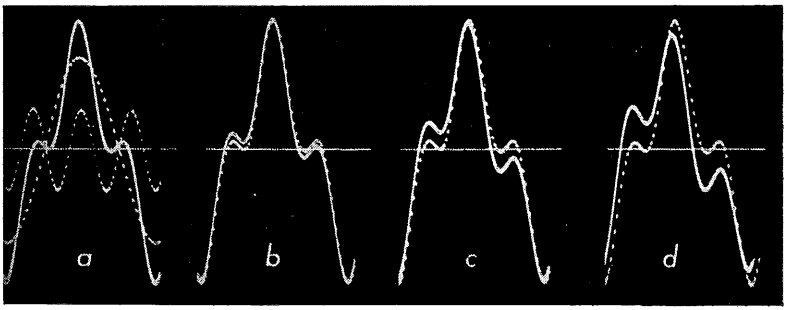

corresponds to a phase shift of 8° (cf. fig. 5–8 and 5–10) it is evident that very high demands must be made on the transfer function of the coupling elements. Fig. 5–13 shows the distortion of a voltage composed of the same frequencies but in which the harmonic is shifted in phase by 180°, as compared with fig. 5–11. The component voltages are shown dotted in a) and the resultant voltage in the initial stage is shown as a full curve. The oscillograms b to g show the waveforms produced when the fundamental suffers a phase shift through coupling networks of 5°, 15°, 30°, 45°, 60° and 75° degrees respectively. For the sake of comparison the waveform of the starting oscillogram is shown dotted in each case.

The rating of coupling networks for *AC* voltages with a *DC* component.

The highest demands on the amplifier are made by voltage waveforms which, in periodically recurring intervals, have a constant value, i.e. a *DC* component (appearing as a horizontal line in the oscillogram).
A typical example is the waveform of an *AC* voltage after half-wave rectification. To ascertain the minimum value of the coupling elements necessary in this case, the *RC* product can be taken (not $\omega \cdot R \cdot C$).
This *RC* product—the time constant—must at least be large enough to prevent the drop in the output voltage of the coupling network (due to the discharging process) from becoming noticeable on the screen during those periods when the voltage persists at a constant value. Otherwise the straightline portions of the oscillogram become tilted or bent, as shown in fig. 5–14*c*—*f*. In this figure are reproduced six oscillograms of two cycles of an *AC* voltage after half-wave rectification, passed through differently rated coupling networks. The drop in voltage at the output of the network is particularly conspicuous in sub-figures e and f. This occurs according to the exponential equation:

$$v_2 = v_1 \cdot e^{-\frac{T}{2R_g \cdot C_g}} \qquad (5\text{–}22)$$

Assuming that the periods of conduction and cut-off in the rectification are equal, we can calculate the required product $R_g \cdot C_g$ according to (5–22) for a voltage decline down to $s = \frac{v_2}{v_1}$, from the equation:

$$R_g \cdot C_g = -\frac{1}{2 \cdot f \cdot \ln s} \qquad (5\text{–}23)$$

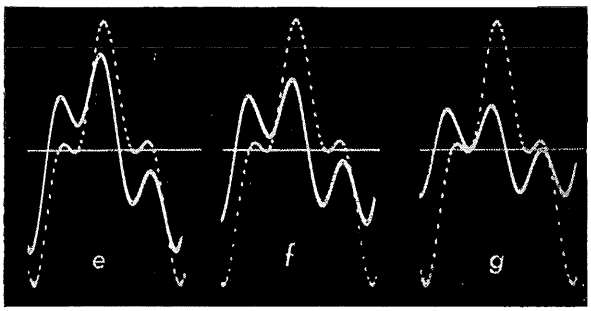

Fig. 5–13.
Oscillograms showing the distortion of a composite *AC* voltage due to a *CR* network, for different phase shifts of the fundamental.

Multiplying both sides of the equation by ω $(= 2\pi f)$ we obtain, referring back to (5–16):

$$\omega \cdot R_g \cdot C_g = -\frac{\pi}{\ln s} = \cot \theta \qquad (5\text{–}24)$$

Thus, for a voltage reduction to $s = 0.9$, we get: $\omega \cdot R_g \cdot C_g = -\frac{3.14}{ln\ 0.9} = 30$; arc cot $30 = 2°$.

Fig. 5–14 will serve to illustrate the process without further calculation. The appertaining data are set out in Table II. For the oscillogram in sub-figure a) the voltage was applied directly. Resistance R_g remained 16 kΩ in all cases while C_g was varied for sub-figures b to f.

Examining these oscillograms more closely and following them from left to right along the time axis, we can already see in b) a slight tilt of the horizontal line. The phase shift here was only $^1/_2°$. According to (5–16) this corresponds to a value of $\omega \cdot R_g \cdot C_g = 115$.

For a coupling network which, for example, must cause at 30 c/s no more than $^1/_2°$ phase difference, the coupling capacitance required when the grid resistor $R_g = 2\text{M}\Omega$ can be calculated as:

$$C_g = \frac{115}{6.28 \cdot 30 \cdot 2 \cdot 10^6} \cdot 10^6 \approx 0.3\ \mu\text{F}$$

This value is considerably larger than that calculated on page 88 for a voltage reduction of 5% (8000 pF). In the light of the foregoing, amplification with faithful phase reproduction requires that $\omega \cdot R_g \cdot C_g \geqq 30$ $(\theta = 2°)$ shall be as nearly as possible > 100.

Limitation of the lower frequency limit.

The lower cut-off frequency obtainable by suitable rating of the coupling components is subject to various limitations. As definite maximum ratings are laid down for the grid resistors of the amplifier valves, the *RC* product required can only be achieved by increasing the value of the coupling condenser. This, on the other hand, must have a high insulation resistance so that no displacement of the working point of the following valves will be caused by the anode voltage of the preceding valves. But high insulation resistance becomes more difficult to obtain the higher the capacitance required.

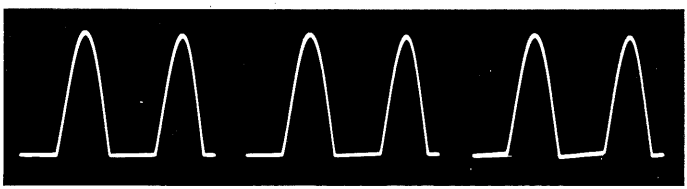

a b c

Fig. 5–14. Distortion of the voltage curve of a half-wave rectified *AC* voltage due to different phase-shifting coupling networks.

Again, the larger dimensions of higher coupling condensers increase the unwanted capacitance with respect to the chassis, thus imposing limitations on the upper cut-off frequency (see "Loss of gain at the upper frequency limit"). Moreover, a large time constant is synonymous with a large period of grid swing. If the amplifier is brought out of voltage balance by a voltage surge (e.g., as a result of applying the input signal or owing to a sudden change in supply voltage), a certain time elapses before it returns to its operating condition. As may be deduced from formula (5–22), the RC product—the time constant—corresponds to the time in which the voltage generated by a voltage pulse on an RC network falls to $\frac{1}{e}$-th (37%) of the peak value. When $RC = 1$ (e.g. $R = 2\ M\Omega$, $C = 0.5\ \mu F$) the voltage will fall to this value after one second, whereas when $RC = 0.1$, only 1/10th of a second is necessary. Sensitivity to voltage surges can be largely reduced by, for instance, connecting the whole amplifier in push-pull and stabilizing the supply voltages. In the vertical amplifier of one oscilloscope, [1], satisfactory operating conditions were achieved in spite of a time constant of $RC = 4$ ($R_g = 2\ M\Omega$, $C_g = 2\mu F$, lower cut-off frequency of the whole amplifier $^1/_{10}$ c/s).

Influence of the cathode and screen-grid condensers.

To obtain the negative bias for the control grid, a resistor is usually included in the cathode lead through which the cathode current (anode current and possibly auxiliary grid current) will flow. The resultant voltage drop is fed in the conventional way to the grid over the grid resistor (R_g in fig. 5–6).

TABLE II

(for fig. 5–14)

Quantity	a	b	c	d	e	f	Remarks
$\omega \cdot R_g \cdot C_g$	—	115	28.6	11.4	3.73	1.73	$= \cot\theta$
$R_g \cdot C_g$	—	57.5	14.3	5.7	1.87	0.87	$\cdot 10^{-3}$ sec
C_g	—	570	143	57	18.6	7.65	10^3 pF
$\frac{v_g}{v_a}$	1.00	1.00	0.999	0.996	0.966	0.866	$= \cos\theta$
θ	0	$\frac{1}{2}$	2	5	15	30	$\theta°$

$R_g = 16\ k\Omega$; $f = 2000$ c/s

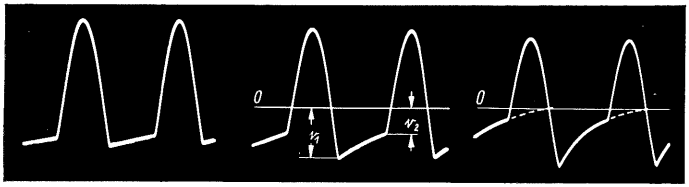

d e f

Since the anode *AC* current also flows through the cathode resistor, an *AC* voltage corresponding to the amplified frequency will reach the grid unless counter-measures are taken. This voltage will be 180° out of phase with the input voltage (excluding additional phase shift) so that the effect would be to decrease the voltage on the control grid and thus to reduce the amplification of the valve (negative or degenerative feedback—see also under "Improving amplifier characteristics by negative feedback").
To avoid this happening, the cathode resistor is shunted by a condenser whose capacitance must be so large that it represents a considerably smaller impedance (larger conductance $= \omega \cdot C$) to the frequency in question than the cathode resistor. In this case the product $\omega \cdot R_k \cdot C_k$ must have a specific value. It should be remembered here that the *AC* voltage appearing across the cathode resistor and short-circuited by the condenser is dependent upon the valve data, particularly upon the mutual conductance [2].
The transfer function of the cathode network is given by:

$$\frac{|G|}{G_m} = \sqrt{\frac{1+x^2}{(1+a)^2+x^2}} \tag{5–25}$$

The additional phase change caused by these circuit components is:

$$\theta = \text{arc tan } \frac{a \cdot x}{1+a+x^2} \tag{5–26}$$

For the sake of brevity, some values in these equations are composite expressions. Thus, $x = \omega \cdot R_k \cdot C_k$ and $a = G_m \cdot \frac{R_k}{R_a}$ or $S_k \cdot R_k$.
For the parameter a, the product $S_k \cdot R_k$ must be used if the screen grid alternating current also flows through the cathode resistor. (The decoupling condenser for the screen grid is connected to the chassis.) If, however, the screen grid condenser (as in fig. 5–6) is connected directly to the cathode, then $a = G_m \cdot \frac{R_k}{R_a}$ is applicable.
The cathode mutual conductance is denoted by S_k. It indicates the change of the total cathode current for a certain change in grid voltage, thus:

$$S_k = \frac{\Delta I_k}{\Delta V_g} \tag{5–27}$$

As a rule this value is not given by the manufacturers of multiple-grid valves but for most calculations it should suffice when, in the case of pentodes for example, the following equation is applied:

$$S_k = S \cdot \frac{I_a + I_{sg}}{I_a} \tag{5–28}$$

The curves calculated for these relationships from formulae (5–25) and (5–26) are given in figs. 5–15 and 5–16 for different values of a.
If fig. 5–15 is compared with fig. 5–7 it stands out that, for small values of $\omega \cdot C_k \cdot R_k$, the gain does not fall back to zero. Even for very low values it does not fall below a certain amount.

In fig. 5–16 it can similarly be ascertained that the phase change for diminishing values of $\omega \cdot C_k \cdot R_k$ reaches a certain maximum figure and then begins to fall again. The conductance figure $\omega \cdot C_k$ of the capacitor C_k, shunted across the cathode resistor, then becomes so small that its phase shifting influence also is reduced.

Taking pentode EF 40 as an example, if $R_k = 500\ \Omega$, $R_a = 50\ \mathrm{k}\Omega$ and $G_m = 100$, then $a = 100 \cdot \dfrac{500}{50{,}000} = 1$. If the gain is not to drop below 5%, then according to fig. 5–15, $\omega \cdot R_k \cdot C_k = 6$. Therefore, for $\omega = 30 \cdot 2 \cdot \pi \approx 200$, C_k must be: $\dfrac{6}{\omega \cdot R_k} \approx 60\mu\mathrm{F}$. The additional phase shift in this case ($f = 30$ c/s) would, according to fig. 5–16, be about 9°. A difficulty arises in the rating of deflection amplifiers when the cathode resistor is particularly small, as is frequently the case when using valves with high mutual conductance. Taking valve EF 80 for example, the following conditions may occur: $R_k = 150\ \Omega$, $R_a = 3000\ \Omega$, $G_m = 20$. Accordingly,

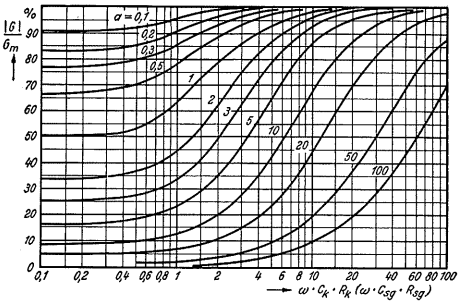

Fig. 5–15. Drop in relative gain at the lower frequency limit due to circuit components in the cathode and screen-grid lead. The parameter "a" should be selected in accordance with the valve data.

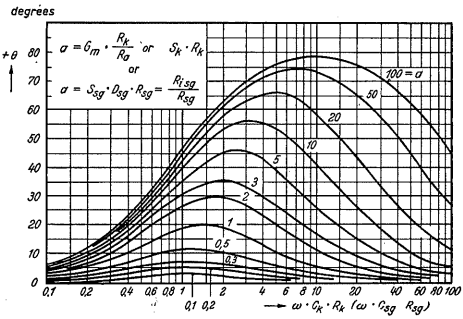

Fig. 5–16. Phase shift of the amplified voltage at the lower frequency limit due to circuit components in the cathode or screen-grid lead.

$a = 20 \cdot \dfrac{150}{3000} = 1.0$. It is required that when $f = 30$ c/s, $\theta \leq 1°$. From 5–16, $\omega \cdot C_k \cdot R_k$ must therefore be at least = 50, and thus we get: $C_k = \dfrac{50}{\omega \cdot R_k} = 1700\mu\mathrm{F}$.

Although it would be possible with the low working voltage given ($V_g = -2\mathrm{V}$) to procure a condenser of this size, it nevertheless appears advisable to choose another way in such cases. If, for instance, the cathode condenser is left out altogether, the gain sinks to about 51% of the maximum value obtainable. At the same time, however, negative current feedback occurs which increases the undistorted drive possible, i.e. permits an increase in the upper frequency limit. It is also possible to earth the cathode and to generate the grid bias by other means. In this way, full amplification is obtained corresponding to $R_a \cdot S$.

To reduce the screen grid voltage to the required value it is often necessary to include a series resistor R_{sg}. Here also an opposing AC voltage would arise if the screen grid were not bypassed by a suitably rated condenser with respect to earth, or better, with respect to the cathode.

For rating these decoupling elements R_{sg} and C_{sg}, the same conditions may be derived as given by equations (5–25 and 5–26) for the cathode circuit components. Corresponding values have only to be inserted for the variable x and for the parameter a, namely:

$$x = \omega \cdot C_{sg} \cdot R_{sg} \text{ and } a = S_{sg} \cdot D_{sg} \cdot R_{sg} = \frac{R_{sg}}{R_{isg}}.$$

The symbols S_{sg}, D_{sg} and R_{isg} refer to the relevant data of the screen grid. These data are not as a rule included in standard valve data but they will be supplied if asked for. On some examples of valve EF 50, values were measured of $R_{isg} = 40\ \text{k}\Omega$. If, for instance, $R_{sg} = 120\ \text{k}\Omega$, then $a = \frac{R_{sg}}{R_{isg}} = 3$. Where the phase shift must not exceed 2° for $f = 30$ c/s, then, according to the curve $a = 3$ in fig. 5–16, $\omega \cdot C_{sg} \cdot R_{sg} = 80$. This gives: $C_{sg} = \frac{80}{\omega \cdot R_{sg}} = \frac{80}{6.28 \cdot 30 \cdot 120{,}000} \cdot 10^6 = 35\mu\text{F}$.

Improvement of amplifier characteristics at the lower frequency limit.

For uniform amplification of the lower frequencies and especially for faithful phase reproduction, it can be seen from the foregoing observations that a fairly considerable outlay in circuit components is required.

Attempts have therefore been made, with a view to economy, to compensate for the loss in gain and the phase shift by a suitable arrangement of the circuit components.

A circuit commonly used for this purpose is shown in fig. 5–17a. An RC combination $C_v R_v$ lies in series with the anode load resistor R_a. The resultant equivalent circuit is shown in fig. 5–17b. The resistor R_v can be neglected provided it is at least ten times larger than the value of $\frac{1}{\omega \cdot C_v}$ for the given frequency range. From a certain frequency onwards the condenser C_v can be regarded as a complete short-circuit, so that it has no influence on the gain. With a falling frequency, however, the total impedance of the anode circuit

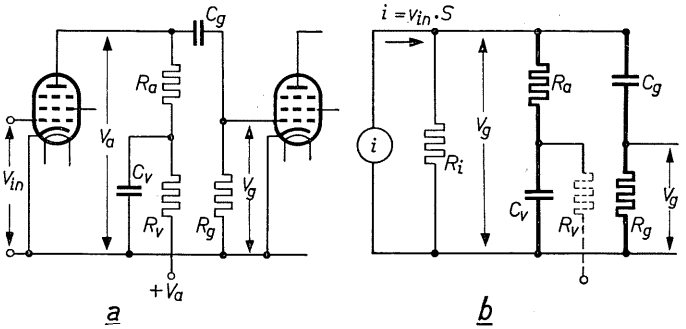

Fig. 5–17. *a*) Circuit for improving the frequency response at the lower frequency limit by means of an RC network in the anode circuit. *b*) Equivalent circuit.

(R_a and C_v in series—$R_g > R_a$) rises and, with a constant alternating current at the anode ($R_i > R_a$) the alternating voltage on the anode, in other words, the gain, rises likewise. In this way, the drop in amplified voltage across R_g at low frequencies can be compensated by suitably rating C_v and R_v.
With a falling frequency, condenser C_v in the anode circuit also increasingly shifts the phase of the amplified voltage. Referring again to the equivalent circuit in fig. 5–17b, it can be seen that this phase shift must be opposed by that caused by the grid network $C_g \cdot R_g$. By means of an RC network in the anode circuit it is thus possible to achieve a large measure of compensation for the frequency response as well as for the phase shifts of the other circuit components in the path of amplification. To remove the effects caused by the grid network $C_g \cdot R_g$, the following condition must be satisfied:

$$C_g \cdot R_g = C_v \cdot R_a \qquad (5\text{–}29)$$

It would not be appropriate, however, to adopt this compensation for each individual stage. It is more advantageous first to rate the circuit components which are decisive for the lower frequencies in such a way that the required amplifying characteristics can be obtained as nearly as possible with a minimum of outlay. The required correction of the frequency response and the phase shift can then be carried out for the whole amplifier in one stage (or in multiple-stage amplifiers, in every second or fifth stage). In this connection, the following must apply according to (5–29):

$$\frac{1}{C_{g1} \cdot R_{g1}} + \frac{1}{C_{g2} \cdot R_{g2}} + \frac{1}{C_{g3} \cdot R_{g3}} + \ldots = \frac{1}{C_v \cdot R_a} \qquad (5\text{–}30)$$

The most suitable method is to select that stage which requires the lowest quiescent anode current. The DC voltage loss at R_v is then kept as low as possible.

Loss of gain at the upper frequency limit.

The basis for these observations is again the circuit of a two-stage RC coupled amplifier given in fig. 5–6. The decoupling condenser C_{sg} for the screen grid and C_k for the cathode and the coupling condenser C_g for the grid can be considered as short-circuits [26] as regards the upper frequency limit and are replaced in the AC equivalent circuit by direct junctions. The resultant equivalent circuit between the anode of the first valve and the grid of the second valve is given in fig. 5–18 [27].
The shunted resistances and capacitances can be condensed into one resistance and one capacitance respectively, producing the simplified equivalent circuit shown in fig. 5–19a. In this case:

[26] It should never be overlooked in practice that the standard types of condensers for this purpose always have a certain amount of series-resistance or inductance in their wrapping. It is therefore essential, especially in deflection amplifiers with a high upper frequency limit, to shunt these capacitances with small, low-loss (ceramic) R.F. condensers of 1000–10,000 pF.

[27] The additional capacitance C_{add} arises by reason of anode reaction ("Miller effect") in the second valve. It consists of $C_{add} = C_{ga}(1 + G)$ in which C_{ga} is the grid-anode capacitance of the valve and G is the gain. With pentodes, C_{ga} and thus C_{add} can, as a rule, be neglected.

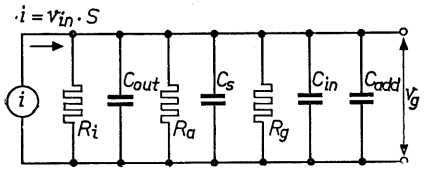

Fig. 5–18. Equivalent circuit of a resistance-coupled amplifier for high frequencies.

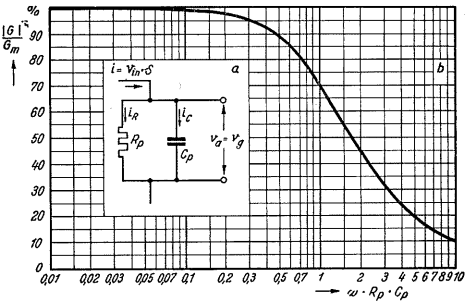

Fig. 5–19. *a*) Simplified equivalent circuit to fig. 5–18 and *b*) relative amplification response at the upper frequency limit.

$$\frac{1}{R_p} = \frac{1}{R_i} + \frac{1}{R_a} + \frac{1}{R_g} \tag{5–31}$$

and

$$C_p = C_{out} + C_s + C_{in} + C_{add} \tag{5–32}$$

In wide-band amplifiers $R_a < R_i$ and $R_g > R_a$, so that, particularly when using pentodes, R_p is for practical purposes equal to R_a. In this case, the amplified AC voltage v_g which reaches the grid of the second valve, is equal to the anode AC voltage v_a.
This voltage is equal to the product of anode alternating current and anode load resistance. The latter is shunted, however, by the capacitance C_p so that the resultant anode impedance decreases with the frequency. Therefore the AC voltage in the anode circuit decreases correspondingly and with it the gain. The impedance of the anode circuit is given by the equation:

$$Z = R_p \cdot \sqrt{\frac{1}{1 + \omega^2 \cdot C_p^2 \cdot R_p^2}} \tag{5–33}$$

As long as C_p plays no part, the mid-frequency gain is:

$$G_m = S \cdot R_p \tag{5–34}$$

For higher frequencies the gain, according to (5–33), is reduced by the factor:

$$\sqrt{\frac{1}{1 + \omega^2 \cdot C_p^2 \cdot R_p^2}} \tag{5–35}$$

The relative gain is thus:

$$\frac{|G|}{G_m} = \sqrt{\frac{1}{1 + \omega^2 \cdot C_p^2 \cdot R_p^2}} \tag{5–36}$$

The curve in fig. 5–19b shows the trend of the relative gain for different values of $\omega \cdot C_p \cdot R_p$ between 0.01 and 10. The cut-off frequency is then given if:

$$R_p = \frac{1}{\omega \cdot C_p} \tag{5–37}$$

In practice the capacitances comprised by C_p are always given in advance so

that for a desired upper frequency limit the maximum permissible value of R_p is also given by the equation (5–37). The gain per stage for ω_u is then:

$$|G| = \frac{S}{C_p} \cdot \frac{1}{\omega_u} \qquad (5\text{–}38)$$

It appears from this that the gain is greater than 1 only when $\omega \cdot C_p < S$.

Special valves for wide-band amplifiers.

Since the capacitance C_p is essentially determined by the sum of the input and output capacitances of the valves used in these stages, wide-band amplifiers should have valves with a large $\frac{S}{C_R}$ ratio ($C_R = C_{in} + C_{out}$). The stray wiring capacitance C_s cannot be suppressed below a certain minimum value so that among several valves with the same $\frac{S}{C_R}$ ratio the valve with the highest mutual conductance is in general the most advantageous.
Valves particularly suitable for this are types EF 42, EF 80 or the long-life valves E 83 F and E 180 F. The $\frac{S}{C_R}$ ratios of these valves are: 0.66, 0.65, 0.66, and 1.17 respectively. For output stages, suitable valves are EL 41 with an $\frac{S}{C_R}$ ratio of 0.555, PL83 with 0.62 or the long-life E 80L with 0.41.
Taking valve EF 42 as an example, $C_{in} = 9.4$ pF and $C_{out} = 4.3$ pF. Assuming the stray wiring capacitance to be 12.3 pF, then $C_p = 26$ pF. If the upper frequency limit is to be 3 Mc/s, then R_p, according to (5–37) must be: $R_p = \frac{1}{6.28 \cdot 3 \cdot 10^6 \cdot 26 \cdot 10^{-12}} \approx 2\ \text{k}\Omega$. The mid-frequency gain G_m of this stage is, according to (5–7) times 18. At 3 Mc/s (cut-off frequency) it falls to 12.7, and at 9 Mc/s to 6, i.e. to one third of the mid-frequency gain.
Nevertheless, it should not be overlooked, taking the 9 Mc/s in this example, that conversely about three times the control voltage on the grid will be necessary for the same anode alternating voltage. As, however, the operating conditions must, for other reasons, always be chosen such that with the maximum undistorted AC anode voltage obtainable at medium frequencies there will also be just sufficient deflection for the beam of the cathode ray tube, there would then be a risk of over-control. These conditions will be discussed later under "Output voltage requirements".
Whereas the lower frequency limit can, as described, be reduced quite considerably by a suitable outlay in circuitry, the upper frequency limit is determined by wiring capacitance and by valve data. There thus exists a "natural limit", so to speak, which is essentially set by the characteristics of the valves available and by the lowest obtainable stray wiring capacitance [3].

Phase shift at the upper frequency limit.

At the upper frequency limit a phase shift of the amplified voltage occurs due to the capacitance C_p. This phase shift increases with increasing frequency.

The total alternating anode current $i_a = S \cdot v_{in}$, divides into currents i_R through resistance R_p and i_c through capacitance C_p (see fig. 5–19a). With an increasing product $\omega \cdot R_p \cdot C_p$, the portion of current through C_p rises and thus the phase of the resultant current will be increasingly determined by the capacitive vector. The voltage increasingly lags behind the current and the phase angle becomes greater in a negative direction. The diagram *a* within the curve field of fig. 5–20*b* shows the composition of these currents. The phase angle θ is given by the relationship between the vectors i_R and i_C. As i_R is inversely proportional to the resistance R_p and i_C to $X_C \left(= \frac{1}{\omega \cdot C_p} \right)$, we obtain:

$$\tan \theta = - \frac{R_p}{\frac{1}{\omega \cdot C_p}} \qquad (5\text{–}39)$$

and from this we obtain the angle:

$$\theta = \text{arc tan} \, (\omega \cdot R_p \cdot C_p) \qquad (5\text{–}40)$$

In the diagram given in fig. 5–20*a*, the vectors for $\theta = 30°$ (i_C and i_R) and 45° (dotted: i_C' and i_R') have been drawn in as examples. For the upper frequency limit $\left(R_p = \frac{1}{\omega \cdot C_p} \right)$ $\theta = -45°$. The curve in fig. 5–20*b* shows the phase angles in dependence upon $\omega \cdot R_p \cdot C_p$ for the range from 0.01 to 10. The drop in gain at the upper frequency limit with reference to the phase angle appears from the diagram, fig. 5–20*a*, by the relationship of i and i_R, as:

$$\frac{|G|}{G_m} = \frac{1}{\cos \theta} \qquad (5\text{–}41)$$

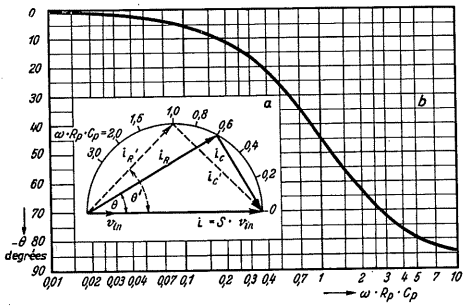

Fig. 5–20. Phase shift of the output voltage at the upper frequency limit.

Generally speaking, therefore, an increase in the ability of an amplifier to deal with phase relationships faithfully presupposes an increase in the upper frequency limit.

Even with an elaborate outlay, additional phase shift cannot be avoided beyond a certain frequency range. One solution of this problem has been found by bringing about, with suitable circuit rating, a frequency-linear increase in the phase shift of the input voltage. This fulfils the condition of equation (5–21), so that the same phase delay occurs at all frequencies. It guarantees true phase reproduction even of voltages rich in harmonics (square waves, etc.) up to high frequencies. As an example of this, fig. 5–21*a* shows the frequency and phase response curve of Philips Oscilloscope GM 5653/02. In fig. 5–21*b* the phase curve at the upper frequency end is reproduced, this time with a linear frequency scale. It can clearly be seen that in this amplifier the phase shift at the upper frequency limit increases linearly (in the negative direction) with the frequency.

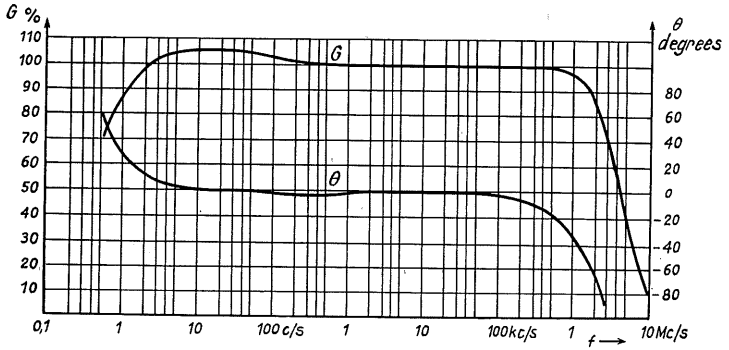

a

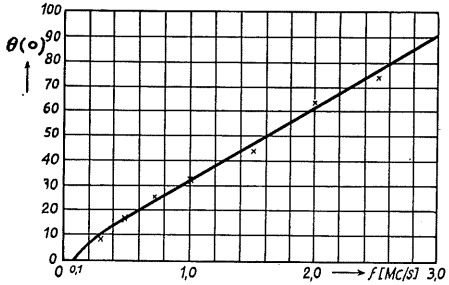

b

Fig. 5–21. Amplification and phase angle of amplifier (oscilloscope GM 5653) in dependence upon frequency. *a*) amplification curve and phase angle conventionally represented. *b*) Phase curve at upper frequency end with linear frequency scale.

Improving gain linearity at the upper frequency limit by resonance.

Various measures have been suggested for improving the linearity of the gain at the upper frequency limit. The feature common to all of them is that the unwanted capacitances C_{out}, C_s and C_{in} are combined with inductances to form an oscillating circuit or networks. In the simplest circuit of this sort, an inductance is connected in series with the anode resistance. It forms together with the capacitances C_p (fig. 5–22*a*) an oscillatory circuit damped by R_a. Parallel as well as series wiring of inductance and capacitance is possible. Making use of the distributed capacitances—on the one side C_{out}, C_s and on the other C_{in} and C_{add}—filter couplings can also be formed. As parallel resonance involves very simple circuitry and as the phase shift of the output voltage shows a most favourable trend as compared to that of other types of coupling, this is the circuit most generally employed. It will therefore be treated here to the exclusion of other types [4].

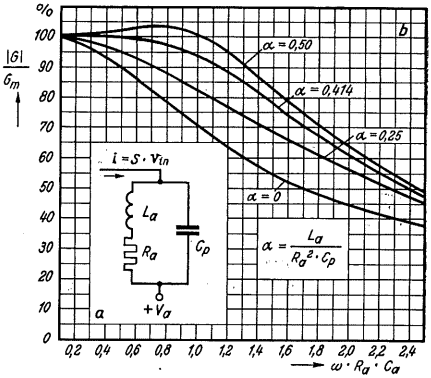

Fig. 5–22. Relative gain at upper frequency limit when using anode resonance.

Owing to the inductance, the anode resistance rises with increasing frequency and therefore the amplification follows accordingly. In this way, the "natural" fall-off of the amplification curve at higher frequency ranges can be displaced. Fig. 5–22*a* represents the simplified circuit of an anode circuit of this sort. The relative gain is now given by the equation:

$$\frac{|G|}{G_m} = \frac{|Z|}{R_a} = \sqrt{\frac{1 + a^2 \cdot \beta^2}{1 + (1 - 2a) \cdot \beta^2 + a^2 \beta^4}} \qquad (5\text{–}42)$$

To make this formula less cumbersome than it would otherwise be, some factors have been compressed into equivalent values a and β, The meanings are:

$a = \dfrac{L_a}{R_a^2 \cdot C_p}$ and $\beta = \omega \cdot R_a \cdot C_p$.

In fig. 5–22*b*, four curves represent the relative gain for four different values of a (0, 0.25, 0.414, 0.5) calculated from formula (5–42). The curve for the value of $a = 0$ is identical with the curve in fig. 5–19*b*. In contrast to this, the abscissa scale for $\omega \cdot R_a \cdot C_a$ ($C_a \approx C_p$) in fig. 5–22*b* is linear in order to show clearly the behaviour of the amplification curve in the region of the frequency limit. It is now to be ascertained how far the improvement of the amplification response can be taken without introducing concomitant disadvantages when using it with the oscilloscope. If, for example, in formula (5–42) the third summand in the denominator—$a^2 \beta^4$—is neglected (which is possible if the frequency is not too high) then the relative gain would be independent of the frequency if a is given such a value that $a^2 = 1 - 2a$. To this would correspond $a = \sqrt{2} - 1 = 0.414$. If, therefore, the inductance is rated $L_a = 0.414\ R_a^2 \cdot C_p$, it is to be expected that the gain will be independent of frequency over a relatively wide range. On the other hand, the inductance cannot be selected as high as one may wish, since otherwise the damping of the anode circuit would become too small. With deflection amplifiers for oscilloscopes it must be taken into account that the signal to be measured may not rise and fall constantly but jumps suddenly, as with rectangular pulses. Such pulses might excite these types of anode circuits into self-oscillation if the damping by R_a does not stand in a definite minimum relationship to the other circuit constants. In other words, the factor $a = \dfrac{L_a}{R_a^2 C_p}$ must not be too large. We

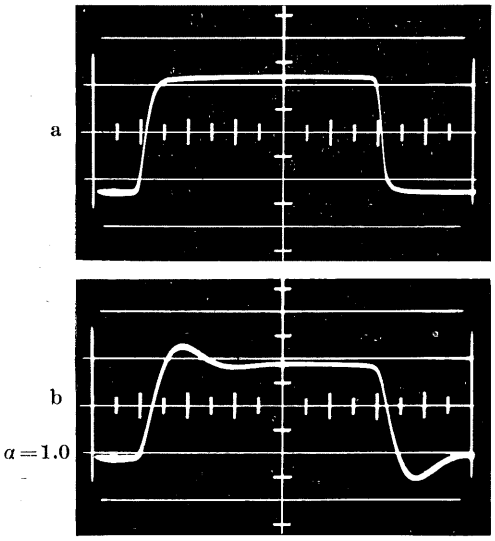

Fig. 5–23. Oscillogram of a rectangular pulse, half-value width 2.5 μs. *a*) Pulse direct from square-wave generator. *b*) Distorted pulse on the anode of an amplifier valve, with circuit elements for $a = 1.0$.

shall consider this process more closely with the aid of oscillograms of a rectangular pulse having a half-value width of 2.5μs and a rise time of about 60μs, recorded with a type GM 5660 pulse oscilloscope (amplifier rise time approx. 35 mμs).

Fig. 5–23*a* shows first the oscillogram of the pulse voltage when the latter is applied directly to the oscilloscope from the pulse generator (GM 2314). In this case the pulse was externally triggered with the control pulse generator in the oscilloscope, the repetition frequency being about 2500 c/s.

For recording fig. 5–23*b* and the oscillograms a . . . . . e in fig. 5–24, this pulse was fed, in negative polarity, to the grid of a separating stage, valve E83F, in the anode lead of which was arranged a circuit as shown in fig. 5–22*a*. The anode resistance was 3.3 kΩ and the total parallel capacitance (including the oscilloscope input capacitance) 60 pF (C_a). By including different values of inductance (L_a) in series with resistor (R_a), various values of α were obtained and then the oscillogram of the alternating anode voltage recorded.

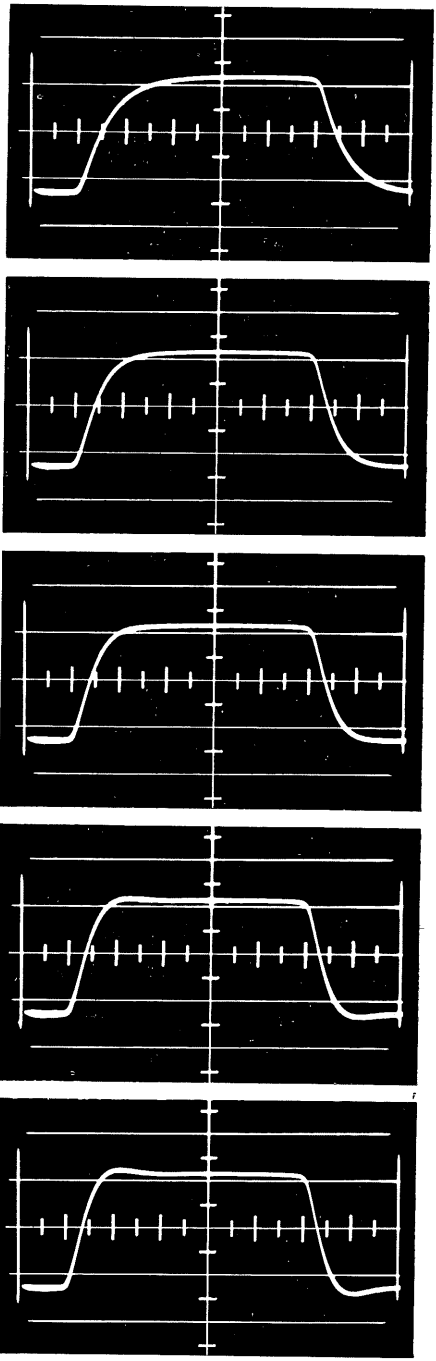

Fig. 5–24. Anode voltage of an amplifier valve, with a rectangular pulse of 2.5 μs width on the grid, at various values of

$$\alpha = \frac{L_a}{R^2_a \cdot C_a}$$

For the oscillogram shown as fig. 5–23*b* the value of a was 1.0. (The picture height in this case was somewhat smaller than for the other oscillograms discussed.) It can be seen that severe overshoot occurs when the voltage reverses polarity; for this reason, such ratings are not generally suitable for the coupling elements of a wide-band amplifier. They were chosen in this case to illustrate this effect more clearly.

The oscillograms in fig. 5–24 show the waveform of the pulse voltage on the anode of valve E83F, the circuit elements being rated at the conventional values for wide-band amplifiers.

Fig. 5–24*a* represents the voltage waveform which appears when there is no inductance. According to formula (5.44) derived in the next paragraph, the rise time T_a can be calculated from the time constant as:

$$T_a = 2.3 \cdot R \cdot C = 2.3 \cdot 3.3 \cdot 10^3 \cdot 60 \cdot 10^{-12} \approx 0.46\ \mu s$$ [28]

At the adjusted deflection velocity of 2.0 cm/μs, 2 mm corresponds to a time of 0.1 μs. For a voltage rise from 10% to 90% of the peak value, 11 mm is found to correspond to 0.55 μs. This is somewhat more than the theoretical value calculated from the formula.

The influence of the shape of the amplifier valve characteristic was not, however, taken into consideration. (See P. A. Neeteson "Electron tubes in pulse technique".)

For the following oscillograms, *b* . . . . . *d*, inductances were connected in series with the resistor, as in fig. 5.22*a*, for the purpose of increasing the upper cut-off frequency; the resultant values of a were respectively 0.25, 0.30, 0.414 and 0.50. At $a = 0.25$ and $a = 0.30$ (fig. 5.24*b* and *c*) an improvement can be seen, due to the inductances, in the leading and trailing edges. At a factor of 0.414 (fig. 5–24*d*) it can be seen that slight overshoot occurs; this therefore represents the reliable limit when high demands are made on the fidelity of reproduction. In practice, the factor $a = 0.36$ is seldom exceeded.

At $a = 0.50$ (oscillogram *e*) the overshoot is excessive.

These oscillograms confirm that the use of inductances to improve the gain at the upper frequency limit should not be taken too far if the amplifier is to satisfy the demands of pulse technique.

For the purpose of comparison, we give below the upper cut-off frequencies for the differently rated circuit elements in the anode lead of the amplifier valve for the individual oscillograms in fig. 5–24.

a	f_{lu}(Mc/s)
0	0.8
0.25	1.14
0.30	1.25
0.414	1.35
0.5	1.44
1.0	1.54

[28] The rise time of the pulse itself (T_{ap}) and of the amplifier (T_{am}) may be neglected for this purpose, since their influence is smaller by one order of magnitude. Provided that the input voltage has no more than 5% overshoot, the total rise time ($T_{a\ total}$) may be derived from the equation:

$$T_{a\ total} = \sqrt{T^2_{ap} + T^2_{am}} = \sqrt{60^2 + 35^2} \approx 0.07\ \mu s$$

(see fig. 5.23*a*.)

By connecting several amplifier stages one behind the other, the rise time and the phase velocity are increased, and, if the overshoot per stage is greater than 5%, the overshoot too is increased. Reference is made in this connection to the book "Television" by F. Kerkhoff and W. Werner (4) in which this subject is dealt with in considerable detail [29].
In this respect it should be added that, as a rule, much higher demands are made on a wide-band amplifier for measurement purposes than on a conventional video amplifier in television receivers. After all, the oscilloscopes intended for this field are used, among other things, for asessing the performance of video amplifiers.

Unit function response curve of an amplifier.

As we saw in the preceding sub-paragraph, a rapid rise of voltage in the amplifier can, depending upon the coupling elements, cause distortion of the voltage curve. The oscilloscope is very often used in pulse technique (television) for investigating voltages with a steeply rising or falling curve, so that it is of general importance to know how a deflection amplifier will behave when called upon to reproduce rapid changes in signal input.
These properties of an amplifier are represented by the *unit function response curve* which indicates the dependency of the output voltage of the circuit components in question (or of the whole amplifier) upon time, when the input voltage rises to a certain value (A) in an infinitely short time. This assumption only applies for the convenience of calculation, as in practice some time, no matter how small, is always required. (Rectangular pulses with a rise-time of $2 \cdot 10^{-8}$ secs. can, however, be achieved in practice.)
Fig. 5–25*a* shows an ideal voltage rise of the sort we are discussing. The rise-time actually required (T_a) is defined as the time taken by the voltage across the element under consideration to rise from 10% to 90% of its maximum value. This process is illustrated by the sketch in fig. 5–25*b*. The rise-time can be calculated by assuming that the RC network in question is to be charged by a voltage rising in an infinitely short space of time. The charge takes place according to the function:

$$v_t = V_o \cdot \left(1 - e^{-\frac{t}{RC}}\right) \qquad (5\text{–}43)$$

For a charging time from 10% to 90% of the output voltage, we obtain for T_a:

$$T_a = 2.3 \cdot R \cdot C \qquad (5\text{–}44)$$

With an anode resistance of 2000 Ω and a capacitance of 25pF, we then arrive at a rise-time of: $T_a = 2.3 \cdot 2 \cdot 10^3 \cdot 25 \cdot 10^{-12} = 11.5 \cdot 10^{-8}$ sec.

[29] It should be pointed out that the factor a is identical with the square of the factor Q $\left(Q = \frac{1}{R}\sqrt{\frac{L}{C}}\right)$ which is used in Kerkhoff and Werner's book "Television". The frequency characteristics shown in fig. 8.5–1 in their book therefore agree essentially with fig. 5–12 in this book. The oscillograms in figs. 5–23*b* and 5.24*a*...*e* likewise correspond to the transient responses given in fig. 8.6–2 of their book, if $a = Q^2$.

Deductions prove [5] that, between the rise-time T_a and the bandwidth B [30] of an RC-coupled amplifier, a relation exists which can be expressed by the equation:

$$B = \frac{0.35}{T_a} \qquad (5\text{–}45)$$

If the upper cut-off frequency of the network under consideration is increased by inductances then, as already shown, "overshoot" may occur (fig. 5–25*c*).

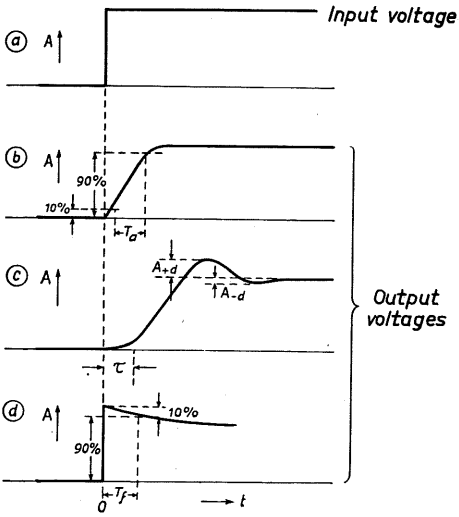

Fig. 5–25. Ideal voltage rise *a*) and unit function response curves of output voltage (*b, c, d*).

This may be an overshoot of amplitude in the positive direction (A_{+d}) as well as, at higher inductances, an overshoot in the negative direction (A_{-d}). The formula applies only if the overshoot does not exceed 5%. If it is greater, then a factor up to 0.45 must be used in place of 0.35. The unit function response curves also show the phase delay time T. (See equation 5–15). At the lower frequency limit there is, furthermore, a certain fall-off in voltage after a rapid voltage rise, as can be seen in fig. 5–25*d*. (See sub-paragraph: "The rating of coupling networks for *AC* voltages with a *DC* component", pages 94–95.)

According to the demands to be met, the time taken by this fall-off—the *drop-time*—is regarded as the decline from the maximum amplitude by 2%, 10% or even 50%.

Thus, from the unit function response curve we can read the behaviour of an amplifier not only as regards frequency response (amplitude in dependence upon frequency) but also as regards phase relationships (delay time). This characteristic is therefore of great importance when assessing the performance of wide-band amplifiers and a study of the comprehensive literature on the subject is very much to be recommended [6] [7] [8] [9].

Improvement of amplifier characteristics by feedback.

Among the different methods of improving the characteristics of an amplifier, a most important place must be assigned to the use of feedback. Negative feedback in particular is universally used because of a number of very beneficial effects which will be discussed in the following pages.

By feedback in an amplifier is understood the transferring of a portion of the

[30] The bandwidth can, for practical purposes, be equal to the upper cut-off frequency as the lower cut-off frequency in oscilloscope amplifiers is always < 50 c/s.

output voltage or of a voltage proportional to the output current to the input circuit. [31]

For this purpose a great number of possible circuits exist. Fig. 5–26 gives in block diagram form two of the circuits commonly used for the purposes under consideration. In fig. 5–26*a*, a portion of the output voltage—$a \cdot v_a'$—is taken from a voltage divider (R_1 and R_2) and fed back to the input circuit. This is *voltage feedback*. In fig. 5–26b, the alternating output current flows through resistance R_k. The voltage across this resistor is used for the feedback. As this voltage is proportional to the amplified current, the term *current feedback* is used for this type of coupling. (Strictly speaking, it is still voltage feedback, but it is now proportional to the output current and not to the output voltage). By these means a portion of the output voltage $a \cdot v_a'$ is superimposed upon the input voltage v_{in} so that the sum of both voltages now drives the amplifier. Thus:

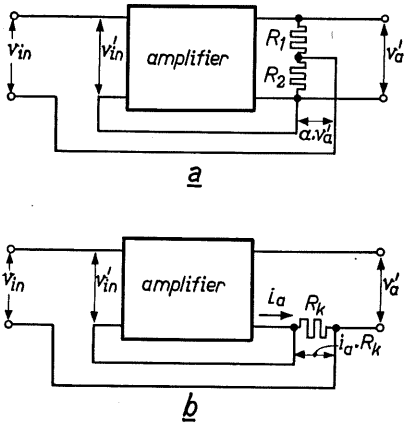

Fig. 5–26. Feedback block-diagrams. *a*) Voltage feedback. *b*) Current feedback (voltage proportional to current).

$$v_{in}' = v_{in} \pm a \cdot v_a' \qquad (5\text{–}46)$$

The factor a indicates which portion of the output voltage is fed back (in fig. 5–26*a*, the resistance ratio: $\frac{R_2}{R_1 + R_2}$). It is therefore known as the *feedback factor*. The feedback may be negative or positive. According to whether the feedback voltage supplements or opposes the input voltage—i.e. whether it is fed back in phase or in anti-phase, the resultant drive voltage v'_{in} and thus the new gain G' will be greater or smaller than in the original state. In the general term "feedback", therefore, a distinction must be made between *positive* or *regenerative* feedback and *negative* or *degenerative feedback*.
Without feedback, the output voltage is:

$$v_a = v_{in} \cdot G \qquad (5\text{–}47)$$

With feedback, the output voltage becomes

$$v_a' = v_{in} \cdot G' \qquad (5\text{–}48)$$

The gain itself in the amplifier remains, of course, unaltered, thus

$$G = \frac{v_a}{v_{in}} = \frac{v_a'}{v_{in}'} \qquad (5\text{–}48a)$$

[31] This is, of course, to be understood in a general sense. The measures discussed can be carried out in the individual amplifier stages as well as actually extended over the whole amplifier. It may also be advantageous to use differently rated feedback couplings in the individual stages.

From (5–48*a*) results

$$v_a' = G \cdot v_{in}' \tag{5–48b}$$

Substituting equation (5–48*b*) for v_a' in (5–46) gives, otherwise arranged,

$$v_{in} = v_{in}' (1 \mp a \cdot G) \tag{5–48c}$$

As, however,

$$G' = \frac{v_a'}{v_{in}} \tag{5–48d}$$

the gain with feedback is

$$G' = G \cdot \frac{1}{1 \mp a \cdot G} \tag{5–49}$$

As the factor $\frac{1}{1 \mp a\,G}$ indicates how and by what amount the gain changes, it is known as the positive (or negative) feedback factor. [32]
If, for example, with negative feedback, $a \cdot G = 2$, then the negative feedback factor is: $\frac{1}{1+a \cdot G} = 1/3$.
The curves in fig. 5–27 give as an example the amplification response of a two-stage amplifier without feedback (curve G_m), with a positive feedback factor of 5 (curve G'_{m1}) and with a negative feedback factor of 1/5 (curve G'_{m2}).
(At the moment we are only concerned with the dotted-line curves). [33]
When using positive feedback, the gain is certainly several times greater,

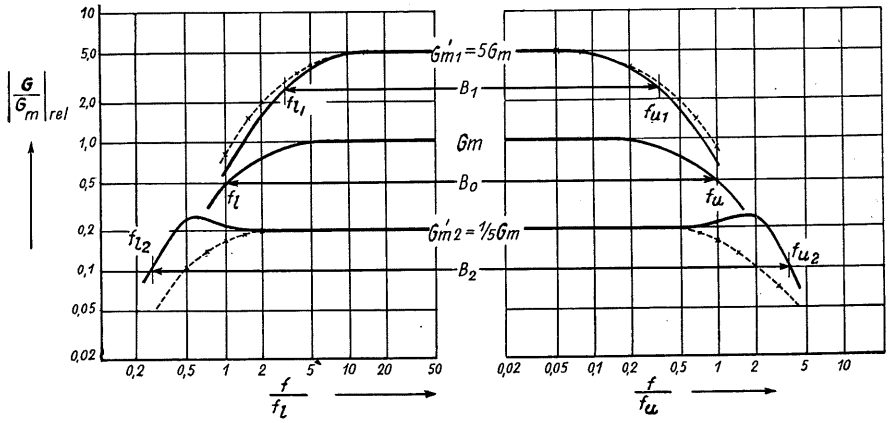

Fig. 5–27. Relative amplification response of a two-stage amplifier without feedback, with five-fold positive feedback and with five-fold negative feedback.

[32] The values applicable with feedback are distinguished from the others by a stroke.
[33] In order to represent the great differences in gain $\left(\frac{G'_{m1}}{G'_{m2}} = 25\right)$ on the same graph, a logarithmic scale has been used for the relative gain also.

corresponding to the feedback factor, but the spacing between the frequency limits f_u and f_l (the frequency response characteristic) becomes smaller by the same extent. With negative feedback, on the other hand, although the gain is reduced, the frequency response characteristic, becomes flatter and wider. For this reason wide-band amplifiers make great use of negative feedback. The middle curve G_m refers to the amplifier without feedback coupling. As two coupling elements have been taken, the drop in gain at the frequency limits is $0.707 \times 0.707 \approx 0.5$, in round figures. The curves shown in dotted lines illustrate the amplification response of a feedback-coupled amplifier in the most conventional way. To calculate this, only the amount of the relative gain— $\frac{G}{G_m}$ —as in figs. 5–7 and 5–19 has been inserted in the expression $\frac{1}{1 \mp \alpha \cdot G}$. This, however, does not always take into account, that an increasing phase shift of the output voltage takes place at the ends of the frequency response characteristic. (See figs. 5–8 and 5–20). This means that at these points of coverage the vector of the feedback voltage not only becomes smaller but suffers additional phase displacement. In consequence, the effect of the feedback is changed. To examine these relationships, it is necessary to represent vectorially the relationship between the voltages v_{in} and $\alpha \cdot v'_a$.

Influence of phase shift caused by coupling networks on the frequency response of feedback amplifiers.

Especially suitable conditions can be obtained by using a feedback amplifier with two coupling networks. [34]
At a corresponding space from the linear amplification characteristic the phase shift approaches the value $2 \times 90° = 180°$ (see figs. 5–8 and 5–20). At these points, in so far as adequate amplification and a sufficiently large feedback factor produce a feedback voltage worth mentioning, this voltage will be fed back shifted 180° in phase with respect to the mid-frequency range. Here, therefore, the feedback will cause exactly the opposite of the effect actually intended; positive feedback has become negative feedback and vice versa. At the area of transition between these extreme frequency ranges and the middle range there will, with positive feedback, be a corresponding reduction in relative gain in the vicinity of the frequency limit and, with negative feedback, an extra increase.
The actual curves resulting from this are shown in full in fig. 5–27. With positive feedback the amplification range B_1 becomes even narrower than it was found to be without taking the phase shift into consideration. With negative feedback B_2 there is not only a considerable widening of the range but even a rise in gain at each limit of the linear portion of the curve. The position of this rise depends upon the number of phase-shifting networks used and its maximum amplitude depends in each case upon the negative feedback factor and the overall gain [10] [11].

[34] The number of circuit elements which cause this phase shift at both ends of the frequency response characteristic must not be mutually equal or equal to the number of amplifying stages.

Limitation of maximum possible feedback.

In an amplifier with positive feedback coupling the quantity $a \cdot G$ must never be more than 1 as otherwise the positive feedback factor would be $\frac{1}{1 - a \cdot G} \rightarrow \infty$ and the amplifier would be driven into self-oscillation.
On the other hand the amplitude of negative feedback may not be indiscriminately high. Using four coupling networks, for example, the total phase shift at the frequency limit is $4 \times 45° = 180°$ and the voltage fed back acts regeneratively. The gain thus increases again in this region and self-excitation will be inevitable. But even at smaller magnitudes of negative feedback a rise in amplification can occur above and below the linear frequency response curve which may be excessive. At all events, careful attention must be paid to the whole frequency range from 0 to far beyond the upper cut-off frequency when rating a feedback amplifier, especially one with negative feedback.
To counter these difficulties, suitable frequency-dependent networks may be incorporated in the amplification or feedback path. This however gives rise to further phase shifts, which must also be taken into consideration. It is evident therefore that a knowledge—at least of the fundamentals—of phase requirements is absolutely essential if the way feedback amplifiers function is to be properly understood.

Phase Shift of the output voltage of a feedback amplifier.

In figs. 5–28a and 5–29a are first of all shown the voltage vectors for the mid-frequency amplification range, without phase shift of the output voltage. Fig. 5–28 represents the phase relationships for positive feedback with $G = 3$ and $G' = 5$ and fig. 5–29 represents those for negative feedback with $G = 5$ and $G' = 3$ [35]. In those frequency ranges where phase shifts of the amplified voltage are occasioned by coupling networks, the feedback voltage $a \cdot v_a$ now also contains this additional phase angle with respect to the input voltage. [36]
In the vector diagrams, fig. 5–28b and fig. 5–29b, the phase angle of the output voltage (without feedback) was taken to be 30° for the lower frequency limit (positive phase angle) corresponding to $\omega \cdot R_g \cdot C_g = 1.73$ (see fig. 5–8). The vector of the feedback voltage $a \cdot v_a$ is to be added at the same angle to the vector of v_{in} for the feedback amplifier. This now results in the actual drive voltage v'_{in} at the input of the amplifier. The feedback voltage supplies at the output a voltage increased by the factor G, namely $a \cdot v'_a \cdot G$, which is in its turn to be added to v_a. This gives finally the vector v'_a of the output voltage which now contains, as opposed to the input voltage, the phase angle θ'. It appears that the original phase angle is increased according to the value of the positive feedback, whereas it is correspondingly decreased by the value of the negative feedback. Negative feedback, therefore, has the further advantage that it provides a means of reducing the phase shift caused by the coupling elements.

[35] The differences between amplifiers without and those with feedback have deliberately been kept relatively small for the sake of clear illustration.
[36] This presupposes that no further phase shift occurs in the feedback path itself. If there are frequency-dependent elements in this path, the phase shifts which they produce must also be taken into consideration.

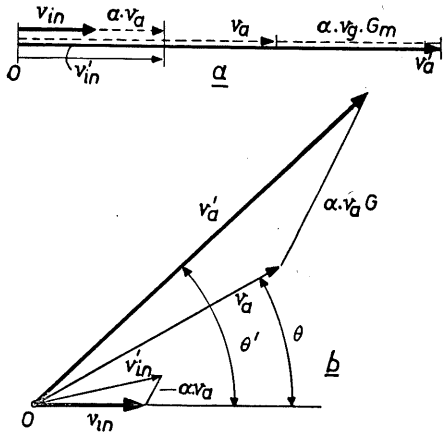

Fig. 5–28. Voltage vectors in an amplifier with positive feedback; *a*) in mid-frequency range and *b*) at a phase shift of 30° (assumed without positive feedback).

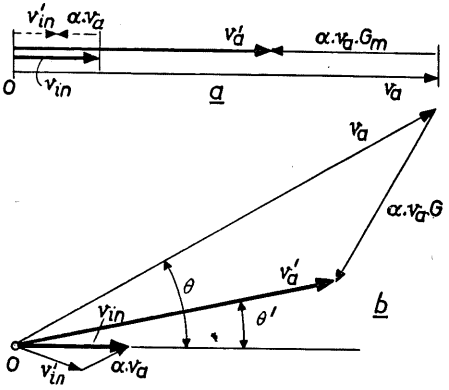

Fig. 5–29. Voltage vectors with negative feedback; *a*) in mid-frequency range and *b*) at a phase shift of 30° (assumed without negative feedback).

Several assumptions have been made in the foregoing for the sake of simplicity. For exact study, reference should be made to specialized publications [12] [13].
The purpose here was merely to show how the amplitude and phase of the output voltage change compared with the input voltage at positive and negative feedback respectively.

Frequency–dependent feedback.

As stated, it is possible by means of frequency-dependent circuit components in the feedback path to influence the feedback voltage very considerably. A reduction of negative feedback at a certain point on the frequency response curve means an increase in the resultant gain. If, for example, the cathode resistor of an amplifier valve is bypassed by only a small condenser, then the negative feedback which occurs at the lower frequencies will be reduced at the upper end of the frequency range. This provides a most convenient method of raising the upper frequency limit, for which reason it is very frequently used. (See fig. 5–41 and condensers C_{12}, C_{17} and C_{21} in the vertical amplifier circuit of Oscilloscope FTO 2, fig. 21–1, and fig. 21–15).
It should not be overlooked, however, that in contrast to the method of increasing the gain by anode resonance, negative feedback produces no increase in the undistorted output voltage at this frequency range. It is a method therefore which is particularly useful in the initial stages of an amplifier but not in output stages where a certain amplitude of voltage is required. When rating the negative feedback circuit in wide-band amplifiers attention must be paid to the limits set out by the amplifier's response to suddenly rising or falling voltages (e.g. rectangular pulses) [14]. Excessive negative feedback might lead here to overshoot.

In certain ranges it is possible to employ positive feedback with frequency-dependent coupling to increase the gain. The disadvantage of negative feedback is that the overall gain is reduced by the factor $\frac{1}{1+a \cdot G}$. For high demands it therefore entails a relatively extensive outlay in amplifier stages. Good results have, however, been obtained with moderately priced, portable oscilloscopes by using frequency-dependent positive feedback coupling.

Distortion and hum in feedback circuits.

Owing to the input voltage waveform being distorted during amplification, caused particularly by non-linearity of the valve characteristic, new frequencies are created. Residual ripple from the supply voltages can also cause frequencies to appear in the amplified output which were not present originally. In a positive feedback circuit these unwanted frequencies are amplified by an amount corresponding to the feedback value. For this reason suitable measures must be taken to keep them as small as possible (e.g. by using valves with a sufficiently large grid spacing).
In a positive feedback circuit it is usually only a matter of a limited increase of the upper frequency range, so that low-frequency ripple voltages will not in any case be magnified.
In a negative feedback circuit, on the other hand, the unwanted voltages are fed back to the input in antiphase. It is clear that these voltages will consequently be reduced at the output, by the negative feedback factor $\frac{1}{1+a \cdot G}$.
This is therefore a further advantage of using negative feedback in wide-band amplifiers.
The distortion-reducing influence of negative feedback may be explained by the linearizing effect it has on the dynamic characteristic of the valve. This linearizing effect can, of course, only be taken as far as the susceptibility of the anode current to further influence permits. In practice the result is that the bends of the dynamic characteristic curve are moved further apart and become correspondingly sharper. This is especially to be observed in output stages which must be heavily driven.
Another way of influencing still further the dynamic characteristic of the valve is to include non-linear networks, auxiliary valves and the like in negative feedback circuits. By the intelligent application of negative feedback, circuits can be built which often lead to fundamental improvements of amplifier characteristics (constant amplification during voltage fluctuations, etc.).

Internal resistance in negative feedback amplifiers.

A change in the effective output and input resistance of an amplifier takes place as a result of feedback.
As negative feedback in particular is extended over the whole amplification range, it is important to mention this effect. A fundamental distinction must here be made between *negative current feedback* (series coupling) and *negative*

voltage feedback (parallel coupling). In the case of negative current feedback, input and output resistance are *increased* according to the feedback factor.

Thus:

input resistance with negative current feedback:

$$R'_{in1} = R_{in}\,(1 + \alpha \cdot G) \qquad (5\text{–}50)$$

and

output resistance with negative current feedback:

$$R'_{out1} = R_{out}(1 + \alpha \cdot G) \qquad (5\text{–}51)$$

In the case of negative *voltage* feedback, input and output resistance are *reduced* according to the feedback factor.

Thus:

input resistance with negative voltage feedback:

$$R'_{in2} = \frac{R_{in}}{1 + \alpha \cdot G} \qquad (5\text{–}52)$$

and

output resistance with negative voltage feedback:

$$R'_{out2} = \frac{R_{out}}{1 + \alpha \cdot G} \qquad (5\text{–}53)$$

Since the aim with regard to deflection amplifiers for oscilloscopes is to achieve a constant *voltage amplification* over as wide a band of frequencies as possible, it is clearly preferable to use negative voltage feedback. Negative current feedback has only a slight influence on the matching conditions when using pentodes since, for reasons already discussed, the impedances of the coupling elements must remain low. They represent therefore, even without negative feedback, only a small fraction of the value of the input or output resistance of the valve. But also the value of the output resistance reduced by negative voltage feedback remains, generally speaking, without appreciable influence on the characteristics of the amplifier. The increase of the input resistance can, however, have a significant effect on the input stage. When the oscilloscope is connected up, the voltage source should be as little loaded as possible; the input of the amplifier must therefore have a high ohmic value. For this reason it is appropriate to use negative current feedback in the first stage and negative voltage feedback in the other stages of a multi-stage amplifier.

Output voltage requirements.

The output stage of the amplifier must be able to supply the voltage necessary for the deflection required without additional amplitude distortion. In this it differs fundamentally from the pre-amplifying stages which are only called upon to deal with small amplitudes of voltage. As according to formula (5–37) the value of the anode resistance must not exceed the calculated amount for a certain upper cut-off frequency, the anode alternating voltage needed can only be obtained by a sufficiently large change in anode current. But the anode current cannot quite be driven by grid control from zero to twice the value of

the quiescent current. In general, the maximum anode current change ($\Delta I_{a\,max}$) will correspond to 1.5–1.8 times the anode quiescent current. Thus:

$$\Delta I_{amax} = (1.5 \ldots . 1.8) \cdot I_{ao} \qquad (5\text{–}54)$$

(With strong negative feedback it is possible to approach the factor 2.)
To achieve a satisfactorily large change in current, powerful output valves must be used in the output stage of a deflection amplifier and their less favourable characteristics as compared with the pre-amplifying pentodes (larger electrode capacitances) will have to be tolerated. With a deflection sensitivity of $DS_{=}$, a deflection voltage V_Y is necessary for the input voltage on the Y plates to produce a certain deflection Y_M.
Thus:

$$V_Y = \frac{Y_M}{DS_{=}} \qquad (5\text{–}55)$$

If, for instance, the deflection sensitivity is $DS_{=} = 0.5$ mm/V, then for a beam deflection of 60 mm, a peak-to-peak voltage will be required of: $\frac{60}{0.5} = 120\ V_{pp}$. In a symmetrical output stage, 60 V_{pp} will then fall to each valve. In the family of curves for PL 83 shown in fig. 5–30*a*, the load line has been drawn in for an anode resistance of 2 kΩ, where the screen grid voltage is 200 V, the supply voltage 280 V and the anode quiescent current 30 mA. For a change in anode current of $\Delta I_a = I_{a\,pp}$ the output voltage is:

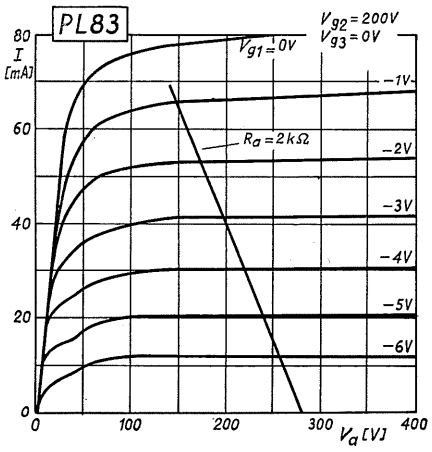

Fig. 5–30. Anode current—anode voltage characteristic of valve type PL 83 with a load line for 2 kΩ.

$$V_{a\,pp} = I_{a\,pp} \cdot R_a \qquad 5\text{–}56)$$

The output voltage of 60 V_{pp} is obtained by driving the anode current from about 15.0 mA to 45 mA.
Any asymmetry is compensated by connecting the output in push-pull. In this case sufficient grid control is obtained by a grid AC voltage of about 3.3 V_{pp}, that is approximately 1.2 V_{rms}.

Balancing the output voltage.

As a rule the input signals to the Y plates are single-pole earthed so that for the symmetry of the deflection plates (see Chapter 2 "Cathode Ray Tube", page 15) there must be a balanced output from the amplifier.
One method of achieving this is by taking a voltage from the anode of the one output valve, divided according to its amplification, and using it to drive the other output valve. In the example shown in fig. 4–25 of a triple-pentode time

base generator, a capacitance-compensated voltage divider is used for this purpose. (Further details of this are given in the following sub-chapter). Another method, which is used in oscilloscope FTO 2, is illustrated in fig. 5–31. Voltage division is effected in this instance by means of a variable resistor in the anode load. This resistor R'_{a1} must be adjusted in such a way that the ratio of the anode AC voltage (v_a) to the portion taken off ($p \cdot v_a$) is equal to the gain factor G of the stage.
Thus:

$$G = \frac{v_a}{p \cdot v_a} = \frac{1}{p} \tag{5–57}$$

This results in a resistance ratio of:

$$p = \frac{R'_{a1}}{R_{a1} + R'_{a1}} = \frac{1}{G} \tag{5–58}$$

and

$$R'_{a1} = \frac{R_{a1} + R'_{a1}}{G} \tag{5–59}$$

If, in the example of PL 83, $G = 18$ for $R_a = R_{a1} + R'_{a1} = 2\text{k}\Omega$ then $R'^{\prime\prime}$ must be $\frac{2000}{18} = 111\ \Omega$.
If an inductance is in circuit to extend the upper frequency range, then, of course, a corresponding portion of the inductance must be in series with R'_{a1}.
The disadvantage of both circuits discussed is the further CR network which has been added. As a result of this the lower cut-off frequency will be higher for the second output valve than for the first, so that the grid drive will be unbalanced at this frequency limit, in so far as it lies at all in the frequency range wanted.
To overcome this disadvantage, a phase inverter stage may be used as shown in basic form by fig. 5–32. In this case the second valve is driven by the

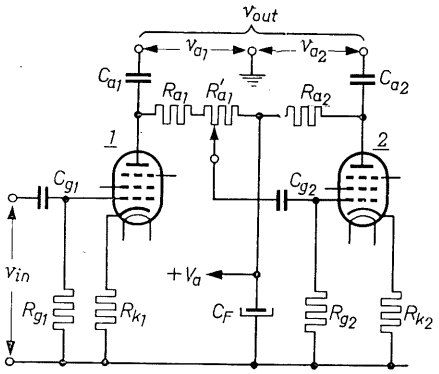

Fig. 5–31. Controlling the second valve of a balanced output stage with a portion of the output voltage of the first valve.

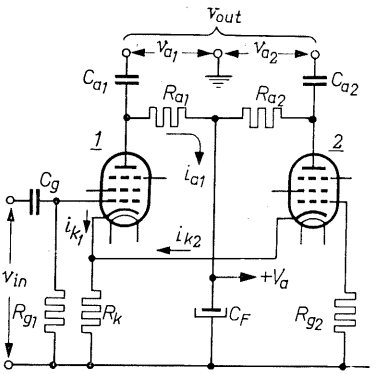

Fig. 5–32. Controlling the second valve of a balanced output stage by means of cathode coupling.

alternating voltage across the common cathode resistor. This circuit is therefore particularly suitable for amplifiers required to pass extremely low frequencies and *DC* voltages too.

The working principle of the circuit in fig. 5–32 may be described as follows. The input voltage v_{in} results in an alternating anode current i_{a1} which also flows through the cathode resistor R_k. The resultant alternating voltage across R_k is in antiphase to the input voltage on the control grid of valve 1 (negative feedback). This voltage is, however, simultaneously operative between grid and cathode of valve 2 whose grid is at earth potential; this valve is therefore controlled in the way desired, namely in antiphase. The alternating current set up in the anode circuit of valve 2 also flows through the common cathode resistor but the resultant *AC* voltage drop is in antiphase to the cathode *AC* voltage caused by the current of valve 1, so that the control voltage for valve 2 is reduced and as a consequence of this, the voltage drop due to the current of this valve is also reduced. This, however, means that the voltage difference on the cathode resistor will be increased, valve 2 will again be driven more heavily, and so on. A state of balance is thus introduced after the amplifier has been switched on, which is achieved for certain valves by suitably rating R_k. If, under certain circumstances, the negative grid bias becomes too large, the operating point can be restored by connecting the grid leak resistors R_{g1} and R_{g2} to an appropriate source of positive voltage.

Thus, the grid drive of valve 2 as well as the negative feedback coupling of valve 1 is effected by the alternating voltage *difference* caused by the cathode currents i_{k1} and i_{k2}. It follows in the nature of things that perfect symmetry cannot be achieved in this way. A simple calculation proves, however, that the asymmetry remains satisfactorily small if the product $S \cdot R_k$ is large with respect to unity.

The relationship between the anode alternating currents is given by the following equation:

$$\frac{i_{a1}}{i_{a2}} = \frac{1 + \beta \cdot S \cdot R_k}{\beta \cdot S \cdot R_k} \quad [37] \qquad (5\text{–}60)$$

If, for example, two valves, type PL 83, are used in this stage with a mutual conductance of 10 mA/V and a cathode resistor of 500 Ω, then:

$$\frac{i_{a1}}{i_{a2}} = \frac{1 + 1.14 \times 10 \times 10^{-3} \times 500}{1.14 \times 10 \times 10^{-3} \times 500} = 1.175$$

The difference of the anode currents and thus of the output voltages is therefore 17.5%. It can, however, be completely compensated if necessary by unequally rating the anode resistances. This circuit can, of course, be used for pre-amplifying stages as well as for output stages. The gain of such a stage is in general approximately one half of the gain obtained by means of the cathode resistor without negative feedback (e.g. with fixed grid voltage and earthed cathode). If, as shown in fig. 5–33, equally large coupling resistors are connected in the anode and cathode leads of a triode, the voltage on the grid of this valve can also be taken off, balanced and in antiphase, from

[37] The factor β expresses the difference between cathode current and anode current (about 1.1 . . . . . 1.3).

cathode and anode. The amplification from input to one output will, of course, always be less than 1, as the entire voltage from the cathode resistor is fed back in antiphase. The disadvantage of this circuit is, therefore, that the maximum amplitude of the output voltage is somewhat smaller than twice the input voltage, so that to drive large output stages it is necessary either to use a valve with a sufficiently large anode current or to interconnect a further symmetrical stage of two valves.
Its advantage is that it offers a high input and a low output impedance (strong negative "current" feedback). In this way, both the output valves may be driven entirely symmetrically.
Other phase inverter circuits for driving push-pull stages are in use [15].

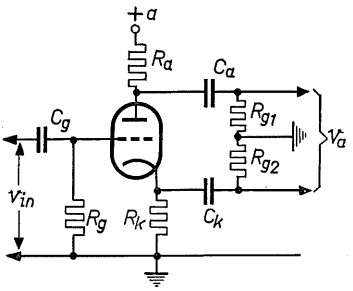

Fig. 5–33. "Catodyne" circuit for voltage symmetry in amplifier.

In oscilloscope "FTO 2", for example, an anode follower is employed for balancing the time base voltage.

Controlling the amplitude of the signal.

There are fundamentally two possible ways of controlling the amount of beam deflection caused by the signal to be investigated.
We may either vary the amplification of the valves or bring about a division of the unamplified or amplified voltage.
The latter method leaves the amplification at its maximum value and effects adjustment by dividing the input voltage. It is the system most widely used at the present day and permits the voltage division to be carried out at the input, between the individual amplifier stages, or at the output. The use of an input potentiometer, as adopted for audio frequency amplifiers, might seem on the face of it to be particularly suitable in this instance. Since, however, the upper frequency limit is mostly much higher in deflection amplifiers for oscilloscopes than in electro-acoustics, attention must be paid to the influence of unwanted capacitances on the voltage division.
A circuit of this sort is shown in fig. 5–34a and the equivalent circuit of an "input potentiometer" is shown in fig. 5–34b. It can be seen that the influence of capacitance C, which is composed of the self-capacitance of the potentiometer, stray wiring capacitance and the input capacitance of the valve, is greatest in the centre of the potentiometer. The voltage division ratio $\frac{v_2}{p' \cdot v_1}$ then appears from the equation:

$$\frac{v_2}{p' \cdot v_1} = \frac{1}{\sqrt{1 + \frac{\omega^2 \cdot C^2 \cdot R^2}{16}}} \qquad (5\text{–}61)$$

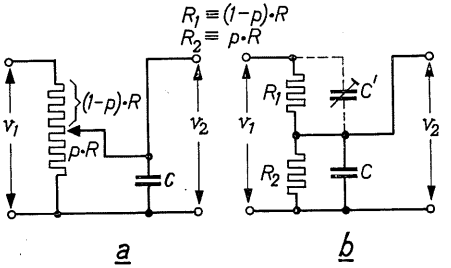

Fig. 5–34. Circuits illustrating the influence of stray wiring capacitance on a voltage divider.

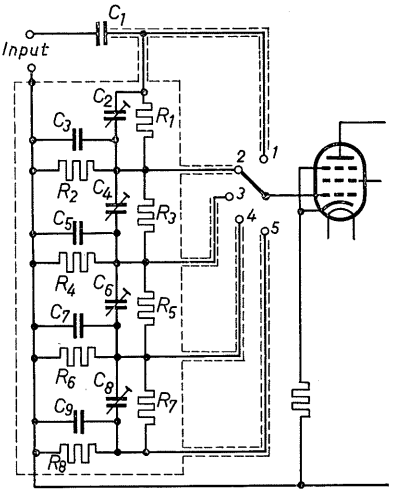

Fig. 5–35. Practical circuit of a step voltage-divider with compensating condensers. Resistors: R_1, R_3, R_5, $R_7 = 0.8$ MΩ. R_2, R_4, R_6, $R_8 = 0.1$ MΩ. Capacitances: $C_1 = 0.2$ μF, C_3, C_5, C_7, $C_9 = 160$ pF. C_2, C_4, C_6, $C_8 = 6$–30 pF (air trimmer).

If, for example, $R = 10{,}000$ ohms, $C = 20$pF and $\omega = 2\cdot\pi\cdot 10^6$ ($f = 10^6$ c/s), then we obtain:

$$\frac{v_2}{p'\cdot v_1} = \frac{1}{\sqrt{1 + \dfrac{4\cdot 9.85\cdot 10^{12}\cdot 400\cdot 10^{-24}\cdot 10^8}{16}}} = \frac{1}{\sqrt{1 + 0.0985}} = 0.953.$$

It thus appears that, as a result of the shunt capacitance C, at a frequency of 1 Mc/s the output voltage v_2 is smaller by about 4.7% than it should be. If $R = 100$ kΩ the error would be 69% and therefore not to be tolerated. For this reason such types of controls must have a low ohmic value, but if they are used in the input, this again entails an impermissible load on the voltage source. A way around the difficulty can be found by shunting a condenser (C' in fig. 5–34*b*) across the "upper" part of the potentiometer. As the frequency increases, extra current flows through C', thus *compensating* the influence of capacitance C which also increases with the frequency. In this way it is possible to build high-ohmic voltage dividers which are to a great extent independent of frequency. The following must apply in this case:

$$R_1\cdot C' = R_2\cdot C \qquad (5\text{–}62)$$

(At the low frequencies, voltage division is effected by the resistances, at the high frequencies by the capacitances.)

In the example quoted, compensation could only apply to that particular setting of the potentiometer; it has not so far been used for continuous voltage adjustment since the capacitance C' would likewise have to be variable and this would lead to complicated control components. Great use is made of it, on the other hand, in step voltage dividers. A practical voltage divider of this sort is shown in fig. 5–35. This circuit also contains *pi* elements but in

general these are dispensed with, and for each attenuator position a voltage divider is switched in between input voltage and amplifier input.
Controlling the amplification by varying the *DC* voltages on the first or second grid is, in general, not to be recommended. The jumps in voltage which are unavoidable with this procedure are transferred in an amplified form to the deflection plates, especially where amplifiers with a very low cut-off frequency are concerned.
It is, however, very convenient to control amplification by means of variable negative feedback. Any other form of adjustment is synonymous with a deliberate worsening of the maximum amplification that can be obtained, while the frequency response of the amplifier remains unaltered. If, on the other hand, the amplification is reduced by means of increasing the negative feedback, then as pointed out earlier in this chapter, the frequency response of the linear characteristic is widened at the same time.
Care must be taken, however, when using variable negative feedback with frequency-dependent circuit components in the feedback path, that no disturbing rise in amplification or tendency to oscillation occurs in the critical areas at the frequency limits.

The cathode follower.

The cathode follower is an ideal means of matching a high input impedance to the low impedances of the coupling elements in a wide-band amplifier, which is of course a fundamental requirement. In this circuit the coupling resistor is in the cathode lead while the anode is connected direct to the *DC* voltage source. Since from the point of view of alternating voltage the anode remains without voltage, this circuit is also referred to as the "anode base" circuit [16] [17] [18].

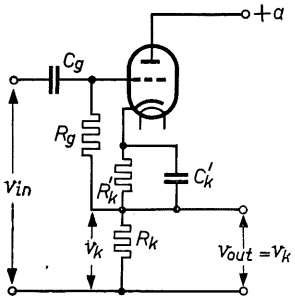

Fig. 5–36. Conventional circuit of a cathode follower.

A conventional circuit of this kind is shown in fig. 5–36. (It includes the circuit components which generate the grid bias, but these have no influence on the amplification.)
Specially characteristic of the cathode follower's properties is the fact that the total output voltage v_k is inversely coupled to the grid. All advantages of the negative feedback amplifier—freedom from distortion, linear frequency response up to high frequencies—are therefore present here in a correspondingly high degree.
The output voltage v_k is obtained from the equation:

$$v_k = S \cdot v_g \cdot \frac{R_i \cdot R_k}{R_i + R_k} \tag{5–63}$$

If the factor $\frac{R_i \cdot R_k}{R_i + R_k}$, which represents the parallel circuit of the internal resistance of the valve with the cathode resistor, is simplified to R_p, and if v_g is represented by:

$$v_g = v_{in} - v_k \tag{5–64}$$

then we arrive at the expression:

$$v_k = S \cdot R_p \cdot (v_{in} - v_k) \tag{5–65}$$

From this we can calculate the gain $G = \frac{v_k}{v_{in}}$ as:

$$G = \frac{S \cdot R_p}{1 + S \cdot R_p} \tag{5–66}$$

The voltage gain will thus always be less than 1. Taking as an example an EF 80 connected as a triode, with an internal resistance of $R_i = 10{,}000\ \Omega$, a cathode resistor of $R_k = 5000\ \Omega$, (thus $R_p = \frac{10{,}000 \cdot 5000}{10{,}000 + 5000} = 3333\ \Omega$) and a working slope of 5 mA/V, the gain is found to be:

$$G = \frac{5 \cdot 10^{-3} \cdot 3333}{1 + 5 \cdot 10^{-3} \cdot 3333} = 0.943.$$

Now the input current is not, as in "anode" amplifiers, given by the quotient $i_g = \frac{v_{in}}{R_g}$. This current is determined in a cathode follower by the voltage difference $v_{in} - v_k = v_g$, so that we obtain the equation:

$$i_g = \frac{v_{in} - v_k}{R_g} \tag{5–67}$$

The effective input impedance is therefore increased. It can be calculated from the equation:

$$Z_{in} = R_g \cdot \frac{1}{1 - G} \tag{5–68}$$

Taking EF 80 again as an example, the input impedance $Z_{in} = R_g \cdot \frac{1}{1 - 0.943} = R_g \cdot 17.5$. If therefore $R_g = 2\ \text{M}\Omega$, the input impedance will be $Z_{in} = 35\ \text{M}\Omega$ [36].

It is clear that with an input impedance as high as this even the slightest currents caused by stray couplings will result in interfering input voltages. In these circuits, therefore, the input terminals and the grid lead must be thoroughly screened.

The output impedance is, in general, resistive and is expressed by the equation:

$$Z_o = R_o = \frac{1}{S \cdot \left(1 + \frac{1}{\mu}\right)} \tag{5–69}$$

in which μ represents the amplification factor of the valve. In most cases $\frac{1}{\mu}$ with respect to 1 can be neglected so that the output impedance is equal to

[38] This increase in impedance does not occur for impedances lying immediately between the input terminals across v_{in}. They, of course, load the voltage source directly.

the reciprocal of the mutual conductance (slope). With EF 80 where $S = 5$ mA/V, we obtain:

$$Z_o = R_o = \frac{1}{5 \cdot 10^{-3}} = 200\ \Omega$$

Equations (5–68) and (5–69) show that with a cathode follower an extremely high input impedance can be matched to a low output impedance.
This "impedance transformation" also means that small alternating input currents can be amplified to appreciable values. A cathode follower, therefore, does not amplify voltage but it does amplify the current of the input voltage source and, since the voltage remains almost constant, it permits a quite considerable power amplification.
For use in oscillograph amplifiers it is important to know the value of the maximum permissible input voltage $v_{in\ max}$. The maximum permissible alternating grid-voltage $v_{g\ max}$ can be obtained from the valve data or family of characteristics. The value of $v_{in\ max}$ is then given by the expression:

$$v_{in\ max} = v_{g\ max} \cdot \frac{1}{1 - G} \qquad (5\text{–}70)$$

If, therefore, the valve in the example is set so that $v_{g\ max} = 0.8\ V_{rms}$ and, as calculated, $\frac{1}{1-G} = 17.5$, then $v_{in\ max} = 14.0\ V_{rms}$. (When establishing the value of $v_{g\ max}$, it must be ascertained whether the maximum peak-to-peak or the r.m.s. value has been determined.)
In another type of cathode follower circuit, shown in fig. 5–37, the grid resistor is connected, not to the cathode, but to the chassis ("0"). This does not result in a reduction of the load due to the grid leak, as previously described, but it has the great advantage that the output impedance is largely independent of the impedance of the voltage source [19] [20] [21] [22]. For this reason, it finds wide application in amplifiers of oscilloscopes which are required to operate with voltage sources of varying output impedance. As in this circuit the voltage drop across the cathode resistor delivers to the grid a voltage that is too high for a proper operating point, this voltage must be controlled by simultaneously applying a suitably high positive voltage (as in the balanced cathode-coupled stage). As shown in fig. 5–37, this can be done quite simply by connecting the grid to the anode voltage source via a resistor. The ratio of the resistances $(R_g + R_{ga}) : R_g$ determines the portion of anode voltage which is to be used as positive counter-voltage. Since this voltage is determined only by the ratio of resistances and can thus be regarded as "fixed", whereas the negative voltage from the cathode resistor amounts to several times the value of the normal grid voltage, the operating point of this valve always adjusts itself automatically and stably to the adjusted value of cathode current.

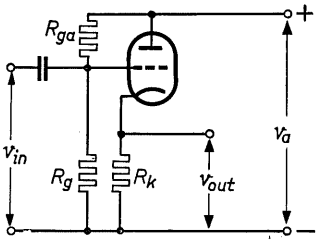

Fig. 5–37. Cathode follower circuit in which the operating point is adjusted by a positive inverse voltage.

DC voltage amplifiers.

For many tasks which the oscilloscope is required to perform it is necessary to amplify *DC* voltages or the *DC* voltage components of complex signals. Amplifiers for this purpose are often employed in supplement to the normal *AC* amplifiers in oscilloscopes (e.g. Philips GM 4530 and GM 4531).
As an example, fig. 5–38 gives the simplified circuit of a single-stage, symmetrical *DC* voltage amplifier with two valves, type EF 42.
The input signal v_{in} is applied directly to the input terminals. Since the cathode resistance $R_{k_{1,2}}$ is small compared with the impedance of the signal source and with the resistance of the grid leak R_{g_1}, practically the entire input voltage appears between grid and cathode of this valve, the anode current of which is

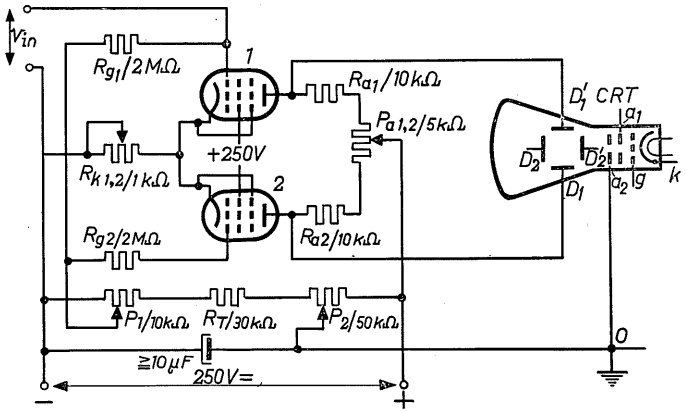

Fig. 5–38. Single-stage *DC* amplifier in push-pull.

driven accordingly. This current, together with the anode current of valve 2, flows through the common cathode resistor $R_{k_{1,2}}$ so that the voltage drop across this resistor is increased. But the same voltage appears also, via P_1 and R_{g2}, between grid and cathode of valve 2 so that if, for example, a positive input voltage arrives, the current in this valve will sink. The anode potential will have risen accordingly, whereas in valve 1, as a result of the increase in current, it will have fallen. Here again, therefore, we have obtained by means of cathode coupling a push-pull relationship between the anodes of both valves, providing the balanced voltage output to the *Y* plates of the cathode ray tube which is necessary if the oscillogram is to be sharp and free from distortion. The symmetrical grid drive of both valves can be achieved by suitably rating the cathode resistor $R_{k_{1,2}}$; it may be useful to make this resistor variable. Since the change in anode current of valve 2 causes a voltage change across the cathode resistor in opposition to that caused by valve 1, the grid drive of valve 2 is, to be exact, the consequence of a certain residual asymmetry of the anode currents. (See also "circuits for balancing the output voltage" pages 115–117.) In general, this will result in a value for the cathode resistor which would produce an excessive quiescent grid voltage. To obtain

the most favourable operating point, the grid leaks are led in this case, not to "0", but to a variable positive voltage on the arm of potentiometer P_1.
Anode symmetry can be adjusted by means of potentiometer $P_{a_{1,2}}$.
The following remains to be noted with regard to the deflection plates of the cathode ray tube when using *DC* voltage amplifiers:
The final accelerating electrode of every cathode ray tube used for measurement purposes (a_2 in the circuit diagram) is earthed in the usual way. Now if the reference point ("0") of the amplifier were also to be earthed, then both deflection plates D_1 and D'_1 would, with respect to a_2, be at the positive potential of the quiescent anode voltage. As, however, the deflection plates in the path of the beam do not represent symmetrically turned electrodes, the result is a distortion of the field which produces severe astigmatism of the spot on the screen. This can be avoided if, instead of the "0" point, a point of the amplifier is tied to the chassis of the oscilloscope which can be adjusted to the same positive potential as that of the anodes of the valves in quiescence. In the circuit diagram, P_2 is used for this purpose. This means in practice, that the spot focus must be adjusted twice, firstly in the usual way and secondly by means of P_2. As long as the voltage divider $P_1 - R_T - P_2$ has not been given a too high ohmic value, there are no resultant difficulties with mains hum or the like. To make quite sure, however, a condenser of about 10 μF can be connected between "0" and earth, as shown in the circuit diagram. Care must be taken at the same time that a corresponding *DC* potential exists between the chassis of the amplifier and the chassis of the oscilloscope.

Some practical AC amplifiers.

The circuit diagrams given in figs. 5–39, 5–40 and 5–41 are practical examples of deflection amplifiers used in some Philips oscilloscopes.
Fig. 5–39 shows the circuit used in the small oscilloscope GM 5655, in which both systems of a triode-hexode are connected in cascade. The voltage-divider across the input consists of a fixed resistor of 1 MΩ and a potentiometer of 0.1 MΩ. Input voltages of up to 50 V_{rms} can be applied direct to the potentiometer (terminals 3 and 4). For voltages greater than 50 V_{rms} (up to 300 V_{rms}) the voltage divider is necessary; these are applied to terminal 5. As compensation for the capacitance between the grid of the first stage and chassis, the voltage divider resistor of 1 MΩ is shunted by a small condenser of about 4.7 pF. This compensation is only effective, however, when the arm of

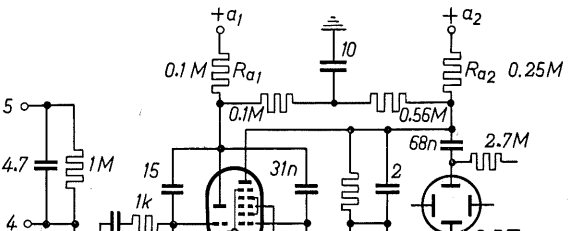

Fig. 5–39. Deflection amplifier in oscilloscope GM 5655.

the potentiometer lies right at the end, at the junction with terminal 4. As an identical amplifier is also available for X deflection, it is necessary, in cases where intermediate positions of the potentiometer are required, first of all to find a setting, with the same AC voltage on both amplifiers, such that the phase difference in both amplifiers will remain sufficiently small. With a maximum deviation of $\pm$ 10%, however, phase measurements can readily be carried out between 6 c/s and 10 kc/s, if the voltages are to be applied to terminals 4 and 3. Using the voltage divider, this applies up to 2000 c/s. The triode system of the valve is used as the pre-amplifier stage. To boost the upper frequency limit, positive feed-back is employed in this stage, using a condenser of 15 pF between anode and grid.

The resistors of 0.56 MΩ and 0.1 MΩ between the anode of the hexode system

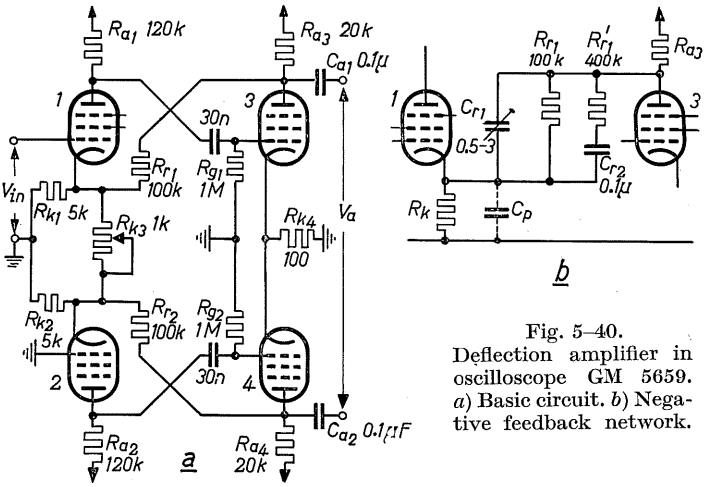

Fig. 5–40. Deflection amplifier in oscilloscope GM 5659. *a*) Basic circuit. *b*) Negative feedback network.

and the anode of the triode system introduce negative feedback for the output stage to increase the undistorted drive voltage for the output. A condenser of 10 pF between the junction of these resistors and the chassis reduces the negative feedback at high frequencies, so that in this way too the amplification curve at the upper frequency end can be boosted. With this amplifier, the deflection factor of cathode ray tube DG 7–6 is 30 V_{rms}/cm. The cut-off frequencies lie at 3 c/s and 50 kc/s [39].

Fig. 5–40*a* and *b* shows the circuits of a balanced two-stage amplifier with four EF 80 type valves as used in the GM 5659 oscilloscope.

The amplitude of the input voltage is regulated in steps by means of frequency compensated voltage dividers, as shown in fig. 5–34b. For every individual attenuator position, a voltage divider (with 5 : 1 ganged divider ratios) can be

[39] In Philips' GM 5655/02 oscilloscope, the deflection amplifiers are each fitted with one ECC 81 and one EF 80. The EF 80 functions as a pre-amplifier, and both systems of the ECC 81 as a push-pull output stage. The cut-off frequencies are 3 c/s and 150 kc/s, the deflection factor 20 mV_{rms}/cm.

switched in between input voltage and amplifier input. The input impedance is thus kept constant and amounts to 1 MΩ in all attenuator positions.
The second side of the balanced amplifier is driven by means of cathode coupling via the delta arrangement of resistors R_{k1}, R_{k2} and R_{k3}. Frequency response correction is provided by frequency-dependent negative feedback over resistors R_{r1} and R_{r2}. These are shown in the circuit diagram as simple resistors but in the actual oscilloscope they consist of a network of resistors and condensers, as shown in fig. 5–40b. The negative feedback resistor proper (R_{r1}) is shunted by condenser C_{r1} and by R'_{r1} and C_{r2} in series. At high frequencies $C_{r2}$is a short circuit so that this circuit element then consists only of the resistors R_{r1} and R'_{r1} in parallel, and C_{r1}.
C_p represents the capacitance between filament and cathode of the valve as well as the stray wiring capacitance. In the mid-frequency range, the negative feedback is independent of frequency when:

$$C_{r1} \cdot \frac{R_{r1} \cdot R'_{r1}}{R_{r1} + R'_{r1}} = C_p \cdot R_k \qquad (5\text{–}71)$$

(R_k = resultant total cathode resistance of the delta circuit). Capacitive compensation, as in the frequency-compensated voltage divider in fig. 5–34b, is thus achieved by means of C_{r1} and C_p.
At low frequencies the reactance of C_{r2} increases, so that the negative feedback decreases and the gain at the lower end of the frequency response characteristic is boosted (f_l = 0.8 c/s).
To improve the frequency response at the upper end of the range the negative feedback is decreased by correspondingly adjusting C_{r1} in relation to C_p.
By varying R_{k3} it is possible to control continuously the negative feedback and inversely change the overall gain in a ratio of 5 : 1 [40]. Together with the step voltage-divider at the input, a gain control in a ratio of 3000 : 1 can be achieved in this way.
The maximum amplification is about × 850 which, in conjunction with C.R.T. DG 7–5, corresponds to a Y deflection factor of about 20 mV_{rms}/cm. (56 mV_{pp}/cm). The maximum permissible input voltage is 500 V_{rms}.
The cut-off frequencies lie at 0.8 c/s and 0.8 Mc/s. This ensures faithful reproduction of voltage pulses from 50 c/s to 50 kc/s, and if the demands are not too high, up to 100 kc/s.
Fig. 5–41 shows the amplifier circuit of Philips Oscilloscope GM 5653. With its cut-off frequencies of 1 c/s and 3 Mc/s, it is an example of a special high-efficiency amplifier.
An EF 42 pentode is connected as a cathode follower triode at the input. The cathode voltage, which is too high to be used for grid bias, is compensated im this case by feeding an equally high negative voltage to the cathode. To

[40] This may be explained as follows: If one first assumes that R_{k3} is not present, then the entire negative feedback, which also drives the appertaining grids, appears across the cathode resistors R_{k1} and R_{k2}. If, on the other hand, one assumes that the cathodes of valves 1 and 2 are directly connected, then the negative feedback voltages across the cathode resistors will cancel each other out, as they are in anti-phase (provided, of course, that both stages are perfectly balanced).
Between these two extremes it is possible, by means of a variable resistor between the two cathodes, to vary continuously the negative feedback and hence the overall gain.

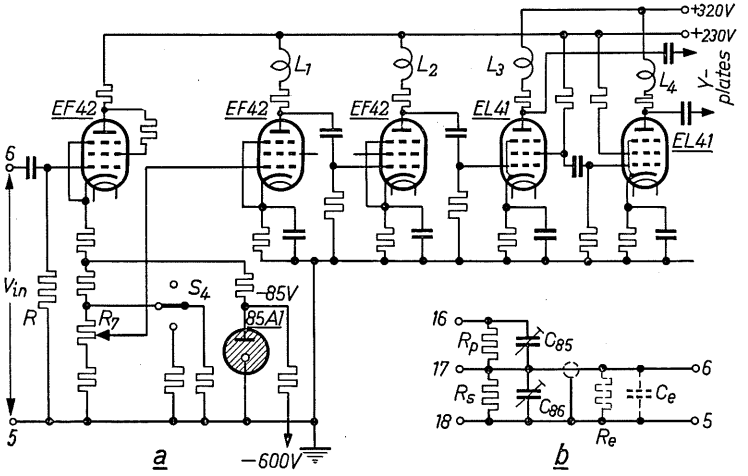

Fig. 5–41.
Deflection amplifier in Oscilloscope GM 5653. *a*) Basic circuit, *b*) voltage divider in probe.

prevent this compensation voltage from leading to supply-voltage surges in the amplification path, it is stabilized by valve 85 A1. In this way the cathode current flows to the source of the negative voltage so that the cathode resistor itself remains void of current for all practical purposes. Thus the risk is avoided of voltage surges arising when regulating the amplification by voltage division in the cathode circuit, surges which, at the extremely low cut-off frequency of the amplifier, might cause annoying fluctuations in the pattern on the screen.

Voltage division is carried out by switching over the cathode resistors in three groups, and a facility for continuous control is provided by potentiometer R_7. Next to the cathode follower come two pre-amplifying stages in cascade. The condensers in the cathode circuits here and in the output stages are small and serve only to boost the gain in the upper frequency band; furthermore, negative current feedback takes place via the cathode resistors. A further increase of the upper frequency limit is brought about by means of inductances L_1 and L_2 and L_3 and L_4 in the anode circuits.

These chokes are amply rated to exclude all possibility of overshoot. In this way too a very good phase characteristic is obtained. (See fig. 5–21a and b.)

The drive of the second valve in the balanced output stage emanates in this circuit neither from the anode resistor nor from the cathode, but from the screen grid of the first valve. The screen grid resistor, which, with respect to the chassis, must not be bypassed with a condenser as is the usual practice, is rated in such a way that the control voltage for the second valve has the same amplitude as for the first, except that it is shifted in phase by 180°. In this stage, type EL 41 output valves are used with their normal anode current of 36 mA in order to obtain sufficiently large deflection voltages with low anode resistors at an upper frequency limit of 3 Mc/s. The output voltages of this vertical amplifier are so large that undistorted oscillograms are possible extending in the Y direction beyond the useful screen of the cathode ray tube.

Thus, details can be observed in the Y direction with increased amplitude, corresponding to the use of a larger screen.
The maximum undistorted input voltage of the cathode follower amounts to 14 V_{rms} (about 40 V_{pp}). For higher input voltages an additional voltage divider is provided in the form of a probe, the circuit of which is given in fig. 5–41*b*. It can be seen that this is another frequency-compensated voltage divider as already described. The ratio of the resistances is arranged to allow a division of voltage in a ratio of 20 : 1, so that *AC* voltages of up to 280 V_{rms} (about 800 V_{pp}) can be observed. In the lower part of the voltage divider, the variable condenser C_{s6} lies in parallel with the input capacitance C_{in} and the capacitance of the cable. The variable condenser C_{s5} is responsible for frequency compensation [41]. The input resistance of the oscilloscope ($R_{in} = 1$ MΩ) is also shunted by the divider resistor R_s. If R_p has a value of 9.5 MΩ, then with a probe input resistance of altogether 10 MΩ, a voltage division of 20 : 1 is obtained. As the input capacitance of the probe only amounts to 8 pF, it is advisable to use the probe whenever possible and most especially with voltage sources having a high internal resistance (television receivers, time base circuits, etc.), as otherwise the input capacitance of the vertical amplifier with direct connection between terminals 5 and 6 will be less favourable (15 pF, input resistance 1 MΩ). The smallest possible deflection factor is 0.3 V_{rms}/cm. with probe and without probe (amplifier direct) it amounts to 15 mV_{rms}/cm. The cut-off frequencies lie at 1 c/s and 3 Mc/s; at 7 Mc/s the gain is still 30% of the average. Voltage pulses are faithfully reproduced from 50 c/s to 200 kc/s, and if the demands are not too high, up to 500 kc/s.
The cathode ray tube employed in this apparatus is the type DG 10–6, with $V_k = -1200$ V and $V_{a3} = +325$ V. The deflection factor amounts, for alternating voltage, to 8 V_{rms} (23.6 V_{pp})/cm, corresponding to a deflection sensitivity of $DS_{\sim} = 1.25$ mm/V_{rms} or $DS_{=} = 0.44$mm/$V_{=}$.

Further examples of deflection amplifiers are contained in part IV of this book, in which more details will be found on the rating of the circuit components, not only for amplifiers but also for the other structural sections.

Direct-voltage amplifiers are often used as independent units supplementary to the *AC* amplifiers incorporated in the oscilloscopes. Fig. 5–42 shows as an example the circuit diagram of the *DC* amplifier, type GM 4531, brought out by Philips.
When designing *DC* amplifiers, care must be taken, more so than when designing *AC* amplifiers with a very low frequency limit, that fluctuations in the supply voltage have no noticeable effect on the output voltage.
This amplifier is therefore designed symmetrically throughout. Moreover the valves in both pre-amplifying stages are heated in series and the heater-current is kept constant by a ferro-hydrogen resistor (8). The screen-grid voltage of the valves in the first amplifying stage is stabilized independently of the supply voltage by means of a type 85 A2 stabilizer valve (7).
The anode current is supplied by two rectifiers and filters in opposite polarity. This makes it possible to connect one pole of the input connections and one

[41] The component numbering is as used in the original circuit diagram.

pole of the output to the chassis. The input is symmetrical; asymmetrical input voltages can nevertheless be applied between sockets 1 and 2 or between 3 and 2.

The amplification of the first pre-amplifying stage with valves 1 and 2 is about 50 ×, having regard to the negative feedback due to the cathode resistors. The output voltage in the anode circuit of these stages must be divided by a ratio of 5 : 1 (resistors R_{20} and R_{21} and resistors R_{22} and R_{23}) in order for the requisite direct voltages to appear on the grids of valves 3 and 4 of the second stage. The resultant "net" gain of the first stage is 10 ×. In the second stage it is about 120 ×.

In the output, two valves, type UL 41 (5 and 6), are circuited as triodes in a cathode follower stage. This arrangement allows the connection to the amplifier not only of oscilloscopes but also of low-ohmic indicating devices (between sockets 4 and 5 minimum 5 kΩ) such as loop galvanometers or paper recording apparatus (Kelvin & Hughes Recorder "FE 104" or "FE 105") for recording slowly changing phenomena. The gain of this stage is about 0.8 ×.

For further stabilization, and to improve the frequency response of the amplifier, a second negative feedback (5-fold) is provided from the cathodes of valves 5 and 6 via resistors R_{16}, R_{17} and condensers C_1, C_2 to the cathodes of

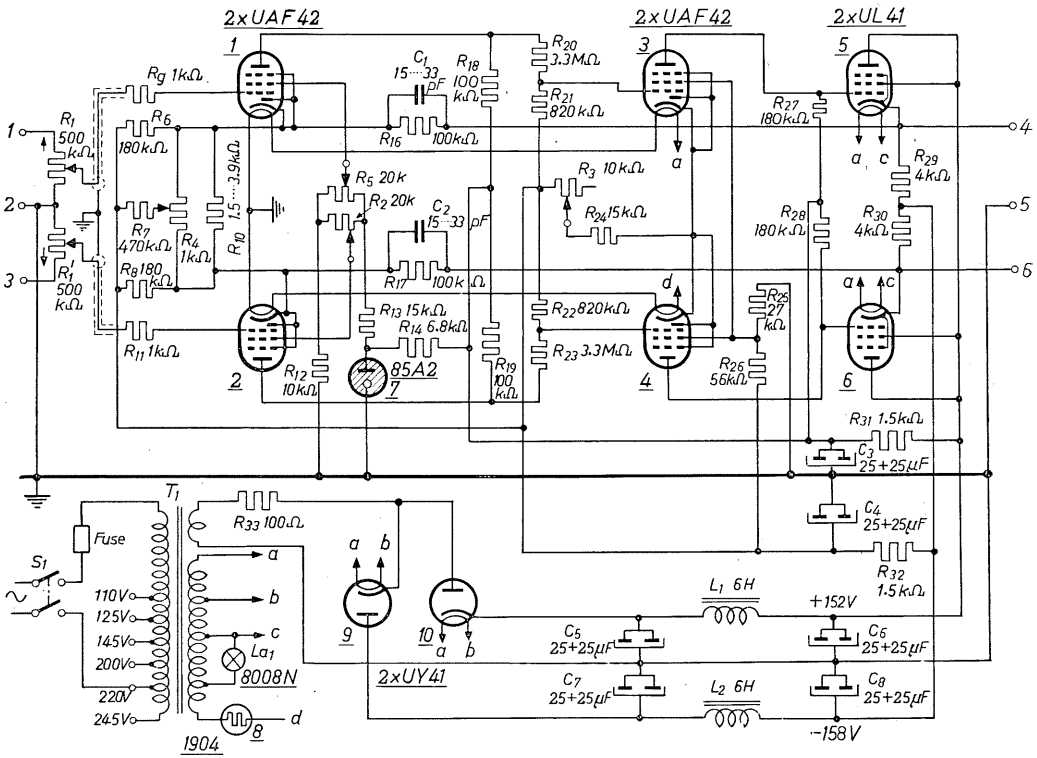

Fig. 5–42. *DC* amplifier, type GM 4531.

valves 1 and 2. The resultant total gain is 200 × with an upper cut-off frequency of 50 kc/s.

By means of potentiometer R_2 the screen grid voltages of valves 1 and 2 can be varied by a certain amount with respect to each other. The output voltage on sockets 4 and 6 is thus correspondingly displaced. The value of this displacement ($\pm$ 250 V_{max}) can be read on the scale beside the control button for R_2. In this way it is possible to adjust on the screen of the cathode ray tube the image of a suitably amplified composite input voltage—the alternating component being relatively small—and to obtain good analysis of the small voltage change. (See footnote 2 on page 137.) In a similar way the value of the *DC* input voltage can be determined directly, taking into account the adjusted gain.

The great constancy of valve working-voltages needed in *DC* amplifiers for still higher amplification involves a very considerable outlay. In Philips' amplifier type GM 4530, whose five stages provide a gain of 3,000 × (with certain limitations, up to 10,000 ×) all anode *DC* voltages are stabilized electronically in an extensive power pack, in addition to the measures described for the type GM 4531 amplifier. (See fig. 3–7.) Further provisions are made to reduce to a minimum the influence of changes in circuit components caused by ambient humidity or variations in temperature.

PART II

General Measuring Technique

6. Taking the Oscilloscope into service; adjustment procedure

Setting up the oscilloscope.

Although quite considerable brilliance of pattern has been achieved on the screens of modern cathode ray tubes, it is nevertheless desirable to set up the oscilloscope in a position where no direct light, either natural or artificial, will fall on the screen. [1]

The oscilloscope should not be set up beside a window where it might be necessary to adjust picture brilliance to an undesirably high value. To prevent light falling on the screen, a visor or light-shield is always to be recommended. Examples can be seen in fig. 6–1 and fig. 1–2. Using these, the operator will automatically be bound to keep the spot and thus the width of the electron beam small, achieving in this way the best pattern definition on the screen.

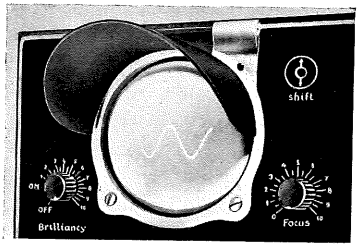

Fig. 6–1. Front panel of an oscilloscope showing visor for shielding the C.R.T. against incident light.

Switching on; brilliance and focus adjustment.

In general no special measures are needed when switching on. The brilliance should be turned right down beforehand to avoid overloading the cathode while the filament is warming up. The filament voltage should have been on for at least one minute before the brilliance control is turned up. If there is no deflection voltage on either of the pairs of deflection plates, what appears on the screen is the reduced image of the cathode. As the accuracy of picture definition is greater the smaller the spot, the voltage on anode a_1 must be adjusted by the focus control to produce the smallest possible spot on the screen. During this process the spot appears in several different shapes and sizes, as may be seen by referring back to fig. 2–7 on page 8. When the input voltage is on the Y plates simultaneously with the time base voltage on the X plates, the resultant oscillogram on the screen is adjusted for optimum definition with the brilliance and focus controls. Typical results are shown in fig. 6–2, which also demonstrate the influence of brilliance on the accuracy of picture definition. In fig. 6–2*a* the trace of the spot, although fine, is too faint to allow the whole pattern to be recorded satisfactorily with the camera. The most favourable brilliance is seen in fig. 6–2*b*, where the whole oscillogram can be observed distinctly without any loss of detail. If a strong presentation of the wave-shape is required, *c* is the right oscillogram. In *d* and *e* the brilliance is too high and the trace of the spot too broad so that certain characteristics of the waveform may well be obscured. Excessive brilliance also

[1] The light from the total charge of fluorescent lamps, with its strong ultra-violet component, can be particularly unfavourable, since this latter excites the entire screen into fluorescence so that it appears brighter than accords with its natural "whiteness".

involves the danger of the trace "burning in" on the screen, and this danger is greater the smaller the surface covered by the spot, that is to say, the greater the specific load on the screen. This fact should especially be borne in mind when there is a possibility of a deflection voltage cutting out for any reason. When large-area waveforms, (for example that of a modulated *RF* voltage) are under investigation, the brilliance must be turned up relatively high. If the signal now cuts out, the high power of the beam will be concentrated on the horizontal trace; this is one of the most frequent causes of burnt-in zero lines on cathode ray tubes.

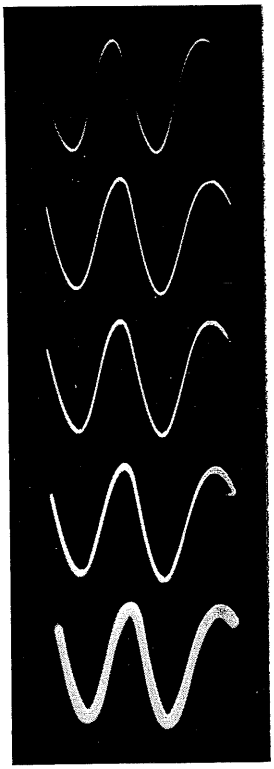

a) Fine definition but brilliance too low.

b) Most favourable setting.

c) Strong waveform.

d) Brilliance too high.

e) Details obscured by excessively thick trace.

Fig. 6–2. Oscillograms showing the influence of brilliance on the waveforms.

Astigmatism.

If there is an alternating voltage on the *Y* plates only, a vertical trace will appear on the screen. When adjusting the sharpness of this trace, we find that the setting of the focus control is different from that which was needed for the horizontal trace, the extent of the difference depending upon the tube in question. This is due to an imperfection in the electron lens of the cathode ray tubes and, by analogy with the corresponding correction error in light optics, is referred to as "astigmatism".

In fig. 6–3, three sections of oscillograms are reproduced, enlarged about $1^1/_2$ times, showing the result in such a case at the junctions of these traces. In a), the horizontal trace is sharply focused and in b), the vertical trace. (A tube with marked astigmatism was chosen for the purpose of illustration.) With such tubes a compromise must usually be struck between both settings (fig. 6–3*c*). The smaller the difference between them, the better will be the overall focus of the pattern. In certain high-duty oscilloscopes a control is provided by means of which the mid potential of the deflection plates can be made to equal that of the final accelerating anode. This avoids the additional

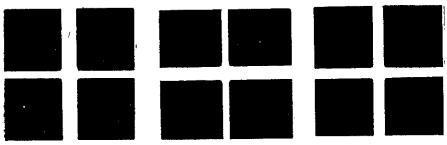

a b c

Fig. 6–3. Co-ordinate traces of an astigmatic cathode ray tube.

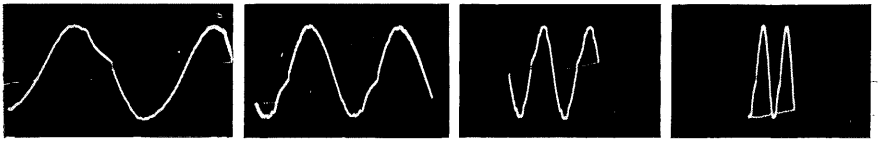

a b c d

Fig. 6–4. Choice of picture width.

astigmatism which might otherwise result from the potential difference between these electrodes.

Picture width.

The width of the pattern on the screen can be adjusted by varying the voltage on the X plates. It is clear that the "time expansion" of the phenomena being observed will be greater the wider the oscillogram can be made (the time base frequency remaining the same, of course). Nevertheless, there are certain limitations.
Fig. 6–4 shows the influence of the picture width on the pattern on the screen. For this oscillogram the time base voltage applied was so high that the waveform under investigation passed beyond the edge of the screen.
The curvature at the edges of the screen then distorts part of the oscillogram. This large width is restricted to special cases. The oscillogram in b) shows the most advantageous width for general purposes, as the whole screen is used for the display without the useful surface being exceeded. The setting as in c) may be preferable for some purposes, although some subtleties of the waveform are lost by compression along the time axis. The pattern shown in d) would be most unfavourable.

Picture height.

Directly connected with the question of the most useful width of picture is the question of the most advantageous height of the picture. This too can be adjusted by varying the amplitude of the signal applied to the Y plates.
Fig. 6–5 gives a number of oscillograms from which it can readily be seen which setting will probably be the most favourable. In a) and b) the waveform again goes beyond the useful surface of the screen. This setting will only be serviceable for special investigations [2]. The wave-

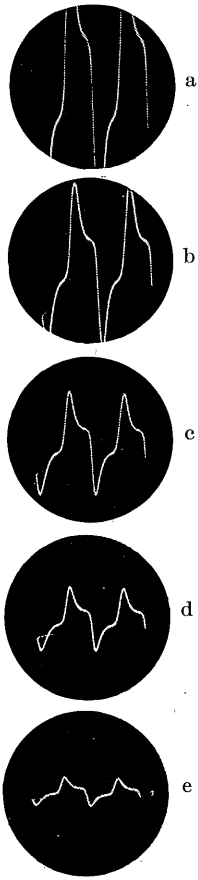

a b c d e

Fig. 6–5. Choice of picture height.

[2] Of course it is possible in this way to observe details in the Y direction which would correspond to observation on a larger type of tube. In fig. 6–5*a*, for example, the centre of the oscillogram appears enlarged. With the vertical shift control one can then observe the other portions of the waveform (top and bottom) by shifting them to the centre of the screen. This method was used to obtain the oscillogram in fig. 15–19 (page 248) which shows the upper peak of the waveform of fig. 15–17*a* (see chapter 15).

forms in c) and d) are clearly the most advantageous; which setting of the two is to be preferred depends upon the intention. In e) not enough details are visible in the Y direction.

Synchronization.

Numerous applications of the oscilloscope are concerned with the observation of periodically recurring phenomena in dependence upon time. If the time base frequency is adjusted to be a whole fraction of the frequency of the signal on the Y plates, the patterns obtained on the screen show in inverse proportion one or more whole cycles of the phenomenon under investigation. If the frequencies are identical, one cycle appears on the screen; if the time base frequency is one half of the frequency on the Y plates, two cycles appear, if one third, then three cycles are shown, and so on.

Only when the time base frequency is a mathematically exact whole fraction of the input signal will the oscillogram be perfectly stationary, drifting neither to the left nor to the right, for only then does the spot describe the trend of the input signal in exactly the same path on the screen. When there is no synchronization, the traces described by the individual cycles of the time base no longer appear one above the other but side by side, resulting in blurred or superimposed oscillograms.

In fig. 6–6a the time base frequency is much too high; as synchronization was nevertheless attempted, the sloping edge typical of over-synchronization can be seen, particularly on the right.

In fig. 6–6b the time base frequency approaches that of the input signal, but synchronization was introduced too soon and too strongly, producing the result as shown with the characteristic slope at the right-hand edge.

Fig. 6–6c is likewise the outcome of premature and excessive synchronization. If the time base frequency had been reduced slightly a steady oscillogram of six cycles of the input signal would have been obtained.

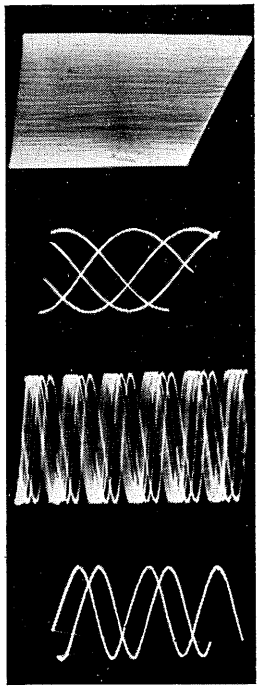

Fig. 6–6. Oscillograms showing the effects of bad synchronization.

In fig. 6–6d, correct synchronization with 2 or 3 cycles of the input signal is only just out of reach.

Choice of the most suitable relationship between input frequency and time base frequency.

The eight oscillograms shown in fig. 6–7 give an idea of these relationships and an indication of the possibilities offered by expanding the display on the screen (time base magnification effect).

Fig. 6–7. Various possibilities of expanding the time base display by a suitable choice of sweep frequency.

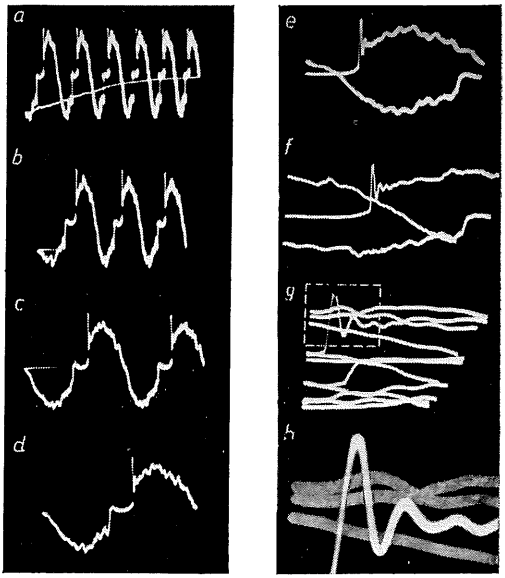

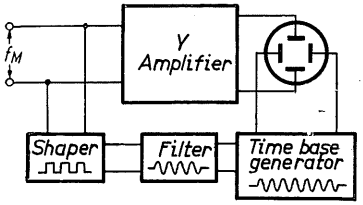

Fig. 6–8. Block diagram of circuit for synchronizing the time base frequency with a multiple of the input frequency.

The oscillograms are of the 50 cycles mains voltage, which was not, however, directly applied. Waveforms of this sort are obtained when a short length of wire is inserted into the input terminal of the vertical amplifier, the other end of the wire being left free. Due to the capacitive coupling of this wire with the mains, a current flows in the input impedance of the amplifier which sets up a corresponding alternating voltage on the grid of the first valve. Everyone who has worked with oscilloscopes is familiar with this phenomenon, often only too well, as the stray coupling can sometimes lead to difficulties when other small voltages from sources with high internal resistance are to be observed. Since the coupling capacitance for this current is small, the fundamental frequency (50 c/s) is weakly coupled while the harmonics that are always present in the mains voltage receive preference. This is therefore a simple means of bringing out harmonics and distortions in the display. Very few details can be perceived in fig. 6–7a, as the six cycles are bunched together too much. Even here, however, short peaks are visible at the crests which become more distinct when the number of cycles displayed is reduced (greater time base expansion). But even with only one cycle it is still not possible to ascertain the trend of the voltage curve at this point.

Whereas it is not easy to synchronize the time base frequency to multiples of the input frequency [3], with most time base generators it is possible, after a little practice, to adjust fairly stationary patterns on the screen when the time

[3] Synchronization is achieved by arranging for the peak value of every first, second, third, etc. cycle of the input signal to trigger the flyback of the time base voltage. However, if the frequency is lower than the time base frequency, then upon one cycle of the input will fall several cycles of the time base, and of these, only that cycle whose peak value coincides with that of the input will be synchronized. The cycles in between will not be influenced.

base frequency is several times higher than the input frequency, thus obtaining an accordingly increased time analysis. In fig. 6–7e the time base frequency, is twice as high. It can now be seen plainly that the peak in the oscillogram corresponds to the behaviour of a damped oscillation. This is plainer still in the next oscillogram where the time base frequency is three times as high. The following pattern, however, is the result of a time base frequency eleven times higher than that of the input, thus 550 c/s. It can easily be calculated from the average length of the time base and the wavelength of this phenomenon that the natural frequency of the damped oscillation, caused by a voltage surge, is about 3800 c/s. It was found that it actually originated from the secondary of a nearby E.H.T. rectifier which had been excited into oscillation by the charging current surges through the valve. The final oscillogram. fig. 6–7h, is an enlarged photographic reproduction (about $2^1/_2$ times) of the indicated portion of fig. 6–7g. This proves that a very great degree of oscillographic analysis is possible with simple means.

If such requirements are frequent, however, a circuit should be built as indicated by the block diagram in fig. 6–8. In this layout the input signal is fed to an auxiliary amplifier, a "shaper", as well as to the vertical amplifier. The operating point of this extra amplifier is adjusted in such a way as to severely distort the voltage waveform and produce as square a wave as possible which, as we know, is rich in harmonics. The shaper is followed by a filter which picks out the harmonic desired and passes it on to synchronize the time base generator. The filter is necessary above all to suppress the fundamental frequency, as this always has the largest amplitude and would otherwise influence the time base in the manner already described. Of course, this method produces an oscillogram in which the individual pictures of one cycle of the signal appear one above the other, as seen in fig. 6–7g and h. A particular section from the total picture of a cycle of the phenomenon under observation can be obtained by triggering, or with the aid of a time base expansion unit. (See chapter 4 under "Time base expansion unit", p. 77, "sawtooth generator for pulse triggering", pp. 72–76, and chapter 22 "A simple time base expansion unit". Oscilloscopes with a facility for triggering the time base by a positive or negative voltage pulse are an ideal means of carrying out investigations of this sort. In so far as the time base is triggered by the output of the vertical amplifier, the picture on the screen begins at the zero line with the positive or negative half cycle, according to choice. If, on the other hand, the part of the input voltage for triggering the time base is fed in externally via a phase shifter, a greatly expanded image can be obtained of any desired part of one cycle of the phenomenon being investigated.

With every good oscilloscope it is possible, to synchronize the time base generator in three ways: with the voltage on the *Y* plates (internal synchronization), with a voltage from an external source (external synchronization) and with the mains frequency (mains synchronization). The intelligent use of these methods of synchronizing the time base opens up many valuable fields of application, but experience shows time and again that use is made only of internal synchronization. Using external synchronization, on the other hand, it is possible with a given voltage to synchronize in a reference phase position. If this synchronization is maintained and, in place of the first

voltage, a second voltage is applied with the same frequency but in a different phase, it will appear on the screen displaced along the time axis in a way exactly corresponding to its phase relationship with the first voltage. (The oscillograms in figs. 5–10, 5–11, 5–12 and 5–13 were recorded in this way.) If these two voltages are then applied alternately to the *Y* plates (electronic switch) pictures will appear one after the other of both voltages in their correct phase relationships. Naturally, more than two voltages can be observed or recorded in this way. An accurate insight into the phase relationships and behaviour of any number of voltages can be obtained by photographing on the same recording-material each voltage in turn. (See figs. 13–6, 13–8 and 13–9.)

7. Simple amplitude measurement

Nature of the display.

A given vertical deflection of the spot on the cathode ray tube screen presupposes a correspondingly large *voltage* applied to the vertical deflection plates.
Since the leak resistors for the deflection plates (as also the input resistors of the amplifier) are in the order of 1–10 Megohms, the current flowing, and thus the load on the circuit under test, is extremely small. The oscilloscope can therefore be regarded in principle as a static voltage indicator [4]. The familiar indicating instruments are, with very few exceptions (static voltmeter), actually *current* meters, as an appropriate value of current is a prerequisite for the information to be indicated. The user of the oscilloscope should always bear these facts in mind, as they open up in themselves alone wide fields of application and lead quite logically to the correct use of the instrument. It is true that with an increasing frequency of the voltage under measurement the capacitance of the deflection plates represents a rising capacitive conductance. When the capacitance of the deflection electrodes (including connection capacitance) is about 10 pF this means that the impedance will be approximately only 160 ohms at 100 Mc/s. However, in most cases it will be possible to include this capacitance in the circuit capacitance so that it will not appear as a load in this sense.

Accuracy of the display and limits of measurement.

In practice the fullest possible use is not always made of the extraordinary advantages offered by the oscilloscope in quantitative investigations, i.e. in determining the absolute value of a quantity or amplitude under test.
It is, of course, necessary to know to what extent the spot deflection is proportional to the voltage applied, what the smallest ascertainable change of spot deflection is (accuracy of definition), and what influence fluctuations of the mains voltage have on the results of the measurement, etc.

[4] With *AC* voltages, the power required for 1 cm deflection with a leak resistance of 5 MΩ is approx. $2 \cdot 10^{-5}$ W. When using a deflection amplifier it drops to 10^{-12} W and lower.

Linearity of the display.

The deflection plates of modern cathode ray tubes are constructed and arranged in such a way as to ensure a linear relationship between the voltage applied and the deflection of the spot over the whole area of the screen. If, for example, for 10 volts *DC* between both plates a deflection is obtained of 4 mm (deflection sensitivity 0.4 mm/V), then for 25 V the deflection is 10 mm, for 50 V it is 20 mm, and so on. This, of course, applies to both directions of deflection, as may be perceived from fig. 7–1. For these illustrations a voltage linear with time was applied to one pair of plates, while on the other a *DC* voltage was raised in steps of 25 V. A photographic recording was then taken of each such position with respect to the other on the same negative. (Fig. 7–1*a* thus consists of 20 and fig. 7–1*b* of 22 separate recordings). In fig. 7–1*a* these deflections were recorded such that they corresponded to the different deflection sensitivities of both pairs of plates. (The vertical deflection plates have a higher sensitivity.)

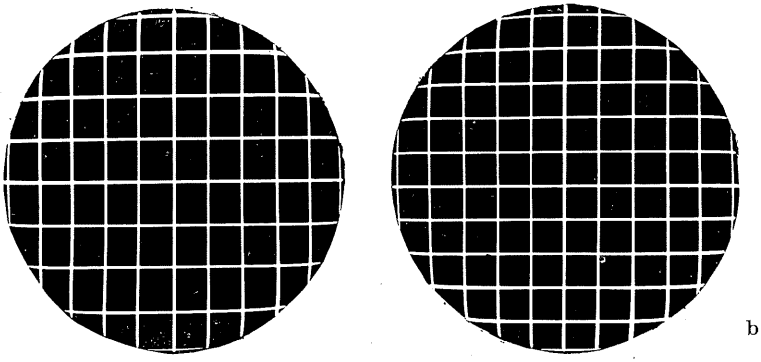

Fig. 7–1. Co-ordinates formed by deflecting a linear trace with *DC* voltages in steps of 25 V; *a*) without sensitivity correction of the *Y* plates, *b*) deflection sensitivity of the *Y* plates matched to the *X* plates by voltage division.

The deflection voltage for producing the trace was chosen high enough to permit ample coverage of the screen; it can thus readily be seen in what area a linear display may be expected and where the curvature of the screen will cause distortion. This is shown more distinctly in fig. 7–1b. In this case the sensitivity of the *Y* plates was reduced to that of the *X* plates, resulting in a quadratic grid. Characteristic of the inertialess functioning of the cathode ray tube is the fact that small voltage changes, which the small indicating instrument used for comparison failed to register after the voltages had been adjusted, are plainly visible on the screen of the oscilloscope. (In fig. 7–1*a*, the second horizontal line above the centre line is rather too low.)

Reading off the display.

The simplest way of reading off the spot deflections is to use a suitable strip of transparent graph (millimetre) paper. Frequently the screen is covered by a

transparent plastic or celluloid sheet bearing a number of crossed lines in the form of a lattice, the distance between the lines being 5 mm or 1 mm. (See fig. 7–2.) In high-grade oscilloscopes flood-lit scales are used, the scale being marked on a thick strip of transparent material which is illuminated from the sides by electric bulbs with variable intensity. Fig. 7–3 shows as an example the scale used on Philips' GM 5660 oscilloscope, with the oscillogram of a pulse 1 μsec wide. (The overshoot visible originated from the voltage source. This was confirmed by a cross-check in which the voltage was applied direct to the deflection plates.)

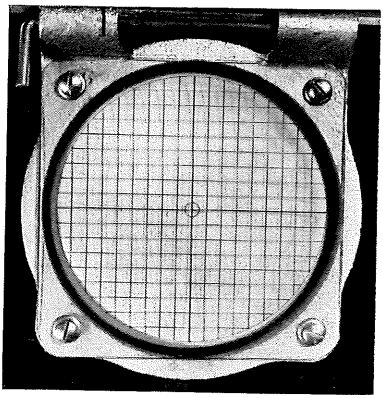

Fig. 7–2. Calibration lattice fitted over the screen of the C.R.T. for amplitude measurements.

A scale of this sort has the great advantage that it does not cover over parts of the screen as the lattice in the photograph does but is perfectly bright and visible together with the phenomena under observation. When the illumination is turned down it becomes almost imperceptible so that it is not troublesome

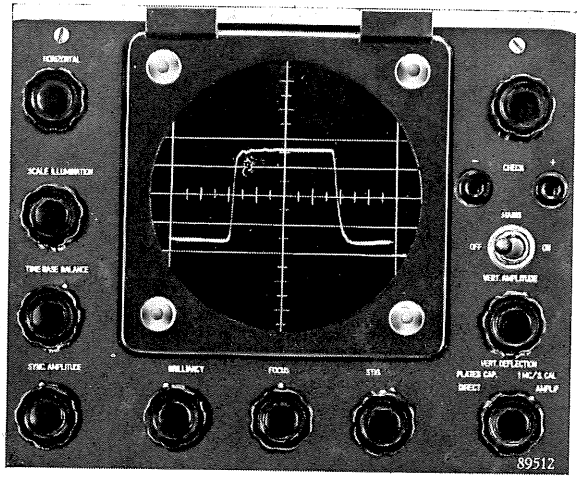

Fig. 7–3. Oscilloscope type GM 5660 with floodlit scale.

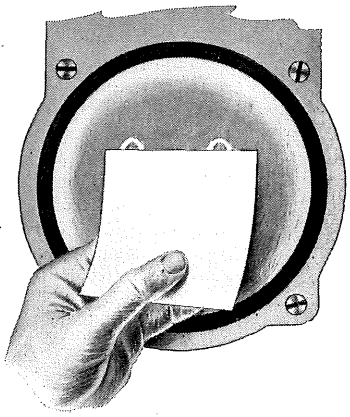

Fig. 7–4. Observing small changes in amplitude.

during tests which require no amplitude measurement. The scale illumination can also be used to indicate whether or not the oscilloscope is switched on. If it is required to observe small changes in amplitude, a practical method is to cover the lower portion of the display with a sheet of thin pressboard or stout paper. Peaking of the crests is then readily observable (fig. 7–4).

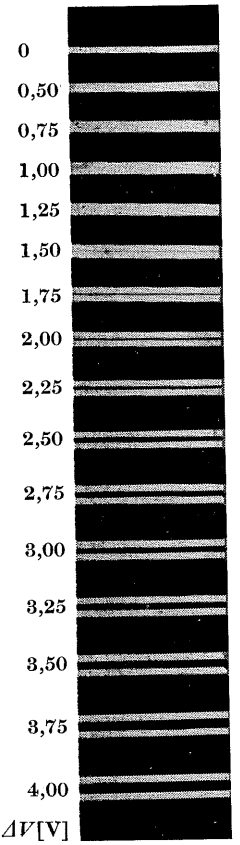

Fig. 7–5. Enlarged sections of photographs of the horizontal trace, first without vertical deflection and then with *DC* vertical deflection increased in each case by ΔV, to determine the accuracy of reading from the screen. (Deflection sensitivity $DS_{=}$ = 0.4 mm/V.)

Accuracy of definition.

The oscillograms in fig. 7–5 are intended to illustrate the maximum accuracy of definition obtainable on the screen. They reproduce sections from the horizontal trace enlarged about $1^1/_2$ times. The first trace above is an extract from the trace in zero position. The second picture actually represents two traces, namely the trace in the zero position and a trace vertically deflected by a *DC* voltage of 0.5 V. In the following oscillograms the zero trace is represented together with its position when vertically deflected by a *DC* voltage $^1/_4$ V larger in each case. We can thus easily ascertain that voltage at which the two traces only just separate from each other. This is clearly the case in the seventh picture from above, at 1.75 V [5].

The spacing between the spot centres is then, therefore, somewhat greater than the diameter of the spot (in this case about 0.7 mm). In the third picture from the bottom one could also find a definition for the readable change of voltage. This recording was taken at a voltage difference of 3.5 V (twice that of the criterion already discussed).

The dark intermediate space is now approximately equal to the thickness of the trace. (See also "Limiting effect of spot diameter on frequency", pp. 68–69.)

Influence of the amplifier on the linearity of the display.

It is understandable that a practical limit is set to all measures aiming at good linearity in conjunction with an adequate output voltage. Thus, the lowest possible anode resistors must be employed if high frequencies are to be uniformly amplified, so that the undistorted voltage drive of the output stages of the amplifier is limited accordingly. In the case of amplifiers with a high upper cut-off frequency one is therefore compelled to make shift with a limitation of the undistorted control voltage amplitude. (See chapter 5 "Deflection amplifiers —output voltage requirements"—page 113.)

As an example, fig. 7–6 shows the dynamic characteristics of the amplifier in the oscilloscope "FTO 2" (see part IV) together with the lattice of the floodlit scale. Characteristics of this sort can be easily obtained by feeding a suitably chosen portion

[5] The procedure adopted here is the practical one. The smallest still readable change of voltage might also be defined theoretically as that value of voltage at which the blackening between the two bright traces of the spot is at the most 1/e = 0.37 times the blackening of the remaining background of the picture.

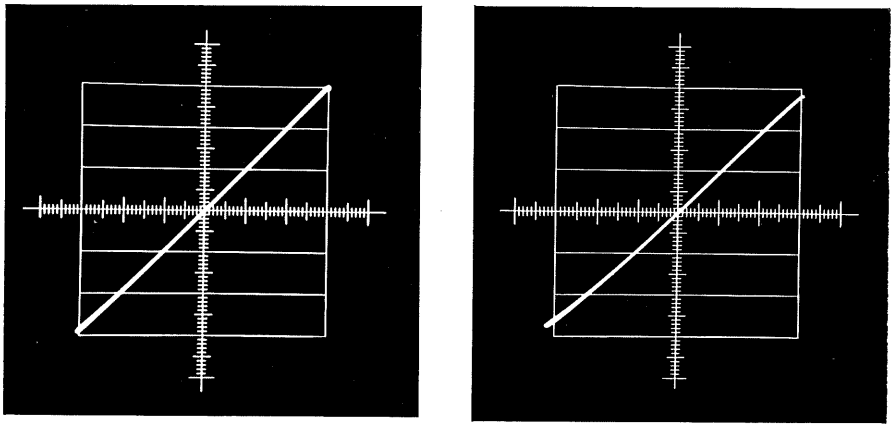

a b

Fig. 7–6. Dynamic characteristics of the vertical amplifier in oscilloscope "FTO 2"; *a*) with +265 V on a_3; *b*) with +1.2 kV on a_3.

of the time base voltage of the oscilloscope to the vertical amplifier. For various values of the time base voltage in the horizontal direction the spot then traces out simultaneously the corresponding deflection in the vertical direction due to the amplified voltage from the amplifier under investigation. If the gain has been adjusted such that the Y deflection is equal to the X deflection, then with an ideal amplifier the spot must trace out a straight line at an angle of 45°. The grid drive limitation of the amplifier, conditioned chiefly by the low anode resistances, expresses itself in a more or less severe S-bend at the ends of the characteristic.

In fig. 7–6a the spot is deflected in the vertical direction only to the maximum permissible "useful drive" for 60 mm picture height. It can readily be seen that up to 40 mm picture height the characteristic may be regarded as straight even for high demands. Up to 60 mm the bend still represents less than 3% distortion. Such slight distortion in the oscillogram of a sine wave would only be ascertainable by very experienced observers.

With the post-acceleration voltage of 1.2 kV in oscilloscope "FTO 2" an approximately 30% higher deflection voltage is necessary, so that greater amplitude distortion will result for the same picture height. However, fig. 7–6b shows that the characteristic up to 40 mm deflection in the Y direction may be regarded, even under these conditions, as sufficiently linear.

Dependence of the deflection sensitivity upon the mains voltage.

For practical work it is important to know the influence of mains voltage fluctuations upon the display. Fig. 7–7 shows in this context the change in the sensitivity of the cathode ray tube alone—curve α—and the sensitivity curve (β) when using the vertical amplifier in oscilloscope "FTO 2". As expected, the deflection sensitivity of the cathode ray tube alone is linearly inversely proportional to the mains voltage. If, therefore, the mains voltage falls by 5%,

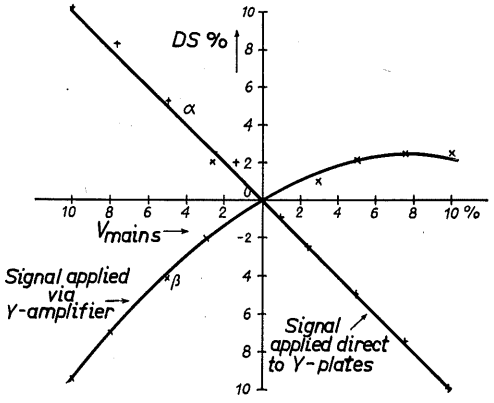

Fig. 7–7. Sensitivity of the C.R.T. in dependence upon changes in mains voltage (in "FTO 2").

the deflection sensitivity will rise by the same extent and vice versa. (See chapter 2 "Cathode Ray Tubes—Deflection of the beam" p. 9.) When the deflection amplifier is used, however, it naturally exerts an influence on the deflection sensitivity. If the mains voltage rises, the mutual conductance of the amplifier valves becomes greater and vice versa, so that according to the number of amplifying stages (or the adjusted gain) a measure of compensation, within certain limits, exists for changes in the sensitivity of the cathode ray tube. Curve β shows that, at small fluctuations of the mains voltage, smaller changes in sensitivity occur. But even the influence of larger fluctuations of the mains voltage is smaller than on the cathode ray tube alone.

The influence of mains voltage fluctuations can be eliminated to a great extent by electronically stabilizing the *DC* supply voltages.

In Philips oscilloscope GM5654, for example, the anode high tension (fig. 3–7) is electronically stabilized as well as the E.H.T. The results of measurement are thus largely unaffected by mains voltage fluctuations, and changes of picture brilliance and deflection sensitivity, which are particularly troublesome when making photographic recordings, are thereby entirely avoided.

Relation between deflections due to *DC* voltages and those due to *AC* voltages.

It has been shown that the deflections of the spot over the whole screen are linearly proportional to the voltage applied. This applies to *DC* as well as to *AC* voltages. With *AC* voltages, however, the maximum amount of deflection due to a voltage whose r.m.s. value has the same amplitude as a given *DC* voltage is several times greater than the deflection due to the *DC* voltage.

As the spot always follows the instantaneous value of the voltage at the frequencies under consideration, it will always be deflected to the *maximum* positive and negative value of an *AC* voltage. By the r.m.s. value I_{rms} of a sinusoidally alternating current with a maximum value I_{max} is, of course, understood that current which generates the same amount of heat in an ohmic resistance as is generated by a corresponding value of direct current, measured with a direct current instrument. Mathematically, the following familiar equations are derived:

$$I_{max} = I_{rms} \cdot \sqrt{2} = I_{rms} \cdot 1.414 \qquad (7\text{–}1)$$

and

$$I_{rms} = \frac{I_{max}}{1.414} = I_{max} \cdot 0.707\,. \qquad (7\text{–}2)$$

The extremes of the deflection with *AC* voltage will therefore lie $2 \times \sqrt{2} = 2.828$ times further apart (in a positive or negative direction according as the direction of current changes) than the deflection by a *DC* voltage of the same value. This means in other words that the deflection sensitivity for *AC* voltage is greater to a corresponding extent, leading to the equation:

$$DS_{\sim} = DS_{=} \cdot 2.828 \qquad (7\text{–}3)$$

These conditions are illustrated in the oscillogram in fig. 7–8. With a *DC* voltage of 50 V, the spot was deflected vertically a) and along the time axis b). Above this the spot traced out its path with an *AC* voltage of 50 V_{rms}. For alternating voltage measurements especially we can also work without time base deflection; a correspondingly long vertical trace is then obtained. If the time base voltage is synchronized to this frequency then it is possible to measure the distance between the crests of the curve ("peak-to-peak—V_{pp}"). If it is only a matter of determining the voltage it may be appropriate to select the time base frequency considerably higher or lower than the frequency of the input signal. This produces a luminous area, the height of which is to be measured.

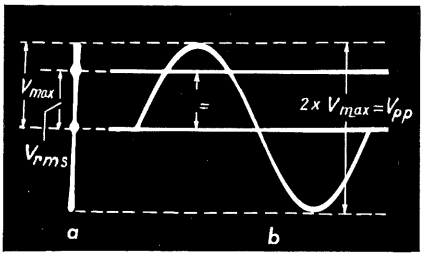

Fig. 7–8. Oscillograms illustrating beam deflection with *DC* and *AC* voltages.

DC voltage measurements.

When the amplitude of the voltage to be tested is adequate, it can be applied directly, that is to say, without amplification, to the *Y* plates. Fig. 7–5 shows that with a deflection sensitivity of $DS_{=} = 0.4$ mm/V and a trace breadth of 0.7 mm, a voltage difference of 1.75 $V_{=}$ can be read off quite distinctly. If we take a maximum deflection of 40 mm from the zero position (corresponding to 100 $V_{=}$) this value can be read off with an accuracy of a good 1.75%. At smaller deflections the degree of uncertainty will indeed be greater, but about 3% should be the expected average.

For measurements of this sort it would certainly be possible to dispense with deflection in the *X* direction; in general, however, it is better to have a time base voltage with a frequency of about 100–1000 c/s describing a short trace. This trace will be moved by the *DC* voltage, just like the pointer of an ordinary indicating instrument. A scale can then be fitted, calibrated according to the deflection sensitivity. Fig. 7–9 shows a scale of this type and the picture on the screen with a *DC* deflection voltage of 43 V. In this way it is possible to

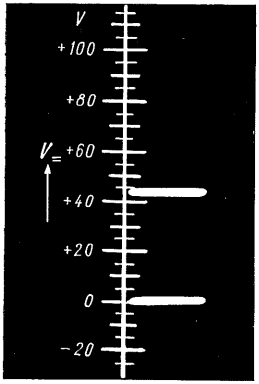

Fig. 7–9. Scale for *DC* measurement; positions of the trace with 0 V and 43 V on the *Y* plates.

measure not only all anode and, above all, screen-grid voltages in radio receivers and amplifiers, but also A.V.C. voltages, grid bias, etc., as long as they are not too small, the polarity of the deflection plates being such that a positive voltage will produce an upward deflection and a negative voltage a downward deflection.

Fig. 7–10 shows the circuit of a device by means of which *DC* voltages can be read off from the minimum perceptible value to 1300 V when using a cathode ray tube with a sensitivity of $DS_= = 0.4$ mm/V. Up to 100 V, intermediate values must be read off a scale on the screen. The accuracy of the reading decreases with diminishing voltage. When a large input impedance is required, the switch *S* is set in position 2 and resistor R_1 is adjusted to its highest value. For voltages higher than 100 V the positions of switch *S* should be chosen as indicated in the circuit. Within the given voltage range, the setting of potentiometer R_1 should now be such that the spot deflection will be just as large as with direct connection of 100 V. From the position of the indicator on potentiometer R_1 the value of the voltage under test can be read off directly, after the angle of rotation has first been

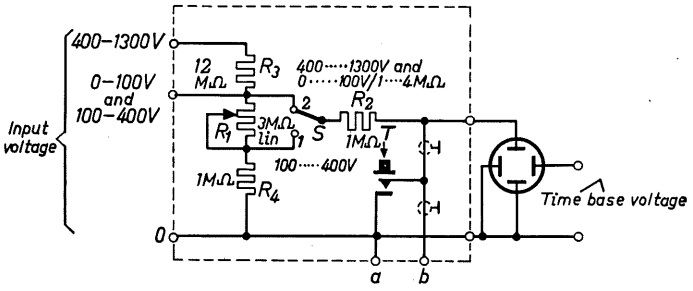

Fig. 7–10. Circuit of auxiliary device for measuring *DC* voltages in ranges of 0–100 V, 100–400 V and 400–1300 V.

calibrated (the ohmic value and the voltage scale run counter to each other). The great advantage of this is that it is now possible to work with the greatest possible accuracy of reading, namely $\leq 2\%$.

By shorting button *T*, the zero starting position can be restored at will, and thus the deflection difference very distinctly ascertained. (The resistor R_2 prevents short-circuiting of the input voltage source.) It may be useful to restore this contact at rapid intervals by means of a relay in conjunction with an electronic switch, so that both positions of the spot can be observed simultaneously. A device of this sort can be connected to terminals a and b [6].

[6] The input terminals and the series resistors must be well insulated and made safe. When measuring *DC* voltages, auxiliary voltages for correcting the zero position should be

In this way it is possible to read distinctly very small deflections of the spot. The cathode ray tube is, as we have seen, a *voltage* indicator. Current measurements are therefore only possible by measuring the voltage drop across a resistance of known value in the circuit. As the voltage loss must be kept small, *DC* measurements are as a rule possible only with the aid of a *DC* voltage amplifier.

AC voltage measurements.

The uses of the oscilloscope in measuring *AC* voltages are very numerous indeed. The vertical amplifier makes it possible to investigate an extremely wide range of voltages, and, with a suitable amplifier, measurements of voltages down to a few millivolts or microvolts can be carried out in a large range of frequencies. With the majority of oscilloscopes the maximum sensitivity of indication is known (the fine adjustment control being fully turned up); intermediate values can be estimated according to the position of the control. For more exact quantitative analysis, comparison with a known 50 c/s voltage,

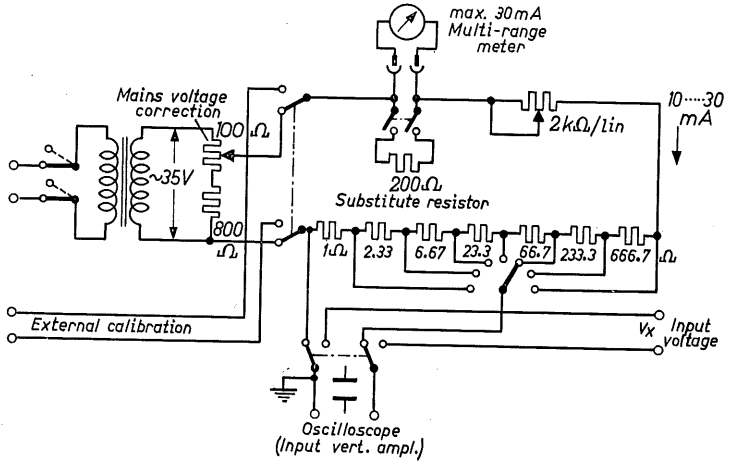

Fig. 7–11. Circuit of a calibration unit for *AC* voltages.

possibly calibrated by a measuring instrument, is very much to the purpose. A facility of this sort is provided in oscilloscopes which are especially intended for the quantitative evaluation of oscillograms (Philips' GM 5660). If no such facility exists, users of the oscilloscope will be well advised to have such a calibration instrument made. Fig. 7–11 shows the circuit of an instrument of this type and fig. 7–12 a photograph of an actual apparatus. Measurement is effected by alternately applying the unknown voltage and the calibration voltage to the input terminals of the oscilloscope.

switched off. As these are fed in via the high-ohmic leak resistors, the effective voltage on the deflection plates would be dependent upon the internal resistance of the input voltage source and the beam deflection would suffer in consequence.

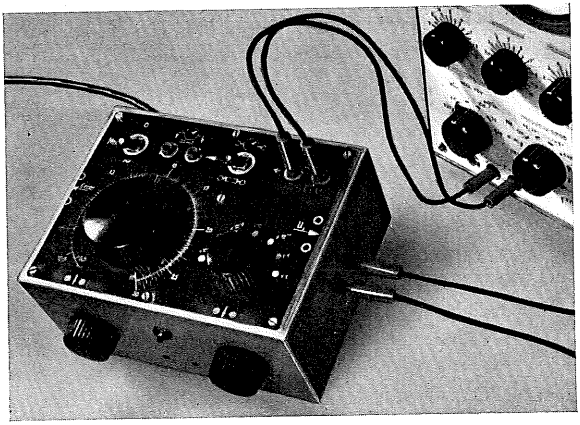

Fig. 7–12. Practical model of calibration unit for *AC* voltages.

By means of the 2 kΩ intermediate control, the amplitude of the calibration voltage is adjusted in such a way that it causes the same peak values as the unknown voltage. In this manner it is possible with the calibration unit to adjust all values of voltage between 10 mV and 30 V (r.m.s.). The instrument shown can also be replaced by a resistor with the value of the instrument resistance, but fluctuations in the mains voltage will then be included in the measurement. A calibration voltage with a square waveform is particularly advantageous. In so far as synchronization with the time base voltage is deliberately avoided, two horizontal traces will be obtained on the screen which lend themselves very well to amplitude calibration. A voltage of this sort can be generated quite simply by means of a glow-stabilizer valve, connected via a resistor across an alternating voltage source with 50 c/s mains frequency. The top of the sine wave will then be clipped at the height of the operating voltage. (See oscillograms fig. 11–19 and fig. 22–3a and b.)
If a stabilizing valve with an especially constant operating voltage is used, as, for example, type 4687, the calibration voltage will be largely independent of the mains voltage and extraordinarily constant during the life of the valve.
To measure alternating currents it is necessary, as with direct currents, to connect a small value resistor with a known resistance in circuit; the voltage drop across this is then observed on the screen. The larger the gain of the vertical amplifier, the smaller may be the resistor and the current.

Determining the voltage amplitudes by vertical displacement of the pattern and measuring the shift voltage.

It has been shown in the foregoing how, by comparison with a sinusoidal voltage whose maximum amplitudes deflect the spot by an equal amount, the peak-to-peak value can be measured even of an irregularly alternating voltage. It is sometimes also necessary, however, to determine the exact values of

individual sections of the voltage curve (in the Y direction), apart from the desirability of increasing the accuracy of reading.

All these measurements can be very conveniently carried out by determining that value of the shift voltage (DC) by which the interesting point on the curve can be moved vertically to the same position on the screen as the zero reference line or to some other point of reference.

Fig. 7–13*a* shows, to begin with, a normally adjusted oscillogram of a sinusoidal voltage with peaky crests.

In fig. 7–13*b* the oscillogram has been shifted so far upwards as to bring the lowest point of the sine wave to lie upon the zero line.

For oscillograms 7–13*d* and 7–13*e*, the appropriate settings for the positive crest of the sine wave and the positive voltage peak were found with shift voltages of —15.5 V and —65 V respectively. According to this the value for the sinusoidal voltage is $v_{\sim} = 31\ V_{pp}$ and that for the peaks is $v_p = 130\ V_{pp}$.

This procedure has proved itself particularly useful for evaluating pulse-shaped oscillograms as frequently occur, for example, in the investigation of blocking oscillators and multivibrator circuits. For this type of quantitative evaluation the type GM 5660 pulse oscilloscope is particularly suitable. As the circuit in fig. 7–14 shows, the DC voltage for the vertical shift is also led from the arms of potentiometers R_{55} and R_{56} to sockets 11 and 12. To these sockets may be applied a high-ohmic voltmeter (Philips' type "P 811") and the shift voltage measured for the purpose described. Quite frequently the amplitude of the test voltage is sufficient for direct connection to the deflection plates, in which case the vertical amplifier—whose frequency limits always restrict the measuring range—may be dispensed with. As regards pulsed voltages with short rise-times, this is most welcome; the faithful reproduction of the waveforms is then limited only by the

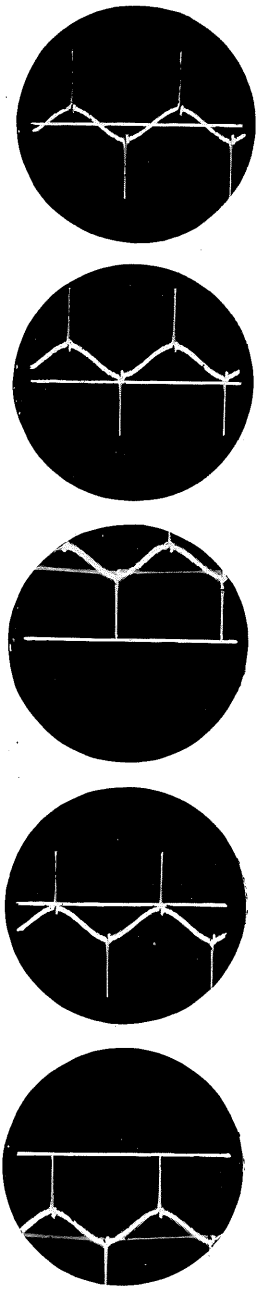

Fig. 7–13. *Oscillograms for evaluating the amplitudes of different sections of an alternating voltage*: *a*) usual setting; *b*) determining the negative crest of the sine wave; *c*) determining the negative voltage peak; *d*) determining the positive crest of the sine wave; *e*) determining the positive voltage peak.

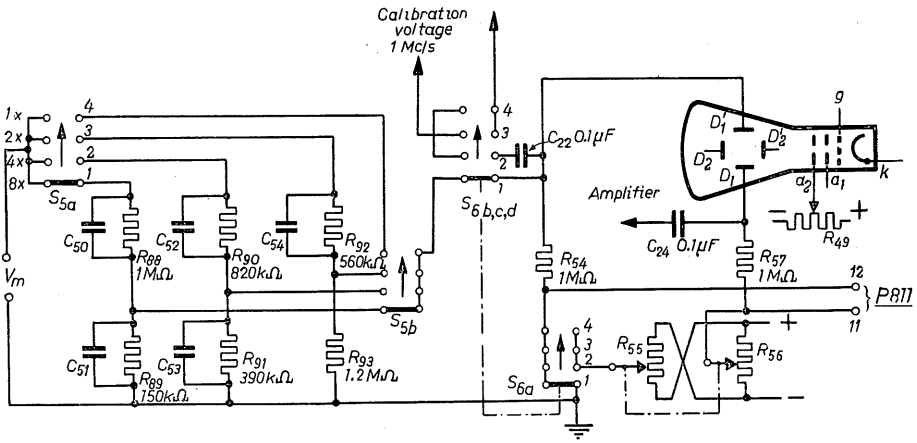

Fig. 7–14. Extract from the circuit of pulse-oscilloscope type GM 5660.

capacitances of the deflection plates and circuit. If the output resistance of the voltage source is low, the picture thus obtained on the screen will conform very closely to reality. Moreover, if the test signal is applied directly (without coupling capacitances) any *DC* component present will also be visible in the oscillogram, and its share can be evaluated in the manner described.

On the type GM 5660 pulse oscilloscope, the first position of the vertical deflection selector-switch is the appropriate one for these measurements. The interesting part of the circuit is shown in fig. 7–14. The input signal reaches the "upper" Y plate D'_1 via the compensated calibration voltage-divider (R_{88}–R_{93} and C_{50}–C_{54}). The *DC* shift voltage from potentiometer R_{56} reaches the other plate D_1 via leak resistor R_{57}.

In this position of the switch S_6, therefore, leak resistor R_{54} of plate D'_1 is tied to the chassis, so that regarded individually, each of these voltages lies asymmetrically on the Y plates (In the other positions of switch S_6, the vertical shift is effected by symmetrical *DC* voltages, i.e. in positions 2, 3 and 4, plate D'_1 receives an opposing *DC* voltage from R_{55} via R_{54}).

In so far, however, as the oscillogram is positioned in or near the middle of the screen, the voltage on both plates—with opposite polarities—must necessarily be almost equal, and thus the mid potential of the plates approximately zero. There will therefore be no astigmatism [7].

But even with the greater shifts needed for evaluating the voltage curve as described, the potential on anode a_2 can be adjusted with R_{49} to equal the mid potential of the deflection plates and thus keep the pattern in focus. This is of particular advantage when, as described in the following, the signal amplitudes are increased to several times the diameter of the screen in order to improve the accuracy of reading.

[7] See also "connection to the deflection plates", page 15 and the remarks on beam positioning and astigmatism, pages 34–35.

Improving the accuracy of reading by increasing the signal amplitude and shifting the pattern on the screen.

The voltage amplitudes can be measured with considerably greater accuracy if the vertical deflections are made to exceed the useful area of the screen [8].

The pattern shift needed for determining a certain potential difference in the voltage curve is correspondingly greater, so that the accuracy of reading is increased by the same extent. In this way the accuracy of measurement is limited in practice only by the accuracy of the *DC* instrument with which the shift voltages are measured.

Fig. 7–15*a*, *b*, *c*, *d*, shows some oscillograms taken with the pulse oscilloscope, type GM 5660, with the switch in position 1 as in fig. 7–14. They refer to the voltage on the anode of an amplifier valve while negative pulses are being applied to its control grid.

Fig. 7–15*a* shows the pattern on the screen in the conventional way. To all these pictures the zero level has been added to make the *DC* component visible. For this particular recording the voltage was divided in the ratio 2 : 1 (switch $S_{5a,b}$ in position 3).

For the other recordings the voltage was applied undivided to the *Y* plates (switch $S_{5a,b}$ in position 4).

The oscillogram in fig. 7–15*b* corresponds to the zero position; the shift voltage was 0 V.

For fig. 7–15*c* the pattern was shifted so as to bring the horizontal voltage "level" to the zero line. In this case, 19 V_{pp} was measured.

In fig. 7–15*d* the upper edge of the oscillogram just touches the zero line. The shift voltage needed was 150 $V_{=}$. Thus, the total amplitude

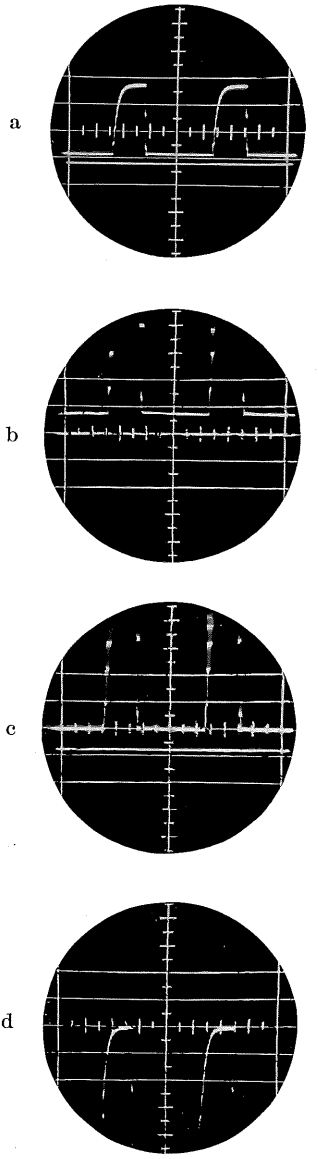

Fig. 7–15. *Oscillograms for accurately reading the voltage amplitudes by shifting the pattern*: *a*) usual oscillogram; *b*) zero setting at twice picture-height; *c*) determining the horizontal *DC* voltage level; *d*) determining the voltage crest.

[8] If the amplitude of the signal is inadequate, an appropriate amplifier must be used. Signals with *DC* components must obviously be passed through a *DC* amplifier. Provided that their frequency limits meet the requirements, Philips' types GM 4530 or GM 4531 may be used. They can be connected directly to the *Y* plates and the pattern may be shifted by means of controls on the amplifiers.

of the measured voltage is 150 V_{pp} with a level component at 19 V_{pp}. With this procedure, which gives an accuracy of reading equivalent to that on a screen several times larger, it is also possible to determine with exactitude the individual modulation levels in the oscillogram of a modulated voltage.

Resistance measurements.

As a typical voltage measuring instrument the oscilloscope is also very suitable for measuring high resistances with *DC* voltage. The simple circuit required is shown in fig. 7–16. There should be a small amplitude of time base voltage on the *X* plates, as for *DC* voltage measurements, in order to produce a short horizontal trace. The value of the unknown resistance R_x is found from the leak resistance—symbolized here as R_n—and from the input voltage $V_=$, according to the equation:

$$R_x = R_n \cdot \left(\frac{V_= \cdot DS_=}{Y} - 1 \right) \qquad (7\text{–}4)$$

If the first term in the bracket is considerably greater than 1 then we can write without disadvantage:

$$R_x = R_n \cdot \frac{V_= \cdot DS_=}{Y} \qquad (7\text{–}5)$$

in which $DS_=$ is the deflection sensitivity of the cathode ray tube for *DC* voltages and Y is the deflection of the spot read on the screen. If, for example, the supply voltage (300 V) of the vertical amplifier is used for this purpose, then when $R_n = 3\,M\Omega$, $DS_= = 0.4$ mm/V and $Y = 0.7$ mm, a value of $R_x \approx 500\,M\Omega$ (only just distinguishable) can be read from the screen.

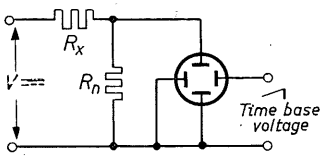

Fig. 7–16. Circuit for measuring high resistances.

This method is particularly suitable for testing the insulation resistance of block condensers. For measuring even higher resistances the anode voltage of the cathode ray tube could also be used. In this case, of course, safety measures must be taken to avoid accidents resulting from the high tension (e.g. a series resistor of at least 1 $M\Omega$ which, if necessary, must be deducted from the result). This would make it possible to test resistances up to $\approx$ 1750 Megohms [9].

Impedance measurements.

Since there is always an amplifier available for alternating voltages, it is also possible to measure small values of resistance to alternating current, that is to say, impedances in general. A sufficiently small ohmic resistance is included in the circuit and, as already described, the voltage drop across it is

[9] Just as small *DC* voltages can be measured on the oscilloscope with the aid of *DC* amplifiers, correspondingly small resistances can, of course, also be measured in the described way.

measured, and thus the current, at a known voltage. In this way impedance measurements can be carried out by comparison with an equally adjusted variable ohmic resistance [2].
A very simple method of power measurement is the following. The voltage from the object under test is applied via the vertical amplifier to the Y plates. The voltage proportional to the current (from a small ohmic resistor in the circuit to the unknown impedance) is used, via the horizontal amplifier, to deflect the spot in the X-direction. As current and voltage are generally not in phase, an ellipse appears on the screen. By calibrating the amplitudes along both co-ordinates, current and voltage can now be determined as described. The distance between the points at which the co-ordinates are bisected is, moreover, a measure of the phase angle θ or of $\cos\theta$ (see chapter 11 "Phase measurements," and especially figs. 11–8b and 11–12, with description).
The power dissipated in the impedance can therefore be found from the relation:

$$W_x = v_x \cdot i_x \cdot \cos\theta \qquad (7\text{–}6)$$

Capacitance measurements.

A particular instance of measuring impedances with the oscilloscope is the measurement of small capacitances. Fig. 7–17 gives the basic circuit for this. The value of the reference capacitance and the input frequency must be such that $\frac{1}{\omega \cdot C_n} \ll R_p$.
The unknown capacitance C_x is found from the equation:

$$C_x = C_n \cdot \frac{v_n}{v_M - v_n} \qquad (7\text{–}7)$$

If $v_n \ll v_M$, the equation can be written:

$$C_x = C_n \cdot \frac{v_n}{v_M} \qquad (7\text{–}8)$$

For $R_p = 3\ \mathrm{M\Omega}$ and $f = 5000$ c/s, C_n can be 1 mμF. If $v_M = 30$ V and $v_n = 10$ mV are still readily measurable, this corresponds to a minimum value for $C_x = 1/3$ pF [10].
This method is therefore particularly suitable for measuring small capacitances (valve capacitances, etc.). Since the voltage on c_n must always be amplified for the display, a vertical amplifier is assumed to be at the position marked with broken lines in fig. 7–17.

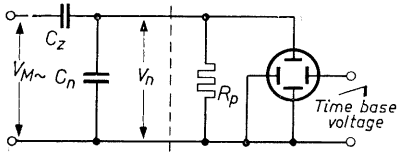

Fig. 7–17. Circuit for measuring small values of capacitance.

The exact value of this voltage is determined as under "AC voltage measurements", page 149.
To summarize, the foregoing examples show that the cathode ray oscilloscope

[10] It may be necessary to take into consideration the input capacitance of the oscilloscope with respect to capacitance C_n, so that it must accordingly be rated smaller.

can be employed for amplitude measurements just as an *AC* or a *DC* thermionic valve voltmeter.
With regard to input voltages requiring amplification, the pass band of the vertical amplifier determines the application of the oscilloscope from the point of view of frequency.

8. The oscilloscope as null-indicator in *AC* bridge circuits

The cathode ray oscilloscope, as a voltage indicator of extreme sensitivity, can be used with great advantage as a null-indicator for *AC* measuring bridges. Its high input impedance is very welcome for this purpose.

Simple null-indicator.

Its simplest application as null-indicator in a "sliding arm" bridge is shown in fig. 8–1. In this circuit the horizontal deflection plates are not used, so that the null voltage, after passing through the vertical amplifier, causes linear vertical

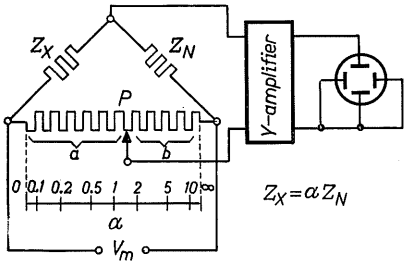

Fig. 8–1. *AC* bridge circuit with oscilloscope as null-indicator.

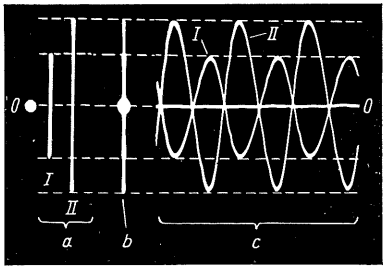

Fig. 8–2. Oscillograms obtained using the oscilloscope as null-indicator; *a*) and *b*) without horizontal deflection *c*) horizontal deflection voltage synchronized to $\frac{1}{3} f_m$.

deflections on the screen, as shown in the oscillograms in fig. 8–2a and b. If the bridge is balanced, the null voltage and the amplitude of deflection disappear; all that is left on the screen is the spot "0". The value of the unknown impedance is then found from the familiar expression:

$$Z_x = \alpha \cdot Z_n \qquad (8\text{–}1)$$

The factor α expresses the ratio of the potentiometer arms a : b, as indicated in fig. 8–1. Traces "I" and "II" appear as a result of arbitrarily varying the setting of potentiometer "*P*" to positions right and left of the null position. In fig. 8–2b these amplitudes of deflection have been recorded superimposed, as they appear to the observer. It must be admitted that this procedure has the disadvantage common to most other conventional indicating methods in *AC* bridges (with the exception of indicating instruments with phase-dependent rectifiers) that when the bridge is unbalanced there is no way of telling whether

the correct position of the potentiometer "P" should be sought further to the left or to the right. At high indicating sensitivities this makes it particularly difficult to ascertain the bridge minimum.

Phase-dependent indication by synchronizing the time base with the bridge voltage.

The disadvantage described can be avoided by applying the linear time voltage to the X plates and synchronizing it securely with the bridge supply voltage, as indicated in the layout in fig. 8–3. What now appears on the screen is the trend of the null-voltage in dependence upon time.
In the oscillogram reproduced in fig. 8–2c, the frequency of the voltage applied to the Y plates was 50 c/s and the time base frequency $16^2/_3$ c/s, resulting in a picture of three cycles. The time base frequency having been firmly synchronized with the input voltage, the oscillogram not only provides information on the amplitude of the null voltage but also, from the phase relations, on the direction in which the unbalance lies. When the bridge potentiometer is operated, the phase position of the null voltage reverses when passing through the point of balance, as may be seen from oscillograms I and II.

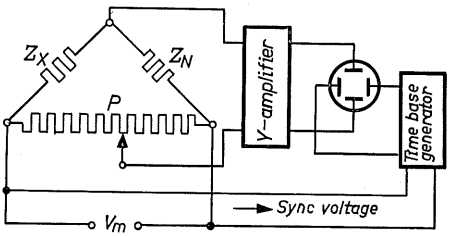

Fig. 8–3. Bridge circuit with oscilloscope; time base synchronized with the frequency of bridge supply voltage.

Null-indication by horizontal deflection with the bridge voltage.

A still more accurate null indication is obtained by applying the bridge supply voltage directly to the horizontal deflection plates in the manner indicated in fig. 8–4a.
Since the voltage to be measured (v_m), that is the voltage on the bridge itself, is hardly sufficient as a rule to achieve a horizontal deflection of 30–60 mm, it must first be brought to the requisite amplitude by a suitable amplifier. Provided that the impedances Z_x and Z_n are of the same type, without phase difference, and that the amplifiers cause no phase shift, the spot deflections in both directions will be in phase and will produce straight-line images on the screen.
When the bridge is balanced the spot will be deflected in the horizontal direction only, resulting in the trace "0" in fig. 8–5.
With an unbalanced bridge the spot is also influenced in the Y direction, so that when the potentiometer is operated, the trace turns about the point "a". As long as the level surface of the screen is not exceeded, the end points of the resultant traces will lie upon straight lines in the vertical direction, indicated by G_1 and G_2 in fig. 8–5.
Traces A_1 and A_2 correspond to different degrees of bridge unbalance on the one side, while A_3 points to a change of balance in the other direction.

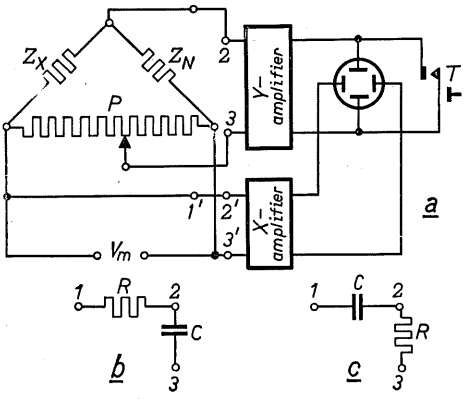

Fig. 8–4. Bridge circuit with oscilloscope for null-indication with rotating trace. Horizontal deflection by voltage under measurement.

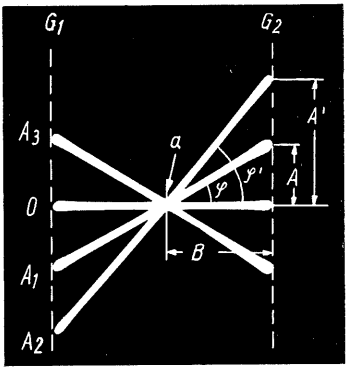

Fig. 8–5.
Oscillograms of null indication with rotating trace.

Correction of the phase relationship between bridge voltage and horizontal deflection voltage.

It is also possible to obtain the deflection voltage for the X plates by transformation of the bridge voltage. Phase shifts are introduced during this process, so that the pattern appearing on the screen is no longer a simple trace but a more or less open ellipse. Employing the mains voltage for measurement, we can use the 50 c/s X-deflection position of the selector switch provided on some oscilloscopes for deflection along the X axis. In this case, too, we must reckon with a phase difference with respect to the bridge supply voltage. When the deflection amplifier also causes a phase shift its effect must be eliminated by turning back the phase to a corresponding extent. This can be done by incorporating a phase shifting network in the null voltage lead to the vertical amplifier (points 1, 2, 3) or in the deflection voltage lead to the X plates (points 1′, 2′, 3′), as indicated in the layout in fig. 8–4b and c. The network must be rated such that when comparing impedances without phase difference a simple trace will appear on the screen as before. (For first adjustment it is better to compare ohmic resistances.) According to the ratio $R : \frac{1}{\omega \cdot C}$, the phase shift when $R = \frac{1}{\omega \cdot C}$ will be 45°. At the same time the voltage at the output of the network will fall to 0.707th of its value.
The output voltage of the network in fig. 8–4b lags behind the input voltage while that of the network in 8–4c leads the input voltage.
If considerable phase correction is necessary, anti-phase shifting networks can be incorporated at the same time between points 1, 2 and 3 on the one side and between points 1′, 2′ and 3′ on the other. In this case, when $R = \frac{1}{\omega \cdot C}$, the phase difference measurable at both networks will be 90°. At all events the essential point here is that the voltage for the X axis need not necessarily

originate direct from the one bridge diagonal but can be taken in other ways from the voltage source. Once the correction has been made, the measurements of complex resistances can be undertaken in a manner which will be described later on in this chapter.

Bridge sensitivity.

If the minimum deflection factor of the available oscilloscope is, to take an example, 1.0 mV_{rms}/cm and the mean diameter of the spot is 0.5 mm, this means that a change of the end point of the indicator by a null voltage of 50 μV will still be readable on the screen. By using a special tuned amplifier, considerably higher null sensitivities can be achieved.
A convenient procedure, especially for observing small amplitudes of deflection, is to short the voltage under measurement either by means of a key (see fig. 8–4) or periodically, by mechanical means or by an electronic switch. The result of this on the screen is the appearance both of the null position "0" and of the pattern deflected by the null voltage.
This idea can be taken further; one can switch over to two pairs of resistances which correspond to certain plus and minus tolerances. Four pictures then appear on the screen:

1. Null trace.
2. Trace with minus tolerance.
3. Trace with plus tolerance.
4. Moving trace corresponding to the amplitude of the voltage being measured.

Since the indication of the bridge ratios is displayed by a rotating trace on the screen, the dependence of the angle of rotation φ upon the null voltage is of interest. The horizontal deflection of the spot by the bridge voltage is constant. (In fig. 8–5 it equals 2 × B). The deflection of the end point in the measuring direction is determined by the (amplified) null voltage. The relation A/B represents here the tangent of the angle θ. The angle of rotation is therefore found from the equation:

$$\theta = \text{arc tan } \frac{A}{B} \qquad (8\text{–}2)$$

By plotting the dependence of the angle of rotation θ upon the relation $\frac{A}{B}$, a curve is obtained as shown in fig. 8–6a. It corresponds to the arc tan curve for the range $\pm$ 90°. As larger angles than $\pm$ 90° are impossible in this arrangement, the other branches of the curve for more than $\pm \frac{\pi}{2}$ of the arc tan function can be left out of consideration.
The important and welcome fact emerges from the curve in fig. 8–6a that the change of angle is greatest for a small change of the null voltage in the vicinity of bridge balance; in this region the curve is at its steepest. (It is determined by the deflection sensitivity of the tube, the amplification and the value of the bridge supply voltage.) A clearer picture is obtained if we plot the change of

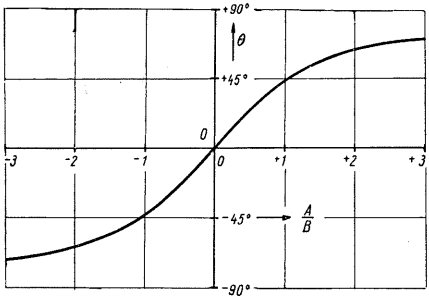

a

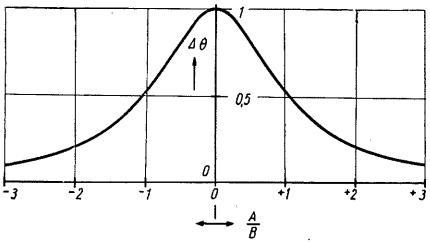

b

Fig. 8–6. Curves showing indication sensitivity of oscilloscope with rotating trace.
a) Angle of rotation in dependence upon A/B (see oscillograms fig. 8–5).
b) Change of angle in dependence upon A/B (= tan of angle of rotation θ).

angle itself in dependance upon the ratio $\frac{A}{B}$, as shown in fig. 8–6b. Mathematically, this curve represents the differential quotient of the arc tan. curve. The appropriate equation is:

$$\frac{d\,(\text{arc tan}\,A/B)}{d\,A/B} = \frac{1}{1 + (A/B)^2} \qquad (8\text{–}2a)$$

One of the essential advantages of this method of measurement is that the acute sensitivity of the null indication declines rapidly with bridge unbalance. This represents a degree of insensitivity to overloading that can scarcely be equalled by any other null-indicating device.

Direct reading of bridge unbalance.

A further advantage of this procedure is that the moving indicator trace can also be used for direct indication of the bridge unbalance. The perpendiculars traversed by the end points of the traces (G_1 and G_2 in figs. 8–5 and 8–7) can be fitted with a scale which may be calculated from the mathematical conditions already considered, although in practice it is simpler to create certain known values of unbalance by means of test resistors and then to calibrate the scale accordingly. This was the method adopted for the scale in fig. 8–7 in which eight different rotating traces are shown on the screen. It is now no longer necessary to balance the bridge; the unbalance can be read off direct and impedance Z_x determined according to equation (8–1). This procedure is particularly useful when, for instance, sorting is required within certain manufacturing tolerances. Since the null voltage on the straight part of the curve in fig. 8–6a is linearly proportional to the unbalance, the divisions of a percentage scale of this type are linear, as can be seen in fig. 8–7.

The measurement of complex impedances.

Still another advantage of the rotating trace method of indication as compared with other systems of null indication in *AC* bridges appears in the measurement of complex impedances. In this case the null voltage is also complex, comprising as it does the two voltage vectors corresponding to the different types of impedance. If, as in fig. 8–8 for example, an electrolytic

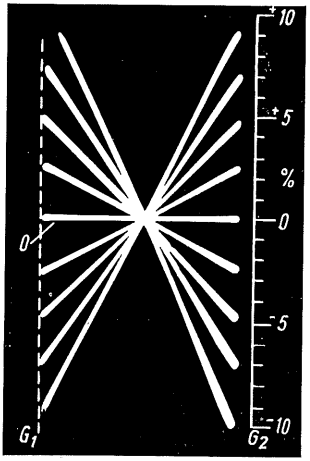

Fig. 8–7. Oscillograms of rotating traces with scale for reading off tolerances.

Fig. 8–8. Bridge circuit for measuring impedances.

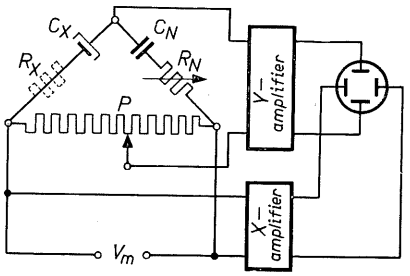

condenser is to be tested, the pattern on the screen when the bridge is off balance will not be a simple trace but an ellipse, as illustrated in figs. 8–9 and 8–10. The bridge can again be balanced by operating potentiometer P, whereupon the ellipse rotates into the position marked 0_{ph}. The two voltage vectors corresponding to the capacitance ratio $C_x : C_n$ have now been balanced, but because of the ohmic "series resistance" of the electrolytic condenser there will still be a residual voltage to contend with. As the vector of this voltage is at right-angles to the vectors of the capacitive voltages of C_n and C_x, the ellipse will remain open even when the bridge is balanced. Only when a variable resistor R_n in series with C_n is adjusted to the appropriate value will the ellipse collapse to the null line "0".
The value of the "leak resistance" R_x is found from the equation:

$$R_x = \frac{1}{a} \cdot R_n \qquad (8\text{–}3)$$

in which a is again the bridge ratio of the potentiometer "P".
It is interesting to note that "bridge balance" and "phase balance" are now completely independent of each other, the influence of the adjustments described being separately recognizable on the screen. Referring to fig. 8–9, when the bridge is unbalanced, the phase balance can first be adjusted to produce the indicator A and afterwards the bridge can be balanced to produce the indicator 0, and vice versa.
This is a unique advantage compared with all other methods used for measurements of this sort. These always require alternate adjustment of "phase balance" and "bridge balance" until the minimum is reached. With the method described here, however, both adjustments can be rapidly and accurately

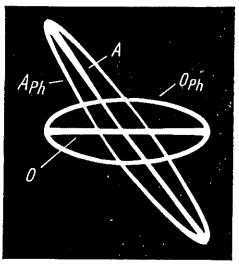

Fig. 8–9. Oscillograms for measuring impedances.

made in complete independence of each other. To illustrate the practical functioning of this procedure, fig. 8–10 shows the null trace "*0*" and the null ellipse "0_{ph}" together with eight different oscillograms of ellipses with an unbalanced bridge.

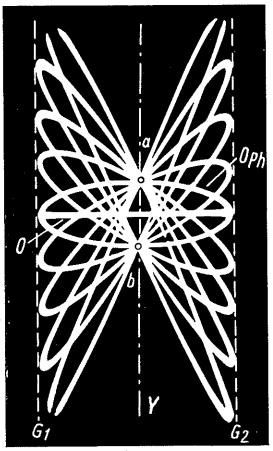

Fig. 8–10. Family of oscillograms showing common points of bisection "*a*" and "*b*".

Direct reading of the power factor of a condenser without phase balance.

A striking fact appearing from fig. 8–10 is that all ellipses without phase balance bisect the Y axis at two common points "*a*" and "*b*". At a certain bridge sensitivity, the spacing between these points is a measure of the ohmic share of R_x on C_x. If it is larger, the ellipses will be wider and thus the spacing between "*a*" and "*b*" greater. An attempt has been made in fig. 8–11 to reproduce these relationships by means of original photographs of two measurements with a different complex component.

It can be seen at once that in order to measure the power factor of a condenser it is not at all necessary to obtain phase balance. It is sufficient to balance the bridge and to read off the opening of the null ellipses at points "a_1" and "b_1" and "a_2" and "b_2" respectively.

If the value of the unknown quantity is not important and it is merely a matter of ascertaining the power factor, it will suffice if the bridge is only approximately balanced. As fig. 8–11 shows, the points of bisection on the ordinate always allow the possibility of reading off the phase angle or its functions [1] [2].

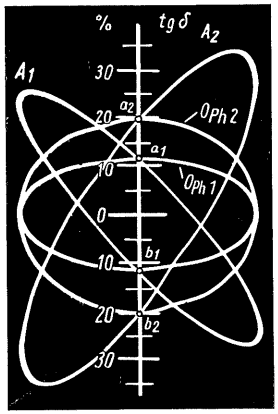

Fig. 8–11. Oscillograms for reading off the power factor of a condenser.

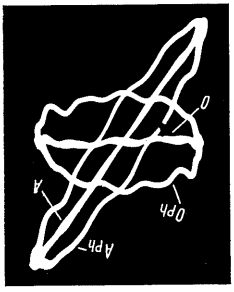

Fig. 8–12. Oscillograms for measuring impedances with voltage containing harmonics.

We have so far only considered measurements with purely sinusoidal voltages which are, of course, a desirable prerequisite for such purposes.

It may, however, happen that the voltage to be measured will contain harmonics. Fig. 8–12 shows the pattern on the screen produced by taking the test voltage straight from the mains without filtering. (Compare with fig. 8–9.) It can be seen that measurements are still possible with such voltages, whereas in other methods of null indication they would produce most equivocal results.

Moreover, in distortion measurements with bridge circuits one can in this way separate the fundamental from the harmonics.

Impedance measurements by voltage comparison.

The oscilloscope often finds useful application in other methods of measurement based on voltage comparison, apart from actual bridge circuits. Fig. 8–13 shows a circuit with which it is easily possible to compare R, C and L impedances. The unknown Z_x and the known Z_n are connected in series to the voltage source v_m. The alternating voltages across these components are fed to one pair of deflection plates each. As the current through both impedances is equal, the voltage drops are proportional to the impedances. To obtain satisfactory deflection, v_m should be about 100 V. This means that without an amplifier this procedure is suitable only for comparing high impedances. If suitable amplifiers are available for both directions of deflection, then, of course, small measuring voltages can be used and correspondingly small impedances compared.

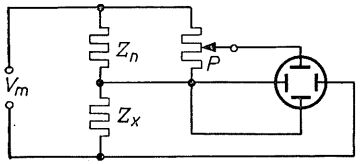

Fig. 8–13.
Circuit for comparing impedances.

If the higher deflection sensitivity of the Y plates is compensated by a voltage divider "P", the picture on the screen when both impedances are equal will be a trace at an angle of 45°. If $Z_x = \infty$, all the voltage will be on the X plates and the trace will be horizontal. When $Z_x = 0$, all the voltage will be across Z_n and thus on the Y plates, resulting in a vertical trace. Thus the trace on the screen will turn according to the ratio $Z_n : Z_x$ and when $Z_n = Z_x$ it will be inclined at exactly 45°. Patterns of this description are shown in the oscillogram in fig. 8–14. It can be seen that the ends of the diagonals lie upon a straight line connecting the end points of the X and Y traces.

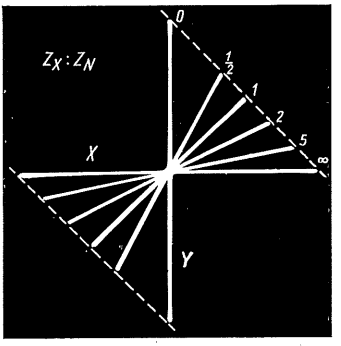

Fig. 8–14.
Oscillograms to fig. 8–13.

Contrary to the bridge method previously described it is not possible with this circuit to increase the indicating accuracy by amplification. However, better use can be made of the surface of the screen and maximum accuracy of reading achieved if the pivotal point of the traces is displaced to the edge of the screen. This can always be done in good oscilloscopes by suitable DC positioning voltages. One can go a step further and turn the cathode ray tube around in such a way that the pivotal point lies bottom centre as shown in fig. 8–15. For a 1 : 1 ratio the indicator now lies in the centre, and the end points move over a straight line which can be fitted with a calibrated scale. This method also has the advantage that the sensitivity is greatest in the middle and declines with increasing values of $Z_x : Z_n$, and vice versa. It is a useful arrangement for rough sorting and is suitable, as already mentioned, for comparing high resistances and inductances as well as small capacitances

where $\frac{1}{\omega C_x}$ is high for a given measuring frequency. Where there is a phase angle between the two impedances, then here also an ellipse appears on the screen instead of a linear trace. The power factor of a condenser, for example, can be determined quite accurately by comparison with a loss-free condenser in the manner previously described for the bridge circuit. This will be considered in more detail in the chapter on phase measurements.

The description given here of the uses of the oscilloscope in bridge circuits has only touched upon the basic possibilities of application. For further and specialized applications the reader is referred to the literature on the subject [3] [4] [5].

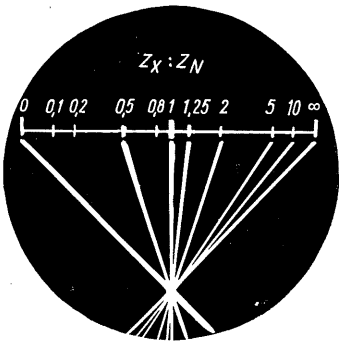

Fig. 8–15.
Family of oscillograms for impedance measurement. Pivotal point at the edge of screen and tube turned 45°.

Bridge circuit for sorting core plates.

One interesting application worth mentioning is a bridge circuit for sorting core plates. The circuit for this is shown in fig. 8–16, with the amplifier omitted.

Two branches of the bridge are formed by coils L_1 and L_2, in which the specimen core plates can be inserted. The coils consist of 15,000 turns of 0.1 mm Cu wire. In the other two branches of the bridge are located resistors R_1 and R_2, the bridge being balanced by varying R_1. Due to resistor R and condenser C, integration of the null voltage takes place $\left(\frac{1}{\omega \cdot C} \ll R\right)$, so that the spot is deflected vertically by a voltage which is directly proportional to the difference of the magnetic fluxes—but not to $\frac{d\Phi}{dt}$. (This will be dealt with more fully in the next chapter concerning the display of hysteresis loops.)

For the purpose of balancing, plates with identical dimensions and of known material are introduced into both coils and "null" is adjusted by means of R_1. If now, in place of one of the plates an unknown plate of the same size is introduced, the pattern on the screen will be seen to change. After some experience it is possible in this simple way to obtain information rapidly on the properties of the unknown material.

It would exceed the scope of the present work to go deeper into this subject; the reader is therefore again referred to the bibliography [6] [7].

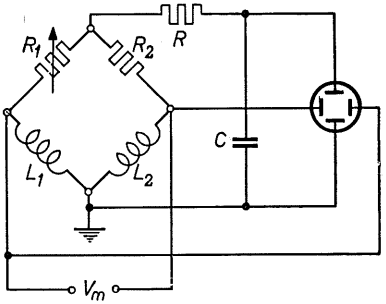

Fig. 8–16.
Bridge circuit for magnetic sorting

9. The display of hysteresis loops

In context with the preceding chapter it will now be shown how the oscilloscope can be used to display the hysteresis loop of magnetic material.
As the reader will be aware, it is a question of representing magnetic induction B as a function of the field strength H, i.e. the interdependence of two quantities is to be shown.
Provided that the iron core is sufficiently well closed (there must be no air gap), the field strength H can be taken as proportional to the number of ampère turns. This means that the primary current i_p can serve to represent the field strength. Two windings are arranged on the specimen core. A resistor R_v is connected in series with the primary winding and the voltage drop across it is used as the deflection voltage for the X plates, as indicated in fig. 9–1.

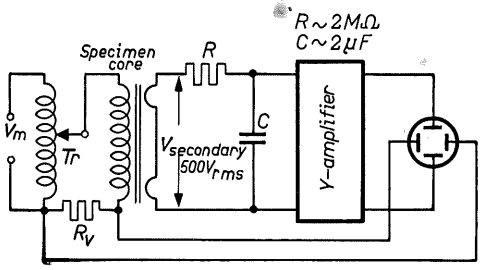

Fig. 9–1. Circuit for displaying hysteresis loops.

When $DS_{X\sim}$ is the deflection sensitivity of the X plates for AC voltage, R_v the value of the series resistor, Z_p the number of primary turns and l the mean length of the lines of force, we obtain as the scale for the horizontal deflection:

$$1 \text{ mm} = \frac{0.4 \cdot \pi \cdot Z_p}{R_v \cdot l \cdot DS_{X\sim}} \text{ [Oersted]} \tag{9–1}$$

The vertical deflection is to be proportional to the magnetic induction B. The secondary winding on the specimen core serves for this, the voltage on it being:

$$v_{sec} = k \cdot \frac{dB}{dt} \tag{9–2}$$

in which k is a constant. This voltage is electrically integrated by feeding it via a large resistor R to a condenser in such a way that $R \gg \frac{1}{\omega C}$. The voltage on the condenser is then:

$$v_c = k' \cdot \frac{B}{RC} \tag{9–3}$$

Due to integration the amplitude of the voltage is small and must be amplified to produce satisfactory deflection.

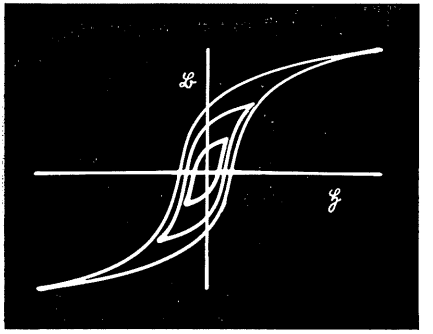

Fig. 9–2. Hysteresis loops (recorded with circuit as in fig. 9–1).

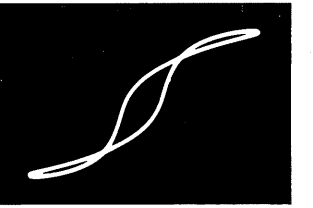

Fig. 9–3.
Hysteresis loop distorted by phase error of vertical amplifier.

The secondary winding is divided in two parts and arranged so that both ends lie outside and have approximately the same capacitance to the primary winding and to the core. Screening is provided between primary and secondary so that the secondary voltage is entirely due to magnetic induction.
If $DS_{Y\sim}$ is the deflection sensitivity of the Y plates for AC voltage, C the value of capacitance in μF, R the resistance in MΩ, Z_s the number of turns of the secondary, Q the cross-section of the core and G the gain, then the scale for the vertical deflection is:

$$1 \text{ mm} = \frac{R \cdot C \cdot 10^8}{Z_s \cdot Q \cdot G \cdot DS_{Y\sim}} \text{ [Gauss]} \qquad (9\text{–}4)$$

Fig. 9–2 shows the patterns of the resultant hysteresis loops on the screen. By varying the input voltage with the variable transformer T_r, different hysteresis loops representing a number of different degrees of magnetization were recorded for this illustration one upon the other.
The pictures of the axes were obtained in each case by switching off the voltage from one pair of plates at the moment of maximum magnetization and then photographing the resultant trace.
The vertical amplifier must cause no phase shift during this test as otherwise a pattern will appear on the screen as shown in fig. 9–3. Small phase errors, however, can be corrected by connecting a phase-shifting network in the amplifier input as in fig. 8–4b or c.
There are, of course, numerous types of hysteresis. Electrical hysteresis received a great deal of attention during the creation of dielectrics with a high ε. These phenomena produce patterns on the screen of the oscilloscope similar to those produced by magnetic hysteresis. On this subject reference is made to special publications [1] [2] [3].
To form a judgment on the properties of different sorts of iron it is not always necessary to record hysteresis loops. As a rule the magnetic sorting bridge already described will be sufficient, particularly in view of the facility it offers for changing the specimen quickly.

10. The uses of intensity modulation

Rating of the circuit components—Time marking.

In the majority of measurements performed by the oscilloscope, the electron beam, and thus the spot, is deflected by the two pairs of deflection plates in co-ordinates at right-angles to each other—the Y and X axes. It may sometimes be required, however, to make a third quantity visible on the screen for which purpose it is possible to have a second trace by using a twin beam oscilloscope or an electronic switch.

However, when it is only a matter of time marking and not of actually portraying the behaviour of a second phenomenon, no additional outlay is necessary, for the oscillogram can be given adequate time marking by simply modulating the intensity of the electron beam. This is done by superimposing the time marking voltage upon the negative grid bias of the C.R.T.

This voltage (usually alternating) can be applied via a condenser, C_g, to the grid in the manner shown in fig. 10–1. The other pole comes to the chassis. The current flowing from this voltage source arrives at the cathode over condenser C_2 and reaches the leak resistor R_g over C_1. The alternating voltage across R_g then controls the grid voltage.

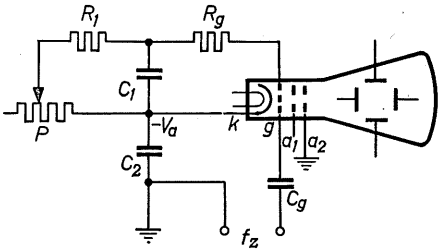

Fig. 10–1.
Circuit for modulating the intensity of the beam.

It should be noted that the grid g is tied via resistors R_g, R_1 and potentiometer P to that pole of the filtering condenser C_2 which is under high tension with respect to the chassis. The coupling condenser C_g must therefore be suitably insulated.

By these means, during each half cycle of the control voltage the spot on the screen will be made brighter or fainter, as the case may be. The resultant "brightness modulation" is clearly to be recognized in the oscillograms in fig. 10–2. In parts b, c, d and e, the alternating voltage "a" was raised in steps and the grid bias increased in each case such that the brilliance peak remained approximately the same.

The variations of brilliance are barely perceptible in the first trace; in the course of the procedure described the interruptions in the trace become increasingly pronounced. This third possibility of influencing the spot is often referred to as the "Z axis", although other measures are necessary for the presentation of three-dimensional oscillograms, and intensity modulation in this case serves only to produce a spatial impression.

Although there may be no objection to the relatively large intervals between the brilliance marking in these oscillograms, it still being possible to determine the centres of the markings or of the darkened trace, interruptions of this kind are nevertheless undesirable since they could mean the loss of certain details in the information displayed.

The markings are therefore kept as close together as possible (fig. 10–2f).

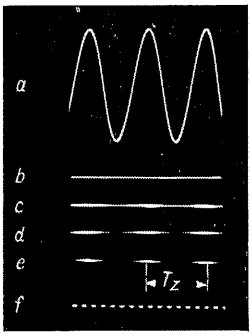

Fig. 10–2. Sinusoidal brightness-modulation with traces of different intensity.

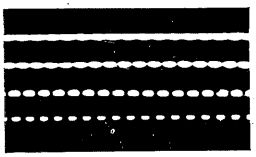

Fig. 10–3. Intensity modulation with closer time markings.

Fig. 10–3 shows four traces with which, as a result of various amplitudes of modulation-voltage and correspondingly higher grid bias, good intensity-modulation is achieved in conjunction with small variations of brilliance. The spacing of the bright points (or of the centres of the darkened trace) corresponds to a time difference T_Z which is equal to the reciprocal of the frequency f_Z, thus:

$$T_Z = \frac{1}{f_Z} \qquad (10\text{–}1)$$

Therefore, at a frequency of 1000 kc/s, the spacing of the points will be: $\frac{1}{1000}$ sec = 1 millisec. The time marking achieved in this way is satisfactory for many purposes.

For the sake of clarity the traces shown in fig. 10–3 have been somewhat enlarged as compared with those in fig. 10–2.

Oscillograms of several different quantities, which can easily be recorded one after the other in one picture, can be clearly distinguished by varying the degrees of intensity modulation. (The time base generator must then be synchronized in fixed phase with the reference voltage.) An example is given in fig. 10–4a; it shows the fundamental frequency of an alternating voltage strongly punctuated and the third harmonic (shifted in phase), less strongly punctuated, together with the unmodulated resultant of both voltages. For comparison, the same curves without intensity modulation are shown in fig.10–4b. The intensity-modulation frequency for modulating the fundamental(50 c/s) was 2200 c/s; that for the harmonic (150 c/s) was 1250 c/s.

Crowding the time markings.

Although bright-dark modulation, as exemplified by the bottom trace in fig. 10–3, is almost invariably used for time marking, it will only be adequate if the writing speed of the beam is reasonably constant. Sudden fluctuations could cause gaps to appear in the oscillogram. However it is apparent from the magnified traces in fig. 10–5 (as seen under a magnifying glass) that it is still possible to count

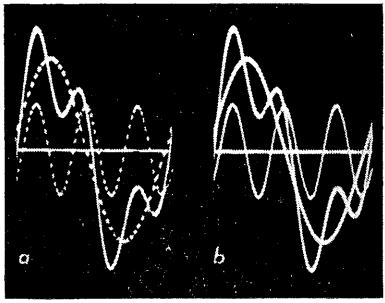

Fig. 10–4. Use of intensity modulation to clarify the presentation of multiple oscillograms.

the time markings with reasonable accuracy even when they are closely crowded together. The section reproduced shows that the bright-dark trace contains six time-marking spaces, whereas the closely modulated trace contains fourteen.
An example of the practical application of this procedure is given in fig. 10–6. The time markings can still be counted even in the steep portion of the

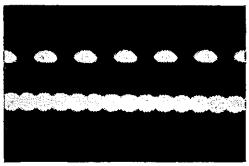

Fig. 10–5. Magnified traces, *a*) with alternate brightening and blanking and *b*) with closely bunched modulation marks.

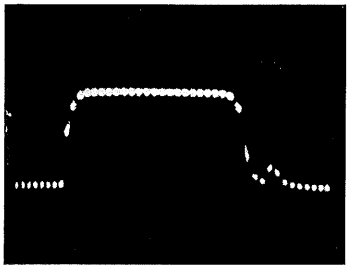

Fig. 10–6. Opening behaviour of a between-lens shutter with time-marking by intensity modulation: $f_Z = 1000$ c/s.

oscillogram, which represents the opening behaviour of a between-lens camera shutter. The opening and shutting time amounted to 3 ms (time marking 1000 c/s). The shutter was open for 20 ms. ($\frac{1}{50}$ sec; 20 time markings). It is interesting to note that, possibly due to rebound, the shutter opened again for about 3 ms approximately 1 ms after closing [11] [1].

Synchronous intensity modulation.

As long as differences, however small, exist between the frequency of the intensity modulating voltage and corresponding multiples of the frequency under observation, the modulation markings will drift along the pattern on the screen. This can make the photographic recording of such oscillograms extremely difficult. It is advisable. therefore, if recordings are to be carried out frequently, not to take the modulating voltage from a second source but to produce it by distorting the actual voltage being measured and by filtering out suitable harmonics. (See fig. 10–7.)
The test voltage is fed not only to the vertical amplifier but also to a distorting stage in which strong harmonics are formed. The desired harmonic (about 10–50 times the fundamental) is filtered out and amplified in an auxiliary amplifier to produce the requisite intensity modulation. By subsequently tuning the filter it is now possible to select the number of time markings wanted. The time markings remain stationary automatically.

[11] The shutter in question belonged to a fairly old camera. In chapter 16 "Measuring the action of between-lens shutters", a number of oscillograms are reproduced of measurements made on more modern shutters.

Another procedure is to excite a poorly-damped tuned circuit into self-oscillation by the flyback of the time base voltage. The circuit oscillates during the time the spot is travelling across the screen, and this voltage, (if necessary after rectification), can likewise be used to modulate the intensity of the beam (brightness modulation or blanking).

Since the starting moment of these oscillations is determined by the flyback pulse, the resultant time markings in the oscillogram remain stationary, irrespective of whether the frequency ratio between the sawtooth and the time marking voltages is a whole-numbered one or not. Changing the frequency relationship merely has the effect of changing the distribution of time markings over the oscillogram.

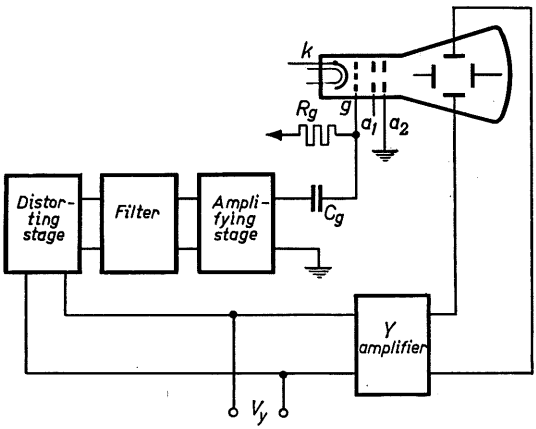

Fig. 10–7. Circuit for intensity modulation with multiples (harmonics) of the input frequency.

An example of this method is given in fig. 10–8 which shows two greatly expanded oscillograms of line synchronizing pulses as used in television technique. (Time base expansion about $\times 800$ and $\times 1700$; see "Time base expansion unit", pages 77–80 and fig. 4–39 on page 73.) The high frequency time marks make it possible to analyse exactly every interesting section of the oscillogram.

According to a method described by Steinberg [2] a punctuated "time line" in the manner of an electronic switch can be traced on a normal, uninterrupted oscillogram. For this purpose a valve circuit is used to blank out the voltage under measurement in each second deflection cycle, and at the same time the horizontal line then appearing on the screen is modulated by the time marking generator, which begins to oscillate at exactly the same moment. This time "scale" can be displaced vertically and horizontally and thus brought to lie on the oscillogram of the process being measured, as indicated in fig. 10–9. If two time-marking

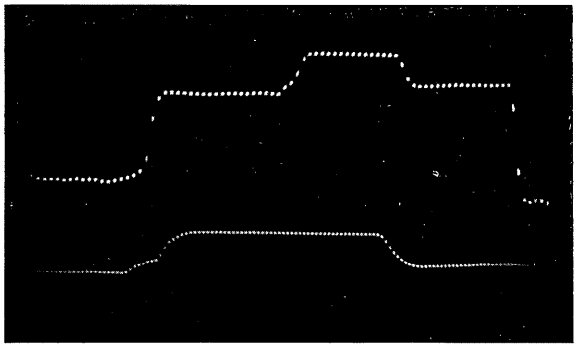

Fig. 10–8. Greatly expanded oscillograms of T.V. line pulses, with time marking by means of synchronous intensity modulation; upper curve: $f_{z1} = 3.2$ Mc/s $= 0.05$ H (H = duration of one line) lower curve: $f_{z2} = 10$ Mc/s $= 0.1 \mu s$.

generators of this kind are available, the accuracy of interpretation can be increased ten-fold according to the vernier principle. The oscillogram is then intensity-modulated by the one oscillator, while the other, whose frequency differs from the first by 10%, serves to intensity-modulate the time scale. The oscillogram is interpreted by counting and comparing the rows of dots.

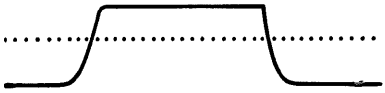

Fig. 10–9.
Intensity-modulated "time scale".

Short brilliance markings without gaps (or short blank-markings).

In some cases it may be necessary to have time marking without blank interspaces. For this purpose, short, sharp voltage pulses are needed.

A great number of circuits exist for generating voltages of this kind. (They are used for instance, in radar units, in electronic computing devices and in television engineering). Most such voltages are generated by differentiation of a square wave. For the following oscillograms a type GM 4581 electronic switch was used as the voltage source, which not only supplies rectangular voltages in a wide range of frequencies but also permits them to be adjusted symmetrically or asymmetrically, as desired. (A pulse and square wave generator—type GM2314—is better suited to the purpose than an electronic switch, which was used here only as a make-shift.)

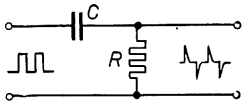

Fig. 10–10.
CR network for differentiation of *AC* voltages.

Differentiation can be effected by a pulse transformer or simply by a *CR* network as illustrated in fig. 10–10. Whereas $\frac{1}{\omega C} \leq \frac{1}{100} \cdot R$ must apply for passing a square wave properly, good differentiation can be achieved when $\frac{1}{\omega C} \gg R$. Good practical results are obtained when $\frac{1}{\omega C} = (3...10) \cdot R$. (The limit frequency applies when $\frac{1}{\omega C} = R$). [3] [4] [5]

This process is illustrated by the oscillograms reproduced in fig. 10–11. Part a) shows three cycles of a rectangular voltage and b) the wave-form of the voltage after a *CR* network, as in fig. 10–10, when $\frac{1}{\omega C} = 3 \cdot R$. During the rise of the square wave a positive peak occurs; as the square wave falls again a negative peak is formed. If the trace on the screen is modulated by this voltage the resultant pattern is as shown in 10–11c). Alternate brightness modulation and blanking takes place. In order to obtain brightness modulation only, the voltage must be full-

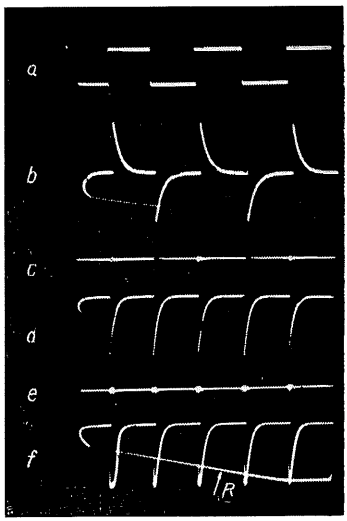

Fig. 10–11. Waveforms of voltages in circuit fig. 10–10, with corresponding traces on the screen.

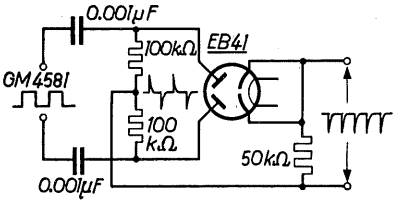

Fig. 10–12. Circuit for full-wave rectification of differentiated voltages (f = 1000 c/s).

wave rectified. (In each cycle of the rectangular voltage there will now be two time markings.) A circuit of this type (as used in conjunction with the GM 4581 electronic switch as the voltage source at a frequency of 1000 c/s) is shown in fig. 10–12. Fig. 10–11d reproduces the waveform of the output voltage and 10–11e the resultant intensity-modulated trace.

One time mark per cycle can be obtained by inserting only one diode (crystal diode) between the two voltage poles—after series resistors—instead of the full-wave rectifier.

With a suitable modulating voltage, semi-punctuated and other types of oscillogram can be obtained. As a practical example, fig. 10–13a shows the pattern of a damped oscillation intensity-modulated by the time marking trace in 10–13b. The differences in spacing give a clear impression of the decreasing speed of the spot.

By changing the polarity of the modulating voltage, short blank markings can be obtained as shown in fig. 10–14a and b.

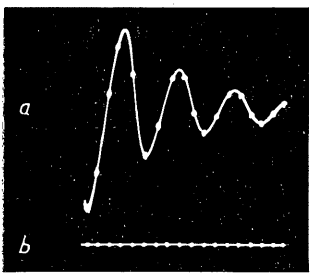

Fig. 10–13. Time-marking by trace brightening.

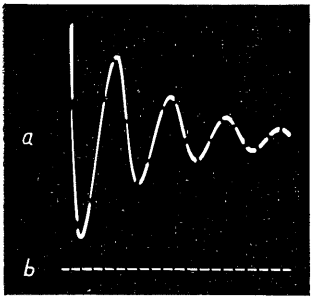

Fig. 10–14. Time-marking by trace blanking.

Intensity modulation proportional to deflection speed.

In practice, oscillograms are not often encountered in which the deflection speed is constant. One has therefore to put up with a trace of varying intensity. However, even when it is only a matter of portraying a simple sine wave, it may be undesirable for the brilliance in the vicinity of the zero axis, where the speed of the spot is greatest, to be essentially less than at the crests of the curves. In this example the speed trend is displaced by 90° according to the cosine function.

The aim must therefore be to modulate the beam intensity in such a way as to achieve a uniform trace. A circuit designed to do this is shown in fig. 10–15. The voltage to be measured (v_Y) is fed via an RC network to the vertical amplifier, the output of which is applied to the Y plates. At the same time v_Y is fed via a CR network to a transformer (a normal A.F. transformer for driving push-pull stages) the secondary of which is centre-tapped. After full-wave rectification, the output is as shown in the oscillogram in fig. 10–16d. The requisite phase difference can be obtained by C_1, R_1 (voltage leading). To avoid causing too high a voltage drop during this process, the

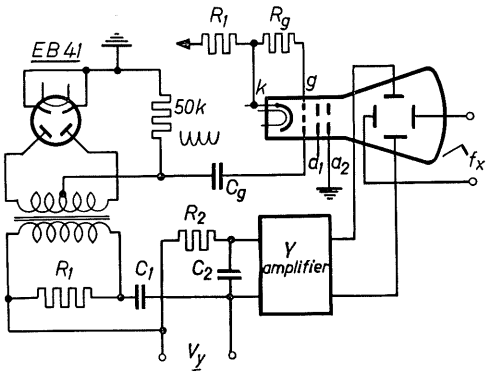

Fig. 10–15. Circuit for speed-proportional brightening of sinusoidal voltages.

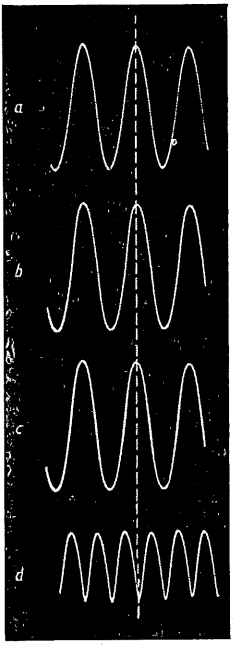

Fig. 10–16. Patterns showing the effect of speed-proportional brightening.

voltage on the Y plates can at the same time be counter-displaced by R_2, C_2 preceding the vertical amplifier, as indicated in the circuit, so that the desired 90° phase difference is achieved in each case with a voltage loss of only 30%. Parts a), b) and c) of fig. 10–16 show the effect of this circuitry. In a) can be seen the normal sine wave without corrective intensity modulation. (See also fig. 6–2a). The differences in brightness between the peaks and the points of zero transition are clearly visible. In b) brightness modulation has been introduced so that the zero transition is approximately equal in brilliance to the peaks. Modulation has been somewhat exaggerated in c) to illustrate the effect distinctly. All waveforms show the same brilliance at the peaks, but different degrees of brilliance on the other portions of the curve. (The reference line permits easier comparison of the time spacings.) Other wave-shapes too can be considerably improved by speed-dependent intensity modulation. In fig. 10–11f, for example, the modulation voltage as in 10–11e was used at the same time for brightness modulation, resulting in a great improvement on the pattern in 10–11d. The flyback, indicated by "R" can now also be seen. If higher demands are made, of course, a greater outlay is needed [6] [7] [8].

Electrical "switching" of the brilliance.

When observing and recording single transients it is especially desirable that the course of the spot on the screen should last no longer than the duration of the transient itself. If the quiescent spot, which is needed to describe a bright trace, were to appear with great brilliance on the screen before hand, it would dazzle the observer or produce a severe blackening halo on the recording material.

This disadvantage can be avoided by blocking the grid with a suitably high negative voltage until just before the recording is to be made. This can be done by

arranging a change-over switch "*S*" in the lead to the arm of potentiometer "*P*", as indicated in fig. 10–17. When the switch is set in position 2, the grid receives from point "a" a biasing voltage sufficient to cut off the tube. In position 1 the preset voltage on the potentiometer arm lies on the grid. Another means of switching is provided in the majority of Philips oscilloscopes. The voltage from a 45 V dry battery is applied to terminals *A* and *B* over a relay contact. (Switch 1–2 can also be a relay change-over contact of course.) Since the internal resistance of the battery is always smaller than the resistor of 0.5 MΩ, the battery will determine the operating point.[12] In this way it is possible, with the aid of further relays or valve circuits, to record single transients in the following sequence:

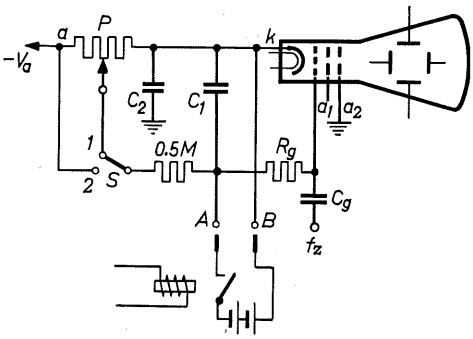

Fig. 10–17. Circuit for electrical "switching" of the brilliance.

1) the spot appears;
2) the time base deflection begins;
3) the transient is released;
4) the transient ends;
5) the time base reaches the end of the screen;
6) the spot disappears.

Fig. 10–6 was recorded in this way, the spot brightness being modulated in addition by an A.F. voltage as time marker.

It has not been possible in this chapter to deal with more than the rudiments of intensity modulation. Its significance in television engineering needs no emphasing, as after all it contains the picture signal itself.

The subject of blanking the flyback was touched upon in the chapter on time base generators.

When making moving-film recordings, (with the Philips-Voigtländer camera "FE 106", for example), it is useful to brighten the spot in the manner described in the foregoing. In this way, the spot, which is stationary before the recording, can be prevented from burning the screen.

Intensity modulation is also used for displaying vector locus diagrams and three-dimensional oscillograms [9] [10] [11] [12] [13] [14] [15].

The functioning of the "stroboscope oscilloscope" for frequencies up to 50 Mc/s is also partly based upon intensity modulation [16].

It can moreover be applied for recording valve characteristics [17] and for representing simultaneously the interdependence of several quantities [18].

It is clear from the foregoing that the appropriate use of intensity modu-

[12] It must always be borne in mind that all these components are under high tension with respect to the chassis. Brightness "switching" can nevertheless be carried out quite safely by means of relays or voltage divider circuits.

lation—influencing the spot in the *third dimension*—opens up innumerable possibilities of application and greatly widens the scope of the apparatus.

11. Phase measurements

Fundamentally, two tasks can be distinguished:

1) the phase difference between two or more given voltages or currents is to be determined, or
2) the characteristics of a circuit unit, of a four-pole network (circuit components, amplifiers, etc.) are to be determined by measuring the phase shift of the output with respect to the input by means of a reference voltage of given frequency.

At this juncture a point of general importance must be made: *every phase measurement is synonymous with a measurement of time difference.*
Thus, every measurement of phase differences allows at the same time the determination of time differences, and vice versa.
The term "phase" means nothing more than the relative time difference between the phenomena under observation.
In the scope of this chapter we shall only be able to deal with the most essential of the great variety of procedures that have been made known up to the present day.

Phase measurement by multiple oscillograms.

When the waveforms of two voltages are displayed simultaneously on the screen of the oscilloscope, the mutual phase difference, that is the time difference between the relative points of the voltage curves, can be read off directly. This is illustrated by fig. 11–1. To read off the phase relations it is best to observe the points at which the voltages pass through zero; the maxima are less suitable for the purpose. The spacing of the zero points of one complete cycle corresponds to 360°, that is to the duration of one alternation T (the time taken to complete one cycle) or 2π.
For investigations of this kind a multibeam oscilloscope is not essential; the vertical deflection plates of a single beam oscilloscope can be switched to two

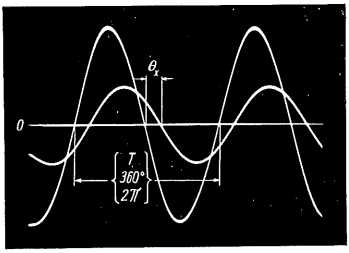

Fig. 11–1. Determining the phase difference between two voltages by a double oscillogram.

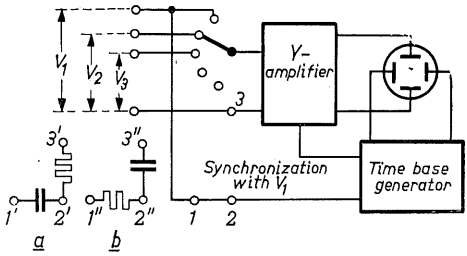

Fig. 11–2. Layout for measuring the phase difference between a number of voltages. Time base firmly synchronized with reference voltage.

or more voltages one after the other. What is essential is that during this process the time base generator must always be synchronized in fixed phase with the reference voltage, as indicated in fig. 11–2 (external synchronization). We can then be sure that the waveforms of the other voltages will represent faithfully the relative phase positions [13].

If switching is carried out rapidly enough (relay switch with at least 20 c/s or rotary switch with 1500 revolutions) in conjunction with long-persistence cathode ray tubes (DN 9–3, DR 10–3) or, still better, types with post acceleration (DN 10–5, DR 10–5, DR 10–6), the observer will obtain a picture of all the different waveforms at one and the same time.

A particularly efficient solution of the switching problem is offered by the electronic switch [14] by means of which the switch-over is adjustable between

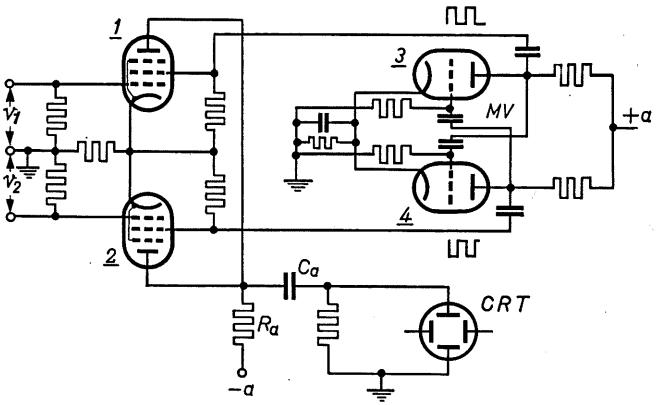

Fig. 11–3. Basic circuit of electronic switch.

frequencies from 2.5 c/s to 40 kc/s with the aid of electronic valves [1] [2] [3] [4] [5].

The basic circuit of this electronic or "amplifying" switching unit is shown in fig. 11–3. The two valves 1 and 2 represent two conventional amplifier stages which, however, possess a common anode resistor R_a. Both input signals v_1 and v_2 are applied to the control grids of these valves. The screen grids do not receive a constant *DC* voltage but a rectangular voltage from a multivibrator *MV*. During the half cycles when the screen grids are driven positive by this voltage the amplifier valves work alternately; that is to say they are switched on in turn during each half cycle of the multivibrator frequency. The amplified input signals appearing across anode resistor R_a are thus applied alternately via C_a to the *Y* plates of the cathode ray tube. In this way two signals

[13] To displace the whole picture sideways if required and to adjust a certain over-all phase position, a corresponding correction is possible by means of phase shifting networks in the sync lead, as shown in fig. 11–2*a* and *b*.

[14] The author recommends the use of the name "amplifier switch" instead of "electronic switch", in view of the fact that it expresses an important aspect of its functioning, namely that amplification also takes place, which can sometimes, indeed, be quite considerable.

can be made simultaneously visible on the screen of a single-beam cathode ray tube (with two electronic switches three signals can be displayed and so on). It is particularly important here that synchronization be carried out directly with an input signal frequency (external synchronization). Otherwise the time base frequency will fall into step with the switching frequency which, of course, lies on the vertical deflection plates, and the pattern will be correspondingly interrupted. For correct synchronization it is only necessary to adjust the switching frequency such that it differs from the integral multiple (or fraction) of the input frequency by more than about $\pm$ 20 c/s. Too great a difference between input and switching frequencies is not advantageous since the undesired patterns will then lie close together and it will be difficult to adjust the suitable switching frequency.

If the multivibrator of the electronic switch can be synchronized externally it is advisable to lock it with the time base voltage of the oscilloscope. This will ensure that the change-over to the second oscillogram always takes place during the flyback of the time base. The oscillogram of the one phenomenon will thus be displayed with one or more whole sweeps of the time base cycle before the change-over takes place.

A special switching device is not absolutely necessary for the photographic recording of multiple oscillograms. As described at the outset, the time base voltage is firmly synchronized with one of the voltages to be observed and this synchronization is then retained for the subsequent recordings. The individual phenomena are now adjusted on the screen at the appropriate amplitude and recorded one after the other on the same photographic material.

This was the method used for recording the oscillograms in figs. 5–10, 5–11, 5–13 and 13–6, 13–8, 13–9 and 13–11.

Measurements by phase marking

With the method just described the actual trend of the phenomena can be observed at the same time. There are some measurements, however, where all that is required is information on the phase difference (time difference).

For this purpose it is expedient to take off phase-dependent pulses from the voltages in question. This can be done magnetically by means of "pulse transformers" or electronically by means of thermionic valve circuits (fig. 11–4). The input voltage to be measured is amplified by valve 1 and the output is then applied to valve 2 in which, by anode and grid rectification, its peaks are clipped in such a way that a rectangular voltage appears in the anode circuit. By correctly rating the following CR coupling network, $\left(\frac{1}{\omega C} > 3\,R\right)$, differentiation is obtained, resulting in the peaky waves indicated. The grid of valve 3 is kept at such a heavily negative potential that only the positive pulses are able to cause a change in anode current (anode rectification). Thus during each cycle, a voltage pulse appears at the output and this pulse is used for phase indication [15].

[15] Phase correction can also be carried out here by connecting phase-shifting networks (RC or CR) to the input of this circuit.

For phase measurement, the time base generator is now adjusted to the frequency of the input signal and synchronized with the reference voltage (fig. 11–5). Both voltage pulses v_1 and v_2 are applied simultaneously to the input of the vertical amplifier. Mutual reaction is avoided in this type of circuit in the simplest possible way by resistors R_1 and R_2. If necessary a buffer stage can be incorporated. (See also fig. 12–15.)
The pulse v_1 synchronizes the time base. Since the sweep frequency is equal

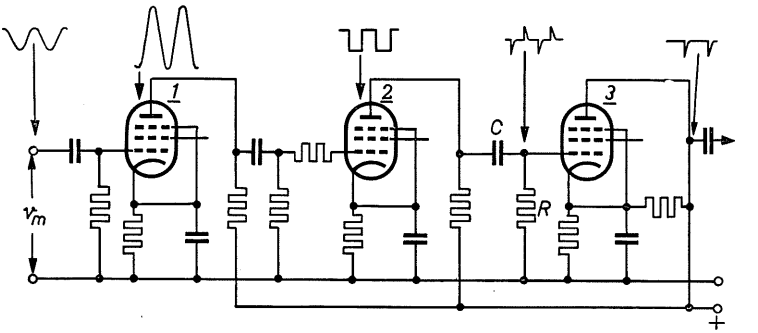

Fig. 11–4. Basic circuit for generating pulses from a sine wave for phase measurements with oscilloscope.

to the signal frequency the total picture-width, as shown in fig. 11–6, corresponds from the point of view of phase to one complete cycle, that is, to 360°. The time base voltage rises linearly with time and thus the phase scale over the whole width of the display is also linear. The phase difference can therefore readily be read off from the distance between the markings v_2 and v_1.
With this procedure, however, just as with that previously described, the accuracy of the reading is not very great, being only between about 5–10°. Improvement is possible by displaying several traces. A second sawtooth

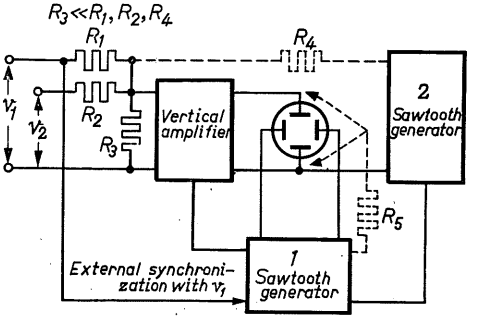

Fig. 11–5.
Layout for phase comparison with pulses according to fig. 11–4.

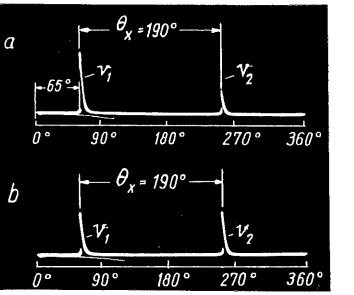

Fig. 11–6. Oscillograms of phase comparison with pulses; *a*) voltage pulses of different amplitude, *b*) pulses of equal amplitude.

generator is used for this purpose, the linear output of which is applied via resistor R_4 (in circuit 11–5) to the Y plates with the frequency of the input signal (synchronize!). If the time base frequency is now adjusted to, say, four times the second sawtooth frequency, four traces or lines will appear on the screen (see fig. 11–7). Each trace corresponds to a phase range of 90° so that the accuracy of reading is now within about 2°.

It can be seen from fig. 11–7*a* that the traces obtained are tilted. This is only a defect of appearance which can be removed by impressing on one of the Y plates a part of the time base voltage proper. This is effected via R_5 as indicated in fig. 11–5 and the correct Y plate must be found by experiment.

The corrected oscillogram is shown in fig. 11–7*b*.

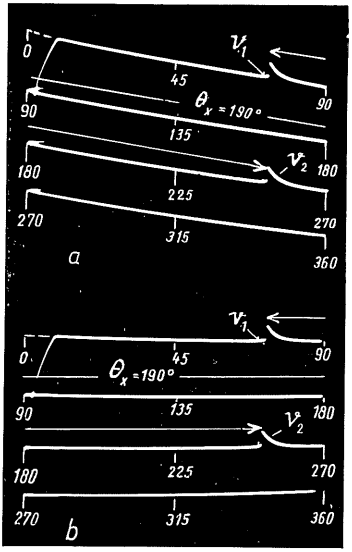

Fig. 11–7. Phase comparison with pulses extended to 4 traces; *a*) tilted traces without correction, *b*) horizontal traces corrected via R_5 as in fig. 11–5.

Phase measurement by Lissajous figures (ellipses).

Because of its great simplicity the measurement of the phase difference between two sinusoidal voltages by the formation of an ellipse has gained great importance. For such measurements the two voltages are simply applied to one pair of deflection plates each (fig. 11–8*a*). The resulting pattern on the screen is known as a Lissajous figure.

For better understanding of the process, some oscillograms are shown in fig. 11–9 to illustrate how the spot behaves when under the influence of in-phase voltages on the deflection plates. In this figure and in fig. 11–10, in which there is a phase difference of 30° between the two signals, thirteen equally spaced points have been marked along the time axes, and by projecting each of these points from the corresponding points on the voltage curves, the formation of the reference pattern is illustrated, which has itself been photographically recorded.

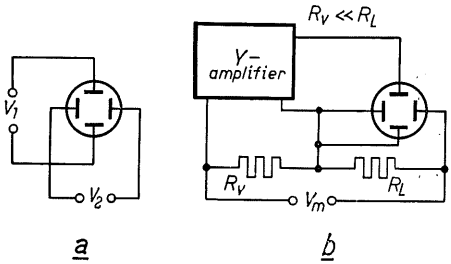

Fig. 11–8. Phase comparison by deflecting the spot in both coordinates to produce an ellipse (Lissajous figure); *a*) basic connections to deflection plates, *b*) layout for measuring the phase difference between current and voltage on a reactive load R_L.

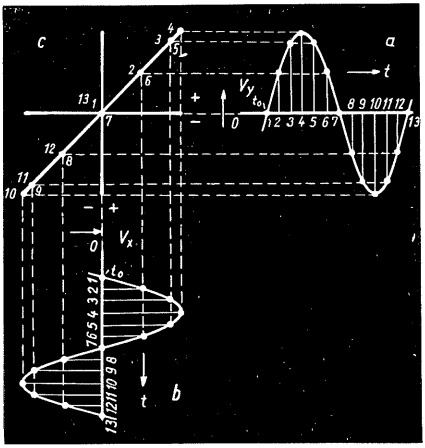

Fig. 11–9. Movement of the spot (*c*) under the influence of two sinusoidal voltages in equal phase (*a*) and (*b*).

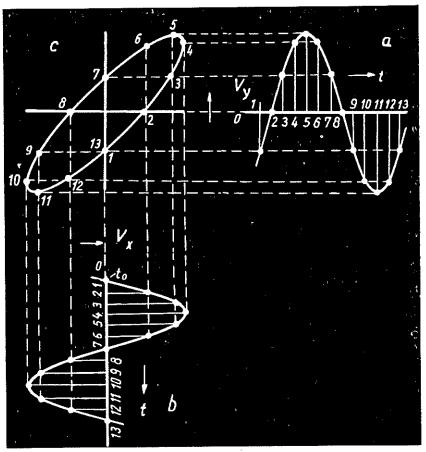

Fig. 11–10. Movement of the spot (*c*) under the influence of two sinusoidal voltages (*a*) and (*b*), with voltage (*a*) lagging.

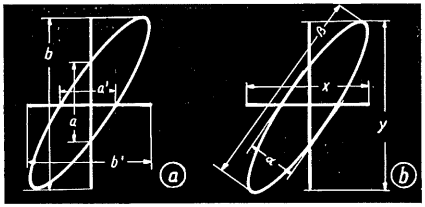

Fig. 11–11.
Determining the phase angle from the ellipse.

Whereas in the course of one cycle the spot in fig. 11–9 travels up and down on a straight diagonal, it describes an ellipse in fig. 11–10. The opening of the ellipse increases with increasing phase difference.
The phase angle can now be determined as shown in fig. 11–11*a* or *b*. The ratio of the part of either axis, ordinate or abscissa, bisected by the ellipse to the length of the projection to the corresponding axis is equal to the sine of the phase angle:

$$\text{sine } \theta = \frac{a}{b} \qquad (11\text{–}1)$$

and the angle θ is thus:

$$\theta = \text{arc sine } \frac{a}{b} \qquad (11\text{–}2)$$

It is a matter therefore of measuring the lengths a and b; the angle corresponding to the quotient $\frac{a}{b}$ can be found in any trigonometric table.
But even this small amount of labour can be made unnecessary by fixing over the face of the screen a sheet of transparent material calibrated with an appropriate scale as shown in fig. 11–12. For measurement, the amplitude of

deflection should be as large as is required for both end points of the scale just to be touched by the ellipse. The phase angle can now be read off directly. [6]

The phase angle can also be calculated from the length of the axes a and β of the ellipse and their projections X and Y according to the equation:

$$\theta = \text{arc sine} \frac{a \cdot \beta}{X \cdot Y} \quad (11\text{–}3)$$

(See fig. 11–11*b*.)

An impression of the patterns resulting from different phase angles is given by the oscillograms in fig. 11–14. It can be seen that the pattern is already ellipsoidal at 1°. In the oscillograms shown so far the amplitude of the deflection in both directions, was equal so that the longitudinal axis of the ellipse always appeared at an angle of 45°. This is not absolutely necessary.

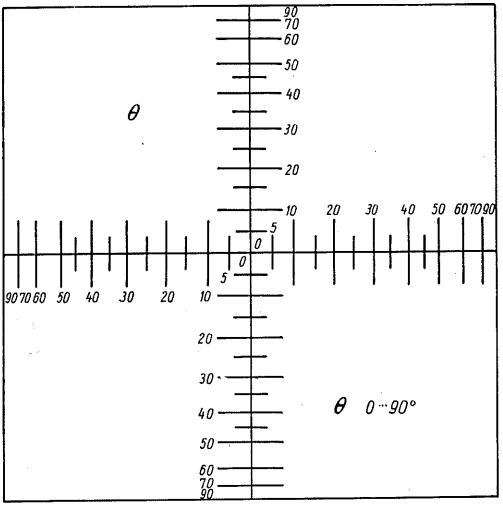

Fig. 11–12. Scale for phase measurement for $\theta < 90°$.

Fig. 11–13*a*, *b* and *c* shows three oscillograms with a phase angle of 30° to illustrate the effect of differences in amplitude between Y and X deflection. What is always decisive is the ratio between the lengths a and b.

The phase angle may not always be of direct interest, however. Very often a function of the phase angle—tan θ or cos θ—is required. This can also be read off directly. A scale with cos θ for $\theta = 0$–90° is given in fig. 11–15, similar to that given in fig. 11–12. It can be calculated from the formula:

$$\cos \theta = \sqrt{1 - \left(\frac{a}{b}\right)^2} \quad (11\text{–}4)$$

It is worth noting in this context that precisely those cos θ values above 0.5, which are of chief interest in practice, become increasingly easy to read as they approach 1.0.

The phase difference between current and voltage in a reactive load R_L can be

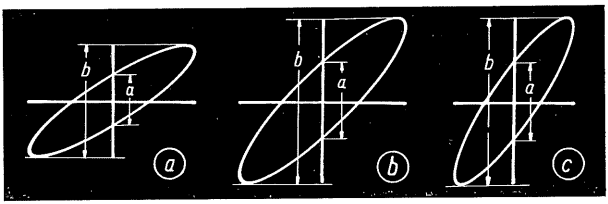

Fig. 11–13. Examples of the independence of phase measurement of deflection amplitude. *a*) Y amplitude smaller than X amplitude; *b*) Y amplitude equal to X amplitude; *c*) Y amplitude larger than X amplitude.

[6] The figure has been reproduced in its present size to enable a copy to be made of it on a similar scale, if so desired (photostat on transparent material or floodlit scale).

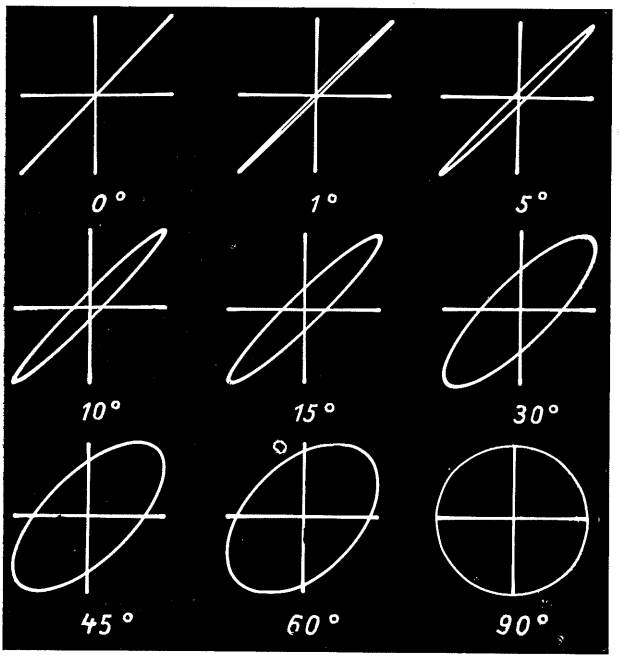

Fig. 11–14.
Nine characteristic oscillograms with varying phase differences.

measured as shown in fig. 11–8*b*. The voltage across R_L is used for the horizontal deflection. The total current flows through a resistor R_v, which is small compared with R_L, and the resultant voltage drop is used, after amplification, for the vertical deflection. (This deflection is thus proportional to the current.) Interpretation of the ellipse appearing on the screen makes it possible to determine at the same time, in the manner already described, current, voltage, cos θ and thus the power of the circuit.

Determining the sign of the phase angle.

From the formation of the ellipse, therefore, the phase difference between two voltages can be ascertained with appreciable accuracy. The oscillograms we have considered do not, however, readily show whether the voltage observed lags or leads the reference voltage.

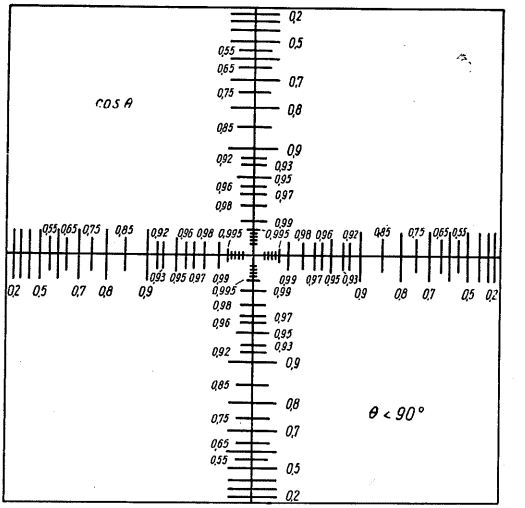

Fig. 11–15.
Scale for direct reading of cos θ.

A method of determining the sign of the phase angle is to introduce into the junction of the voltage with unknown phase angle a phase shifting network as in fig. 11–2*a* and *b*, in which the direction of phase change is known. (In fig. 11–2*a* the output voltage leads and in 11–2*b* it lags). If as a result of this network the ellipse is widened, then the phase shift of the unknown voltage will have the same direction and if it is narrowed, it will have the reverse direction. It is better to use a *CR*-network for this purpose (fig. 11–2*a*—output voltage leading.) The resistance R can be formed, in the AF band at least, by the input impedance of the oscilloscope so that in practice it is only necessary to connect up a suitably rated condenser.

If the phase difference is greater than 90°, the ellipse inclines towards the left side of the screen, as can be observed in the series of oscillograms given in fig. 11–16. At 180°, a straight diagonal forms as at 0°, but inclined towards the left of the screen (seen as a mirror image). As the phase difference increases, the ellipse widens again until at 90° and 270° a circle appears. If no special measures are taken the patterns up to 270° will be the same as those between 90° and 180°, just as the patterns between 270° to 360° will be the same as those between 0° and 90°.

Various measures have been devised for making these oscillograms free from ambiguity. The method proposed in fig. 11–17 is particularly simple. The grid of the cathode ray tube is supplied, via phase-shifting networks, with a portion of the reference voltage (not of the voltage whose phase changes) in such a way that at phase differences between 0–180° the right of the pattern on the screen is brightened and the left dimmed. This method was used for the oscillograms in fig. 11–16. If the phase difference exceeds 180°, the situation is reversed and the left of the picture is brightened. Thus in the examples shown in fig. 11–16 we can easily distinguish between the patterns representing phase differences of 15° and 345°, 45° and 315°, 90° and 270°, 135° and 225°, and 165° and 195°.

The most favourable value of the phase-shifting components R and C depends upon

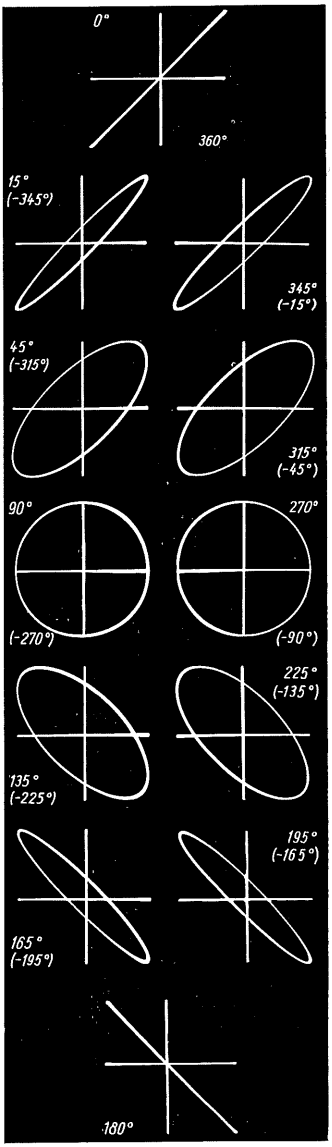

Fig. 11–16.
Oscillograms for phase measurement with intensity modulation, for unambiguously interpreting all patterns from 0° to 360°.

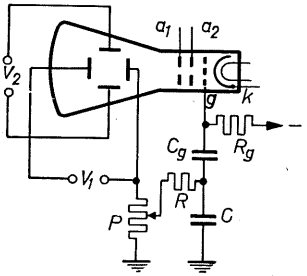

Fig. 11–17. Circuit for unambiguously interpreting ellipses by intensity modulation with the voltage with reference phase.

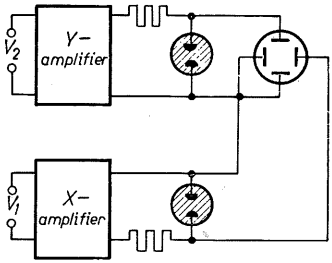

Fig. 11–18.
Phase measurement by means of glow-tube circuit.

the values of the grid network R_g, C_g, and must be found by experiment for a given signal frequency. The intensity modulation can be varied if necessary by potentiometer P. In this way it is possible to see from the oscillogram whether one has to do with a leading or lagging phase relationship (θ less than or greater than 0° or 360°).

Obviously, the accuracy with which phase measurements can be interpreted from the patterns on the screen depends also upon the sharpness of spot focus. A phase angle of 1° is still clearly readable. Measurement naturally is made more difficult and less accurate if the voltage curves are distorted [6].

Another interesting method of unambiguously determining phase-angles from oscillograms obtained with sinusoidal voltages is shown by the circuit in fig. 11–18. Both voltages, the reference voltage and the voltage to be compared, are brought by transformation or amplification to an amplitude higher than the ignition potential of a glow-tube. The voltages on both glow-tubes are switched alternately to both deflection plates. When the voltage on the glow-tube circuit during one half cycle reaches the ignition potential the voltage, after ionization, falls to the operating value v_B as indicated in the oscillogram in fig. 11–19, so that each time the peak P is formed. If the value of the peak voltage v_p is at least $2 \times v_B$, the remaining portion of the sine wave will be almost even. As a result of two such voltages on the deflection plates, angular patterns

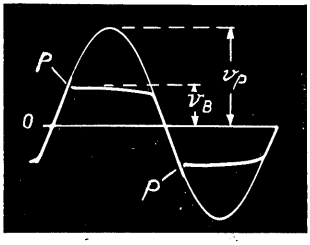

Fig. 11–19.
Operating voltage waveform of a glow-tube circuit as in fig. 11–18.

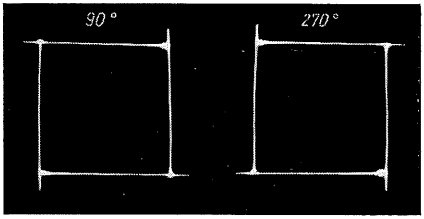

Fig. 11–20.
Patterns on the screen for $\theta = 90°$ and $\theta = 270°$ in measurements with a circuit as in fig. 11–18.

with peaks appear on the screen, and the length of their sides is a measure of the phase difference. At the same time, the peaks at the ends of the figure indicate the direction of the phase difference. Two characteristic patterns are shown in fig. 11–20, for $\theta = 90°$ and $\theta = 270°$ (or $-90°$).

Brightness modulation is another means of obtaining an accurate indication of the phase angle. If, as shown for example in fig. 11–21, the ellipse is intensity-modulated with an alternating voltage whose frequency is $\frac{360}{5} \cdot f_x$, a brightness marking will result at every 5°, making altogether 72 points. To determine the phase angle under 90°, it is only necessary to count the points falling into quadrants II or IV. The number of the points $\times$ 5° gives the phase angle. In the example reproduced it is therefore $5^1/_3 \times 5 = 26^2/_3°$.

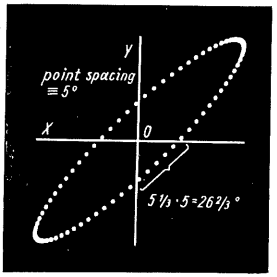

Fig. 11–21.
Phase measurement with brilliance marking.

It is expedient to produce these modulation markings by multiples of the input signal frequency, as was described in chapter 6 and illustrated in fig. 6–8. In this way the markings remain stationary and the pattern can be interpreted with ease.

Measuring the phase difference with a sharply bent sine wave.

An interesting method of particular value for measuring small phase angles is the following one [7]. The input signal is led over two cross-circuited diodes (valves or crystal diodes) which receive a small bias from battery *B*, as in fig. 11–22. Without bias both half-cycles of the sine wave would be passed through unattenuated. The result of the bias is to prevent current from flowing for a short period in the vicinity of the zero transition points. The resultant voltage appearing across the output resistor has a waveform as shown in fig. 11–23*a* for $\theta = 0°$.

Applying this voltage now to a circuit element (*CR*-network, amplifier) in which the phase change occurs which is to be measured, then these "steps" become displaced, the displacement "*A*" being a measure of the phase change. In fig. 11–23 the oscillograms above "*a*" show corresponding patterns for phase angles of 0°, 1°, 5°, 15° and 30°. For this process, therefore, no comparison voltage with a reference phase is required.

In extension of this idea, other possibilities present themselves. For example, without horizontal deflection (fig. 11–23*b*) the bends in the curve cause two points to appear in the vertical trace, and the distance between them is likewise a measure of the phase difference. In fig. 11–23*a* the horizontal deflection frequency was half as great as the signal on the *Y* plates to produce the pattern observed. But even when the time base frequency is deliberately not synchronized with the vertical deflection frequency but is appreciably higher or lower, patterns are obtained which can still be interpreted (fig. 11–23*c*). On a luminous area, which becomes darker towards the middle, two horizontal traces appear, the spacing of which can also serve to indicate the phase

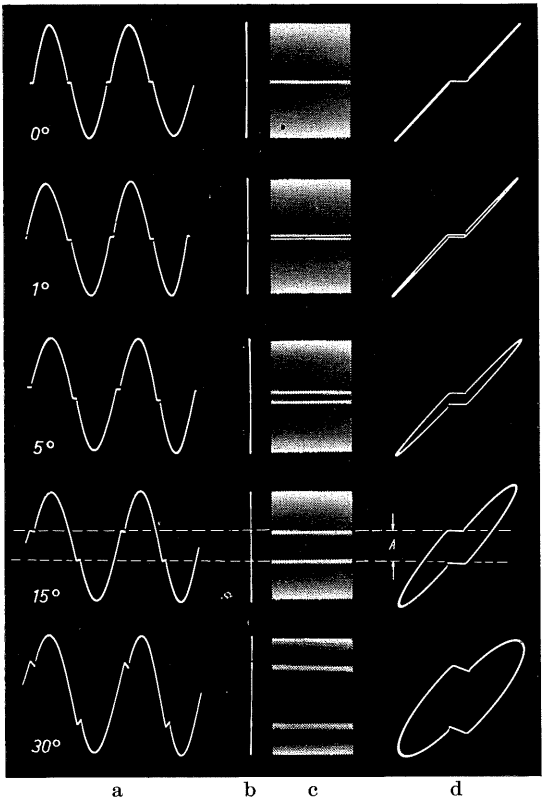

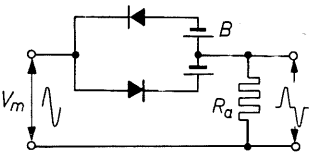

Fig. 11–22.
Circuit for generating a "bent" sine wave.

Fig. 11–23.
Oscillograms for measurement with a "bent" sine wave.

difference. It is also possible to dispense with the time base generator altogether and to effect the horizontal deflection by means of the "unbent" input signal (amplified if necessary) as shown in the circuit in fig. 11–24. The patterns then obtained on the screen are, as reproduced in fig. 11–23*d*, "bent" ellipses—ellipses with a short, horizontal portion in the centre. The spacing of these portions of the curve is again a measure of phase.

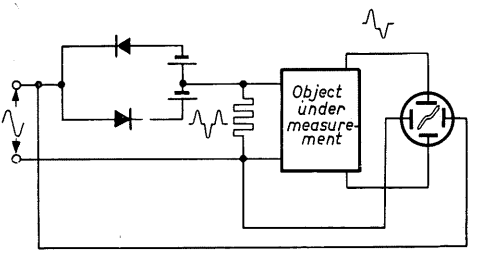

Fig. 11–24. Circuit for phase measurement with bent sine wave for patterns as in fig. 11–23*d*.

Phase measurement on a circular scale.

The use of a circular scale to indicate the phase angle between two alternating voltages is particularly expedient since it allows direct presentation in electrical degrees of angle. One method of achieving this is as follows. The reference voltage v_1 is impressed upon both pairs of deflection

plates such that both component voltages have a phase difference of 90°. The circuit generally to be recommended is shown in fig. 11–25, in which the comparison voltage v_1 is applied across the series arrangement of a resistor R with a condenser C. If $\frac{1}{\omega C} = R$, then the phase difference between the voltages v_C and v_R is very nearly 90°. With equal amplitudes of deflection in the X and Y directions, the pattern appearing on the screen at exactly 90° phase shift will be a circle.

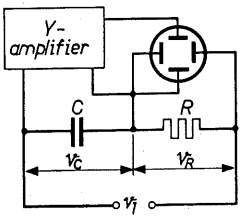

Fig. 11–25.
Circuit for generating a circular trace.

The prerequisite here is, of course, that v_1 shall be symmetrical with respect to earth. As this is seldom the case, the circuit usually employed is as illustrated in fig. 11–26. In this circuit the deflection voltages for both pairs of plates are mutually displaced by minus or plus 45° by means of an *RC* or a *CR* network. In the process the voltages drop to 0.707 of the amplitude of the input voltage. In this example the mains voltage is employed for v_1. (Since a variable auto-

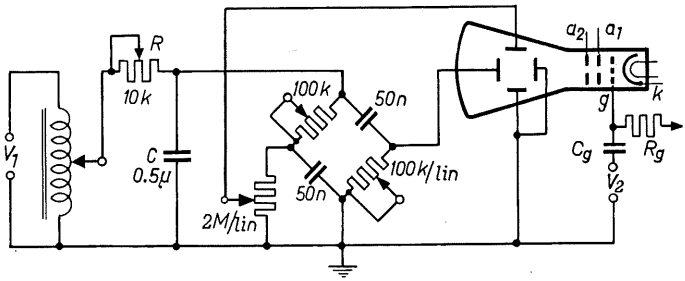

Fig. 11–26.
Circuit for a circular trace — v_1 single-pole earthed.

transformer with one winding is used at the input, attention must be paid to correct polarity.)

The harmonics always present in mains voltages must be filtered out by an *RC* network as otherwise severe distortion of the circle will appear. (The circle

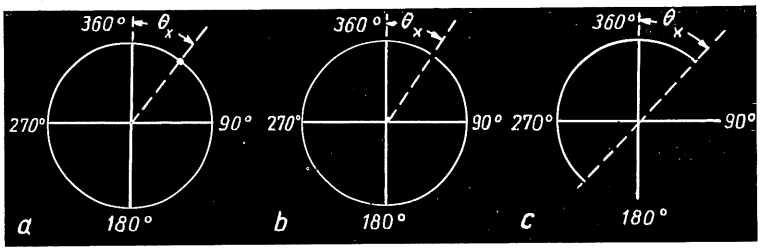

Fig. 11–27. Oscillograms for phase measurement with a circular trace; *a*) brilliance marking, *b*) blank marking, *c*) brightening of semi-circle.

is an ideal criterion for harmonics.) The size of the circle can be adjusted by the input transformer. The phase and thus the circle itself can be adjusted by the two variable resistors of 100 kΩ and the symmetry of the pattern can be regulated by the 2 MΩ potentiometer.

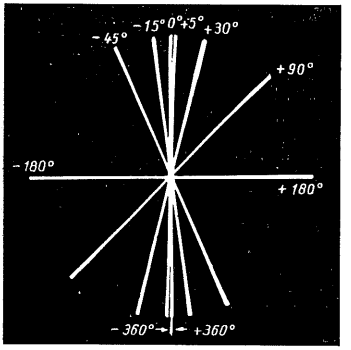

Fig. 11–28.
Phase measurement with rotating trace.

A pulse is now generated (as described by fig. 11–4) from voltage v_2, whose phase difference with respect to v_1 is to be measured, and this pulse is impressed upon the grid of the cathode ray tube so that, according to polarity, a bright marking or an interruption appears on the circumference of the circle, as shown in fig. 11–27*a* and *b*. The marking for $\theta = 0$ can be easily ascertained by connecting v_1 itself to the device for generating the pulse (fig. 11–4). The output position on the circumference of the screen can be corrected as desired by means of phase-shifting networks at the input of the pulse-former. The distance of the measuring mark from the zero mark on the circumference of the circle gives the phase angle directly in degrees up to 360°.

The oscillogram in fig. 11–27*c* indicates another, similar method, which is to take a rectangular voltage from the second valve in the circuit in fig. 11–4, and to apply it to the grid of the cathode ray tube. The result is that exactly one half of the circle is brightened. The chord connecting the end points of the semi-circle likewise gives a phase scale in degrees of angle. The degree of accuracy in interpretation using these methods with standard cathode ray tubes is about 2° [8] [9].

A number of circuits, "phase bridges", have also been made known, with which a trace is formed that rotates in dependence upon the phase difference between both voltages [10] [11] [12] [13]. (An identical circuit is described in the following chapter on frequency measurements "circuit for the representation of cycloids".) A prerequisite is that the amplitudes of these voltages shall be entirely equal. The phase angle can then be read from a circular scale covered by a rotating trace as illustrated by fig. 11–28, which shows a number of traces representing certain phase angles.

It can be seen that phase angles are indicated of max. +360° or —360°.

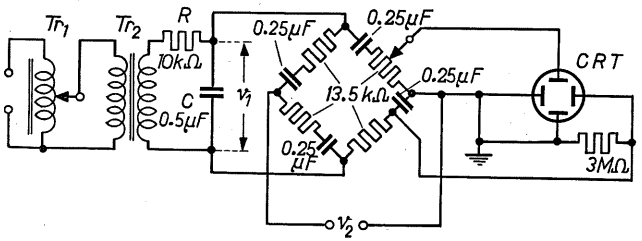

Fig. 11–29.
Bridge-circuit for producing a rotating trace.

The phase angle corresponds to twice the angle of rotation of the trace. Thus if α is the angle of rotation and θ is the phase angle, then:

$$\theta = 2 \cdot \alpha \qquad (11\text{–}5)$$

The relevant circuit is shown in fig. 11–29. In this example the phase difference between the voltages v_1 and v_2 at mains frequency was observed. The voltage was taken from the mains after regulation by Tr_1, separation by Tr_2 and smoothing by R and C. For the elements of the bridge circuit, $\frac{1}{\omega C}$ must be equal to R. The values given in the circuit provide satisfactory results.
It must be added that this method of indication is ambiguous, that is to say the trace for 0° can also be 360°, that for 90° also —270° and that for 180° may be —180°. The method is most suitable for the measurement of large phase angles. The accuracy of reading remains constant over the whole range of 360°, being about 5°.
If the two voltages v_1 and v_2 are taken from different AC generators, then without perfect synchronization a rotating trace is obtained, from which the synchronization of the generators can be very simply and clearly adjusted.
It should be noted that, where sufficient voltage is available, no more than a few inexpensive circuit elements are needed for the purpose, apart from the cathode ray tube and its power supply (no vertical amplifier and no time base generator). In this way phase measurements can readily be carried out even at frequencies as high as 1 Mc/s [14].
The circuit for the phase bridge is, as in most measuring arrangements given here, rated for a specific frequency. If phase measurements are to be carried out within a certain frequency range, however, it is necessary to include in each voltage lead a mixer valve for frequency transposition. The frequency-determining elements of this stage should be rated such that the output frequency is always equal to the bridge frequency.

Phase measurement with a rectangular voltage.

With the aid of a symmetrical rectangular voltage it is possible to investigate with excellent results the phase-shifting influence of individual circuit elements or of an entire amplifier, especially when the phase differences are small.
Alternating voltages of this kind can either be generated in multivibrator circuits, in a square-wave voltage generator (e.g. Philips' GM 2314 or GM 2324) or obtained by "clipping" a sinusoidal voltage.
The voltage is applied with a suitable amplitude to the object under measurement and the wave-form of the output voltage is observed on the oscilloscope. The oscilloscope amplifier must naturally be able to pass this waveform faithfully at the frequency in question. One should first, therefore, make quite sure on this point by connecting the input signal directly to the oscilloscope. As we saw in chapter 5 (fig. 5–14) square waves make very high demands on an amplifier.
The behaviour of the voltage in relation to time is then observed (preferably two cycles) with a linear voltage on the X plates.

The resultant patterns of the most important gradations of phase difference are shown in the series of oscillograms in fig. 11–30*a*. Viewing these pictures from the side we can perceive as early as $^1/_2{}^\circ$ a faint tilt of the straight portions of the waveform. (The vertical portions could not be recorded owing to the extraordinarily high deflection speed.)

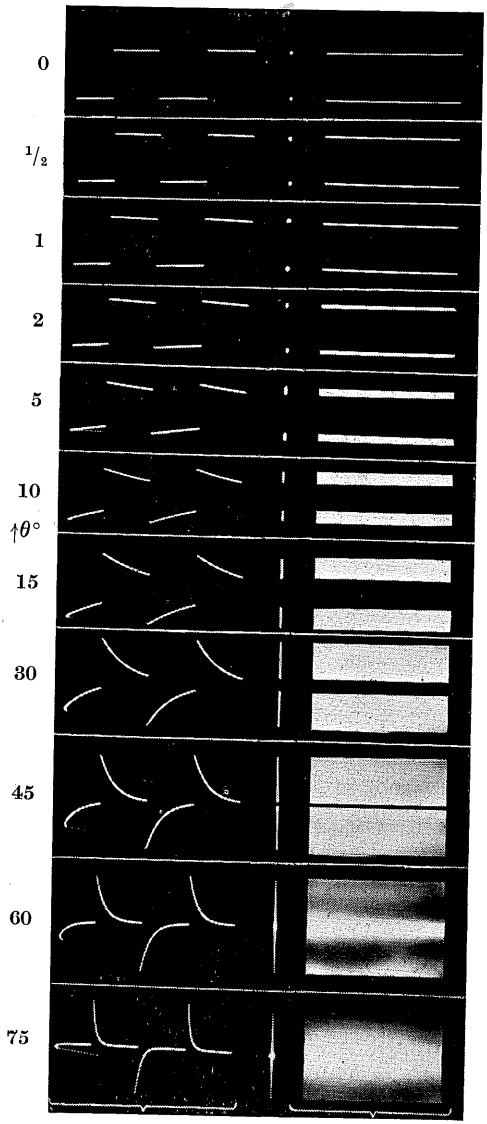

Fig. 11–30. Oscillograms for phase measurement with square waves; *a*) patterns of two cycles, *b*) without time base, *c*) time base frequency higher than signal frequency and not synchronized.

In addition to this familiar procedure, two other possibilities are indicated in the series of oscillograms *b*) and *c*). In series *b*) the voltage on the X plates was switched off: for this purpose the time base generator can be dispensed with entirely.

This results in the appearance of points, or strokes, whose height in relation to the total picture height is a measure of the phase difference.

In series *c*), although the time base generator was in use, the frequency was much higher than the input frequency and not synchronized. Traces or strips of different thickness now appear whose breadth in relation to the whole picture height can again serve as a measure of the phase difference.

The distortion of a square wave by phase shift.

To be able to judge the oscillograms thus obtained we must first know the causes of this distortion.

As is known, a square wave can be built up according to Fourier from a fundamental sine wave and an appropriate number of sinusoidal harmonics in certain phase relationships. For a square wave voltage beginning at zero with the positive maximum value of amplitude A the following equation applies:

$$y = \frac{4 \cdot A}{\pi} \sum_{n=1}^{n=\infty} \frac{1}{2n-1} \cdot \text{sine}\,(2n-1)\,x \qquad (11\text{–}5a)$$

or

$$y = \frac{4 \cdot A}{\pi} \cdot \left[\text{sine } x + \frac{1}{3}\text{sine } 3x + \frac{1}{5}\text{sine } 5x \ldots\right] \qquad (11\text{–}5b)$$

The amplitude relationships are as follows:

Fundamental:		amplitude	1
3rd harmonic:		,,	$^1/_3$
5th ,,	:	,,	$^1/_5$
7th ,,	:	,,	$^1/_7$
9th ,,	:	,,	$^1/_9$
11th ,,	:	,,	$^1/_{11}$ and so on.

This means that a voltage of this shape contains the 101st harmonic with still 1% the fundamental.
In a circuit element which determines the low-frequency end, the output voltage leads the fundamental frequency of the input voltage.
In a circuit element which determines the upper frequency end, the output voltage lags the input voltage. Since at the low-frequency end the harmonics, corresponding to the frequency, are appreciably less shifted in phase, and

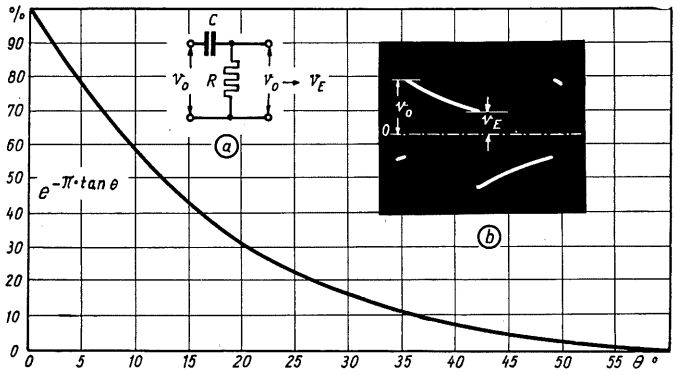

Fig. 11–31. Dependence of attenuation factor $e^{-\pi \cdot \tan\theta}$ upon phase angle θ. *a*) *CR* network, *b*) oscillogram distorted by phase shift.

since, moreover, their "wavelength" is only a fraction of the fundamental, the instantaneous values change such that the horizontal portions of the voltage curve become tilted in the direction of the time axis.
In a circuit element determining the upper frequency limit the harmonics are influenced more strongly than the fundamental (as a rule attenuation occurs too) and the portions of the curve become rounded counter to the direction of the time axis.
To gain a picture of the change in waveform at a certain phase shift we could draw the fundamental together with its harmonics and construct the

sum curve for the characteristic cases. But this would take up far too much time. We can, however, find the connection between phase difference and change of the square wave from the following consideration.
At the beginning of each half cycle of the signal, condenser C (fig. 11–31*a*) is charged up [5].
Until the arrival of the following half cycle, condenser C can discharge through resistor R. The voltage decay is given by the time constant $\tau = R \cdot C$, to which the familiar equation for the discharge curve of a CR circuit applies:

$$v_E = v_o \cdot e^{-\frac{t}{C \cdot R}} \tag{11–6}$$

As indicated in fig. 11–31*a*, v_o is the initial voltage and v_E is the voltage at the end of the half cycle.
The time t is in this case (symmetrical signal) equal to half the reciprocal of the rectangular-voltage frequency, thus:

$$t = \frac{1}{2f} \tag{11–7}$$

It is now necessary to show the voltage v_o and v_E on the one hand and the phase angle on the other hand in their mutual dependency. We should recall in this context the equation: $\cot \theta = \omega \cdot R \cdot C$, which was derived as (5–16) for coupling elements of this sort in chapter 5.
If we now insert in equation (11–6) equations (11–7) and (5–16) and substitute $\frac{1}{\tan \theta}$ for $\cot \theta$, we obtain:

$$v_E = v_o \cdot e^{-\pi \tan \theta} \tag{11–8}$$

Fig. 11–31 shows the curve for the dependence of the attenuation factor $e^{-\pi \tan \theta}$ upon the phase angle θ, calculated according to (11–8). We can read from this, for a given phase angle, the voltage decay at the end of the half cycle or inversely the phase angle corresponding to a given fall in amplitude. [6]
Oscillograms 11–30 *b* and *c* are particularly suitable for this measurement, being so easy to interpret.
The oscillograms reproduced in fig. 11–30 correspond to the prerequisites mentioned so that they can readily be used as a kind of scale for practical comparisons.
For this reason a fairly comprehensive series of oscillograms was selected to provide the reader with a basis of comparison for a given case. It is worth making an attempt to memorize these characteristic patterns.
In series *a*), especially in the lower pictures, it can be seen that the total

[5] For the lower frequency limit the corresponding circuit elements of an amplifier can be combined to form the equivalent circuit of a CR network. In a similar way, the upper frequency limit can generally be characterized by the parallel circuiting of a suitable resistor and an "equivalent" capacitance.

[6] A scale can also be constructed from this curve to enable the phase angle to be read straight from the screen. It is only necessary in this case to adjust the picture height so that the end marks are reached above and below.

picture height increases with increasing phase-shifting influence of the circuit elements present. This can be explained as follows.

If the RC time constant is so large that no noticeable phase change appears, then the voltage amplitude is so high that as a result of "recharging", the spot jumps from the given minus deflection to the plus deflection and vice versa as in fig. 11–32*a*. The voltage source thus overcomes the voltage difference $2 \cdot v_{max}$. If, however, the time constant is so small that the zero line is reached *before* the end of the half cycle, as shown in fig. 11–32*b* (the condenser can practically discharge itself within this time), then the voltage source again allows the output voltage to rise to the value $2 \cdot v_{max}$, but this time from the zero line. At the next half cycle it falls by the same amount after it has first again become zero, so that about twice the amplitude of the voltage peaks occurs as before. This applies to the case where $\theta < 60°$. Where $\theta > 60°$ (75° etc.), the decay of the amplitude of the fundamental becomes noticeable, so that the total picture now becomes smaller. If the value of the CR network is such that the condenser can partly but not wholly discharge, then of course various intermediate values of amplitude are found, as may be seen from the pictures in fig. 11–30 from about $\theta \geq 10°$ onward.

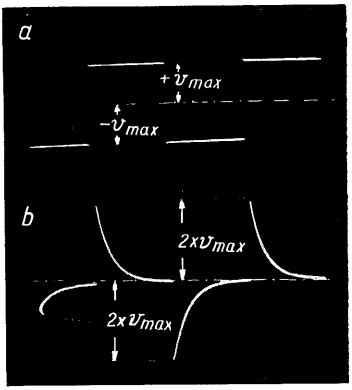

Fig. 11–32. Oscillograms to explain increase of amplitude at large phase angles; *a*) phase angle $\theta = 0°$, *b*) phase angle $\theta = 60°$.

Electrical differentiation.

With increasing phase shift the oscillogram corresponds less to the course of the input voltage itself than to its change or to the slope of the curve at each moment. As a curve of this kind represents the differential quotient of the original curve, the possibility of electrical differentiation arises. For the picture in which $\theta = 60°$, $\frac{1}{\omega C}$ was equal to $1.8 \cdot R$ and for $\theta = 75°$, $\frac{1}{\omega C}$ was equal to $4 \cdot R$. It can be seen that from about $\frac{1}{\omega C} = 3 \cdot R$, this effect becomes sufficiently distinct for interpretation. In this way, from any voltage corresponding to a changing phenomenon an oscillogram can be obtained which represents mathematically the first derivation of the process. Referring to the circuit as in fig. 11–31*a*, if we make $\frac{1}{\omega C} \gg R$, then the current i flowing through these circuit elements will be determined mainly by C.

The voltage v_c across this condenser is then for practical purposes equal to the input voltage v_o, thus $v_o \approx v_c$. As is known, the current through a condenser is proportional to the voltage change $\frac{dv}{dt}$, and thus the current here is pro-

portional to $\frac{dv_o}{dt}$. The voltage drop v_E is then equal to:

$$i \cdot R = v_E \approx R \cdot C \cdot \frac{dv_o}{dt} \qquad (11\text{–}9)$$

The output voltage v_E in a circuit rated in such a way is given by the product of a constant ($k = RC$) and the differential quotient of the input voltage. It is thus proportional to the first derivation of the input voltage.

Phase measurement with half-wave rectified sinusoidal voltages.

Since there may not always be a voltage source available for square waves of variable frequency, it should be mentioned that similar measurements are possible with a half-wave rectified *AC* voltage. In fig. 11–33 oscillograms are set out similar to those for square waves in fig. 11–30. Here also we can work without horizontal deflection and obtain patterns as in series *b*). With a higher, non-synchronized time base frequency, patterns result as shown in series *c*). With a voltage curve of this sort, however, phase changes of less than 2° are not readily perceptible.

Investigations on circuit elements with lagging phase.

Square waves can also be used to investigate the influence of an *RC* network (fig. 11–34*a*) on phase relations. A series of oscillograms for such a case are shown in fig. 11–35. The voltage across the condenser now reaches its maximum value after a delay. The larger the *RC* time constant, the slower the voltage rise. Since the influence of the circuit in 11–34*a* is equivalent to the circuit in 11–34*b*, under certain conditions which apply in amplifying technique [15] [16], these results can also be applied to investigations on the upper frequency limit of circuit elements or amplifier stages. According to fig. 11–35 the amplitude of deflection does not increase in this case but always decreases, as opposed to the case of a *CR*-network.

Electrical integration.

As the picture for $\theta = 75°$ in fig. 11–35 shows, an almost exact triangular wave has been formed from the square wave. Thus, during each half cycle of the rectangular voltage the output voltage rises constantly, and falls likewise during the next half cycle. But this corresponds to the integrated curve of the input voltage. Therefore, with a circuit as in fig. 11–34*b* electrical integration is possible. For this purpose R must be $> 3 \cdot \frac{1}{\omega C}$.

Referring to the circuit in fig. 11–34*a*, if we make $R \gg \frac{1}{\omega C}$ then the current i flowing through these circuit components is for practical purposes determined by the value of R. In first approxmation, therefore, $i = \frac{v_o}{R}$. The voltage v_C across condenser C caused by the alternating current i is given by the equation $v_E = \frac{1}{C}\int i \cdot dt$. (The capacitance integrates the current i over the time t).

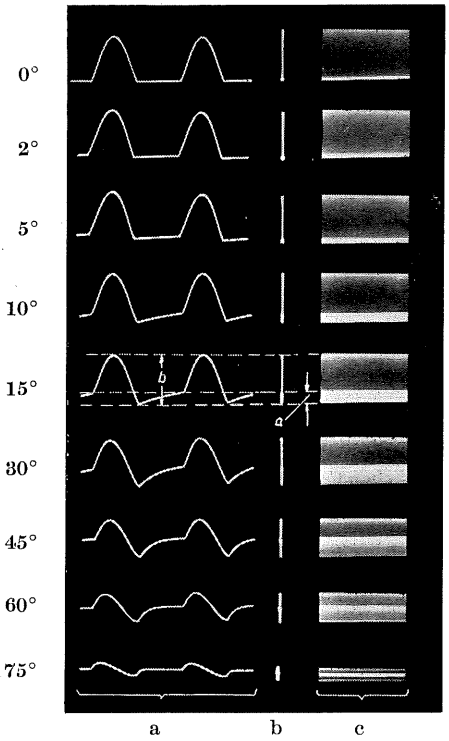

Fig. 11–33. Oscillograms for phase measurement with half-wave rectified sine waves; *a*) with time base, *b*) without time base, *c*) with high, non-synchronized time base frequency.

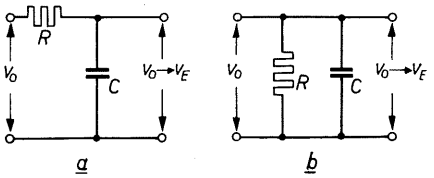

Fig. 11–34. *RC* circuit *a*) and equivalent circuit with resistor and capacitor in parallel *b*).

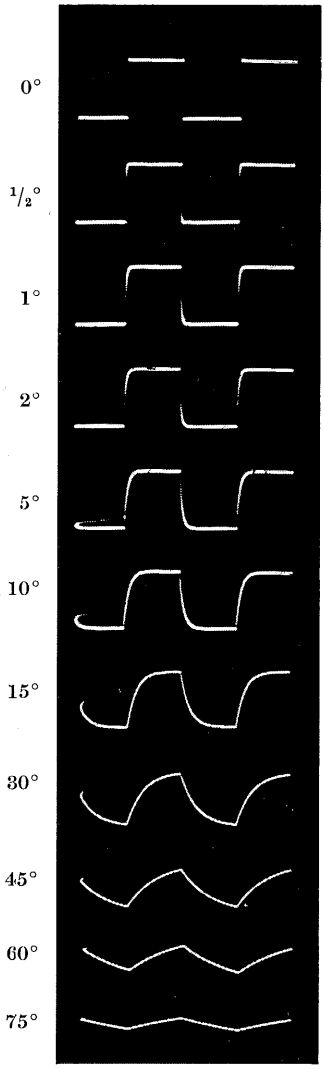

Fig. 11–35. Oscillograms for phase measurements at negative phase angle.

Provided that $i = \frac{v_o}{R}$, the voltage across the condenser is obtained from the equation $v_E = \frac{1}{RC} \cdot \int v_o \cdot dt$. It corresponds to the integral of the voltage v_o over time t.

In this way the voltage corresponding to any other change in condition (e.g. the velocity of a movement) can again be converted into a voltage proportional to the time integral of this voltage (the amplitude of a movement). See also the relevant references to the literature in chapter 10 "The uses of intensity modulation" [2] [3] [4].

It can be seen from the oscillograms in fig. 11–36 that half-wave rectified sinusoidal voltages are less suited for investigating circuit elements with a phase lag. Particularly noticeable is a rounding of the trailing edge of the voltage peak and a displacement of the half-wave peak due to increasing phase lag of the fundamental. These changes are not so marked however as with a square wave.

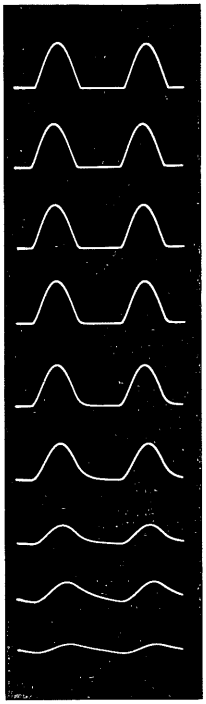

Fig. 11–36. Phase measurement with half-wave rectified sine waves with negative phase angle for the fundamental.

The use of square waves for assessing the properties of electrical transmission systems.

It was mentioned in chapter 5, with regard to the unit function response of an amplifier, that a very clear general idea of the essential characteristics of a deflection amplifier can be obtained by observing its behaviour during sudden periodically rising or falling input voltages.

We have further seen in this chapter how phase changes can be observed with the aid of square waves.

The combination of such results has shown that square waves, which can be regarded as a periodic sequence of switching on and off, can provide information on all the essential characteristics of the object under measurement, i.e. frequency response, phase distortion, overshoot, etc.

For such purposes, asymmetrical rectangular voltages are sometimes used to allow the system under test a longer time to swing out in accordance with its time constants after the pulse of the shorter part of the cycle.

Contrary to frequency-response testing with sine waves, which requires a whole sequence of measurements, often only one measurement suffices for ascertaining whether a certain square wave is undistorted, or distorted to a certain known extent, in order to be able to form a sufficiently accurate judgment of the characteristics of the transmission system in question. A special oscillographic technique has been developed from this which finds particular application in pulse technique and in the field of television.

The principle is also applied in locating faults in cables and overhead lines [17] and for ultrasonic testing for defects in manufactured parts [18].
For a through treatment of these subjects the reader is referred to the relevant publications [19—29]. A work by J. Müller [24] deserves special attention in view of the wide survey it offers. (See also chapter 19.)

12. Frequency measurements

Frequency measurement — frequency comparison.

The cathode ray oscilloscope by itself is not a device for measuring frequency, but it makes possible frequency *comparison* with a measure of accuracy which can hardly be equalled by other means. (For absolute frequency measurement, see page 223 et seq.)
The only limit set to the accuracy of the reading is the "absolute" limit at which the observer is still able to determine with sufficient precision changes in the pattern on the screen. The higher the frequency, the higher the accuracy of reading.
The oscilloscope being fundamentally a voltage-actuated device, the following pages will deal mainly with investigations on actual electrical potentials, but it should be recalled that quite generally every change of condition, mechanical, optical, thermic and so on, can always be converted by a suitable transducer into a proportional voltage and displayed on the screen of the oscilloscope. In this way, for example, very accurate measurements of rotation speeds are possible. The rotating part can be scanned by a light beam and a photocell, so that no mechanical connection or loading is necessary.
In a similar manner the time-keeping of a watch can be checked and adjusted in a surprisingly short space of time [1].

Frequency measurement by comparison with the time base frequency.

The time base frequency first suggests itself as a means of determining the unknown frequency, since it is after all adjustable within the individual ranges. As a rule, however, the scale adjustment only approximately coincides with the actual frequency of the time base (it can be dependent upon the supply voltage, amplitude, etc.) so that without further measures being taken it is not to be recommended if absolutely reliable results are required. [1]
On the other hand, exact measurements are immediately possible if the time base frequency is firmly synchronized with a suitable standard frequency. The standard frequency should be equal to, or a small integral multiple of, the time base frequency required for the measurement.
To proceed, therefore, the frequency of the time base generator is adjusted so that it is equal to or a fraction of the standard frequency. Once synchronization

[1] Certain oscilloscopes, especially those for pulse measurement, are being fitted nowadays with calibrated scales for time-base expansion. These can of course be used straight away for frequency measurements—within the limits of accuracy indicated.

is firmly established we have the assurance that the time base has the accuracy of the standard frequency.

The voltage with the unknown frequency is then applied, amplified or not, to the Y plates. The circuit for a frequency comparison of this kind is shown in fig. 12–1. What now appears on the screen is the waveform of the voltage with known frequency. In the following examples sinusoidal voltages will generally be used. Zig-zag wave shapes and other forms may also appear, however, and be similarly interpreted. If the number of cycles appearing on the screen is equal to N_{fx}, and if the known frequency is f_n, then, if the frequency ratios are whole-numbered the unknown frequency will be:

$$f_x = N_{fx} \cdot f_n \cdot p \qquad (12\text{–}1)$$

The factor "p" represents the ratio—time base frequency : reference frequency. If they are equal, it is then equal to 1. Otherwise it will always be a fraction or an integral multiple of unity. In the series of oscillograms given in fig. 12–2, the patterns "e" to "i" represent those cases where the unknown frequency is exactly equal to or an integral multiple (1, 2, 3, 5 and 10×) of the time base frequency. If, on the contrary, the unknown frequency is only an integral fraction of the time base frequency then during each time base cycle only a portion of the waveform of the unknown frequency will appear. The whole picture of one cycle of this voltage now appears during a certain number of time base cycles in sections one above the other, as shown in fig. 12–2 a to d for integral frequency ratios of $^1/_{10}$ to $^1/_2$.

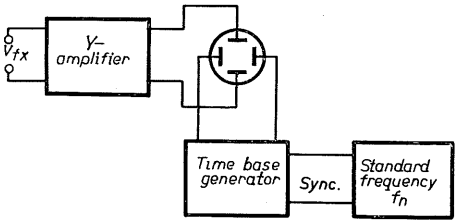

Fig. 12–1. Layout for frequency measurement by comparison with the synchronized time base.

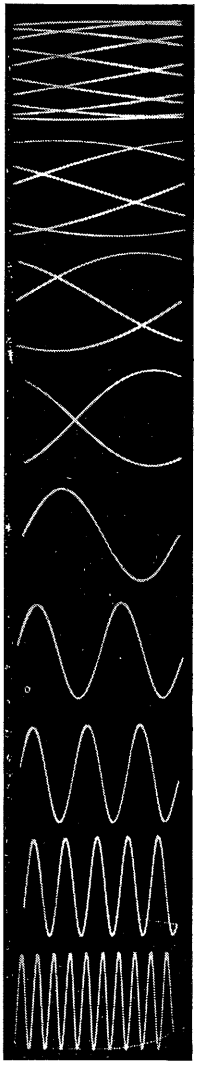

Fig. 12–2. Oscillograms obtained with a circuit as in fig. 12–1.

$f_x : f_n =$	a	b	c	d	e	f	g	h	i
	$^1/_{10}$	$^1/_5$	$^1/_3$	$^1/_2$	1	2	3	5	10

The unknown frequency is found from patterns of this kind as the quotient of the known frequency f_n and the number of curve sections N_s of the unknown frequency, as:

$$f_x = \frac{f_n}{N_s} \cdot p \qquad (12\text{–}2)$$

Useful results can still be obtained from patterns where the frequency ratios are not even numbered. Fig. 12–3 reproduces an arbitrarily chosen number of the innumerable figures resulting from a frequency ratio between 2 : 1 and 3 : 1 (fig. 12–2 between f and g). If the comparison frequency $f_n = 50$ c/s (mains) and the time base frequency is synchronized in the ratio 1 : 1, then these patterns correspond to values of f_x as given in the last column of table 12–I. The frequency ratios for these patterns are set out in fractions and decimals in order to show how, with a single comparison frequency, any desired number of intermediate values in the frequency adjustments can be found, which is particularly expedient when making continuous calibrations.

To interpret such patterns it is best to think of the figure as being enclosed in a rectangle and then to count the number of points at which the loops touch the horizontal tangent (above or below) and the number of loops touching the vertical tangent (left or right), as illustrated in fig. 12–4. The unknown frequency is now given by:

$$f_x = f_n \cdot \frac{N_l}{N_s} \cdot p \qquad (12\text{–}3)$$

in which N_s is again the number of curve sections and N_l the number of loops touching the tangents.

Symbol	$f_x : f_n$	f_x (in c/s) (for $f_n = 50$ c/s)
a	$^{17}/_{6} = 2^{5}/_{6} = 2{,}833$	$141^{2}/_{3}$
b	$^{14}/_{5} = 2^{4}/_{5} = 2{,}800$	140
c	$^{11}/_{4} = 2^{3}/_{4} = 2{,}750$	$137^{1}/_{2}$
d	$^{8}/_{3} = 2^{2}/_{3} = 2{,}667$	$133^{1}/_{3}$
e	$^{5}/_{2} = 2^{1}/_{2} = 2{,}500$	125
f	$^{7}/_{3} = 2^{1}/_{3} = 2{,}333$	$116^{2}/_{3}$
g	$^{9}/_{4} = 2^{1}/_{4} = 2{,}250$	$112^{1}/_{2}$
h	$^{11}/_{5} = 2^{1}/_{5} = 2{,}200$	110
i	$^{13}/_{6} = 2^{1}/_{6} = 2{,}167$	$108^{1}/_{3}$

Table 12–I (to fig. 12–3)

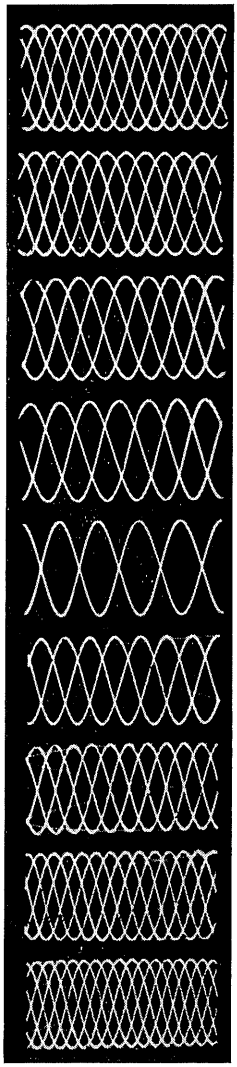

Fig. 12–3. Oscillograms with odd-numbered frequency ratios (3....2; Table 12–I).

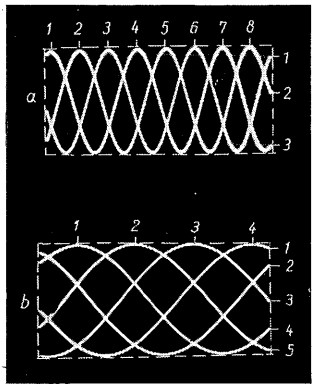

Symbol	$f_x : f_n$	f_x (in c/s) (for $f_n = 1000$ c/s)
a	$^7/_{16} = 0{,}438$	$437^1/_2$
b	$^3/_7 = 0{,}428$	$428^4/_7$
c	$^5/_{12} = 0{,}417$	$416^2/_3$
d	$^2/_5 = 0{,}400$	400
e	$^5/_{13} = 0{,}385$	$384^8/_{13}$
f	$^3/_8 = 0{,}375$	375
g	$^4/_{11} = 0{,}364$	$363^7/_{11}$

Table 12–II (to fig. 12–5)

Fig. 12–4.
Counting the patterns at frequency ratios: $f_x : f_n =$ *a*) $^8/_3 = 2^2/_3$; *b*) $^4/_5$.

In fig. 12–4*a*, $f_n = 50$ c/s, $f_x = 50 \cdot {}^8/_3 = 133^1/_3$ c/s. The equation (12–3) also applies, however, to frequency ratios at which $\frac{N_l}{N_s}$ is < 1. In the example given in fig. 12–4*b*, $\frac{N_l}{N_s} = {}^4/_5$, $f_n = 50$ c/s and $f_x = 50 \cdot {}^4/_5 = 40$ c/s.

The fact that numerous intermediate values can also be found for frequency ratios smaller than unity is demonstrated by the arbitrarily selected oscillograms in fig. 12–5, which appear between the frequency ratios $^1/_2$ and $^1/_3$. Assuming again that the time base is synchronized in the ratio 1 : 1, with $f_n = 1000$ c/s, frequency ratios and intermediate values are obtained as set out in table 12–II.

Interpretation of these patterns is limited by the ability to count the number of loops N_l touching the tangents. It should also be noted that, if the number of curve sections is too large, some of them may be lost owing to the flyback time. The patterns in figs. 12–3 and 12–5 particularly may appear at first rather confusing and difficult to interpret, but after some practice it will soon be found that patterns such as those in 12–3*e* and 12–5*d*, for example, stand out very clearly. Usually it is not even necessary to count them in this way. When calibrating a scale, it is found by continuously varying the unknown frequency that characteristic patterns of this kind appear quite distinctly, so that these points can readily be established as calibration marks between the integral frequency ratios. It was mainly to draw attention to these in-

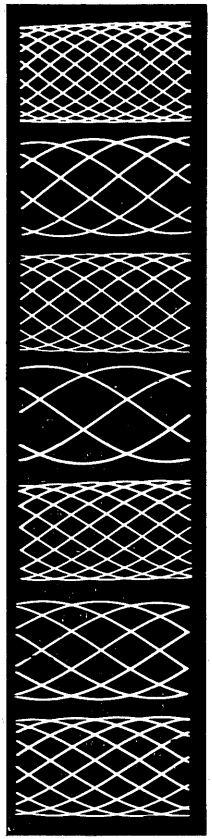

Fig. 12–5.
Oscillograms with odd-numbered frequency ratios ($^1/_2 \ldots . {}^1/_3$, Table 12–II).

frequently exploited possibilities that the oscillograms reproduced have been discussed at such length.

Frequency measurement with several traces (lines).

The oscillograms discussed in the foregoing make it apparent that for large frequency ratios the screen should be able to accommodate a widely extended picture. For this purpose, as already described in the chapter on phase measurements, it is possible with two linear time base voltages to trace

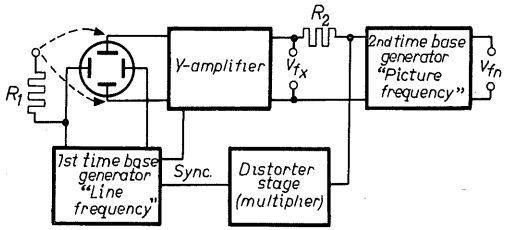

Fig. 12–6.
Block diagram for frequency comparison with several traces.

horizontal lines on the screen and superimpose on them the voltage with the unknown frequency. The relevant circuit is shown in fig. 12–6 which largely resembles the circuit in fig. 11–5 in chapter 5.
The sawtooth oscillator for the "picture" frequency is synchronized with the standard frequency. By means of a distorting stage (shaper) multiples of the "picture" frequency are generated, filtered and used to synchronize the line frequency oscillator. If, for example, the standard frequency is 50 c/s, then it is quite possible to observe in five lines a frequency one hundred times that of the standard frequency, i.e. 5000 c/s. By an appropriate choice of lines one can in this way—with one "picture" frequency and various line frequencies—cover a wide band of frequencies. Where a standard frequency equal to or a multiple of the line frequency is available, we can then, in inverse order, use it to synchronize the first sawtooth oscillator and from this we can synchronize the second. The shaper with filter elements can then be dispensed with.

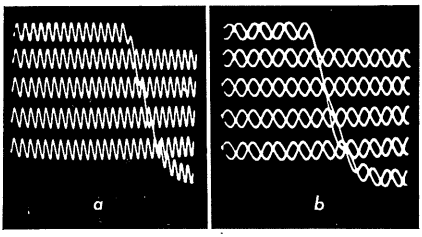

Fig. 12–7. Oscillograms with several traces (lines) for frequency comparison: *a*) 5 traces; $f_x : f_p = 127$; *b*) 5 traces; $f_x : f_p = {}^{83}/_2 : 1 = 41^1/_2$; f_p = picture frequency.

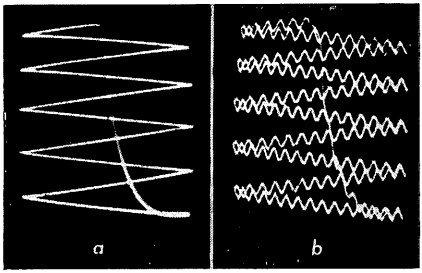

Fig. 12–8. Frequency comparison with trace produced by triangular voltage: *a*) pattern of the base line; *b*) with the frequency to be measured $f_x : f_p = 141$.

Typical patterns are shown in fig. 12–7*a* and *b*. In order to obtain horizontal lines, here again a portion of the line frequency voltage was fed to the Y plates over resistor R_1. A point to be noted in this context is that when there are a large number of lines a not unappreciable part of the unknown frequency pattern is sacrificed to the flyback.
In such cases it is better to use a triangular instead of a normal sawtooth line voltage. Voltages of this sort can be produced by integration of a rectangular voltage [2]. (See also chapter 16 "Measuring the action of between-lens shutters", figs. 16–2*c* and 16–3.) In place of the first sawtooth voltage oscillator, an arrangement should be visualized of a square-wave generator, an integration network and perhaps an amplifier, in circuit following each other (fig. 12–6). Examples of the result of this arrangement are shown in fig. 12–8. Trace and flyback are now equalized so that the patterns can be evaluated in both directions without any portions remaining unseen.

Frequency comparison by double oscillograms.

If a twin-beam oscilloscope, or a single-beam oscilloscope with an electronic switch, is available, frequency comparison can be undertaken by directly comparing the patterns of both voltages. The time base is now to be synchronized again with the standard frequency. With a twin-beam oscilloscope the same time base voltage can be used for both systems, as it must be in any case with a single-beam oscilloscope. The voltage of the comparison frequency is applied to one input of the electronic switch and the voltage with the unknown frequency to the other. The waveform of the known frequency then remains stationary, and shows immediately whether the time base frequency is equal to or a fraction of the comparison frequency.

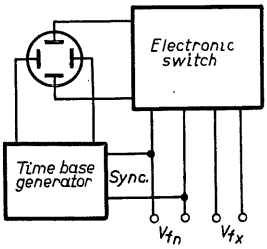

Fig. 12–9. Block diagram for frequency comparison with electronic switch.

Fig. 12–9 shows the basic layout for this method of frequency comparison. By comparing the number of cycles of the unknown frequency N_{fx} with the number of cycles of the known frequency N_{fn}, the unknown frequency is:

$$f_x = f_n \cdot \frac{N_{fx}}{N_{fn}} \qquad (12\text{–}4)$$

Fig. 12–10 shows a double oscillogram of this kind (f_x above, f_n below) for an integral frequency ratio of 4 : 2. In fig. 12–10*b* the frequency ratio was not an integral one, being 5 : 2.
If the waveform of the reference frequency is not a simple figure but looks like those in fig. 12–3, then in accordance with equation (12–3) the factor "p" must be introduced for N_{fn} (fig. 12–10*c*-top). The same applies when the waveform of the voltage with unknown frequency is not a simple figure (see fig. 12–5).

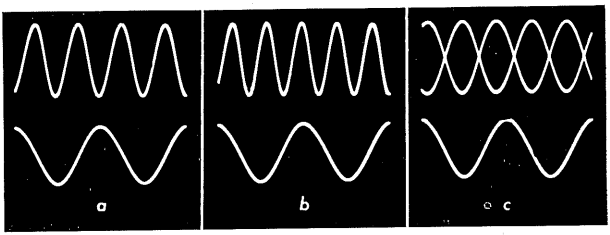

Fig. 12–10. Double oscillograms using electronic switch:
a) $f_x : f_n = 2$;
b) $f_x : f_n = {}^{5}/_{2} = 2{}^{1}/_{2}$;
c) $f_x : f_n = \frac{{}^{5}/_{2}}{2} = 1{}^{1}/_{4}$.

Frequency comparison by anode-voltage modulation of a circle.

A circular trace is obtained, as already described, by applying two voltages displaced 90° with respect to each other to both pairs of deflection plates. The basic circuit is again shown in fig. 12–11.
If the anode voltage of the cathode ray tube is now modulated sufficiently by the voltage with the unknown frequency, the sensitivity of the deflection plates will vary in such a way that the circle will be rhythmically widened and narrowed.
For this purpose the second anode of the C.R.T. is not directly earthed but connected to the chassis over a resistor. To this resistor is applied the voltage with the unknown frequency, and the result on the screen is as shown in fig. 12–12.

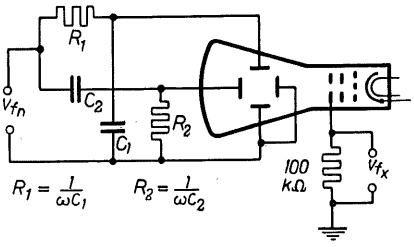

Fig. 12–11.
Circuit with anode-modulated C.R.T. for frequency measurement with circle.

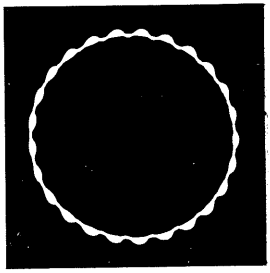

Fig. 12–12.
Circular trace with anode-modulated C.R.T.

It should be added that modulation of the anode voltage also affects the sharpness of spot focus. It must therefore not be too large. Good spot focus in conjunction with the possibility of stronger modulation can be achieved by modulating simultaneously the other electrodes (a_1, g_2), in proportion to their share of *DC* voltage. The unknown frequency is found from the number of radial displacements N_{fx} on the circumference of the circle, thus:

$$f_x = f_n \cdot N_{fx} \qquad (12\text{–}5)$$

(The "circle" frequency is then equal to f_n).

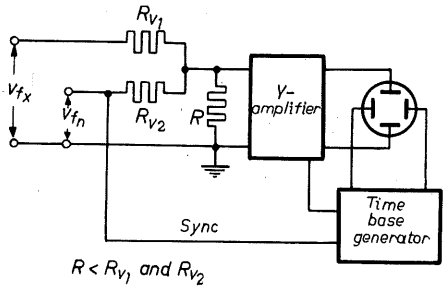

Fig. 12–13. Circuit for frequency comparison by addition of v_{f_x} and v_{f_n}.

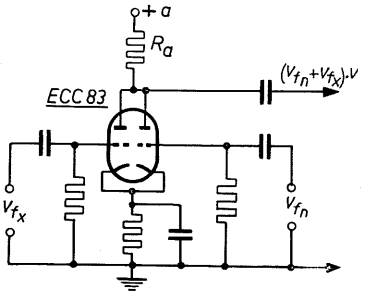

Fig. 12–15. Circuit for addition with a double valve.

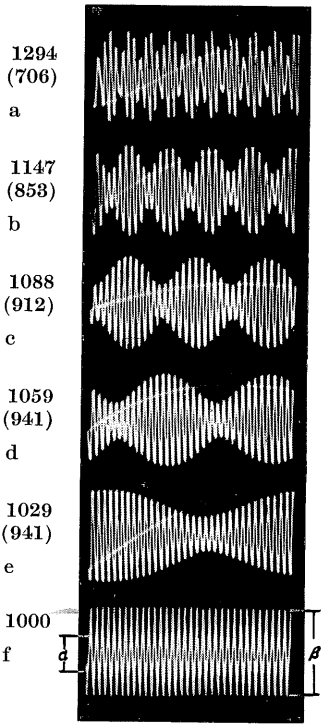

Fig. 12–14. Oscillograms for frequency comparison by addition. The figures beside the patterns apply to $f_n = 1000$ c/s and $f_n = f_X = 34$.

Frequency comparison by adding the voltage of unknown frequency and the comparison frequency.

In this process both voltages are applied together to the input of the vertical amplifier, as shown in fig. 12–13. To avoid mutual reaction on the voltage sources, there should be at least two series resistors, R_{v1} and R_{v2}, as indicated, and the common input resistor R should be small with respect to them. In the circuit used when recording the oscillograms in fig. 12–14, $R_{v1} = R_{v2}$ were 800 kΩ and R was 170 kΩ. A better method of adding the two voltages is to use a double valve, as shown in fig. 12–15 (ECC 40 or ECC 83). Since both anode connections contain the common load resistor R_a, the voltages v_{fn} and v_{fx}, amplified in both systems, are added in the anode circuit. The possibility of reaction is thus extremely slight. If necessary it could be reduced still further by using pentodes. The input voltages for measurement should preferably have approximately the same amplitude. The time base generator should be firmly synchronized with the reference voltage v_{fn} so that its frequency will

not change if, during measurement, amplitude fluctuations appear on the deflection plates (external synchronization).

As long as the two frequencies do not stand in any integral relation to each other the patterns on the screen will drift one through the other. When frequency equality is achieved, however, the pattern of the reference voltage appears again, but the amplitudes fluctuate in the rhythm of the frequency difference, i.e. a beat frequency occurs. This is illustrated by the oscillogram, in fig. 12–14*f*; the amplitude fluctuations from α to β were photographed employing a long exposure in conjunction with a small aperture.

Should the unknown frequency deviate from the comparison frequency, on the other hand, symmetrical variations of amplitude appear above the waveform of the standard frequency, which, at certain frequency-differences, appear as stationary beating patterns (amplitude modulation).

Oscillograms illustrating this phenomenon are shown in fig. 12–14*a*) to *e*). If N_{fn} is the number of cycles adjusted via the time base, corresponding to the quotient of the comparison and time base frequencies, thus:

$$N_{fn} = \frac{f_n}{f_X} \qquad (12\text{–}6)$$

then the unknown frequency f_x, which, with the reference frequency, causes the beating, is found by:

$$f_x = f_n \pm f_n \cdot \frac{N_{beat}}{N_{fn}} \qquad (12\text{–}7)$$

in which N_{beat} is the number of beating patterns in the picture. The interesting fact emerges from this that one can thus very easily obtain fixed frequency points in the vicinity of a standard frequency at a spacing of:

$$\pm f_n \cdot \frac{N_{beat}}{N_{fn}}$$

By the choice of N_{fn} (the cycles of the reference frequency adjusted on the screen) the frequency spacing can be chosen within very wide limits.

In the oscillograms in fig. 12–14, $N_{fn} = 34$.

At larger frequency spacings the patterns are not always so easy to interpret but, after a little practice, equally accurate results can be obtained from them.

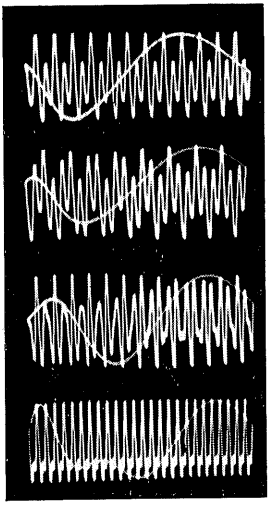

Fig. 12–16.
Oscillograms with large spacings between the known and unknown frequencies.

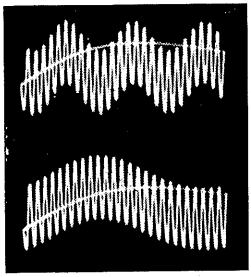

Fig. 12–17.
Oscillograms for *a*) $f_x = 3 f_X$ and *b*) $f_x = f_X$.

In fig. 12–16*a*), for example, $f_x = {}^1/_2\, f_n$, [2] in *b*) $f_x = {}^1/_3\, f_n$, in *c*) $f_x = 1{}^1/_2\, f_n$ and in *d*) $f_x = 2\, f_n$.

Useful results can also be obtained when the unknown frequency is so low that it is equal to or a multiple of the time base frequency. The amplitudes of v_{fn} now vary in the rhythm of $\frac{f_x}{f_X}$. The frequency can be determined in the same way as described under "Frequency measurement by comparison with the time base frequency", page 197.

In this case, however, the ratio $f_n : f_X$ can be read straight from the screen from the number of cycles N_{fn}. The unknown frequency is found from the equation:

$$f_x = \frac{N_{fx}}{N_{fn}} \cdot f_n \qquad (12\text{–}8)$$

The factor N_{fx} now represents the number of variations due to f_x.

In fig. 12–17*a* the unknown frequency f_x was equal to $3f_X$ and in *b*), $f_x = f_X$. When $N_{fn} = 26$ and $f_n = 1000$ c/s, the unknown frequency is $115^5/_{13}$ c/s and $38^6/_{13}$ c/s respectively.

These examples make it clear how, in a simple manner, it is possible with one standard frequency to make accurate frequency measurements in a wide range.

Frequency comparison with Lissajous figures.

When two voltages whose frequency ratio is to be determined are applied one to the Y plates and the other to the X plates of the cathode ray tube, the spot under their influence will trace on the screen patterns known after their originator as Lissajous figures.

The elementary layout for this is shown in fig. 12–18. If both frequencies are equal, a simple figure with no cross-over appears on the screen, as already described in the chapter on phase measurements and illustrated in figs. 11–14 and 11–16 (pages 182, 183). The resultant patterns are ellipses, the inclination and opening of which depend upon the phase difference and amplitude relationship of the two voltages. For an analytical evaluation of these figures the interested reader is referred to the relevant publications [3] [4].

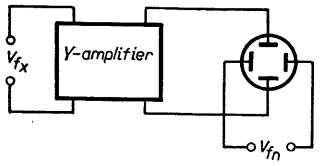

Fig. 12–18. Layout for frequency comparison by Lissajous figures.

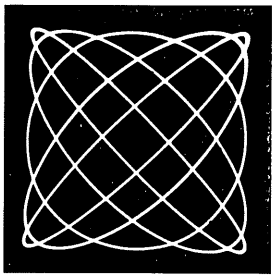

Fig. 12–19. Composite oscillogram: frequencies equal but differences of phase. Phase differences of individual figures: 15°, 45°, 90°, 105° and 135°.

[2] Otherwise expressed, the oscillogram represents the picture of a sine wave with its first harmonic in a certain phase relationship.

At small differences of frequency the oscillogram passes in a certain space of time through all the patterns for phase relationships from 0° to 360°.

Fig. 12–19 shows a composite oscillogram representing phase differences of 15°, 45°, 90°, 105° and 135°, where the amplitudes of deflection in both directions were equal. The frequency difference Δf can, if small, be determined by checking on a stop watch the time taken for the phase to pass through 360° (one cycle). The reciprocal of this time T (in seconds) is then directly equal to the frequency difference:

$$\Delta f_{(c/s)} = \frac{1}{T(\mathrm{s})} \qquad (12\text{–}9)$$

In this way very slight frequency differences, amounting to small fractions of one cycle, can be ascertained accurately. If the frequency ratio is an integral multiple, the familiar Lissajous figures with crossed loops appear which, depending on the initial phase relations of both voltages, can also pass through a great variety of different shapes.

In fig. 12–20 a number of original oscillograms are set out to illustrate how different patterns are produced in the individual phase positions [3] of the voltage on the Y plates (higher frequency) when the frequency ratio is 2 : 1. It can be seen that there are certain patterns which repeat themselves and are thus susceptible of more than one interpretation. The figure for a phase difference $\theta = 0°$, for example, also appears at $\theta = 180°$, that for $\theta = 45°$ can also be $\theta = 135°$, and so on.

The oscillogram for 90°, which inversely repeats itself at 270° and which, when the curves coincide, also appears in a

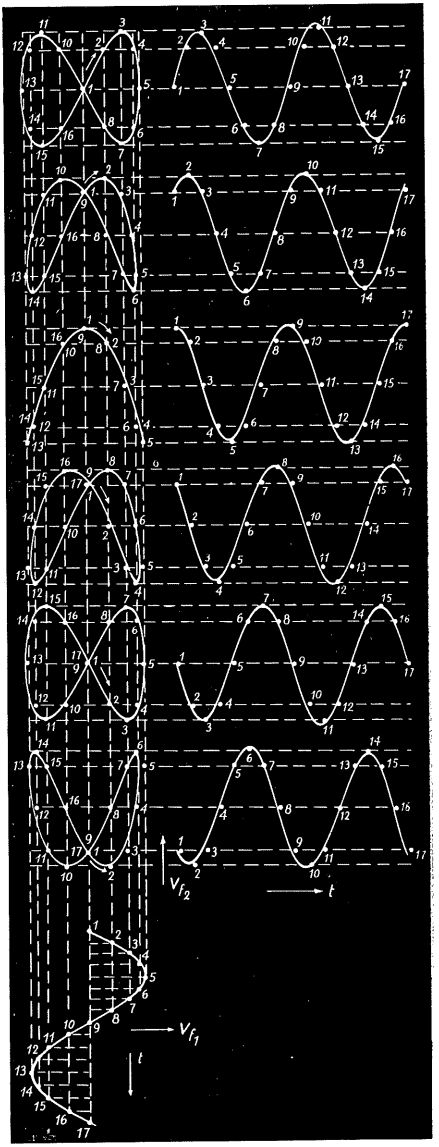

Fig. 12–20. Lissajous figures at 2 : 1 frequency ratios for different initial phase position of the higher frequency. The oscillograms are set out in steps of 45° between 0° and 225°. The arrow indicates the direction of movement of the spot from the starting point.

[3] The term "phase position" refers in this context to the initial phase of the voltage with the higher frequency. A phase difference of 360° means, therefore, a cycle of the voltage with the *higher* frequency.

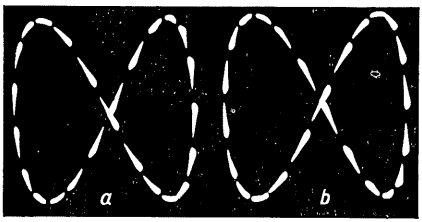

Fig. 12–21. Non-linear intensity modulation to clarify ambiguous patterns *a*) 0°, *b*) 180°.

correspondingly transformed shape at higher even-numbered frequency-ratios, is identical with what is known as the "Tschebyscheff function" [5]. Here too it is possible to obtain unambiguous patterns by means of intensity modulation with a reference voltage, as shown in fig. 11–16 in the preceding chapter. For this purpose an asymmetrical voltage waveform of a higher frequency is the most suitable. The sawtooth voltage in the time base generator of a second oscilloscope can be used with advantage. The effect of this intensity-modulation is shown in fig. 12–21*a* and *b*, where the frequency ratio is 2 : 1 at phase differences of 0° and 180°. A wedge-shaped brightness-

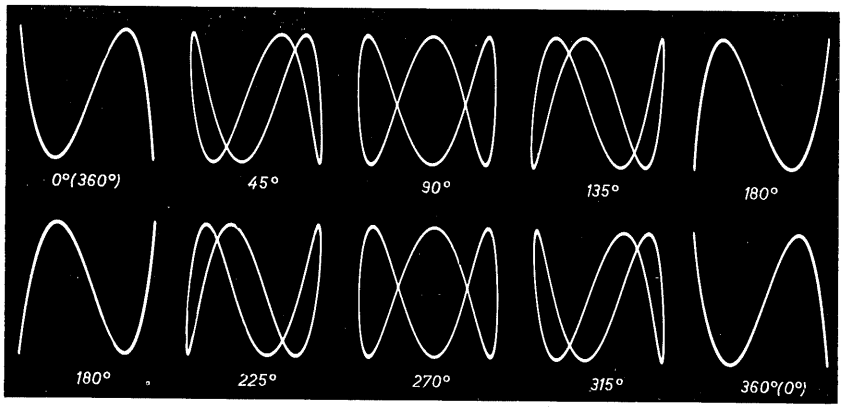

Fig. 12–22. Lissajous figures for 3 : 1 frequency ratio at different phase conditions.

marking is produced, the direction of which, when the patterns for 0° phase difference are known, allows the other phase positions to be unambiguously distinguished.

Of course, at higher frequency ratios too the oscillograms pass through the

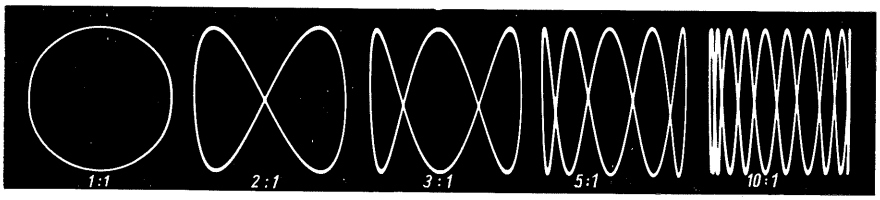

Fig. 12–23. Lissajous figures for whole-numbered frequency ratios: 1 : 1, 2 : 1, 3 : 1, 5 : 1 and 10 : 1.

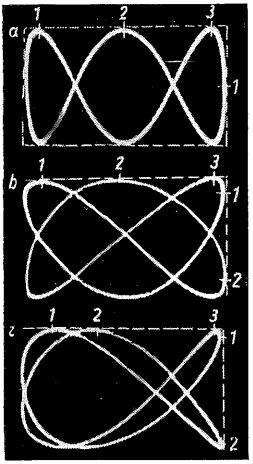

Fig. 12–24.
Method of counting on Lissajous figures: *a*) 3 :1, *b*) and *c*) 3 : 2.

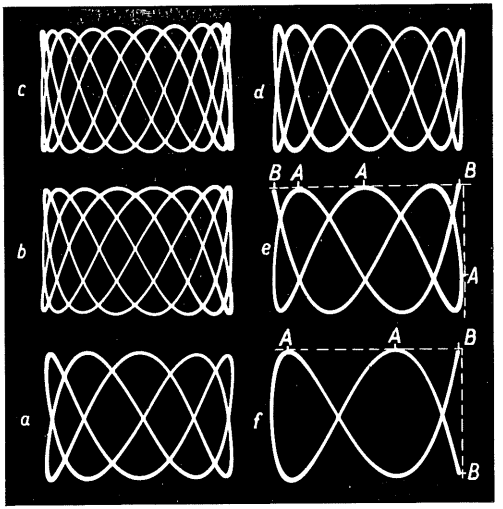

Fig. 12–25. Lissajous figures for odd-numbered frequency ratios (f_X for f_n = 50 c/s): *a*) $^5/_2 = 2^1/_2$; f_x = 125 c/s; *b*) $^8/_3 = 2^2/_3$; $f_x = 133^1/_3$ c/s; *c*) $^{10}/_3 = {}^1/_3$, $f_x = 166^2/_3$ c/s; *d*) $^7/_2 = 3^1/_2$, f_x = 175 c/s; *e*) as for *b*) $^8/_3$, different phase relations; *f*) as for *a*) $^5/_2$, different phase relations.

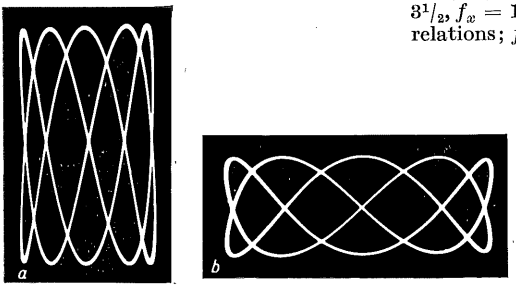

Fig. 12–26. Choice of the most suitable presentation of pattern, corresponding to the frequency ratio: *a*) unfavourable; *b*) correct (frequency ratio 5 : 2).

patterns corresponding to the different phase differences. In fig. 12–22 this is exemplified by a series of oscillograms in which the frequency ratio is 3 : 1 and the phase differences are given in steps of 45° from 0° to 360°. For an exact analysis of such figures the reader is referred to a publication on the subject [6]. Typical Lissajous figures for the frequency ratios: 1, 2, 3, 5 and 10 are shown in fig. 12–23.

To interpret these patterns, the method, as already described, is to think of the oscillogram as being surrounded by a rectangle whose sides are tangent to the loops of the patterns. The number of points at which the loops touch two adjacent tangents is a direct indication of the frequency ratio of the voltages on both pairs of plates. For example, in fig. 12–24*a*, the ratio of the vertically deflected to the horizontally deflected voltage is 3 : 1.

Frequency ratios that are not even numbers can, as long as they correspond to rational fractions, also be determined by Lissajous figures.

In fig. 12–24*b* and *c*, oscillograms are reproduced for a frequency ratio of 3/2 in two different phase relationships. A number of typical patterns for odd-numbered frequency ratios are also given in fig. 12–25. The figures in *a*), *b*), *c*) and *d*) are *open* loops representing frequency ratios of 5/2, 8/3, 10/3 and 7/2. The figures in *e*) and *f*) represent the same frequency ratios as in *a*) and *b*) but they are shown at the moment when the loops were coinciding. In such cases the number of loops or peaks (A) on two adjacent tangents must be counted twice and the points of contact of the beginning and end of these figures (B) counted once.

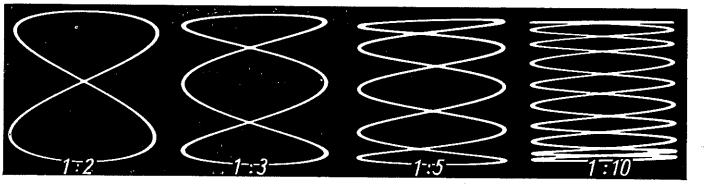

Fig. 12–27. Lissajous figures for frequency ratios < 1.

The patterns shown in figs. 12–19, 12–20, 12–21, and 12–22 are given within the form of a square. The other patterns, however, are given within the form of an oblong, corresponding to the frequency ratio. Such pictures are easier to interpret, as may be seen by comparing the two oscillograms in fig. 12–26. In all the oscillograms so far discussed the frequency of the Y deflection was higher than that of the X deflection. If the reverse is the case, patterns are obtained which, although they have the same shape as those considered, will be turned by 90°. Fig. 12–27 shows a series of oscillograms for frequency ratios of 1/2, 1/3, 1/5 and 1/10.

Lissajous figures with elliptical trace.

With increasing frequency differences, and particularly when the frequency ratios are not even numbers, it becomes increasingly difficult to interpret the resultant patterns. The range of measurements can be considerably extended if the path of the spot, there and back, is separated by means of a part of the sinusoidal voltage shifted in phase by 90°, in common with the unknown frequency on the Y plates. The forward-moving trace and the return trace will not then move in a straight line but will describe an ellipse, so that the picture of the otherwise intersecting paths of the spot will also be separated.
Fig. 12–28 shows a suitable circuit for this type of measurement. The comparison voltage with the low frequency—in this case taken as the reference frequency f_n—is used for the horizontal deflection. From this voltage, as already described, two components inversely phase-shifted by 45° are produced by means of R_1, C_1 and R_2, C_2.
The voltage from R_2 lies on the X plates while the 90° phase-shifted component from C_1 is fed, together with the frequency to be measured, over resistors R_{v1} and R_{v2} through the vertical amplifier to the Y plates. By

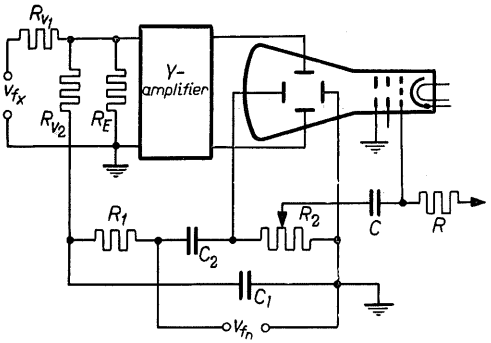

Fig. 12–28. Layout for frequency comparison by Lissajous figures on elliptical trace.

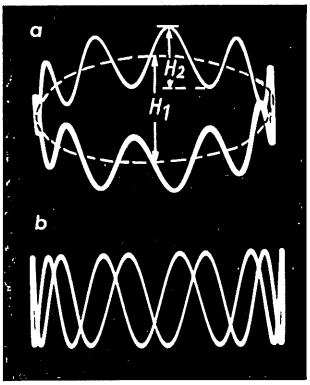

Fig. 12–29. Improvement of readability by elliptical trace: *b*) linear deflection; *a*) elliptical trace at equal frequency ratio.

controlling the gain of the amplifier the opening of the elliptical trace ("H_1" in fig. 12–29) can be adjusted as required. The height of the curve traced by the voltage with the unknown frequency (H_2) is best adjusted by this voltage itself. The result is shown in fig. 12–29. With a frequency ratio of 10 : 1 the figure is much easier to interpret on an elliptical trace than in the conventional display.

Moreover, it is possible, as indicated in the layout in fig. 12–28, to feed a portion of the X deflection voltage to the grid of the cathode ray tube in such a phase that one half of the pattern will be brightened (see fig. 12–29a). This gives the oscillogram a certain depth, so that the observer believes he can distinguish between foreground and background, an effect which makes interpretation easier.

In fig. 12–30 three oscillograms are shown, illustrating how odd-numbered frequency ratios can be determined by this method.

If only the *frequency difference* is to be ascertained, and if the frequency ratio is large, good results can be achieved by simply increasing the deflection voltage on the X plates. The movement of the spot in the horizontal direction may then amount to several times the diameter of the screen. This effect is shown clearly in fig. 12–31*a* and *b*. At small frequency fluctuations the pattern

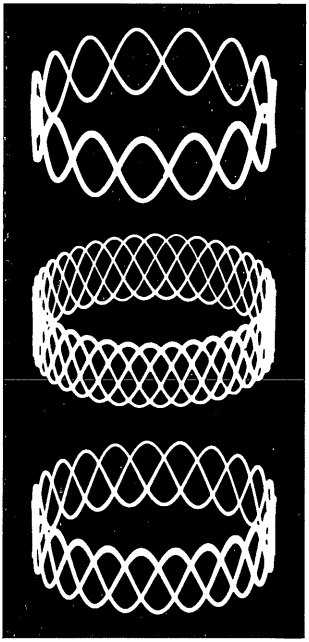

Fig. 12–30. Determination of odd-numbered frequency ratios with Lissajous figures on elliptical trace ($f_n = 50$ c/s); *a*) $^{15}/_2 = 7^1/_2$, $f_x = 375$ c/s; *b*) $^{37}/_5 = 7^2/_5$, $f_x = 370$ c/s; *c*) $^{23}/_3 = 7^2/_3$, $f_x = 383^1/_3$ c/s.

drifts in a horizontal direction (top and bottom in opposite directions). By making a mark (shown as "M" in fig. 12–31*b*) the time required for the completion of one cycle can be checked with a stopwatch and thus the frequency difference determined.
At faster frequency changes, the cycles passing within a certain time can be counted in order to arrive at the frequency difference. These methods are used for checking the frequency of broadcasting stations with a standard frequency, and for time measurements in general.
Particularly large frequency ratios can be bridged by means of an auxiliary frequency f_a. A pattern is then formed between f_n and f_a, by one of the methods described, and then with the auxiliary frequency and f_x, a second is formed. For this purpose one can use two oscilloscopes, a twin-beam oscilloscope or an

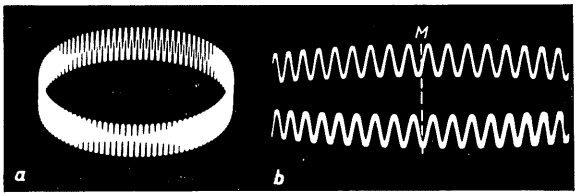

Fig. 12–31.
Determining large frequency differences by increasing the X deflection voltage.

oscilloscope in conjunction with an electronic switch. It is possible in this way to compare frequencies in a ratio of F^2_{max}, i.e. the square of the maximum frequency ratio measurable with the method used [7].
Methods of frequency measurement working with radial deflection are ideal for circular screen surfaces. Anode voltage modulation is unserviceable, as we saw in fig. 12–12, because of the periodically recurring unsharpness of focus it produces.
It is true that, owing to the bunching together at the ends of the Lissajous figure, an upper limit is found beyond which interpretation becomes uncertain. In fig. 12–30*b* and *c*, for example, it would be difficult for the inexperienced observer to count the voltage loops or peaks at these positions.
Contrary to the opinion often expressed that, for radial deflections, only polar-coordinate cathode ray tubes are suitable (but which are only to be used for this purpose), it should be pointed out that, with relatively simple circuitry, "polar" oscillograms can also be obtained with standard cathode ray tubes with two pairs of plates for deflection in rectangular coordinates. Useful results from simple circuitry are obtained by the method of producing cycloids on the screen, sometimes known as the "Roulette method" because of the shape of the resultant patterns.

Frequency measurement with cycloids on a circular trace.

The "function" of a quantity to be measured can also be presented by means of what is known as the "polar coordinate method" in which a circular trace is described by a radius rotating at a constant angular velocity. The length of the

radial vector from a zero point is plotted in dependence upon its angle of rotation. In polar coordinates, therefore:

$$r = f(\theta) \qquad (12\text{–}10)$$

These curves begin in general at a centre point with zero amplitude. A great number of circuits have been made known [8] with which oscillograms of this kind can be obtained using standard cathode ray tubes with two pairs of deflection plates. Since, however, they almost invariably demand special deflection-amplifiers, they need hardly fall within the scope of this book. Very great importance, on the other hand, is attached to frequency measurements with cycloids, which may also be described as circular oscillograms. They require the simplest of circuitry, consisting only of resistors and condensers; nevertheless they allow a wide range of measurements of even-numbered frequency ratios as well as an extraordinarily precise determination of odd-numbered frequency ratios.
The following considerations are based on a very comprehensive work on this subject by W. Bader [9] which also deals exhaustively with the geometric analysis of these patterns.

Circuit for frequency comparison with cycloids (roulette patterns).

The basic idea of a circuit for this type of measurement is shown in fig. 12–32. The two voltages for comparison, v_{f1} and v_{f2}, are each applied to the series arangement of a resistor with a condenser. The condenser is rated such that for the frequency concerned the capacitive reactance $\frac{1}{\omega C}$ is equal to the value of the ohmic resistance in series with it. As a result of this, the voltages applied to the pairs of deflection plates are 90° out of phase with each other in each case. This means that either of these voltages alone will describe a circular trace on the screen with a circumferential velocity which is determined by its frequency and amplitude. If now both voltages are applied simultaneously, the spot will describe a path representing the sum of two circles. Fig. 12–33 illustrates the vectors of both voltages v_{f1} and v_{f2}. While the vector with the lower frequency, in this case v_{f1}, is rotating, the vector of the voltage with the higher frequency is rotating around the peak of the first vector. The path of the spot corresponds to the path of a point on the radius of a circle described by the vector of the voltage with the higher frequency, which, in its turn, revolves around the circumference of the circle described by the slower vector. The pattern thus appearing on the screen is of a basic circular path, fringed by loops or cusps. If the faster vector rotates in the same direction as the slower vector then, in simple figures, one loop less will be

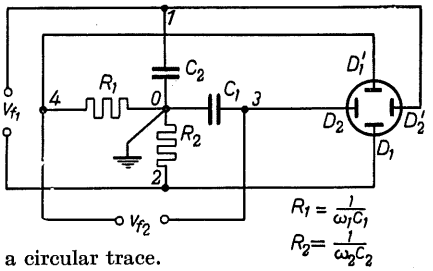

Fig. 12–32.
Basic circuit for producing cycloid patterns on a circular trace.

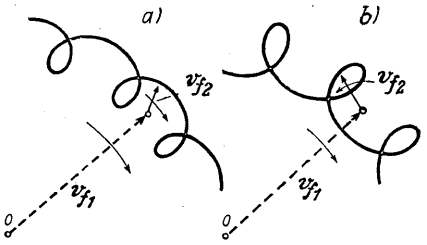

Fig. 12–33. Formation of a cycloid pattern by the addition of two rotating vectors: *a*) epicycloid, *b*) hypocycloid.

described than corresponds to the frequency ratio (the point on the small circle runs counter to the large circle), and the cusps or loops point inward. Curves of this sort are known as *epicycloids.* (Fig. 12–33*a*). If the faster vector rotates counter to the slower vector (the point on the smaller circle leads the larger circle), then, in simple figures, one loop more is described during one rotation of the slower vector than corresponds to the frequency ratio. The loops or cusps point outward. These types of curve are known as *hypocycloids.*

Referring again to the circuit arrangement, the Y plates are in the first place connected to points 2 and 4 and thus receive the "ohmic" component of both voltages from resistors R_1 and R_2. At the same time the X plates receive from points 1 and 3 the 90° phase-shifted component of these voltages from condensers C_1 and C_2. If the Y plates are connected across 1 and 4, they will then receive the "ohmic" component (R_1) of voltage v_{f2} and the capacitive component (C_2) of voltage v_{f1}. The X plates now receive from 2 and 3 the capacitive component of v_{f2} from C_1 and the non-phase-shifted component of v_{f1} from R_2. A provision for reversing polarity is made in the circuit used for carrying out these tests, shown in fig. 12–46. In this arrangement the voltages of the "ohmic" components can be switched over, thus allowing a choice of either hypocycloids or epicycloids. (These oscillograms are also known as roulette patterns.)

Interpreting cycloid patterns.

The process described is illustrated by oscillograms in fig. 12–34. The two initial circles "A" and "B" are shown on the same picture, together with their oscillographic sum "C". (In these recordings the ratios of the circles to each other were not equal.)

The frequency ratio concerned is $f_x/f_n = 4$ [4].

Fig. 12–35 sets out a series of cycloid patterns for whole-numbered frequency ratios of $f_x/f_n = 2, 3, 5, 10, 21, 30$ and 51.

If the unknown frequency is equal to the reference frequency, or only slightly different, then, in an epicycloid, a circle appears which beats with the frequency difference. In fig. 12–36*a* the two initial circles for this are shown (the signals to be measured are not equal), together with the background pattern. The limits of this area are given by the sum and difference of the peak values of both voltages. If the two voltages are equal in amplitude, there will obviously be only one initial circle, and the limits will be found at the centre point, or at twice the diameter, as shown in fig. 12–36*b*.

[4] In the following, the lower frequency will always be taken as f_n. For all oscillograms recorded it was 50 c/s. Bearing this in mind, f_x will sometimes be indicated to emphasize the possibilities of counting by this method.

In the case of hypocycloids there will generally—for unequal amplitudes—be an ellipse, which will rotate according to the difference-frequency. When the signal amplitudes are equal there will be a rotating trace or straight line, which can also be used as an indicator of the phase difference (see "Phase measurements on a circular scale", fig. 11–28). The phase angle is equal to twice the rotation angle of the trace.

The patterns in fig. 12–36*c*) and *d*) are composite photographs showing the initial circles, the rotating traces and the area covered by the traces in a hypocycloid circuit [10]. An arrangement of this sort can serve for checking phase equality in machines connected in parallel [11].

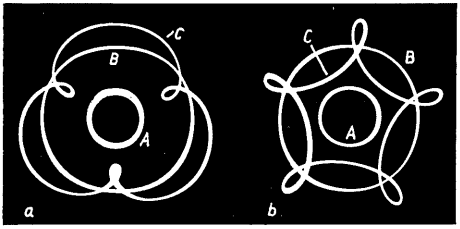

Fig. 12–34. Geometric composition of cycloid patterns: *a*) epicycloid, *b*) hypocycloid.

The desirability of having a smaller signal amplitude for the higher than for the lower frequency is illustrated by the oscillograms in fig. 12–37. In *a*), this requirement has been met, but in *b*) the signal amplitudes are equal, while in *c*) the amplitude of the signal with the higher frequency is greater than that of the signal with the lower frequency. These types of figures could under certain circumstances lead to confusion with the patterns of odd-numbered frequency ratios. By the choice of voltage amplitudes the pattern can be given the form most favourable for correct interpretation. It can be seen that, in general, loops appear on the screen, but reducing the amplitude of the voltage with the higher frequency results in the appearance of peaks, or cusps, as

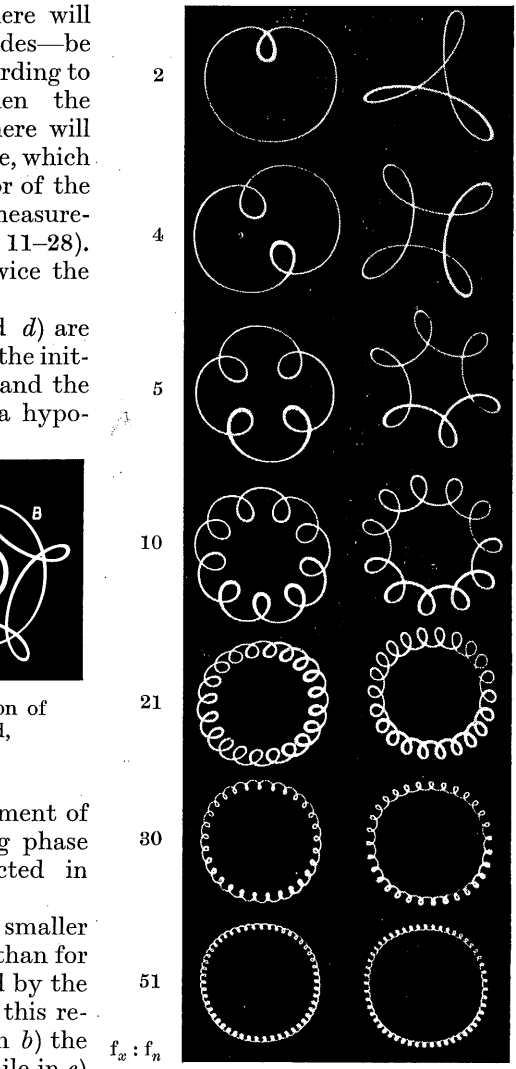

Fig. 12–35. Frequency comparison by cycloids: simple figures.

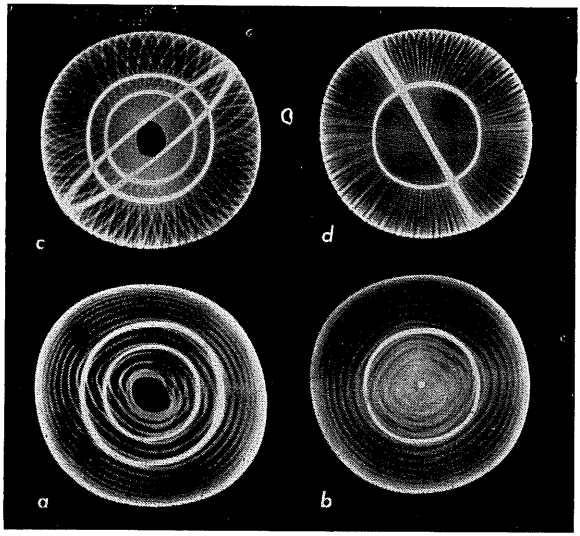

Fig. 12–36.
Cycloid patterns at approximately equal frequencies:
a) epicycloid; different amplitudes of comparison voltage;
b) epicycloid; equal amplitudes of voltage;
c) hypocycloid; different amplitudes of voltage;
d) hypocycloid; equal amplitudes of voltage.

shown in fig. 12–38, which are perhaps easier to read, or even in the appearance of figures with straight sides, as illustrated in fig. 12–39. (The figures in question are hypocycloids with frequency ratios of 2 and 3.)
If the figures are not stationary, the frequency-difference can be determined, with respect to the ratio which would correspond to the stationary pattern, by counting the number of peaks (backwards and forwards) that pass a given point in the unit of time, just as in the case of Lissajous figures with an elliptical trace [9].
This process also lends itself particularly well to the determination of odd-numbered frequency ratios. Fig 12–40 shows oscillograms of an epicycloid and a hypocycloid for a frequency ratio of: $m = {}^5/_2 = 2^1/_2$. In general terms, the frequency ratio m_H or the frequency f_{xH} can be found from hypocycloids when s is the number of loops or cusps and when p indicates whether the figure is traced in a single or multiple form, from the equations:

$$m_H = \frac{s - p}{p} \qquad (12\text{–}11)$$

and

$$f_{xH} = f_n \cdot \frac{s - p}{p} \qquad (12\text{–}12)$$

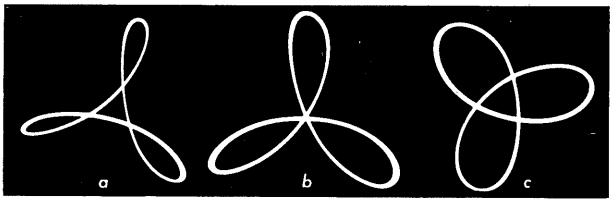

Fig. 12–37.
Influence of signal amplitudes on hypocycloids.

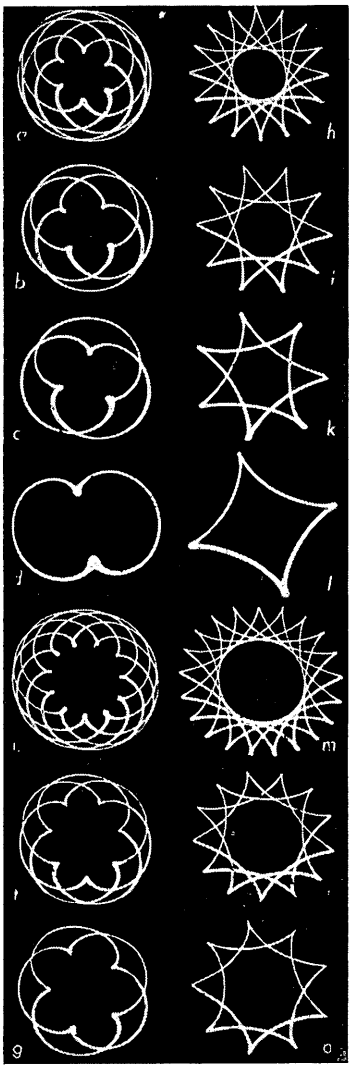

Fig. 12–38.
Cycloid patterns illustrating gradations of reading in the vicinity of frequency ratio 3.
(Multiple figures).

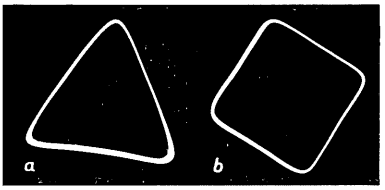

Fig. 12–39.
Straight-sided hypocycloids resulting from certain voltage ratios.

For epicycloids the equation is:

$$m_E = \frac{s + p}{p} \qquad (12\text{–}13)$$

and

$$f_{xE} = f_n \cdot \frac{s + p}{p} \qquad (12\text{–}14)$$

In this way, it is possible with a fixed standard frequency, to achieve extraordinarily delicate gradations in the determination of unknown frequencies. Some typical oscillograms for frequency ratios between 1 and 2 are shown in fig. 12–41. It can be seen from the patterns *a*) and *b*), however, as well as from the oscillograms in fig. 12–38 (*h* and *m*) that it may be difficult in the case of multiple-figure hypocycloids to determine the factor p (the number of outlines of the figures). Epicycloids are more convenient

Fig. 12–40. Cycloid patterns with $^2/_5$ frequency ratio: *a*) epicycloid, *b*) hypocycloid.

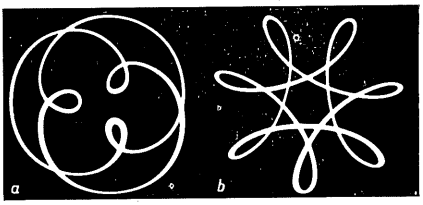

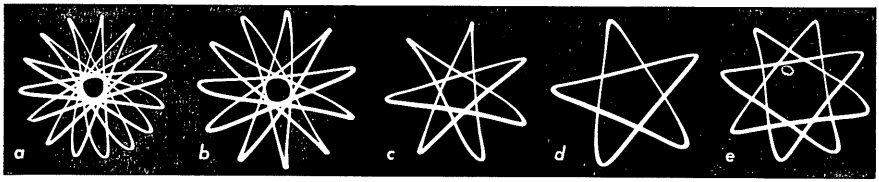

$f_x/f_n = {}^8/_7 = 1^1/_7$	$^6/_5 = 1^1/_5$	$^4/_3 = 1^1/_3$	$^3/_2 = 1^1/_2$	$^5/_3 = 1^2/_3$
f_x [c/s] $= 57^1/_7$	60	$66^2/_3$	75	$83^1/_3$

Fig. 12–41. Straight-sided hypocycloids at odd-numbered frequency ratios.

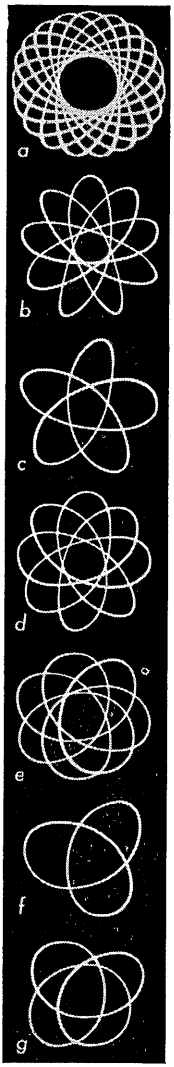

$f_x : f_n$	f [c/s]
$^9/_{10}$	45
$^4/_5$	40
$^2/_3$	$33^1/_3$
$^3/_5$	30
$^2/_5$	20
$^1/_3$	$16^2/_3$
$^1/_4$	$12^1/_2$

Fig. 12–42. Hypocycloids at $f_x/f_n < 1$; easy to interpret.

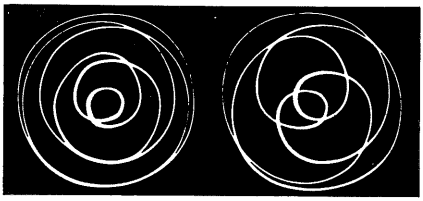

Fig.12–43.
Epicycloids at $f_x/f_n < 1$;
unfavourable.

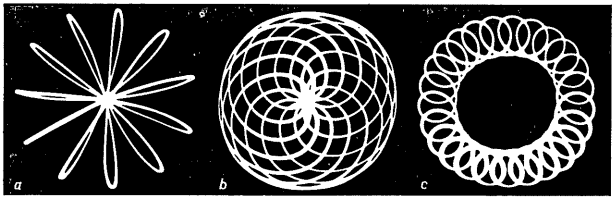

Fig. 12–44. Unfavourable adjustment of voltage ratios.

in this respect, as the corresponding oscillograms in fig. 12–38 show, especially when the cusps are drawn in towards the centre as in figures *a*) and *c*). These considerations suggest, therefore, that epicycloids are, as a rule, the more expedient of the two [5].

On the other hand, epicycloids are less suitable at frequency ratios where f_x/f_n is less than unity, as illustrated by the two oscillograms in fig. 12–43, whereas hypocycloids can be interpreted just as well as before. This is demonstrated by seven oscillograms in fig. 12–42. The asymmetry noticeable at extremely low frequencies is caused by relatively slight distortions of the waveform of the comparison voltage.

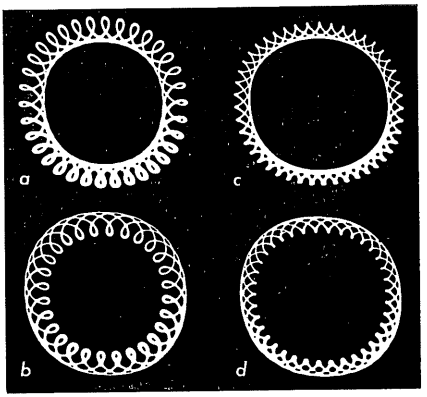

$m = 10^1/_3$	$m = 10^1/_4$
$f_x = 516^2/_3$ c/s	$f_x = 512^1/_2$ c/s

Fig. 12–45. Cycloid patterns illustrating fine gradations of reading at a frequency ratio of 10 : 1.

Examples of unfavourable settings are given in fig. 12–44. The hypocycloid in *a*) represents an odd-numbered frequency ratio and equal amplitudes of signal; since the inside loops rotate in the centre of the pattern, interpretation is impossible. The epicycloid in *b*) also represents equal amplitudes of signal, so that the loops which are needed for counting are seen to overlap in the centre. The epicycloid in *c*) can indeed be interpreted ($m = 25$, $p = 1$, $f_x = 1250$ c/s for $f_n = 50$ c/s), but it could quite easily be mistaken for a double pattern. A smaller amplitude of the signal with the higher frequency is always to be preferred.

The oscillograms in fig. 12–45 show how fine gradations of reading can be achieved at greater frequency ratios. The three-fold pattern in *a*) contains 34 loops, in *b*) 28 loops. According to equations (12–11) and (12–12) and (12–13) and (12–14), the frequency ratios are:

$$m_H = \frac{34 - 3}{3} = 10\tfrac{1}{3} \text{ and } m_E = \frac{28 + 3}{3} = 10\tfrac{1}{3}$$

and the unknown frequency is $516^2/_3$ c/s ($f_n = 50$ c/s).

In the hypocycloid in fig. 12–45 *c*) there are 45 cusps and in the epicycloid in *d*), 37 cusps (quadruple figure). The frequency ratios are thus:

$$m_H = \frac{45 - 4}{4} = 10\tfrac{1}{4} \text{ and } m_E = \frac{37 + 4}{4} = 10\tfrac{1}{4}$$

and the unknown frequency is: $512^1/_2$ c/s.

[5] To determine the factor p, it is advisable to start counting from the centre of the figure and to move out along a radius cutting the points of intersection. (At these points the number to be counted is "2".)

Practical circuit arrangement.

As already mentioned, the reference frequency used in these examples was 50 c/s. Fig. 12–46 shows the circuit with the ratings of the components employed, based on the circuit given in fig. 12–32. An RC network of 10 kΩ and 1μF is incorporated to filter out the mains harmonics. The input voltage is applied via a transformer to a potentiometer of 50 kΩ, which permits adjustment of the signal amplitude. In both branches of the comparison voltages two potentiometers of 0.5 MΩ/lin., each in parallel, form a resistance network. The one potentiometer is circuited as a variable resistor $R = \frac{1}{\omega C}$ to adjust the circular pattern. Since a reference frequency of only 50 c/s is used, one condenser of 0.1 μF suffices for C_1. If the whole audio frequency range is to be taken into account, provision must be made for switching over C_1 in the same way as C_2. By means of two switches, not shown in this circuit, the two signals can be alternately switched off, and the appropriate pair of deflection plates directly connected. By three switching operations it is thus possible to adjust the two circles individually one after the other and then to switch over to both signals to produce the sum pattern. The switchable condensers in the branch for v_{fx} make it possible over the entire AF range to fulfil the condition $R_2 = \frac{1}{C_2\omega_2}$. Change-over switch S enables a choice to be made between epi-

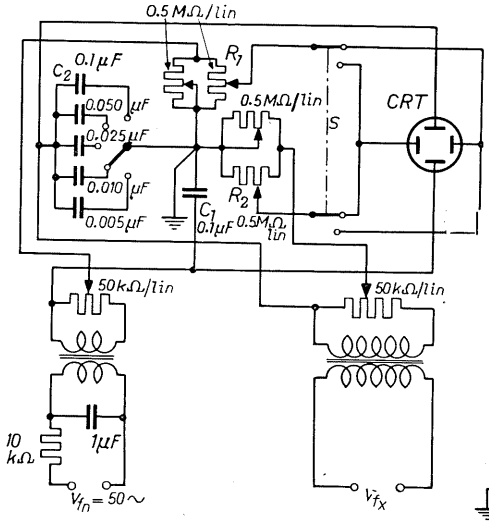

Fig. 12–46. Practical circuit for producing cycloid patterns.

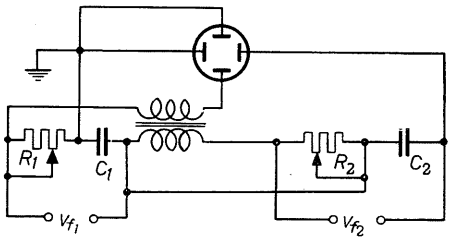

Fig. 12–47. Circuit for cycloids: C.R.T. with single-pole earthed deflection plates.

cycloids and hypocycloids. Another circuit arrangement is illustrated in fig. 12–47. in which a cathode ray tube with asymmetrically operated deflection plates is used. It is identical with the arrangement described by Reich in 1937 [12] [13]. Rangachari also drew attention to circuits of this kind in 1928 [14] [15].
It has been demonstrated that frequency comparison with cycloid patterns offers a number of advantages over other methods of comparison. The construction of the simple circuit required is therefore very much to be recommended if frequency measurements over wide ranges are frequently carried out. As the oscillograms show, calibration points up to 50 times the standard frequency and fractions thereof can be read off quite distinctly.
Trace brightening, by using the comparison voltage with the higher frequency to intensity-modulate the beam, can also serve in many ways for frequency measurements.

Frequency measurement by intensity-modulating the oscillogram of the voltage with unknown frequency.

The most obvious method is to brighten, by intensity modulation, the waveform of the voltage with the unknown frequency.
For this purpose the signal is applied in the conventional way to the Y plates and the pattern adjusted on a time base of suitable frequency. The comparison frequency is applied between the grid of the cathode ray tube and the chassis of the oscilloscope.
If the comparison frequency is adjustable (e.g. by a signal generator), fairly stationary points are obtained, which can be counted, as illustrated in fig. 12–48. For exact measurements, especially at large frequency differences, photographic recording is necessary. From the number of points in the oscillogram of the voltage with the unknown frequency we find:

$$f_x = \frac{N_{fx}}{N_p} \cdot f_n \qquad 12\text{–}15)$$

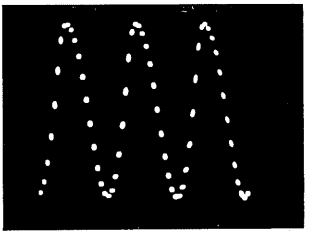

Fig. 12–48. Intensity modulation of the voltage with unknown frequency.

in which N_{fx} is the number of cycles of the unknown frequency and N_p the number of brightness markings, or points. In fig. 12–48, $f_n = 100$ c/s, $N_{fx} = 3$ and $N_p = 60$; according to (12–15) this makes $f_x = 5$ c/s. The example shows clearly that this method lends itself particularly well to the measurement of lower frequencies. In the case considered, an ordinary AF generator, the frequency range of which usually begins at 20–30 c/s, was used for the measurement of a frequency of only 5 c/s.

Intensity modulation of a circular trace by a voltage with the second frequency.

The circuit illustrated in fig. 12–49 is used for this measurement. In the manner described on several previous occasions, a circular trace is produced with the voltage of unknown frequency, v_{fx}, and a voltage of known frequency, v_{fn}, displaced in phase by 90°. The voltage with the known frequency v_{fn} is applied between the grid of the cathode ray tube and chassis. It should be noted that the time constant of the RC coupling network must be sufficiently

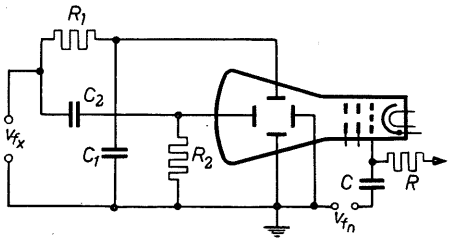

Fig. 12–49. Layout for intensity-modulating a circular trace by a voltage with the known frequency.

large to deal with low frequencies of v_{fn}. If the waveform of v_{fx} is not sinusoidal enough, the harmonics should first be filtered out, but this need not be taken too far, since a slight lack of constancy in the circular trace has no effect at all on the measurement. Regularly spaced brightness markings now appear on the circular trace, which remain stationary if the frequency ratio is an exact integral, and which are a direct indication of the frequency ratio itself. When the frequency ratio is not quite integral, the brightness markings will be seen to move around the circle. Typical sinusoidally intensity-modulated oscillograms are shown in fig. 12–50*a*) to *f*) for $f_n : f_x$ of 1, 2, 3, 5, 10 and 103.

If f_x is greater than f_n, the voltages v_{fx} and v_{fn} must, of course, be changed over. The ratio $f_x : f_n$ is then found directly from the number of brightness markings.

Thus it is possible with one standard frequency to span a wide measurement range (at least 1 : 10 and 10 : 1, i.e. a total of 1 : 100).

In addition to integral frequency ratios, intermediate values can also be ascertained, as demonstrated by fig. 12–51 with oscillograms in the neighbourhood of a 4 : 1 ratio. Table 12–III shows that the number of brightness markings on the circle comes into the numerator of the fraction which indicates the frequency ratio. The number for the denominator, however,

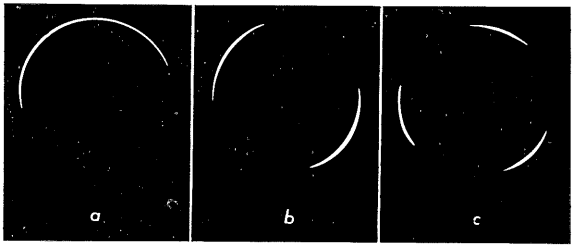

Fig. 12–50. Frequency measurement by intensity-modulation of a circular trace.

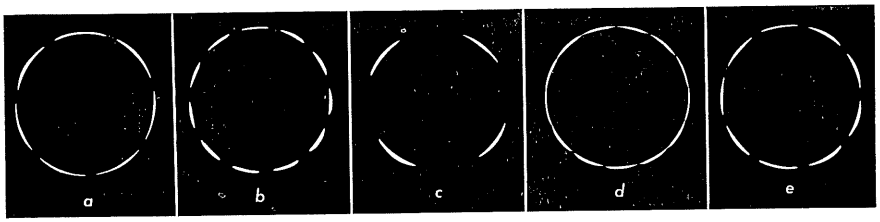

Fig. 12–51.
Intensity-modulated circular traces at odd-numbered frequency ratios (except *c*) in the neighbourhood of $f_x/f_n = 4$.

Pattern	Frequency ratios $f_x:f_n$	f_x at $f_n = 50$ c/s
a	$^7/_2 = 3.500$	175 c/s
b	$^{11}/_3 = 3.667$	$183^1/_3$ c/s
c	$4 = 4.000$	200 c/s
d	$^{13}/_3 = 4.333$	$216^2/_3$ c/s
e	$^9/_2 = 4.500$	225 c/s

Table 12–III (to fig. 12–51)

is not to be found from the number of loops or peaks as in frequency measurement with Lissajous figures, or by comparison with the time base frequency. Nevertheless, if calibration is carried out by progressively varying one of the frequencies under comparison, as is usually done, the number for the denominator can be found exactly by means of simple experiment. There will always be only one whole number which will provide a possible frequency ratio. These patterns differ at once from the oscillograms for integral frequency ratios by the small spacing between the bright parts of the picture. The spacing diminishes the more the frequency ratio deviates from a whole-numbered ratio, so that patterns are ultimately found in which the circle is entirely filled in. Such patterns can, of course, no longer be interpreted.

Intensity modulation of line patterns.

The intensity modulation of line patterns (similar to television scanning) with the voltage of unknown frequency makes frequency comparison possible over a very wide range. To this end, two sawtooth generators are required.
The relevant circuit is shown in fig. 12–52. The sawtooth oscillator for the vertical-deflection frequency (low) is synchronized with the horizontal deflection frequency. The sawtooth oscillator for this (a multiple of the vertical

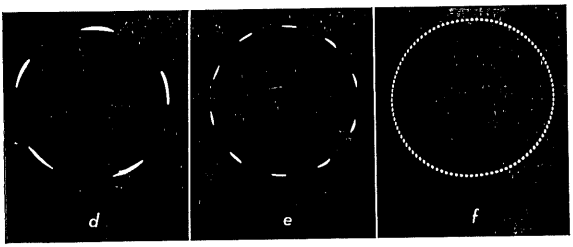

frequency) is synchronized with a standard frequency which can again be a multiple of ten or less.

If the unknown frequency is equal to or an integral multiple of the *vertical frequency*, then one or correspondingly more patches of brightness will appear during one pattern in a *horizontal* direction, as shown in fig. 12–53. If the unknown frequency is equal to or an integral multiple of the *horizontal* frequency, one or more patches of brightness will appear during the tracing of one line in a *vertical* direction, as can be seen in fig. 12–54.

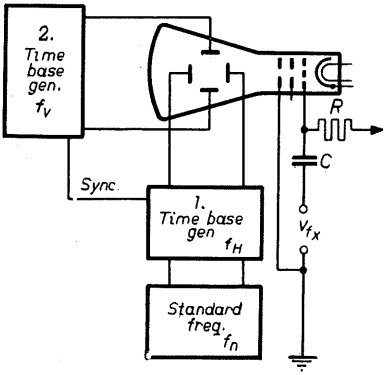

Fig. 12–52.
Circuit for frequency measurement by brightness-modulation of line patterns.

In the oscillograms reproduced, the vertical frequency f_V was equal to 100 c/s and there were 60 lines (i.e. $f_H = 6000$ c/s), therefore the patterns shown in figs. 12–53 *a–e* and 12–54 *a–e* correspond to frequencies of 100, 200, 300, 500 and 1000 c/s and 6, 12, 18, 30 and 60 kc/s respectively.

The interesting fact appears that in this way two separate frequency ranges can be embraced with one standard frequency. A gap exists between the two, which can be selected within wide limits according to the ratio f_H/f_V. The method is thus particularly suitable for adjustments at the frequency limits of an amplifier, for example. The frequencies under investigation can be read off quickly and clearly in definitely determined steps.

Should the unknown frequency not stand in an exact integral relationship to the horizontal or vertical frequency, the bright patches will no longer appear exactly above or beside each other, but will drift, or, at small deviations,

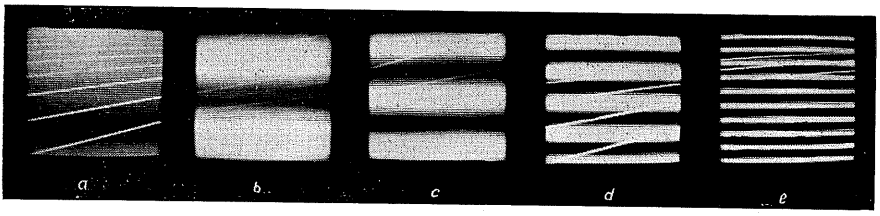

Fig. 12–53. Oscillograms at multiples of vertical frequency.

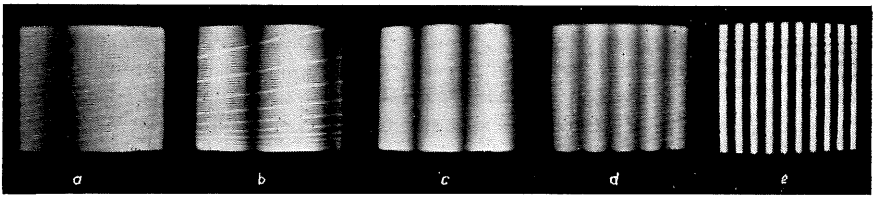

Fig. 12–54. Oscillograms at multiples of horizontal frequency.

appear at a slant. This is illustrated by the oscillograms in fig. 12–55 representing in *a*) and *b*) f_H/f_V ratios slightly deviating from 2 and in *c*) and *d*) from 11. The unknown frequency in each case was somewhat lower or higher than the indicated frequency ratio.
As long as the frequency ratio differs from the comparison frequency by less than one complete cycle, an additional phase difference exists. The slant of the pattern markings can then serve as a direct measure of the phase.
The foregoing is also meant to show how an interfering frequency in a television picture and its cause can be determined by means of the known horizontal and vertical frequencies.

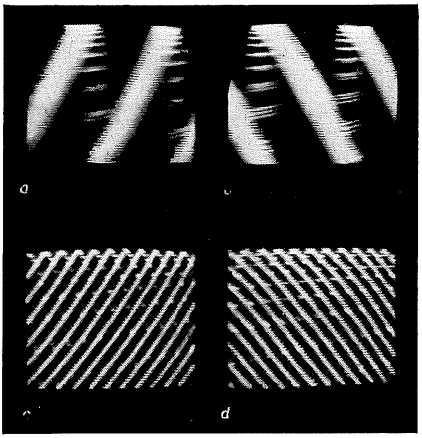

Fig. 12–55. Oscillograms of intensity-modulated line patterns when the unknown frequency is somewhat less or more than a multiple of the horizontal frequency: *a*) and *b*) unknown frequency deviates slightly from twice the horizontal frequency; *c*) and *d*) unknown frequency at 11 times the horizontal frequency.

Absolute frequency measurement with rotating trace

Method of measurement.

All the methods of frequency measurement described so far are based on the comparison of an unknown with a known frequency. Other methods have been indicated, however, by which a direct indication of the unknown frequency is obtained.

In a circuit patented by E. T. Jaynes (16) the alternating voltage with unknown frequency is applied via phase shifting elements to both pairs of deflection plates in such a way that the phase difference between the voltages amounts to 180°. This can be done with *RC* and *CR* networks in a manner similar to that already described for producing a circular movement of the spot with two alternating voltages of identical frequency and displaced by 90° with respect to each other. (See figs. 11–26, 12–11 and 12–28).

Circuit.

The circuit with examples of component ratings is shown in fig. 12–56. The components are rated such that each element produces a phase shift of 45° for 200 c/s (cut-off frequency).

As two elements are provided in each branch, the voltage arriving at the input of the *Y* amplifier is displaced by —90° and has somewhat less than half the amplitude of the input voltage. The voltage at the input of the *X* amplifier is attenuated by the same amount but has a phase shift of +90°. Since the phase shifting elements are directly coupled, certain slight corrections because of reaction are needed to bring about the desired phase difference of 180°. With the circuit in fig. 12–56, for example, the only correction needed was to increase condenser C_2 to 0.036 μF.

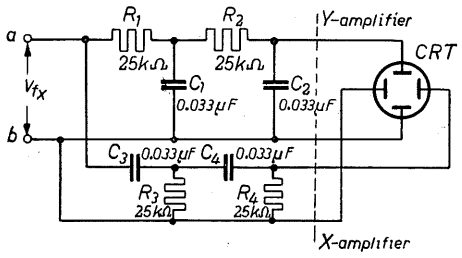

Fig. 12–56. Circuit for absolute frequency measurement with rotating trace.

In general the voltage with unknown frequency must be amplified —for both deflections—to obtain a sufficiently large image on the screen. A type GM 5654 oscilloscope was therefore used for the measurements about to be described, as this permits amplification in both directions. As the input impedance for the *X* deflection in this oscilloscope is 50 kΩ, R_4 was rated for 50 kΩ likewise to obtain from the two in parallel the desired value of 25 kΩ at the end of this filter.

The oscillograms and the method of evaluating them.

By these means a diagonal trace is obtained on the screen of the cathode ray tube, from top left to bottom right. (See fig. 11–16, last oscillogram, for 180°.) At the limit frequency of the circuit components, and with equal amplitudes of deflection in both directions, the trace would have an inclination of 45°. Changes in the input frequency produce changes in the phase and amplitude of the output voltages of the filters. Elements R_1, C_1 and R_2, C_2 form a low-pass filter; its output voltage decreases with increasing frequency (see fig. 5–19*b*). Condensers C_3, C_4 and resistors R_3, R_4 represent, on the other hand, a high-pass filter, the output voltage of which increases with increasing frequency (see fig. 5–7). The phase difference remains constant at 180° (see

figs. 5–8 and 5–20). The result is always a diagonal trace, but one which appears to rotate on its axis following the changes in the amplitude of the voltages, as described in the previous chapter and illustrated in fig. 11–28. In this case, however, the end points of the trace do not describe a circle but a hyperbolic curve, as shown in fig. 12–57. To make this quite clear the oscillograms reproduced were photographed while varying the frequency as smoothly as possible from 25 c/s up to 2,500 c/s, the exposure time being 4 secs. and the aperture small (f 11). The deflection amplifiers were so adjusted as to have the almost vertical 25 c/s trace the same length as the almost horizontal 2,500 c/s trace. With the gain selected, the trace inclined at 45° corresponds to 250 c/s.

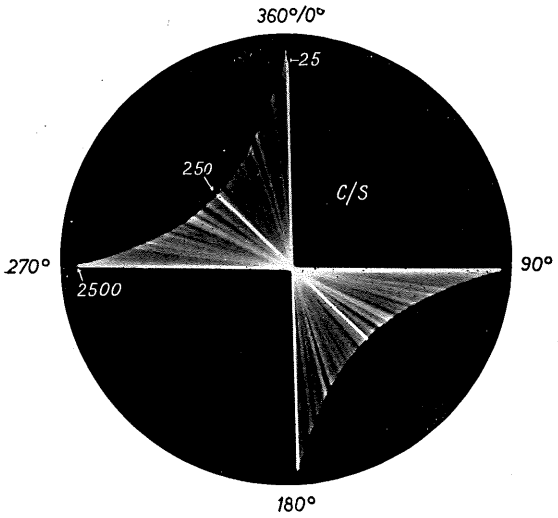

Fig. 12–57.
Oscillogram for absolute frequency measurement.

It should be stressed that an absolute frequency indication is obtained in this way, the accuracy of which depends only upon the accuracy and constancy of the circuit elements—apart from the constancy of amplification. Thus, after the frequency range has once been calibrated, no voltage source with a reference frequency is needed.

The accuracy of the reading can be improved if the pivotal point of the trace is moved to the edge of the screen. The reading is further facilitated if the cathode ray tube is rotated 45° (to the right). The resultant picture on the screen when this action is taken is illustrated in fig. 12–58, which shows the positions of the trace corresponding to 29 different frequency settings.

With the circuit as in fig. 12–56 a frequency scale is obtained that reads from right to left. Of course, by reversing the connections to the X plates a trace can be obtained that reads conventionally from left to right. For the sake of convenience, fig. 12–58 and all subsequent oscillograms in this chapter are simply enlargements of the negatives reversed.

Choice of measuring ranges.

With a relatively large frequency range as in fig. 12–58 the scale obtained is found to crowd together at the ends; the accuracy of reading is greatest in the middle (about 2%). By adjusting the gain of the amplifiers, the frequency range can be influenced and thus the accuracy of the scale reading improved.

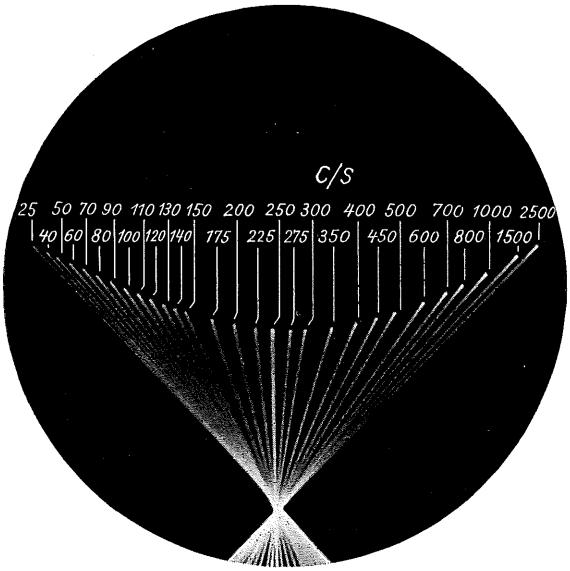

Fig. 12–58.
Pivotal point of rotating trace displaced to the edge of the C.R.T.; tube turned 45° to the right.

Fig. 12–59, which was also taken with the circuit shown in fig. 12–56, illustrates an almost linear scale in the range from 20...160 c/s with an accuracy of reading of about 1%. As a further variation, fig. 12–60 represents a frequency

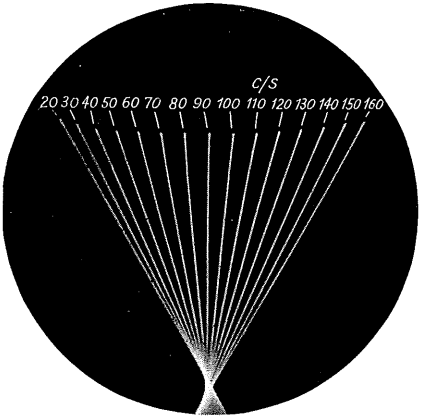

Fig. 12–59.
Almost linear frequency scale.

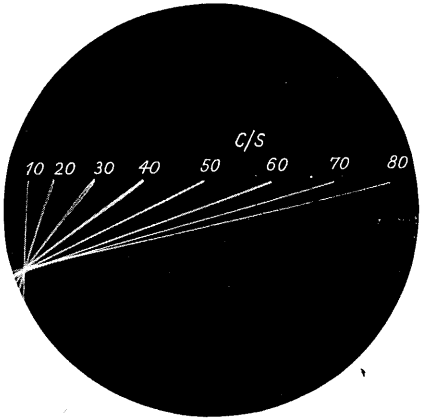

Fig. 12–60. Accuracy of reading increases with the frequency.

range from 10...80 c/s, in which the accuracy of the scale reading increases with the frequency (about 1%).

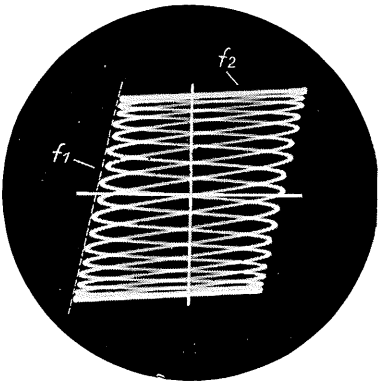

Fig. 12–61.
Simultaneous determination of two frequencies: $f_1 = 60$ c/s, $f_2 = 650$ c/s.

Simultaneous measurement of several frequencies.

It is possible in the same way to determine simultaneously the frequencies of two and more alternating voltages. If two alternating voltages with different frequencies and similar amplitudes are applied to input sockets *a*, *b* for v_{fx}, the resultant image on the screen is an oblique Lissajous figure, as shown in fig. 12–61. (The voltage with the higher frequency serves for the horizontal deflection.) [6]

The inclination of the sides of this oscillogram is a measure of the frequency in question, just as in the case of the rotating trace with a single frequency. (The amplitudes of the frequency components must of course be taken into account.)

The reference co-ordinates in these figures were recorded separately to facilitate the reading. To do this, the voltages on the pairs of X and Y plates were switched off alternately.

As a rule the frequencies do not stand in a whole-numbered or rational relationship to each other. The picture on the screen is therefore not a Lissa-

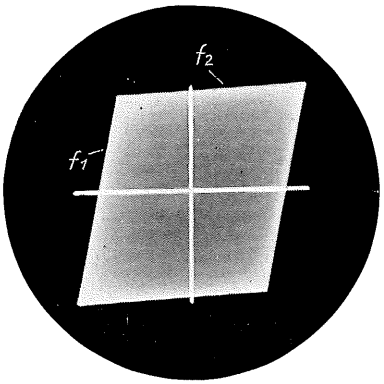

Fig. 12–62.
Simultaneous determination of two frequencies not rationally related to each other.

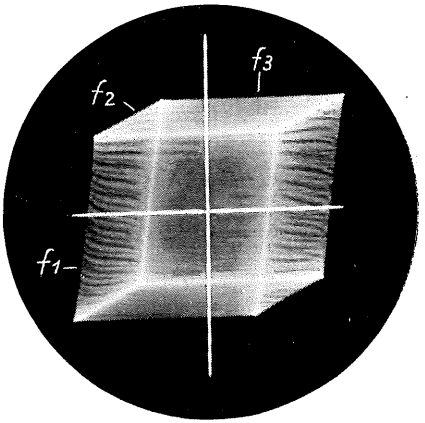

Fig. 12–63.
Simultaneous determination of three frequencies; $f_1 = 50$ c/s; $f_2 = 150$ c/s; $f_3 = 1000$ c/s.

[6] Two or more voltages can very simply be added by means of a resistance T network, as described with fig. 4–42 on page 77 and fig. 12–13 on page 204.

jous figure with recognizable contours but simply a luminous area with straight sides, as illustrated by the oscillogram in fig. 12–62.
Three alternating voltages of differing frequencies produce a hexagon as in fig. 12–63. Here again the inclination of the sides is a measure of the corresponding frequencies.

Special advantages and applications.

Since this method allows both the frequency and the amplitude to be read from the oscillogram, it will plainly be very useful in frequency analysis. As pointed out at the beginning of this chapter, all the methods of frequency measurement described can, with the aid of suitable transducers, be used also for measuring mechanical vibrations, speeds of revolution and other non-electrical phenomena.
In view of the absolute indication it gives, the method of measuring one frequency described in the foregoing is especially suitable for observing mechanical vibrations or the speed of a motor.

PART III

Practical Examples

13. Recording the waveforms of luminous flux, current and voltage of fluorescent lamps

General.

To the illumination engineer it is particularly important to know the nature and extent of the alternations of the luminous intensity of fluorescent lamps during one cycle of the mains voltage (the stroboscopic effect). Since the oscilloscope is actually a voltage indicator, it is necessary, in order to observe the behaviour of light, to use a photocell for supplying a voltage proportional to the luminous intensity or to the alternation of luminous intensity.
The basic layout for this type of investigation is illustrated in fig. 13–1. The distance of the light source L from the photocell F must be adjusted such that the maximum permissible density of radiation for the photocell is not exceeded. In practice, however, this applies only to incandescent lamps, the radiation density of fluorescent lamps being relatively small. It is essential for the purposes of the investigation to know the relationship between "direct light" and "alternating light". For this reason care should be taken that the

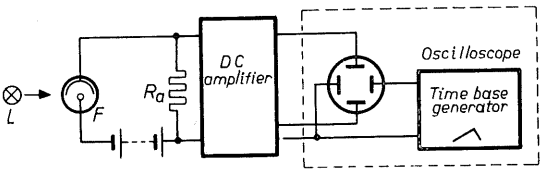

Fig. 13–1.
Arrangement for displaying on the oscilloscope the luminous flux of sources of illumination.

direct voltage components from the photocell are also presented for display. As oscilloscopes often contain only *AC* voltage amplifiers, a *DC* voltage amplifier is therefore needed in addition (e.g. Philips GM 4531 or oscilloscope GM 5656). For the recordings dealt with in this chapter, an amplifier of the type illustrated in fig. 5–38 was used. This amplifier is connected direct to the Y plates of the oscilloscope and the time base generator is connected to the X plates.

Incandescent lamps.

To provide a practical basis of comparison for investigations on fluorescent lamps, an example is first given in fig. 13–2 of the patterns obtained in this way of the luminous flux variations in the case of incandescent lamps of 40 W and 200 W during one cycle of the 50 c/s mains. In these, as in the subsequent recordings, approximately the same amplitude for the average brightness was adjusted in all oscillograms. A clear picture is thus obtained of the relative proportion of flux alternation with the various light sources. These oscillograms cannot, however, be a measure of the absolute values of luminous flux. Two cycles of the mains voltage are shown in all cases, extended over the whole width of the screen. To make easy comparison possible, the parts of the waveforms extended beyond one cycle have been blanked out.

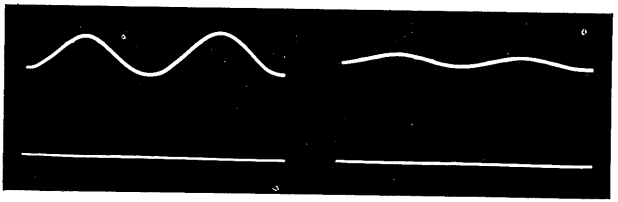

a b

Fig. 13–2. Luminous flux of incandescent lamps during one cycle of the mains voltage.
a) 40 W/220 V lamp;
b) 200 W/220 V lamp.

The luminous intensity of the 40 W lamp fluctuates around the mean value by about ± 19 % and that of the 200 W lamp by about ± $5^1/_2$ %.

Fluorescent lamps.

Waveforms of the luminous flux of low-pressure fluorescent lamps during one cycle of the *AC* mains are reproduced in fig. 13–3. Waveform *a*) represents the flux of the mercury-vapour light of the lamp *without* fluorescent material. It fluctuates by approximately ± 90 vH about the mean value. The light thus follows almost perfectly the course of the current, with twice the frequency.
Fig. 13–3*b* shows the luminous flux waveform of a "TL" "Daylight" lamp. The fluctuation of the luminous flux amounts to about ± 52 %.
The luminous flux waveform of the "white" "TL" lamp is shown in fig. 13–3*c*. The fluctuation in this instance amounts to ± 33 %. Finally, fig. 13–3*d* shows the flux waveform of the "warmtone" "TL" lamp with a "ripple" of ± 27 %.

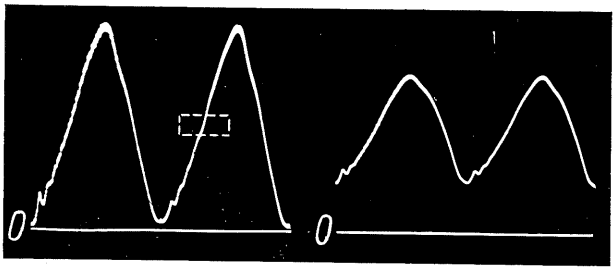

a b

Fig. 13–3. Luminous flux of fluorescent lamps.

a) Lamp without fluorescent material.
b) "Daylight" lamp.

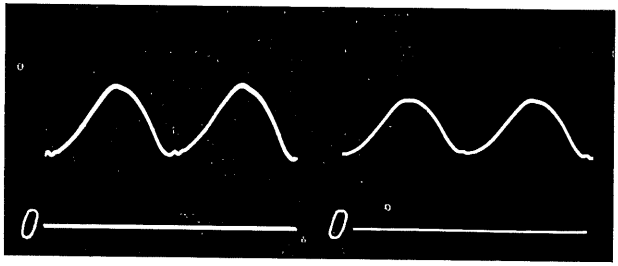

c d

c) "White" lamp.
d) "Warmtone" lamp.

It can at once be seen how the fluctuation of the luminous flux can be influenced by the fluorescent material. In this respect rapid development is being made and progressive improvement may be expected. [1]
A further interesting detail emerges from the waveform of the mercury-vapour light in fig. 13–3*a*. Using large time-base expansion and photographic

Fig. 13–4.
"Time expanded" and photographically enlarged section of waveform from fig. 13–3*a*.

enlargement of a section of this waveform, it appears, as shown in fig. 13–4, that the whole oscillogram contains a small superimposed low-frequency flux variation of about 22,000 c/s. This is due to processes taking place during the gas discharge.

Current and voltage waveforms of fluorescent lamps.

Fluorescent lamps, as is known, are usually employed with a pre-connected choke. This gives rise to an undesired phase shift between current and voltage so that the power factor cos θ in this arrangement is only 0.5 ..... 0.6.
Fig. 13–5 reproduces a circuit with which, according to the position of switch S, patterns can be produced on the oscilloscope one after the other of the current, the voltage on the lamp and the mains voltage. To obtain the current waveform, an ohmic resistor R_v of about 10 ohms is connected in the

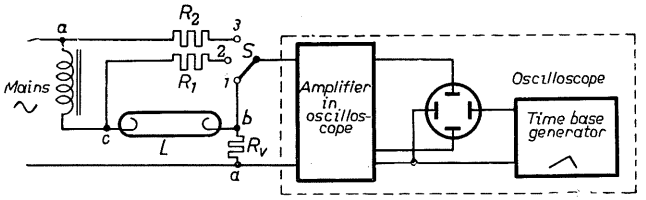

Fig. 13–5. Arrangement for displaying the current and voltage curves of fluorescent lamps.

main circuit. The voltage drop across this resistor is applied to the vertical amplifier and amplified sufficiently to produce the desired deflection.
In the second position of the switch the lamp voltage lies over resistor R_1 at the input of the amplifier, and in position 3, the mains voltage lies across the input of the amplifier via R_2. The values chosen for the resistors should be such that the desired deflection is obtained on the screen without the necessity of further adjusting the gain control. A value of 2 MΩ is appropriate if, as in the present instance, the input impedance of the amplifier is 150 kΩ. When R_1 and

[1] These oscillograms were recorded some appreciable time ago.

R_2 are equal, a direct impression is received from the oscilloscope of the relationship between mains voltage and lamp voltage.
With the time base frequency synchronized to the mains voltage, the waveforms of lamp current, lamp voltage and mains voltage appear on the screen displaced with respect to each other in a way exactly corresponding to their actual phase relationships. (In most oscilloscopes a special switching position exists for investigations of this kind.)
The result of this measurement is illustrated in fig. 13–6*a*.

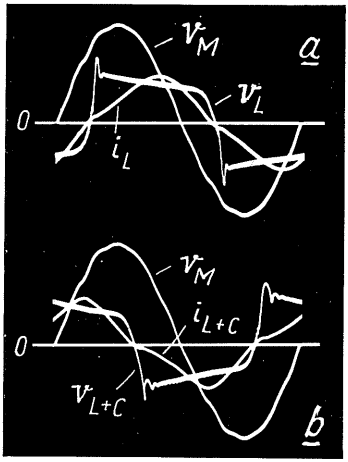

Fig. 13–6. Current and voltage waveforms of fluorescent lamps; *a*) lamp with "inductive" ballast, *b*) lamp with "capacitive" ballast.

Fluorescent lamps connected in duo.

Endeavours were very soon made to improve the poor power factor of fluorescent lamps and also to reduce the variations of luminous flux and thus the stroboscopic effect.
A large measure of improvement in these respects was achieved by the "duo" arrangement of fluorescent tubes as shown in fig. 13–7 [1]. One lamp functions in the normal circuit with an interconnected choke. The current and voltage relations of this circuit were discussed with reference to fig. 13–6*a*. The current and voltage of the lamp lag behind the mains voltage.
The second lamp is preceded by the combination of a condenser with a choke, which is rated in such a way that it has a capacitive character, the current thus leading the mains voltage. The relationships in question can be seen in fig. 13–6*b*. (It will be noticed that the waveform of the mains voltage contains severe harmonics.)
The oscillograms in fig. 13–8 show the relationships to the mains voltage v_M of the lamp currents i_L and i_{L+C} individually and of the total current i_T. As appears from *c*), the phase shift of the total current with respect to the mains voltage is small. The power factor for this arrangement is given as 0.95.

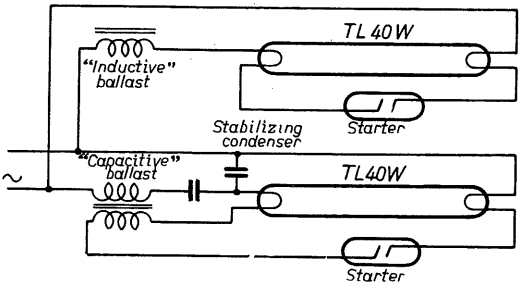

Fig 13–7. "Duo" arrangement of fluorescent lamps.

This is not, however, the only advantage of the duo arrangement. The mutually phase-shifted currents of the two lamps also result in a corresponding phase shift of the variations of luminous flux. This means that when the flux of one lamp declines, the flux of the other increases accordingly, and vice versa. These conditions are shown by the oscillograms in fig. 13–9 for "daylight" lamps. The luminous flux of each lamp is shown individually—Φ_L and Φ_{L+C}—together with the sum of both $\Phi_L + \Phi_{L+C}$.

The brightness variation of the light of both lamps now only amounts to $\pm 18\,\%$; it is thus only as large as with a 40 W incandescent lamp, as opposed to $\pm 52\,\%$ with a single fluorescent lamp.

Two further oscillograms of the duo arrangement are given in fig. 13–10, showing the luminous flux of "white" and "warmtone" lamps, for which the flux variations were calculated at $\pm$ 16 % and $\pm$ 11% respectively. These values are even less than those of a 40 W incandescent lamp. The oscillograms also prove that by means of the duo arrangement a power factor [2] of 0.95 is within easy reach.

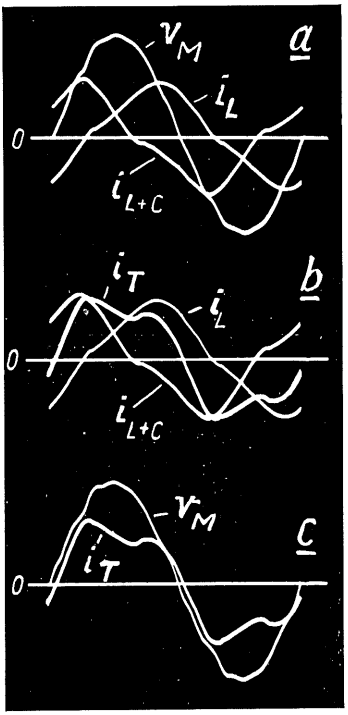

Fig. 13–8. Current and voltage waveforms of fluorescent lamps in "duo". *a*) Mains voltage v_M and currents i_L and i_{L+C} of lamps individually. *b*) Currents of individual lamps and sum current i_T. *c*) Waveforms of mains voltage and total current.

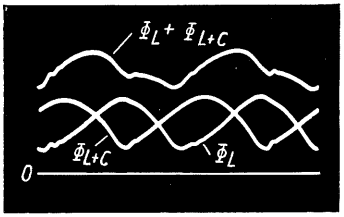

Fig. 13–9. Luminous flux of two "daylight" lamps —individually Φ_L and Φ_{L+C}—and their sum $\Phi_L + \Phi_{L+C}$ (duo arrangement).

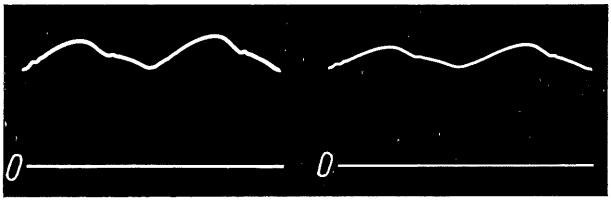

a b

Fig. 13–10. Luminous flux of fluorescent lamps in "duo";
a) "white"
b) "warmtone"

Lamp current and luminous flux waveforms of electronically controlled lamps.

It is frequently necessary to control the brightness even of fluorescent lamps. Since they have a relatively high ignition potential and a practically constant working voltage, control is not possible, as it is with incandescent lamps, by varying the voltage. A solution of the problem was found by connecting an antiparallel arrangement of two thyratrons in series with the fluorescent lamp and its ballast. By changing the phase of the grid voltage responsible for ignition, the current is made to flow only during an adjustable portion of the half cycles. In this way the mean current of the lamp can be reduced quite considerably without extinguishing the lamp [3].

The oscillograms in fig. 13–11*a* show the current waveforms of a lamp controlled in this manner at settings of 1200, 600, 300, 150 and 75 mA (measured with a standard multirange meter calibrated in r.m.s. values). They were recorded in the way described on several previous occasions, with the time base synchronized in fixed phase with the mains frequency, so that the same reference phase position was assured for all composite photographs. The corresponding oscillograms of the luminous flux are shown in fig. 13–11*b*. It might be assumed, since adjustment to a lower current means a shorter time of current flow, that the stroboscopic effect would be increased. Experience shows, however, that the light fluctuates just as little at reduced brightness as at normal working current. The explanation for this curious behaviour is to be found in the flux waveforms in fig. 13–11*b*.

It can clearly be recognized that the afterglow of the fluorescent material, which at normal current (top curve) is hardly noticeable, represents at decreasing current a progressively increasing part of the total light.

The foregoing observations show that the oscilloscope can provide a thorough insight not only into the behaviour of the lamps themselves but also into the entire principle of thyratron control.

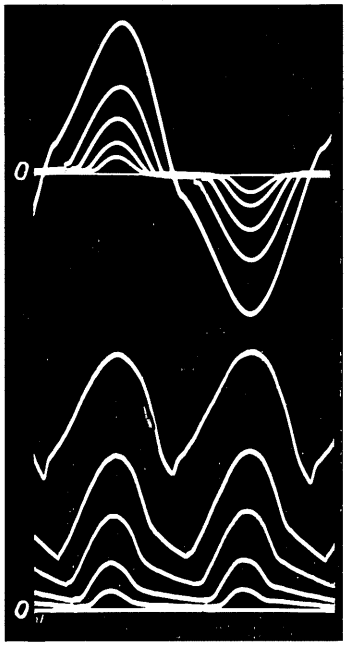

Fig. 13–11. Current and luminous flux waveforms for fluorescent lamps, with electronic control in five different stages of adjustment.

14. Investigating switching phenomena on electric light bulbs

What happens in radio receivers and amplifiers after they have been switched on is fairly well known. In any case it is now generally recognized that the cathode ray oscilloscope can display all the information that may be required. Less interest seems to be shown, however, in what happens during the actual processes of switching on and switching off. And yet numerous examples might be quoted of occasions when an exact knowledge of switching phenomena could lead either to greater safety of operation or to greater economy.
The investigations about to be described were carried out, by way of example, on electric light bulbs, as used on radio receivers. The results are, of course, valid for incandescent lamps in general.
Using an oscilloscope (Philips GM 3156) recordings were made of the course of the current through the lamp as well as of the luminous flux at the moment of switching on. Naturally, both processes could have been displayed simultaneously on a twin-beam oscilloscope or with the aid of an electronic switch. Since, however, the phenomena repeat themselves indentically, it was quite sufficient to join the recordings together afterwards, especially as they were made on the same apparatus and with the same time base expansion.
The circuit used is shown basically in fig. 14–1. The bulb is fed, either from an accumulator or from the secondary of a mains transformer, via contact K_3 and resistor R_v. The value of this resistor must be small in relation to the cold resistance of the lamp, as otherwise the switching process might be falsified.
The voltage drop on resistor R_v is proportional to the current through the bulb. After amplification in the *DC* vertical-amplifier, it is applied to the

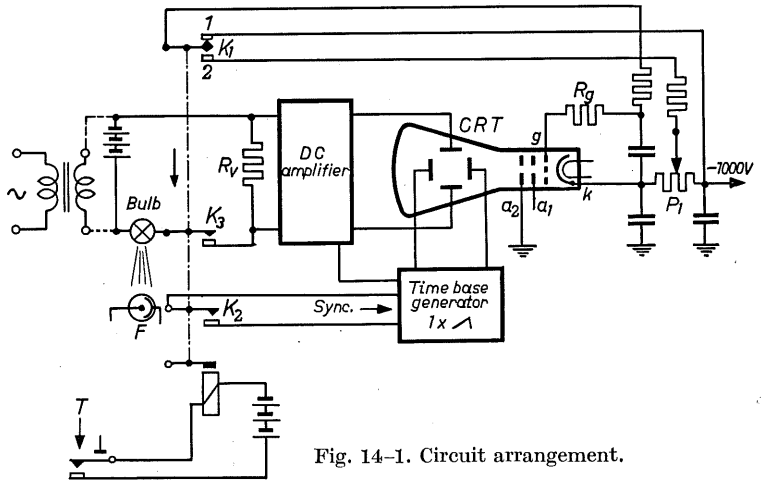

Fig. 14–1. Circuit arrangement.

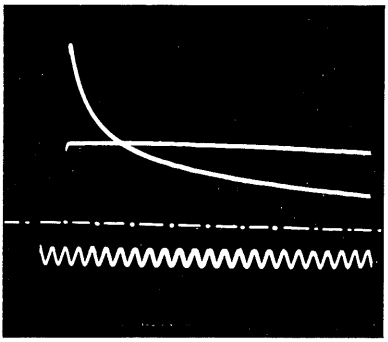

Fig. 14–2. Current of a 6.3 V/0.15A bulb at the moment of switching on (*DC* operation). The broken line represents zero, the horizontal full line a constant current of 0.5 A. The sinusoidal frequency for the time scale is 2500 c/s.

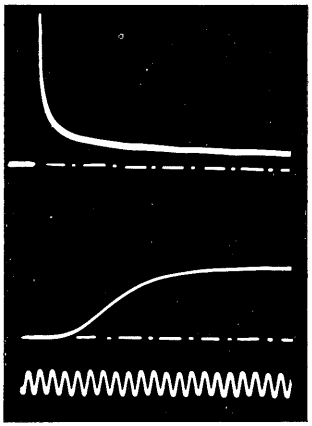

Fig. 14–3.
Above: Switching-on current under conditions identical with those for fig. 14–2. Centre: trend of the luminous flux. Below: time scale 200 c/s.

Y plates of the cathode ray tube. For this measurement the time base generator must be adjusted for a single sweep. To avoid premature exposure of the film and to ensure correct timing of the recording the necessary switching processes are effected by a relay with several contacts. The relay is switched on for the recording by button T. The armature of the relay is then actuated and closes, one after the other, contacts K_1, K_2 and K_3. This sequence is arranged by suitably adjusting the contacts. In the quiescent state no spot is to be seen on the screen, the Wehnelt cylinder being at full cut-off potential. When K_1 closes, the grid receives only a partial voltage from potentiometer P_1. Now K_2 closes and a single time base is triggered, after which K_3 switches on the current for the bulb. K_3 should preferably be a double contact to avoid "chatter" when the relatively high peak current is switched on. For recording the behaviour of the luminous flux the light of the bulb is directed on to a high-vacuum photocell during the process of switching. The voltage drop on the

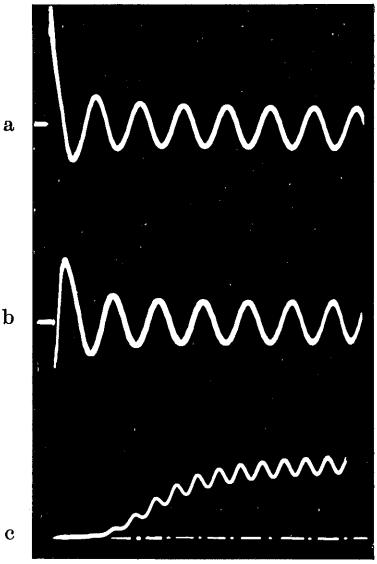

Fig. 14–4. At *AC* operation the height of the current surge depends upon the voltage phase at the moment of switching on.
a) Switching on in the positive peak.
b) Switching on at a smaller amplitude.
c) Rise of the luminous flux.

working resistance, which is proportional to the luminous flux, is fed via a *DC* amplifier to the *Y* plates. To provide a time scale for these curves, an alternating voltage of known frequency was recorded below the waveforms under investigation. In order also to have a measure of the current, a further recording was made, for which the bulb was replaced by a rheostat in series with an ammeter, and the current to be recorded was adjusted to 500 mA. The oscillograms thus obtained for the first 10 milliseconds with a bulb of 6.3 V/0.15 A are shown in fig. 14–2. The time-marking frequency was 2500 c/s. In fig. 14–3 the period of time represented is longer, at the end of which the lamp has certainly reached its stable condition. In this instance the frequency of the time scale chosen is 200 c/s. The interesting fact appears that, at the moment of switching on, the current rises to around nine times the nominal value of the current. It is further interesting to note that light radiation only begins after the current has reached its nominal value. The time in the case under investigation is about 15 ms. After a further 50 ms the luminous flux has attained its normal value.

Observing the switching-on current with *alternating voltage* in the oscillograms in fig. 14–4 we can see that the height of the initial peak depends upon the phase of the voltage at the moment of switching on. In pattern *a*) it is plain that the moment of switching on lay in the vicinity of the positive peak; a maximum value was therefore reached similar to that of the direct voltage. In pattern *b*), on the other hand, only a small current peak is observed. The luminous flux shown in *c*) naturally retains a ripple of about 15% of the basic light with twice the frequency of the supply current. No time marking was necessary for this recording, the time scale being given by the known frequency of the supply current (50 c/s) or of the luminous flux (100 c/s).

15. Investigations on television receivers

General.

To be able to form a judgment on the operation of a television receiver, whether it be for the purposes of development, servicing or general study, it is of fundamental importance to have a clear knowledge of the behaviour of the various signal voltages with respect to time.

The actual waveform is usually of more interest than the absolute value of the voltage.

The oscilloscope presents the information required for these investigations in an extraordinarily clear and comprehensive way, and for this reason it has become an indispensable tool of the television engineer.

As long as it is not a matter of solving problems of development, oscilloscopes with an amplifier having an upper frequency limit of about 1 Mc/s are quite sufficient for these investigations (e.g. Philips GM 5659 or GM 5650). An oscilloscope of this standard can display satisfactorily rectangular waveforms at frequencies many times higher than the line frequency.

The oscillograms in fig. 15–1*a* and *b* show to what extent the pattern of higher modulation frequencies is influenced by the upper frequency limit. For these

examples the ouput voltage of Philips GM 2887C pattern generator during two cycles of the horizontal deflection was recorded with the addition of eleven modulation (bar) pulses (eleven vertical pulses in one line). In fig. 15–1*a*, the upper frequency limit is 3 Mc/s and in *b*), 0.8 Mc/s. It can be seen that the reproduction of these modulation pulses is perfectly satisfactory for most investigations, at least on deflection voltages or currents. What is most essential is the lower frequency limit, which should where possible be as low as 1 c/s. If this is not so, the phase of the frame pulses may be badly distorted. A high input impedance is also of decisive importance; it should be at least 1 MΩ but using a probe voltage-divider it can be made as high as 10 MΩ.

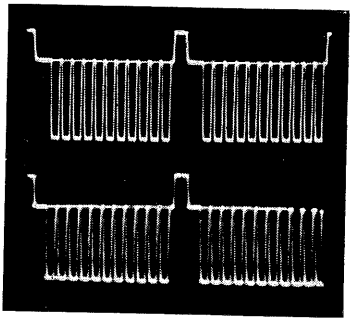

Fig. 15–1. Pattern generator signal during two cycles of the horizontal deflection, reproduced via vertical amplifiers with upper cut-off frequencies of *a*) 3 Mc/s and *b*) 0.8 Mc/s.

The vertical amplifiers of the oscilloscopes on which the investigations about to be described were carried out, types GM 5653 and GM 5654, both have a band-pass of 1 c/s to 3 Mc/s. The normal oscillograms were recorded without any particular post-acceleration voltage, whereas +2 kV were used for the expanded waveforms.

This chapter will deal first with the most essential types of oscillogram, all obtained using the Philips type TD 2312A "Home Projection Receiver" as a practical example. The simple time base expansion unit described in chapter 22 was used for the "time expanded" oscillograms.

In addition to these, a number of oscillograms are reproduced which were taken from Philips Direct View Table-Model TD 1420 U. The expanded recordings were made with a type GM 4584 time base expansion unit, with which is was possible to reproduce separately the pulse sequences of both fields of a frame one above the other on the screen.

Investigations on TV projection receiver "TD 2312A".

Fig. 15–2 shows the circuit diagram of receiver TD 2312A.

The working principle of receiver TD 1420 U is fundamentally the same as that of TD 2312A. Differences will be pointed out as occasion arises [1] [2].

The circled numbers found at various points in the circuit diagram of TD 2312A refer to oscillograms. They are given the same designation in the servicing data and are also marked at the side of the relevant waveforms reproduced in this chapter.

The reception signal employed was in most cases the aerial voltage of the West Berlin television transmitter with a test pattern as shown in fig. 15–3, but occasionally the H.F. voltage of the GM 2887C pattern signal generator was also used.

Where appropriate, the oscillograms are marked with the peak-to-peak value of

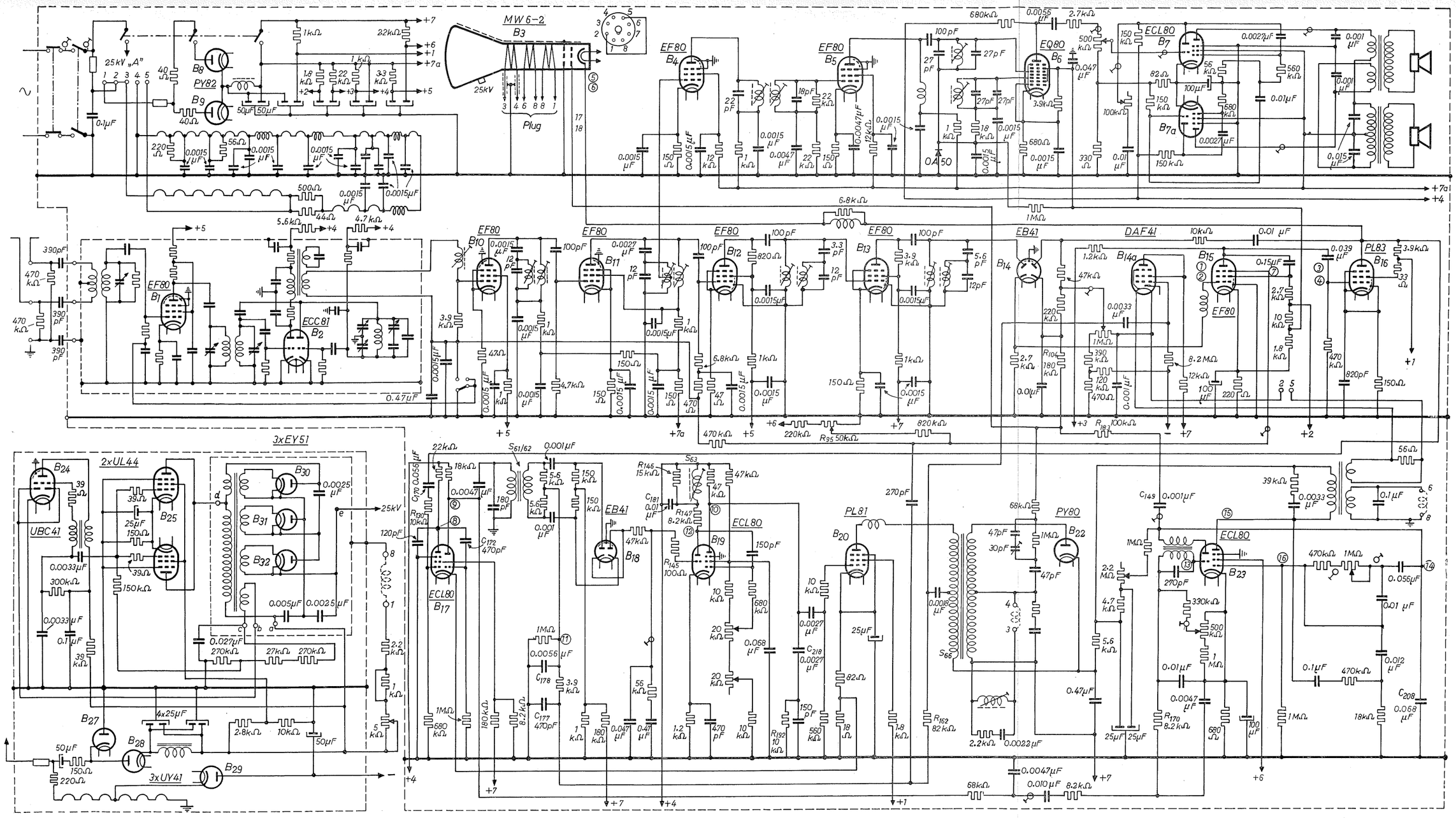

Fig. 15–2. Circuit diagram of Philips television projection receiver, type TD 2312 A.

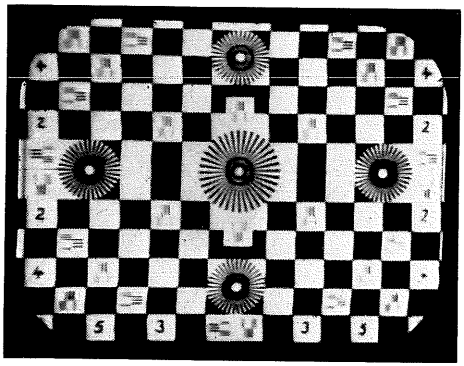

Fig. 15–3.
Test pattern transmitted from West Berlin, used for oscillograms up to fig. 15–22.

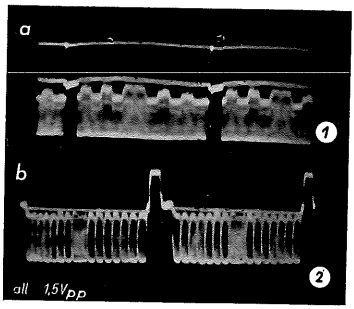

Fig. 15–4. Video signal on the grid of pre-amplifier EF 80: *a*) two cycles of the frame deflection; *b*) two cycles of the line deflection.

voltage found at the appertaining setting of the receiver. It was obtained by comparing the maximum vertical deflection caused by the signal with an equal deflection caused by a 50 c/s sinusoidal voltage and by measuring its r.m.s. value ($\times 2.83$).
The measurements start at the video detector stage or at the grid of the video pre-amplifier valve, where the demodulated signal is already available. The observations to follow will be summarized for the individual stages.

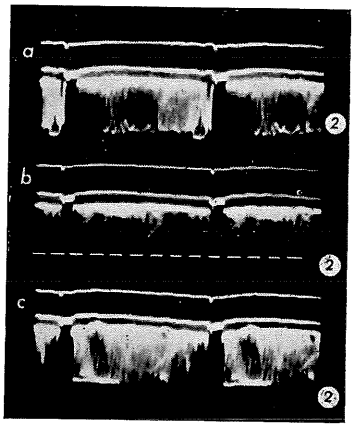

Fig. 15–5. Video signal as in fig. 15–4*a*) but with varying intensity of picture modulation.

Video detector and video amplifier.

The video signal appears across the cathode resistor of one section of the double-diode EB 41 (B_{14}). Its phase is negative, as shown in the oscillograms in fig. 15–4.
For fig. 15–4*a* the time base frequency was equal to half the frame (vertical) frequency and in fig. 15–4*b* equal to half the line (horizontal) frequency during reception of the television test pattern transmitted from West Berlin, as illustrated in fig. 15–3. The oscillograms in fig. 15–5 show three different patterns with the frame frequency during the normal picture transmission. The pattern in *a*) shows the presence of a great deal of "white" in the lower part while the upper part contains dark patches. In *b*) the whole pattern is relatively dark; the limit of "white" modulation possible is indicated by a dotted line. In *c*), on the other hand, the upper part of the pattern is at maximum brightness and the lower part is dark. It must, of course, be remembered in observations of this kind that the oscillograms represent the sum of the modulation voltages at the corresponding vertical and horizontal deflections during the time of per-

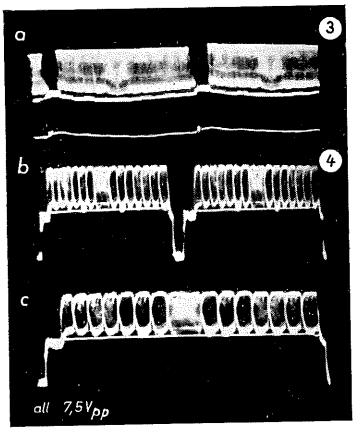

Fig. 15–6. Composite signal on the grid of the video output pentode PL 83: *a*) two cycles of the frame deflection; *b*) two cycles of the line deflection; *c*) the same, but during one cycle.

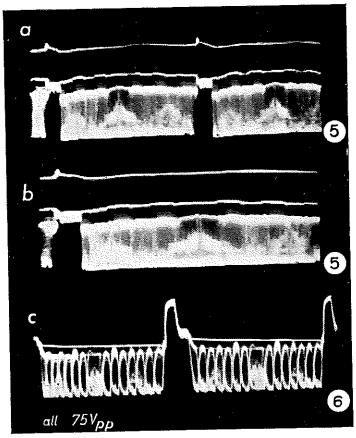

Fig. 15–7. Oscillograms on the cathode of picture tube MW 6–2: *a*) composite signal during two cycles of the frame deflection; *b*) the same, but during one cycle; *c*) composite signal during two cycles of the line deflection.

ception, or the exposure time of the recording. For more analytical observation it is possible to display the modulation content of one single line [3]. This subject will be touched upon at a later stage in this chapter.

The video signal reaches the grid of the video pre-amplifying valve EF 80 (B_{15}) in the same form and appears amplified at the anode with its phase reversed. From this point it is passed practically unchanged via coupling elements to the grid of the video output stage, valve PL 83 (B_{16}). The oscillograms of the voltages at this point corresponding to those in fig. 15–4, are shown in fig. 15–6. In fig. 15–6*c* a further oscillogram is reproduced of the pattern during one cycle of the line frequency; from this the modulation content in this time may be compared with the test pattern in fig. 15–3.

The amplified, composite video signal from the anode of the video output stage PL 83 controls the cathode of the picture tube MW 6–2. The relevant oscillograms are shown in fig. 15–7. The pattern in *b*) now represents one cycle of the frame signal with modulation, to be compared with the test pattern in this direction.

To form a clear impression of the synchronization measures in the deflection circuits it is essential to be able to observe what distortions (wanted or unwanted) of the sync pulse-train take place in the individual stages.

Referring to the oscillograms in figs. 15–4, 5, 6 and 7, it can be seen that the relatively simple line pulse presents no difficulties of interpretation, even in a normal oscillogram. With regard to the frame pulse the situation is different. As is known, the actual frame sync pulses, each with 6 or 5 equalizing pulses respectively, and an appropriate series of line pulses are sent out by the transmitter during the vertical blanking, which in oscillograms of this kind only amounts to a few millimetres in width.

The way these pulses are dealt with in the television receiver is decisive for proper functioning, good line-interlace, etc. To observe them satisfactorily they must be expanded along the time axis by a time base expansion unit.

A simple apparatus of this kind, which is however only suitable for mains-coupled composite television-pulses, is described in chapter 22.
Fig. 15–8 shows oscillograms, expanded 25-fold by this apparatus, which represent the beginning of the vertical blanking pulse measured on the cathode of the MW 6–2 picture tube. The oscillogram in *a*) shows the test pattern transmitted from Berlin, and that in *b*) the corresponding pulse train from the type "GM 2887C" pattern generator. The shaping of these composite sync pulses will be shown by further oscillograms, expanded along the time base. It should be noted that with this simple time base expansion unit, which works on the 50 c/s mains, the pulse trains of the two fields of the lineinterlace process appear covering each other in the oscillogram. The pattern generator delivers a simple pulse sequence only (no line interlace).

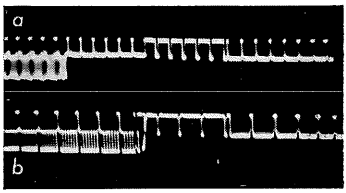

Fig. 15–8. Expanded oscillogram with 50 c/s time base frequency at the beginning of the vertical sync pulse on the cathode of the picture tube: *a*) composite signal from Berlin test pattern; *b*) voltage from pattern generator GM 2887C with 11 vertical bars.

Automatic Gain Control.

In the receivers investigated, the control voltage fed to the *RF* amplifier EF 80 (B_1) and to the *IF* amplifiers EF 80 (B_{10} and B_{12}) has two components: one constitutes the positive voltage adjustable by the contrast control R_{95}, and the other the automatic control voltage proper, which is obtained by rectification of the positive flyback pulses on the third grid of the video pre-amplifier EF 80 (B_{15}). The third grid of this valve, together with the cathode, forms a diode section whose internal resistance is dependent upon the strength of the signal. The oscillogram of the positive horizontal flyback pulse on the third grid of the video pre-amplifier is shown in fig. 15–9.

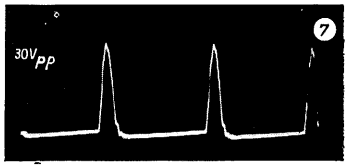

Fig. 15–9. Line flyback pulses on grid 3 of EF 80 for generating the control voltage.

Synchronization separator.

This receiver uses a double valve—ECL 80 (B_{17})—for simultaneous pulse separation and pulse amplification.
The complete composite signal in which, as

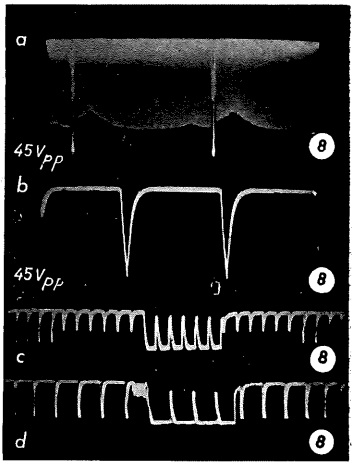

Fig. 15–10. Sync pulses on anode of pentode section of the synchronization separator. Time base expansion: *a*) half frame frequency; *b*) one third of line frequency; *c*) and *d*) 50 c/s expanded oscillograms corresponding to fig. 15–8 *a* and *b*.

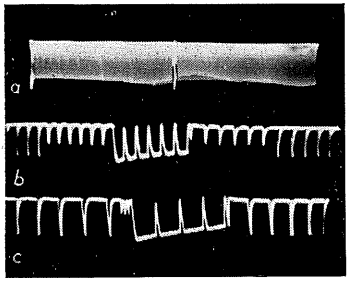

Fig. 15–11. Pulse train on grid of triode section of the synchronization separator. Time base expansion as in fig. 15–10.

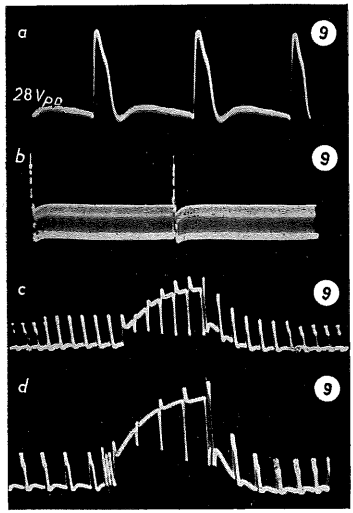

Fig. 15–12. Sync pulses on anode of triode section of the synchronization separator. Time base expansion: *a*) one third of line frequency; *b*) half frame frequency; *c*) and *d*) oscillograms taken with time base expansion unit.

the oscillograms in figs. 15–7 and 8 show, the sync pulses are positive-going, is taken from the anode of the video output stage and fed via condenser C_{170} and resistor R_{130} to the control grid of the pentode section of an ECL 80. Grid detection is effected by suitably rating the time constant of the grid circuit, while the screen grid potential is kept extremely low. The control range of the pentode is thus very limited, so that the modulation content is clipped and only the sync pulses are further amplified; they appear at the anode of the valve inverted in phase.

In fig. 15–10*a* the time base frequency of the oscilloscope is again equal to half the frame frequency, and in 10*b* equal to one third of the line frequency. These oscillograms, it must be added, merely disclose information on whether frame or line pulses are contained at all in the amplified voltage. A clear insight into the particularly interesting part in the neighbourhood of the vertical sync pulse is obtained only by using a time base expansion unit. Examples are shown in fig. 15–10*c* and *d*, corresponding to the signal forms of fig. 15–8. Comparing these with the oscillograms of the horizontal pulses in fig. 15–10*b*, one can see that the form of the line pulse is identical, except that the deflection in the Y axis is smaller in fig. 15–10 *c* and *d*.

These pulses are now fed over a coupling condenser of 470 pF (C_{172}) to the grid of the triode section of the ECL 80. The value of the grid leak resistor is 1 MΩ. The time constant of this grid network causes slight distortion of the frame pulse, as can be observed in fig. 15–11. The pattern in 15–11*a*) represents the normal oscillogram with a time base frequency of half the frame frequency, while *b*) and *c*) again show the pulse train expanded twentyfive-fold along the time axis.

The amplified pulses now appear at the anode of this stage (see fig. 15–12), with the distortion likewise amplified. The oscillogram in *a*) is reproduced this time with one third of the line frequency, *b*) with one half of the frame frequency, while *c*) and *d*) are shown with a reduced picture height, just as in the expanded patterns in fig. 15–10*c* and *d*.

Line deflection generator (horizontal deflection).

This deflection generator is made up of the following: a multivibrator employing an ECL 80 (B_{19}), an output valve PL 81 (B_{20}) with output transformer, a booster diode PY 80 (B_{22}) and a phase discriminator stage employing a double diode EB 41 (B_{18}). A sawtooth voltage, as shown in fig. 15–13*a*, appears across the output condenser C_{218} from the cathode-coupled multivibrator, which oscillates at the line frequency. By adding this sawtooth voltage to a voltage whose waveform corresponds to the charging current of C_{218} and which appears across a series resistor R_{192} (fig. 15–13*b*), the voltage is obtained which is needed for driving the line output valve PL 81 (fig. 15–13*c*). For synchronizing the line deflection generator the "flywheel synchronizing" circuit is used, which is characterized by its high degree of insensitivity to interference. The pulses coming from the synchronization separator ECL 80 (B_{17}) are not simply differentiated and then immediately employed for synchronization, but are fed via a coupling condenser and a balancing transformer—S_{61}, S_{62}—to the anode and cathode respectively of the series-connected sections of the double diode EB 41 (B_{18}), the phase discriminator. In this stage the relative phase of the sync pulses is compared with a sawtooth voltage originating from the deflection generator and which is obtained by double integration of the voltage from the winding S_{66} via the network R_{162}–C_{177} and R_{137}–C_{178}. The sawtooth voltage in question is shown in fig. 15–14*b*. The phase discriminator delivers a control voltage which is dependent upon the relative phase of the sync pulse with respect to the sawtooth voltage. This results in a stable state of balance if the sync pulse coincides with the middle of the steep edge of the sawtooth.

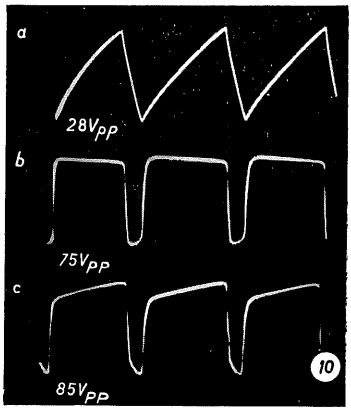

Fig. 15–13. Generation of the drive voltage for the line output stage: *a*) sawtooth voltage from multivibrator; *b*) current waveform of charging condenser in multivibrator circuit; *c*) drive voltage for line output.

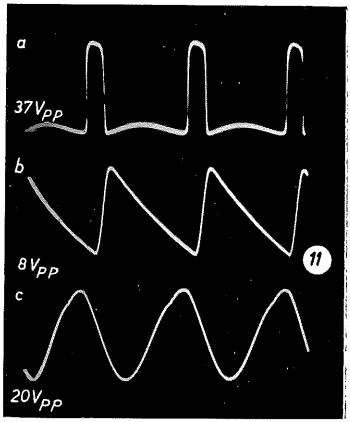

Fig. 15–14. Voltages in line deflection generator: *a*) waveform on anode resistor of multivibrator; *b*) integrated voltage of line flyback pulse from line output transformer; *c*) voltage on flywheel circuit

The control voltage is fed through a resistor of 100 Ω (R_{145}) to the grid of the multivibrator-triode section of the ECL 80, and by influencing the frequency of

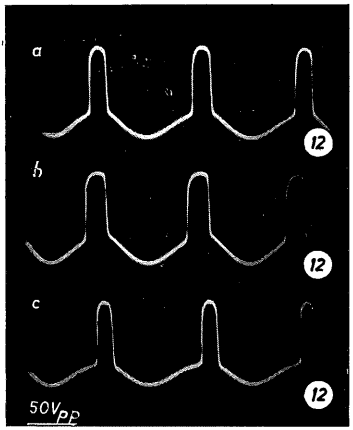

Fig. 15–15. Voltage waveform on anode of ECL 80 triode section of multivibrator.

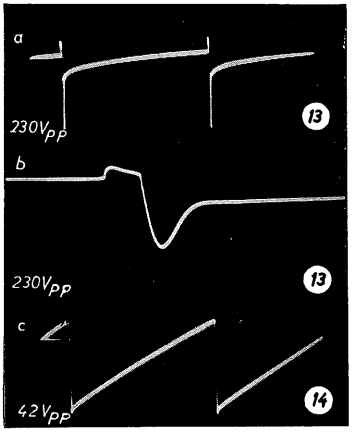

Fig. 15–16. Generation of the drive voltage for the frame output stage: *a*) voltage on grid of blocking oscillator; *b*) the same expanded along the time axis; *c*) charging condenser voltage.

the multivibrator it enforces the necessary synchronization between the transmitter and the deflection circuit of the receiver. A rectangular voltage (fig. 15–14*a*) appears across a resistor of 8.2 kΩ (R_{147}) in the anode circuit of this stage. In series with R_{147} lies (at the "cold end") the flywheel synchronizing circuit proper (S_{63}, C_{181}, R_{146}), across which a voltage appears as shown in the oscillogram in fig. 15–14*c*. The sum of the voltages on the anode of the triode system of the ECL 80 (B_{19}) is shown by the oscillograms in fig. 15–15. In *a*) the resonant frequency of the flywheel synchronizing circuit is in full agreement with the line frequency; the multivibrator pulse rests exactly upon the peak of the voltage curve from the synchronizing system. Variation of the line frequency results in different relative phase positions as depicted by the oscillograms in *b*) and *c*).

Frame deflection generator (vertical deflection).

The voltage for generating the deflection current is produced with a triode-pentode ECL 80 (B_{23}), whose triode section works as a blocking oscillator. The oscillogram in fig. 15–16*a* shows the voltage waveform on the grid of this valve during two cycles of the frame frequency. What really takes place is seen in the expanded oscillogram in *b*). This shows plainly that the incidence of grid current sharply limits the increase in grid voltage. The voltage can only swing in the negative direction in a manner which results in the appearance of a sawtooth voltage across the 68,000 pF charging condenser (C_{208}) of the blocking oscillator (fig. 15–16*c*). The blocking oscillator is grid-synchronized with a voltage pulse which is obtained by triple integration of the composite pulse taken from the anode of the synchronization separator (fig. 15–12). Fig. 15–17 shows a normal and an expanded oscillogram of the voltage on the first integration network. The pulse from the blocking oscillator results in a strong downward deflection, so that even in the expanded oscillogram (fig. 15–17*b*) only few details are observable in this direction. If, however, the blocking oscillator is put out of

action, it is possible to obtain an expanded oscillogram of the frame-pulse waveform on the integration networks and to make the influence of the equalizing pulses as clear as it appears in fig. 15–18. The experienced television technician can recognize at once from these oscillograms that the interlace is working properly.
The pulses of the two fields coincide on their steep edge. If there were no interlace, the edges would appear separately, adjacent to each other [4].
Where an oscilloscope is available with a particularly high *Y* deflection and a facility for zero correction (e.g. GM 5653), a similar pattern can be obtained with the blocking oscillator running (fig. 15–19).
A number of different settings for the frame frequency are reproduced, among which the oscillogram in fig. 15–19*a* represents an unstable condition. The parts of the waveform in fig. 15–17*a* corresponding to the oscillograms in figs. 15–18 and 15–19 are circumscribed by a dotted line to illustrate the extent of time base and amplitude expansion employed. Fig. 15–20*b* shows the waveform of the voltage on the grid of the pentode section of ECL 80, and 20*a* the waveform of the anode voltage. The parabolic component [1] can be seen in the grid voltage waveform, although its scale is reduced in the reproduction owing to the peaky amplitude of the pulse.

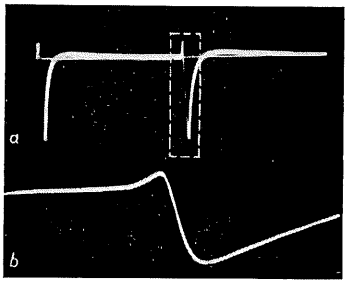

Fig. 15–17. Voltage waveform on first integration condenser for vertical sync pulses. Time base expansion: *a*) two frame cycles; *b*) section with time base expansion unit.

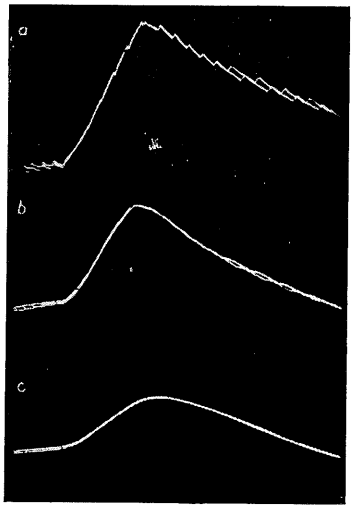

Fig. 15–18. Expanded oscillograms from the integration networks, with blocking oscillator out of operation: *a*), *b*) and *c*) first, second and third networks.

Suppressing the flyback.

Additional blanking of the flyback traces, independently of the blanking pulses received from the transmitter, is effected by taking pulses from the line and frame deflection generators and using them to cut off the anode current of the picture tube during the respective flyback periods. The line flyback is suppressed by applying the voltage appearing in the secondary of the line output transformer, via smoothing and phase-correcting networks, to the grid of the

[1] This pre-distortion of the anode current is necessary in order to obtain a sawtooth current in the deflection coils of the anode circuit in spite of the influence of the limited primary inductance of the output transformer.

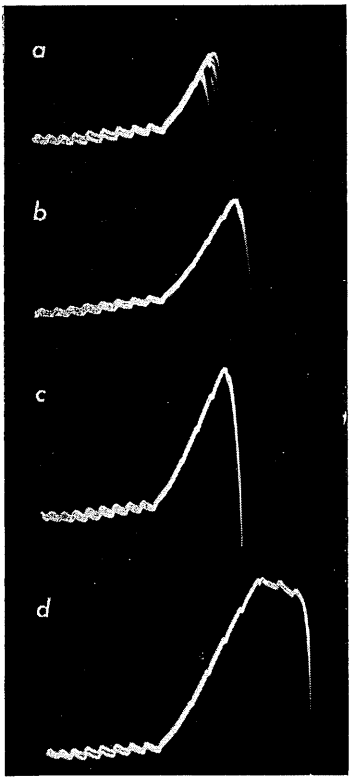

Fig. 15–19. Voltage on first integration network with blocking oscillator in operation and with different settings of the frame frequency.

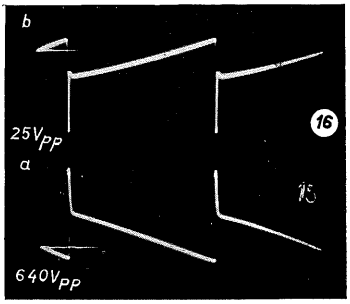

Fig. 15–20. Voltage waveforms on *a*) anode (15) and *b*) grid of frame output stage.

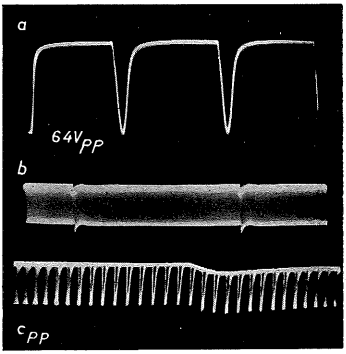

Fig. 15–21. Additional suppression of flyback (frame and line). Time base expansion: *a*) one third of line frequency; *b*) half frame frequency; *c*) time-base expanded oscillogram.

picture tube. Fig. 15–21*a* shows the waveform of this voltage during three cycles of the line frequency.

To suppress the frame flyback, the sawtooth voltage on condenser C_{208} (fig. 15–16*c*) is differentiated by a *CR* network of 1000 pF and 180 kΩ (C_{149}, R_{183}, R_{104}) and, since the MW 6–2 has a triode system, it is also applied to the Wehnelt cylinder.

Fig. 15–21*b* shows the relevant waveform during two cycles of the frame frequency, and *c*) shows a part of the same waveform near the frame sync pulse expanded along the time axis. In this case the line blanking is relatively stronger than the frame blanking, but the latter is also quite sufficient for additional blanking of the correctly adjusted picture.

Extra High Tension Supply.

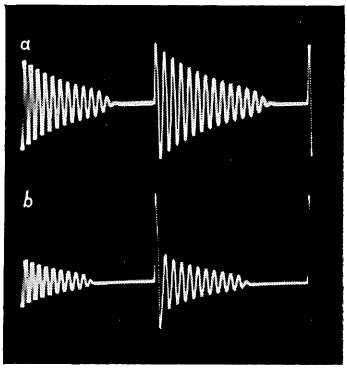

Fig. 15–22 Voltage waveform for E.H.T.; *a*) receiver picture dark, low load; *b*) bright picture.

The extra high tension of 25 kV required for operating the picture tube is obtained by means of a separate aggregate. The triode section of a UBC 41 (B_{24}) works as a blocking oscillator and generates a sawtooth voltage of about 1000 c/s, which is fed to the control grids of two pentodes UL 44 connected in parallel. The operating point of these valves is adjusted in such a way that a sawtooth current with a very steep trailing edge flows through the primary of the transformer in the anode circuit. As a result of the rapid changes of current the anode circuit, which consists of inductance and winding-capacitance, is excited into self-oscillation, and this is renewed with the arrival of each surge. The stepped-up voltage peaks of these oscillations on the secondary of the transformer amount to about 8.5 kV with a characteristic frequency of about 20 kc/s. This voltage is rectified and smoothed by a voltage-tripler circuit employing three EY 51 diodes. The relevant waveforms are shown in fig. 15–22. The time base frequency in this picture is 550 c/s and thus the frequency of the damped oscillations is 17 kc/s.

Oscillograms of the Direct-View Table-Model, receiver "TD 1420 U".

The input signal employed for the following oscillograms was again in accordance with the West Berlin test pattern shown in fig. 15–3. The "time expanded" oscillogram of a pulse train of this kind during the vertical blanking on the cathode of the picture tube (anode video output stage PL 83) was reproduced in fig. 4–44*a*).

The voltage waveform on the anode of the synchronization separator (ECL 80) is shown in fig. 15–23*a* and *b*). In *a*) the pulse trains of both fields appear expanded along the time axis one above the other in the vicinity of the frame sync pulse. In this case there are respectively seven and five equalizing pulses present. (A type GM 4584 time base expansion unit was used for these recordings.) Fig. 15–23*b* shows a normal oscillogram during three cycles of the line deflection. The form of this voltage can also be recognized at the ends of the pulse trains in the expanded oscillogram in fig. 15–23*a*.

This voltage is amplified by the triode section of an ECL 80. The waveforms of the voltages at the anode of this valve system are shown by the oscillograms in fig. 15–24*a* and *b*. In *a*) can again be seen the expanded pulse trains of the fields in the neighbourhood of the frame sync pulse and in *b*) the normal ocillogram during three cycles of the line deflection. In this recording, six leading and six lagging equalizing pulses are present.

This pulse train is now fed via the discriminator transformer to a phase discriminator stage. The oscillograms in fig. 15–25*a*, *b* and *c* show the voltage waveform on the primary of this transformer.
Fig. 15-25*a* shows the voltage pattern during two cycles of the frame deflection and *b*) the pattern during two cycles of the line deflection. The expanded oscillogram in *c*) shows the pulse train again near the frame sync pulse.
In this receiver a control voltage is generated by means of two germanium diodes OA 51 which is dependent upon the relative phase position of the

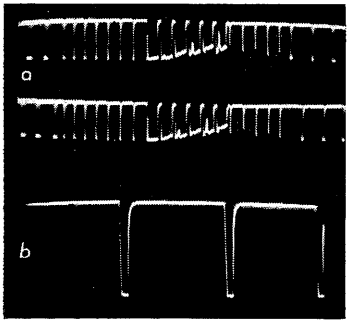

$25V_{pp}$

Fig. 15–23. Voltage waveform on anode of synchronization separator. (Receiver "TD1420U"): *a*) expanded oscillogram; *b*) three cycles of line deflection.

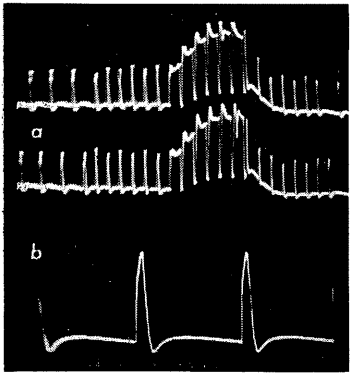

$45V_{pp}$

Fig. 15–24. Voltage on anode of amplifier triode section of sync-separator: *a*) time base expanded; *b*) three cycles of line deflection.

$80V_{pp}$

$55V_{pp}$

$80V_{pp}$

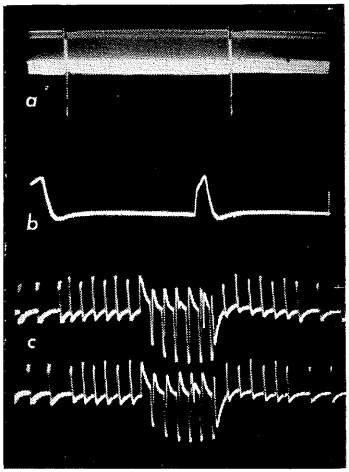

Fig. 15–25. Voltage on primary of discriminator transformer:
a) two cycles of frame deflection;
b) two cycles of line deflection;
c) expanded oscillogram.

$18V_{pp}$

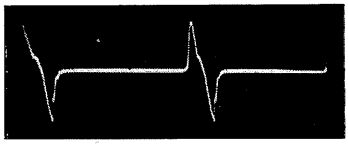

Fig. 15–26.
Voltage waveform at centre tap of discriminator transformer secondary.

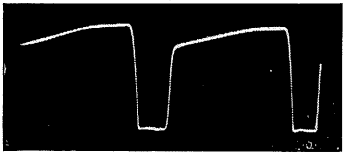

Fig. 15–27. Voltage on anode of pentode section of ECL 80 in line time base generator ($75V_{pp}$).

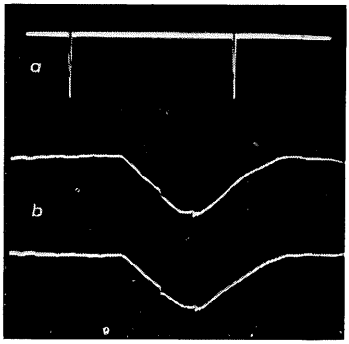

Fig. 15–29. Voltage on grid of vertical sync amplifier: *a*) two cycles of frame deflection; *b*) expanded oscillogram ($7.5V_{pp}$).

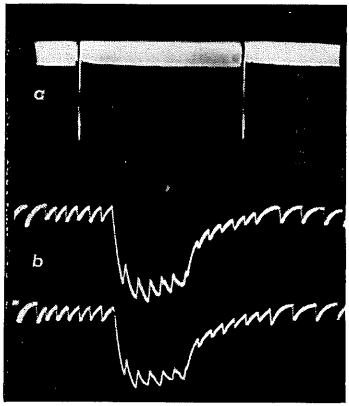

Fig. 15–28. Waveform of vertical sync pulse on first *RC* network: *a*) two cycles of frame deflection; *b*) expanded oscillogram ($25V_{pp}$).

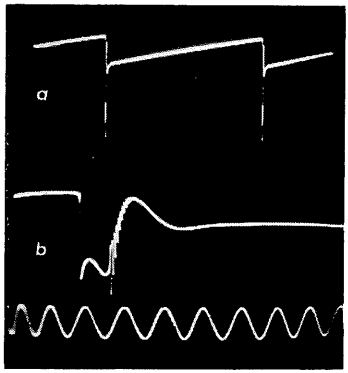

Fig. 15–30.
Anode voltage of blocking oscillator for frame deflection:
a) two cycles of frame deflection;
b) time base expanded; time-marking 10 kc/s; ($150V_{pp}$).

sync pulses with respect to a pulsed voltage fed back from the line deflection generator. The germanium diodes are oppositely connected to the symmetrical secondary winding of the discriminator transformer. The voltage waveform at the centre tap of the secondary during two line cycles is shown by the oscillogram in fig. 15–26.
The control voltage, which represents the difference voltage of the two diodes, controls the inductive reactance of the triode system of the ECL 80. It thereby effects a frequency change of the sine-wave generator in the pentode system and thus enforces the necessary synchronization between transmitter and

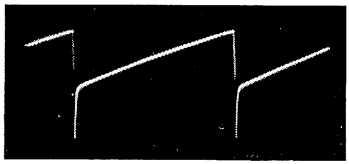

Fig. 15–31. Voltage on charging condenser of blocking oscillator ($90V_{pp}$).

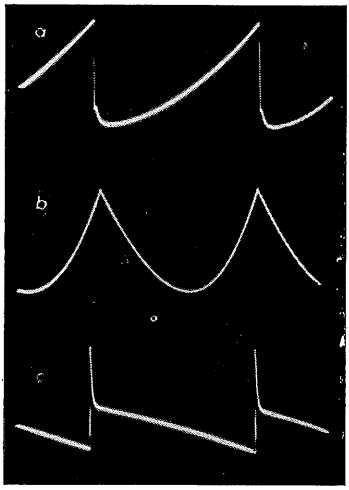

Fig. 15–32. Voltages in line output stage: *a*) waveform on the grid ($7.5V_{pp}$); *b*) parabolic component of cathode voltage ($\sim 0.4V_{pp}$); *c*) waveform on the anode ($1500V_{pp}$).

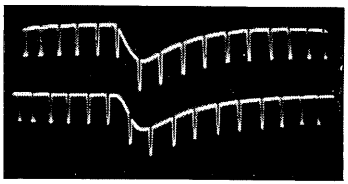

Fig. 15–33. Voltage waveform for flyback blanking on grid of picture tube ($45V_{pp}$ and $65V_{pp}$).

receiver. The form of grid voltage required for driving the line output valve PL 81 is obtained by adding the asymmetrical rectangular voltage generated by the multivibrator circuit to a sawtooth voltage which is produced by integration of a part of the rectangular voltage in an *RC* network. Fig. 15–27 shows the waveform of this voltage at the anode of the pentode section of the ECL 80.

The sawtooth voltage for the frame deflection is generated in the triode section of an ECL 80, working as a blocking oscillator. For synchronization, pulses are again taken from the anode of the synchronization separator triode ECL 80 and passed through two *RC* networks to filter out the line pulses. Fig. 15–28*a* reproduces the voltage waveform on the condenser of the first network for two frame pulses. The "time expanded" oscillogram in 15–28*b* shows the pulse trains of both fields. The corresponding voltage waveform on the condenser of the second network can be seen in fig. 15–29*a* and *b*. This voltage lies on the grid of the pentode section of the ECL 80. Here it is amplified, separated and reversed in phase so that the voltage from the anode of this system appears as positive pulses on a winding of the transformer in the blocking oscillator circuit and is used for synchronization.

The normal oscillogram of the anode voltage waveform during two cycles of the frame frequency is shown in fig. 15–30*a*. The actual trend of the voltage pulse only becomes clearly visible after time base expansion as shown—single this time—in fig. 15–30*b*. A sinusoidal voltage with a frequency of 10 kc/s has been included in the oscillogram for the purpose of determining the frequency of the overshoot visible. Interpretation of the patterns shows the overshoot to have a frequency of approximately 175 kc/s.

Here again, a sawtooth voltage appears across the charging condenser in the blocking oscillator circuit, which, due to the operation of the oscillator, has a negative peak superimposed upon it, as shown in fig. 15–31.

A parabolic component is added to this voltage in the familiar manner by means of *RC* networks in the grid circuit of the output stage PL 82. The actual voltage on the grid is shown by the oscillogram in fig. 15–32*a*. The shape of the parabolic voltage can be observed on the cathode resistor, as in fig. 15–32*b*, and the corresponding anode voltage is shown in *c*). To blank the flyback traces on the screen of the picture tube MW 36–44, the grid receives a pulse with the line frequency from the line output transformer as well as a pulse with the frame frequency from the anode of the blocking oscillator triode section of the ECL 80. The "time expanded" oscillograms of the pulse trains in fig. 15–33 represent the waveform of these voltages on g_1 of the picture tube in the vicinity of the vertical blanking pulse. It can clearly be seen that the vertical blanking of both fields occurs in phase, whereas the line blanking, as desired, is displaced by a distance of half the spacing between the pulses. (Compare also fig. 15–21*a*, *b* and *c*.)
The oscillograms reproduced in this chapter represent only an arbitrary selection from the most essential voltage waveforms in the television receiver. It scarcely needs to be repeated that a clear knowledge of these waveforms is of fundamental importance in television engineering.
For certain types of investigation an even more far-reaching insight into what takes place in a television receiver is possible by employing a time base expansion unit, with the aid of which the individual voltage components of the video signal can be clearly observed together with all the pulse-shaping processes during any given cycles of the line frequency.

"Time expanded" oscillograms compared with selected lines of the picture.

When observing normal oscillograms which show the composite signal during one or more cycles of line deflection (figs. 15–4*b*, 15–6*b* and *c*, and 15–7*c*) it is usual to speak of "line patterns". It should always be remembered, however, that what one sees is the sum of the voltages of *all* 625 lines of both fields during the time of perception or during the time taken to record the oscillogram. This produces the well-known "veil" between the line pulses, which fluctuates with the instantaneous values of the video signal voltages or move in a horizontal direction. In this way the sideways movement of an object in the television receiver can be recognized in an oscillogram of the horizontal deflection (line) cycles.
However, using a time base expansion unit to produce a greatly expanded oscillogram in the rhythm of the frame frequency, a single curve can be observed which represents the actual voltage waveform of the signal-pulse composition during only one cycle of the line frequency. With a moving scene the voltage curve will, of course, vary in amplitude according to the variations in brightness, and will also move horizontally, corresponding to the sideways movements of the bright or dark patches. Nevertheless there will always be single lines only. When the picture is stationary as, for instance, with a test pattern, the oscillogram will naturally also be stationary. Moreover, if at the same time the appropriate lines in the receiver picture are brightened by an intensity-modulating pulse from the time base expansion

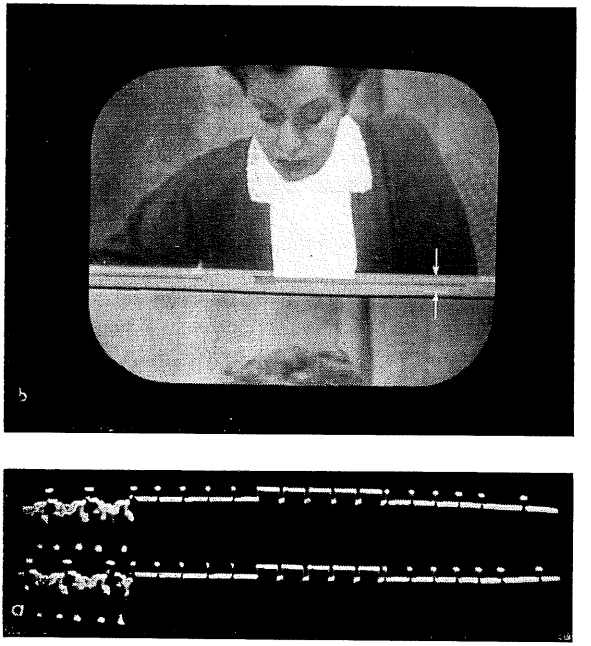

Fig. 15–34. Receiver picture *b*) together with expanded oscillogram *a*) at the beginning of vertical blanking.

unit, as described in detail in chapter 4, pages 77 et seq., an extraordinarily clear and useful means of comparing oscillograms with picture becomes available. The following figs. 15–34, 35, 36, 37, 39 and 40 illustrate the possibilities offered by this method. They were recorded during normal reception of the test pattern broadcast by the West Berlin television transmitter.

The voltage fed to the vertical amplifier of the oscilloscope was taken respectively from the anode of the video output stage PL 83 and from the cathode of the picture tube MW 36–44 in a Philips television receiver, type TD 1422A.

Fig. 15–34*a* shows a double oscillogram, expanded over some twelve cycles of the line frequency, with the frame sync pulse at the beginning of the vertical blanking. The corresponding picture on the receiver is reproduced in 15–34*b* with the frame frequency adjusted in such a way as to make visible on the receiver screen the gap in the picture during vertical blanking. (See also fig. 4–41*b*.)

The intensity modulation makes clearly apparent that the section under observation ends within the vertically blanked gap, indicated by arrows in 15–34*b*.)

In fig. 15–35*a* a double oscillogram of some five cycles of the line frequency is observed in conjunction with a test pattern on the picture screen. Fig. 15–35*b* reveals that the oscillogram corresponds to the lines at the transition point from the simple alternation of black and white squares to those squares which are further subdivided for test purposes. The pulse train during the first five line-cycles (in the oscillograms *both* fields counted from the left) shows in its essentials only the regular rectangular voltages corresponding to the black-white alternations of the large squares. In the fifth cycle, however, at the point marked with an arrow, the voltage form that produces the smaller squares is already visible. In the following cycles the amplitudes of this voltage increase in accordance with the further lines of the scan.

In this case the time base expansion is not sufficient to show the details of

these voltage forms. On the other hand, the extreme expansions along the time axis obtained with a type GM 4584 time base expansion unit allow a clear insight into voltage waveforms of less than half a picture-line in width. Thus, with the same test pattern in fig. 15–36, we can now investigate the voltage form of the line which passes over the centre of the small squares, through the 200 lines fan and through the figures 2, 0, 0. Comparing the oscillogram in fig. 15–36*b* with the brightened line in the test pattern, we can easily distinguish the connection between the black-white alternations and the upper part of the oscillogram. The voltage fluctuations for scanning the small squares are now quite easy to follow. In those parts of the oscillogram that show the 200 lines fan, or that scan the number "200", it can be seen, it is true, that they no longer represent 100% modulation of the video signal. Experiments have proved that this fact is neither to be attributed to excessive frequency-dependence of the receiver nor to a too low upper frequency limit of the oscilloscope. Identical oscillograms were obtained even when using an especially well-tuned receiver in conjunction with a type GM 5660 oscilloscope having an upper frequency limit of 10 Mc/s. [2]

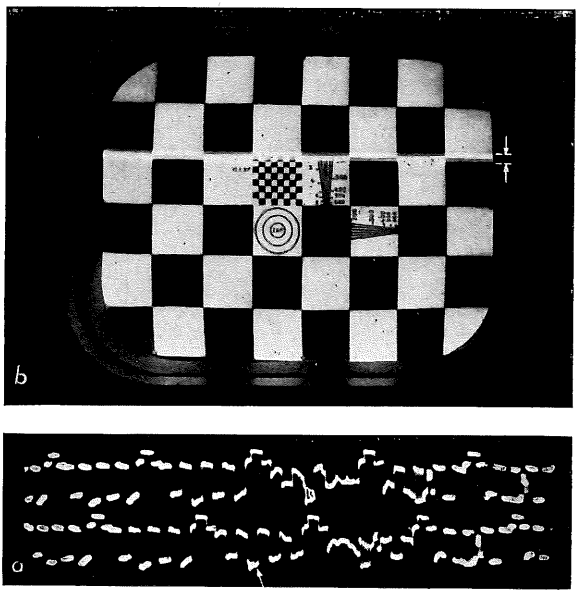

Fig. 15–35. Test pattern *b*) with oscillogram *a*) of five intensity-modulated lines of both fields.

In fig. 15–36, the expanded oscillogram in *b*) is compared with a normal oscillogram in *a*) with the line frequency periodically expanded. To ensure that the line pulse for this comparison started definitely at the left-hand edge of the picture, the time base generator of GM 5660 was not synchronized in

[2] When assessing these oscillograms, as also those in figs. 15–37*a* and 15–39*a*, it must be remembered that they can only correspond to the usual conditions during practical television reception. They naturally differ from oscillograms recorded in short-circuit operation from a dia-scanner or from a monoscope installation [5] [6]. Practical experience nevertheless shows that satisfactory pictures can be obtained by efficiently regulating the basic brightness and contrast in conjunction with the gradation characteristic of the TV screen. Closer examination of the test pattern in fig. 15–36*c* and particularly in fig. 15–37*b* reveals that the black parts of the fans are not quite so dark as the squares. Similarly, the intermediate spaces of the fans are not so white as the white squares. The oscillograms make this quite understandable.

the normal way but *triggered* by the line pulse. Since these oscillograms are approximately as wide as the receiver picture the corresponding sections along the horizontal axis can be directly compared.

Figs. 15–37 and 15–39 are intended to demonstrate the possibilities as well as the limitations of extreme time base expansion. It should first of all be pointed out that oscillograms of this kind are faint, so that their deficiency of light must be compensated by particularly favourable conditions during photographic recording. These oscillograms (figs. 15–37*a*, 15–39*a* and 15–40) were recorded with the following equipment:

Oscilloscope:	Philips "GM 5654"
Time base expansion unit:	Philips "GM 4584"
Cathode ray tube:	DB 10–6 (blue fluorescent screen) (Anode voltage: $V_k = -1.2$ kV, $V_{a2} = +2$ kV)
Camera:	Tenax II (lens Sonnar 1 : 2) maximum aperture. (Scale of picture 4 : 1. Exposure time: $^1/_{10}$ sec.)
Film:	$^{21}/_{10}°$ DIN Pan.
Developer:	Rapid (Gevaert 230, X-ray developer)
Enlargement paper:	Silver bromide – extra hard.

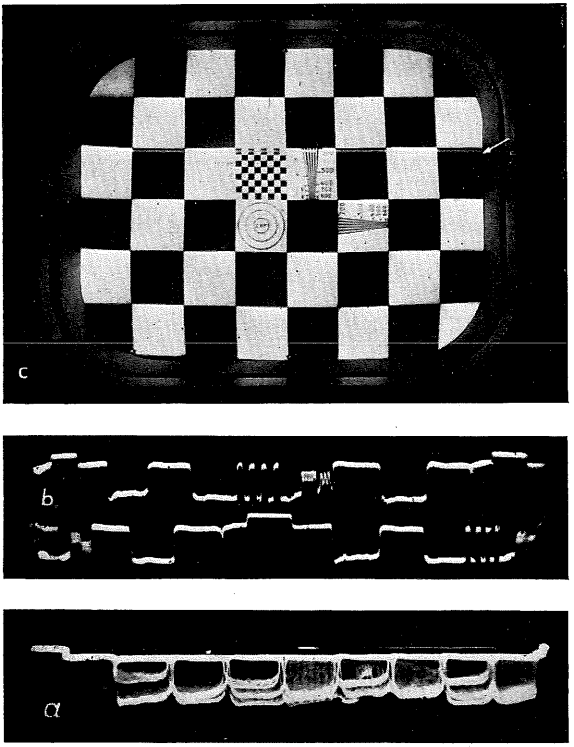

Fig. 15–36. Test pattern *c*) with oscillogram *b*) of one line each of both fields; *a*) normal oscillogram during one line deflection.

The oscillogram in fig. 15–37*a* shows the voltage waveform during less than half a picture line of both fields, while in fig. 15–37*b* can be seen the relevant section of the pattern on the TV screen. It can now be observed distinctly that the voltage alternations corresponding to the small squares are still quite rectangular, and the scanning of the 200 lines fan and the numbers 2, 0, 0 is far clearer than in fig. 15–36*b*.

The sync pulse and its surroundings are shown likewise expanded in the oscillogram of the second field, which clearly reveals the difference between black and blanking level. A similar section is given in fig. 15–39 of a test pattern from the West German Bundespost transmitter (fig. 15–38)

together with an oscillogram of the voltages which modulate the line selected. Here again, the connection between the oscillogram and the black-white alternations of the receiver picture can be followed quite distinctly [2]. It can be seen that there is 100% white to black level modulation of the 1 Mc/s bars. The pulses pertaining to the number "1" and to the cross-over points of the letters "M", "H" and "z" do not, however, reach the black level, but then they correspond to a rectangular voltage of 3 Mc/s. Fig. 15–40 shows for the purpose of comparison with fig. 15–37 the expanded oscillogram of the same line, but this time under more difficult transmission conditions. It is evident that in this case overshoot takes place after each rise of voltage, which adversely affects the edge resolution of the waveforms.

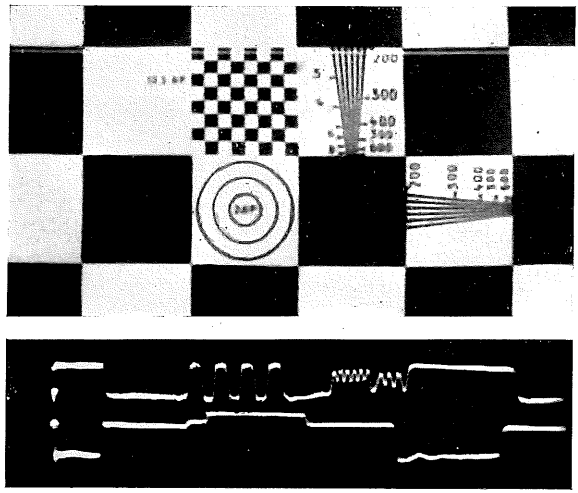

Fig. 15–37. Oscillogram *a*) with section of test pattern *b*) of fig. 15–36*c*), showing maximum time base expansion.

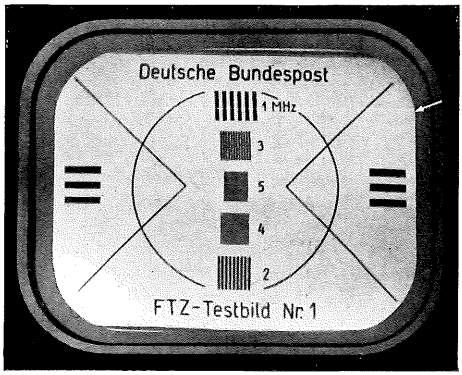

Fig. 15–38. Test pattern of German Bundespost transmitter.

These oscillograms, and particularly those in figs. 15–37*a*, 15–39*a* and 15–40 are intended not only to demonstrate the possible applications of the oscilloscope in television engineering and servicing but also to stress that it is possible by these means to study clearly, objectively and critically all transmission processes in television, whether in new plants or in actual operation.

[3] Small differences in the oscillograms, especially at the beginning, may be attributed to a certain non-linearity of the time base voltage due to the extreme time base expansion, which exceeds the value indicated in the catalogue for the type GM 4584 time base expansion un.t. Small non-linearities of this kind at the beginning of the sawtooth sweep are typical of the transitron circuit. For exact measurements one can, of course, use one of the time-marking methods already described, e.g. intensity modulation with either 1 Mc/s or 10 Mc/s.

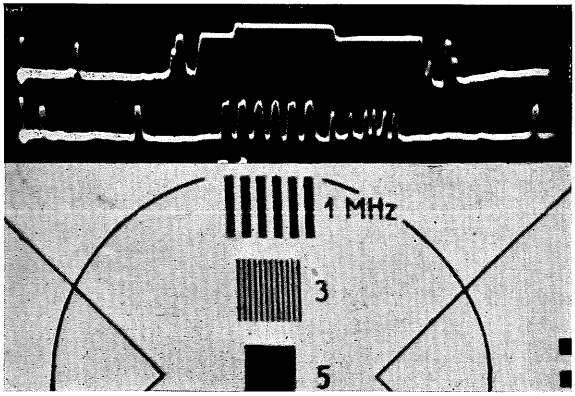

Fig. 15–39. Maximum "time expanded" oscillogram, with corresponding section of test pattern in fig. 15–38.

Fig. 15–40. Oscillogram of test pattern in fig. 15–37*b*; as fig. 15–17*a*, but with inferior transmission quality.

16. Measuring the action of "between-lens" shutters

The growing popularity of synchronized flashlight photography has made it more important than ever before to have an exact knowledge of the action of camera shutters. Of the many existing methods for measuring the opening-time of camera shutters, the clearest and most accurate results are obtained by measurement with the cathode ray oscilloscope.

There are essentially two methods.

a) The shutter to be tested is built into a camera, with which a photograph is taken of the path traced on the screen of the oscilloscope by the spot travelling at a known speed.

b) The shutter is placed between a source of light and a photocell. During the opening of the shutter, light falls upon the photocell. This then delivers a proportional voltage which serves to deflect the spot in the vertical direction.
By simultaneously deflecting the spot in the horizontal direction with a voltage linear with time, the complete picture of the shutter-action versus time function appears on the oscilloscope screen.

Measuring the opening-time by direct recording of an oscillogram.

With the first of these methods the measurement will be more accurate the longer the line traced on the screen. The most convenient way with the means usually available in laboratories and testing stations is to produce a sinusoidal trace, [1] which can be done quite simply by applying the alternating voltage

of a beat-frequency oscillator to the vertical deflection plates. The 50 c/s mains voltage will be quite sufficient for shutter times between $^1/_5$ and $^1/_{100}$ sec., which are the most suitable for this method. The basic layout for the measurement is shown in fig. 16–1. The frequency of the time base generator is adjusted so that three to six cycles of the voltage on the Y plates appear on the screen, and made stationary by synchronization as specified in the instructions for using the oscilloscope.

The frequencies for the vertical and horizontal deflection must be chosen such that the duration of the whole pattern, and thus the reciprocal of the time base frequency, will be greater than the expected opening-time of the shutter. When the pattern is photographed with a camera containing the shutter being tested, the photo will not show the complete oscillogram; there will be a gap, and where this gap lies depends entirely upon the moments at which the shutter opens or shuts during the path of the spot. From the measuring frequency f_M and the number of cycles photographed N_M (including fractions of cycles, if any), the opening time T_O is given by:

$$T_O = \frac{N_M}{f_M} \qquad (16\text{–}1)$$

Fig. 16–2*a* shows an oscillogram recorded in this way. With a nominal opening time of $^1/_{25}$ sec., and a measuring frequency of 80 c/s, the number of cycles counted is $3^1/_4$, so that according to the formula (16–1) the actual opening time is 40.7 (40) ms, (the nominal time being included in brackets, as it will be

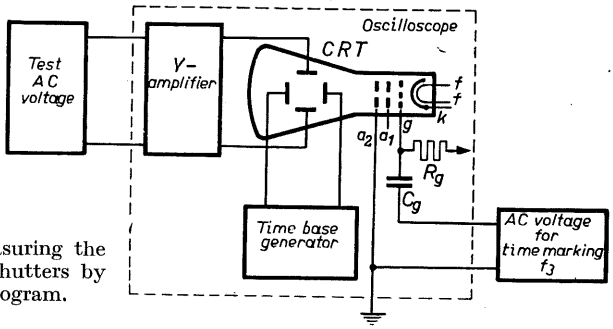

Fig. 16–1. Layout for measuring the opening time of camera shutters by direct recording of an oscillogram.

in the remainder of this chapter). It is clear from this recording that interpretation cannot be very accurate when simply using a sinusoidal voltage on the Y plates without time-marking. The speed of the spot is not constant since, of course, it follows the cosine function.

As we have already seen in chapter 10 on the applications of intensity modulation, it is possible in every oscilloscope to control the brightness of the trace by simply modulating the beam with an alternating voltage of known frequency. This results in a punctuated instead of a continuous trace. The interval between the dots appearing on the screen as a consequence of the time-marking frequency f_Z corresponds to the time T_Z, given by the reciprocal of this frequency:

$$T_Z = \frac{1}{f_Z} \qquad (16\text{–}2)$$

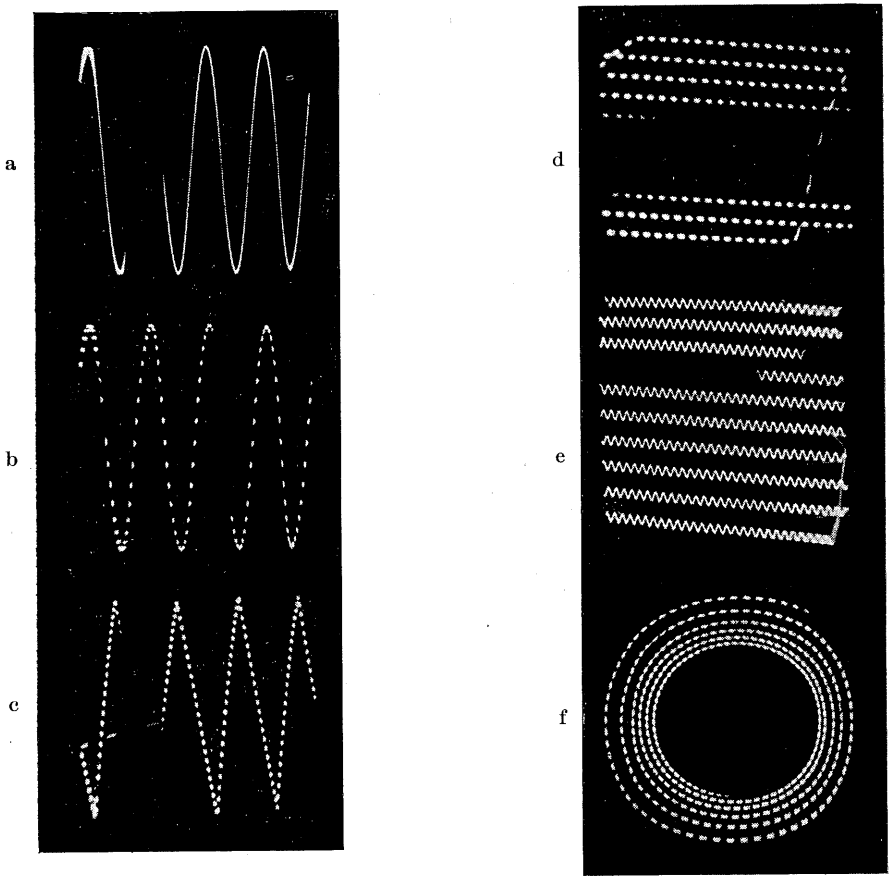

Fig. 16–2. Oscillograms for determining shutter times with traces of known duration.

In the example reproduced in fig. 16–2*b*, the measuring frequency is 50 c/s and the time-marking frequency 1000 c/s. The shutter to be tested was set at $^1/_{10}$ s, corresponding to 100 ms. To interpret the pattern it is only necessary to count the number of dots recorded. The quotient of the number of dots D in the oscillogram and the time marking frequency f_Z (in kc/s) gives the actual opening-time T_O (in milliseconds), thus:

$$T_O = \frac{D}{f_Z} \qquad (16\text{–}3)$$

In the example selected we therefore find: $\frac{116}{1} = 116$ ms. An undesired property of a sinusoidal voltage for the vertical deflection is that the speed decreases at the peaks, where the time marking dots consequently crowd together, whereas in the rest of the oscillogram the dots are widely spaced. This sets a limit to the accuracy of the measurement, but this drawback can

be avoided by using a voltage with a linear rise and fall, that is to say, a voltage with a triangular waveform. Waveforms of this kind can be obtained by using electronic generators specially developed for the purpose. Usually, however, rectangular voltage sources will be available (electronic switch or a special square-wave generator, such as Philips' type GM 2314 or GM 2324). The triangular voltage can then be obtained quite simply by integration of a rectangular voltage. The simplest way to do this is to use an *RC* network as shown in fig. 16–3. As a guide to the rating of such an integration circuit, it should be pointed out that $R \geqq 5 \cdot \frac{1}{\omega C}$, in which ω is equal to $2\pi f_M$.

Table 16 – I gives the appropriate values of R and C for the frequency ranges concerned. They are the values which were used for these recordings. The intended effect is obtained only when the condenser has a quality grading of *I*.

Fig. 16–3.
RC network for electrical integration of rectangular to triangular voltages.

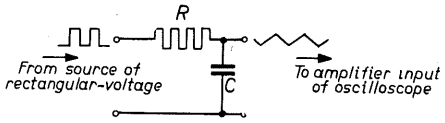

Table 16–I
Rating of the integration circuit
(fig. 16–3)

Frequency Range (c/s)	R (MΩ)	C
5.....50	3.0	0.1 μF
50....250	3.0	0.025 μF
250....750	1.0	0.010 μF
750...2000	1.0	0.002 μF

The condenser and the leads to the vertical amplifier usually require electrostatic screening against the stray fields from the mains voltage, which are always present. This also applies to the condensers in the phase-shifting circuits for producing a spiral-shaped trace, which will be mentioned later in this chapter (fig. 16–5).

Fig. 16–2*c* shows the oscillogram of a triangular voltage recorded in this way. What particularly stands out in comparison with fig. 16–2*b* is the spacing of the dots, 155 of which can be counted, without any crowding at the peaks. For this test the exposure time was adjusted to $^1/_{50}$ sec. = 20 ms and the time-marking frequency was 8.4 kc/s. According to (16–3) the opening-time was therefore: $\frac{155}{8.4} = 18.5$ ms.

To obtain a long trace it is possible, with simple means, to produce a raster-shaped oscillogram, similar to a television picture. To do this, sawtooth voltages are applied to both pairs of deflection plates in the cathode ray tube. The ordinary time base generator will of course be used for the horizontal deflection. For the vertical deflection a second sawtooth voltage generator is required. If another oscilloscope is available when this measurement is being made, the

necessary voltage can be taken from its sawtooth generator. Its frequency must be adjusted so that the duration of the pattern is again somewhat larger than the expected opening-time of the shutter. (The frequencies for the two directions of deflection can also be changed over, so that vertical instead of horizontal lines appear.) The time base generator with the lower (frame) frequency is synchronized with the "line" frequency to keep the lines stationary on the screen.

An oscillogram of this kind is shown in fig. 16–2*d*. The exposure time adjusted for this recording was $^1/_{100}$ s = 10 ms and the number of dots counted was 153. With a time-marking frequency of 12.5 kc/s, the opening time is therefore: $\frac{153}{12.5} = 12^1/_3$ ms.

When time-marking by brightness modulation of the trace is not possible or, for some reason or another, is not desirable, the time marking voltage can also be used for additional deflection of the spot. When properly adjusted it

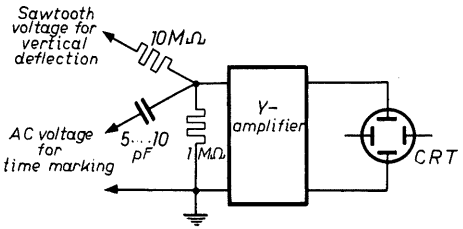

Fig. 16–4.
Addition of a sinusoidal voltage for time-marking in the oscillograms in figs. 16–2*e* and 16–6.

creates a ripple over the trace on the screen. The distance between the peaks of what is usually a sinusoidal voltage again corresponds, according to (16–2), to the time $T_Z = \frac{1}{f_Z}$. The pulsed voltages from time markers can be used in the same way. For the typical oscillogram reproduced in fig. 16–2*e*, the voltage of a beat-frequency oscillator (Philips' type GM 2308) was applied together with the voltage for the vertical deflection to the input of the vertical amplifier. The basic arrangement is shown in fig. 16–4. To avoid reaction, both voltages are fed in together over high impedances. The small condenser of about 6 pF for the time-marking voltage can, of course, always be replaced by a high ohmic resistor with an appropriate value. For this oscillogram the alternating voltage for the time-marking was 2,500 c/s and the adjusted exposure $^1/_{10}$ s = 100 ms. The count showed the cycles of the time-marking frequency to be 276 and thus the opening-time T_O is 110 ms. In patterns with sinusoidal or triangular vertical deflection voltages it is expedient, for additional horizontal movement of the spot, to add the time-marking voltage to the time base voltage of the oscilloscope. Connection must then always be made via a small coupling capacitor to keep possible *DC* voltages at this point in the oscilloscope away from the *AC* voltage source for the time marking.

In order to get the longest possible oscillogram on the circular screen it is obviously convenient to produce a circular trace, in the manner previously described. The idea of a circular trace can be further developed into a spiral-

shaped oscillogram, many times longer than the circumference of the largest possible circular trace. For this purpose, the damped oscillation of an oscillating circuit excited by a periodic voltage pulse is applied to one pair of plates via an *RC* element so as to give it a phase shift of —45°. The same voltage is

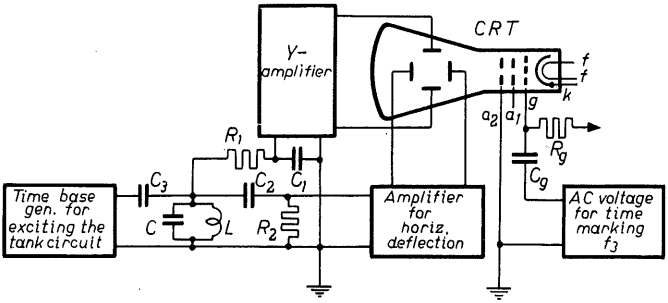

Fig. 16–5. Layout for producing a spiral-shaped oscillogram (fig. 16–2*f*).

applied to the other pair of plates via a *CR* element and shifted +45° in phase, so that between the two voltages there is a phase difference of 90°. When the deflections in both directions are equally matched, the voltage pulse produces a regular logarithmic spiral on the screen [2] [3]. The time base generator in the oscilloscope can be used to excite the oscillating circuit, but its voltage must not lie on the deflection plates. These receive only the phase-shifted voltage from the *LC* circuit, as in the layout shown in fig. 16–5. The resultant periodic pulses form a stationary pattern of the spiral.

Here again, time-marking is introduced by intensity modulation, giving a pattern on the screen as exemplified in fig. 16–2*f*. The exposure time for this recording was $^1/_{25}$ s = 40 ms, and with a time-marking frequency of 10 kc/s, 371 dots were counted. (The trace described on the screen was altogether about 60 cm long.) The opening-time of the shutter was, therefore:

$$\frac{371}{10} = 37.1 \text{ ms}.$$

The oscillogram in fig. 16–6 was obtained by the method described for fig. 16–2*e*. The exposure time was $^1/_{200}$ s with a time-marking frequency of 15 kc/s. It can be seen that it is now rather difficult to count the opening-time, since the beginning and end of the oscillogram are not sharply defined. This is due to the fact that the opening and closing times of the shutter are no longer negligibly short in relation to the "open time". When this happens, the trace appears gradually instead of suddenly, so that one is in doubt as to where to start and stop counting for the actual "open time".

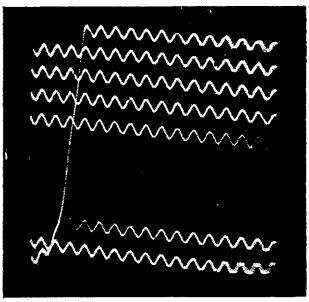

Fig. 16–6. Oscillogram as in fig. 16–2*e*, but for $^1/_{200}$ sec.

From this oscillogram the shutter time might be estimated at 6.5 ms (5.0 ms). For investigating

short opening-times it is better, therefore, to employ the method *b*) mentioned at the beginning of this chapter, as it furnishes a clear picture of the whole process.

Measuring the action of the shutter with a light source and a photocell.

The layout required for this measurement is represented in fig. 16–7. The shutter is arranged between a light source and a photocell. When the shutter is opened, light falls upon the photocell and the photo-electric current thereby produced causes a proportional voltage drop on the anode resistor R_a. This voltage is then used, after passing through a *DC* amplifier, for vertically deflecting the spot.
Since it is a non-recurring phenomenon that has to be recorded it is necessary

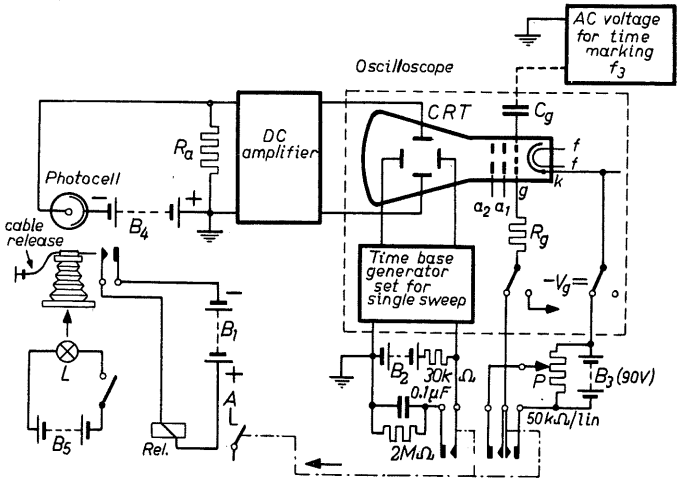

Fig. 16–7. Layout for recording the opening-time with a light source and a photocell.

to use a single-stroke time-base deflection as described in the directions for use of the oscilloscope. To avoid premature exposure by the quiescent spot of light, it must either be deflected beyond the area of the screen or, as indicated in fig. 16–7, the beam must be blocked by the negative voltage of a dry battery B_3. (No battery is required if a Philips oscilloscope type GM 5653 is employed.) Using the GM 3156 oscilloscope for this measurement, the single-stroke time base is triggered by short-circuiting terminals 3 and 4. In the layout in fig. 16–7 this is not done directly, but via a condenser of 0.1 μF which is shunted, to enable it to discharge, by a resistor of 2 MΩ. After the various contacts of the relay have been properly adjusted, then, upon the cable release being depressed, the armature "A" is actuated, whereupon the spot is released, the single time-base starts, the shutter opens and the opening process is recorded.

Fig. 16–8 shows an oscillogram obtained in this way of a between-lens shutter at an opening-time of $^1/_5$ sec. The time-marking used in this case is a second oscillogram of a voltage with a frequency of 100 c/s, recorded below the pattern of the opening-process. Interpretation shows the opening-time to be 190 (200) ms. Of course, time marking can also be effected with this method by modulating the brightness of the trace with an alternating voltage of known frequency, as already described (fig. 16–2*b*, *c*, *d* and *f*). This possibility is also indicated in fig. 16–7.

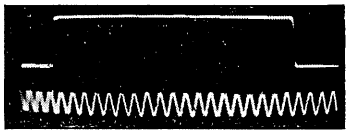

Fig. 16–8. Oscillogram of the action of a camera shutter for $^1/_5$ s. Time-marking frequency: 100 c/s.

Two further oscillograms are reproduced in fig. 16–9 which were recorded on a miniature camera for times of $^1/_{250}$ s and $^1/_{500}$ s respectively. It should be noted that the opening-time indicated represents the mean value. This means that to assess the shorter times the points were counted from half the height of the oscillogram. The values for the "open time" (shutter fully open) lie in the region of 3.4 and 2.2 ms respectively. The mean opening-time in this case was 4.2 (4.0) and 2.85 (2.0) ms respectively.

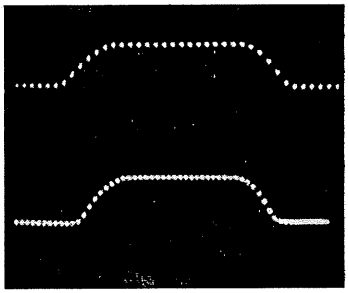

Fig. 16–9. Opening-time curve of shutter in a miniature camera: above: $^1/_{250}$ s. $f_Z = 5000$ c/s. $T_0 = 4.2$ ms (mean); below: $^1/_{500}$ s. $f_Z = 10{,}000$ c/s. $T_0 = 2.8$ ms (mean).

In the first method described in this chapter (figs 16–2 and 16–6) cathode ray tubes with the shortest possible afterglow are required, as, for example, Philips' types DB 10–5, DB 10–6 or DB 13–2. In the second method, on the other hand, it is advantageous to use tubes with long persistence screens so that the non-recurring phenomena will remain visible for a while after its occurrence. Suitable tubes are Philips' types DR 10–5, DR 10–6 or DR 13–2. On the extremely long-persistence tube, type DP 10–6, the trace remains fluorescent, even after 80 seconds with $^1/_{1000}$ of the original intensity of luminescence. This value is amply sufficient to allow good observation of the waveform. To avoid glare from the bright spot of light during the measurement it is advisable to fit an orange-yellow filter over the screen.

Employing long-persistence tubes of this kind, working observations can be carried out without the necessity of photographic recording.

17. Recording the waveforms of the luminous flux and ignition current of flash-bulbs

Importance of knowing the behaviour of the luminous flux.

In contrast to the eye, which reacts to the radiant *output*, a photographic emulsion reacts to the *work performed* by the light. For the eye, only the intensity is important. The photographic emulsion, on the other hand, accumulates the effect of radiant energy over a period of time; the film density corresponds, therefore, to the product of luminous intensity and time—the work done by the light.
By daylight and incandescent light it is possible, by adjusting the exposure time, to determine the amount of work to be performed by the light. With flashlight the situation is different. Here the maximum exposure time is predetermined by the burning time of the material within the flash-bulb and by the course of its burning. This applies equally to the "open-flash" process as to synchronized flashlight photography with "*X*" contacts and, subject to certain limitations, with "*M*" contacts.
Only with a cathode ray oscilloscope is it possible to get a true picture of the behaviour of the luminous flux in flashlight photography and thus of the amount of luminous work available. The oscillogram can again be provided with time markings at any characteristic points of the curve.

Recording the luminous flux.

The layout for the measurement is fundamentally the same as that given in fig. 16–7. In place of the shutter, the flash-bulb is now arranged near the photocell, preferably at a distance of just over three feet, and a grey filter used, to avoid overloading the photocell or the amplifier. The release contacts are adjusted in such a way that the electron beam is released before the flash and then the time-base started. A *DC* amplifier is again required to amplify the photocell voltage to the value needed for satisfactory deflection of the spot. Using this arrangement, the luminous flux versus time curves of Philips' Photoflux

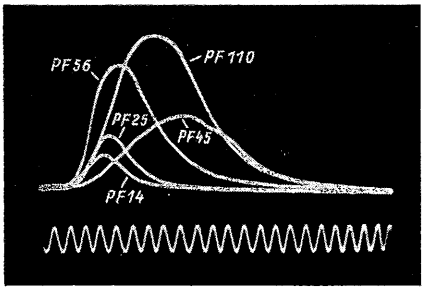

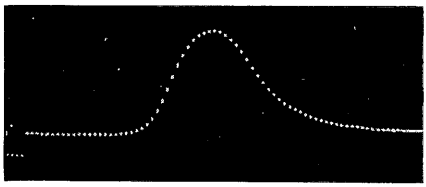

Fig. 17–2. Luminous flux waveform of Photoflux Lamp PF 3N. Time-marking by intensity modulation: 2000 c/s.

Fig. 17–1. Luminous flux waveforms of different flash-bulbs. Time-marking: 200 c/s = 5 ms

lamps PF 14, PF 25, PF 45, PF 56 and PF 110 were recorded one above the other on a single photograph as shown in fig. 17–1. Time marking is again provided by further recording below the oscillogram the pattern of a sinusoidal voltage of 200 c/s, naturally with the same expansion along the time axis. The distance between the peaks corresponds to 5 milliseconds. This method of presentation allows good comparison of the individual lamps, but it should be borne in mind that oscillograms of this sort only reproduce what happens to be the characteristic of the particular example. To make a general assessment, the usual manufacturing deviations must be taken into account. They must not be confused with the curves published by the makers, which represent the average values measured over large series of production samples.

The oscillogram in fig. 17–2 represents the luminous flux of the small PF 3N flash-bulb; in this case, brightness modulation of the trace has been used for time marking. To judge the behaviour of the flux curve in flashlight photography it is important to have an exact marking of the moment at which the bulb is switched on for ignition. It is obtained by taking a portion of the ignition voltage from the igniting battery and feeding it over a high-value resistor to the grid of the input valve in the vertical amplifier. The resulting voltage division depends on the ratio of the series resistor to

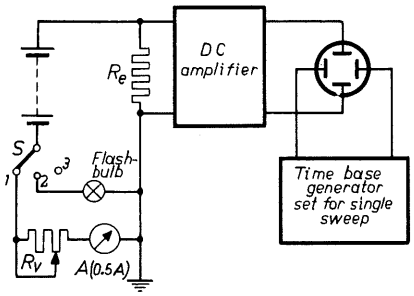

Fig. 17–4. Layout for the display of ignition current waveforms.

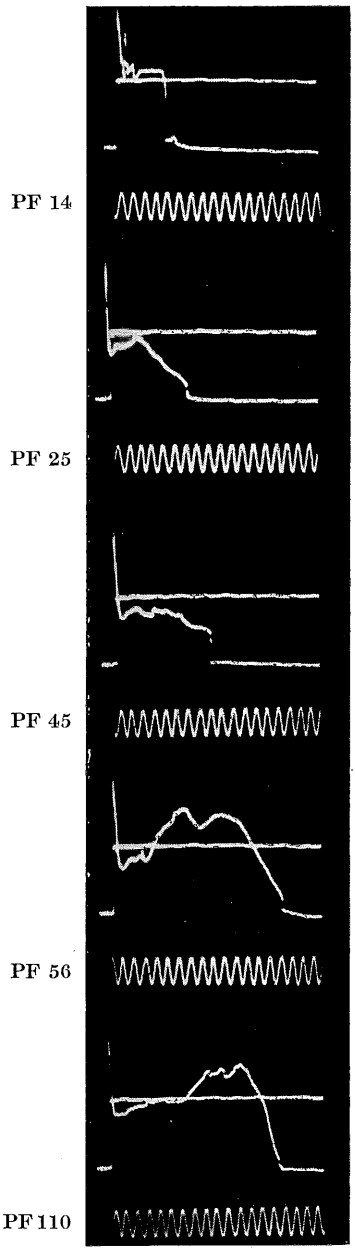

Fig. 17–3. Oscillograms of ignition current in flash-bulbs. Time-marking: 200 c/s.

the grid resistor, and it must be such that the oscillogram is vertically displaced by an amount sufficient to allow clear interpretation, The significant times can be obtained by counting the dots from this "threshold" ($f_Z = 2000$ c/s). In this case, for example, the ignition time is $t_{ign} = 14^1/_4$ ms, the peak time $t_p = 18^1/_2$ ms, and the light emission time $t_l = 8^3/_4$ ms.
It need hardly be stressed that care must be taken during the measurement to prevent the flashlight from falling, directly or indirectly, upon the screen of the cathode ray tube. This would completely blank out the oscillogram. For continuous recordings it is safest to install the oscilloscope in an adjoining room.
To obtain the correct conditions for ignition it is important to know the value of ignition current required, or the electrical work in watt-seconds needed for ignition. This information is clearly provided by the oscillogram of the ignition current during the time of switching on.

Recording the waveform of the ignition current.

The basic layout for this measurement is represented in fig. 17–4. Reference should also be made to the remarks on the layout in fig. 16–7. Ignition is caused by four nickel-iron accumulator cells which supply a voltage of about 3.3 V. A resistor R_e of 0.5 Ω is connected in the ignition circuit, across which a voltage linearly proportional to the current appears. The voltage is passed through the *DC* amplifier and applied to the *Y* plates for vertical deflection. Resistor R_e increases at the same time as the internal resistance of the voltage source, so that the ignition conditions resemble those for ignition with dry batteries. To assess the current intensity from the vertical deflection a calibration current is provided by changing-over switch *S* to position 1 and adjusting ammeter "*A*" with R_v to 0.5 A.
The displaced zero line resulting from this is recorded separately and added to the oscillogram. In this way information is also given on the absolute peak of the current surge. Fig. 17–3 shows a representative selection from a large series of oscillograms recorded in this manner, the waveforms being characteristic of Photoflux lamps PF 14, PF 25, PF 45, PF 56 and PF 110 respectively. The horizontal line near the centre of the pictures is the 0.5 A current marking. At the moment of switching on, when the internal resistance of the bulb in its cold state is only about 1 ohm, a steep current surge of over 1 amp appears. This, however, very rapidly declines and remains at a value of approximately 0.5 A for a certain time, which varies according to the size of the individual types of bulb.
In view of the steep portions of these curves, time marking by intensity-modulation was dispensed with, and instead, a third oscillogram of a 200 c/s sinusoidal voltage was recorded beneath the waveform under investigation. The time marking corresponds to 5 milliseconds. Here again it should be stressed that these recordings are not to be judged as manufacturers' mean values but only as the results which happened to be ascertained on single examples.
The burning-times that can be read from these oscillograms for PF 14, PF 25, PF 45, PF 56 and PF 110 are: 23, 32.5, 42.5, 80 and 72.5 ms respectively. Assuming that the voltage on the lamp during ignition was approximately

3.0 V, the electrical work required for the ignition can be calculated from the oscillograms as: 38, 32, 36, 144 and 122 mWs respectively.

18. Investigations on flash-bulb synchronizers

To examine the action of synchronizer contacts an oscillogram is generally sufficient which shows the beginning of the contact process marked upon the curve representing the action of the camera shutter. This can be simply achieved by arranging for the synchronizer contact to create, via a small condenser, a connection between the input of the vertical amplifier, which amplifies the voltage from the photocell, and a direct voltage source of a few volts. If the other pole of the voltage source is connected to the casing of the camera, the surge by the charging current of the condenser appears on the oscillogram as a peak or blip when contact is made. In all other respects the layout used is fundamentally the same as in fig. 16–7.

The oscillogram in fig. 18–1*a* is the result of testing the "*X*" contact of the between-lens shutter in a 6×6 camera; the time marking voltage used was 500 c/s. The moment at which the "*X*" contact closes coincides with the beginning of the peak in the curve of the shutter opening-time and is marked by a downward blip. (The exposure time is $^1/_{25}$ s.) As expected, therefore, the contact closes only after the shutter is fully open.

Fig. 18–1*b* reproduces the enlarged luminous flux versus time curve of a PF 14 Photoflux lamp. The step at the beginning of this curve, the moment at which the synchronizer contact closes and the corresponding blip in the curve of the shutter opening-time all occur at the same time. The mean "open time" of the shutter embraces 21 cycles of the 500 c/s time-marking voltage, corresponding to 2×21 = 42 (40) ms. The peak time of 17 ms and the time of light emission—

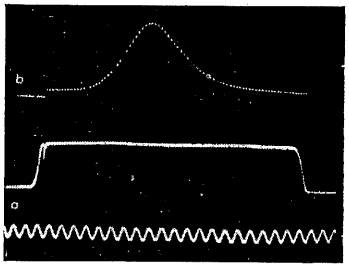

Fig. 18–1. Shutter-time curve for $^1/_{25}$ sec exposure, and luminous flux of type PF 14 flash-bulb with "blip" marking the beginning of ignition with "*X*" contact. Time-marking: 500 c/s = 2 ms.

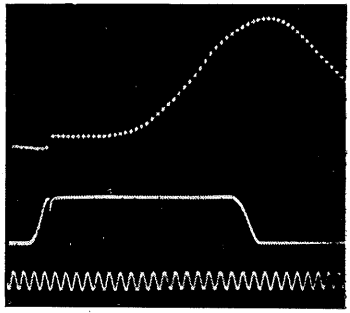

Fig. 18–2. Shutter-time curve for $^1/_{50}$ sec exposure, and luminous flux of type PF 25 flash-bulb synchronizing with "*X*" contact. Time-marking: 1000 c/s = 1 ms.

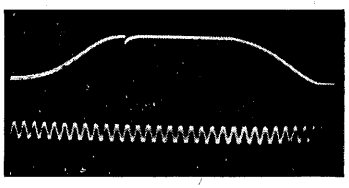

Fig. 18–3. Shutter-time oscillogram for $^1/_{500}$ sec, with "*X*" contact synchronization. Time marking: 5000 c/s = 0.2 ms.

11 ms both lie well within the open time of the shutter. This indicates that the total light is used when taking the photograph.
At an exposure of $^1/_{50}$ sec the situation is different. The relevant oscillograms are shown in fig. 18–2, with time marking in this instance of 1000 c/s. The moment at which the synchronizer contact closes after the shutter has opened can be recognized more distinctly. The mean "open time" is 19 (20) ms.
The luminous flux versus time curve of a PF 25 type flash-bulb, again enlarged corresponding to the time scale, is shown above the curve of the shutter opening-time. Its peak time of 21 ms and light emission of 15.5 ms are set against a shutter "open time" of only 17 ms. Since the flash-bulb does not reach its peak intensity until 21 ms after switching on, the shutter closes before half the available light has been made use of. The result will be a badly under-exposed negative. This is why, when using standard flash-bulbs of 16–20 ms peak time with *X* contacts, one is always advised never to work with exposure times shorter than $^1/_{25}$ sec.

It is of interest to the users of flash-tube apparatus to know exactly when the contact closes at even shorter exposures. Information on this is given in the oscillogram reproduced in fig. 18–3 for an exposure of $^1/_{500}$ sec with time marking of 5000 c/s corresponding to 0.2 ms. The results are: mean shutter opening-time 3.7 (2.0) ms, "open time" (shutter fully open) 2.2 (2.0) ms. After the synchronizer contact closes, the shutter remains open for nearly 2.0 ms. Since the emission time of flash-tube apparatus is only about $^1/_5$–$^1/_2$ ms, this "open time" is amply sufficient. The oscillograms reproduced in fig. 18–4 were recorded when testing the between-lens shutter of a miniature camera with an "*M*" contact. They represent exposures of $^1/_{25}$, $^1/_{50}$, $^1/_{100}$, $^1/_{250}$ and $^1/_{500}$ sec. respectively. The time-marking voltage is 500 c/s corresponding to 2 ms. The blip appearing when the "*M*" contact closes now occurs 16 ms *before* the shutter opens. The luminous flux versus time curve of a PF 14 flash-bulb has been arranged above these oscillograms in such a way that the marking for the moments of contact for flash-bulb and camera lie exactly one above the other. In this way it

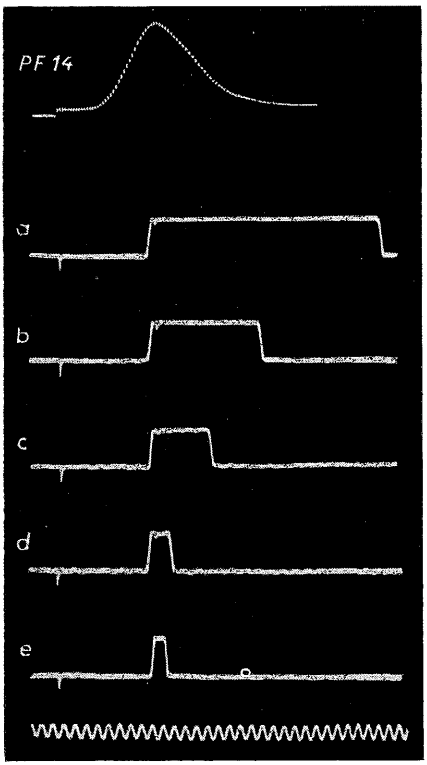

Fig. 18–4. Shutter-time curves with "*M*" contact synchronization and luminous flux of type PF 14 flash-bulb.

is possible to observe immediately the agreement of the peak time of $18^3/_4$ ms and the emission time of $12^1/_2$ ms with the shutter time of the camera.

Apart from the beginning of the moment of contact, it is also interesting to examine the total duration of the contact process. This process can be displayed on the oscilloscope by applying, instead of a pulse, an alternating voltage of suitably small amplitude and appropriate frequency through the synchronizer contact to the input of the vertical amplifier. The effect of this is that, during the time the contact is closed, a ripple is superimposed on the oscillogram of the shutter time. The peaks of this ripple represent a time marking corresponding to $1/fz$. Some typical oscillograms are reproduced in fig. 18–5 for the same exposure times as in fig. 18–4, but for this purpose enlarged to produce oscillograms expanded along the time axis. The frequency of the voltage used for marking the contact times has also been adapted to the different time base expansions. It can be seen from these recordings that the "X" contact also closes. This has no bearing on the ignition process, however, the flash-bulb having already been ignited by the "M"-contact.

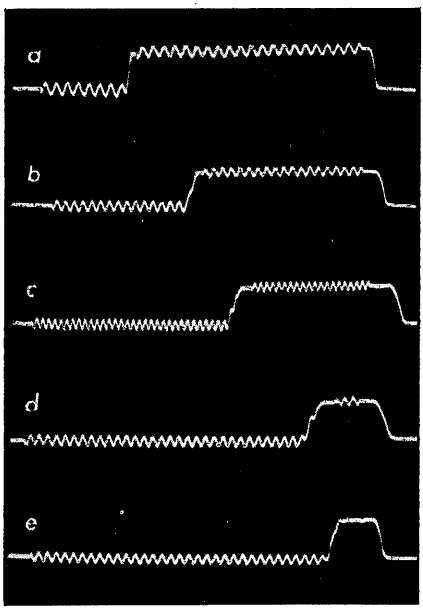

Fig. 18–5. Shutter-time oscillograms with superimposed ripple to mark the closed time of "M" and "X" contact.

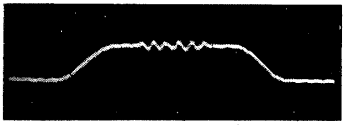

Fig. 18–6. Shutter-time curve for $^1/_{500}$ sec, with ripple to mark the closed time of "X" contact alone.

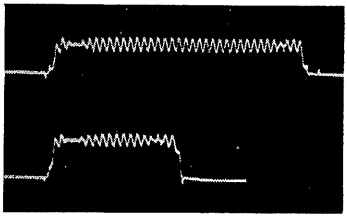

Fig. 18–7. Shutter-time curve with ripple to mark the closed time of an imperfectly working "X" contact. Above: $^1/_{25}$ sec. Below: $^1/_{50}$ sec.

Even at $^1/_{250}$ sec and $^1/_{500}$ sec, corresponding ripple is found at the peaks of the oscillograms, although not very distinctly at $^1/_{500}$ sec. Fig. 18–6 shows a greatly time-expanded oscillogram prepared especially for investigating the "X" con-

tact at a shutter time of $^1/_{500}$ sec with a time-marking frequency of 5000 c/s corresponding to 0.2 ms. It appears from this that the contact is closed for almost exactly 1 ms, which is quite sufficient when using a flash-tube apparatus. Contact is made in this case for approximately 0.6 ms after the shutter is fully open.

It is obvious that the time-marking for the contact process can also be used for interpreting the whole oscillogram of the shutter action. The deflection along the horizontal axis is, after all, linear with time, so that the time scale obtained in this way can be carried over to the whole pattern. The values ascertained from the oscillograms in figs. 18–5 and 18–6 are set out in the following table:

Table 18–I

Exposure	Opening-time	Time-marking
a) $^1/_{25}$ sec	45.2 (40) millisecs.	500 c/s
b) $^1/_{50}$,,	21.9 (20) ,,	1000 ,,
c) $^1/_{100}$,,	14.2 (10) ,, [1]	2000 ,,
d) $^1/_{250}$,,	4.2 (4) ,,	2000 ,,
e) $^1/_{500}$,,	2.8 (2) ,,	2000 ,,
$^1/_{500}$,,	2.85(2) ,,	5000 ,,

These examples show the variety of information that can be obtained from oscillograms of this kind on the action of synchronizer contacts.

In conclusion, fig. 18–7 presents two oscillograms for observing the contact times of an *X* contact subsequently built into a camera by hand. The shutter times are $^1/_{25}$ and $^1/_{50}$ sec respectively. They show clearly that the contact is interrupted shortly after the shutter opens and shortly before it closes. It is evident that the action of this contact bears no comparison with that of manufactured contacts in cameras of repute, as illustrated by the oscillograms in figs. 18–4 and 18–5.

19. Measuring the travel time in four-terminal networks and investigating line matching conditions with pulsed voltages

Methods of measurement.

The use of rectangular voltages for assessing the characteristics of electrical transmission systems has already been touched upon in chapter 11 (page 194). In the bibliography to that chapter the reader is also referred to numerous publications which deal with the subject comprehensively. For observing the voltage waveforms before and after a four terminal network (cable), use is

[1] This opening time was inadmissibly long. It should again be stressed that these oscillograms represent individual results only, obtained on cameras which happened to be at the disposal of the author. It is not the object of these observations to make a critical evaluation or comparison of the properties either of the camera shutters or of the flash-bulbs.

always made of a pulse oscilloscope driven by a square-wave generator. The oscillogram provides the required information with unique clarity and detail. Apart from the dynamic characteristics, other properties of four terminal networks can be investigated with a similar measuring arrangement.
It is important to know not only the form of the voltage at the exit of the network but also the travel or propagation time of the signal in a transmission system. The time needed by a signal to travel through the network can be ascertained quite simply and clearly with the aid of the oscilloscope.
All other methods provide the results only indirectly, which means that the measurement is seldom entirely reliable.
In the oscillographic method of determining the travel time, the time difference between the leading edge of the pulse at the beginning and end of the network is measured by rigidly synchronizing the oscilloscope with the pulse and using a specific time base expansion. This procedure also enables a very thorough study to be made of line-matching problems [1] [2].
With regard to the steadily increasing demands being made on the bandwidth and transmission quality of communication systems, such methods of measurement are gaining considerable importance. Although it is sometimes necessary for this purpose to use special generators for providing extremely short pulses, it is nevertheless quite sufficient for a great many such measurements to use a pulse with a half-value width of 0.2 μs, as supplied by Philips' type GM 2314 universal square-wave generator.
In the following, a simple layout will be described, and illustrated by oscillograms, to make clear the principles upon which these measurements are based.
Further oscillograms show the voltage trend with relatively long pulses under identical conditions.

Circuit.

The measurements described were carried out on a length of delay cable for which a travel time was specified of 1.9 μs/m. As cables of this kind are so constructed that, with a minimum of damping, the travel time of a pulse is several times longer than that in a normal cable, a short length serves the purpose. The pulse used was the approximately 0.2 μs (half-value width) voltage pulse from the type GM 2314 universal square-wave generator, which was fed via a separating stage with an E83F valve to the cable input, as shown in fig. 19–1. As a result of the negative pulses on the grid of this valve, the anode current drops accordingly and positive pulses appear at the anode and at the cable input directly connected with it [1].
With this separator valve it is possible to make the pulse-voltage source a very high resistance with regard to the cable input.
For these measurements the square-wave generator should be externally triggered by a control pulse-generator [2].

[1] The earth connection of the pulse-voltage source to the cathode is effected via the output capacitance C_{out} of the anode-voltage generator.
[2] Philips' type GM 5660 pulse oscilloscope contains a pulse-generator of this kind. The half-value width of the control pulse is approx. 1 μs, the rise-time approx. 0.1 μs.

The individual cycles of the time base are triggered in the oscilloscope in the same way [3].

For these oscillograms the pulse repetition frequency was about 2000 c/s; the patterns thus obtained are quite bright enough (post-acceleration voltage +2 kV). In the examples shown, the voltage trend was observed at the cable input, to which the vertical amplifier of the oscilloscope was accordingly connected [4].

By means of switch S_1 the cable input can either be left "open" or switched to a resistor of 2.7 kΩ corresponding to the characteristic impedance of the

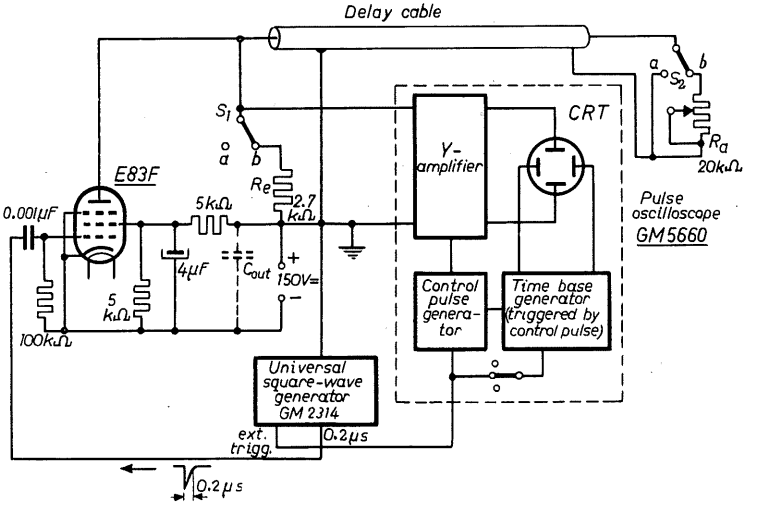

Fig. 19–1. Circuit for measuring the travel time and investigating the matching conditions in cables.

cable ($Z = 2.7$ kΩ). By means of switch S_2, the cable output can either be short-circuited (position "*a*") or switched to a variable resistor (position "*b*"). If this resistor is adjusted to 2.7 kΩ, the cable is then terminated by its characteristic impedance. If the resistor is adjusted to its maximum value (20 kΩ) the output end of the cable is then, for matching purposes, "open".

Results.

Some of the oscillograms obtained in this way are shown in figs. 19–2*a*, *b*, and *c* and 19–3. For the patterns in fig. 19–2, the cable input was matched to

[3] See fig. 4–39. By means of a delay network (not shown in this circuit) a time delay of about 0.25 μs is introduced between the triggering of the time base and the arrival of the control pulse, which in its turn triggers the pulse to the *Y* plates. Thus, a part of the zero line always appears before the pattern of the pulse is traced, and this appears in its entirety from the start.

[4] Rise-time of vertical amplifier 0.04 μs.

2.7 kΩ. For fig. 19–2*a* the switch was set at *b* at the cable end and the variable resistor set at 20 kΩ i.e. the cable end was, for practical purposes, "open". After the primary pulse *A* can be seen the reflected pulse *B*. From the time scale of 1 Mc/s in fig. 19–2*d* the travel time τ [5]—there and back—is found to be 3.3 μs. The travel time in one direction is thus 1.65 μs.

According to the specific nominal travel time, this gives a cable length of 0.87 m. If the resistor at the cable end is adjusted to the value of the characteristic impedance, the reflections disappear and an oscillogram is obtained as shown in fig. 19–2*b*.

With the cable end short-circuited, the reflected pulse is negative, as can be seen from fig. 19–2*c*. If the

[5] Measured at the base of the pulse at 10% of the maximum pulse height.

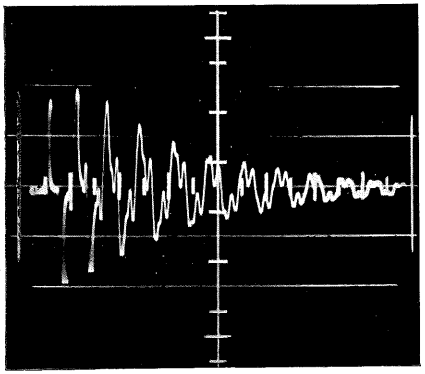

Fig. 19–3. Oscillogram with cable input open and output short-circuited.

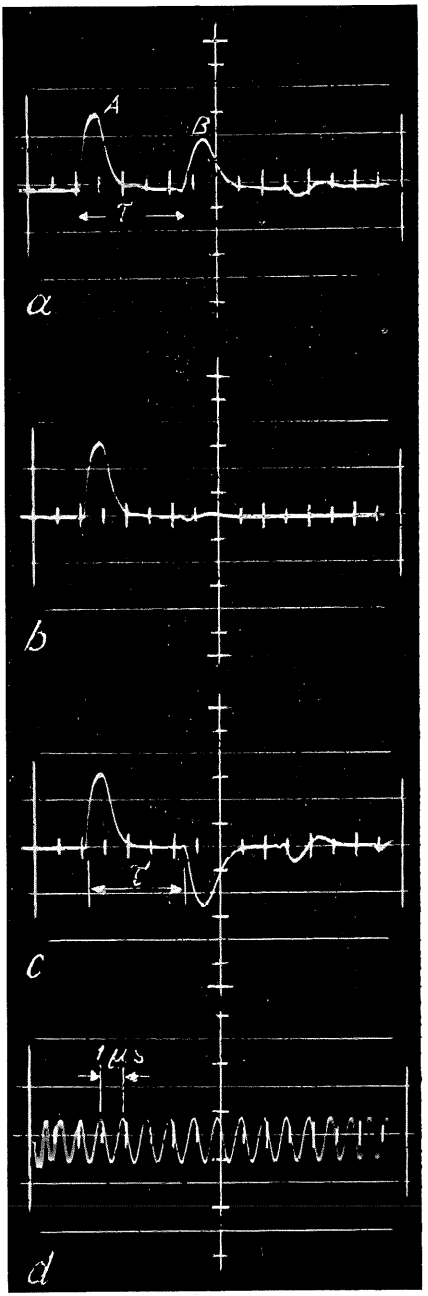

Fig. 19–2. Oscillograms for determining the travel time and matching conditions: *a*) end of cable open; *b*) end of cable terminated by characteristic impedance; *c*) end of cable short-circuited; *d*) time calibration: 1 Mc/s = 1 μs.

cable output is short-circuited but the input open, the reflected energy of the pulse swings to and fro until it is dissipated by the damping of the cable. Fig. 19–3 shows an oscillogram thus obtained. The time base of 1.6 μs/cm used for the oscillograms in fig. 19–2 was reduced in this case to 11 μs/cm in order to be able to observe the damping process as a whole.

Oscillograms with a relatively long rectangular pulse.

As explained in the foregoing, the pulses used for measuring the travel time in cables should be as short as possible. Their duration must be short in relation to the travel times to be ascertained in the object under test.

As soon as the pulse duration becomes equal to or longer than twice the travel time of the pulse (there and back) overlapping occurs of the input and reflected voltage. Obviously, conclusions can also be drawn from these oscillograms with regard to matching conditions and travel times. However, measuring arrangements of this kind are very frequently used in order, with suitably selected control pulses, to generate pulses of a desired shape using delay cables or networks and specific matching conditions. An example of just such a long, negative pulse is shown by the oscillogram in fig. 19–4*a*. From the time calibration of a 1 Mc/s circuit, recorded as a second oscillogram, the pulse duration is found to be 46 μs. This pulse generates in the same circuit as given in fig. 19–1 a correspondingly long positive pulse in the anode of valve E 83 F, which then appears at the cable input. If both switches, S_1 and S_2 are set in position *a*, the cable input will be open and the output short-circuited.

As shown in fig. 19–4*b*, there now arises at the cable output a negative pulse which, after twice the travel time, appears at the cable input. Since this is open, the pulse energy swings to and fro in this way for the whole duration of the input pulse, as can be seen in the oscillogram, after a short pulse, in fig. 19–3. At the end of the input pulse a similar line pulse is released, which swings to and fro in the same manner.

If the output resistance has a specific value (> 0, $< Z$) only a part of the voltage surge arriving will be reflected. It becomes superimposed on the input pulse, which now appears with a part of its amplitude, as the oscillogram in fig. 19–4*c* shows for an output resistance of 0.7 kΩ.

If the output resistance of the cable is identical with its characteristic impedance—in this case 2.7 kΩ—the reflections disappear. The picture of the pulse with full voltage amplitude is now ascertained at the input of the cable [6], as shown by the oscillogram in fig. 19–4*d*.

If the output resistance is several times larger than the characteristic impedance of the cable, and if the input resistance is high also, then a voltage surge will pass through the cable whose magnitude will correspond to that part of the input voltage which is due to the ratio of the characteristic impedance to the internal resistance of the voltage source (in this case the output resistance of valve E 83 F).

[6] The amplitude relationships shown in the various oscillograms are only approximately equivalent to those actually occurring. For better patterns it would be necessary to compensate for large voltage differences by correcting the amplification.

An example is given in fig. 19–5*a* for an output resistance of 10 kΩ. The surge coming from the end of the cable possesses the same polarity. Its voltage is again added to the voltage at the input after twice the travel time, thus forming the second step at the beginning of the oscillogram. As the input pulse still persists, a charge continues to flow in the cable which again causes an increase in voltage at the input after twice the travel time. The charging current always being determined by the difference between the input voltage and the voltage at the start of the cable at the same moment, steps are formed the mean values of which rise in accordance with an e-function.

The discharge of the cable at the end of the input pulse takes place in a similar way. After twice the travel time the charge falls in each case by a certain amount.

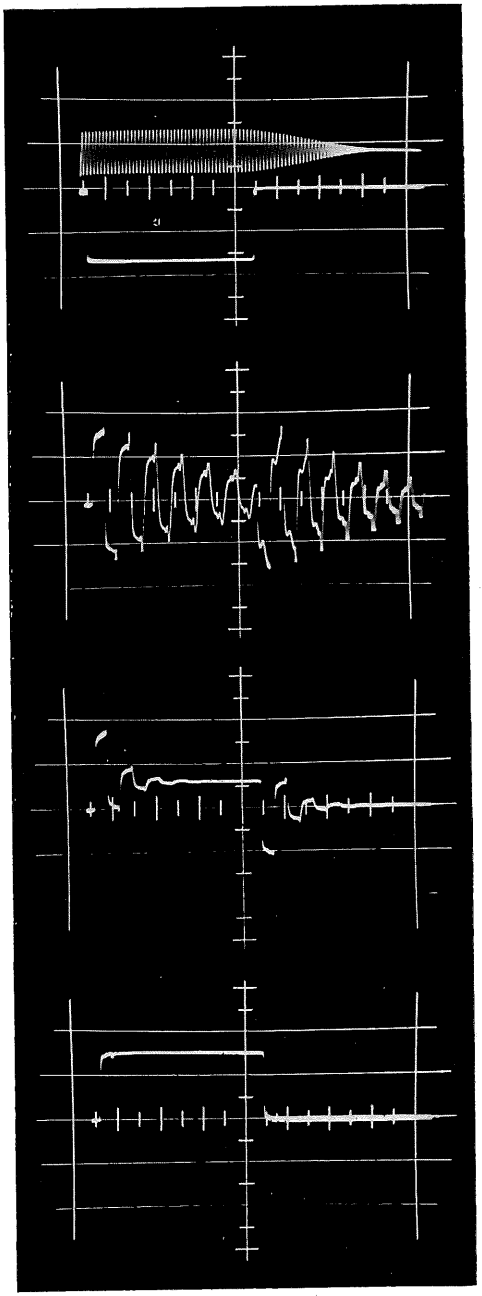

Fig. 19–4. Voltage waveform at cable input with a 46 μs rectangular pulse: *a*) negative rectangular pulse from generator and 1 Mc/s time-marking; *b*) cable input open, cable output short-circuited; *c*) cable input open, output resistance 0.7 kΩ; *d*) cable input open, output resistance $R_{out} = Z = 2.7$ kΩ.

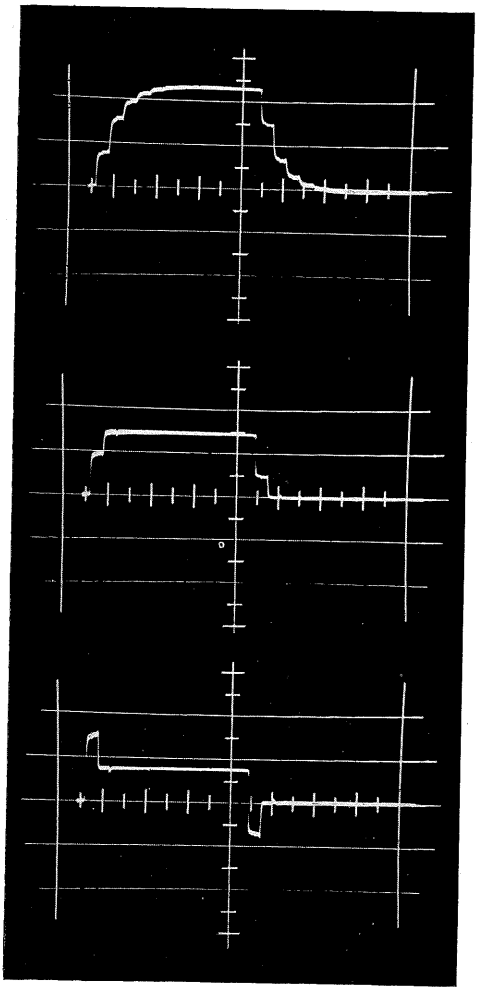

a

b

c

Fig. 19–5. Voltage waveform at cable input with a 45 μs input pulse: *a*) input open, output resistance 10 kΩ; *b*) input resistance $R_{in} = Z = 2.7\,\text{k}\Omega$, output resistance 10 k$\Omega$; *c*) input resistance $R_{in} = Z = 2.7$ kΩ, output resistance 0.7 kΩ.

In the event that the cable is terminated at the output with a multiple of the characteristic impedance ($R_{out} = 10\,\text{k}\Omega$) and at the input with a resistance equal to the characteristic impedance ($R_{in} = Z$) the voltage waveform will be as shown in fig. 19–5*b*. At the beginning and end of the input pulse from the square-wave generator only one step now appears. If the input and output of the cable are terminated with a resistance equal to the characteristic impedance ($R_{in} = R_{out} = Z = 2.7\,\text{k}\Omega$) a picture of the positive pulse is obtained like that shown in fig. 19–4*d*. Its amplitude will, however, only be half that shown, as the total voltage in this arrangement falls in equal parts to input and output resistance.

Further reducing the output resistance to a fraction of the characteristic impedance ($R_{out} = 0.7\,\text{k}\Omega$) results in an oscillogram as shown in fig. 19–5*c*. A positive pulse appears at the beginning and a negative pulse at the end. Its width again corresponds to twice the travel time. The amplitude relationships are given by the relationships of input and output resistance and by the characteristic impedance of the cable [1].

These examples show how, by means of a delay cable with a suitable termination resistance and by the use of a specific control pulse, it is possible to generate voltage pulses with a predetermined and complicated form.

[1] The question of quantitative pulse relationships cannot be dealt with here. However, the literature on the subject is extensive. Special reference is made to the book "Principles of Radar" [3] which treats all aspects of the subject very thoroughly and clearly.

PART IV

Circuit-designing

20. Small oscilloscope.

General data and valve complement.

Vertical amplifier:

1 c/s.... 220 kc/s frequency limits
30 c/s.... 8 kc/s (Phase error $< 2°$)
Deflection factor: min. 150 mV_{rms}/cm

Time base:

Frequency: 20 c/s.... 20,000 c/s (8 ms/cm.... 8 μs/cm approx.)
Picture width: approx. 3.... 6 cm, adjustable
Flyback suppression: fixed.

Valve complement:

Cathode ray tube:	DG 7–6
Power supply:	2 × AZ 41
Vertical amplifier:	EF 42
Time base generator:	EF 40, EC 50.

Dimensions: 20 × 11 × 24 cm.
Weight: 4.75 kg.
Power consumption: approx. 35 W.

Power supply.

As far as possible, standard radio components are used for the power pack. As shown by fig. 20–1, it consists of two rectifier and filter sections connected in series. One section supplies a full-wave rectified voltage of about +410 V to the second filtering condenser. The anode current for the time base and vertical amplifier is taken from this point. The other section supplies an extra voltage of about 310 V for the anode voltage of the cathode ray tube, which requires a potential of between 500 and 800 V. The current delivered by this second rectifier is small, so that satisfactory filtering is possible by simple means with half-wave rectification. Standard electrolytic condensers are quite sufficient for the purpose [1].

The mains transformer should preferably be made specially for the oscilloscope, although two suitable transformers from radio receivers could conceivably be used. The winding T_5 in the transformer with windings T_3, T_5 and T_6 would, however, have to be very well insulated (750 $V_=$). Moreover, the heater winding T_8 for the EC 50 thyratron must be thoroughly screened and have as little capacitance as possible. Table 20–I sets out the rating data for the windings in numerical order. The shape of the transformer core is illustrated in fig. 20–2. It consists of sheet-iron 0.5 mm thick, stacked to a height of

[1] The accelerating anode a_2 of the cathode-ray tube is under tension with respect to earth in this circuit. For this reason it is not possible to apply *direct* voltages for measurement to the deflection plates. This restriction was necessary for the sake of economy in outlay.

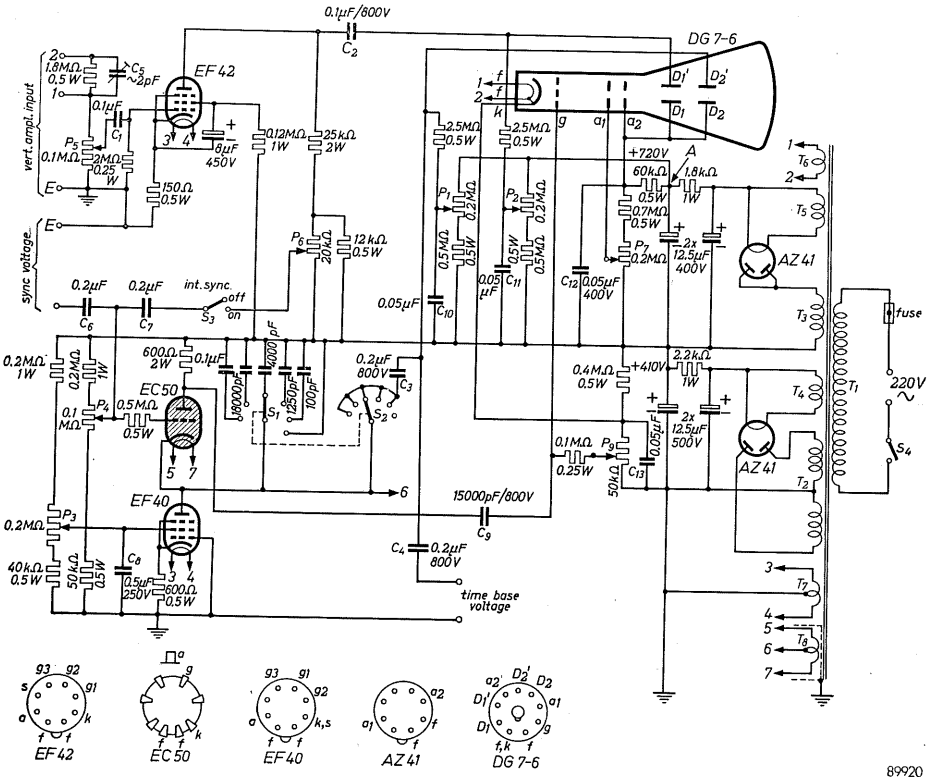

Fig. 20–1 Circuit diagram

Table 20–I
Data for the mains transformer

Winding No:	Number of turns	Diameter of wire (mm)	Voltage (V)
T_1	1100	0.28	220
T_2	2 × 1950	0.08	2 × 390
T_3	1200	0.06	1 × 240
T_4	21	0.50	4.0
T_5	21	0.50	4.0
T_6	33	0.35	6.3
T_7	2 × 17	0.45	2 × 3.15
T_8	2 × 17	0.70	2 × 3.15

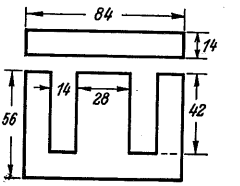

Fig. 20–2
Section of iron core for power transformer

28 mm. Two AZ 41 valves are used for rectification, although type EZ 80 is also suitable. Any other small valve is serviceable for the rectifier connected to winding T_3, since the current to be rectified amounts to only a few milliamperes.

The voltages for the auxiliary anode and the grid of the cathode ray tube are taken from a voltage divider which has the total voltage across it. Spot focus and brilliance are controlled by potentiometers P_7 and P_9 respectively.
The primary circuit of the transformer should be provided with a mains switch and a fuse.

Beam positioning.

The displacement of the spot from the centre of the screen is effected by applying a *DC* voltage to one plate of each pair of deflection plates in such a way that it can be varied with respect to the other plate between a positive and negative value.
A resistor of 60 kΩ lies between anode a_2 of the cathode ray tube and point "*A*" with the highest potential in the power supply. The current flowing to the voltage divider causes a voltage drop on this resistor of about 30 V. The anode a_2, and with it the deflection plates D_1 and D_2, are therefore more negative by that amount than point "*A*". Between point "*A*" and the positive pole of the first rectifier, two voltage dividers with potentiometers P_1 and P_2 are connected. These latter are to be rated such that in the centre setting the voltage on the arms will be approximately equal to the voltage on anode a_2. If the arms are moved upwards, as illustrated in the circuit diagram, their voltage will be more positive than a_2 and thus more positive than D_1 and D_2. If moved downwards, they will be more negative.
The leak resistors of 2.5 MΩ for the deflection plates D'_1 and D'_2 are not, therefore, tied directly with D_1 and D_2 but connected to the arms of P_1 and P_2. This permits zero correction of the spot on the screen by about $^3/_4$ cm in both directions of deflection [1].
If zero correction is dispensed with, there is no further need of potentiometers P_1 and P_2, the resistors of 0.5 MΩ in series with them and the pre-resistor of 60 kΩ.
The leak resistors for plates D'_1 and D'_2 are then connected directly to point "*A*".

Time base generator.

This apparatus uses the familiar thyratron circuit. Coarse control of the time base frequency is effected in five stages by switching between the differently rated charging condensers. Fine control is effected by varying the anode current of charging valve EF 40. This is done by controlling the screen grid voltage by means of potentiometer P_3. With full trace length (about 60 mm), a time base frequency range of approximately 20 c/s to 20,000 c/s can be covered. The maximum frequency depends upon the stray wiring capacitance. In certain circumstances it is necessary to try out the most favourable value of the charging condenser indicated as 100 pF, and if the wiring capacitance alone is large, it may even have to be omitted altogether.
The other capacitances should also be found by practical experiment to

[1] No noticeable distortion of the pattern is caused by this additional potential difference between a_2 and the deflection plates, since it only amounts to roughly 5% of the anode voltage.

ascertain the most suitable overlap of the individual frequency ranges. In the last position of the time base frequency-switch the charging circuit is shorted (no time base voltage). The second pole of the switch simultaneously switches off the coupling condenser C_3 from the X plate D'_2, and an external voltage for deflection along the X axis can now be applied to the time base sockets. For 1 cm deflection of the beam, 15 V_{rms} are required. In all other positions of the switch, the time base voltage proper can be taken from these sockets for controlling other apparatus (wobbulators) or for testing amplifiers.
To synchronize the time base frequency with the amplified input signal, this latter is taken from potentiometer P_6 in the anode circuit of the amplifier valve (switch 3 closed) and fed via condenser C_7 to the grid of the thyratron. If an external voltage is to be used for synchronization (sockets "sync"), potentiometer P_6 is turned back far enough for the switch S_3 coupled with it to open.
During the discharge (flyback of the spot), a voltage pulse appears across the 600 ohm resistor in the anode circuit of the thyratron EC 50. This pulse is passed through condenser C_9 to the grid of the cathode ray tube, and since it is negative with respect to the cathode, the tube is cut off for the duration of the pulse and thus the flyback blanked out.
The cathode resistor of the charging valve EF 40 is not bypassed (negative current feedback). Its internal resistance is therefore high, resulting in good linearity of the time base voltage. As the horizontal deflection plates of DG 7–6 were designed for asymmetrical voltages, it is unnecessary to balance the time base voltage.

Amplifier for vertical deflection.

For optimum results the vertical deflection plates of these tubes should, it is true, receive symmetrical voltages. However, as the deflection in the Y direction is usually much smaller than in the X direction, simplifications can be made and an unbalanced amplifier used without any noticeable deterioration of the pattern. A single pentode with high mutual conductance is chosen as the amplifier, a valve of this kind giving good amplification even

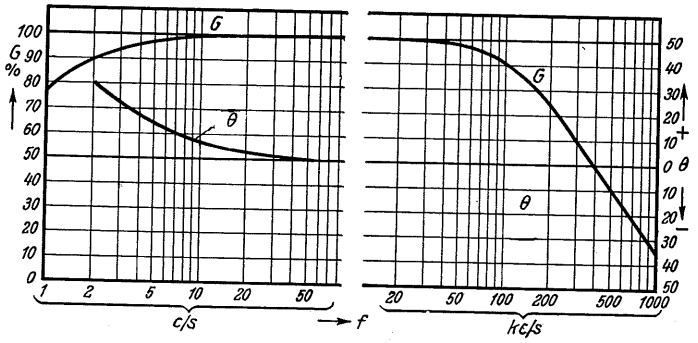

Fig. 20–3 Amplification and phase curves of vertical amplifier

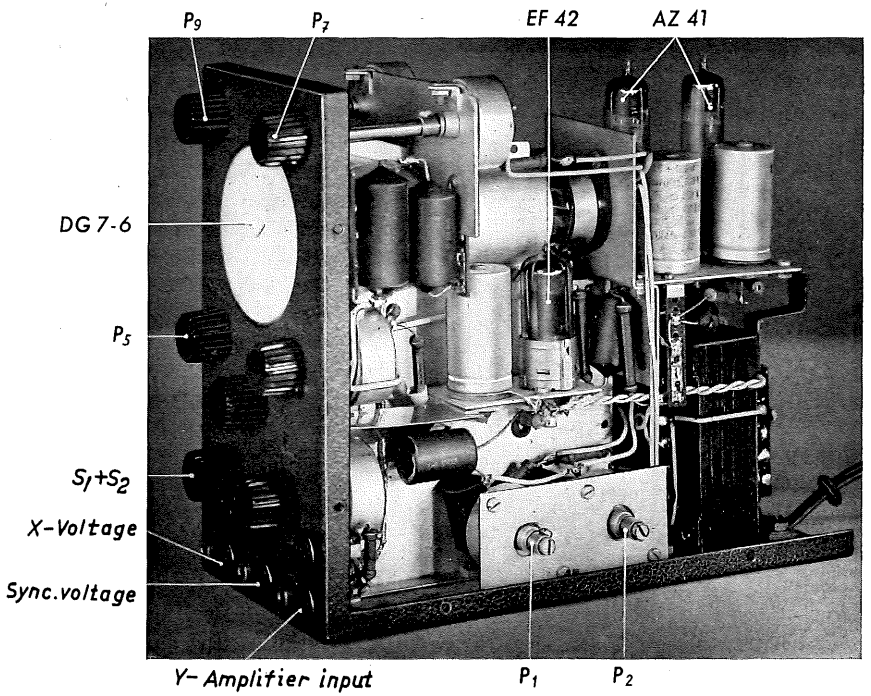

Fig. 20–4 Interior view: amplifier and supply sections

with negative feedback. A sufficiently large, undistorted output and a favourable compromise between gain and bandwidth are achieved with an anode resistor of 25 kΩ and a non-bypassed cathode resistor (negative current feedback). The EF 42 has an amplification of about 90 $\times$, so that with a deflection factor of 13.6 V_{rms}/cm in C.R.T. type DG 7–6, the deflection factor with amplifier is: $DF_{\sim} = 150$ mV_{rms}/cm.

The vertical signal may be reduced to the required amplitude on the screen by an input voltage divider preceding the control grid of the valve. Voltages of up to 50 V_{rms} can be applied direct to potentiometer P_5 of 0.1 MΩ via sockets "1" and "E". With the control fully turned up, the gain and phase curve is as illustrated fig. 20–3. The gain deviates by less than 2% between about 7 c/s and 75 kc/s. In the range between about 30 c/s and 8,000 c/s, the additional phase shift is also less than 2%. Undistorted measurements are thus possible over the whole audio-frequency range. But also at 500 kc/s there is still 40% of the mean amplification and even at 1 Mc/s, deflections of approximately 15 mm can still be obtained with a voltage of 1 V. This oscilloscope can therefore find application in radio engineering for investig-

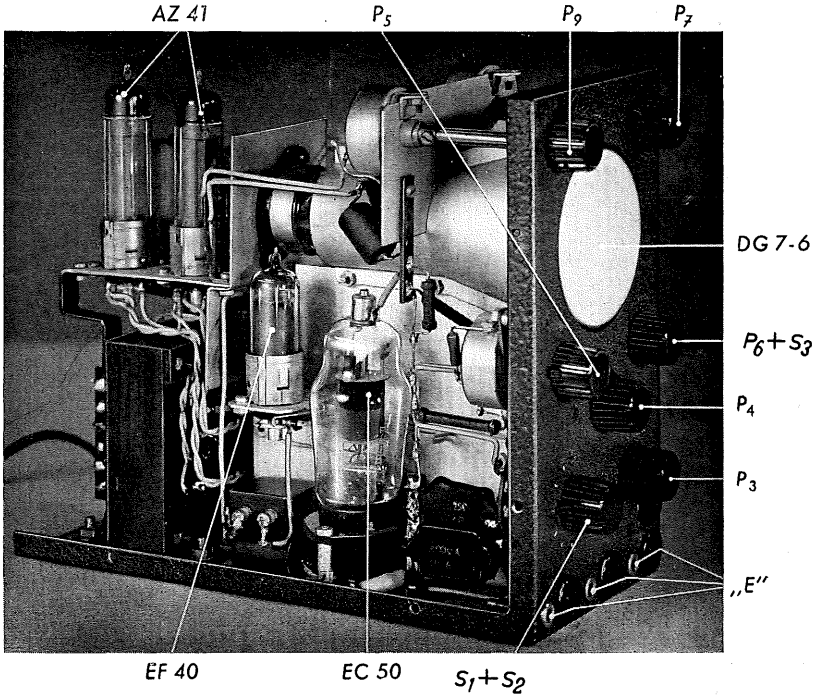

Fig. 20–5 Interior view: Time-base and rectifier sections

ations in the long-wave and intermediate frequency ranges and over a large part of the medium wave ranges. Voltages higher than 50 V_{rms} must be fed in via the 1.8 MΩ resistor across sockets "2" and "*E*", resulting in an additional voltage division of roughly 1 : 20. Since this input resistor forms a filter together with the input capacitance of the valve, the upper limit of the linear amplification range decreases to about 25 kc/s and the limit of phase-accurate reproduction to 1500 c/s. The capacitance in parallel with the input potentiometer (valve, wiring and potentiometer capacitance) reduces the voltage division at higher frequencies. To compensate for this, the input resistor must be shunted by a capacitor of 1 . . . 2 pF. In its simplest form this may consist of two insulated and multistranded wires and it must be adjusted in such a way that the same voltage division occurs at high frequencies as in the region of 1000 c/s.

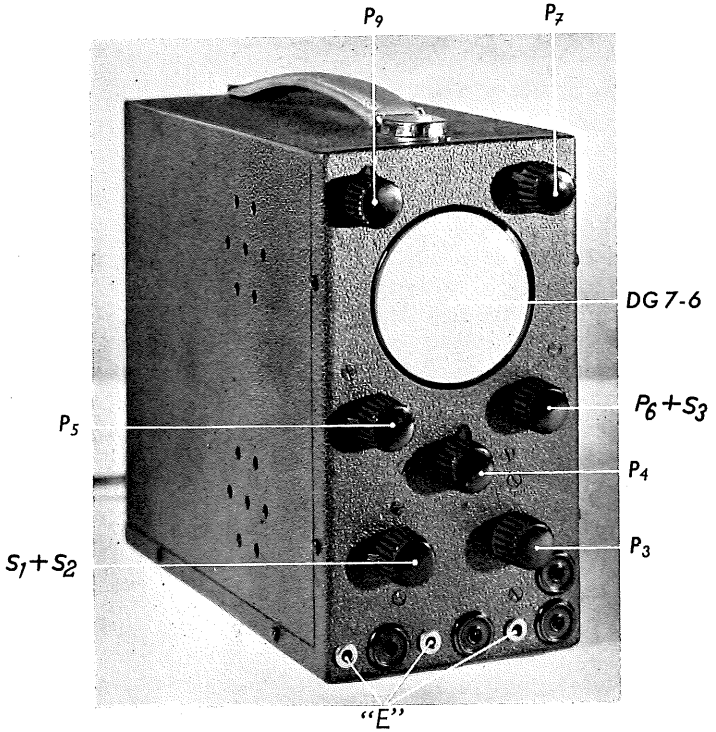

Fig. 20–6 The finished model.

Construction.

The layout of this model can clearly be seen in figs. 20–4, 20–5 and 20–6. Steel plate 1 mm thick should be used for the casing. The screening for the cathode ray tube should consist of malleable cast-iron approximately 4 mm thick or mu-metal with a sectional thickness of 0.5 mm. As shown in fig. 20–4, the two potentiometers for the beam positioning are assembled at the right-hand side in such a way that they can be adjusted through slits with a screw-driver. It should be particularly stressed that the wiring capacitance in the time base section and most especially in the amplifier section must be kept as low as possible. In the last resort, the upper frequency limit of the amplifier depends upon the wiring capacitance.
All potentiometers in this model are rated for a maximum load of 0.5 W.

21. Special duty oscilloscope "FTO-2"

General remarks.

Unlike the small oscilloscope described in the preceding chapter, this apparatus can only be built with any prospect of success by those who have completely mastered the whole technique of time base construction, wide-band amplifiers, etc. Moreover, it will be necessary to have a certain number of high-grade measuring instruments and apparatus at hand in order to be able properly to carry out the sensitive measurements required, especially with regard to the alignment of the vertical amplifier.

It should be expressly emphasized that the design of this model was based entirely on the considerations contained in the first section of this book.

With regard to circuitry, as little as possible was borrowed from industrially manufactured oscilloscopes, since, of course, the conditions are fundamentally different when building one's own apparatus. Whereas in industrial makes every single detail is developed to the last degree by specialists with all the resources of a modern laboratory at their disposal, a circuit design of this sort can only be more or less the work of an individual. He has to rely upon standard commercial components, while the apparatus industry is in a position to produce and use components specially rated for a particular purpose. On the other hand, an individual circuit design is better able to provide for certain additional devices, switches, connections and so on, which tend to make the apparatus more suitable for a given application, whereas an industrially developed oscilloscope must be adapted to a wide variety of applications and must dispense with specialized devices which might make the cost of the product prohibitive.

Although, as mentioned at the outset, the number of persons able to construct this apparatus will be very limited, this chapter has nevertheless been included in order to elucidate by a practical example the detailed considerations which must apply when building a high-grade oscilloscope. It also makes it possible to critically assess the limits of efficiency of the apparatus which, for obvious reasons, could not be done without restrictions when discussing an industrial product.

Experience has shown that, in descriptions of this kind, data are often requested with regard to modifications in the valve complement and the like. It must therefore be pointed out at once that in this type of apparatus only those modifications can be recommended which have been thoroughly tested and proved in practice. Since this is not practicable for any conceivable variation of, for instance, the valve complement, builders are expressly advised to abide by the data given. With this in mind, the makes have often been indicated for the various structural components; the valve complement consists of Philips' types.

Electrical data.

Cathode ray tube: DG 10–6.

Deflection factors: *Y* axis —5.5 V_{rms}/cm (with 265 V post-acceleration) or 5.0 V_{rms}/cm (without post-acceleration) or 7.0 V_{rms}/cm (with 1.2 kV post-acceleration).
X-axis —6.65 V_{rms}/cm (with 265 V post-acceleration) or 6.15 V_{rms}/cm (without post-acceleration) or 8.2 V_{rms}/cm (with 1.2 kV post-acceleration).

All deflection plates can be switched to sockets for external connection.
Input capacitances: 10 pF (C_{D1}, C'_{D1}) and 12 pF (C_{D2}, C'_{D2}).
Z-axis (grid): from approx. 10 c/s to 0.3 Mc/s; min. 1.5–3.0 V_{rms}.
Input impedance: 100 kΩ/53 pF.

Vertical deflection amplifier:

Three-stage with cathode follower input.
Lower cut-off frequency: approx. 3 c/s.

Upper cut-off frequency	*Minimum deflection factor*
0.70 Mc/s	5 mV_{rms}/cm
2.6 Mc/s	15 mV_{rms}/cm
7.5 Mc/s	50 mV_{rms}/cm.

Phase error from 50 c/s onward: $< 1°$.
Good reproduction of rectangular voltages up to 2–3 kc/s, 50 kc/s and 250 kc/s respectively.
Voltage divider on cathode follower: 3 switching positions:

0.15 V_{rms}/cm
0.5 V_{rms}/cm
1.5 V_{rms}/cm
} upper cut-off frequency 7.5 Mc/s.

Load to signal voltage: 1.5 MΩ/23 pF; max. 15 V_{rms}.
Further attenuation: 20 : 1 via special socket.
Input impedance: approx. 5 MΩ/8 pF; input voltage: max. 300 V_{rms}.
Intermediate values of gain 3 : 1 continuous control.
Valves: 3 × EF 42; 2 × PL 83.

Time base generator.

Oscillator: 1 × EF 42 in transitron Miller circuit.
Balancing stage: 1 × EF 42.
Frequency range: 1.25 c/s. . .100 kc/s.
Sweep range: 0.1 sec/cm. . . . 1.2 μsec/cm.
Flyback suppression with 1 × EA 50; can be switched off.
Synchronization: Internal, external and mains.
Switchable as *X* amplifier: frequency limits: 3 c/s—225 kc/s.
Phase error $< 1°$ between 30 c/s and 30 kc/s. (at 3c/s 15° phase shift).
Input impedance: 25 kΩ/ 55 pF.

Power Supply:

High Tension:

a) Time base generator 1 × EZ 80. 285 V/16 mA.
b) Vertical amplifier 2 × EZ 80. 265 V/120 mA.
1 × 150 B2.

Extra High Tension:

a) 1 × EY 51 —1000 V for C.R.T. cathode.
b) 1 × EY 51 +1200 V for C.R.T. post-acceleration anode.

Fig. 21–1 The finished model – FTO 2.

Mechanical structure of the oscilloscope.

The individual structural sections of the oscilloscope, the power pack, the vertical amplifier, the time base generator and the X amplifier are built in separate compartments separated by 1.5 mm duraluminium sheet, thus combining effective screening with robust construction.
Fig. 21–1 shows the exterior view of the finished apparatus. Contrary to the practice with most manufactured oscilloscopes, the vertical amplifier input is

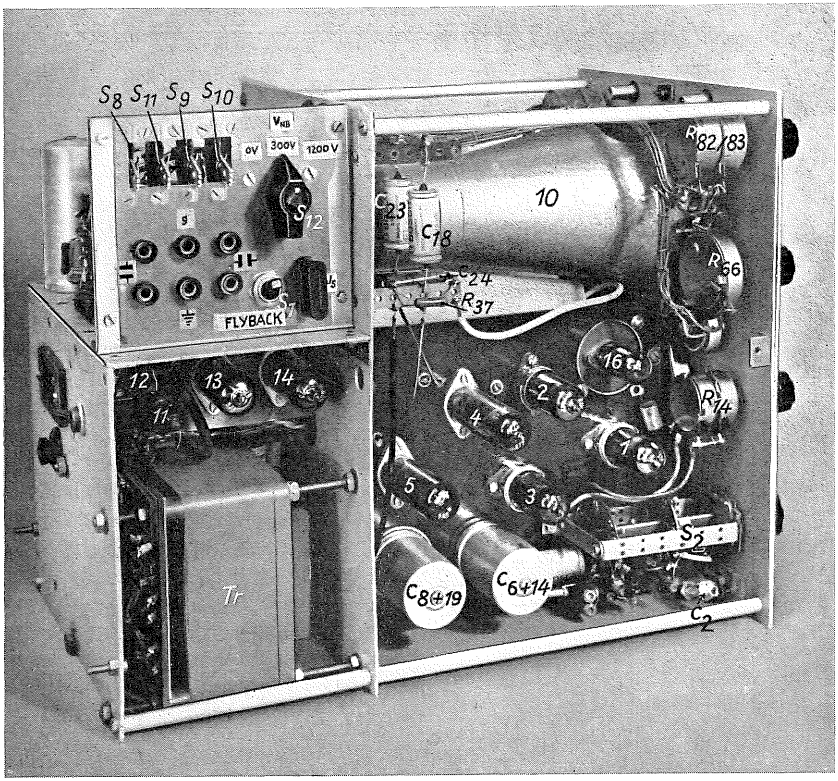

Fig. 21–2 Chassis with vertical amplifier, power pack and side connection panel.

arranged at the left of the front panel. The consideration that led to this measure being taken was that in a measuring set-up the general rule is: voltage source on the left, object under test in the centre and indicating device (in this case the oscilloscope) on the right. For the sake of short connections and an accessible layout it is therefore convenient to have the connection sockets for the vertical amplifier on the left of the front panel.
The vertical amplifier section and the power pack with the rectifier valves can be seen in fig. 21–2 while fig. 21–3 shows the interior of the power pack with the rear chassis-plate removed. The time base generator and the horizontal amplifier section with smoothing choke, E.H.T. condensers and rectifier valve EZ 80 for the supply section of the time base generator can be recognized in fig. 21–4. Fig. 21–5 shows a side and rear view of the casing, with the mains connection, fuse and switch (S_6) as well as the input panel on the left side

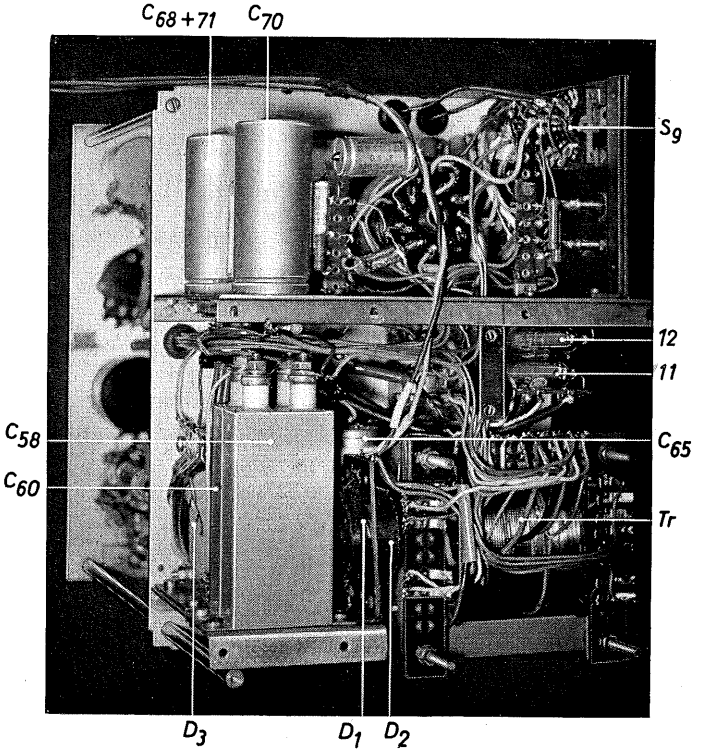

Fig. 21–3 View of power pack with rear panel removed.

with the sockets for direct connection to the deflection plates, for brightness modulation and for measuring the beam current. The front view with the control panel is shown in fig. 21–6.

In view of the high cost which would have been involved in having the front panel specially etched or engraved, the inscriptions and scales were first drawn clearly on paper and a photographic reproduction later made on high-gloss paper of cardboard thickness. It is protected against mechanical damage by a cellophane sheet 1 mm thick. This simple panel fulfils its purpose in every respect.

The photograph in fig. 21–7 gives a view into the apparatus from underneath and that in fig. 21–8 a view from above. The scale drawings in figs. 21–9, 10, 11, 12, 13 and 14 reproduce the exact dimensional relationships and arrangement of the most important structural sections.

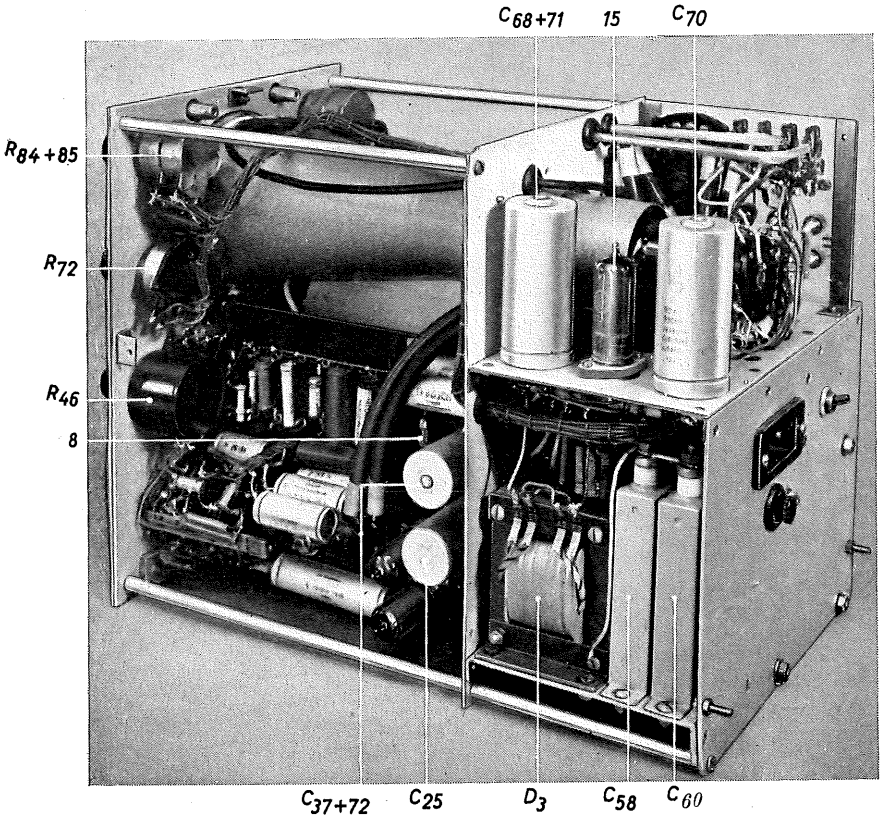

Fig. 21–4 Chassis with time-base generator and power pack.

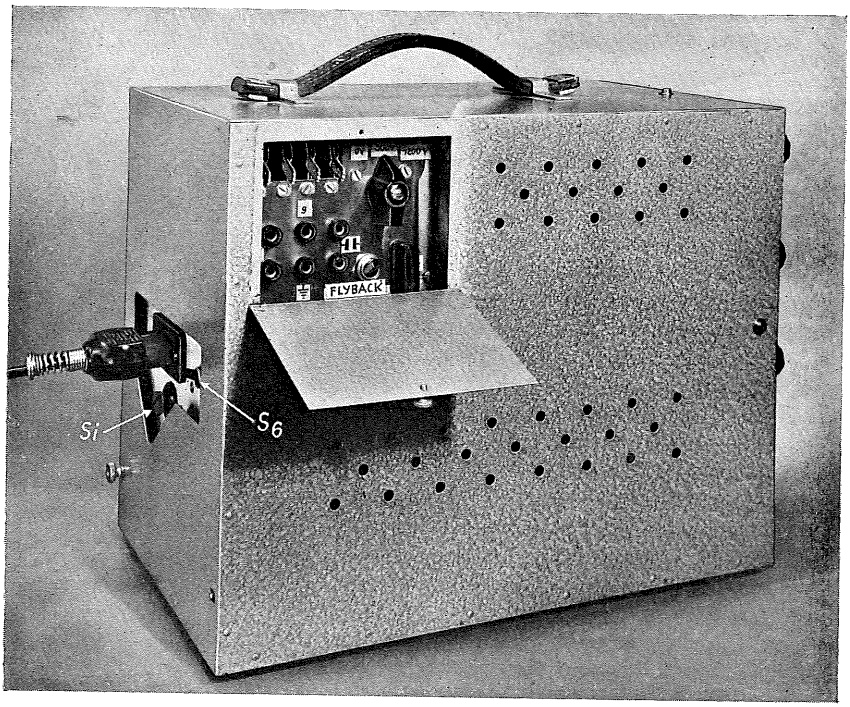

Fig. 21–5 Rear and side view, showing connection panel, mains lead, fuse and switch.

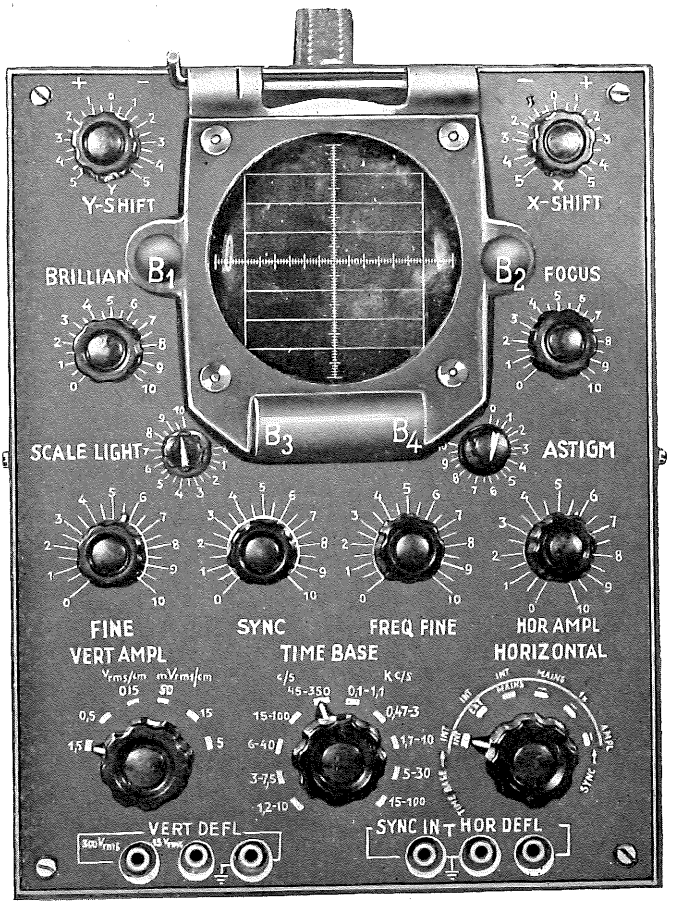

Fig. 21–6 Control panel of FTO-2.

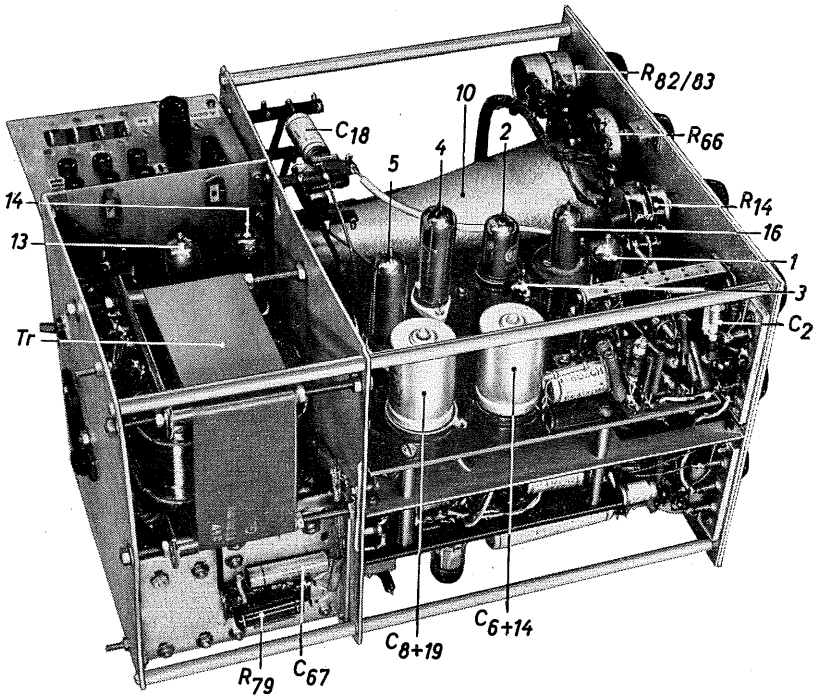

Fig. 21–7 Chassis: view from underneath.

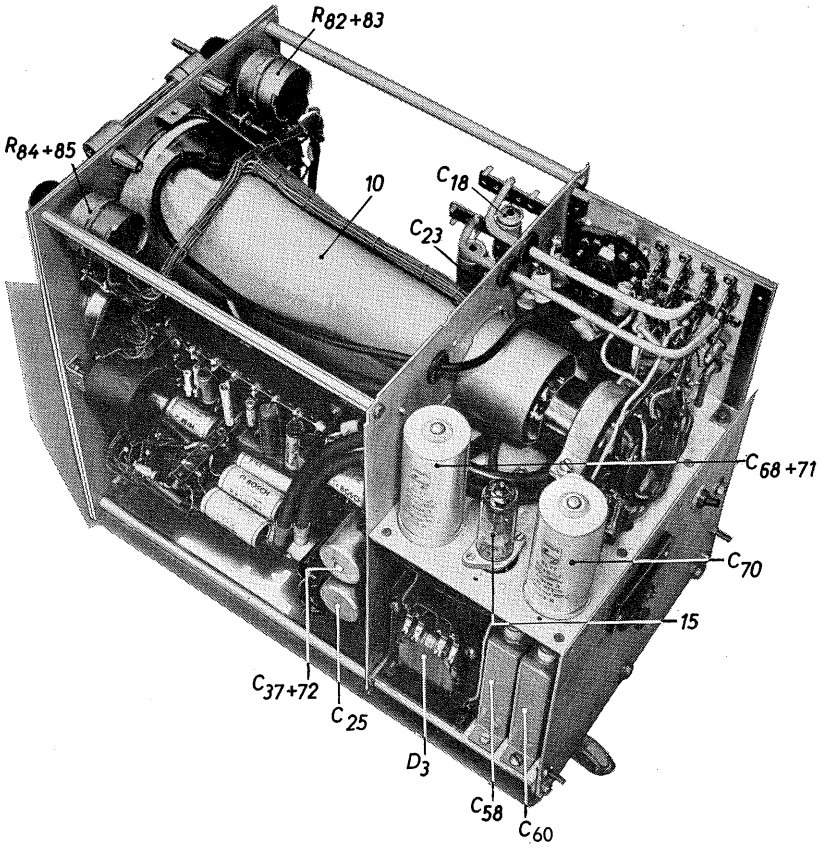

Fig. 21–8 Chassis: view from above.

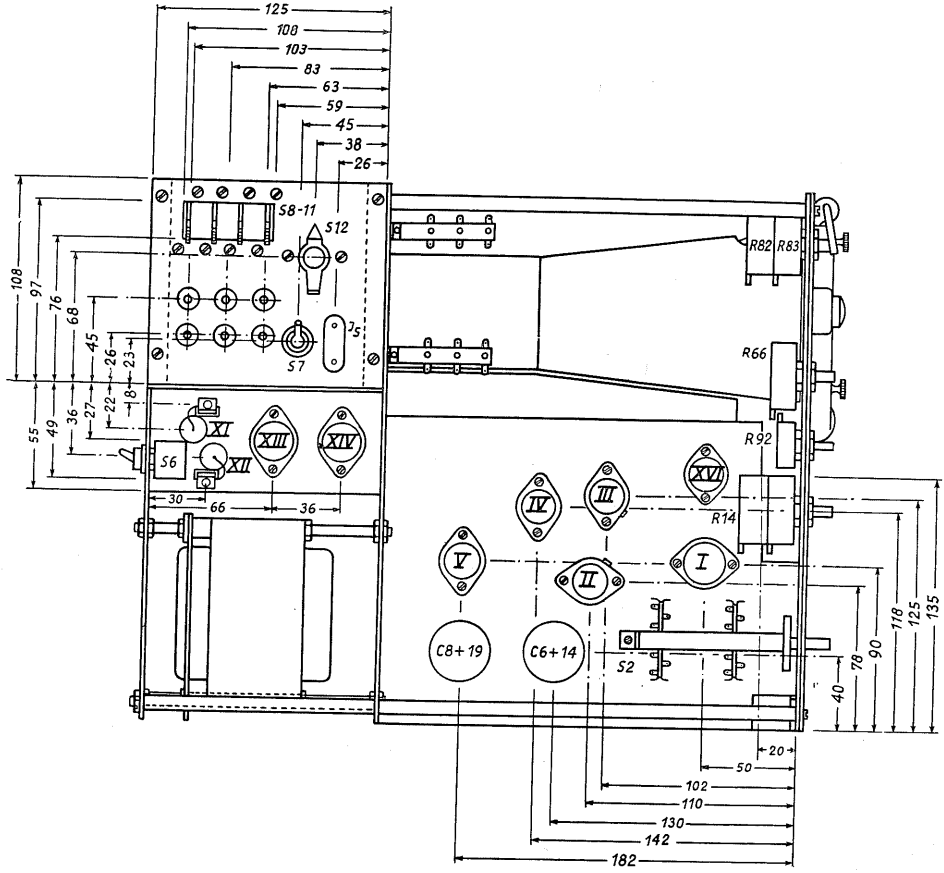

Fig. 21–9 Scale drawing of chassis with vertical amplifier.

Fig. 21–10 Scale drawing of rear panel with connection strips for C.R.T.

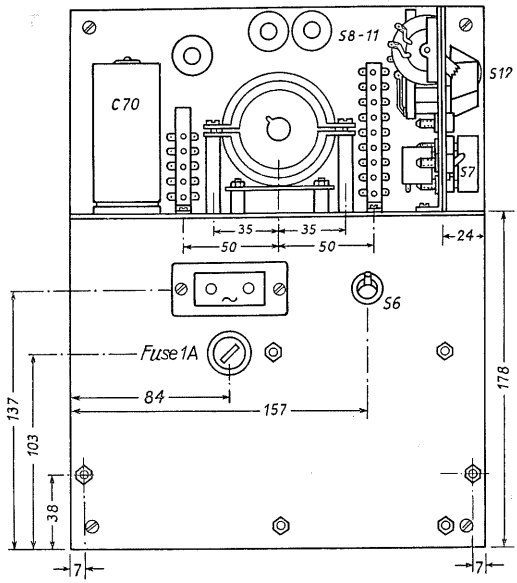

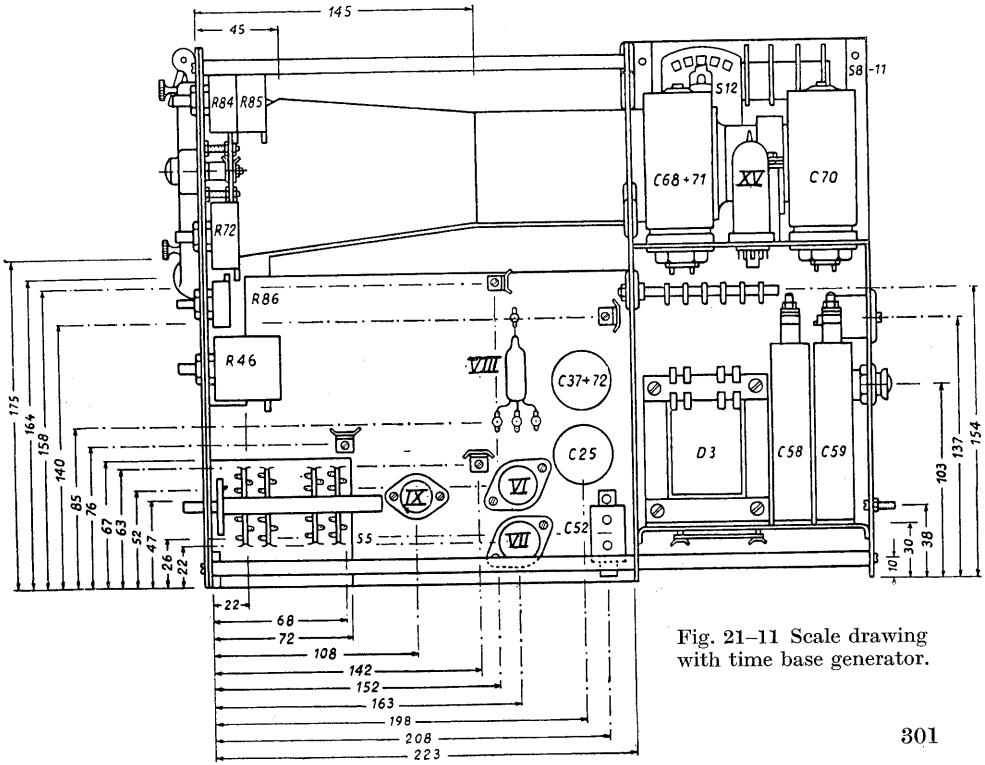

Fig. 21–11 Scale drawing with time base generator.

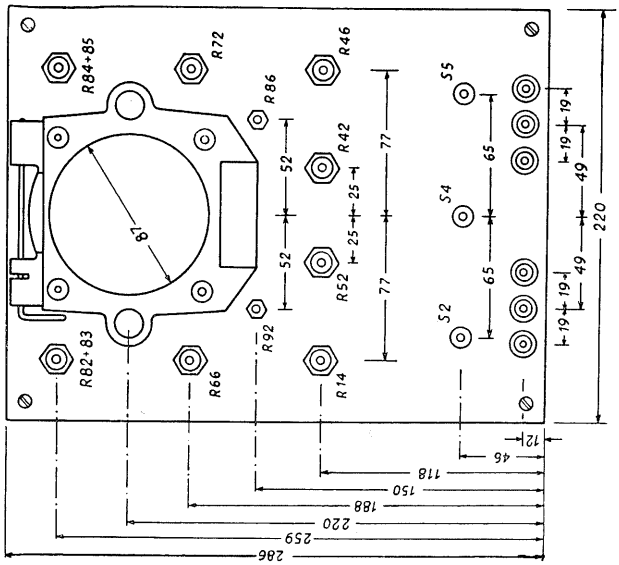

Fig. 21–13 Scale drawing of front panel.

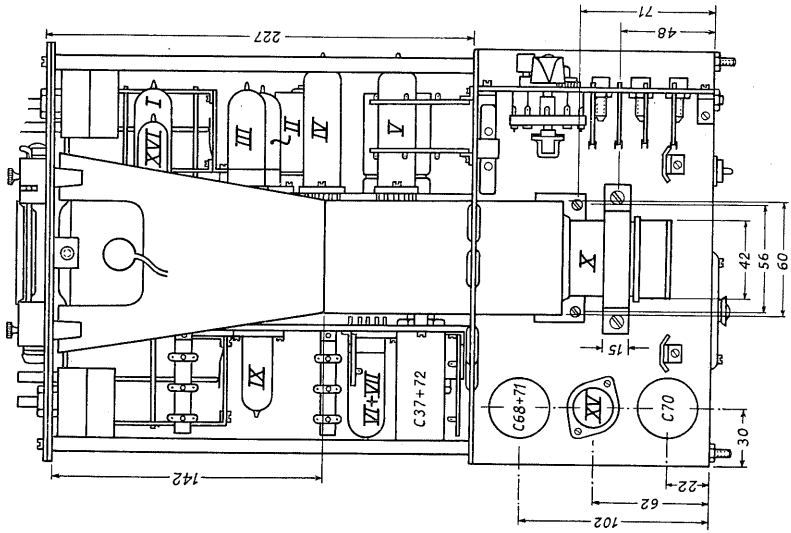

Fig. 21–12 Scale drawing of view from above.

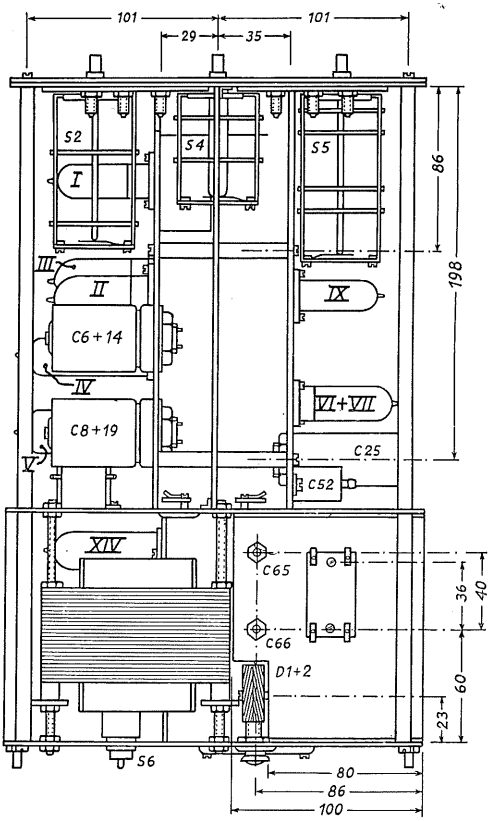

Fig. 21–14 Scale drawing of view from underneath.

Cathode ray tube and power supply.

Cathode ray tube.

The tube chosen for this apparatus is Philips' type DG 10–6, which, with its symmetrical deflection plates for symmetrical deflection voltages, satisfies the highest demands.

This tube also has a post-acceleration anode which, by means of switch S_3 in the circuit diagram, shown in fig. 21–15, can be connected either to the chassis (0 V), to the filter condenser for supplying the anode voltage to the vertical amplifier (+265 V) or to a special E.H.T. source (+1200 V). In this way it is possible to make the most favourable compromise between deflection sensitivity on the one hand and brilliance or focus on the other, depending upon the work in hand. In deviation from the data given for this tube, the

voltage on a_2 is in this case only 1kV instead of 2kV. This is in order to achieve the highest possible deflection sensitivity.
Of course, full advantage can only be taken of the good characteristics of the tube (spot focus, etc.) when the post-acceleration voltage is 1.2 kV. The deflection sensitivity is still higher at this voltage than it would be if the potential of a_2 and a_3 with respect to the cathode were 2 kV. In this way the following deflection factors for *AC* voltages are obtained:

without post-acceleration voltage: 5.0 V_{rms}/cm
with + 265 V post-acceleration: 5.5 V_{rms}/cm
with +1200 V post-acceleration: 7.0 V_{rms}/cm.

The cathode ray tube is screened from the stray magnetic field of the power transformer by enclosing it in a mu-metal cylinder.

Anode voltages for vertical amplifier and time base generator.

All the alternating voltages needed are supplied by the transformer T_r. For generating the anode voltages for the vertical amplifier and the time base generator two special rectifiers with their own filters are used in order to exclude all risk of the time base voltage interfering with the amplifier, even at the lowest frequencies. Since the current consumption of the time base generator does not exceed 20 mA, it is sufficient for this portion of the anode voltage to use one valve, type EZ 80, and a *CRC* network for filtering consisting of a 2 kΩ resistor and two electrolytic condensers of 50 μF each. The ripple voltages measured amount to 3.0 V_{pp} and 35 mV_{pp} respectively. In view of the high current of 120 mA drawn by the vertical amplifier it is necessary to use two EZ 80 valves in parallel, or one EZ 81, and a smoothing choke together with two condensers of 50 μF and 100 μF each respectively. The ripple on the 50 μF reservoir condenser is approximately 12 V_{pp} and on the 100 μF filter condenser about 36 mV_{pp}. Both windings on the choke are wired in parallel in order to ensure the lowest possible voltage loss with the relatively high current.

E.H.T. section.

Two EY 51 rectifier valves are used for generating the extra high tension. The circuit is as shown in figs. 3–9 and 3–10 on page 33. The E.H.T. of —1000 V for the C.R.T. cathode is smoothed by a *CRC* filter with 1 μF condensers and with a total R of about 50 kΩ. A resistor of 20 kΩ precedes the reservoir condenser in order to protect the rectifiers [1].
Controlling the brightness of the oscillogram by varying the negative voltage on grid "*g*" with potentiometer R_{68}, and adjusting the spot focus by varying the positive potential on a_1 with potentiometer R_{72} is effected in the manner described in detail in the chapter on the power supply. The difference in brightness appearing when the flyback blanking is switched on and off is compensated by providing resistor R_{67} with a switch (S_7).

[1] Although, according to the valve data, 100 kΩ are required in this case, this value was chosen, with the risk it involves, since with a 100 kΩ pre-resistor only 700 $V_{=}$ were measured on the reservoir condenser. No detrimental results were ascertained when the oscilloscope was taken into service.

The second EY 51 supplies the post-acceleration voltage of +1200 V over a *CRC* filter with two 0.1 μF condensers and one filter resistor. It is possible to use such small values of capacitance with a resistance of 500 kΩ as the total current consumption never exceeds 150 μA (voltage drop max. 75 V).
To ensure fairly quick and sure discharge of the condensers, four 7.5 MΩ resistors—in all 30 MΩ—are connected in series across the voltage output. A continuous current of 40 μA flows through these resistors. A further effect of this is to reduce the dependence of the output voltage upon the current drain so that there is no disturbing fluctuation of the acceleration voltage and thus of the deflection sensitivity (picture size) when controlling the brightness.

Control voltages for adjusting the position of the pattern on the screen.

Tandem potentiometers R_{82}, R_{83} and R_{84}, R_{85} are provided in order to be able to correct the central position of the pattern on the screen and above all to make it possible to adjust the pattern when the input voltages are asymmetrical. They form a voltage divider together with resistors R_{71}, R_{72}, R_{86} and R_{87}, which lie between —1000 V and about +200 V. In this way direct voltages can be fed to the pairs of deflection plates so as to allow any desired adjustment of the pattern over the whole surface of the screen. (See also fig. 3–11*b*.) These voltages are symmetrical as a result of using two cross-connected tandem potentiometers. When the voltage on one plate of the pair of plates in question is adjusted to a certain positive value, the voltage on the other plate drops automatically to an equivalent negative value; the mean potential on the pair of plates should always remain zero. Thus, in all positions, the adjusted focus is retained.

Astigmatism control.

In so far as the voltage divider discussed is correctly rated so that the mean potential of the pairs of plates always remains zero, subsequent adjustment should not really be necessary. For this reason no provision is made for it in the majority of industrially manufactured oscilloscopes. The voltage divider is set for optimum focus at normal working voltages. In this oscilloscope, however, a facility is provided for additional adjustment of the mean potential of the deflection plates. By means of R_{86} it is possible to find the best position of focus if the working voltages should change or the relationships in the voltage divider should be altered. It also permits adjustment to optimum focus in cases where it is desired to apply an asymmetrical *AC* signal (via a coupling condenser) to one of the *Y* plates. (In such cases the leak resistors must, of course, remain connected to the plates).

Direct connection to the deflection plates.

To apply input voltages which are beyond the frequency range of the vertical amplifier, the *Y* plates can be switched from the amplifier output to the external connection sockets by means of the low-capacitance switches S_8 and S_{11}. This is particularly desirable in *DC* voltage measurements. If necessary an

additional *DC* amplifier can be connected to these sockets. The switches used for this model were the types often found at the rear of Philips' radio receivers for switching over the loudspeakers. Their self-capacitance is small, amounting to about 1 pF. The horizontal deflection plates, too, can be switched in this way to external sockets. Since these connections also disconnect the plates from the leak resistors, provision must always be made, when applying external voltages, for direct coupling to the chassis of the oscilloscope. If this is not done through the voltage source itself (connection via capacitances), additional leak resistors to the chassis must be provided.

R.F. filter in the mains lead.

To prevent harmonics of the time base voltage from being radiated over the power supply and causing radio interference, R.F. chokes (Ch_1 and Ch_2) are included in the mains lead in the way they are frequently used in radio receivers for R.F. decoupling from the mains. They should be effective down to 150 kc/s to exclude the possibility of interference in the long-wave range. In this manner the harmonics of the time base voltage are also kept away from the input of the vertical amplifier where they would lead to distortion of the oscillogram. (See oscillograms fig. 4–37*c* and *e*.)

Connection for measuring $I_{a3}(I_s)$.

Since the adjustment of the brightness control is relatively coarse, it was found expedient for the purpose of photographic recordings to measure the current on anode a_3 and to work accordingly. Sockets "I_s" are provided for this, which are normally bypassed by means of a shorting plug. When photographs are to be taken, a micro-ammeter can be connected here (measuring range 0–10 μA or, for high degrees of brightness, 0–100 μA). When using a post-acceleration voltage it must be remembered that the micro-ammeter is under this tension with respect to the chassis.

Vertical amplifier.

General.

The range of applications of an oscilloscope is determined by the frequency range of the vertical amplifier and by the minimum deflection factor which can be obtained with it. This section therefore received the greatest attention during development.

The individual stages will be discussed in the following with reference to the circuit diagram in fig. 21–15. As can be seen from this, a cathode follower input-stage is followed by two pre-amplifier stages and an output stage in push-pull.

The valves used for cathode follower and pre-amplifiers are types EF 42 [2] while two valves PL 83 are used for the output stage.

[2] The S/C ratio of the EF 80 is admittedly more favourable, but since the wiring capacitance represents the largest share of the harmful capacitance, and the EF 42 has the higher mutual conductance, the latter was found to be preferable.

Input and cathode follower stage.

A cathode follower stage is employed in order to obtain the highest possible input impedance. In addition to the earth socket there are two sockets for the input voltages (asymmetrical). If connection is made to the socket marked "15 V", contact S_1 is interrupted and the voltage divider R_1—R_2 switched off so that the signal passes to the grid of the cathode follower over condenser C_1. With a total cathode resistance of 2 kΩ and a cathode current of 12 mA, the input voltage may amount to 15 V_{rms} before any deterioration in the linearity of the dynamic characteristic becomes noticeable. Since the *DC* voltage drop on the cathode resistor is then 24 V and therefore represents too high a bias on the grid, it must be compensated by simultaneously applying a positive voltage of +22 V to the grid. This brings about the correct operating point at —2,0 V. It is obtained quite simply by connecting a resistor of 8.8 MΩ between the grid and a potential of +150 V. A voltage divider is thus formed with R_3 and R_4 by means of which the operating point of the valve can be adjusted.
As a result of the high cathode potential a certain "over-automatic" negative grid voltage exists, so that the working point can be kept constant within wide limits. If, for any reason, the anode current begins to change, a counter-change of the bias is the immediate consequence; this has the effect of keeping the anode current constant, and is determined exclusively by the rating and stability of resistors R_3 and R_4. The most favourable value of R_3 is best found by experimentally selecting or combining several resistors while observing the anode current of the valve. In the apparatus described, two resistors are connected in series. To suppress all influence from mains fluctuations the positive anode voltage is stabilized with a stabilizer valve type 150 B2. The voltage gain of this stage was found to be 0.94.
Voltages higher than 15 V_{rms} must be fed in via the socket marked "300 V". Contact S_1 then automatically connects the voltage divider R_1—R_2 to condenser C_1 so that the voltage is fed, attenuated in a ratio of 20 : 1, over C_1 to the grid of valve 1. In order for the same ratio to hold good over the whole frequency range of the amplifier, this voltage divider also must be compensated by condensers C_2—C_3. At lower frequencies the voltage division is effected by the resistors but, as the frequency increases, it is effected more and more by the condensers. For C_2 a ceramic tube trimmer of max. 8 pF is used.

Rating the amplifier stages and controlling the gain.

The maximum upper cut-off frequency is determined chiefly by the output stage, which must supply a sufficient amplitude of voltage for vertically deflecting the spot with a minimum of distortion.
A high anode current is necessary in order that the requisite anode resistors may remain as low as possible. For these reasons, two PL 83 valves are used for the output stage; they are especially suitable for the purpose, having been developed for the video output stages of television receivers. Extensive tests during construction showed the most favourable value for the anode resistors

to be 1.5 kΩ. The cathode resistors R_{27} and R_{33} of 90 Ω are bypassed by only small values of capacitance in order to improve the upper frequency response. In the lower and middle frequency ranges, in which these condensers represent high impedances, negative current feedback occurs, which improves the possibility of driving the output stage. The dynamic characteristics thus obtained are reproduced in fig. 7–6*a* and *b* (page 145).

The major requirement when constructing a vertical amplifier, particularly with regard to the output stage, is to *reduce the wiring capacitance to an absolute minimum.* It must be remembered that it is this which directly determines the maximum upper cut-off frequency obtainable. In the model under discussion it was possible to keep these capacitances at the output of the last stage at about 30 pF. With an anode resistance of 1.5 kΩ, the frequency limit can then be calculated from formula (5–37) to approximately 3.5 Mc/s. By including chokes $L_5 + L_6$ and L_7 of 13.0 + 7.0 μH and 20.0 μH respectively in the anode circuits, and by bypassing the cathode resistors with condensers of 530 pF each, the maximum upper cut-off frequency of the amplifier is brought to approximately 7.5 Mc/s. With 20.0 μH a factor a is obtained for the circuit elements in the anode lead of ≈ 0.3 (see pages 103–5). As can be seen in the circuit diagram, the antiphase drive of valve 5 is effected by taking a portion of the voltage from the anode resistor of valve 4, which must correspond to the amplification of valve 5, in the manner shown in fig. 5–31. To retain the symmetry right up to the upper cut-off frequency, the inductance in the anode circuit of valve 4 must also be partly connected in series with resistor R_{29}. The gain of each stage was found to be approximately $\times 7.5$ and thus $\times 15$ for the whole output stage.

The pre-amplification stage should be rated such that with a satisfactorily small deflection factor (at the most 50 mV_{rms}/cm) fullest possible advantage is taken of the whole bandwidth of the output stage. It appeared that this was not possible with one pre-amplifying stage alone; two pre-amplifiers are therefore used in this circuit. Whereas, most types of gain control entail a reduction of the maximum gain, an attempt is made here, while tolerating a somewhat lower upper cut-off frequency, to obtain for special purposes a step-by-step boosting of the total gain. This is done by switching the anode resistor of the second valve from 750 Ω to 2.55 kΩ and 8.0 kΩ respectively. The gain of this stage, which is about $\times$ 3 with 0.75 kΩ, can thus be boosted to $\times$ 10 and $\times$ 30 so that the total gain is boosted in a ratio of 1 : 3 : 10. The upper frequency limits then lie at 7.5 Mc/s, 2.6 Mc/s and 0.70 Mc/s respectively, as shown by the curves in fig. 21–16*b*. To correct the frequency response at the upper limits, resonant chokes L_2, L_3 and L_4 are connected in series to the anode resistors. The frequency response is improved by bypassing the cathode resistor (R_{21}) with a condenser of 150 pF. The most favourable values of these circuit elements must be determined from case to case. When constructing this particular model the wiring capacitances and the inductance of the resonant chokes were measured with an "Elomar" LC measuring apparatus, type MB 2025. A Philips measuring bridge, type GM 4144, was used for measuring the other capacitances. The frequency response was measured with a GM 2653 signal generator together with a GM 6016 HF-millivolt meter.

The first pre-amplifier works with an anode resistor of 700 Ω, which provides

an amplification of approx. $\times 2.6$. The total gain at maximum bandwidth is therefore: $0.94 \times 2.6 \times 3.0 \times 15 = \times 110$.
With a deflection factor of 5.5 V_{rms}/cm (post-acceleration voltage +265 V), this corresponds, with amplifier, to a deflection factor of 50 mV_{rms}/cm. By switching over the anode resistor of valve 3, the deflection factor can be reduced to 15 mV_{rms}/cm and to a minimum of 5 mV_{rms}/cm (maximum gain thus $\times 1100$). No electronic stabilizing of the anode voltages is used; further boosting of the gain is not therefore expedient since, in consequence of the lower cut-off frequency of about 3 c/s, the amplifier becomes very sensitive to voltage surges. Electronic stabilization of the anode voltages for the vertical amplifier and the time base generator was not employed in this model, as measures of this kind exceed the scope of this design. Moreover, increasing use is being made of *AC* voltage stabilizers (e.g. Philips type 7776) with which the supply for an entire test layout can be made practically insensitive to interference from mains fluctuations.
When circuiting this amplifier, the rules regarding the earth connections for the frequency ranges concerned must be carefully observed. More stringent conditions apply than, for instance, in an *RF* resonance amplifier in radio receivers. The latter can come into unwanted oscillation with only one frequency, the tuned frequency, whereas a wide-band amplifier of the sort we are concerned with can become unstable quite arbitrarily within a range of less than 1 c/s to 15 Mc/s. It not infrequently occurs that very high frequency oscillations are set up in the first place which, after rectification, result in a lowering of the operating points of the valves and further in the appearance of extremely low-frequency relaxation oscillations. For these reasons, earth loops must be carefully avoided and all important points must be earthed at central points.
It is very difficult to achieve continuous control of the gain of vertical amplifiers. After extensive tests it was decided in this case to make the cathode

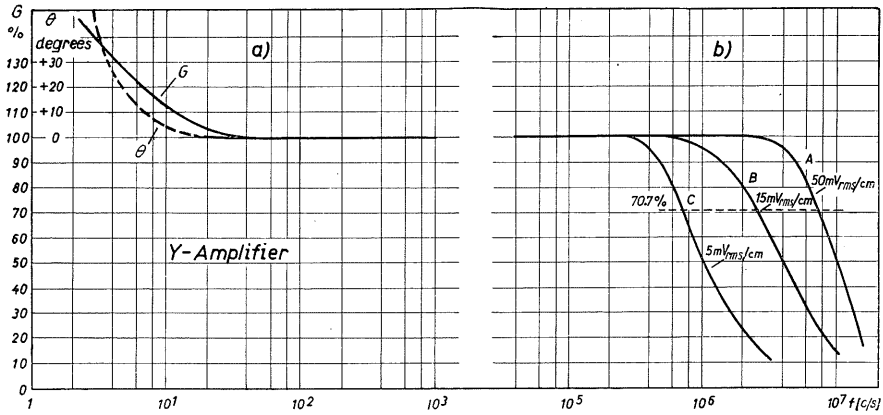

Fig. 21–16 Frequency response of vertical amplifier.
a) lower frequency limit with phase curve "θ"; *b*) upper frequency limit.

resistor of the pre-amplifier valve variable. This admittedly causes a certain fluctuation of the pattern during adjustment, but it has the advantage of being both simple and convenient.

The gain is reduced both by displacing the operating point for valve 2 in areas of reduced transconductance and by simultaneously increasing the negative feedback due to the cathode resistor. With a resistor (R_{14}) of max. 500 Ω, the gain can be stepped down about 3.5 : 1. This provides good bypassing of the stepped variation of the indication sensitivity, which is always in a ratio of 3 : 1. The potentiometer R_{14} has a logarithmic characteristic, so that the gain control is relatively linear with the angle of rotation [3].

For input voltages up to 15 V_{rms}, the reduction of gain for the desired amplitude of the pattern is effected by means of switch S_2, whereby appropriate voltages are taken from the cathode resistor. Higher input voltages must be fed in via socket "300 V" as already described. In this way, from 30 mV_{rms} for 60 mm deflection, all voltages up to 300 V_{rms} can be adjusted to any desired vertical deflection up to a maximum of 60 mm (see fig. 7–6*a* and *b*).

All essential working voltages or currents for the valves are detailed in the circuit diagram. Compensation at the lower frequency limit of the amplifier is effected by an *RC* network R_{16} — C_8 (3.3 kΩ — 50 μF) in the anode circuit of the first pre-amplifier stage (valve 2). The relatively high value of C_8 is to be explained by the low value of the anode resistor R_{15} (700 Ω). It should be noted that R_{16} has only a subordinate influence on the compensation. Since electrolytic condensers with the required favourable values are not always available, the final correction is made in this case by selecting the value of C_{10}, which, of course, also influences the frequency and phase response at the lower end [4, 5].

The curves in fig. 21–16*a* show the gain G and the phase-angle θ in dependence upon the frequency. It can be seen that, owing to the effect of the compensation network, the gain increases at the lower frequency end—as far as could be observed—as low as 3 c/s. (The voltage source used for the measurement was Philips *RC* generator "FE 211".)

The oscillograms in fig. 21–17 indicate the limits of efficiency of this amplifier with rectangular voltages. The photograph in *a*) represents a square wave with a frequency of 50 c/s while that in *b*) represents a rectangular voltage with a frequency of 250 kc/s, pulse width 2 μsecs. The overshoot visible in the latter originates from the voltage source itself. (See also fig. 7–3.) With a deflection factor of 15 mV_{rms}/cm, the maximum frequency for the true reproduction of a rectangular voltage is 50 kc/s. Owing to the high value of L_4, a peak is obtained with rectangular voltages down to several kc/s when

[3] A tandem potentiometer of 2 × 1000 Ω/log was used with both sliding arms connected in parallel, in order to reduce gain fluctuations during adjustment to a minimum.

[4] Most favourable results are obtained when the time constant of the coupling elements at the anode is small. This is why the coupling condenser C_{10} is rated at only 0.070 μF and not at 0.22 μF as for the other valves.

[5] The new, very small electrolytic condensers of 50 + 50 μF brought out by Philips proved most suitable for use in this apparatus. (The former types would have been difficult to accommodate because of their height.) They were used for C_6, C_8, C_{14} and C_{19}. (See figs. 21–2 and 21–7.)

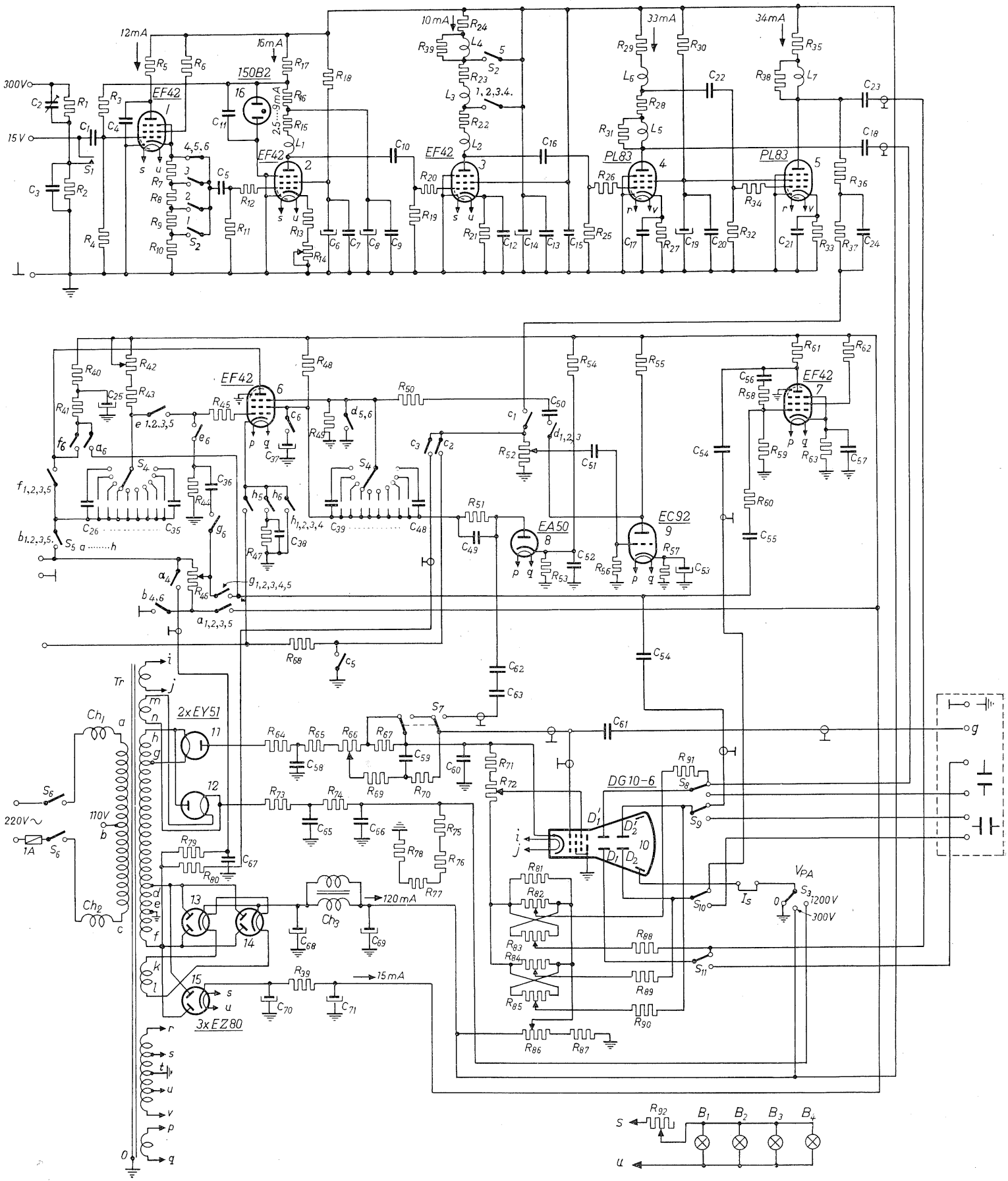

Fig. 21–15 Main circuit diagram of FTO-2.

the deflection factor is 5 mV_{rms}/cm. This setting is therefore less suitable for square waves.

Horizontal deflection: Time base generator.

The maximum desirable velocity of the time base.

When the vertical amplifier is in use, its upper frequency limit indirectly determines the maximum expedient velocity of the time base. There would be little point, for instance, with a vertical amplifier whose frequency dependence is as shown in curve *A*, fig. 21–16*b*, in having a maximum time base frequency of $^1/_{10}$ of the upper frequency limit, that is, about 750 kc/s, if one wishes to observe in detail the waveform of a voltage with a frequency of 7.5 Mc/s (10 cycles in the oscillogram). The waveform is, after all, only interesting when it deviates from a sine wave, that is to say when it contains harmonics. However, since these are always multiples of the fundamental frequence, they are severely suppressed in consequence of the frequency-dependence of the amplifier at the upper frequency end; the vertical amplifier then acts as a low-pass filter. This means that harmonics which, as a rule, have only a fraction of the amplitude of the fundamental, will not be visible at all. Nothing would therefore be gained by a high time base velocity, since only sine waves would appear on the screen of the oscilloscope [6].

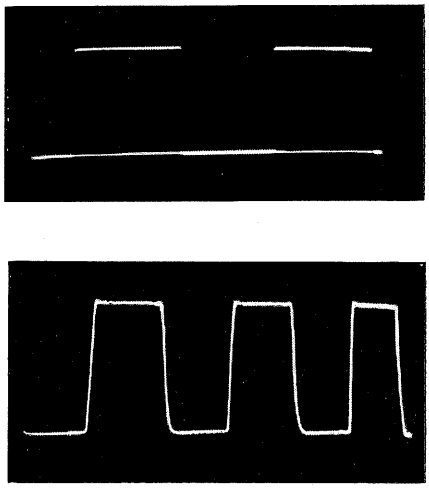

Fig. 21–17 Limits of efficiency of vertical amplifier with rectangular voltages. *a*) 50 c/s *b*) 250 kc/s.*
* The slight non-linearity visible only occurs in the end position of the time base fine frequency control. The voltage waveform is linear below 50 kc/s time base frequency.

With these considerations in mind the greatest attention was devoted to the vertical amplifier when constructing "FTO 2", and the transitron-Miller circuit was employed for the time base generator. This allows a maximum time base frequency of 100 kc/s. By taking advantage of the flyback blanking, the visible section of the pattern can be made somewhat shorter than would correspond to the frequency ($< 10\ \mu$sec). The oscillogram in fig. 21–17*b*, represents a time base velocity of $1^1/_4\ \mu$s/cm.

[6] If the input signal is large enough to produce satisfactory deflections when applied directly to the vertical deflection plates, then, of course, a time base generator with a high velocity can indeed be of value.

Circuitry.

The way in which the transitron-Miller circuit functions was dealt with in detail in chapter 4 on time base generators (page 62) to which reference should be made. Switching over condensers C_L and C_1 in the basic circuit diagram given in fig. 4–34 (in fig. 21–15, C_{26}–C_{35} and C_{39}–C_{48}) provides coarse control of the time base frequency. Fine adjustment is effected by varying the resistor between grid and anode supply (R_{42} in fig. 21–15). A range from 1.2 c/s to 100 kc/s is thus obtained in the following steps:

1.2 c/s	10 c/s	0.17 kc/s	1.1 kc/s
3 c/s	25 c/s	0.47 kc/s	3.0 kc/s
6 c/s	40 c/s	1.7 kc/s	10.0 kc/s
15 c/s	100 c/s	5.0 kc/s	30.0 kc/s
45 c/s	350 c/s	15.0 kc/s	100.0 kc/s.

The amplitude is controlled by taking different amplitudes of voltage from the anode resistor of the oscillator, using a potentiometer (R_{46}) and applying them via condenser C_{64} to the X plate D'_2 and simultaneously via condenser C_{55} and resistor R_{60} to the grid of the second valve, EF 42. This valve is in circuit as an "anode follower" [1]. By this is understood a grounded cathode amplifier stage with such large negative feedback that its gain is equal to unity. As opposed to the cathode follower, whose output is in phase with its input, the output of the anode follower is inverted in phase as in all grounded cathode circuits. It serves this purpose in the present circuit. The strong negative feedback enables relatively large amplitudes of the sawtooth voltage to be passed without distortion. The output is taken from its anode and applied via condenser C_{54} to the X plate D_2, thus achieving symmetrical operation of the deflection plates for the horizontal direction also. Since the voltage from the oscillator is doubled by the inverter stage, amplitudes of voltage are obtained sufficient to deflect the spot horizontally 50% beyond the useful surface of the screen. This makes possible a relatively large expansion of the oscillogram along the time axis and thus an exact observation of details in the waveform.

Synchronization.

The sync voltage is fed to the third grid. To keep the load (also capacitive) on the output of the vertical amplifier as low as possible during internal synchronization, a special sync amplifier stage is provided (triode EC 92).
Three types of synchronization are carried out with this:

a) With the voltage on the Y plates.
The voltage from the anode of valve 5 reaches potentiometer R_{52} via resistors R_{36} and R_{37} and condenser C_{24}. The grid of valve 9 thus receives an adjustable portion of the input signal.

b) With an external frequency.
Contact c_1 is interrupted. From the socket "sync", the voltage of an external source then passes via contact c_2, now closed, to potentiometer R_{52} and thence to the grid of valve 9 for amplification, after which it is used for synchronization.

c) With the mains frequency.
Contacts c_1, c_2 are interrupted and c_3 is closed, so that a small amplitude of the mains voltage reaches potentiometer R_{52} over R_{80}.

Suppressing the flyback: trace brightening.

In this oscillator circuit there is no voltage available on the individual electrodes that can be used directly for blanking the flyback. However, the course of the voltage on grid 2 during the time when the voltage on the anode is linearly falling is almost constant in the positive direction, so that it is suitable for *brightening* the trace. (See fig. 4–35*b*). To ensure that the trace-brightening will really be constant, this voltage is clipped by diode EA50 (see fig. 4–35*c*). Its cathode therefore receives a positive voltage of about 150 V from the voltage divider R_{53}—R_{80}.

Single-stroke time base.

To be able to observe the behaviour of single transients it must be possible to trigger the time base for one cycle only. This is effected in the following way The third grid of the relaxation oscillator is tied to earth (contact d_5). The cathode of this valve now lies across earth via contact h_5, resistor R_{68} and contact c_5, so that g_1 carries a large negative potential and the valve is cut off from oscillation. If now the sync socket is connected for a brief period to earth by means of a contact or a key, the time base can be released for a single sweep.

Horizontal amplifier.

Apart from the observation of one quantity in its dependence upon time, there are numerous instances when the interdependence of two quantities is primarily of interest. In phase measurements, for example, the voltages corresponding to the two phenomena are applied to both pairs of deflection plates in the cathode ray tube. In such cases it is often desirable to be able to amplify the voltage for deflection along the horizontal axis. In the oscillo-

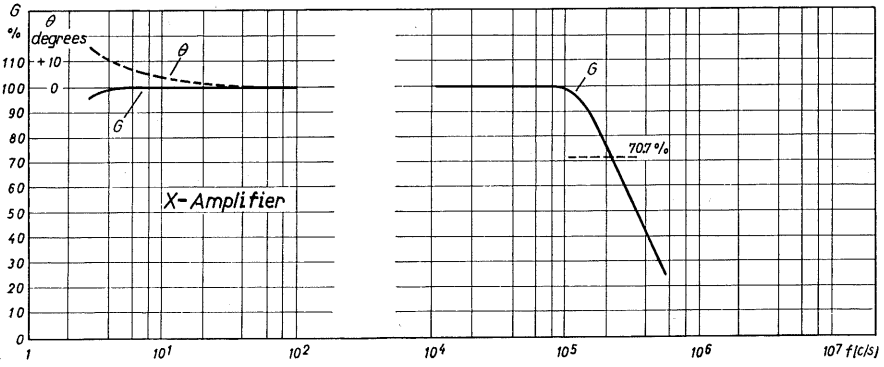

Fig. 21–18 Frequency response of horizontal amplifier.

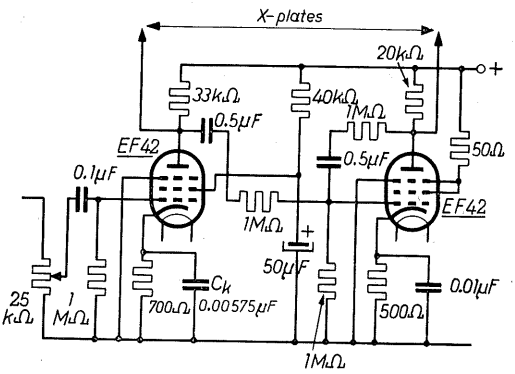

Fig. 21–19 Basic circuit diagram of horizontal amplifier.

scope under discussion this is done by providing a means of switching over a valve to work together with valve 7 as a symmetrical amplifier. To keep the number of elements to be switched over to a minimum, it was found necessary to use a part of those in the oscillator circuit, which meant that entirely optimum working conditions could not be obtained for this amplifier. Nevertheless, with the circuit elements used, it was possible to obtain a frequency response as shown by the curve in fig. 21–18. The smallest possible deflection factor is 125 mV_{rms}/cm. The circuit for the horizontal amplifier is shown individually in fig. 21–19. The input impedance is: 25 kΩ, 55 pF.

Sinusoidal horizontal deflection with the mains frequency.

In position 4 of switch S_5 (contact $b_{1,\ 2,\ 3,\ 5}$), the time base generator is wholly switched off and a voltage with the mains frequency is fed via contact a_4, potentiometer R_{46}, contact g and resistor R_{79}, to deflection plate D'_2 and via the phase inverter, valve 7, to D_2. Since the secondary voltage of the power transformer is distorted by the pulsed loading of the anode winding during the charging current on the first filter condensers, the harmonics must be filtered out with R_{79} and C_{67} in order to obtain a really sinusoidal 50 c/s X deflection.

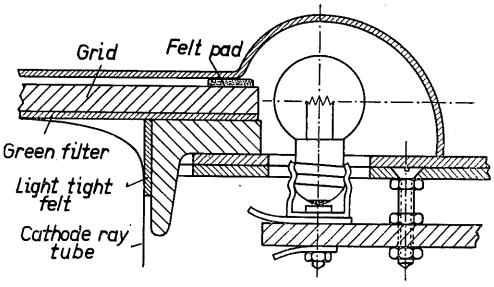

Fig. 21–20 Arrangement of illumination bulbs and floodlit scale.

Floodlit scale.

As already mentioned, this oscilloscope is fitted with a floodlit scale. The light from the illumination bulb falls sideways on to the perspex, as indicated by the sketch in fig. 21–20. Further details are hardly necessary, the principle being the same as used nowadays in most radio receivers. The arrangement on the screen of the cathode ray tube is shown in figs. 21–1 and 21–6. The only feature to which attention should be drawn is that a yellow-green filter must always be fitted between the "perspex" scale and the screen. The scale on the sheet of "perspex" was originally scratched in by the author. When done carefully, and if the requirements are not too high, a scale of this sort should generally suffice. The "perspex" scale together with the light-shield and the arrangement of the

illumination bulbs (B_1—B_4) around the screen can be recognized clearly in fig. 21–6. After many experiments it was found preferable, for the sake of uniform illumination of the scale, to use four bulbs 6.3 V/0.3 A. If the available space allows it, it is advisable to arrange the four bulbs diametrically on the co-ordinates. The light from the bulbs in the example described is sufficient, using Pan film of 21/10° DIN with a reduction of 3 or 4 : 1, an aperture of 4.0 and an exposure of $^1/_2$ sec, to obtain an amply exposed scale. It is still sufficient at an exposure of $^1/_5$ sec. Since these conditions are similar to those required for recording most oscillograms, the scale and the oscillogram can be photographed simultaneously in one recording. If this is not possible, oscillogram and scale must be exposed individually, under the conditions most favourable to each, as a double recording.

Mains transformer.

Fig. 21–21 shows the windings on the special transformer used in this model.

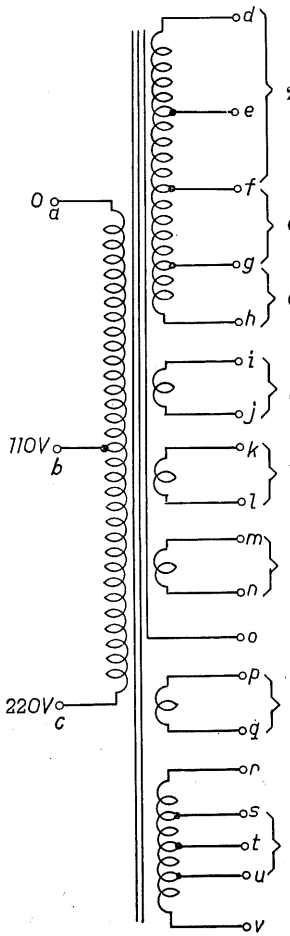

Fig. 21–21 Power transformer used in oscilloscope FTO 2.

2 × 270 V/135 mA		*DC* voltage for anodes in vertical amplifier and timebase generator
650 V/2.5 mA		with *e-f* for extra high tension-1200 V for C.R.T. (DG 10–6)
6.3 V/0.1 A		Heating for E.H.T. rectifier EY51. (–1200V = with respect to chassis!)
6.3 V/0.3 A		Heating for C.R.T. (DG 10–6)
12.6 V/0.6 A		Heating for H.T. rectifiers 2 × EZ 80 (filaments in series)
6.3 V/0.1 A		Heating for E.H.T. rectifier EY51 (± 1200 V with respect to chassis and 2400 V with respect to "g").
Screen winding		
6.3 V/1.0 A		Heating for time base generator.
6.3 V/2.0A*	15.0 V/0.6A	Heating for vertical amplifier 3 × EF 80 and 2 × PL 83.

* Also for scale illumination bulbs

Parts List

a) Resistors

R_1 = 5 MΩ/0.5 W; ± 2%
R_2 = 0.3 MΩ/0.25 W; ± 2%
R_3 = 8.8 MΩ (5.0 MΩ/1 W + 3.8 MΩ/1W, selected)
R_4 = 1.5 MΩ/0.25 W
R_5 = 50Ω/0.25 W
R_6 = 100Ω/0.25 W
R_7 = 1,33 kΩ/0.5 W
R_8 = 467Ω/0.25 W
R_9 = 133Ω/0.25 W
R_{10} = 67Ω/0.25 W
} ; select experimentally to ± 2%
R_{11} = 1.0 MΩ/0.25 W
R_{12} = 50Ω/0.25 W
R_{13} = 100Ω/0.25 W
R_{14} = 500Ω, Potentiometer 2 × 1000Ω/log. parallel
R_{15} = 700Ω/1.0 W
R_{16} = 3.3 kΩ/2.0 W
R_{17} = 6.0 kΩ/3.0 W
} ; select experimentally to ± 2%
R_{18} = 1.5 kΩ/1.0 W
R_{19} = 1.0 MΩ/0.25 W
R_{20} = 100Ω/0.25 W
R_{21} = 100Ω/0.25 W
R_{22} = 750Ω/1.0 W
R_{23} = 1.8 kΩ/2.0 W
R_{24} = 5.5 kΩ/3.0 W
} ; select experimentally to ± 2%
R_{25} = 1.0 MΩ/0.25 W
R_{26} = 50Ω/0.25 W
R_{27} = 90Ω/1.0 W
R_{28} = 1.32 kΩ/4.0 W (2 resistors 2.66 kΩ/2 W parallel)
R_{29} = 180Ω/1.0 W
} select exp. to ±2%
R_{30} = 3.3 kΩ/2.0 W
R_{31} = 2.0 kΩ/0.25 W
R_{32} = 1.0 MΩ/0.25 W
R_{33} = 90Ω/1.0 W
R_{34} = 100Ω/0.25 W
R_{35} = 1.5 kΩ/4.0 W (2 resistors 3.0 kΩ parallel); select experimentally to ± 2%
R_{36} = 50 kΩ/1.0 W
R_{37} = 1.0 MΩ/0.5 W
R_{38} = 2.0 kΩ/0.25 W
R_{39} = 2.0 kΩ/0.25 W
R_{40} = 20 kΩ/2 W
R_{41} = 33 kΩ/2 W
R_{42} = Potentiometer 3 MΩ/lin; 1 W
R_{43} = 0.3 MΩ/1 W
R_{44} = 1.0 MΩ/0.25 W
R_{45} = 100Ω/0.25 W
R_{46} = Potentiometer 25 kΩ/lin; 2 W
R_{47} = 700Ω/0.5 W
R_{48} = 40 kΩ/1.0 W
R_{49} = 20 kΩ/0.5 W
R_{50} = 100 kΩ/1.0 W
R_{51} = 220 kΩ/1.0 W
R_{52} = Potentiometer 100 kΩ/lin; 0.5 W
R_{53} = 100 kΩ/1 W
R_{54} = 100 kΩ/1 W
R_{55} = 4.7 kΩ/2 W
R_{56} = 1 MΩ/0.25 W
R_{57} = 160Ω/0.25 W

R_{58} = 1 MΩ/0.25 W
R_{59} = 1 MΩ/0.25 W
R_{60} = 1 MΩ/0.25 W
R_{61} = 20 kΩ/2 W
R_{62} = 50 Ω/0.25 W
R_{63} = 500 Ω/0.25 W
R_{64} = 20 kΩ/2 W
R_{65} = 27 kΩ/2W
R_{66} = Potentiometer 25 kΩ/lin; 0.5 W
R_{67} = 500 Ω/1 W
R_{68} = 20 kΩ/1 W
R_{69} = 1 MΩ/0.25 W
R_{70} = 0.1 MΩ/0.25 W
R_{71} = 80 kΩ/1 W
R_{72} = Potentiometer 0.5 MΩ/lin; 1 W
R_{73} = 20 kΩ/2 W
R_{74} = 500 kΩ/2 W
R_{75} = R_{76} = R_{77} = R_{78} = 7.5 MΩ/0.5 W
R_{79} = 50 kΩ/2 W
R_{80} = 6.8 MΩ/1.0 W
R_{81} = 100 kΩ/1 W
R_{82} = R_{83} = R_{84} = R_{85} = two tandem potentiometers, each 2 × 2 MΩ/lin; 1 W
R_{86} = Potentiometer 25 kΩ/lin; 0.5 W
R_{87} = 500 kΩ/2 W
R_{88} = R_{89} = R_{90} = R_{91} = 3 MΩ/0.5 W
R_{92} = Wire-wound variable resistor 10 Ω/lin; 2.5 W

b) Condensers

C_1 = 0.22 µF/250 V=; paper (quality grading 1)
C_2 = ceramic tube trimmer Philips max. 8 pF
C_3 = 60 pF; ceramic
C_4 = 5 kpF; ceramic
C_5 = 0.22 µF/250 V=; paper
C_6 = 50 µF/350 V=; electrolytic (1 kpF = 1000 pF = 0.001 µF.)
C_7 = 5 kpF/350 V; ceramic
C_8 = 50 µF/350 V=; electrolytic
C_9 = 5 kpF/350 V=; ceramic
C_{10} = 50 kpF/350 V=; paper (quality grading 1)
C_{11} = 5 kpF; ceramic condenser (C 4000)
C_{12} = 150 pF; ceramic
C_{13} = 5 kpF; ceramic
C_{14} = 50 µF/350 V= electrolytic condenser
C_{15} = 5 kpF; ceramic
C_{16} = 0.22 µF; paper (quality grading 1)
C_{17} = 530 pF; ceramic
C_{18} = 0.5 µF/350 V=; metal paper
C_{19} = 50 µF/350 V=; electrolytic
C_{20} = 5 kpF; ceramic
C_{21} = 530 pF; ceramic
C_{22} = 0.22 µF; paper
C_{23} = 0.5 µF/350 V=; metal paper
C_{24} = 500 pF; ceramic
C_{25} = 50 µF/350 V=; electrolytic
C_{26} = 0.25 µF/350 V=; metal paper
C_{27} = 0.1 µF/850 V=; metal paper
C_{28} = 50 kpF/350 V; paper
C_{29} = 20 kpF/350 V; paper
C_{30} = 6 kpF/350 V; ceramic
C_{31} = 2 kpF/350 V; ceramic
C_{32} = 700 pF/350 V; ceramic

C_{33} = 220 pF/350 V; ceramic
C_{34} = 70 pF/350 V; ceramic
C_{35} = 10 pF/350 V; ceramic
C_{36} = 0.1 μF; paper
C_{37} = 50 μF/350 $V_{=}$; electrolytic
C_{38} = 5750 pF; ceramic (selection or combination)
C_{39} = 2.0 μF/350 $V_{=}$; metal paper
C_{40} = 0.5 μF/350 $V_{=}$; metal paper
C_{41} = 0.25 μF/350 $V_{=}$; metal paper
C_{42} = 0.1 μF/350 $V_{=}$; metal paper
C_{43} = 30 kpF/350 $V_{=}$; paper
C_{44} = 10 kpF/350 $V_{=}$; ceramic
C_{45} = 5 kpF/350 $V_{=}$; ceramic
C_{46} = 1 kpF/350 $V_{=}$; ceramic
C_{47} = 500 pF/350 $V_{=}$; ceramic
C_{48} = 250 pF/350 $V_{=}$; ceramic
C_{49} = 50 pF; ceramic
C_{50} = 0.5 μF/350 $V_{=}$; paper
C_{51} = 10 kpF/250 $V_{=}$; ceramic
C_{52} = 2 μF/250 $V_{=}$; metal paper
C_{53} = 50 μF/350 $V_{=}$; electrolytic
C_{54} = 0.5 μF/350 $V_{=}$; metal paper
C_{55} = 0.5 μF/350 $V_{=}$; metal paper
C_{56} = 0.5 μF/350 $V_{=}$; metal paper
C_{57} = 10 kpF; ceramic
C_{58} = 1 μF/1.6 $kV_{=}$; paper
C_{59} = 0.1 μF/150 $V_{=}$; metal paper
C_{60} = 1 μF/1.6 $kV_{=}$; paper
C_{61} = 0.1 μF/1.2 kV; paper
C_{62} = C_{63} = 0.25 μF/500 $V_{=}$; metal paper
C_{64} = 0.5 μF/500 $V_{=}$; metal paper
C_{65} = C_{66} = 0.1 μF/1.6 kV; paper
C_{67} = 0.15 μF/500 $V_{=}$; metal paper (0.10 + 0.05 μF)
C_{68} = C_{70} = 50 μF/350 $V_{=}$; electrolytic
C_{69} = 100 μF/350 $V_{=}$; electrolytic
C_{71} = 50 μF/350 $V_{=}$; electrolytic

c) Chokes

Ch_1 = Ch_2 = RF chokes
Ch_3 = 4 H/100Ω (Iron-core with air gap) Görler D 524 B
L_1 = 6 μH;
L_2 = 6 μH;
L_3 = 75 μH;
L_4 = 1.25 mH
L_5 = 13 μH
L_6 = 7 μH
L_7 = 20 μH
} Air choke on ceramic tube

d) Transformer

Tr = Special construction as in fig. 20–21; Görler Nr. 47648; M 102b

e) Valves

1 = 2 = 3 = EF 42
4 = 5 = PL 83
6 = 7 = EF 42
8 = EA 50[1]
9 = EC 92
10 = DG 10–6
11 = 12 = EY 51
13 = 14 = 15 = EZ 80
16 = 150 B 2
} Philips

[1] Alternatively, type EAA 91 (EB 91)

22. Simple time base expansion unit

for displaying phenomena with the mains frequency and mains-coupled television pulses.

A very simple time base expansion unit can be built if the demands made upon it are restricted to the display of phenomena having the frequency of the mains or of phenomena synchronized with the mains frequency, as, for instance, television pulses from mains-coupled transmitters. The *AC* mains voltage, which can easily be stepped up and controlled in phase, can be used for the time base deflection.

Circuitry

The simplified circuit of the apparatus is represented in fig. 22–1. The series arrangement of a condenser C_1 and a resistor R_1 lies across an auto-transformer connected directly to the mains. This circuit, which is also known from descriptions of grid-controlled current gating circuits [1], has the characteristic

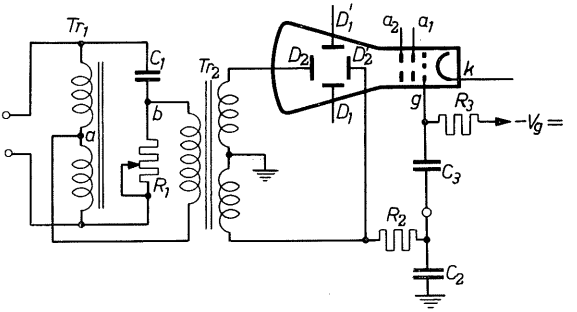

Fig. 22–1 Basic lay-out of simple time base expansion unit.

that by varying R_1, the vector of the voltage on points a and b can be changed in phase by almost 180°, while the amplitude—and this is the great advantage of the circuit—remains practically constant.

This voltage is applied to the primary of transformer Tr_2, where it is stepped up, the high voltage on the secondary serving to deflect the spot along the X axis. A voltage is taken from the appropriate pole of the secondary and fed through an RC network R_2, C_2 where it is shifted in phase by 90° and, at the same time, reduced in amplitude such that, when impressed upon the grid of the C.R.T. (via condenser C_2) it brightens one half cycle of the trace and suppresses the other half cycle.

The higher the deflection voltage on the X plates, the greater is the expansion of the voltage on the Y plates. By changing the phase with R_1, any desired section from the whole cycle of a pulse train or the like can be accurately adjusted on the screen. By additionally reversing the polarity of the deflection voltage it is possible to shift the phase by a total of 360°.

Details of the practical circuit are shown in fig. 22–2. In the model constructed by the author, the primary of the mains transformer from a radio receiver, with a tap for 110 V, was used as the auto-transformer. The potentiometer

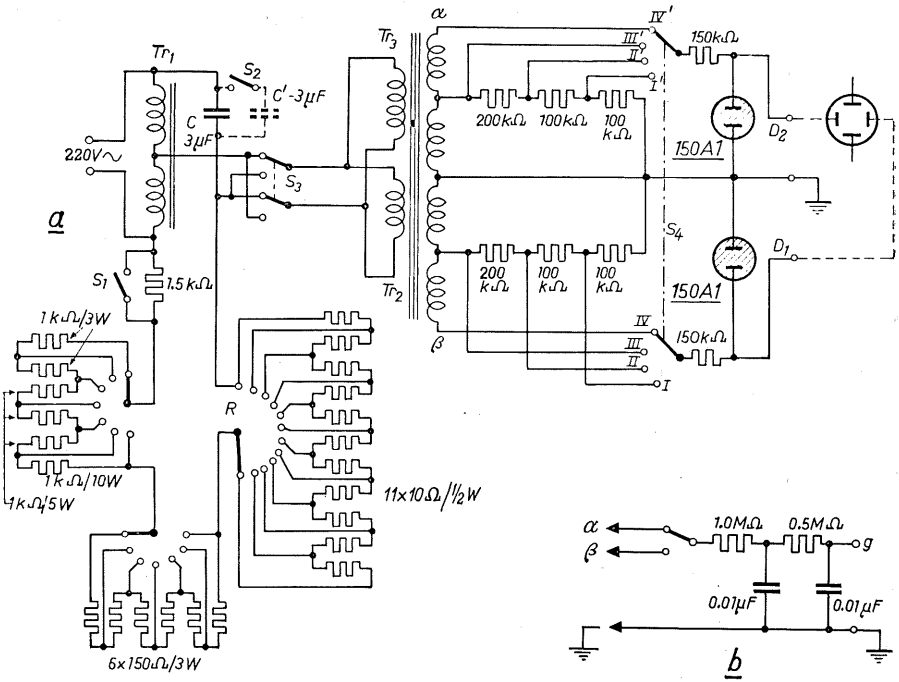

Fig. 22–2 Circuit of simple time base expansion unit: *a*) deflection generator; *b*) phase-shifting circuit for intensity modulation.

for shifting the phase should have a logarithmic characteristic and should be initially rated for a heavy loading-current. Variable resistors of this sort are difficult to obtain, so that in this case the change of resistance is effected by switching over three and four groups of fixed resistors respectively. It is particularly important for the first resistor in the 1 kΩ group to be rated for a high load (about 0.1 A) and condensers C and C' must be able to withstand continuously the relatively high reactive current which, at 220 V potential, can amount to a maximum of 0.2 A in each case. In order to approach as nearly as possible the theoretically obtainable phase-shift of 180°, a resistor of 7.5 kΩ is connected in series with the three groups of resistors; this can be short-circuited by switch S_1. If a condenser C' also of 3μF is connected to condenser C together with switch S_2 (not absolutely necessary) the phase shift of 180° can be achieved to within a few degrees (with switch S_3 therefore $2 \times 180° = 360$). For stepping up the phase-shifted voltage a transformer is required with the highest possible input impedance and transformation ratio. But these two requirements contradict each other. In this unit, therefore, the primaries of two transformers are connected in parallel and their secondaries in series. An intermediate transformer from a power amplifier was used with a transformation ratio of $1 : 2 \times 2$. (A special transformer for this purpose could, if desired, be tuned to 50 c/s by suitable capacitors connected in parallel.) To be able rapidly to find the interesting part of a whole cycle from a phenomenon with unknown phase relationships, it was found expedient to have a means of redu-

cing the time base expansion at the beginning of the investigation. This purpose is served by the double-pole switch S_2, by means of which the X plates can be connected either to the maximum voltage or in three steps to one half of the preceding voltage in each case. The first division is effected by switching to the centre taps on the secondaries of both transformers. For further reduction of the deflection voltage two resistive voltage dividers are used, which on the one side are connected to the centre taps and on the other to the chassis. Voltage gradations are thus obtained as shown in the oscillogram in fig. 22–3*a*. The values of the alternating voltages in the individual steps I.....IV are approximately: 80, 160, 320 and 640 V_{rms}. Since, in most oscillosocopes, the maximum permissible voltage for external deflection is 500 V_{rms}, the voltage peaks are clipped in this circuit by connecting two discharge lamps over series resistors of 150 kΩ parallel to the output terminals.

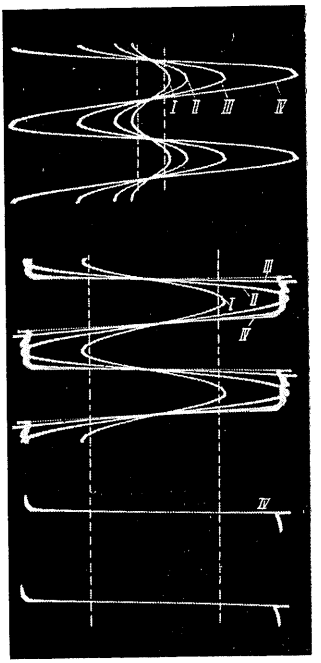

Fig. 22–3 Oscillograms of 50 c/s time-base voltage.

The lamps used are of the "150 A1" type with an operating voltage of 150 V and a maximum stabilizing current of 4 mA. The output peak voltage is then limited to twice the value of the operating voltage of the lamps, as illustrated by the oscillograms in fig. 22–3*b* for the voltage steps I–IV. The voltage sufficient to produce a satisfactory deflection in tube DG 10–6 in Philips oscilloscope GM 5663 (without external post-acceleration) is indicated by broken lines. To obtain only one trace, the flyback is suppressed by a voltage, shifted 90° with respect to the deflection voltage, applied to the grid of the cathode ray tube. The circuit is represented in fig. 22–2*b*. The phenomenon under investigation can also be observed on the flyback, the forward trace being this time suppressed. This is done by switching over the trace-brightening voltage to points α and β of the maximum voltage. Thus, one half cycle of the clipped voltage is brightened and the other suppressed, as can be seen in the oscillogram in fig. 22–3*c* for two cycles of voltage step IV. Naturally, the luminous intensity of the oscillogram is lower than that of a normal oscillogram, since the spot is on the screen for a mere fraction of a whole cycle. It is therefore expedient to use for this purpose a tube with a post-acceleration of 1–2 kV (e.g. DN 9–5, DN 10–5, DG 10–6). The built-in post-acceleration voltage source of 400 V in the GM 5663 is sufficient for direct observation.

With oscilloscope "FTO–2", which can also be used with advantage, it is only necessary to switch over to 1.2 kV post-acceleration. The brightness of the pattern on the screen is then quite sufficient for maximum time base expansion.

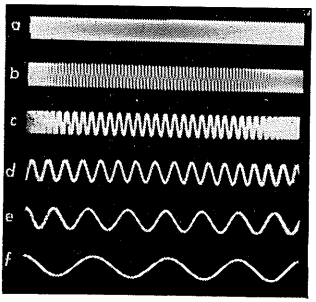

Fig. 22–4 Oscillograms of a 5000 c/s voltage: *a*) time base 25 c/s; *b*) time base 50 c/s; *c*) *d*) *e*) and *f*) expanded time-base in steps I, II, III and IV.

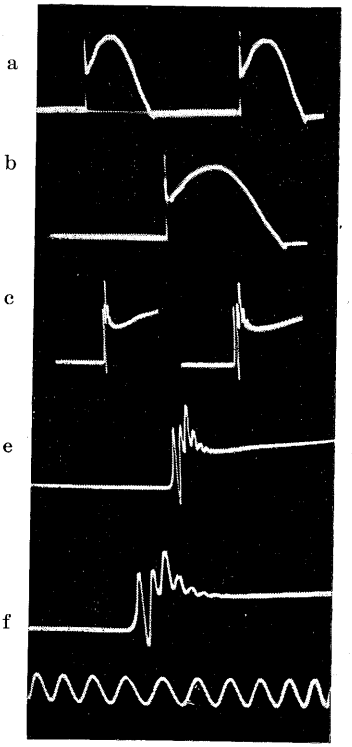

Fig. 22–5 Oscillograms of a half-wave rectified 50 c/s voltage on an inductive load: *a*) time base 25 c/s; *b*) time base 50 c/s; *c*), *d*), *e*) and *f*) expanded time-base in steps I, II, III and IV; time marking with 10,000 c/s.

Practical applications of the time base expansion unit.

To illustrate the time base expansion obtainable in comparison with normal oscillograms, a series of patterns of a 5000 c/s voltage under differing conditions is set out in fig. 22–4. In *a* the voltage is shown in the usual way for a 50 c/s pattern with a linear time base voltage of 25 c/s. Two hundred cycles thus fill the whole width of the screen. The individual alternations lie so close together that only a band of light is visible, without details. For the oscillogram in *b* the time base frequency is 50 c/s, which would allow the display of one whole cycle of the mains frequency; in this instance therefore, one hundred cycles of the 5000 c/s frequency are accommodated on the screen. Some individual cycles can now be discerned, in the centre at least.

The remaining oscillograms in fig. 22–4 represent the patterns produced by expanding the 5000 c/s voltage along the time axis with the 50 c/s voltage of the time base expansion unit in the four steps I, II, III and IV. In fig. 22–4*c* the curves crowd together at both ends of the oscillogram, corresponding to the sinusoidal deflection (Lissajous figure).

Step II produces, as can be seen in *d*, a deflection across the screen almost linear with time, since only the nearly linear part of the sine wave falls to the visible deflection. The total picture width with $16^1/_2$ cycles of 5000 c/s corres-

ponds to a period of time of about 3.3 ms, that is to say a sixth of the whole cycle (20ms) of a normal 50 c/s deflection.
In step III (oscillogram *e*), $7^3/_4$ cycles are obtained, representing 1.6 ms and thus one thirteenth of the whole deflection cycle. The final oscillogram in *f* (step IV) represents the greatest enlargement of signal possible with this apparatus. With four cycles of 5000c/s on the screen, the whole width of the display corresponds to a time of only 0.8 ms and thus to a section of one twenty-fifth of the total trace with normal 50 c/s deflection. In other words the signal has been expanded by twentyfive along the time axis as compared with the picture of a whole cycle.

Application for expanding the display of 50 c/s phenomena.

The oscillograms in fig. 22–5*c*, *d*, *e* and *f* reproduce the four steps of expansion obtainable with this simple unit for the normal oscillograms shown in 22–5*a* and *b*. The waveform in question represents the voltage on a load with strong inductive components in the circuit of a mercury vapour rectifier. As can be seen from *a*, the waveform is fundamentally that of a half-wave rectified voltage, except that it begins with a very steep rise. Examining the single cycle shown in *b* one might well assume that it was a matter of a simple voltage peak with no oscillations in it. Absolute certainty and a clear insight into the details of the peak can only be obtained by considerably greater expansion of the signal along the time axis. To get the interesting part into the centre of the screen—*e* and *f*—it was necessary to adjust the phase of the time base voltage. To provide a time scale, the pattern of a 1000 c/s alternating voltage was recorded at the same time and can be seen below the oscillogram in *f*.
It now becomes quite clear that an oscillatory phenomenon lay concealed in this "peak". The frequency of the oscillation can be calculated fairly accurately from the time scale at 35,000 c/s, that is, the 700th harmonic of the fundamental. (This oscillation also remained stationary on the screen.)

Application in television pulse technique.

In fig. 22–6 the form of the frame sync pulse from Philips' small television signal generator GM 2887C is displayed for examination, with particular reference to the vertical blanking. Fig. 22–6*a* shows in the usual way two pulse trains at a time base frequency of 25 c/s and in *b* one pulse train is shown on a linear time base of 50 c/s. The oscillograms in c, *d* and *e* represent expansions in steps I, II and III respectively. In *e* it is already possible to perceive the "content" of the frame blanking pulse with the line sync pulses and the width of the frame sync pulse proper. The pattern only just includes the whole width of the frame blanking. As a result of the great expansion in step IV the whole picture is filled out by about 15 to 16 line pulses, so that still further details are made visible. To investigate the entire frame blanking, it is necessary to proceed in sections by shifting the phase. A number of such sections of the pulse train are joined together in fig. 22–7 in such a way

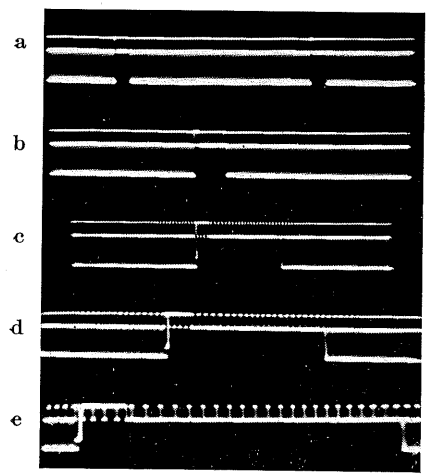

Fig. 22–6 Composite signal from Philips television signal generator GM 2887 *C* with vertical blanking: *a*) time base 25 c/s; *b*) time base 50 c/s; *c*), *d*), and *e*) expanded time base in steps I, II and III.

as to produce a complete oscillogram of the whole of the frame blanking. (Its total width corresponds to somewhat more than three separate recordings.)

At the beginning and end of this oscillogram a number of line pulses are visible with "picture content". This consists here of a rectangular voltage, which supplies $6^1/_2$ vertical bar pulses in the television picture. Four such "lines" are reproduced, optically magnified, in fig. 22–8*a* and, for the sake of comparison, fig. 22–8*b* shows the usual oscillogram of two lines with the same content. Since, in the small signal generator, the line frequency is not coupled with the frame frequency, the line pulses drift for the most part over the screen. To record them photographically, therefore, a moment had to be chosen when they had become stationary. Fig. 22–9 reproduces (step IV expansions joined together in the same way) the pulse pattern of the test

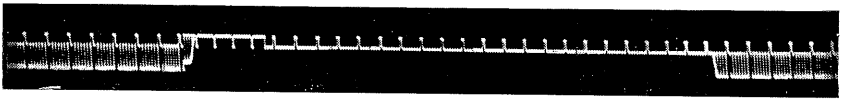

Fig. 22–7 The whole vertical blanking pulse from the GM 2887 *C*, expanded in step IV. Several recordings, with different phase of time base voltage, joined together.

transmission from West Berlin (see fig. 15–38). The voltage was taken from the video output of Philips' table receiver "TD1410 U" (In this case the ratio of amplitude of the sync pulses to video content is not according to standard.) Since the time base frequency is 50 c/s, and thus corresponds to the vertical frequency, whereas the transmitter is sending out pulses for the line interlace,

both fields of the frame, with their line pulses phase-shifted by 180°, are obtained one above the other. The sequence of the line pulses appears at half pulse spacing. This can be recognized from the fact that the oscillogram of the line pulses is not, as in fig. 22–7, open underneath, but is in each case covered over at the height of the blanking level. The equalizings are clearly perceptible in the standard composite signal; their edges appear a little brighter than the line pulses themselves.

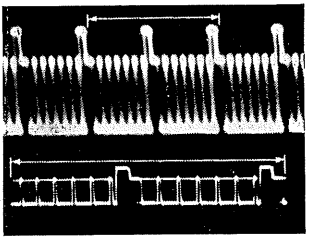

Fig. 22–8 Line pulse from the GM 2887 *C*, as in oscillogram 22–7: *a*) enlarged section of line pulse before blanking pulse; *b*) normal oscillogram of two lines with the same "bar" modulation as in *a*.

Displaying the pulse sequences of both fields of a television frame.

In order to build the simplest possible unit, one which would work without a *DC* supply section, the time base frequency was limited, as emphasized at the outset, to the mains frequency. In consequence of this, however, the two fields of the television frame overlap since, of course, they occur at 50 c/s. They can be displayed separately by periodically switching over the time base, with the aid of a rectangular voltage, to two different heights on the screen (similar to the action of an electronic switch).

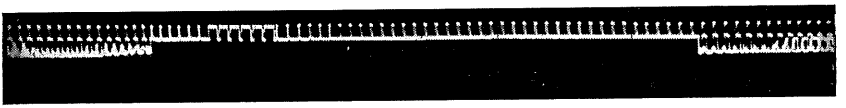

Fig. 22–9 Blanking pulse from west Berlin television transmitter.

If the switching frequency is accurately set to 25 c/s, then one field will be traced at a higher level during the one half cycle of the switching frequency and the other field lower during the other half cycle.
This is the manner in which the Philips time base expansion unit GM 4584 works, described on page 77.
Further oscillograms obtained using the unit described in the present chapter are to be found in chapter 15, "Investigations on television receivers".

CONCLUSION

The cathode ray oscilloscope is finding steadily increasing application in all branches of engineering and has become an indispensable tool in workshop and laboratory alike. Nevertheless, experience repeatedly confirms that the great variety of uses to which this versatile measuring apparatus can be put are only seldom fully realized and exploited. More often than not its application is restricted to a small number of tasks for which the oscilloscope is, in any case, the only solution.

With this in mind, the author has devoted considerable space to practical examples, particularly to measurements on television receivers, showing how the use of time base generators for extreme expansion of the display enables far more details of a signal to be observed than is possible with a normal oscillogram. The various ways in which the oscilloscope is able to solve a given problem of measurement have been discussed in detail, and special attention has been devoted in each case to the methods of interpreting and evaluating the results. The reader will find reference to further possibilities and special measurements in the bibliography to the individual chapters.

The measurements described deal mainly with investigations of electrical phenomena. It has been stressed, however, that the oscilloscope is just as capable of displaying information on any other phenomenon or change of condition. To this end, all that is needed is to generate, by means of a suitable transducer, a voltage proportional to the phenomenon in question and to feed it to the cathode ray oscilloscope. It is possible in this way to effect considerable improvements on older, familiar methods of measurement and, what is more, to establish new processes of investigation far more revealing and instructive than ever before.

It is the author's hope that this book will not only make its own modest contribution to a more extensive use of the cathode ray oscilloscope in electrical engineering, where it is at home, but will also act as a stimulus to its wider application in other fields of technology and science.

Bibliography

2. The cathode ray tube

1. *Pieplow, H.*, "Meßgenauigkeit und Meßgrenzen technischer Elektronenstrahloszillographen", ATM, I. May [1949], J 8340–5 und II. Jan. [1950], J 8340–6
2. *Garlick, G. F. J.*, "The Physics of Cathode Ray Tube screens", Electronic Engineering, Aug. [1949]
3. *Custers, J. F. H.*, "The recording of rapidly occurring electric phenomena with the aid of the cathode ray tube and the camera", Philips' Tech. Review, Vol. 2, page 148
4. *Blok, L.*, "An apparatus for the measurement of scanning speeds of cathode ray tubes", Philips' Tech. Review, Vol. 3, page 216
5. *Czech, J.*, "Kamera-Aufnahmen von Elektronenstrahloszillogrammen", Zeitschrift für angewandte Photographie, Vol. III, Nr. 5, pp. 65–71
6. *Gier, J. de*, "A cathode ray tube with post-acceleration", Philips' Tech. Review, Vol. 5, page 245
7. *White, W. G.*, "Cathode-Ray Tubes with Post-Deflection Acceleration", Electronic Engineering, March [1949], pp. 75–79
8. *Allard, L. S.*, "An Ideal Post Deflection Accelerator C.R.T.", Electronic Engineering, Nov. [1950], pp. 461–463
9. *Czech, J.*, "Großprojektion von Oszillogrammen", Funk und Ton, Vol. 6, Verlag für Radio-foto-Kinotechnik GMBH, Berlin-Borsigwalde, July and Sept. [1952], Nr. 7, pp. 363–368 and 492–493
   And *Czech, J.*, "Elektronenstrahlröhren", Handbuch für Hochfrequenz- und Elektro-Techniker, Vol. II., Verlag für Radio-Foto-Kinotechnik GMBH, Berlin-Borsigwalde [1953], pp. 280–299

3. Power supply

1. *Dammers, B. G., Haantjes, J., Otte, J.* and *Suchtelen, H. van*, "Application of the Electronic Valve in Radio Receivers and Amplifiers. (A.F. Amplification – The output Stage-power Supply). Design Calculation of high-tension rectifiers. Book V. Philips' Technical Library [1951], pp 362–401
2. *Kammerloher, J.*, "Hochfrequenztechnik", Part III, Gleichrichter, Verlag Wintersche Verlagshandlung, Leipzig [1942], pp. 189–236

4. The time base generator

1. *Richter, H.*, "Elektrische Kippschwingungen", Verlag S. Hirzel, Leipzig [1940]
2. *Puckle, O. S.*, "Time Base Scanning Generators", Chapman & Hall Ltd., London, 2. edition [1952]
3. *Jager, J.*, "Comments on Circuits for Generation of Time-Base Voltages", Philips' Electronic Application Bulletin, Vol. X, Dec. [1948], Nr. 1, pp. 15–29
4. *Kinne, E.*, "Kippgerät für Fernsehempfänger", Funk und Ton, Vol. 6, Aug. [1952], Nr. 8, pp. 429–434
5. "Ein Kippspannungsgerät für Kathodenstrahloszillographen", Philips' Technische Monatshefte, Nr. 33, Jan. [1936], pp. 45–50
6. *Aschen, R.*, und *Chambas, R.*, "The Transitron Effect in H.F. Pentode Type EF 42", Philips' Electronic Application Bulletin, Vol. X, Oct. [1949] Nr. 10, pp. 211–226
7. *Briggs, H. B.*, "The Miller-Integrator", Electronic Engineering, Aug., Sept. and Oct. [1948], pp. 243–247, 279–284 and 325–329
8. *Brunetti, C.*, "The Transitron Oscillator", Proc. I.R.E., Vol. 27 [1939], Nr. 2, p. 88
9. *Cocking, W. T.*, "Linear Saw-Tooth Oscillator", Wireless World, Nr. 6 [1946], p. 176
10. *Kerkhof, F.*, and *Werner, W.*, "Television" [1952], Philips' Technical Library
11. *Hartog, H. den*, und *Muller, E. A.*, "Oscilloscope Time-Base Circuit", Wireless Engineer, Oct. [1947], pp. 287–292
12. *Ferguson, A. E.*, "Feedback in Time-Base Circuits", Electronic Engineering, June [1952], pp. 280–281
13. *Dammers, B. G.*, "A Time-Base Generator for Frequencies of 1 to 100 Mc/s", Philips' Electronic Application Bulletin, Vol. X. June [1949], Nr. 7, pp. 157–166

14. *McQueen, I. G.*, "The Monitoring of High-Speed Waveforms", Electronic Engineering, Oct. [1952], pp. 436–441
15. *Kretzmann, R.*, "Industrial Electronic Handbook", (second edition) 1956, Philips' Technical Library.
16. *Velthoven, Th. M. W.*, "The Oscilloscope, Type GM 5660", Communication News, Vol. XIII June [1953], Nr. 4, pp. 139–146
17. *Bruyer, E. M.*, "Line Selector Checks on Television Waveforms", Electronics, Sept. [1953], pp. 153–155
18. *Czech, J.*, "Besondere Zeitdehnungsverfahren bei Elektronenstrahl-Oszillografen", FTZ, July [1954], Nr. 8, pp. 425–430

5. Deflection amplifiers

1. *Bruin, S. L. de*, and *Dorsmann, C.*, "The investigation of rapidly changing mechanical stresses with the cathode ray oscillograph", Philips' Tech. Review, Vol. 5, page 26
2. *Rothe, H.*, and *Kleen, W.*, "Elektronenröhren als Anfangsstufenverstärker", Bücherei der Hochfrequenztechnik, Vol. 3, Chapter: Breitbandverstärker, Akademische Verlagsgesellschaft Geest & Portig KG., Leipzig, 2. ed. [1948]
3. *Strutt, M. J. O.*, "Verstärker und Empfänger", section: Vorverstärkerstufen, Springer-Verlag, Berlin [1943], pp. 104–109
4. *Bartels, H.*, "Grundlagen der Verstärkertechnik", Chapter V: Vorverstärker, Section 5: Verstärker für breite Frequenzbänder, 2. ed., Verlag S. Hirzel, Leipzig [1944], pp. 158–163
5. *Macek, O.*, "Die Bedeutung der Frequenzkennlinie und Anstiegszeit bei modernen Breitbandoszillografen", Radio Mentor [1952], Nr. 11, pp. 541–542, and "Die Bedeutung der Signal-Laufzeit im Verstärker bei modernen Breitbandoszillografen", Radio Mentor [1952], Nr. 12, pp. 596–597
7. *Kerkhof, F.* and *Werner, W.*, "Television". Chapter VIII Wide-band amplifiers. Philips' Technical Library [1952], pp. 206–301.
7. *Haantjes, J.*, "Judging an amplifier by means of the transient characteristic". Philips' Tech. Review, Vol. 6, page 193
8. *Bedford, A.V.*, "Analysis, Synthesis and Evaluation of the Transient Response of Television Apparatus". Proc. of the I.R.E., Oct. [1942], pp. 330–457
9. *Sloten, J. van*, "Experimental testing of electrical networks by means of the unit function response", Philips' Tech. Review, Vol. 12, page 233
10. *Brück, L.*, "Gegenkopplungsschaltungen", Telefunkenzeitschrift, Nr. 77 [1937], pp. 9–23
11. *Brück, L.*, "Frequenzgang und Schwingneigung gegengekoppelter Verstärker", Telefunkenröhre, Nr. 14 [1938], pp. 237–253
12. *Tellegen, B. D. H.*, "Inverse feed-back", Philips' Tech. Review, Vol. 2, page 289
13. *Deketh, E. T. H. J.*, "Fundamentals of Radio-Valve Technique", Book I. Negative Feedback. Philips' Technical Library. Chapter XXVII, pp. 377–406
14. *Müller, J.*, "Die Übertragung der Sprungfunktion durch den gegengekoppelten Verstärker", FTZ [1951], Nr. 12, pp. 547–551
15. *Dammers, B. G.*, *Haantjes, J.*, *Otte, J.* and *Suchtelen, H. van*, "Application of the Electronic Valve in Radio Receivers and Amplifiers". Book V. (A.F. Amplification – The output Stage-Power Supply). Article: Phase inverters and splitters. Philips' Technical Library. 1951, pp. 18–30
16. *Sowerby, J. Mc. G.*, "Electronic Circuitry", Wireless World, Sept. [1948], p. 321, and "Der Ausgangswiderstand des Katodenverstärkers", Funk und Ton, Vol. 2 [1948], Nr. 12, pp. 657–658
17. *Geyger, W.*, "Der Katodenverstärker", Funk und Ton, Vol. 2 [1948], Nr. 3, pp. 119–124
18. *Rothe, H.*, und *Kleen, W.*, "Elektronenröhren als Anfangsstufenverstärker", Vol. 3, Akademische Verlagsgesellschaft Geest & Portig KG., Leipzig [1948], pp. 198–201
19. *Amos, S. W.*, "Valves with resistive Loads", Wireless Engineer, Apr. (1949], pp. 119–123
20. *Ross, S. G. F.*, "Design of Cathode-coupled Amplifiers", Wireless Engineer, July [1950], pp. 212–215
21. *Dillenburger, W.*, "Der Kathodenverstärker", Funk und Ton, Vol. 5 [1951], Nr. 4, pp. 190–193
22. *Flood, J. E.*, "Cathode-Follower Input Impedance", Wireless Engineer, Vol. 28, Nr. 335, Aug. [1951], p. 231

7. Simple amplitude measurement

1. *Pieplow, H.*, "Meßgenauigkeit und Meßgrenzen technischer Elektronenstrahloszillografen", ATM, May [1949], J 8340–5
2. *Round, H. J.*, "Impedance Measurement, Comparison Method with C. R. Indicator". Wireless Engineer, May [1950], pp. 154–158
3. *Emschermann, H. H.*, und *Zinke, O.*, "Messung von Kapazitäten bei Hochfrequenz", ATM, Sept. [1951], V 3533–2

8. The oscilloscope as null-indicator in *AC* bridge circuits

1. *Oetker, R.*, "Das Braunsche Rohr als Indikator für Wechselstrombrücken", Frequenz, Febr. [1951], Nr. 2, pp. 33–38
2. *Brailsford, H. D.*, "Measuring Coil Characteristics without an Impedance Bridge", Electronics Manual for Radio Engineers, Vol. 20, Febr. [1949], pp. 239–242
3. *Holleufel, W.*, "Oszillograf als einfacher Nullindikator in Wechselstrombrücken", Die Elektro-Post, Nr. 10 [1952], pp. 191–192
4. *Cole, R. H.*, "Use of the Cathode-Ray Tube for Comparison of Capacities", Review of Scientific Instruments, June [1941], pp. 298–300
5. *Frommer, I. C.*, "*AC* Null Indicator", Electronics, Oct. [1951], pages 136, 138, 140, 160 and 164
6. *Suchtelen, H. van*, "Comments on magnetic sorting bridges", Philips' Electronic Application Bulletin, Nr. 12 [1949], pp. 261–273, and *Wilson, W.*, "The Cathode Ray Oscillograph in Industry", Chapman & Hall Ltd., London [1948], pp. 155–157
7. *Crowhurst, N. H.*, "Transformer Iron Losses", Electronic Engineering. Oct. [1951], pp. 396–403

9. The display of hysteresis loops

1. *Jonker, G. H.* and *Santen, J. H. van*, "The ferro-electricity of titanates". Philips' Tech. Review, Vol. 11, page 183
2. *Ettinger, G. M.*, "Butterfly Curve Tracer for Magnetic Materials", Electronics, March [1953], pp. 119–121
3. *Griessen, B.*, and *Zwaag, H. v. d.*, "Aufnahme der Wechselstrommagnetisierungskurven mit Hilfe elektronischer Meßgeräte", Philips' Elektronisch Messen, Vol. 3 [1953], Nr. 10, pp. 2–11

10. The uses of intensity modulation

1. *Czech, J.*, "Exact Measuring of the Opening Time of Camera Shutters with a Cathode Ray Oscillograph", Philips' Electronic Measuring, Vol. 8., Nr. 8 [1953].
2. *Tucker, M. J.*, "A Note on Electronic Analogue Integration and Differentiation", Electronic Engineering, Jan. [1953], p. 35
3. *Klein, P. E.*, "Elektronenstrahloszillographen", Vol. 1, Weidmannsche Verlagsbuchhandlung, Berlin [1948], Differenzierung, Integrierung, pp. 102 and 103
4. *Janssen, J. M. L.* and *Ensing, L.*, "The electro-analogue, an apparatus for studying regulating systems". Philips' Tech. Review. I. Components and functions, Vol. 12, Page 257; II. The electrical execution, Vol. 12, page 319
5. *Wilson, W.*, "The Cathode Ray Oscilloscope in Industry, Automatic Brilliancy Control", Chapman & Hall Ltd., London [1948], p. 46
6. *Rochelle, R. W.*, "Cathode-Ray-Tube Beam Intensifier", Electronics, Oct. [1952], pp. 151–153
7. *Klerk, I. de*, "Automatic C.R.T. Trace Brightening for Varying Amplitude R.F. Signals", Electronic Engineering, Sept. [1953], pp. 388–389
8. *Niesten, I. G.*, und *Wijnterp, W.*, "Het registreeren van polaire diagrammen van enkele electrische grootheden bij constante frequentie met behulp van electronenstraaloscillograaf en camera", De Ingenieur, 58, Jg. [1946], Nr. 32, pp. 33–38, and "Berekening en registratie van enkele polaire stroomfiguren aan een autotransformator met variabele overzetting, welke met een constanten weerstand is belast", De Ingenieur, Vol. 59, June [1947], pp. 23–27
9. *Sulzer, P. G.*, "Vector Voltage Indicator", Electronics, June [1949], pp. 107–109

10. *Mac Kay, D. M.*, "Projective Three-dimensional Displays", Electronic Engineering, July [1949], pp. 249–254, and Aug., pp. 281–286
11. *Admiral, D. J. H.*, "Tracing Vector Locus Diagrams by Means of a Cathode-Ray Oscilloscope", Philips' Electronic Application Bulletin [1950], Nr. 1, pp. 2–14
12. *Schäfer, O.*, "Ortskurvenschreiber für den Tonfrequenzbereich", ATM, June [1952], I 036–8, pp. 137–138
13. *Genç, Selahattin*, "Ein Kathodenstrahloszillograph zur Untersuchung von Functionen zweier Variabelen", Technische Mitteilungen PTT [1950], Nr. 9, pp. 342–348
14. *Grevel, R., Grundlach, F. W.*, and *Herklotz, H.*, "Die Erzeugung von dreidimensionalen Meßdiagrammen mit dem Kathodenstrahloszillographen", ATM, Nov. [1951], J 8344–6
15. *Janssen, J. M. L.*, and *Michels, A. J.*, "An experimental "stroboscopic" oscilloscope for frequencies up to about 50 Mc/s", II. Electrical build-up, Philips' Tech. Review, Vol. 12, page 73.
16. *Foster, B. C.*, "A simple Valve Comparator", Electronic Engineering, May [1952], pp. 220–223
17. *Classen, R., Gundlach, F. W.*, and *Lentze, F.*, "Ein Bildrasterverfahren zur gleichzeitigen Abbildung meherer Vorgänge mit dem Elektronen-Einstrahl-Oszillographen", ATM, Sept. [1951], J 8344–5

11. Phase measurements

1. "Gleichzeitige Wiedergabe meherer Vorgänge auf dem Leuchtschirm eines Oscillographen", Philips' Elektronisch Messen, Vol. 2. [1948], Nr. 4, pp. 2–16
2. *Dorsman, C.*, and *Bruin, S. L. de*, "An electronic switch". Philips' Tech. Review. Vol. 4, page 267
3. *Carpentier, E. E.*, "An electronic switch with variable commutating frequency". Philips' Tech. Review. Vol. 9, page 340
4. *Firestone, W. L.*, und *Bloniarz, R. M.*, "Non-distorting CRO Switch", Electronics, July [1952], pp. 139–141
5. *Mackay, R. St.*, "Switch Provides Reference Display", Electronics, Dec. [1952], pp. 122 and 123
6. *Benson, F. A.*, and *Carter, A. O.*, "Phase-Angle Measurements", Electronic Engineering, June [1950], pp. 238–242
7. *Sabaroff, S.*, "Technique for Distortion Analysis", Electronics, June [1948], pp. 114–117
8. *Nijenhuis, W.*, "Measurement of phase angles with the help of the cathode ray tube". Philips' Tech. Review. Vol. 5, page 208
9. *Patchett, G. N.*, "A Versatile Phase-Angle Meter", Electronic Engineering, May [1952], pp. 224–229
10. *Bartels, H.*, "Grundlagen der Verstärkertechnik", Verlag S. Hirzel, Leipzig [1949], Messung des Phasenmaßes, pp. 24–27
11. *Thiede, H.*, "Die Umwandlung zweier phasenverschobener Spannungen in zwei phasengleiche Spannungen mit einem durch die Phase bestimmten Spannungsverhältnis", Funk und Ton, Vol. 2 [1948], Nr. 3, pp. 111–118
12. *Grübel, G.*, "Phasenmesser für Labor und Prüffeld", Funk und Ton, Vol. 3 [1949], Nr. 6, pp. 315–319
13. *Grübel, G.*, "Zwei einfache Summe-Differenzschaltungen", Funk und Ton, Vol. 3 [1949], Nr. 11/12, pp. 591–593
14. *Ruhrmann, A.*, "Hochfrequenz-Phasenmessung mit direkter Anzeige", ATM, May [1950], V 3631–3, T 52/53
15. *Pitsch, H.*, "Lehrbuch der Funkempfangstechnik", Akademische Verlagsgesellschaft Geest & Portig KG., Leipzig [1948], Stromquellen-Ersatzschaltung, pp. 6–7
16. *Günther, H.*, "Tafeln zur Umwandlung von Reihenschaltungen komplexer Widerstände in äquivalente Parallelschaltungen", Funk-Technik, Verlag für Radio-Foto-Kinotechnik GMBH, Berlin-Borsigwalde, Vol. 6 [1951], Nr. 2, pp. 52–53
17. "Eine neue Meßmethode zur Fehlerortung in Kabeln und Freileitungen", Frequenz, Vol. 6 [1952], Nr. 7, pp. 213–215
18. *Reverey, G.*, "Die zerstörungsfreie Prüfung von Isolatoren", ETZ, Ausg. A, Vol. 73 [1952], Nr. 14, pp. 451–455
19. *Terman, F. E.*, "Radio Engineers' Handbook", McGraw-Hill Book Company Inc., New York and London [1943], Square-wave Testing, pp. 968–971

20. *Moss, H.*, "Cathode Ray Tube Traces", Electronic Engineering, London, Sept. [1949], pp. 52–55
21. *Schiffel, R.*, "Empfängerprüfung mit dem Multivibrator", Das Radio Magazin [1949], Nr. 9, pp. 254–256
22. *Köhler, A.*, "Verstärkerprüfung mit Rechteckschwingungen", Das Radio Magazin [1949], Nr. 13, pp. 379–382
23. *Meyer-Eppler, W.*, "Die Messung der Frequenzcharakteristik linearer Systeme durch einmalige oder wiederholte Schaltvorgänge", TFZ [1951], Nr. 4, pp. 174–182
24. *Müller, J.*, "Die Bestimmung des Amplituden- und Phasenganges von linearen Übertragungssystemen mit Hilfe von Rechteckwellen", FTZ [1951], Nr. 5, pp. 211–220
25. *Schlegel, H.*, "Elemente der Impulstechnik", I. Rechnerische Behandlung der Impulse und ihrer Verzerrungen durch einfache Vierpole, Radio Mentor [1951], Nr. 4, pp. 183–189, II. Der Impulsübertrager, Nr. 7, pp. 336–340, and III. Impulsverstärker, Nr. 11, pp. 554–558
26. *Zimmermann, H.*, "Der Anteil des ZF-Verstärkers am Einschwingvorgang eines Fernsehempfängers", FTZ [1951], Nr. 12, pp. 537–542
27. *Bryan, H. E.*, "Square Wave Testing Simplified", Audio Engineering, Oct. [1951], pp. 14–15
28. *Hershler, A.*, and *Seidman, A. H.*, "General Purpose Short-Pulse Generator", Electronics, Aug. [1953], pp. 182–183
29. *Müller, J.*, "Die Prüfung von Fernsehübertragungssystemen mit Hilfe von Rechteckwellen", Funk und Ton, Vol. 6 [1952], Nr. 12, pp. 617–631

12. Frequency measurements

1. *Suchtelen, H. van*, "Measuring the rate of watches with a cathode-ray oscillograph". Philips' Tech. Review. Vol. 9, page 317
2. *Briggs, B. H.*, "The Miller-Integrator", Electronic Engineering, Aug., Sept., Oct. [1948], pp. 243–247, 279–284 and 325–329; also Funk und Ton, Vol. 2 [1948], Nr. 12, pp. 653–655
3. *Barkhausen, H.*, "Einführung in die Schwingungslehre", Verlag S. Hirzel. Leipzig [1940.] pp. 53–59
4. *Moller, W.*, "Die Braunsche Röhre", IV. edition [1949], pp. 176–194
5. *Feldtkeller, R.*, "Einführung in die Theorie der Rundfunk-Siebschaltungen", Verlag S. Hirzel, Leipzig, 3. edition [1945], pp. 54–61, Fig. 29a, b, c, d and Fig. 31
6. *Kanberg, H.*, "Die Breite des Mitnahmebereichs bei der Steuerung eines selbsterregten Röhrengenerators durch ganze Vielfache seiner Eigenfrequenz" Funk und Ton, Vol. 3 [1949], Nr. 9, pp. 497–505
7. *Laporte, H.*, "Die Messung von elektrischen Swingungen aller Art nach Frequenz und Amplitude", Verlag Knapp, Halle [1949]
8. *Klein, P. E.*, "Zeit- und Kurzzeitmessungen mit Elektronenstrahloszillographen", Weidmannsche Verlagsbuchhandlung, Berlin, Aug. [1949]
9. *Bader, W.*, "Frequenzvergleich durch Zykloiden", Archiv für Elektrotechnik, XXXIV. Vol. [1948], Nr. 2/3, pp. 115–124
10. *Czech, J.*, and *Rodrian, G.*, "Darstellung von Vorgängen der analytischen Mechanik mit dem Elektronenstrahloszillografen", Funk und Ton, Vol. 4 [1950], Nr. 5, pp. 239–249
11. *Wilson, W.*, "The Cathode Ray Oscillograph in Industry", Chapman & Hall Ltd., London [1948], Directional synchroscope, Fig. 67, p. 90
12. *Lewer, S. K.*, "The Cathode-Ray Tube Handbook", Sir Isaac Pitman & Sons Ltd., London [1947], Comparison of Frequencies, p. 86, Fig. 32
13. *Reich, H. J.*, "Circuits for oscillographic frequency comparison", Review of Scientific Instruments, Vol. 8, Sept. [1937], p. 348
14. *Rangachari, T. S.*, "The Harmonic Comparison of Radio Frequencies by the Cathode-Ray Oscillograph", Exper. Wireless and Wireless Eng., Vol. 5, May [1928], p. 264
15. *Rangachari, T. S.*, "The Super-position of Circular Motions", Exper. Wireless and Wireless Eng., Vol. 6, April [1929], p. 184
16. *Dorf, H.*, "Audio Patents", Audio Engineering, May [1951], pp. 2–4, and *Jaynes*, E.T. USA-Patent Nr. 2,541,067

13. Recording the waveforms of the luminous flux, current and voltage of fluorescent lamps

1. *Oranje, P. J.*, "Gas discharge Lamps". Philips' Technical Library [1951]
2. *Endler, H.*, "Die Betriebstechnik der Leuchtstofflampe", Elektrotechnik, Vol. 34., Nov. [1952], Nr. 45, pp. 3–5
3. *Kretzmann, R.*, "Industrial Electronics Handbook" (second edition) [1956]. Philips' Technical Library

15. Investigations on television receivers

1. Funk-Technik, Vol. 7 [1952], Nr. 4, pp. 111 and 112
2. Funk-Technik, Vol. 8 [1953], Nr. 1, pp. 15 and 16
3. *Fisher, J.*, "Television Picture Line Selector", Electronics, March [1952], pp. 140–143
4. *Kerkhof, F.*, and *Werner, W.*, "Television", Separation of the composite synchronizing signal, Philips' Technical Library [1952], pp. 96–99.
5. *Demus, E.*, "Untersuchungen an Fernseh-Studio-Einrichtungen mit Hilfe von Synchronisierimpulsen veränderlicher Phasenlage", FTZ [1953], Nr. 5, pp. 208–213
6. *Bruyer, E. M.*, "Line Selector Checks Television Waveforms", Electronics, Sept. [1953], pp. 153–155

16. Measuring the action of between-lens shutters

1. *Wilson, W.*, "The Cathode-Ray-Oscillograph in Industry", Chapman & Hall Ltd., London, "Timepieces" [1948], pp. 112–113
2. *Blok, L.*, "An apparatus for the measurement of scanning speeds of cathode ray tubes". Philips' Tech. Review, Vol. 3, page 216
3. *Czech, J.*, "Darstellung abklingender Schwingungen als stehendes Bild auf der Kathodenstrahlröhre", VDI-Zeitschrift, Vol. 84 [1940], Nr. 5, pp. 83–85, Fig. 6

19. Measuring the travel time in four-terminal networks, etc.

1. *Röschlau, H.*, "Die Anwendung der Impulstechnik zur Prüfung von Fernseh-Übertragungseinrichtungen". NWDR-Hausmitteilungen, 5 [1953], pp. 187–190
2. *Kaden, H.*, "Über das Verhalten von Kabeln mit Wellenwiderstandsschwankungen bei Fernseh- und Meßimpulsen". Archiv der elektr. Übertragung, Vol. 7 [1953], pp. 157–162
3. *Reintjes, J. F.*, Principles of Radar, Koate G. T. third edition, 1952. McGraw–Hill Book Company – New York

21. Special duty oscilloscope "FTO–2"

1. *Czech, J.*, "FTO 1 Elektronenstrahl-Oszillograf", Funk-Technik, Vol. 5 [1950], Nr. 10, 11 and 12, pp. 306–308, 342–344, 374–376 and 382
2. *Briggs, B. H.*, "The Anode Follower", R.S.G.B. Bulletin, Vol. 22 [1947], pp. 138–143

22. Simple time-base expansion unit

1. *Kretzmann, R.*, "Industrial Electronics Handbook" (second edition) [1956]. Philips' Technical Library
2. *Huggins, P.*, "Changing the Phase of a Low Frequency Sinusoid", Electronic Engineering, Oct. [1952], pp. 462–464
3. *Moeller, F.*, "Strom-, Spannungs- und Phasenregelung für Meßzwecke", Verlag G. Braun, Karlsruhe, 1. ed. [1949]

Index

S

T

PHILIPS TECHNICAL LIBRARY

Philips' Technical Library comprises 4 series of books:

a. Electronic Valves
b. Light and Lighting
c. Miscellaneous
d. Popular series

Series *a*, *b* and *c* in cloth binding 6″ × 9″, gilt. The dimensions of the popular series, coloured "integral" binding, are $5\frac{3}{4}$″ × $8\frac{1}{4}$″.
Most of these books are published in 4 languages: English, French, German and Dutch.

a. Series on ELECTRONIC TUBES

Book	I	"Fundamentals of Radio-Valve Technique", by J. Deketh
Book	II	"Data and Circuits of Receiver and Amplifier Valves"
Book	III	"Data and Circuits of Receiver and Amplifier Valves", 1st Suppl.
Book	IIIA	"Data and Circuits of Receiver and Amplifier Valves", 2nd Suppl., by N. S. Markus and J. Otte
Book	IIIB	"Data and Circuits of Receiver and Amplifier Valves", 3rd Suppl., by N. S. Markus and J. Vink
Book	IIIC	"Data and Circuits of Television Receiving Valves", by J. Jager
Book	IV	"Application of the Electronic Valve in Radio Receivers and Amplifiers", Volume I, by B. G. Dammers, J. Haantjes, J. Otte and H. van Suchtelen
Book	V	Ditto, Volume 2
Book	VII	"Transmitting Valves", by P. J. Heyboer and P. Zijlstra
Book	VIIIA	"Television Receiver Design" 1, by A. G. W. Uitjens
Book	VIIIB	"Television Receiver Design" 2, by P. A. Neeteson
Book	IX	"Electronic Valves in Pulse Technique" by P. A. Neeteson
Book	X	"Analysis of bistable Multivibrator Operation", by P. A. Neeteson
Book	XI	"U.H.F. Tubes for communication and Measuring Equipment"
Book	XII	"Tubes for Computers"
Book	XIII	"Industrial Rectifying Tubes"

Book IIIB and XIII are in active preparation.

b. Series "LIGHT AND LIGHTING"

1. "Physical Aspects of Colour", by P. J. Bouma
2. "Gas Discharge Lamps", by J. Funke and P. J. Oranje
3. "Fluorescent Lighting", by Prof. C. Zwikker c.s.
4. "Artifical Light and Architecture", by L. C. Kalff (size 7″ × 11″)
5. "Artificial Light and Photography", by G. D. Rieck and L. H. Verbeek (size 7″ × 11″)
6. "Manual for the Illuminating Engineer on Large Size Perfect Diffusors", by H. Zijl
7. "Calculation and Measurement of Light", by H. A. E. Keitz
8. "Lighting Practice", Volume I, II and III, by Joh. Jansen
9. "Illuminating Engineering Course", by H. Zijl

Book 4 in German only. The English edition of book 8 is in preparation.

c. Series "MISCELLANEOUS"

a. "Television", by Fr. Kerkhof and W. Werner
b. "Low-Frequency Amplification", by N. A. J. Voorhoeve

c. "Metallurgy and Construction", by E. M. H. Lips
d. "Strain Gauges", by Prof. J. J. Koch
e. "Introduction to the study of Mechanical Vibrations", by G. W. v. Santen
f. "Data for X-Ray Analysis", I, by W. Parrish and B. W. Irwin (size 8.2″ × 11.6″), paper bound
g. "Data for X-Ray Analysis" II, by W. Parrish, M. G. Ekstein and B. W. Irwin (size 8.2″ × 11.6″), paper bound
h. "X-Rays in Dental Practice", by G. H. Hepple
i. "Industrial Electronics Handbook", by R. Kretzmann
j. "Introduction to TV-Servicing" by H. L. Swaluw and J. v. d. Woerd
k. "From the Electron to the Superhet", by J. Otte, Ph. F. Salverda and C. J. van Willigen
l. "How Television works" by W. A. Holm
m. "The Cathode Ray Oscilloscope" by J. Czech
n. "Industrial Electronics Circuits" by R. Kretzmann
o. "Medical X-Ray Technique" by G. J. van der Plaats and L. Penning
p. "Electrical Discharges in Gases" by F. M. Penning
q. "Tube Selection Guide compiled" by Th. J. Kroes

Books l, o and p are in active preparation.

"POPULAR SERIES"

Our "Popular Series" is intended to meet the growing demand for works on technical subjects written in a way that can be readily understood by the less advanced reader. Popular as used here does not mean superficial, but intelligible to a wider public than is catered for by the other more specialized books in Philips Technical Library.

1. "Remote Control by Radio", by A. H. Bruinsma
2. "Electronic Valves for L. F. Amplification", by E. Rodenhuis
4. "Battery Receiving Valves", by E. Rodenhuis
5. "Germanium Diodes", by S. D. Boon
6. "Introduction to the Cathode Ray Oscilloscope", by Harley Carter
7. "From Microphone to Ear", by G. Slot
8. "Valves for A. F. Amplifiers", by E. Rodenhuis
9. "Robot Circuits", by A. H. Bruinsma

Books 4 and 9 are in preparation.

PHILIPS JOURNALS

a. Philips Technical Review
b. Philips Research Reports
c. Philips Telecommunication Review
d. Philips Serving Science and Industry
e. Medicamundi
f. Electronic Applications